ISBN 0-315-53253-X

PARAMETRIC ANALYSIS OF CAPWAP RESULTS

A parametric analysis and evaluation of the uniqueness of the CAPWAP solution and the impact of parametric variation on the results

Mohamad Mozher Hamzeh

A Thesis

Submitted under the supervision of

Dr. Bengt H. Fellenius

Professor

in partial fulfillment

of the requirement for the degree of

Master of Applied Science

Department of Civil Engineering
Faculty of Science and Engineering
University of Ottawa
Ottawa, Ontario
Canada

June 9, 1989

And lower unto them the wing of submission through mercy, and say: My Lord, Have mercy on them both as they did care for me when I was little.

(Quran, s.XVII, v.24)

To mother and father . . .

ACKNOWLEDGEMENTS

I would like to express my sincere gratitude to my wife Saff for her support, patience, and understanding during the course of writing this thesis. I would like also to thank my colleagues Mr. A. Alta'i, Mr. H. Hachem, and Mr. N. Khan, for their enlightening and challenging discussions of my work during the course of analysis. Special thanks are expressed to Dr. V. Garga, and Dr. E. Evgin for their assistance in broadening the views of my geotechnical education. The efforts of the support staff of the Civil Engineering Department are kindly acknowledged for their willing help and continued assistance during my residence at the university. Additional gratitude is expressed to my colleague and friend Mr. H. Hachem for willingly being my contact with the university during my residence outside Ottawa. Last, but not least, I would like to express my sincere gratitude to Mr. R. A. Gould for his comments on my work and helpful advice during the final stages of writing this report.

This reaserch has been financially supported by an NSERC grant. The field data have been provided by Terratech Limited of Montreal. The final report of this research has been produced using the computing facilities of Golder Associates, London, Ontario.

SUMMARY

The CAPWAP is a Wave Equation Analysis technique which utilizes dynamic measurements taken at pile head during driving to estimate pile bearing capacity among other things. The practical reliability of the CAPWAP have caused its promotion as an alternative to the static loading test. While the popularity of the method is increasing, questions are being raised about the parametric interdependence of the CAPWAP, and its effects on the estimated results. This research is a parametric study aimed to investigate the effects of parametric interdependence on the CAPWAP solution.

The CAPWAP method is a development of the Wave Equation Analysis procedure introduced by Smith in 1960. The basic soil model utilized in the CAPWAP recognizes two components of soil resistance: static and dynamic. The static soil resistance is modelled as a frictional spring charterized by two quantities: maximum soil resistance, and quake (limit of elastic deformation). The dynamic soil resistance is modelled as a linear dashpot where dynamic resistance is directly proportional to pile element velocity through a damping coefficient. In addition to Smith parameters, The CAPWAP soil model was expanded to include unloading quakes, unloading soil resistance, toe gap, soil plug, and soil toe damper.

The CAPWAP method utilizes dynamic measurements of strain (force) and acceleration (velocity) at pile head during driving. The force measurements are iteratively simulated using the measured velocity and assumed soil properties. The analysis terminates when a good agreement is achieved between the measured and computed force traces. The soil parameters assumed are then considered representative of actual soil properties.

The parametric analysis of the CAPWAP method was carried out using dynamic data from four industrially monitored piles. Three of the piles analyzed were steel pipe piles, while one pile was a steel H pile. The soil conditions at the sites of two piles, labelled JI and JA, were similar to those encountered at many piling sites. The soil conditions at the site of JI Pile generally consisted of 26 m of clayey postglacial deposits underlain by glacial till. The JA Pile was driven through sandy soils. The soil conditions at the site of AM Pile consisted of very sensitive Champlain clays, and the blow analyzed for the pile was extracted from restrike records. Unorthodox conditions, however, existed at the site of LW Pile which was driven through weathered sandstone. The weahthered rock probably crumbled into sand as the pile toe advanced.

The criterion for selection of analysis blows insured that mobilization of ultimate soil resistance was attained. Some deficiencies were observed in the quality of data processed. However, no adjustments were provided to improve the quality of the data except for

static force shifts. Such adjustment insured that the force records at pile heads had values of zero prior to the beginning of loading

The analysis procedure consisted of first obtaining a very good match for each pile analyzed. A predefined resistance increment was then added to the estimated soil resistance. This, obviously, destroyed the match. The destroyed match was restored by varying the program parameters other than the total static resistance. The addition of resistance increments followed by restoration of the match was repeated until rematching was no longer possible. This defined what is believed to be the upper bound of the CAPWAP solution. The lower bound of the solution was similarly obtained by applying resistance decrements.

The parametric analysis of the record blows resulted in a range of ultimate soil resistance for each pile analyzed. For JI Pile, ultimate soil resistance ranged from 900 to 1500 KN. Ultimate soil resistance ranged from 450 to 650 KN, and from 1275 to 1725 KN for JA and AM Piles, respectively. Larger variation was obtained for LW Pile with a corresponding ultimate soil resistance ranging from 300 to 1125 KN. Verification of the estimated pile capacities, except for AM Pile, was not possible due to the lack of static loading tests. The reported AM Pile capacity as estimated from a static loading test ranged from 1500 to 1900 KN (Fellenius, 1988). The variation of pile capacities, expressed as a percentage of the difference of maximum or minimum obtained Rult to the average Rult value, ranged from ±15 to ±58 percent. Based on the results of the four piles analyzed, the variation of estimated ultimate soil resistance may be expected to be less than ±58 of the average Rult value, or more appropriately, less than ±25 percent of the average Rult value if LW Pile results were disregarded. Due to unusual soil conditions, and analytical evidence to follow, the results of LW Pile were not considered quantitatively representative.

The variation of ultimate soil resistance was due to variations of other CAPWAP parameters, of which, the variation of damping had the most noticeable effects. The decrease in ultimate soil resistance was concurrent with a corresponding increase in Smith damping coefficient values. This indicates a deficiency in the capacity of CAPWAP in filtering out the static and dynamic components of resistance. However, the deficiency is limited to the range of ultimate soil resistance obtained for each pile.

The Smith damping coefficients obtained for pile shafts ranged from 0.0 to 0.9 s/m with typical values ranging from 0.1 to 0.2 s/m. The corresponding Smith damping coefficients for pile toes ranged from 0.4 to 2.3 s/m, but had values of typically 0.6 to 0.8 s/m. The Smith damping coefficients obtained for LW Pile toe ranged from 2.2 to 14.1 s/m. Such values are excessively large, and cannot be correlated to any existing practical experience. The large damping values for the pile toe resulted in relatively low static toe resistance. Due to the unconventional soil conditions at the site of the pile, and the lack of static loading test correlation, the quantitative implications of the CAPWAP results obtained for LW Pile were cautiously utilized.

The quake values obtained from the analysis of a single pile did not exhibit any relation to the variation of ultimate soil resistance. Generally, the quake values obtained for pile shafts ranged from 0.5 to 5.0 mm, while the quake values obtained for pile toes ranged from 1.5 to 6.5 mm. The typical quake values obtained for pile shafts and pile toes were 2.5 and 5.0 mm, respectively. However, the compilation of quake results obtained from the four piles indicated a general trend of increasing quakes with ultimate soil resistance. This relationship did not contribute to the parametric interdependence of CAPWAP results in any of the cases analyzed. But, it was an indication of the global properties of soil quakes.

The results of variation of secondary CAPWAP parameters such as unloading quakes and shaft resistance, toe gap, and toe soil damper, indicated random variation of these quantities within the range of ultimate soil resistance obtained for a given pile. The effects of secondary CAPWAP parameters, with the exception of toe gap, were observed to be cosmetic. The variations of these parameters served to enhance the general appearance of the match without, practically, affecting the estimated pile capacity. The toe gap parameter was observed to contribute significantly to the parametric interdependence of the pile toe results. The parameter was observed to substitute either or both, the static and dynamic soil resistance of the toe element. This is due to the sharp lowering of the computed force trace in the pile toe reflections region associated with a toe gap. Thus, the rising of the computed trace associated with soil resistance can be effectively counterbalanced.

The results of static resistance distribution estimated from CAPWAP were generally consistent with the results of effective stress principles and the expected behavior of the soil at the sites of the piles. The static resistance distribution of JI Pile indicated lower capacity in the portion of the pile above depth 26 m. This was expected due to generation of excess pore pressures in the postglacial clayey deposits at the site above that depth. The shaft resistance for JA Pile generally increased with depth consistent with expectations of pile shaft resistance in sandy deposits. The shaft resistance distribution for AM Pile linearly increased with depth in the upper portion of the pile. However, very low capacity was estimated in the lower portion of the shaft. This is due to soil setup following the end of initial driving, and the gradual remolding of the soil during restrike which probably originated in the lower portion of the pile. The resistance distribution for LW Pile generally increased with depth. However, the estimated toe resistance was very low, typically, 11 percent of the total pile capacity. Such low toe resistance is considered unreasonable, and the misestimate, if any, may be due to incorrectly determined magnitudes of dynamic resistance.

The variation of CAPWAP parameters have caused coherent variations in the maximum compression and tension forces, maximum element velocities, and maximum elements displacements computed in the pile. The variation of these quantities was observed to increase with depth. The maximum variations of these quantities, except for tension forces, was less than the variation of ultimate soil resistance estimates. The variation of computed tension forces was significantly larger. the coefficients of variation (percent standard deviation to average value) computed for tension forces ranged from 0 to 245 percent. The coefficients of variations obtained for the other dynamic quantities ranged from 0 to 16 percent.

TABLE OF CONTENTS

CHAPTER CONTENTS

CHAPTER CONTENTS (Continued)

CHAPTER CONTENTS (Continued)

CHAPTER CONTENTS (Continued)

LIST OF TABLES

LIST OF TABLES (Continued)

LIST OF FIGURES

LIST OF FIGURES (Continued)

LIST OF FIGURES (Continued)

LIST OF FIGURES (Continued)

LIST OF FIGURES (Continued)

LIST OF FIGURES (Continued)

LIST OF FIGURES (Continued)

CHAPTER 1

INTRODUCTION

1.1 General

For centuries, piles have been installed by means of impact hammers. The pile capacity has traditionally been estimated from penetration resistance (blow-count) recorded at the end of driving. This technique is subject to much uncertainty and its use makes pile foundation design inarticulate. During the last twenty years, representative modelling of pile driving has been incorporated into several computer programs. However, these programs rely on assumed and unsubstantiated input data. About fifteen years ago, the advent of CAPWAP (CAse Pile Wave equation Analysis Program) provided a solution to this problem.

The CAPWAP applies a comprehensive model to simulate pile driving and makes use of two quantities recorded at pile head during driving: acceleration and strain (force). A digital computer, the so-called Pile Driving Analyzer (PDA) receives these two quantities in analog form. The PDA integrates acceleration into velocity and stores it, together with the force signal, onto a magnetic tape. In the laboratory, the field measurements are played back and loaded into a computer used in conjunction with the CAPWAP program.

Using the velocity as a boundary condition, the force generated in the pile during a hammer blow is simulated and compared to the force recorded during driving.

The CAPWAP input consists of soil parameters, such as resistance, limit of elastic deformation (quake), and viscous damping as assumed acting along the pile. For the first computation, there is little agreement only. However, guided by the nature of disagreement between the computed and measured force, the operator adjusts the input parameters. After several successive calculations (trials), an agreement or a match is achieved. The soil parameters applied as input for the last program run are considered representative for the actual soil conditions at the site during driving.

1.2 Statement of the Problem

One of the most important uses of the CAPWAP analysis is to determine the soil resistance and its distribution, i.e., pile capacity. However, it has been found that the CAPWAP's numerical solution is not unique. For instance, when changing marginally one parameter, say soil resistance, the resulting mismatch between the calculated and measured force traces can be corrected by changing either or both the quake and damping parameters. Because the CAPWAP analysis is being promoted to replace the static loading test, determining the degree of interdependence of the CAPWAP parameters becomes important.

1.3 Objectives of the Investigation

The objectives of the research are to investigate the parametric interdependence of the CAPWAP results, and the extent of uniqueness of the CAPWAP solution.

1.4 Scope of the Study

Representative dynamic data from four industrially monitored piles have been digitized, processed, and analyzed.

For each one of the monitored piles, several blows from a depth were selected and digitized. For three of the four piles, the blows were selected from initial driving at a depth slightly above refusal. For the other pile, the blows were selected from restrike records. One blow was processed for each pile to obtain Case Method estimate and to prepare for CAPWAP analysis.

For each blow analyzed, a very good match was first established and labelled Reference Match. Then, a resistance increment of 5 percent of the utimate soil resistance was added to the computed soil resistance. Naturally, this destroyed the match. The match was subsequently restored by adjusting the other parameters. Adding resistance increments and restoring the match was repeated until restoring the match was not possible. This established the solution's upper bound. The lower bound was established in a similar manner by subtracting resistance increments. Knowing the upper and lower bounds, the range of solutions indicated the expected CAPWAP reliablility range.

1.5 Outline of the Report

The material presented in this report is organized as follows:

- Historical review of pile dynamics school of thought.
- Introduction to the basics of wave equation with emphasis on the Smith model. Brief introduction to two computer programs using the Smith model: The TTI and WEAP.
- Introduction to the dynamic monitoring of pile driving. The Pile Driving Analyzer and data acquisition system. Data digitizing and processing.
- The CAPWAP model and philosophy. Description of variables not available in the Smith model. Matching techniques. The nature of CAPWAP traces and regions of influence of different parameters.
- Description of field data.
- Parametric analysis of the CAPWAP model.
- Discussion of the results and the CAPWAP analysis.
- Conclusions.

CHAPTER 2

THEORETICAL BACKGROUND

2.1 General

The origin of pile foundations is lost in antiquity. In very early times, if the subsoil was obviously too weak for the support of a structure, rows of stakes were driven into the ground to provide a more firm bearing. Pile foundations were used by the Aztecs in North America before the coming of the Europeans. In Europe, the art of pile driving was well established in Roman times. Details of piled foundations were recorded by Vitruvius in 59 A.D. (Peck et al., 1966). The piles were originally relatively short, and the driving equipment was primitive. The drop hammer is the earliest type of pile driving equipment.

Early pile drivers were powered by men or animals and ropes were used to lift the rams. Those rams were limited to about 3 KN in weight. At the end of the 19th century, steam hammers were used to power light rams with a weight of about 8 KN at the most. At the beginning of the 20th century, electrically driven machines were in use, and the weight of the ram was increased typically to 12 KN. In the 1930s, diesel hammers and pile drivers with rams up to 30 KN were common (Flodin and Broms, 1981). Pile driving hammers are being improved constantly to meet the vast variety of conditions under which piles are being driven. Complex and sophisticated equipment is now available. Naturally, the complexity of these systems increased the complexity of pile driving analysis and design.

2.2 Bearing Capacity of Piles

Many types of pile foundations exist. The analysis and design procedures are dissimilar for different types. However, bearing capacity is an important aspect common to all types.

Initially, the pile bearing capacity was determined from the penetration resistance, that is, the number of blows required to drive the pile a given distance into the ground. This method is highly empirical, and depends on the experience of the engineer with the particular soil and equipment used.

Probably, the first person to discuss a comprehensive method of pile driving analysis was a Swedish engineer by the name of Christopher Polhem. In connection with the construction of lock Slussen and The Royal Palace in Stockholm about 1740, Polhem discussed the bearing capacity of piles. He wrote (translated from old Swedish by Flodin and Broms, 1981):

> One must know three things, namely the weight of the ram, the distance it travels to the pile head during the blow, and how much the pile sinks under the blow.

Polhem explained, without deriving a theoretical relationship, that if one relates these three factors, then one could get a measure of the bearing capacity of the pile and calculate the number of piles needed.

2.3 The Pile Driving Formulae

A pile driving formula is an attempt to evaluate the resistance of the pile by equating the energy available to drive the pile with the work produced by the pile penetration into the ground.

In 1851, Sanders (U.S. Army Corps of Engineers) proposed the first dynamic pile driving formula (Lowery et al., 1969). By the turn of the century, a large number of different dynamic formulae were available. Among them, the Engineering News formula is the simplest and one of the most widely used.

During pile driving, the available potential energy is equal to the weight of the ram multiplied by its height of fall (stroke). At impact, the converted kinetic energy is consumed by the work done to push the pile in the ground and by some losses in the system. This is expressed algebraically as follows:

$$\text{Driving energy} = \text{Work of pile penetration} + \text{losses}$$

$$E_r = W_p + L_s \tag{2.3-1}$$

where:

E_r denotes potential energy of the ram.
W_p denotes the work of the pile.
L_s denotes the losses in the system.

but

$$E_r = \text{weight of the ram x height of fall (stroke)}$$
$$= W_{ram} \times S_{stroke} \tag{2.3-2}$$

and

$$W_p = \text{soil resistance (Rult) x pile penetration (Set)}$$
$$= R_{ult} \times S_{set} \tag{2.3-3}$$

and

L_s = losses proportional to soil resistance (Rult) by a coefficient, C_{coef}
$= R_{ult} \times C_{coef}$ (2.3-4)

substituting Eqs. 2.3-2 trough 2.3-4 into Eq. 2.3-1:

$$W_{ram} \times S_{stroke} = R_{ult} \times S_{set} + R_{ult} \times C_{coeff} \qquad (2.3\text{-}5)$$

therefore, the pile resistance can be isolated as:

$$R_{ult} = \frac{W_{ram} \times S_{stroke}}{S_{set} + C_{coeff}} \qquad (2.3\text{-}6)$$

converting the stroke into inches and applying a safety factor of 6, one obtains the Engineering News formula:

$$R_{ult} = \frac{2 \times W_{ram} \times S_{stroke}}{S_{set} + C_{coeff}} = \frac{2WH}{S+C} \qquad (2.3\text{-}7)$$

where:

R_{ult} = pile capacity in tons
W = weight of ram in tons
H = hammer stroke in inches
S = pile set in inches
C = empirical constant

The empirical constant C in Eq. 2.3-7 has been assigned the following values (Teng, 1962):

C = 0.1 for steam hammers.
= 1.0 for impact hammers.

The use of dynamic formulae has been severely criticized for being inaccurate and unreliable. It is believed that dynamic formulae cannot model pile driving because they neglect the longitudinal stress waves generated during impact. The use of dynamic formulae has persisted in spite of this due to their simplicity and lack of alternatives.

2.4 A Review of Wave Equation Analysis

When digital computers were introduced, a new era started. With their ability to handle arithmetic operations fast and accurately, computers have permitted different approaches to problem solving. Solutions impossible without the help of a computer were introduced. In 1955, E.A.L. Smith proposed a mathematical model to solve the problem of pile driving (Smith, 1960). The numerical solution he described uses the computer to simulate pile driving the same way a T.V. camera simulates motion by animation. In his paper he commented:

> Obviously the rules for making such a set of motion picture drawings are these:
>
> 1. Time is divided into intervals of 1/24 s each
>
> 2. No motion can be shown in any drawing
>
> 3. Motion is depicted by making each successive drawing differ from the preceding drawing by just enough to represent the changes occurring during one interval
>
> The rules for making a numerical pile calculation are almost identical and may be stated thus:
>
> 4. Time is divided into small intervals such as 1/4000 s
>
> 5. It is assumed that all velocities, forces, and displacements will have fixed values during any particular interval
>
> 6. The velocities, forces, and displacements for each interval will be computed so as to differ from those existing in the preceding interval by just enough to represent the change occurring during one interval
>
> If these two sets of rules are compared rule by rule, it will be found that there is no essential difference.

In his main paper, Smith (1960) introduced a comprehensive model to simulate pile driving and to calculate pile capacity and stresses from observations made in the field. The method is based on wave propagation theory, and is since known by the "Wave Equation Analysis of Pile Driving".

In the following years, the Texas Transportation Institute at Texas A&M University in cooperation with the U.S. Department of Transportation (FHWA) developed a computer program to calculate pile capacity from penetration resistance based on Smith model (Lowery et al., 1969). The program enjoyed success and became known as the TTI program.

The TTI program was the most widely used wave equation program in the United States. However, difficulties were encountered in that unrealistic stresses were sometimes obtained for analysis of piles driven by diesel hammers. Based on extensive studies and measurements on pile driving, the Federal Highway Administration contracted with G. G. Goble and F. Rausche to prepare a wave equation program which would accurately model the diesel hammer. This program became known as the WEAP program (Goble and Rausche, 1976).

The results of the wave equation analysis are a function of the operators choice of input parameters. Due to the variable nature of the problem, it is often difficult to select representative values for a given parameter. For instance, cushion stiffness varies substantially during driving due to the hardening of the material under hammer blows. It was necessary to introduce a more reliable method based on field measurements to analyze pile behavior during driving. Such a method, known as the CAPWAP method, was introduced by Rausche in 1972 (Rausche et al., 1972).

2.5 Basics of The Wave Equation

Mechanical waves originate in the displacement of some portion of an elastic medium causing particle vibration. Because of the continuity of the medium, the disturbance is transmitted to adjacent layers until the whole medium is affected (neglecting wave decay). The particles do not travel with the wave, but oscillate about their position of equilibrium. For a particle in an elastic body, equilibrium position is conserved after the wave has passed.

One can distinguish two kinds of mechanical waves by considering the direction of particle movement. As illustrated in Fig. 2.1, particles in a longitudinal wave oscillate back and forth in the direction of wave propagation. The particle velocity vector, v_p, is parallel to the wave velocity vector, v_w. In a transverse wave, the particles oscillate in a direction perpendicular to the direction of wave movement. Thus, the vector v_p is perpendicular to the vector v_w.

Two or more waves can travel in the same medium independently of one another. When waves meet at a given point, the net displacement of that point is the algebraic sum of displacements due to each individual wave. When the waves are separated, each keeps its original identity. Consider the two waves illustrated in Fig. 2.2. Each wave is characterized by two properties, its shape and its sign (positive or negative). Assuming the rectangular wave of positive sign, and the elliptical wave of negative sign, at time zero, t_0, these waves are moving toward each other. At a later time, t_2, the two waves are at the same location and superimpose each other. The magnitude and shape of the resulting wave is the algebraic sum of the two waves. When the waves are separated at time t_3, each retains its original properties.

2.5.1 Differential Equation of Motion

Waves associated with mechanical vibrations are generally a function of space and time. In a solid rod that is straight, homogeneous, elastic, and having constant cross-sectional area, longitudinal wave propagation can be described by the following partial differential equation (Timoshenko and Goodier, 1970):

$$\frac{\partial^2 u}{\partial t^2} = c^2 \frac{\partial^2 u}{\partial x^2} \tag{2.5-1}$$

or

$$\ddot{u} = c^2 u'' \tag{2.5-2}$$

$\ddot{u}$ = second partial derivative of displacement with respect to time, i.e, acceleration.

u'' = second partial derivative of displacement with respect to x, i.e, strain gradient in the x direction.

c = wave speed expressed as:

$$c^2 = E/\rho \tag{2.5-3}$$

E = Young modulus of elasticity
ρ = density of the material

The equation of motion in Eq. 2.5-1 is derived from Newton's second law of motion and Hooke's law. Consider an elastic rod subject to a longitudinal stress wave as illustrated in Fig. 2.3. At Time t, a point A on the rod is displaced a distance u from its original position. Another point, Point B at a distance dx from Point A is displaced a distance u+($\partial u/\partial x$)dx from its position of origin, where $\partial u/\partial x$ is the strain or rate of displacement in segment dx. According to Newton's second law of motion, the sum of dynamic forces on a body must be equal to zero or,

$$F = ma \tag{2.5-4}$$

for the case of elastic rod in consideration,

F = summation of external forces acting on the rod
$= (\sigma + (\partial\sigma/\partial x)\, dx - \sigma)\, A$
$= (\partial\sigma/\partial x)\, A\, dx$ (2.5-5)

A = cross sectional area of the rod
$(\sigma + (\partial\sigma/\partial x)$ = rate of change in stress in the segment dx
and

m = mass of segment dx of the rod
$= \rho\ A\ dx$ (2.5-6)

and

a = particle acceleration in segment dx of the rod
$= \partial^2 u/\partial t^2$ (2.5-7)

Substituting Eq. 2.5-5 through Eq. 2.5-7 into Eq. 2.5-4, one obtains

$$\frac{\partial^2 u}{\partial t^2} \rho\, A\, dx = \frac{\partial \sigma}{\partial x} A\, dx \tag{2.5-8}$$

However, according to Hooke's law, stress in a one dimensional body is proportional to strain by means of the Young modulus of elasticity, E, or

$$\sigma = E\ \varepsilon \tag{2.5-9}$$

where

σ = stress at point A of the rod

ε = strain or rate of deformation in segment dx
$= \partial u/\partial x$

Substituting Eq. 2.5-9 into Eq. 2.5-8 and eliminating dx from both sides of the equation

(2.5-10)

or more conveniently

$$\ddot{u}\, A\, \rho = u''\, A\, E \qquad (2.5\text{-}11)$$

The wave equation in Eq 2.5-2 can thus be obtained by dividing both sides of Eq. 2.5-11 by Aρ.

2.5.2 Solution of the Wave Equation

The homogeneous differential equation of Eq. 2.5-1 is referred to as the linear one-dimensional wave equation. Its numerical solution for pile driving purposes is presented by many researchers among which are Smith (1960), Forehand and Reese (1964), Lowery et al. (1969), and Rausche et al. (1985). Using d'Alembert's integration method (Kreyszig, 1979), the closed form general solution is as follows:

$$u(x,t) = f(x-ct) + g(x+ct) \qquad (2.5\text{-}12)$$

which implies that a displacement pattern in the rod consists of two components: f and g. As illustrated in Fig. 2.4, the function f describes a wave of magnitude u that is travelling in the positive x direction at a speed c. The function g describes a wave travelling in the negative x direction at a corresponding speed -c. The waves thus described coexist, and are shifting position with time without changing shape.

2.5.3 Wave Equation Application to Pile Driving

For a pile embedded in an elastic medium and subject to soil resistance, the basic wave equation (Eq. 2.5-2) needs to be modified to account for the soil resistance.

To the wave equation in Eq. 2.5-11, a term representing static soil resistance is added,

$$A\, \rho\, \ddot{u} = A\, E\, u'' + R_{stat} \qquad (2.5\text{-}13)$$

where R_{stat} is proportional to the relative displacement, u, between the pile and the soil. The coefficient of proportionality between the static soil and relative pile displacement is denoted k, and is known as the soil stiffness.

$$R_{stat} = k\, u \qquad (2.5\text{-}14)$$

If the soil is additionally modelled as a viscous material, the dynamic component of resistance, R_{dyn}, should also be considered,

$$A \rho \ddot{u} = A E u'' + R_{dyn} + R_{stat} \tag{2.5-15}$$

where R_{dyn} is directly proportional to the rate of deformation (pile particle velocity), $\dot{u}$, by means of a damping coefficient j.

$$R_{dyn} = j \dot{u} \tag{2.5-16}$$

Substituting Eq. 2.5-14 and Eq. 2.5-16 into Eq. 2.5-15, one obtains:

$$A \rho \ddot{u} = A E u'' + j \dot{u} + k u \tag{2.5-10}$$

Equation 2.5-10 represents the wave equation in an infinitely long elastic pile subject to visco-elastic soil resistance along the entire shaft. Its solution requires elaborate mathematical manipulation and is best assessed using numerical techniques.

2.6 Smith Model

Smith (1960) method of representing the pile analytically is shown in Fig. 2.5. Smith reasoned that the ram and the pile cap are usually short and heavy objects that can be reasonably modelled as rigid masses. The capblock is usually made of wood, plastic, or similar material that is light and elastic. The cap is therefore modelled as a massless spring. The pile is a heavy and compressible object and is represented by a series of masses and elastic springs. Each mass and spring represent a section of the pile usually 1 to 2 metres in length. Where applicable, soil elements are attached to pile elements to represent soil resistance along the pile shaft. One additional soil element is added in the toe area to model toe resistance.

2.6.1 Soil Representation in Smith Model

Smith modelled the soil as an elasto-plastic material with viscous damping as illustrated in Fig. 2.6.

The elasto-plastic load-deformation characteristics of the soil are modelled using frictional springs. Two soil parameters, Quake and RMAX, are defined to determine soil stiffness and the stress level at which plastic flow occurs. The soil quake is the magnitude of elastic deformation taking place before plastic yield. RMAX is the maximum static resistance a soil element can provide against pile movement. Pile ultimate resistance (Rult) is the summation of all static resistance provided by the different soil elements.

The viscous behavior of the soil accounts for the dynamic resistance encountered during pile movement. Viscosity is traditionally modelled using a dashpot. The corresponding dynamic resistance is assumed linearly proportional to pile element velocity, v, by means of a damping coefficient, j. It should be noted, however, that dynamic resistance is a function of velocity and disappears as soon as the motion stops. Smith argued that toe damping must be greater than shaft damping, because around a pile toe, the soil is being displaced, while along the shaft there is only relative movement between the pile and the soil.

In his 1960 paper, Smith proposed typical values of soil damping and soil quakes. Subsequent attempts have also been made to correlate these parameters with results from statics and dynamic tests (Forehand et al., 1964, Authier and Fellenius, 1980b, and Rausche et al., 1985).

2.6.2 Wave Equation Analysis Using Smith Model

Wave Equation Analysis in Smith Model is initiated by simulating the action of a hammer ram falling a given distance called stroke above pile head (Fig. 2.5). At impact, the ram's kinematic energy is transferred to pile head through the capblock and pile cushion elements, and the pile head element is consequently accelerated. The impulse of pile head element is transmitted to the second pile element and so on. In each step of the analysis, the stress position, and velocity of each pile element is computed from the following forces applied upon it:

1. forces due to the compression of neighboring elements

2. static and dynamic soil resistance

3. gravity forces on the element

The analysis terminates when the velocities of all pile elements drops to zero.

2.6.3 Accuracy of Smith's Numerical Solution

Smith claimed the accuracy of his numerical solution to be within 5% of the closed form solution. However, he warned that if too long pile segments are used, or if the time interval chosen between the steps of analysis is not adequate, the accuracy of the numerical solution might be reduced or even the solution might become unstable. He derived a relation for the time interval recommended for analysis based on the minimum time required by the wave to travel the length of one pile segment (Smith, 1960).

2.6.4 Significance of Smith Model

Smith model was proposed for the following applications:

- o Determination of pile set under a specific hammer blow.
- o Determination of driving stresses.
- o Determination of soil resistance from observed pile sets.
- o Driving analysis of non uniform piles or unusual site conditions.

2.6.5 Determination of Pile Set

The pile set under a hammer blow is the net displacement of toe element at the end of analysis. Knowledge of this quantity is useful in selecting pile driving equipment.

A typical procedure for utilizing Wave Equation Analysis is as follows: For the same pile, driving equipment, and soil resistance distribution, different magnitudes are assumed for the ultimate soil resistance Rult. A wave equation analysis is run for each assumed Rult, and the corresponding net pile penetration is computed. These values are plotted on a bearing graph as illustrated in Fig. 2.7. If the blow count required to achieve a certain pile capacity is too large, the driving hammer is refused and replaced by another hammer that can achieve the desired capacity at a reasonable blow count.

2.6.6 Determination of Driving Stresses

Since forces, velocities, and displacements are calculated at each pile element for each time increment of the analysis, maxima of these quantities can be used to estimate the expected stresses during driving. Pile damage due to excessive stresses can thus be controlled.

Following the procedure described in the previous section to construct the bearing graph, a plot of maximum stresses versus penetration resistance is constructed to show the expected maximum stresses in the pile during driving. If these stresses are high enough to induce pile damage, the hammer can be replaced by another hammer that can drive the pile while generating lower stresses.

2.6.7 Determination of Pile Capacity

Bearing graphs are primarily used to estimate pile bearing capacity from observations of penetration resistance. Following pile driving, a bearing graph is generated using available information regarding pile, driving equipment, and soil properties. Subsequently, the pile bearing capacity can be directly estimated from this bearing graph based on the pile penetration resistance observed in the field. It should be noted, however, that since soil resistance is not the only input to the model, the program solution is a function of many factors. Hammer efficiency, properties of cushion and capblock materials, and soil parameters can affect the computed results significantly (Authier and Fellenius, 1983). Figure 2.8 shows a typical variation in the solution due to hammer efficiency.

2.6.8 Allowance for Variation

Smith model can be used in a wide range of situations. For uniform piles, pile elements are all similar. For tapered piles, the mass and stiffness of the different pile elements can be changed with depth to accommodate the change in pile properties. The soil resistance distribution can assume any shape to fit site conditions. The wide range of situation which can be simulated by Smith model made pile driving analysis more reliable and more comprehensive.

2.7 The TTI Program

The TTI program was developed by Texas A&M University for the U.S. Federal Highway administration. It improves on the Smith model by using a better estimate of the ram impact velocity and introduces pile damping to account for internal pile friction.

Different hammers, including drop hammers, air/steam, and diesel hammers, were modelled to evaluate the ram impact velocity. Dashpots were used to model the internal pile resistance to wave propagation, known as the pile damping.

The typical output of the TTI is a bearing graph. Since driving stresses and hammer stroke are also computed during the analysis, they can be plotted against penetration resistance to show the maximum pile stresses and hammer strokes expected for different values of penetration resistance.

The TTI was the most accepted and most widely used wave equation analysis program in the United States. However, unrealistic stresses were computed by the TTI program for piles driven by means of diesel hammers.

2.8 The WEAP Program

Similar to the TTI program, the WEAP (Wave Equation Analysis Program) uses a modified version of Smith model to analyze pile behavior during driving. The WEAP differs from the TTI program by improving the modelling of diesel hammers. Furthermore, additional parameters were introduced to the soil model proposed by Smith.

The output of the WEAP program is similar to that of the TTI. Typically, a bearing graph with a plot of hammer stroke and driving stresses versus penetration resistance is produced.

The WEAP benefits from the results of extensive investigations carried out to study the behavior of available pile driving hammers in the United States. Based on the results of the investigations, an extensive library of pile driving hammer data was made available for the use of WEAP program. Any hammer model in the library can be modified by the user to simulate specific conditions different from the conditions assumed by the library. The library can also be updated to include additional hammers, or to modify the data of a previously defined hammer.

2.8.1 WEAP Soil Model

Smith Model introduced three major parameters to model soil behavior; static resistance, damping, and quake. The WEAP program adopted Smith parameters for the the soil model and additionally introduced new ones.

The WEAP introduced a dimensionless coefficient, named Case damping coefficient, to replace Smith damping (Goble and Rausche, 1976). According to Smith (1960), the dynamic soil resistance is proportional to the static soil resistance by means of the product of the pile velocity and a damping factor, j_{smith}, named Smith damping coefficient.

$$R_{dyn} = j_{smith} \, V \, R_{stat} \tag{2.8-1}$$

where,

R_{dyn} = dynamic soil resistance
j_{Smith} = Smith damping coefficient
V = pile element velocity
R_{stat} = maximum static resistance of the soil element

Case damping suggests that the dynamic soil resistance is proportional to pile impedance by means of the product of the pile velocity and a dimensionless damping coefficient, j_{case}, named Case damping coefficient.

$$R_{dyn} = j_{case} V Z \qquad (2.8\text{-}2)$$

where,

R_{dyn} = dynamic soil resistance
j_{Case} = Case damping coefficient (dimensionless)
V = pile element velocity
Z = pile impedance

Case damping was reported to be more suitable for modelling soil viscosity in contrast to Smith damping which is insensitive to the soil type and dynamic properties (Ramey and Hudgins, 1977, and Authier and Fellenius, 1983).

2.8.2 Unloading Parameters

In Smith model, soil behavior during unloading is assumed similar to its behavior during load application. However, soils often exhibit dissimilar behavior during loading and unloading.

Two unloading parameters were introduced in the WEAP program to model the behavior of soil during pile driving; unloading soil resistance, and unloading quakes (Fig. 2.9).

Unloading soil resistance is a quantity expressed as a percentage of static soil resistance. The maximum magnitude of unloading soil resistance is limited to the magnitude of ultimate soil resistance.

Similar to unloading resistance, unloading quakes are also expressed as a percentage of loading quakes. Their maximum value is limited to the value of loading quakes.

2.9 Soil Resistance From Pile Head Measurements

In a solid rod that is straight, homogeneous, and elastic, with constant cross-sectional area, stress and velocity developed due to longitudinal wave propagation are correlated as follows (Timoshenko and Goodier, 1970):

$$V = \sigma c/E \qquad (2.9\text{-}1)$$

If the equation is multiplied by the rod's cross sectional area one obtains:

$$F = (EA/c)\ V \tag{2.9-2}$$

where the term EA/c is usually symbolized by the letter Z and is referred to as the rod impedance. Eq. 2.9-2 indicates that force and velocity in the rod should remain proportional. However, in the case of driven piles, the proportionality between force and velocity is disturbed due to wave reflections.

In an elastic rod subject to longitudinal strain wave, fixed end conditions occur when the rod extremity is restrained from moving. A fixed end is defined as an extremity that has zero velocity at all times. Free end conditions occur when the pile extremity is subjected to no force.

Force and velocity are reflected in opposite manners at the rod boundaries. A generally acceptable sign convention considers compression stress as well as downward particle velocity to be positive. Thus, when a compression wave is induced at the pile head, the resulting force and and particle velocity are both positive.

The force is directly proportional to velocity according to Eq. 2.9-2. If the compression wave encounters a fixed end condition at the pile toe (Fig. 2.10), it will be reflected as a compression wave, that is, the force in the reflected wave retains its positive sign. However, the particle velocity associated with the compression wave will be directed upward, which is negative according to the sign convention utilized, that is, it changes sign. If, instead, a free end condition exists at the pile toe, the reflected wave will be a tension wave. Accordingly, the force becomes negative, and the particle velocity retains its downward direction and positive sign.

Soil resistance has a similar effect on wave reflections. Consider a compression wave travelling downward at a wave speed, c, and encountering a soil resistance element, R, at a distance, x, from the pile head (Fig. 2.11). Two waves are subsequently generated at the soil resistance element: one is compressive and directed toward the pile head, the other is tensile and directed toward the pile toe. The magnitude of force in each of these waves is equal to R/2. The magnitude of the particle velocity is proportional to the force and is equal to (R/2)/Z. In the compression wave travelling upward, the force is positive but the particle velocity, which is directed upward, is negative. This wave reaches pile head at time 2c/x. Knowing wave speed, c, the distance, x, can be calculated.

If the velocity at pile head is multiplied by pile impedance EA/c and plotted, together with the force at pile head using a force versus time scale as illustrated in

Fig. 2.12, the magnitude of soil resistance that has generated the resistance wave can be obtained from the difference between the force and velocity traces. By monitoring the behavior of force and particle velocity at the pile head, soil resistance and its distribution can therefore be estimated.

2.10 Advantages of the Wave Equation Analysis

Smith model is probably the father of all wave equation analysis programs. Wave equation analysis of pile driving provides a practical and comprehensive method to analyze impact pile driving, select pile driving equipment, and obtain preliminary estimates of pile bearing capacity. With the advent of microcomputers, the method became readily available to every foundation engineer (Goble et al., 1976).

Wave equation analysis was initially aimed to replace the dynamic formulae in estimating pile bearing capacity. Several researchers have reported that despite the wealth of experience that supports the dynamic formulae, wave equation analysis has proven more reliable in this domain (Hannigan, 1986).

Wave equation analysis can analyze most impact pile driving situations independent of pile and soil conditions. The method is also able to estimate the driving stresses in the pile which, in the case of concrete piles, is a dominant factor in the structural design of the pile. The method is equally valuable in selecting the pile driving hammer. Wave equation analysis can test the adequacy of a certain hammer in driving a certain pile. If the number of blows required to drive the pile is excessive, a heavier or more efficient hammer would be chosen to save time, and to reduce the damage induced by impact stresses at pile head. Wave equation analysis can also help monitoring the hammer performance. For instance, if hammer strokes for a given analyzed situation are lower than the computed theoretical values, it might be that hammer efficiency is impaired (Goble et. al., 1980).

A strong literature background supports wave equation analysis. The potential of the method has stimulated the interest of researchers and engineers in using and developing it.

2.11 Difficulties with Wave Equation Analysis

Pile driving analysis using the wave equation involves many unknowns. Two types of which exist: Unknowns related to the driving system, and unknowns related to the soil data.

Practical experience showed that good modelling of the driving system is essential in obtaining reliable results from wave equation analysis. The method, consequently, integrated the results of several studies which helped provide better and more comprehensive models of the air/steam and diesel hammers. Deficiencies persisted, however, when attempts were made to model certain components of the driving system. The modelling of cushioning materials, for instance, faces an intrinsic difficulty. The cushion wood changes properties under the cyclic impacts of the hammer during the course of pile driving. It is consequently difficult to choose a representative value for the pile cushion parameter. Because pile cushions greatly affect the energy transferred to the pile, their properties have a significant effect on the results of wave equation analysis (Hirsh and Edwards, 1966).

The soil model used for wave equation analysis presents an additional difficulty. The parameters or properties used to model the dynamic behavior of soils, such as damping and quakes, cannot be readily measured using routine laboratory testing. Additionally, damping and quake are not common geotechnical parameters. An experienced geotechnical engineer who is novice at using the wave equation cannot intuitively select meaningful quake or damping values. Many such engineers would then accept the recommended values given in the user manual which, consequently, reduces their confidence in the results. Unless wave equation analysis is used steadily, which is unlikely in an average nonspecialized geotechnical office, acquiring the necessary experience to run a comprehensive wave equation analysis may prove difficult.

Early attempts have been made to define the quake and damping of different soils based on the results of static loading tests (Forehand and Reese, 1964). More recent attempts made use of dynamic monitoring data and Case method estimate to define Case damping values for clays, silts, and sands (Rausche et. al., 1985). Such studies, an exmaple of which is presented in Fig. 2.13, are valuable in determining typical values of these parameters.

CHAPTER 3
DYNAMIC MONITORING

3.1 General

Dynamic monitoring provides measurements of strain and acceleration in a pile subjected to driving. A significantly higher degree of accuracy can be obtained from wave equation analysis when used in conjunction with these field measurements.

3.2 Apparatus for Dynamic Monitoring

Stress measurements are usually obtained using strain transducers attached to pile head. Acceleration measurements are obtained by means of accelerometers. A typical arrangement of these devices is shown in Fig. 3.1.

The signals from the transducers are transmitted during driving to a nearby data acquisition system (Fig. 3.2). A so-called Pile Driving Analyzer (PDA) processes these signals into force and velocity traces versus time. A typical illustration of such traces is presented in Fig. 3.3. The force trace is calculated directly from the strain readings, and the velocity trace is integrated from the acceleration signals. The data obtained are used, by means of the Pile Driving Analyzer, to make on-site estimates of the pile capacity, pile integrity, and hammer performance. It can also be stored on a magnetic tape for later additional analysis (Fig. 3.4).

3.3 Case Method Estimate of Pile Capacity

Case Method is a simplified method that uses a closed form solution to estimate pile bearing capacity using the force and velocity measurements. The assumptions behind the Case Method are as follows (Authier and Fellenius, 1983):

- the pile material is ideally elastic
- the pile is of uniform cross section
- the soil resistance shows rigid plastic behavior and is concentrated to the pile toe

Based on the above assumptions, and the theory of wave propagation in uniform rods, the total soil resistance mobilized at the pile toe can be computed from the following equation (Goble et al., 1980):

$$R_{total} = \tfrac{1}{2}(F_1+F_2) + \tfrac{1}{2}(V_1-V_2)Z \qquad (3.3\text{-}1)$$

where,

F_1 = Force in pile head at impact
F_2 = Force in pile head at time 2L/c
V_1 = Velocity of pile head at impact
V_2 = Velocity of pile head at time 2L/c
Z = Pile impedance expressed as Mc/L
M = Pile mass
c = Wave speed in pile material
L = Pile length.

In words, Eq. 3.3-1 states that the mobilized total soil resistance is the average of force measured at the time of impact and at 2L/c later, plus the impedance of the pile times half the difference between the velocity values at impact and 2L/c later.

The soil resistance computed using Eq. 3.3-1 is the sum of static and dynamic resistance. The dynamic component of resistance is temporary and is due to soil damping (Section 2.6.1). The static soil resistance, called Case Method estimate, can only be estimated if the dynamic component is correctly separated from the total soil resistance. The dynamic resistance due to pile toe damping can be expressed as follows,

$$R_{dyn} = j_{Case} V_{toe} Z \qquad (3.3\text{-}2)$$

Where,

R_{dyn} = Dynamic soil resistance
j_{case} = Dimensionless Case damping constant
V_{toe} = Toe velocity estimated from measured head velocity
Z = Pile impedance expressed as Mc/L

and

$$R_{stat} = R_{total} - R_{dyn} \qquad (3.3\text{-}3)$$

The dimensionless damping factor J_{Case} is an operator entered variable. The results of Case Method depend on the value selected for this parameter.

A sample Case Method computations is presented in Fig. 3.5.

3.4 Pile Integrity Control

Dynamic measurements can be used to evaluate pile damage and integrity based on the concepts of the Wave Equation.

When excessive driving stresses induce pile damage, a change of pile impedance occurs. For instance, a crack developing in a concrete pile will result in a reduction of the cross sectional area and pile impedance around the damaged portion of the pile.

Changes in pile impedance generate resistance waves similar to the resistance waves generated by soil resistance. Fig. 3.6 shows force and velocity traces recorded during the dynamic monitoring of a concrete pile. Blow 1 was recorded prior to any damage occurring to the pile. The subsequent blows show the progressive failure of the pile. When the pile is completely broken, wave reflections similar to pile toe wave reflections are recorded at a time earlier than 2L/c indicating that the pile is shorter than its presumed length.

3.5 Laboratory Manipulation of Dynamic Measurements

As mentioned in an earlier section, the data obtained in the field during the dynamic monitoring of pile driving are saved on magnetic tape for further analysis in the laboratory. Such technology of information storage requires that the data be stored in an analog form compatible with the recording equipment and the storage medium used. However, these data are analyzed by means of digital computers which cannot readily use the analog data saved in the field. Consequently, and intermediate step of data manipulation is required to digitize and process the analog data into a computer usable digital form.

A schematic representation of analog and digital dynamic data is shown in Fig. 3.7. In analog form, the trace is continuous and defined at every point of time within the duration of hammer blow. Consequently, the trace comprises an infinite number of mathematical points. However, for practical analysis purposes, and due to limitations in digital computers capability, it is neither necessary nor possible to analyze the data at every point in time. When digitized, the trace is represented by a series of single points selected from the analog trace at a predefined frequency called Digitizing Frequency.

The digitizing frequency controls the time interval separating two consecutive data points. When the digitizing frequency is increased, the time interval between the two points is reduced and vice versa. Higher digitizing frequencies result in more precise representation of the analog trace by allowing more points to be sampled. In practice, the dynamic data are digitized at a frequency of 8000 to 10,000 points per second.

Data digitizing is done using appropriate electronic circuits called digitizers. When installed on a microcomputer, the digitizer accepts data from the tape recorder through an appropriate direct wire connection. By means of a software package, the operators controls the digitizer's operation. The digitized data is then saved on a flexible diskette in digital form.

When the data is stored in the field, electronic limitations of the recording instrument may require that the data be reduces or magnified to achieve accurate information storage. When the data is played back for digitizing, reduction or magnification of the data may also be required depending on the play back electronic equipment utilized. Consequently, the magnitude of the digitized data does not usually correspond to its natural magnitude in the field due to this reduction/magnification processes during storage and play back operations.

During data processing, the data are scaled back to their natural magnitude by means of calibration factors. The factors are computed from information on how much the data were reduced or magnified during storage and play back. For instance, if the data were reduced to half magnitude during storage, then magnified 1.5 times during play back, the resulting net reduction factor is then 0.5 x 1.5 = 0.75. To bring the data back to its natural scale one need to multiply the digitized records by the inverse of the net reduction factor 1/0.75 = 1.333. Similarly, if the data were reduced to half magnitude during storage, then magnified 2.0 times during play back, the resulting net reduction/magnification factor is 0.5 x 2.0 = 1.0. The resulting calibration factor is then 1/1.0 = 1.0.

Sometimes, due to magnetic noise in the tape, direct current offsets, or imperfections during recording and playback, the calibrated force and velocity traces do not take an acceptable physical form. Such minor impurities in the digitized data can also be fine tuned during data processing to insure that,

o Force and velocity at the beginning of the blow are both zero (Fig. 3.8(a)).

o Force and velocity are proportional up to the peak impact force since soil resistance waves prior to that time are insignificant and usually neglected. (Fig. 3.8(b)).

o No phase lag exist between force and velocity traces (Fig. 3.7(c)).

When the data are digitized and processed, quantities such as maximum force, acceleration, velocity, as well as Case Method estimate can be readily obtained. A report of such quantities is usually generated by the computer at the end of processing. The data is then stored for use by the CAPWAP program. The CAPWAP analysis has the purpose of estimating pile bearing capacity using the measurements taken during dynamic monitoring.

CHAPTER 4

THE CAPWAP METHOD

4.1 General

The advantages of wave equation analysis and the field measurements taken during dynamic monitoring have been combined in a computer program called CAPWAP (CAse Pile Wave Analysis Program). The CAPWAP analysis method was developed by Rausche et al., 1972. The method is more superior to conventional wave equation analysis because it does not require any assumption of soil properties such as damping and quakes. Instead, the field measurements taken during dynamic monitoring are used to compute the soil parameters and ultimate resistance.

4.2 The CAPWAP Method

The CAPWAP analysis makes use of the force and velocity obtained by means of dynamic monitoring. The early CAPWAP model used a lumped mass system of masses and springs similar to the model originally proposed by Smith in 1960 (Fig. 4.1). Later, Smith model was replaced by the continuous pile model shown in Fig. 4.2.

The analysis commences by identifying the pile properties such as elasticity, mass, and cross-sectional area, as well as variations of these parameters along the pile length to establish the pile impedance profile. The pile is divided into several elements as illustrated in Figure 4.1. Each pile element is about 1 metre in length. Soil elements are assigned to the pile elements to represent soil resistance and soil resistance distribution along the pile shaft. For each soil element, assumptions are made at first about the soil parameters: damping, quake, and maximum resistance.

The digitized measured velocity is input to the CAPWAP as a loading condition at the pile head. The wave propagation in the pile due to pile head acceleration is subsequently simulated. Time is divided into increments called analysis steps. In every analysis step, the force, velocity, and displacement of every pile element is computed using the concepts of wave equation. The analysis usually covers a time interval of 4L/c to 5L/c following the first peak velocity which identifies hammer impact.

The force trace computed in the pile head element is subsequently compared to the force trace measured in the field. At first, there is a little agreement, only. Guided by the discrepancy between the computed and measured force traces, the user adjusts the input parameters such as soil resistance, quake, and damping. The analysis is repeated and another force trace is computed. When the best possible match between the computed and measured force traces is achieved, the analysis is terminated. The soil parameters used for the last run are considered representative to the actual soil conditions existing in the field during the driving of the pile. An example of iterative CAPWAP matching is shown in Fig. 4.3.

4.3 CAPWAP Model

4.3.1 Pile Model

The pile model shown in Fig. 4.1 was initially used for CAPWAP analysis. The model consists of a series of masses connected by means of elastic springs. The driving system was eliminated from the CAPWAP model since its role was replaced with actual field measurements.

For uniform homogeneous piles, subdividing the pile into several segments according to the lumped mass approach suggested by Smith results in uniform segments of equal length. For non-uniform piles, or for piles made up of different materials, the equal length segments imposed by the lumped mass model have variable mass, stiffness, and travel time. CAPWAPC (CAse Pile Wave Analysis Program - Continuous Version) is a development of the original program. CAPWAPC uses a continuous pile model (Fig. 4.2) which has several major advantages over the lumped mass model. Primarily, the speed of computation was increased in addition to improving the accuracy of wave propagation analysis.

The pile is divided into a number of segments of equal travel time, i.e, it takes the wave a constant time interval, dt, to travel through any pile element of length dL_i.

$$dL_i = dt\ c_i \tag{4.3-1}$$

where,

dL_i = length of pile element i.
dt = time increment used for wave equation analysis.
c_i = wave speed through pile element i.

For non-homogeneous piles, the wave speed changes in accordance with changes in pile density and elasticity as indicated in Eq. 2.5-3. The length of continuous pile segments are varied to conserve a constant time travel, dt.

The CAPWAP (as well as the CAPWAPC), used dashpots to model internal pile material damping.

4.3.2 Soil Model and CAPWAP Extensions

Smith introduced three major parameters to model soil behavior, static resistance, damping, and quakes. Unloading soil parameters, such as unloading soil resistance and unloading soil quakes, were introduced in the WEAP program. The CAPWAP used the soil model of the WEAP and extended it by further including the additional soil parameters described in the following sections.

4.3.2.1 Reloading resistance

Reloading coefficients were introduced to model the reduction in resistance associated with soil softening due to remolding. The reloading soil resistance is limited to the the value of soil resistance and expressed as a ratio of it.

Reloading values have very little effect on the results, and can be neglected in most cases.

4.3.2.2 Toe gap

When a pile rebounds after a hammer blow, the pile toe usually becomes separated from the bearing soil. During the following hammer blow, the toe has to travel the separation distance before engaging the static soil resistance. This phenomenon occurs in hard driving of toe bearing piles driven in soils providing little shaft resistance. To model this behavior, a toe gap parameter was included.

As illustrated in Fig. 4.4, the quake model for the toe soil element was modified to account for the toe gap. The gap is modelled as rigid plastic deformation preceding the elastic displacement associated with the soil quake.

4.3.3.3 Soil plug

A soil plug is a mass of soil that coagulates during driving between the flanges of H piles or inside the shaft of open-toed pipe piles. The soil plug often forms in the area of pile toe. To model this phenomenon, a soil plug parameter was included in CAPWAP analysis.

The soil plug results in a change in pile impedance. As described in Section 3.4, changes in pile impedance results in reflection waves similar to those produced due to soil resistance. The soil plug exerts a resistance against pile movement proportional to the product of the mass of soil plug, and toe acceleration. The CAPWAP models this effect as an external dynamic force in accordance to Newton's second law of motion (Eq. 2.5-4).

4.3.3.4 Toe soil damper

According to the elasto-plastic model adopted by Smith, the force in the spring of the toe soil element is expected to increase during elastic compression when the pile toe moves downward. However, the driving of piles to rock induces a wave in the rock which makes the resistance versus pile toe displacement behavior very different from the elasto-plastic Smith approach. One characteristic of such a resistance-displacement curve, (Fig. 4.5a), is a decreasing static soil resistance with increasing pile toe displacement (CAPWAPC, 1986).

The CAPWAP program models the curve in Fig. 4.7a by adding a dashpot underneath Smith model for pile toe (Fig. 4.7b). The static resistance can thus decrease (spring expands) even though the pile moves downward. Pile movement is due to the compression of toe soil damper under static and dynamic toe forces.

4.4 CAPWAP Unknowns

The CAPWAP reduces the number of unknowns in a conventional wave equation analysis by eliminating the role of driving system, and by introducing field measurements. However, the problem of pile driving analysis using the CAPWAP method is still statically indeterminate. The unknowns in a CAPWAP analysis are divided into two categories: pile material unknowns, and soil resistance unknowns.

The pile is divided into N_p segments, each about 1 m in length. Usually, pile material data are accurately defined.

Soil resistance is represented by N_s soil elements added to every second pile element in the embedded portion of the pile (about 2 m apart). Every soil element is represented by 3 unknowns: maximum resistance, damping, and quake. Thus, with N_s soil elements and including those at the pile toe, there are $3(N_s+1)$ unknowns. However, in most instances, damping and quakes can be assumed constant along the shaft reducing the number of unknowns to N_s+5 distributed as follows: N_s+1 resistance values, quake and damping for the shaft, and quake and damping for the toe.

The extensions of the CAPWAP add more unknowns to the problem. Unloading quakes contribute to two additional unknowns: shaft unloading quakes and toe unloading quakes. The following parameters also contribute to one unknown each:

unloading shaft resistance, reloading shaft resistance, reloading toe resistance, toe gap, soil plug, and toe soil damper. Therefore, the total number of unknowns in the soil model is N_s+13 unknowns.

4.5 Matching Techniques

To obtain an agreement between the measured and computed force at pile head, good estimates have to be made regarding the unknowns described in Section 4.4. Unless the influence of different parameters is qualitatively known, a CAPWAP match becomes a random search for one combination through an infinite number of permutations. Fortunately, the nature of parametric influence on the calculated traces is readily known. The engineer can use this knowledge to systematically improve the CAPWAP match.

4.5.1 Periods of Parametric Influence

Normally, a CAPWAP analysis is carried out on a trace about 4L/C long in time. A good agreement match should extend at least to about 3L/C in time. A lower agreement quality may be accepted for the last L/C.

A CAPWAP trace can be divided into four periods as shown in Fig. 4.6.

Period 1 extends from peak impact to about 2L/C. It is highly governed by shaft resistance. Close to impact, this region traces the early wave reflections. It is the easiest portion of the trace to match.

Period 2 exists in the vicinity of 2L/C, and has a duration of about 3 ms plus the rise time of impact, t_r. It is governed by toe properties which are: resistance, damping, quake, gap, and soil plug. All these parameters can be significant in this portion of the trace.

Period 3 has a duration of about 5 ms. It is separated from the time 2L/C by a period equivalent to the rise time of impact t_r. This period is slightly complex, and is mostly governed by damping and ultimate soil resistance. Period 3 overlaps Periods 2 and 4.

Period 4 occurs following Period 2 and extends to the end of the trace. Wave reflections become very complex. The period is usually affected by all program parameters. Most unloading takes place during Period 4 which makes it possible to obtain a good match by adjustment of the unloading parameters.

4.5.2 Influence of shaft resistance

The effect of resistance distribution is most significant in the first 2L/c period of the record which makes it the easiest to match. Assuming certain values for quake and damping, the individual static resistance values can be easily adjusted to obtain a match. For instance, if the measured and computed force curves are parallel between Elements 3 and n as shown in Fig. 4.7a, then the soil resistance for these elements has been correctly determined. However, static soil resistance must be added over the first three elements to obtain a good match. Sufficient accuracy will probably be obtained from,

$$R_1 = R_2 = R_3 = d/3.$$

By analogy, the resistance of element 7 in Fig. 4.7b should be reduced by an amount d to correct the match.

4.5.3 Effect of Ultimate Soil Resistance

In general, a good match can be easily obtained within Period 1 if the total soil resistance has been correctly determined. As described in Section 2.5.3, total soil resistance is the sum of two components, static and dynamic. Damping represents the dynamic component of resistance, and can substitute static soil resistance in the first 2L/c of the record. However, as the dynamic resistance is proportional to pile element velocity, it is temporary and most of its effect fades in Period 3 leaving the wave reflections associated with the static soil resistance, only. The validity of ultimate soil resistance assumed can be directly determined from Period 3 of the trace. If the computed force in Period 3 is too low, more static resistance should be added to the pile; if the computed force is high, the ultimate soil resistance previously assumed must be reduced.

Figure 4.8 illustrates the case where total soil resistance has been correctly determined as suggested by the good match in the first 2L/c of the record. The disagreement in Period 3 indicates that not enough static soil resistance has been assumed. The static soil resistance should be increased accordingly. However, damping should be reduced to preserve the good match in Period 1 of the record.

4.5.4 Effect of damping

Damping usually acts for a relatively short time compared to static resistance. Since dynamic resistance is directly proportional to velocity, it is best seen when the velocity of pile element is maximum, that is, in the first period of the record. Within the first 2L/C time period, damping can substitute static soil resistance.

The best indication that damping parameters are not correctly determined can be obtained by comparing the measured and computed curves in Periods 1 and 3 of the record. If a good match is achieved in Period 1, it indicates that the assumed total resistance is correct. However, if the computed curve does not match the measured curve in Period 3 of the record, it is an indication that the assumed static soil resistance is not correctly determined. The static soil resistance have to be increased or reduced to match the curves. Damping constants should also be modified accordingly to preserve the magnitude of correctly determined total soil resistance.

Damping also works as a shock absorber. Consequently, it effectively smoothens high frequency oscillations in the computed curve. For the example case given in Fig. 4.9, additional damping would increase the computed force in Period 1 of the record. It would also smoothen out the high frequency oscillations computed in Period 4.

4.5.5 Effect of Quakes

Quake controls the rate at which the force is transmitted from one element to its adjacent. An element force cannot be fully mobilized unless the displacement has exceeded the quake. The obtained solution is a lower bound solution if pile element displacements are smaller than quake values.

Quakes affect the rate of force transfer to the spring in the soil model. Larger quakes, for example, will result in slower rate of loading of soil elements. During CAPWAP matching, quakes can be used to delay or accelerate the rise (or decline) of the computed force trace. For instance, if the quakes are increased for the example illustrated in Fig. 4.10a, the rise of the force trace will be delayed to improve the match.

Quakes influence the later portion of the record primary because they affect the speed of unloading. A change of quake may be necessary if a mismatch in Period 4 of a record cannot be corrected by other means (Fig. 4.10b). If changing the quakes is undesired, only unloading quake values can be modified. Smaller unloading quakes will more rapidly lower the computed curve, since unloading forces are of negative values.

4.5.6 Effect of Unloading Shaft Resistance

Unloading shaft resistance affects the later portion of the record, Period 4, where the unloading of forces takes place.

If, for a given CAPWAP match, the computed force trace is lower than the measured trace in Period 4 of the record (Fig. 4.11), unloading shaft resistance may need to be reduced. Since the reflection, at pile toe, of the initial compression wave is usually a tensile wave, the forces computed at pile head after time 2L/c are mostly negative. Reducing the unloading shaft resistance will usually reduce the magnitude of negative resistance waves generated in period 4. That will result in a slower decline of the computed force trace.

4.5.7 Effect of Toe Gap

When a pile with low shaft resistance is driven to a hard layer, it often rebounds so that the toe looses contact with the bearing soil. Under the next hammer blow, the pile will move a certain distance equivalent to the toe gap without engaging any toe resistance.

When a toe gap exists beneath a pile toe, the reflections of pile toe resistance will be usually delayed. The result of this delay on the measured force trace will be similar to those shown in Fig. 4.12. A pile with a toe gap will usually show a sudden drop in the force trace around time 2L/c.

4.5.8 Effect of Soil Plug

Soil often plugs between the flanges of H piles and at the toe of pipe piles driven open-toe. The weight from pile shoes and pile toe plates can also be modelled as soil plugs.

A soil plug is a mass attached to pile toe element. It produces a dynamic resistance force on the pile toe element proportional to the product of soil mass in the plug and pile toe acceleration.

Unlike static soil resistance at pile toe, dynamic resistance acting on the toe element can assume negative values. The dynamic resistance due to the soil plug has the general effect of increasing the computed force just before 2L/C, where toe acceleration is positive, and reducing it just after 2L/C when toe acceleration is negative (Fig. 4.13).

Adding a soil mass smaller than 20% of the mass of the toe element usually has very little effect on the computed trace. Adding more than three times the weight of toe element has an effect similar to adding toe damping (CAPWAPC, 1986).

4.5.9 Effect of pile properties

Pile properties are used to determine the wave speed and pile impedance and stiffness.

Most piles have simple linear elastic behavior where force is proportional to velocity. For piles including cracks or splices, compression or tension slacks may be used to model the soft spots.

Pile damping usually smoothens the computed curve. Common damping values are known to range between 1 to 5 percent. If too much damping was assumed for pile material, the wave decay becomes very fast as shown in Fig. 4.14a. Within the mentioned range, pile damping has insignificant effect on the computed trace.

Pile stiffness also effects wave speed. Although it is usually determined to a good accuracy, pile stiffness may change during driving due to formation of a soil plug around the shaft or at the toe. If pile stiffness is not correctly estimated, a phase lag will result between the computed and measured force traces as shown in Fig. 4.14b.

4.6 Parametric Interdependence of the CAPWAP

Recent studies of the effects of parametric interdependence on the CAPWAP results have been reported.

A parametric study to investigate the direct effects of variation of a single parameter on the obtained match were reported by M. Hussein (1986a). The study comprised obtaining a CAPWAP match for a 37 m steel pipe pile. The effects of changing a single CAPWAP parameter were then demonstrated through the destroyed match. This procedure was repeated for all CAPWAP parameters.

The results of a more comprehensive study were reported by Balthus and Kielbassa (1986). The aim of Balthus and Kielbassas was the investigation of user-independent capacity of CAPWAP at seperating the dynamic and static components of resistance. The procedure described entailed the construction of a fully automated CAPWAP program where matching is achieved by computerized procedure to minimize the area between measured and computed force traces. Simplified resistance envelopes (triangular or rectangular) were used to reduce the number of CAPWAP unknowns and iterations. The results of the study indicated that a local minimum was obtained in a toe damping - shaft damping - ultimate resistance space. In other words, the CAPWAP method resulted in a unique solution when all program parameters, other that damping and static resistance, were maintained constant. The study, however, did not indicate if this local minimum, which was based on force matching, corresponded to a similar minimum obtained from velocity matching. When all other program parameters were involved, the research concluded that the CAPWAP method can seperate static from dynamic resistance with limited accuracy, only.

A more recent study of the CAPWAP solution as a function of the operator was reported by Fellenius (1988). Dynamic data from four industrially monitored piles were compiled and distributed to 20 individuals who were asked to perform and return a CAPWAP analysis for every pile. Statistical survey of the data returned by 18 individuals generally indicated quantitative agreement between the pile capacities individually estimated.

CHAPTER 5
FIELD DATA

5.1 General

The parametric analysis of the CAPWAP method was carried out using dynamic data from four industrially monitored piles.

The first pile, labelled JI, is a test pile driven for the pile testing program at the Jones Island water treatment plant on the shore of Lake Michigan. The second pile, labelled JA, is a bridge abutment pile driven in Jasper, Alberta. The third pile, labelled AM, is a foundation pile driven at the national Aviation Musem on the shore of Ottawa River, Ottawa, Ontario. The fourth pile, labelled LW, is a bridge abutment pile driven on the shore of Lake Wahum, Ontario.

5.2 Pile Data

All four piles analyzed were steel piles. Three piles were thin walled pipe piles, while the fourth pile was a wide flange beam, also known as H pile. The pile data presented in the following subsection are summarized in Table 1.

5.2.1 JI Pile Data

The JI Pile is a closed-toe pipe pile with an outside diameter of 324 mm and a wall thickness of 9.5 mm. The JI Pile is 42.2 m long with a cross sectional area of 94 cm^2. For the blow analyzed, the JI Pile had an embedment depth of 35.2 m and an observed penetration resistance of 25 blows per 0.3 m.

5.2.2 JA Pile Data

The JA Pile is an H pile with a nominal webb length of 310 mm and a nominal flange width of 79 mm. This pile is a structural unit usually known as a wide flange W310x79 section. The JA Pile is 28.9 m long with a cross sectional area of 101 cm^2. For the blow analyzed, the pile had an embedment depth of 21.6 m and an observed penetration resistance of 50 blows per 0.3 m.

5.2.3 AM Pile Data

The AM Pile is a closed-toe pipe pile with an outside diameter of 245 mm and a wall thickness of 14 mm. The AM Pile is 58.4 m long with a cross sectional area of 100 cm^2. For the blow analyzed, the pile had an embedment depth of 58.2 m and an observed penetration resistance of 100 blows per 0.3 m.

5.2.4 LW Pile Data

The LW Pile is also an open toe pipe pile with an outside diameter of 406 mm and a wall thickness of 13 mm. The LW Pile is 18.6 m long with a cross sectional area of 157 cm^2. For the blow analyzed, the LW Pile had an embedment depth of 14.6 m and an observed penetration resistance of 60 blows per 0.3 m.

5.3 Soil Profiles

The soil conditions encountered at the sites of the analysis piles are presented in Tables 2 through 5. The soil conditions, which are subject to local variations, are summarized in terms of major soil strata encountered in the field during borehole drilling.

5.3.1 JI Pile, Soil Data

A borehole drilled at the site of the JI Pile encountered 6 m of miscellaneous earth fill at ground surface. The fill had a unit weight of 18 KN/m^3 and an established angle of internal friction of 30 degrees.

Underlying the fill, the borehole encountered strata of soft to stiff compressible postglacial silty clay and clayey silt with a thickness of 19.5 m. The silty clay and clayey silt strata had a unit weight of about 17 KN/m^3, undrained shear strength of 40 KPa, and an effective friction angle of 37 degrees.

Underlying the silty clay and clayey silt, layers of mixed glacial soils were encountered. The glacial soils consisted of alternating layers of sand, sandy silt, and clayey silt. The glacial soils had a thickness of 56 m, unit weight of 18 KN/m^3, undrained shear strength of 200 KPa, and an effective friction angle of 37 degrees.

Beneath the glacial soils, the borehole was terminated in dolomite bedrock.

5.3.2 JA Pile, Soil Data

A borehole drilled at the site of the JA Pile encountered a layer of sandy gravel fill with lenses of frost at ground surface. The fill had a thickness of 1.3 m, and was underlain by 2.3 m of coarse to medium coarse sand with layers of silty sand and lenses of frost.

Beneath the sand, the borehole encountered 0.7 m of sandy gravel underlain by 18.6 m of fine to medium sand. The fine to medium sand was compact and brown in color. The stratum contained layers of fine silt.

Beneath the fine to medium sand, the borehole was terminated in a layer of fine to medium sand, trace silt which it penetrated to 5 m.

5.3.3 AM Pile, Soil Data

A borehole drilled at the site of the AM Pile encountered 1.3 m of sand and clay fill at ground surface.

Beneath the fill, the borehole encountered 0.5 m of loose to dense silty fine sand. The silty fine sand was underlain by 16.2 m of soft to stiff grey fissured silty clay.

Underlying the fissured silty clay, a 30 m thick layer of stiff to very stiff grey clay was encountered. The borehole was terminated at depth 48 m in a dense soil underlying the clay.

5.3.4 LW Pile, Soil Data

A borehole drilled at the site of the LW Pile encountered 0.4 m of peat at ground surface. The peat was underlain by 2.7 m of silt.

Underlying the silt, the borehole encountered 7.4 m of stiff to firm grey silty, sandy clay overlying 3.1 m of brown weathered sandstone with silty clayey shale. The borehole was terminated in bentonitic sandstone which it penetrated to 2.1 m.

5.4 Pile Driving Data

5.4.1 Driving of the JI Pile

The pile driving diagram for the JI Pile is presented in Fig. 5.1.

The pile encountered easy driving in the fill and the cohesive postglacial deposits above depth 26 m. In these strata, most pile penetration was due to the combined weights of the hammer and pile materials. The pile penetration resistance in the underlying glacial deposits increased with depth until the pile met refusal at 37.5 m below ground surface. The JI Pile had a penetration resistance of 190 blows for the last 0.3 m driven.

5.4.2 Driving of the JA Pile

The pile driving diagram for the JA Pile is presented in Fig. 5.2.

The JA Pile, which was driven in sandy soils, encountered a penetration resistance linearly increasing with depth. The pile was embedded in sand at depth 22.4 m. For the last 0.3 m driven, the pile had a penetration resistance greater than 50 blows per 0.3 metres.

5.4.3 Driving of the AM Pile

The driving record of the AM Pile is not available above depth 47 m. The driving record for the last ten metres driven is presented in Fig. 5.3.

The driving of the AM Pile was terminated at depth 57 m below ground surface. For the last metre driven, the pile had a penetration resistance greater than 45 blows per 0.3 m.

The AM Pile was restruck, and the pile driving resistance during the restrike is presented in Fig. 5.3. The blow analyzed for the AM Pile is the tenth blow of restrike.

5.4.4 Driving of the LW Pile

The pile driving diagram for the LW Pile is presented in Fig. 5.4.

The LW Pile was driven through weathered sandstone below depth 10.4 m. Pile driving was terminated in bentonitic sandstone where the pile met refusal at depth 15.6 m. For the last 0.3 m driven, the LW Pile had a penetration resistance greater than 170 blows per 0.3 m.

5.5 Dynamic Data

For each pile analyzed, field measurements recorded during the dynamic monitoring of pile driving were stored on magnetic tapes. The tapes received by the University of Ottawa contained analog signals of the force and velocity recorded at pile head during driving. Several blows were digitized for each pile, and one representative blow per pile was selected for analysis. The dynamic records of the four blows analyzed are shown in Figures 5.5 through 5.8.

CHAPTER 6

ANALYSIS AND RESULTS

6.1 General

This chapter presents the procedure and results of the parametric analysis of the CAPWAP method. The material presented in this chapter is organized as follows:

1. Criterion for selection of analysis blows.
2. Data digitizing procedure.
3. Data processing input and results.
4. Results of Case Method estimate.
5. Parametric analysis procedure.
6. Presentation of the analysis results.

The results are presented by reference to tables and figures compiled from raw analysis data. The detailed raw data are presented in Appendix A (included under seperate cover). A discussion of the results is presented in Chapter 7.

6.2 Data Digitizing

For each pile analyzed, several blows were digitized as selected from a depth close to refusal depth. The blows were selected such that enough pile movement occurred during the blow to insure the mobilization of ultimate soil resistance. The depths at which the blows were digitized are shown on Figs 5.1 through 5.4. The digitizing of analog force and velocity signals was performed on an IBM-PC microcomputer using a digitizing hardware circuit. The data were played back from the tapes on which they were stored, and were transmitted through a direct connection to the digitizing circuit installed on the motherboard of the IBM-PC. Several blows were digitized and processed for each pile and one of these blows was selected for analysis.

6.3 Data Processing

6.3.1 Input Data

The input sheets required by the data processing program, DATPRO, for the selected analysis blows are presented in Tables 6.1 through 6.4. The input data presented in each table is divided into five different categories: .

1. Physical properties of the pile.

2. Processing information

3. Data adjustment information

4. Plotting format information

5. Case Method computational information

It should be noted that no data adjustment has been incorporated in this parametric analysis. An elaborate description of the input variables extracted from DATPRO user manual is provided in Appendix B under seperate cover (CAPWAPC, 1986).

6.3.2 Data Processing Results

The output of the DATPRO program is presented in Table 7 (CAPWAPC, 1986). The output includes the maximum dynamic quantities observed or computed for the pile during the hammer blow presented as AMAX, VMAX, DMAX, FMAX, and EMAX.

AMAX describe the maximum acceleration recorded at pile head during the hammer blow. Similarly, VMAX, DMAX, and FMAX denote the maximum velocity, displacement and force at pile head, respectively. EMAX denotes the maximum energy recorded, and is computed from the integration of the product of force and velocity at pile pile head throughout the time record (CAPWAPC, 1986).

The output of DATPRO also includes a listing of the force and velocity, FT1 and VT1, recorded at pile head at the time of first velocity peak. The corresponding proportional velocity, VEAC, is computed and a ratio, F/V, is obtained to indicate the degree of proportionality between force and velocity at the beginning of the analysis.

The results of Case Method estimate are shown in Table 7 as RT and RS-1 through RS-4. The variable RT represents Case Method estimate for zero damping. The variables RS-1 through RS-4 represent Case Method estimates for selected damping coefficients. In the case of the piles analyzed, the damping coefficients were set to 0.1 through 0.4 for RS-1 through RS-4, respectively.

The pile integrity numbers, BETA, are also shown in Table 7. The corresponding distance from pile head where damage is anticipated are shown under B-PL. It should be noted that DATPRO results indicate a slight change in impedance for LW Pile at 5.7 m from pile head.

Following processing, the selected blows were ready for CAPWAP analysis.

6.4 Parametric Analysis Procedure

A systematic procedure was adopted for determining the range of acceptable CAPWAP solutions for each of the blows selected. All of the analyses were based on force trace matching. Velocity matching, also known as WAPCAP analysis, was performed following the force match (CAPWAP match) using the same set of parameters. The procedure undertaken to identify the range of acceptable CAPWAP solutions for each of the analysis blows was as follows:

1. A very good CAPWAP match was first obtained for the analyzed blow. The match was labeled "Reference Match". The corresponding ultimate soil resistance was labeled "Reference Rult". Five per cent of the Reference Rult was labelled "Resistance Increment".

2. One Resistance Increment was added to the Reference Rult. This, obviously, destroyed the match previously achieved.

3. The destroyed match was restored by varying the program parameters other than the total static soil resistance. However, the distribution of the static soil resistance was changed as found required.

4. When a rematch was achieved, one additional Resistance Increment was added to the total static soil resistance and step 3 was repeated.

5. Steps 3 and 4 were repeated until rematching was no longer possible. This defined what is believed to be the upper bound of the CAPWAP solution.

6. The lower bound of the CAPWAP solution was identified by repeating Steps 2 through 5 for negative Resistance Increments, Resistance Decrements, until rematching was no longer possible.

7. The range of ultimate soil resistance within which good CAPWAP matches were possible was recorded.

6.5 Parametric CAPWAP Analysis

The pile profiles used by the CAPWAP program to model the analysis piles are shown in Table 8. The pile profiles and material properties, i.e., modulus of elasticity, unit weight, and pile damping, were kept constant throughout the parametric analysis.

6.5.1 Analysis of the JI Pile

The Reference Match for the JI Pile was found at an ultimate soil resistance of 1000 KN. The corresponding CAPWAP and WAPCAP matches are presented in Fig. 6.1. The parametric analysis of the JI Pile indicated that the pile ultimate soil resistance could be increased to 1500 KN or reduced to 900 KN and still be able to obtain acceptable CAPWAP matches for the analyzed blow. The CAPWAP solutions obtained while determining this range are presented in Figs. 6.2 through 6.13. The corresponding WAPCAP matches are presented in Figs. 6.14 through 6.25.

6.5.2 Analysis of the JA Pile

The Reference Match for the JA Pile was found at an ultimate soil resistance of 575 KN. The corresponding CAPWAP and WAPCAP matches are presented in Fig. 6.26. The parametric analysis of the JA Pile indicated that the pile ultimate soil resistance could be increased to 650 KN or reduced to 450 KN and still be able to obtain acceptable CAPWAP matches for the analyzed blow. The CAPWAP solutions obtained while determining this range are presented in Figs. 6.27 through 6.34. The corresponding WAPCAP matches are presented in Figs. 6.35 through 6.42.

6.5.3 Analysis of the AM Pile

The Reference Match for the AM Pile was found at an ultimate soil resistance of 1500 KN. The corresponding CAPWAP and WAPCAP matches are presented in Fig. 6.43. The parametric analysis of the AM Pile indicated that the pile ultimate soil resistance could be increased to 1725 KN or reduced to 1275 KN and still be able to obtain acceptable CAPWAP matches for the analyzed blow. The CAPWAP solutions obtained while determining this range are presented in Figs. 6.44 through 6.49. The corresponding WAPCAP matches are presented in Figs. 6.50 through 6.55.

6.5.4 Analysis of the LW Pile

The Reference Match for the LW Pile was found at an ultimate soil resistance of 900 KN. The corresponding CAPWAP and WAPCAP matches are presented in

Fig. 6.56. The parametric analysis of the LW Pile indicated that the pile ultimate soil resistance could be increased to 1125 KN or reduced to 300 KN and still be able to obtain acceptable CAPWAP matches for the analyzed blow. The CAPWAP solutions obtained while determining this range are presented in Figs. 6.57 through 6.74. The corresponding WAPCAP matches are presented in Figs. 6.75 through 6.92.

6.5.5 Parametric Variations

The values of different parameters obtained while determining the ranges of ultimate soil resistance for the different piles were compiled and presented in Tables 9 through 12. Additionally, the data are presented graphically in Figs. 6.93 through 6.117. The row data, from which these tables and figures were compiled, are presented in Appendix A under seperate cover.

The tables and figures show how the values of different parameters were varied to obtain a good CAPWAP match for a given ultimate soil resistance value. Standard statistical quantities, such as maxima, minima, averages, and standard deviations, were also computed and tabulated in the corresponding tables.

6.5.5.1 Variations of static resistance

The variations of shaft and toe static soil resistance for the four blows analyzed are presented in Tables 9 through 12, and in Figs. 6.93 through 6.96.

The ultimate static soil resistance for the JI Pile varied between 900 and 1500 KN. Consistently, more than 50 percent of this resistance was due to shaft resistance. The variations of shaft and toe resistance during the analysis of the pile are shown in Fig. 6.93. The computed shaft resistance for the pile varied between 582 and 875 KN, while the toe resistance varied between 289 and 632 KN.

The variations of shaft and toe resistance for the JA Pile are presented in Table 10 and Fig. 6.94. The ultimate soil resistance of the pile varied between 450 and 650 KN during the parametric analysis. The soil resistance along the pile shaft was found to account for more than 70 percent of the ultimate static resistance of the pile. The static soil resistance along the pile shaft varied between 321 and 481 KN, while the pile toe resistance varied between 129 and 195 KN. The computed average values for shaft and toe resistance were 404 and 146 KN, respectively.

The parametric variations for the AM Pile are presented in Table 11. The variations of the shaft and toe static soil resistance are presented in Fig. 6.95. The range of ultimate soil resistance obtained from the parametric analysis of the pile was 1275 to 1725 KN. More than 60 percent of this resistance was due to soil resistance along the pile shaft. The AM Pile shaft resistance varied between 882 and 1155 KN, while the pile toe resistance varied between 391 to 667 KN. The computed average values for shaft and toe resistance were 1005 and 495 KN, respectively.

The ultimate soil resistance for the LW Pile varied between 300 and 1125 KN. The corresponding variations of the CAPWAP parameters for the analyzed blow are presented in Table 12. The variations of the shaft and toe static soil resistance are presented in Fig. 6.96. The ratio of pile shaft resistance to pile ultimate resistance was almost constant at a value of 87 percent. With little toe bearing, the LW Pile toe capacity ranged from 40 to 139 KN during the parametric analysis of the blow.

6.5.5.2 Variations of damping

The variation of Case and Smith damping coefficients for the four blows analyzed are presented in Tables 9 through 12. The variations of Case damping coefficients are graphically presented in Figs. 6.97 through 6.100.

The Case damping coefficients for the JI Pile varied between 0.00 and 0.15 for the shaft and between 0.50 and 1.20 for the toe with average values of about 0.07 and 0.79 for the shaft and toe damping, respectively. The corresponding Smith damping coefficients varied between 0.00 and 0.10 s/m for the shaft and between 0.60 and 1.09 s/m for the toe. The average Smith damping coefficients computed for the JI Pile were 0.04 and 0.75 s/m for the pile shaft and pile toe damping, respectively.

The pile shaft Case damping coefficients obtained for the JA Pile were consistently greater than those obtained for the toe. However, the computed Smith damping coefficients for the pile shaft were generally smaller than those computed for the pile toe. The Case damping coefficients for the pile shaft ranged from 0.62 to 0.77 with an average value of 0.70. The Case damping coefficients for the pile toe ranged from 0.24 to 0.76 with an average value of 0.47. The corresponding Smith damping coefficients varied between 0.55 and 0.91 s/m for the shaft and between 0.49 and 2.35 s/m for the toe. The average computed Smith damping coefficients for the JA Pile were 0.70 and 1.34 s/m for the pile shaft and pile toe, respectively.

The variations of Case damping coefficients for the AM Pile are presented in Fig. 6.99. Little variation was observed for the pile toe damping which ranged between 0.65 and 0.75 with an average value of 0.69. The variation of the pile shaft damping was relatively greater with a range of 0.14 to 0.65 and an average value of 0.38. Smith damping coefficient for the pile varied between 0.05 and 0.30 s/m for the shaft, and between 0.45 and 0.75 s/m for the toe. The average computed Smith damping coefficients were 0.16 and 0.58 s/m for the pile shaft and pile toe, respectively.

The Case damping coefficients obtained for shaft damping and toe damping of the LW Pile were compatible in magnitude. However, shaft damping coefficients were slightly greater. The variations of Case damping coefficients for this pile are presented in Fig. 6.100. The Case damping coefficients for the pile shaft ranged from 0.53 to 0.91 with an average value of 0.71. The Case damping coefficients for the pile toe ranged from 0.50 to 0.95 with an average value of 0.66. Unlike the Case damping coefficients, the Smith damping coefficients for the pile shaft were considerably smaller that those of the toe. The Smith damping coefficients for the LW Pile varied between 0.33 and 2.18 with an average value of 0.52 s/m. The Smith damping coefficients for the pile toe varied between 2.24 and 14.07 with an average value of 5.56 s/m.

6.5.5.3 Variations of toe soil damper

The variations of the soil toe damper coefficient for the four blows analyzed are presented in Tables 9 through 12, and in Figs. 6.101 through 6.103.

The soil toe damper coefficient for the JI Pile varied between 0 and 817 KN/m/s with an average value of 240 KN/m/s. The soil toe damper coefficient was not utilized during the analysis of the JA pile and its value was set to zero throughout the parametric analysis of the blow. Similarly, the analysis of the AM Pile did not make use of the soil damper coefficient except for the match at 1725 KN where the soil damper was assigned a value of 2 KN/m/s. The analysis of the LW Pile also made little use of the soil damper coefficient. The coefficient was assigned a value of 1.9 KN/m/s during the matching of LW Pile force trace at 1080 and 1125 KN, only. For the balance of the parametric analysis of the LW Pile, the soil damper coefficient was set to zero.

6.5.5.4 Variations of quake values

The variations of quake values are presented in Tables 9 through 12, and in Figs. 6.104 and 6.107.

In general, the quake values obtained for the pile shafts were smaller than those obtained for pile toes.

The quake values obtained during the analysis of the JI Pile are presented in Fig. 6.104. The quake values for the pile shaft ranged from 2.0 to 5.5 mm with an average value of 3.6 mm. The toe quakes for the pile ranged from 3.0 to 5.0 mm with an average value of 4.7 mm.

The quake values obtained during the analysis of the JA Pile had relatively little variations. Typical values for the pile shaft and pile toe quakes were 2.5 and 5.0 mm, respectively, as shown on Fig. 6.105.

The analysis of the AM Pile resulted in no variation in the shaft quakes throughout the parametric analysis of the blow. The quake values obtained during the analysis of the pile are presented in Fig. 6.106. The shaft quakes assumed a constant value of 2.5 mm. The pile toe quakes were generally stable, also. At lower ultimate soil resistance, the toe quakes were set to 6.5 mm, and were lowered to 5.1 mm for higher Rult.

The quake values obtained during the analysis of the LW Pile were also stable. The pile toe quakes had a constant value of 5.0 mm throughout the analysis. The pile shaft quakes were subject to little variation, but generally assumed a value of 2.5 mm.

6.5.5.5 Variations of unloading quake

The unloading quakes obtained during the parametric analysis are presented as a percentage (ratio) of the loading quakes in Tables 9 through 12, and in Figs. 6.108 to 6.111.

The unloading quake ratios for the JI Pile are presented in Fig. 6.108. The unloading quake ratios obtained for the pile shaft ranged from 3 to 60 percent of the loading quakes with an average value of 30 percent. The corresponding unloading toe quakes ranged from 25 to 100 percent of the loading quakes with an average value of 77 percent.

The unloading quake ratios obtained during the analysis of JA Pile are presented in Fig. 6.109. The unloading quake ratios for the pile shaft did not vary during the analysis and assumed a constant value of 100 percent. The unloading quake ratios for the pile toe were also constant with a value of 5 percent except for the solution at 450 KN where the unloading toe quake ratio had a value of 100 percent of the corresponding loading quake.

The results of unloading quake ratios obtained from the analysis of the AM Pile are presented in Fig. 6.110. Little variations were obtained for the unloading quakes for this pile. The unloading shaft quake ratios ranged from 90 to 100 percent, while the unloading toe quake ratios ranged from 30 to 40 percent.

The unloading quake ratios obtained for the LW Pile are presented in Fig. 6.111. The unloading shaft quake ratios for the pile ranged from 0 to 100 percent with an average value of 28 percent of the loading shaft quakes. The unloading quake ratios for the pile toe ranged from 40 to 100 percent with an average value of 75 percent of the loading toe quakes.

6.5.5.6 Variations of unloading shaft resistance

The results of unloading shaft resistance are presented as a percentage (ratio) of the loading shaft resistance in Tables 9 through 12, and in Figs. 6.112 through 6.114.

The unloading shaft resistance ratios for the JI Pile ranged from 0 to 100 percent of the loading shaft resistance but mostly had a value of 100 percent. The values of this parameter obtained from the analysis of the JA Pile ranged from 0 to 60 percent with a typical value of 0 percent. The unloading shaft resistance ratios obtained from the analysis of the AM Pile ranged from 4 to 31 percent, but mostly had a value of 31 percent. The analysis of the LW Pile did not make use of the unloading shaft resistance parameter which was set to zero throughout the analysis of the pile.

6.5.5.7 Variations of soil plug

The analysis of the JI Pile, JA Pile, and AM Pile, did not make use of the soil plug parameter which was set to zero throughout the analysis of these three piles. For the analysis of the LW Pile, a soil plug of 0.55 KN was assumed throughout the parametric analysis of the pile.

6.5.5.7 Variations of toe gap

The variations of the toe gap parameter are presented in Tables 9 through 12, and in Figs. 6.115 throughout 6.117.

The toe gaps obtained during the analysis of the JI Pile ranged from 1.5 to 4.0 mm with an average value of 1.9 mm. The typical value of toe gap utilized during the analysis of the pile was 1.5 mm. The toe gaps obtained from the analysis of the JA Pile ranged from 0.0 to 3.5 mm with typical values of about 0.0 or 1.0 mm. The analysis of the AM Pile resulted in a range of 0.0 to 5.0 mm for the toe gap parameter with an average value of 1.0 mm. The larger toe gap values obtained for the AM Pile were associated with larger ultimate soil resistance. However, in the cases of the JI and JA Piles, the larger toe gaps were associated with lower ultimate soil resistance. The analysis of the LW Pile did not make use of the toe gap parameter which was set to zero throughout the parametric analysis of the pile.

6.5.5.8 Variations of pile resistance distribution

The variation of static soil resistance in the individual soil elements for the four piles analyzed are compiled and presented in Tables 13 through 16. Statistical quantities, such as maxima, minima, and averages, are also presented in the tables for each individual soil element. These statistical quantities are further presented graphically in Figs. 6.118 through 6.121. The variations of load transfer in each of the four piles were also compiled and presented in Tables 17 through 20, and in Figs. 6.122 through 6.125.

6.5.6 Variations of the Computed Dynamic Quantities

The variations of CAPWAP parameters have caused coherent variations in the dynamic quantities computed by the wave equation program. The variations of maximum computed compression and tensile forces in the piles, as well as the maximum velocities and displacement of individual soil elements were compiled from the corresponding CAPWAP (force matching) results and presented in Tables 21 through 36. The data are also presented graphically in Figs. 6.126 through 6.141.

CHAPTER 7

DISCUSSION

7.1 General

Driven piles are installed for a variety of reasons. In view of many uncertainties involved in the analysis of pile foundations, it has become customary, and in many cases mandatory, to perform a certain number of full-scale pile loading tests at the site as believed required. The purpose of these tests is to verify, experimentally, the load-displacement characteristics of the pile, and the pile bearing capacity. Although the test piles may be reused following the testing program, static loading tests are sometimes referred to as "destructive tests", and are known to be operationally and financially inconvenient. However, the static loading tests are physical tests supported by field measurements, and therefore, are readily accepted by the foundation engineering communities.

The CAPWAP method, and other signal matching techniques, are applications of Wave Equation Analysis to pile driving. The CAPWAP method makes use of force and velocity time histories measured at pile head during driving. By means of combining the wave equation and the field measurements, the CAPWAP method is used to make satisfactory estimates of the pile bearing capacity among other things. The data required to perform a CAPWAP analysis can be obtained during the driving of the pile at a relatively low cost, and without disturbance to the pile driving operation. Supported by its reliability, low cost, and convenience, the method is being promoted as an alternative to the static loading test.

While the principles of wave equation are well defined, a competent CAPWAP analysis necessitates specialized education, good practical experience in the field of piling installation, and extensive training in the use of the technique and interpretation of the results. It has been claimed, however, that within the limitations of the soil model assumed, the iterative CAPWAP analysis will ultimately guide the engineer to a unique set of parameters. These are assumed to correctly and uniquely describe the soil behavior during the driving of the pile (Rausche et. al., 1985).

As detailed in Chapter 4, the iterative CAPWAP analysis is terminated when the analyzing engineer is satisfied that a good match has been achieved between the force trace measured in the field, and the force trace computed based on the velocity measurements and the operator's input. A final check is usually made by producing a WAPCAP match (velocity trace match) using the same set of input parameters. However, due to human subjectiveness, the analysis may be terminated before the ultimate CAPWAP match has been achieved. Alternatively, and despite the claims regarding the uniqueness of the CAPWAP solution, one may wonder if several matches of the same quality may be produced using different sets of input parameters. In other words, is the CAPWAP solution subject to parametric interdependence, and if so, what is the range within which the program parameters may be changed and still be able to produce a good quality match ? Finally, what is the affect of parametric interdependence on the estimated bearing capacity of the pile ?

To shed light on these questions, a study of the parametric interdependence of the CAPWAP results was undertaken. The results of the investigation were presented in previous chapters of this thesis. This chapter provides a discussion of the results.

7.2 Bearing of Soil Conditions on the CAPWAP Results

The soil conditions at the sites of the four piles are presented in Tables 2 through 5. The soil conditions at the sites of JI and JA Piles are similar to those found at many piling sites. The soils at the site of JI Pile generally consist of soft to stiff postglacial cohesive deposits to a depth of 26 m, underlain by glacial till. Consequently, the driving of the JI Pile is expected to generate pore pressures which would temporarily reduce and alter the pile shaft resistance and its distribution during driving. The JA Pile was driven in sandy soils where the pile resistance is expected to increase linearly with depth (Fig. 5.2).

The sites of the AM and LW Pile are more unusual. The AM Pile was driven in a sensitive clay deposit which completely liquefies during driving. Several undocumented sources of information reported cases where piles have actually moved upward as much as 1 m due to buoyancy following the removal of the hammer from the pile. The CAPWAP analysis was carried out on a blow selected from restrike record of the AM Pile. The blow analyzed was the 10^{th} blow of restrike at which time the pile had moved 25 mm due to preceding blows. The movement of the pile insured the mobilization of ultimate soil resistance. However, the remolding of the soil which accompanied the blow is believed to have changed soil properties (resistance, damping, and quakes) during the time history record of the blow.

The LW pile was mostly driven through a weathered sandstone which probably crumbled into sand as the pile toe advanced. The elasto-plastic soil model of the CAPWAP may appear adequate to simulate such conditions. However, the viscous or damping effects of such soil are not readily defined.

7.3 Comments on the Data Utilized

The dynamic data utilized for the study were obtained from four industrially installed and monitored piles. The data received by the university of Ottawa were stored on magnetic tapes. The tapes were six years old, and had been stored in a standard office environment

It is known that the quality of magnetic tapes, and the stored information, may be affected by a variety of factors. Examples of these are exposure to magnetic fields, humidity, temperature, dust, and hand manipulation. Consequently, under very reasonable storage conditions, the quality of information stored on any magnetic medium will eventually be affected.

The quality of the data received ranged from fair to poor. The data were digitized and processed and the better quality blows were selected. However, a certain static force offset was observed at the origin of the JI, JA, and AM Pile traces. Although the policy undertaken by this research was not to provide any data adjustment, a static force shift was provided, as found necessary, to ensure that the force traces had values of zero prior to the beginning of loading. Otherwise, and although it sometimes felt necessary during the analysis, no data adjustment have been provided.

The data processing results also shed some light on the quality of the data analyzed. As shown in Table 7, the maximum forces, FMAX, and force values at peak hammer impact, FT1, were dissimilar except for the case of JI Pile. This indicates that the first velocity peak defining the peak hammer impact does not precisely coincide with the peak force at pile head. Visual examination of the dynamic traces presented in Figs. 5.6 through 5.8 indicate that the peak force magnitude occurs within 0.5 milliseconds of the peak velocity magnitude. Since the analysis time increment for these piles was typically 0.2 milliseconds, the imperfection was considered negligible, and the CAPWAP program did not perform any automatic time shift correction on the data. Instead, the analysis was carried out with a theoretical phase lag of one or two time increments between the force and velocity traces.

The proportionality between force and velocity at peak hammer impact is shown in the Table 7 as F/V. Theoretically, 100 percent proportionality should be observed. However, the ratio of force to proportional velocity, VEAC, ranged from 98 to 103 percent. The error involved is also considered negligible, but could have been corrected by changing the scaling factor of either force or velocity. In such a case, the output of the Pile Driving Analyzer obtained in the field during the dynamic monitoring of the piles is most valuable in determining which scaling factor need be modified. The trace obtained in the laboratory should have the same magnitude of the trace observed in the field.

The integrity number, BETA, for the LW Pile indicates another potential problem. A slight change in the pile impedance is detected at depth 5.7 m from the point of gage assembly at pile head. The pile length below gages was 17.5 m, while the embedded length of the pile was 14.6 m. The change in pile impedance was then detected some 2.8 m below ground surface at the time of the blow. The reflections of such impedance change should be observed at pile head at time 0.65 L/c following the peak hammer impact. Visual examination of the dynamic traces in Fig. 5.8 indicate a sudden drop in the force trace at that time, and a more subtle change in pile acceleration. The force and velocity traces meet shortly (1 milliseconds) following their separation. This behavior may be due to an improperly constructed splice where the soil around the pile shaft formed a plug and caused the change in impedance. The length from pile head to the detected point of damage, approximately 6 m (20 feet), supports this assumption. If the assumption of a change in impedance is eliminated in this steel pipe pile, wave equation principles suggest that the reduction in the separation between force and velocity traces may be due to negative shaft resistance or early unloading in the upper portion of the pile shaft. However, early unloading of the pile is considered unlikely due to the relatively short length of the pile, the depth below ground surface, and the soil type (silt) within which the problem was detected. Finally, the problem may also be related to poor quality data.

Additional problems with phase lag were furthermore detected in the JA Pile traces. Visual examination of the traces presented in Fig. 5.6 indicate that a second velocity peak is observed at pile head at time 2L/c. This may be due to either pile toe reflections, or a rebound in the drop hammer - pile cap assembly. If the velocity "blip" was indeed due to hammer rebound, a corresponding increase in the force trace should have been observed as well. However, the velocity peak was concurrent with a sudden reduction in the measured force. This may suggest that soil resistance at pile toe is so little that free end conditions almost exist. This is very unlikely for the case of JA pile. The possibility of a toe gap developing due to pile rebound is then considered. As may be measured from Fig. 5.6, the time elapsed during the force drop is approximately 1 millisecond. The computed maximum velocity at pile toe ranged from 2.1 to 2.6 m/s with an average value of about 2.3 m/s (Table 30). Therefore, the maximum magnitude of the toe gap required to produce such drop in force may be computed as 2.3 mm. The assumption of a developed toe gap is then reasonable, and the pile toe has to freely travel the distance of the gap before engaging any soil resistance. However, in this case, the peak of the velocity blip should have coincided with the negative peak (minimum) of the force blip. Yet, a phase lag of approximately 1 milliseconds exists between the two peaks.

The quality of the data have immediate effects on the CAPWAP results. However, and despite the imperfections, the data were considered good enough for a meaningful parametric analysis.

7.4 Results of the Analysis

Based on the parametric study, the results of the investigation may be divided into several categories:

1. Uniqueness of the solution and quality of matches obtained.
2. Variation of ultimate soil resistance
3. Variation of basic CAPWAP parameters
4. Variation of secondary CAPWAP parameters.
5. Influence of parametric variation on the computed dynamic quantities.

7.4.1 Uniqueness of the Solution

Prior to discussing the uniqueness of the solution, it may be beneficial to discuss what a "unique CAPWAP solution" means.

The purpose of the CAPWAP analysis is to determine the soil resistance and properties along the pile during the hammer blow. This is achieved by obtaining the best possible match between the force trace measured in the field, and the force trace simulated in the laboratory. The best possible match is theoretically achieved when the area between the two traces is minimized. Since a CAPWAP analysis is usually carrier out over a time period of 4L/c to 5L/c, this procedure would dictate minimizing the area between the measured and computed traces over the full time record analyzed. It is known that the first 3L/c time period is much more significant than the remaining of the record. Additionally, the trace matching around time period 2L/c is most viable in the correct determination of toe resistance. Consequently, an unintelligent procedure which aims for absolute minimization of the area between the measured and computed traces may, in fact, sacrifice the match in more important areas of the trace. To avoid this mishap, CAPWAP users rely on visual examination of the trace to decide whether or not a match is acceptable. Often, the accepted match does not correspond to the absolute "area minimization" match. Based on this discussion, it is probably not appropriate to address a unique CAPWAP solution due to the subjectiveness of procedure.

The investigation of a theoretical unique CAPWAP solution would require the minimization of the area between the traces in a multi-dimensional space. The dimensions of the space required would be equal to the number of CAPWAP unknowns. No such study is known to exist at present time, but a simplified attempt has been reported by Balthus and Kielbassa (1986). The procedure described used simplified soil resistance envelopes (rectangular or triangular), and assumed single damping and quake values for the pile shaft. An automatic procedure was then used to minimize the area between the computed and measured force traces. Based on the results of the study, a local minimum was obtained in a shaft damping - toe damping - ultimate resistance space. In other words, when fixing all other CAPWAP parameters, a unique solution was obtained when varying only damping and static resistance. The publication, however, did not discuss if this local minimum corresponded to a similar minimum for WAPCAP analysis.

7.4.2 Obtained Matches

The criterion for accepting a match in this study was based on visual examination. The matches obtained are presented in Figs. 6.1 through 6.92. For each pile analyzed, a very good CAPWAP match was first obtained. the match was then destroyed by increasing or reducing the soil resistance. Subsequently, the match was restored by varying the program parameters other than the soil resistance. This procedure was repeated until the restoration of the match was no longer possible.

Examination of the reference match obtained for JI Pile (Fig. 6.1) indicate that excellent agreements were achieved for both CAPWAP and WAPCAP analyses. The CAPWAP matches presented in Figs. 6.2 through 6.14 are the restored matches obtained for an ultimate soil resistance ranging from 900 to 1500 KN. The CAPWAP match presented in Fig. 6.11 was the least quality match among all matches for the JI Pile. At higher Rult, the match quality significantly decreased. The CAPWAP match presented in Fig. 6.13 corresponds to the analysis at 900 KN. Attempts to reduce the soil resistance below this value resulted in unstable solutions and automatic abortion of the program. This may be due to unrealistic large computed numbers which exceeded the numerical capacity of the microprocessor chip. However, the exact reason which forced analysis termination is not readily defined. The WAPCAP matches presented in Figs. 6.14 through 6.25 for JI Pile are all of good quality.

The reference matches obtained for JA Pile are presented in Fig. 6.26. It may be seen that the quality of the reference matches is not as good as those of JI Pile. This is especially true for the WAPCAP match, Fig. 6.26(b). A discussion of the force drop and velocity peaks observed in the traces at time 2L/c was provided in Section 7.3. The discussion also addressed a phase lag that exists between the measured traces as a result of poor quality data. Consequently, relatively lower quality matches were obtained. The phase lag is obvious in the computed force trace at time 2L/c. However, the velocity peak at time 2L/c was not matched. Attempts to match this blip in the velocity trace were not successful. The ultimate soil resistance of the JA Pile varied between 450 and 650 KN. The corresponding rematches are presented in Figs. 6.27 through 6.42. It may be seen that the quality of the matches at 650 KN and 450 KN presented in Figs. 6.29 and 6.34, respectively, is not very satisfactory. In view of the poor quality of data, these matches were accepted.

The reference matches obtained for AM Pile are presented in Fig. 6.43. The CAPWAP matches obtained during the parametric analysis of the pile are shown in Figs. 6.44 through 6.49. The corresponding WAPCAP matches are presented in Figs. 6.50 through 6.55. The estimated ultimate soil resistance ranged from 1275 to 1726 KN. The quality of the matches obtained for the pile was generally good, both for CAPWAP and WAPCAP analyses. The quality of the matches decreased as the soil resistance approached the limits of the accepted range of solutions (Figs. 6.46, 6.49).

The analysis of LW Pile resulted in a relatively wide range of variation for the static soil resistance. Good matches were obtained at ultimate resistance ranging from 300 to 1125 KN. The reference matches presented in Fig. 6.56 were obtained at ultimate soil resistance of 900 KN. The quality of the matches gradually decreased as the soil resistance was increased to 1125 KN as may be seen in Figs. 6.57 through 6.61, and 6.75 trough 6.79. However, the quality of the match actually improved as the soil resistance was decreased to 610 KN (Fig. 6.67). Further reduction in soil resistance resulted in gradual reduction in the match quality (Figs. 6.62 through 6.74, and 6.79 through 6.92).

7.4.3 Variation of Ultimate Soil Resistance

The parametric variations obtained from the study are compiled in Tables 9 through 12. The ranges of ultimate soil resistance, together with average and reference Rults, are summarized in Tables 37 and 38.

Table 37 presents a summary of deviation of ultimate soil resistance from the average Rult obtained for a pile. The deviation is computed as a percent ratio (percentage) of the difference between maximum and average Rults to the average Rult. The deviations ranged from ±15 percent for AM Pile to ±58 percent for LW Pile. The average deviation obtained for the four piles was 29 percent. These results are presented graphically in Fig. 7.1.

The results of an alternative method for analyzing Rult variation are presented in Table 38. The variation of ultimate soil resistance is presented as a percent ratio of maximum and minimum Rults to the Reference Rult corresponding to the Reference match. For comparative purposes, the results of this method, together with the results of the deviation method, are presented in Fig. 7.1.

As may be noted from the figure, the variation of Rult for JA and LW Piles is greater in the negative side of the Reference Rult. If the Reference Rult is assumed to be the "correct" ultimate soil resistance, then, for these two pile, the probability of underestimating pile bearing capacity using the CAPWAP method is greater than the probability of overestimating it. Under the assumption given, this error is to the safe side. Based on the same assumption, the results of JI Pile indicate a greater probability of making an overestimate. However, it is not really known if the Reference Rult is indeed the correct ultimate soil Resistance. Ideally, this should be verified from the results of a static loading test. It is unfortunate that such verifications are not possible for the case of JI, JA, and LW Piles since no static loading tests are available for the piles. However, Fellenius (1988) reported the results of a static loading test performed on the AM Pile one day prior to the restrike from which the record blow was obtained. The capacity of the pile reported ranged from 1500 to 1900 KN, or 1800 to 1900 KN if the potential error in jack load was disregarded. Based on these results, the range of ultimate soil resistance estimated from the CAPWAP corresponds to a small underestimation, and an error to the safe side.

Another alternative approach for analyzing the variation of ultimate soil resistance is to consider the coefficients of variations of the results. The coefficient of variation is defined as the percent ratio of standard deviation to the average value. This method of analysis is probably less meaningful for the ultimate soil resistance parameter since the variation of Rult was not obtained from a statistical survey. Instead, the different values of Rult for a given pile were systematically obtained by adding or subtracting a prefixed resistance increment to the ultimate resistance obtained from the reference match. However, for comparative purposes, the averages and standard deviations for Rult were computed and presented in Tables 9 through 12. The coefficients of variations for the ultimate soil resistance, together with the coefficients of variations for other CAPWAP parameters, are presented in Table 39 and Fig. 7.2. The coefficient of variation for Rult ranged from 10 to 36 percent and had an average value of 19 percent for the four piles analyzed.

All of the analysis methods presented indicate that the variation of LW Pile results are relatively high. This is probably due to the soil conditions at the site of the pile. As discussed in earlier section, the LW Pile was driven through weathered sandstone which probably crumbled into sand as the pile toe advanced. The application of elasto-plastic soil model in such conditions is coherent. However, the extent of applicability of damping parameters is not as clear. The Case and Smith damping coefficients obtained for the four piles are presented in Figs. 7.3 and 7.4, respectively. The Case damping coefficients obtained for LW Pile toe ranged from 0.50 to 0.95 (Table 12). The corresponding Smith damping coefficients ranged from 2.24 to 14.07 s/m. Although such values for Case damping coefficient are not uncommon, the magnitude of Smith damping coefficients are alarming. The maximum computed velocities for the toe element of LW Pile ranged from 2.7 to 1.9 m/s. Consequently, and according to Eq. 2.8-1, the maximum dynamic soil resistance of the toe element ranged from 6 to 27 times the static resistance of the pile toe. Considering the energy required to break down the sandstone in the toe area into granular sand, this may seem realistic. However, the final static toe resistance is relatively too low which contradicts this argument. Commercially, such unusual case should be supplemented by a static loading test.

Based on the results of analysis presented in this section, it may be concluded that the ultimate soil resistance obtained from the reference match should not be considered a datum for analyzing the variation of Rult due to the lack of calibration with static loading tests. The maximum variation of ultimate soil resistance obtained from CAPWAP for the four piles analyzed was within ±58 percent of the average Rult value. This variation is reduced to a maximum of ±25 percent if the results of LW Pile were disregarded.

7.4.4 Variation of Shaft and Toe Resistance

The results of variation of static shaft and toe resistance are compiled and presented in Fig. 7.5. As may be noted from the results, both shaft and toe resistance generally increased as the ultimate soil resistance increased. To study the relative variation of these results, the percent ratio of shaft and toe resistance to the ultimate soil resistance were computed and presented in Tables 40 through 43, and in Figs. 7.6 through 7.9. For the four piles analyzed, the CAPWAP estimates indicate that the larger portion of static soil resistance is due to pile shaft resistance. The band of relative variation for the JI Pile was the largest and had a magnitude of 16 percent as shown in Fig. 7.6. The band of relative variation of shaft and toe resistance for LW Pile had the lowest magnitude of 3 percent (Fig. 7.9). The low band of variation for LW Pile is due to the fact that both shaft and toe resistance were proportionally increased, or decreased, as the ultimate soil resistance was modified.

The coefficients of variation for the shaft and toe resistance of the four piles are computed and presented in Table 39 and Fig. 7.2. These results reflect the fact that, for all analysis cases, the shaft resistance was estimated to contribute to most ultimate soil resistance. The coefficients of variation obtained for shaft resistance were comparable to those obtained for Rult.

Based on the results of this discussion, the variation of resistance distribution between pile shaft and pile toe as estimated from CAPWAP analysis was less than ±8 percent. However, such conclusion lacks the support of more elaborate statistical evidence and calibration with telltaled static loading tests. Alternatively, the coefficients of variation generally indicate a similarity between the variation of Rult and that of pile shaft and pile toe resistance. Consequently, it would be more prudent to assume a range of variation for resistance distribution between pile shaft and pile toe similar to that obtained for Rult (±25 percent excluding LW Pile results).

7.4.5 Variation of Damping

The values of Case and Smith damping coefficients obtained during the study are summarized in Figs. 7.3 and 7.4, respectively. The results generally indicate larger damping values for the toe elements, with the exception of JA Pile results. The range of Case damping values obtained for JI and AM Piles were within the suggested range of values for the soil conditions encountered at the sites of the piles (Fig. 2.13). The Case damping values for the LW File correspond to unusual soil conditions and may not be correlated. The Case damping values obtained for JA Pile were higher than the range of values recommended for sandy soil conditions. However, as may be noted from Fig. 7.3, the range of Case damping values for the pile toe were comparable to the range of values observed for the parameter, as shown in the chart of Fig. 2.13.

The values of Smith damping coefficient obtained are summarized in Fig. 7.4. It may be noted from the figure that the analysis generally resulted in Smith damping values of smaller than 1 s/m. The Smith damping values obtained for LW Pile were exceptional, and were discussed in Section 7.4.3. Smith damping coefficients obtained for the toe element of JA Pile exceeded 1 s/m as the ultimate resistance of the pile was reduced below 600 KN. Such results are also considered unusual, and commercially , should be confirmed by a static loading test. However, the compiled results presented in Fig. 7.4 indicate that there is a general trend of increased dynamic resistance as the static soil resistance was reduced. This argument is further supported by the results of a statistical survey of CAPWAP results as a function of the operator (Fellenius, 1988). The four blow records presented in this thesis were compiled and distributed to 20 individuals. Eighteen individuals performed and returned a CAPWAP analysis for each blow. A compilation of basic CAPWAP results obtained from the survey are presented in Table 44. The pertinent results of Smith damping variation were extracted and presented, together with computed best fit regression lines, in Fig. 7.10.

Based on these results, it may be concluded that the substitution of static resistance by dynamic resistance contributes significantly to the parametric interdependence of the CAPWAP method. This conclusion is further supported by the results of Balthus and Kielbassa (1986) who concluded that, based on the results of their study, the CAPWAP method can only filter with a limited accuracy the dynamic component of soil resistance.

7.4.6 Variation of Quakes

The quake values obtained from the study are presented in Tables 9 through 12 together with computed averages and standard deviations. The quake results are further compiled and presented in Fig. 7.11. The coefficients of variation of quake values for the piles analyzed are presented in Table 39 and Fig. 7.2. The coefficients of variation obtained ranged from 0 to 35 percent, and averaged to 18.5 and 13.5 percent for the shaft and toe quakes, respectively. Coefficients of variation computed for the results published by Fellenius (1988), however, indicate larger variation for the quake values, typically in the range of 50 percent.

The variation of quake values obtained from the analysis of any single pile indicate random variations. Nevertheless, the combined results of the four piles indicate a general trend of increasing quakes with increasing ultimate soil resistance (Fig. 7.11). This observation is further supported by the results of the survey compiled by Fellenius (1988). The pertinent results of quake variations obtained from the survey are presented in Figs. 7.12 and 7.13. The corresponding best fit regression lines were also computed and included in the figures. As may be noted from Fig. 7.12, there is a good indication of increasing shaft quakes with increasing Rult. The results presented in Fig. 7.13, however, indicate a larger scatter, but generally support the same conclusion. Based on these results, it may be concluded that the quake values generally increase with increased soil resistance, and this relationship is an intrinsic property of the quake parameter. However, the soil stiffness is defined as the ratio of Rult to the soil quake. If soil quakes actually increased with increased Rult, one may wonder about the effects of such relationship on the computed soil stiffness. To shed light on such questions, Fellenius results (1988) were used to compute soil stiffness as a ratio of Rult to shaft quakes. The results of computed soil stiffness are presented in Fig. 7.14. As may be expected, the data indicate increased soil resistance with increased stiffness. This validates the usefulness of quake data obtained, and the usefulness of conclusions drawn from them.

7.4.7 Variation of Secondary CAPWAP Parameters

The parameters of the CAPWAP method may be divided into two categories: The basic wave equation parameters introduced by Smith (1960), and the additions to the model introduced by the WEAP and CAPWAP programs. The basic CAPWAP parameters are considered to include soil resistance, damping, and quakes. The unloading parameters, soil plug, toe gap, as well as the recently introduced toe soil damper, are considered secondary parameters.

Based on the results of this study, the variation of unloading quantities, such as unloading quakes and unloading shaft resistance, were observed to have cosmetic effects on the computed traces in the later portions of the records. The variations of these quantities are presented in Tables 9 through 12, and in Figs. 6.108 through 6.117. The data, converted from percentage to physical units, are further compiled and presented in Figs. 7.15 and 7.16. As may be observed from these figures, the variations of unloading quantities do not appear to follow any general trend. The coefficients of variation obtained for the unloading quantities are presented in Table 39 and Fig. 7.17. The magnitude of coefficients of variation obtained reflect the randomness of the results.

The toe gap parameter was observed to have a significant effect on the quality of the match at time 2L/c of a record. The parameter was observed to contribute significantly to the parametric interdependence of the results in the ranges of ultimate soil resistance obtained. The parameter was observed to substitute either or both, the static and dynamic soil resistance of the pile toe element. The parameter has the general effect of sharply lowering the computed trace at time 2L/c, and hence, it is able to counterbalance the rising of computed curve due addition of soil resistance. The values of toe gaps obtained from the study are presented in Figs. 6.115 through 6.117, and are further compiled in Fig. 7.18. The values of toe gaps obtained ranged from 0 to 5 mm, but were generally less than 3 mm. The relative variation of the results as indicated from the coefficients of variation presented in Table 39 and Fig. 7.17 is quite large. Similar to the case of unloading parameters, there is an indication of randomness in the toe gaps obtained.

The variation of the toe soil damper parameter was observed to have negligible effects on the computed traces. However, the variation of the parameter had considerable effects on the computed final displacement, and computed blow count. The values obtained for the parameters are presented in Tables 9 through 12, and in Figs. 6.101 through 6.103. The computed coefficients of variation for this parameter ranged from 0 to 292 percent, as shown in Table 39 and Fig. 7.17.

The soil plug parameter was required only in the case of LW Pile which was driven open toe. A soil plug value of 0.55 KN was utilized throughout the parametric analysis of the pile. Assuming a compacted unit weight of 20.0 to 20.4 KN/m^3 (125 to 130 pcf) for the resulting sandy soil at the site of the pile, the length of the corresponding soil plug inside the pile may be computed as 240 mm.

7.4.8 Variation of Soil Resistance Distribution

The variation of static resistance distributions obtained from the parametric analysis are presented in Figs. 6.118 through 6.121. The corresponding load transfer diagrams are presented in Figs. 6.122 through 6.125.

The load distribution curves computed for JI Pile indicate little shaft resistance mobilized in the postglacial cohesive soils above depth 26 m. This is consistent with expectations of reduced effective stresses due to generation of excess pore pressures in this soil. For JA Pile which was driven through sandy soils, effective stresses are expected to increase linearly with depth. The load distribution curves computed for the pile generally indicate shaft resistance linearly increasing with depth, consistent with the principles of effective stresses. The load distribution curves obtained for LW Pile generally indicate a soil resistance increasing with depth. However, the toe resistance estimated is very low.

The load distribution curves computed for AM Pile are shown in Fig. 6.124. As may be noted from the figure, the computed shaft resistance increased with depth, then abruptly decreased to insignificant magnitudes below depth 35 m. This behavior may be due to the remolding of soil in the lower portion of the pile during restrike. Following the end of driving of the pile, the dissipation of excess pore pressures resulted in soil setup, and linearly increasing soil resistance as observed at the upper portion of the pile shaft. During restrike, the soil resistance gradually broke down due to remolding of soil. The remolding appears to have originated in the lower portions of the pile.

The general shape of resistance distributions obtained did not vary significantly, as may be seen in Figs. 6.118 through 6.121. This may be due to the fact that shaft resistance and its distribution directly affects the quality of the match during the first 2L/c period of the record. The CAPWAP program permits the selection of different damping and quake values for the different soil elements along the pile shaft. However, to reduce the number of parameters analyzed, similar values of damping and quake were assumed for all the shaft soil elements. Consequently, it may be considered that the stability of soil resistance distribution is partially due the fixing of damping and quake values along the pile shaft. Larger variation should be expected if soil damping and quakes for the different soil elements were individually selected and varied.

7.4.9 Variation of Computed Dynamic Quantities

The variation of CAPWAP parameters have caused coherent variation in the dynamic quantities computed for the pile during the hammer blow. These computed quantities include pile element displacements, pile element velocities, and maximum compression and tension forces in the pile.

The dynamic quantities obtained from CAPWAP (force) matching are compiled and presented in Tables 21 through 36 and in Figs. 6.126 through 6.141. As may be observed from the figures, there is a general trend of increased deviation with depth. Subsequently, the coefficients of variation for these quantities were computed and normalized over depth. The corresponding results are presented in Table 45 and in Figs. 7.19 through 7.23.

The coefficients of variation obtained for maximum element displacements, velocities, and compression forces are shown in Figs. 7.19, 7.20, and 7.21, respectively. The coefficients obtained confirm increased variation with depth, as may be seen from the figures. The maximum coefficients of variation obtained ranged from 11 percent for element velocities, to 23 percent for maximum compression forces. The variation of these dynamic quantities is relatively smaller than the variations of basic CAPWAP parameters. However, the variation of maximum computed tension forces is more diverse, especially for the case of AM Pile.

The coefficients of variation obtained for the maximum computed tension forces are presented in Fig. 7.22. As may be noted from the figure, the trend of increased variation with depth is less consistent. Additionally, the coefficients of variation obtained are larger, especially for AM Pile. As may be noted from Table 28, CAPWAP estimates indicated no tension forces in AM Pile except for the solution at 1725 KN. if this particular match was excluded from the analysis, the coefficients of variation for tension forces in the pile would have had values of zero. Consequently, coefficients of variation for maximum tension forces in the piles, excluding AM Pile, were plotted in Fig. 7.23. The results indicate variations of 0 to 72 percent, with an average coefficient of variation of 19 percent. However, based on the results obtained, one should expect relatively larger variations in the maximum tension forces obtained from a CAPWAP analysis. If, during a commercial analysis, suspicious tension forces are computed for a given pile, a parametric analysis should be provided to confirm the validity of the results obtained.

CHAPTER 8

CONCLUSIONS

The results of analysis obtained from this parametric study confirm the parametric interdependence of the CAPWAP method. Subsequent to obtaining a good agreement between the measured and computed force (or velocity) traces, the mismatch resulting from changing the ultimate soil resistance may be restored by modifying the values of other program parameters. This parametric interdependence is restricted, however, to a certain range of ultimate soil resistance which varied for the different piles analyzed.

The parametric interdependence of the CAPWAP method is mainly due to the interdependence of dynamic and static soil resistance. The effects of secondary CAPWAP parameters other than toe gap were observed to be limited to cosmetic improvements to the match, and practically, had no significant effects on the computed ultimate soil resistance.

The CAPWAP method was least accurate in filtering out the static and dynamic components of resistance for the case of LW Pile. The application of the method to the analysis of piles driven into similar soil conditions should tolerate significant variations in the computed ultimate soil resistance. In such cases, the provision of at least one static loading test would be most helpful in the calibration of results, and proper determination of expected magnitudes of dynamic soil resistance.

The results of the study, excluding the results of LW Pile, indicate that the maximum variation of estimated ultimate soil resistance would be within ±25 percent of the average soil resistance obtained from the parametric analysis of the pile. If the results of LW Pile were to be included, the maximum variation expected would be within ±58 percent of the average soil resistance obtained.

The results of static resistance distributions estimated from the CAPWAP method generally appeared to agree with the principles of effective stresses, and the expected soil behavior at the sites of the different piles.

Based on the results of theoretical analysis presented, there is a statistical evidence of increased quake values with increased ultimate soil resistance.

The variations of secondary CAPWAP parameters were observed to be random within the ranges of ultimate soil resistance obtained. The effects of these parameters, with the exception of toe gap, are considered negligeable on the estimated pile capacity. The toe gap, however, contributed significantly to the parametric interdependence of pile toe results.

The variations of dynamic quantities, such as compression forces, element displacements, and element velocities, estimated from the CAPWAP method were observed to increase with depth. The maximum relative variation of these quantities, however, was less than the relative variation of ultimate soil resistance. The variation of computed tension forces was significantly larger. Caution should be exercised when using the values of tension forces estimated from a CAPWAP analysis, unless a parametric analysis is provided.

REFERENCES

REFERENCES

ASTM, 1986. **Proposed new standard method of high-strain dynamic testing of piles.** American Society for Testing and materials, 13 p.

AUTHIER, J., and FELLENIUS, B. H., 1980a. **Dynamic measurements as an inspection tool for discovering damage to spliced and unspliced precast concrete piles. Two case histories.** Proceedings International Seminar on the Application of Stress-Wave Theory on Piles, 1980, H. Bredenberg Editor, A. A. Balkema, Rotterdam, pp. 121-127.

AUTHIER, J., and FELLENIUS, B. H., 1980b. **Quake values determined from dynamic measurements.** Proceedings International Seminar on the Application of Stress-Wave Theory on Piles, 1980, H. Bredenberg Editor, A. A. Balkema, Rotterdam, pp. 197-216.

AUTHIER, J., and FELLENIUS, B. H., 1981. **Pile integrity and soil set-up and relaxation.** Second Seminar on the Dynamics of Pile Driving, Pile Research Laboratory, University of Colorado, Boulder, 9 p.

AUTHIER, J., and FELLENIUS, B. H., 1983. **Wave equation analysis and dynamic monitoring.** Civil Engineering for Practicing and Design Engineers, Pergamon Press Ltd., Vol. 2, No. 4, pp. 387-407.

BALTHUS, H. G., and KIELBASSA, S., 1986. **Numerical modelling of pile driving.** 2nd International Symposium on Numerical Models in Geomechanics, Ghent, pp. 487-495.

Beringen, F. L., van Hooydonk, W. R., and Schaap, L. H. J., 1980. **Dynamic pile testing: An aid in analyzing driving behavior.** Proceedings International Seminar on the Application of Stress-Wave Theory to piles, Stockholm, 1980, H. Bredenberg, Editor, A. A. Balkema, Rotterdam, pp. 108-130.

BREDENBERG, H., and HOLM, G., 1985. **Evaluation of pile driving criterion from Case measurements.** Proceedings, International Symposium on Penetrability and Drivability of Piles, San Francisco, Vol. 1, pp. 159-162.

CAse Pile Wave equation Analysis Program (CAPWAP), 1984. **CAPWAP system documentation.** Software Manual, IBM - PC version, Goble, Rausche, Likins and Associates (GRL), Software Products, Cleveland, 315 p.

CAse Pile Wave equation Analysis Program - Continuous Version (CAPWAPC), 1986. **The CAPWAPC program, user's manual.** Software Manual, IBM - PC version, Goble, Rausche, Likins and Associates (GRL), Software Products, Cleveland, 206 p.

Canadian Foundation Engineering Manual (CFEM), 1985. **Second edition, Part 3: Deep Foundations.** Canadian Geotechnical Society, Technical Committe on Foundations, BiTech Publications, Vancouver, pp. 269-373.

CHELLIS, R., 1951. **Pile Foundations.** McGraw-Hill Book Co., pp. 28-33, 449-450, 525-538.

FELLENIUS, B. H., SAMSON, L., THOMPSON, D. E., and TROW, W. A., 1978. **Dynamic behavior of foundation Piles and driving equipment.** Final report, Research Contract No. 1ST00045, Terratch Ltd. and the Trow Group Ltd. to the Department of Supply and Services, Canada, 520 p.

FELLENIUS, B. H., 1984. **Geotechnically allowable stress for driven piles.** American society of Civil Engineers, ASCE, Journal of Civil Engineering, November 1984, Vol. 54, No. 11, pp. 72-75.

FELLENIUS, B. H., RIKER, R. E., O'BRIEN, A. J., and TRACY, G., 1985. **CAPWAP analysis and static testing in a soil exhibiting set-up.** Seminar on Dynamic Monitoring of Pile Driving and Its Application in Foundation Design and Construction Control, University of Colorado, Boulder, Colorado, Department of Civil and Architectural Engineering, March 28 and 29, 1985. 25 P.

FELLENIUS, B. H., 1988. **Variation of CAPWAP results as a function of the operation.** Proceedings, Third Stress Wave Conference, Ottawa, 1988, pp. 814-825.

FLODIN, N., and BROMS, B., 1981. **History of civil engineering in soft clay.** Soft Clay Engineering. Editors, E. W. Brand, and R. P. Brenner, Elsevier Scientific Publishing company, pp. 26-156.

FORHAND P. W., and REESE J. L., 1964. **Prediction of pile capacity by the wave equation.** American Society of Civil Engineers, ASCE, Journal for Soil Mechanics and Fondation Engineering, SMFE, Vol. 90, No. SM2, pp. 1-25.

GOBLE, G. G., RAUSCHE, F., and MOSES, F., 1970. **Dynamic studies on the bearing capacity of piles. Phase III.** Report No. 48, Vol. 1 and Vol. 2, Division of Solid Mechanics, Structural and Mechanical Design, Case Western Reserve University, 325 p.

GOBLE, G. G., and RAUSCHE, F., 1976. **Wave equation analysis of pile driving. WEAP program.** Vol. 1 - Background, Vol. 2 - User's Manual, Vol. 3 -Program Documentation, US Department of Transportation, Federal Highway Administration, FHWA, Office of Research and Development, Implementation Division, Washington, D.C., 371 p.

GOBLE, G. G., RAUSCHE, F., and LIKINS, G. E., 1980. **The analysis of pile driving. A state-of-the-art.** Proceedings, International Seminar on the Application of Stress-Wave Theory to Piles, Stockholm, 1980, H. Bredenberg, Editor, A. A. Balkema, Rotterdam, pp. 131-162.

GRAVARE, C. J., GOBLE, G. G., RAUSCHE, F., and LIKINS, G. E., 1980. **Pile driving construction control by the Case method.** Ground Engineering, Vol. 13, No. 2, pp. 20-25.

GRAVARE, C. J., and HERMANSSON, I., 1980. **Practical experience of stress wave measurements.** Proceedings, International Seminar on the Application of Stress Wave Theory on Piles, Stockholm, 1980, H. Bredenberg Editor, A. A Balkema, Rotterdam, pp. 131-162.

HANNIGAN P. J., 1986. **Dynamic pile testing and analysis.** 11th Annual Fundamentals of Deep Foundation Design. STS Consultants, Ltd., Fairfax, Virginia, 59 P.

HIELY A., 1930. **Pile driving calculations with notes on driving forces and ground resistance.** American Society of Civil Engineers, ASCE, Journal of Structural Engineering, Vol. 8, July, 1930, pp. 246-259.

HIRSH, T. J., and EDWARDS, T. C., 1966. **Impact load -deformation properties of pile cushioning materials.** Research Report No. 33-4, Pilling Behavior, Research Project No. 2-5-62-33, Texas Transportation Institute, Texas A&M University, College Station, Texas, 12 p.

HIRSH, T. J., CARR, L., and LOWERY, L. L., 1976. **Pile driving analysis. Wave equation user's manual. TTI program.** Vol. 1 - Background, Vol. 2 - Computer Program, Vol. 3 - Program Documentation, US Department of Transportation, Federal Highway Administration, FHWA, Office of Research and Developement, Implementation Division, Washington, D.C., 308 p.

HOLLOWAY, D. M., CLOUGH, G. W., And VESIC, A. S., 1979. **A rational procedure for evaluating the behavior of impact-driven piles.** American Society for Testing and Material, ASTM Symposium on Behavior of Deep Foundations, R. Lundgren, Editor, Special Technical Publication, STP 670, 1978, pp. 335-357.

HUSSEIN, M., 1986a. **CAPWAPC - A parameter study.** Paper Presented to the Eighth Pile Driving Analyzer User's Seminar, Kungsbacka, Sweden, 25 p.

HUSSEIN, M., 1986b. **Qualitative evaluation of pile force and velocity records.** Paper Presented to the Eighth Pile Driving Analyzer User's Seminar, Kungsbacka, Sweden, 20 p.

ISAACS, D. V., 1931. **Reinforced concrete pile formulae.** Transactions of the Institution of Engineers, Australia, Vol. XII, No. 370, pp. 312-323.

KHAN, N., 1987. **Load distribution in test loaded instrumented steel piles.** M.A.Sc. **Thesis.** Department of Civil Engineering, Faculty of Engineering, University of Ottawa, Ottawa, 176 p.

KREYSZIG, E., 1979. **Advanced engineering mathematics.** John Wiley and Sons, Fourth Edition, pp. 468-538.

LOWERY, L. L., HIRSH, T. J., EDWARDS, T. C., and SAMSON, C.H., 1969. **Pile driving analysis, State-of-the-art.** Research Report 33-13, Research Study No. 2-5-62-33, Texas Transportation Institute, Texas A&M University, 79 p.

LOWERY, L. L., 1983. **Pile driving analysis by the wave equation. User's manual. TTI program.** Utilization Manual for Data Building and Checking Program, Vol. 1 - Background, Vol. 2 - Computer Program and sample problems, Wild West Software Inc., 325 p.

PECK, R. B., HANSON, W. E., and THORNBURN, T. H., 1966. **Foundation Engineering.** John Wiley and Sons, Inc., pp. 175-188.

RAMEY, G. E., and HUDGINS, A. P., 1977. **Sensitivity and accuracy of the pile wave equation.** Ground Engineering, Vol. 10, No. 7, pp. 45-47.

RAUSCHE, F., MOSES, F., and GOBLE G. G., 1972. **Soil resistance prediction from pile dynamics.** American Society of Civil Engineers, ASCE, Journal of Soil Mechanics and Foundations Division, Vol. 98, No. SM9, pp. 917-937.

RAUSCHE, F., GOBLE, G. G., and LIKINS, G. E., 1985. **Dynamic determination of pile capacity.** American Society of Civil Engineers, ASCE, Jornal of Geotechnical Engineering, Vol. 111, No. 3, pp. 367-383.

RAUSCHE, F., LIKINS, G. E., and HUSSEIN, M., 1986. **Dynamic Analysis of Impact Piles By WEAP86.** Report Prepared for Office of Implementation Federal Highway Administration, McLean, Virginia, 40 p.

RAUSCHE, F., 1986. **CAPWAPC principles and limitations.** Unpublished Paper. Goble Raushe Likins and Associates, Inc. Cleveland, 24 p.

SMITH, E. A. L., 1960. **Pile driving analysis by the wave equation.** American Society of Civil Engineers, ASCE, Journal for Soil Mechanics and Foundation Engineering, Vol. 86, No. SM4, pp. 35-61 (Discussion in Vol. 87, No. SM1, pp. 63-75).

TENG, W. C., 1962. **Pile foundations.** Civil Engineering and Engineering Mechanics Series, N. M. Newmark and W. J. Hall, Editors, Prentice-Hall Inc., pp. 193-252.

THOMPSON, C. D., and THOMPSON, D. E., 1985. **Real and apparent relaxation of driven piles.** Americal Society of Civil Engineering, ASCE, Journal of Geotechnical Engineering, Vol. 111, No. 2, February, pp. 225-237.

TIMOSHENKO, S. P., and GOODIER, J. N., 1970. **Theory of elasticity.** Engineering Societies Monographs, McGraw Hill Book Company, Third edition, pp. 485-514.

T A B L E S

Table 1. Pile Data

Pile	JI	JA	AM	LW
Material	Steel	Steel	Steel	Steel
Shape	Pipe	H pile	Pipe	Pipe
Size	-	W310x79	-	-
O.D. (mm)	324	-	245	406
Wall (mm)	9.5	-	14	13
Length (m)*	42.7	28.9	57.4	17.5
Area (cm^2)	94	101	100	157
Pile toe	Plate			Open
PRES (Bl/0.3 m)+	25	50	100	60
Embedment (m)	35.0	21.6	57.0	14.6

+ Penetration resistance for the blow analyzed (blows/0.3 m)
* Pile length below gauges

Table 2. Soil Profile, JI Pile

(embedment 35.2 m)

Depth (m)	Type	Thickness (m)	Unit weight (KN/m^3)	Cu (KPa)	Friction angle (Deg)
0.0	Miscellaneous earth fill	6.0	18	-	30
6.0	Soft to medium stiff compressible postglacial silty clay and clayey silt	19.5	17	40	37
25.5	Mixed glacial soil: sandy silt, sand, clayey silt	56.0	18	200	36.5
81.5	Dolomite bedrock. End of borehole	-	-	-	-

Table 3. Soil Profile, JA Pile

(embedment 21.6 m)

Depth (m)	Type	Thickness (m)
0.0	Sandy gravel fill with lenses of frost	1.3
1.3	Coarse to medium coarse sand with layers of silty sand and lenses of frost	2.3
3.6	Sandy gravel	0.7
4.3	Medium to fine compact brown sand with layers of fine silt	18.6
22.9	Medium and fine compact sand, trace silt	5.0
27.9	End of borehole	

Table 4. Soil Profile, AM Pile

(embedment 58.2 m)		
Depth (m)	Type	Thickness (m)
0.0	Fill: sand and clay with pieces of weathered shale	1.3
1.3	Loose to medium dense silty fine sand	0.5
1.8	Medium soft to stiff fissured silty grey clay	16.2
18.0	Stiff to very stiff silty grey clay	30.0
48.0	Dense soil End of borehole	

Table 5. Soil Profile, LW Pile

(embedment 14.6 m)

Depth (m)	Type	Thickness (m)
0.0	Surface layer of peat	0.4
0.4	Silt	2.7
3.1	Stiff to firm grey silty, sandy clay	7.4
10.4	Brown weathered sandstone with silty clayey shale	3.1
13.5	Bentonitic sandstone	2.1
15.6	End of borehole	

Table 6.1 DATPRO Input for JI Pile

JI PILE					kN	METR			
AREA	94.2	LENG	42.7	WEIG	31.5	EMOD	20925.	WSPD	5120.
SPCW	78.300	MC/L	385.0	EA/C	385.0	2L/C	16.6		
VCAL	1.38	FCAL	2.62	IDEL	200.	ISAV	824.	FREQ	9250.
JSTA	100.	JSTP	578.	JINT	1019.				
PSET	1.18	IADJ	2.	STAT	.00	WRAM	.00	WCAP	.00
VSMO	0.	FSMO	0.	VSHI	0.	FSHI	0.	IOFF	0.
NGRD	2.	NAXS	4.	DIST	4.50	NPLT	1.	PFST	2.
VSCL	.00	FSCL	.00	DSCL	.00	ASCL	.00	ESCL	.00
WSCL	.00	RSCL	.00	MSCL	.00	TSCL	5.00		
DAM1	.10	DINC	.10	DMAX	.00				
VTRG	.30	NPEK	1.	JDEL	.00	XTEN	.00	TDGE	2.00
IENG	0.	REPR	1.	FSTA	4.	FSTP	4.	TITC	0.
FOPT	0.	OMIT	0.	IPWP	0.	ECOM	0.	PORD	0.

Table 6.2 DATPRO Input for JA Pile

JA PILE kN METR

AREA	101.0	LENG	28.9	WEIG	22.4	EMOD	20000.	WSPD	5061.
SPCW	76.600	MC/L	399.1	EA/C	399.1	2L/C	11.4		
VCAL	1.15	FCAL	2.00	IDEL	200.	ISAV	824.	FREQ	8500.
JSTA	100.	JSTP	416.	JINT	1019.				
PSET	.61	IADJ	2.	STAT	.00	WRAM	.00	WCAP	.00
VSMO	0.	FSMO	0.	VSHI	0.	FSHI	0.	IOFF	0.
NGRD	2.	NAXS	4.	DIST	4.50	NPLT	1.	PFST	2.
VSCL	.00	FSCL	.00	DSCL	.00	ASCL	.00	ESCL	.00
WSCL	.00	RSCL	.00	MSCL	.00	TSCL	5.00		
DAM1	.10	DINC	.10	DMAX	.00				
VTRG	.30	NPEK	1.	JDEL	.00	XTEN	.00	TDGE	2.00
IENG	0.	REPR	1.	FSTA	3.	FSTP	3.	TITC	0.
FOPT	0.	OMIT	0.	IPWP	0.	ECOM	0.	PORD	0.

Table 6.3 DATPRO Input for AM Pile

AM PILE kN METR

AREA	100.3	LENG	57.4	WEIG	44.6	EMOD	20400.	WSPD	5082.
SPCW	77.500	MC/L	402.7	EA/C	402.7	2L/C	22.6		
VCAL	1.19	FCAL	1.99	IDEL	200.	ISAV	824.	FREQ	8200.
JSTA	100.	JSTP	749.	JINT	1019.				
PSET	.36	IADJ	2.	STAT	.00	WRAM	.00	WCAP	.00
VSMO	0.	FSMO	0.	VSHI	0.	FSHI	0.	IOFF	0.
NGRD	2.	NAXS	4.	DIST	4.50	NPLT	1.	PFST	2.
VSCL	.00	FSCL	.00	DSCL	.00	ASCL	.00	ESCL	.00
WSCL	.00	RSCL	.00	MSCL	.00	TSCL	5.00		
DAM1	.10	DINC	.10	DMAX	.00				
VTRG	.30	NPEK	1.	JDEL	.00	XTEN	.00	TDGE	2.00
IENG	0.	REPR	1.	FSTA	2.	FSTP	2.	TITC	0.
FOPT	0.	OMIT	0.	IPWP	0.	ECOM	0.	PORD	0.

Table 6.4 DATPRO Input for LW Pile

LW PILE kN METR

AREA	157.0	LENG	17.5	WEIG	21.1	EMOD	20000.	WSPD	5054.
SPCW	76.800	MC/L	621.2	EA/C	621.2	2L/C	6.8		
VCAL	1.17	FCAL	1.28	IDEL	200.	ISAV	824.	FREQ	8500.
JSTA	100.	JSTP	347.	JINT	1019.				
PSET	.50	IADJ	2.	STAT	.00	WRAM	.00	WCAP	.00
VSMO	0.	FSMO	0.	VSHI	0.	FSHI	0.	IOFF	0.
NGRD	2.	NAXS	4.	DIST	4.50	NPLT	1.	PFST	2.
VSCL	.00	FSCL	.00	DSCL	.00	ASCL	.00	ESCL	.00
WSCL	.00	RSCL	.00	MSCL	.00	TSCL	2.50		
DAM1	.10	DINC	.10	DMAX	.00				
VTRG	.30	NPEK	1.	JDEL	.00	XTEN	.00	TDGE	2.00
IENG	0.	REPR	1.	FSTA	1.	FSTP	1.	TITC	0.
FOPT	0.	OMIT	0.	IPWP	0.	ECOM	0.	PORD	0.

Table 7. Data Processing Results

PILE		JI	JA	AM	LW
ID		4	3	2	1
BN		16	13	10	1
AMAX	g	340	338	452	361
VMAX	m/s	2.54	3.00	4.88	3.17
DMAX	mm	33	13	26	11
FMAX	KN	1074	1251	2038	2042
EMAX	KN-m	26.8	9.7	32.0	14.4
FT1	KN	1074	1181	1952	1984
VT1	m/s	2.54	3.00	4.88	3.17
VEAC	KN	978	1199	1967	1967
F/V	%	103	98	99	101
RT	KN	1355	1153	2468	2459
RS-1	KN	1285	1030	2322	2309
RS-2	KN	1215	907	2177	2160
RS-3	KN	1145	784	2032	2011
RS-4	KN	1076	662	1887	1861
RTMN	KN	1341	1150	2353	2182
C-MN	m/s	5231	5013	4902	4311
RSMX	KN	1359	1194	2479	2460
JADD		78	50	93	29
RTUN	KN	1355	1243	2777	2533
TF	KN	0	0	0	0
T-PL	m	0	0	0	0
BETA	%	99	99	99	90
B-PL	m	0	0	0	5.7
SK F	KN	972	951	1240	1429
SKUN	KN	972	1041	1549	1503
FMIN	KN	78	-7	11	-11
RAUT	KN	920	259	1395	235
WDX	KN	658	355	674	865

Table 8. Pile Profiles for CAPWAP Analysis

PILE	I	DEPTH	AREA cm^2	ELAS. MOD. KN/cm^2	SPEC. WT. KN/m^3
JI	1	0.00	94.20	20925.00	78.30
	2	42.65	94.20	20925.00	78.30
	3	42.65	889.00	20925.00	78.30
	4	42.70	889.00	20925.00	78.30
JA	1	0.00	101.00	21013.80	76.60
	2	29.00	101.00	21013.80	76.60
AM	1	0.00	100.30	20400.00	77.50
	2	57.40	100.30	20400.00	77.50
LW	1	0.00	157.00	20000.00	76.80
	2	17.50	157.00	20000.00	76.80

- Pile damping is 5.00 % for all piles

Table 9. Parametric Variations, JI Pile

		Resistance		Case damping		Smith damping		Toe soil damper
	Rult	Shaft	Toe	Shaft	Toe	Shaft	Toe	
	KN	KN	KN	-	-	s/m	s/m	KN/m/s
Min.	900	582.3	288.8	0.000	0.500	0.000	0.603	0.0
Avg.	1200	790.2	409.8	0.071	0.791	0.037	0.754	240.1
Max.	1500	874.9	632.3	0.149	1.200	0.098	1.091	817.1
Std.	187	90.6	113.7	0.045	0.215	0.026	0.135	220.2
	1500	867.7	632.3	0.100	1.173	0.044	0.714	217.9
	1450	862.9	587.1	0.062	1.200	0.028	0.787	223.3
	1400	857.3	542.7	0.100	0.930	0.045	0.660	228.8
	1350	874.9	475.1	0.100	0.900	0.044	0.729	217.9
	1300	866.7	433.3	0.000	0.770	0.000	0.684	272.4
	1250	833.3	416.7	0.000	0.750	0.000	0.693	326.8
	1200	800.0	400.0	0.007	0.680	0.004	0.655	408.6
	1150	850.0	300.0	0.054	0.700	0.025	0.898	408.6
	1100	789.6	310.4	0.100	0.500	0.049	0.620	817.1
	1050	730.8	319.2	0.056	0.500	0.030	0.603	0.0
	1000	696.0	304.0	0.100	0.580	0.055	0.735	0.0
	950	661.2	288.8	0.100	0.700	0.058	0.933	0.0
	900	582.3	317.7	0.149	0.900	0.098	1.091	0.0

Table 9. Parametric Variations, JI Pile (Continued)

	Rult	Quakes Shaft	Quakes Toe	Unloading quakes Shaft	Unloading quakes Toe	Unloading shaft res. Rs-/Rs+	Soil plug	Toe gap
	KN	mm	mm	%	%	%	KN	mm
Min.	900	2.0	3.0	3.0	25.0	0	0.0	1.0
Avg.	1200	3.6	4.7	29.7	76.9	70	0.0	1.9
Max.	1500	5.5	5.0	60.0	100.0	100	0.0	4.0
Std.	187	1.2	00.6	20.5	30.2	45	0.0	0.7
	1500	5.5	5.0	60	100	10	0.0	1.5
	1450	5.0	5.0	60	100	0	0.0	1.5
	1400	5.0	5.0	45	100	100	0.0	1.5
	1350	5.0	5.0	30	100	100	0.0	1.5
	1300	4.0	5.0	30	100	100	0.0	1.5
	1250	3.7	5.0	30	100	100	0.0	1.5
	1200	3.7	5.0	30	100	100	0.0	1.0
	1150	3.7	5.0	60	25	0	0.0	1.7
	1100	3.0	5.0	15	25	0	0.0	1.7
	1050	2.0	4.0	3	100	100	0.0	2.5
	1000	2.0	4.0	3	50	100	0.0	2.5
	950	2.0	5.0	5	50	100	0.0	2.0
	900	2.0	3.0	15	50	100	0.0	4.0

Table 10. Parametric Variations, JA Pile

	Rult	Resistance Shaft	Resistance Toe	Case damping Shaft	Case damping Toe	Smith damping Shaft	Smith damping Toe	Toe soil damper
	KN	KN	KN	-	-	s/m	s/m	KN/m/s
Min.	450	321.0	129.0	0.623	0.240	0.547	0.491	0.0
Avg.	550	403.6	146.4	0.696	0.473	0.704	1.336	0.0
Max.	650	481.2	195.3	0.772	0.761	0.909	2.354	0.0
Std.	65	53.0	18.1	0.046	0.152	0.124	0.515	0.0
	650	454.7	195.3	0.623	0.240	0.547	0.491	0.0
	625	481.2	143.8	0.664	0.300	0.551	0.833	0.0
	600	450.4	149.6	0.681	0.408	0.604	1.089	0.0
	575	431.7	143.3	0.685	0.415	0.633	1.155	0.0
	550	412.9	137.1	0.704	0.421	0.681	1.227	0.0
	525	384.6	140.4	0.734	0.550	0.761	1.563	0.0
	500	356.7	143.3	0.753	0.558	0.843	1.553	0.0
	475	338.9	136.1	0.772	0.600	0.909	1.759	0.0
	450	321.0	129.0	0.650	0.761	0.808	2.354	0.0

Table 10. Parametric Variations, JA Pile (Continued)

	Rult	Quakes Shaft	Quakes Toe	Unloading quakes Shaft	Unloading quakes Toe	Unloading shaft res. Rs-/Rs+	Soil plug	Toe gap
	KN	mm	mm	%	%	%	KN	mm
Min.	450	0.5	1.5	100	5	0	0.0	0.0
Avg.	550	2.1	4.3	100	16	9	0.0	0.7
Max.	650	2.5	5.0	100	100	60	0.0	3.5
Std.	65	0.7	1.3	0	30	19	0	1.1
	650	1.3	0.25	100	5	0	0.0	1.0
	625	2.5	0.50	100	6	20	0.0	0.0
	600	2.5	0.50	100	6	60	0.0	0.0
	575	2.5	0.50	100	6	0	0.0	0.0
	550	2.5	0.50	100	6	0	0.0	0.0
	525	2.5	0.50	100	5	0	0.0	1.0
	500	2.5	0.50	100	5	0	0.0	1.0
	475	2.5	0.50	100	5	0	0.0	0.0
	450	0.5	1.5	100	100	0	0.0	3.5

Table 11. Parametric Variations, AM Pile

	Resistance			Case damping		Smith damping		Toe soil damper
	Rult	Shaft	Toe	Shaft	Toe	Shaft	Toe	
	KN	KN	KN	-	-	s/m	s/m	KN/m/s
Min.	1275	881.5	390.7	0.137	0.650	0.052	0.453	0.0
Avg.	1500	1004.9	495.1	0.380	0.690	0.158	0.577	0.3
Max.	1725	1155.2	666.7	0.650	0.750	0.297	0.745	0.3
Std.	150	81.5	88.8	0.169	0.035	0.080	0.095	0.7
	1725	1058.3	666.7	0.137	0.750	0.052	0.453	2.0
	1650	1155.2	494.8	0.170	0.675	0.059	0.550	0.0
	1575	1040.8	534.2	0.330	0.700	0.128	0.528	0.0
	1500	968.8	531.2	0.418	0.651	0.174	0.494	0.0
	1425	970.4	454.6	0.455	0.673	0.189	0.597	0.0
	1350	959.3	390.7	0.500	0.650	0.210	0.670	0.0
	1275	881.5	393.5	0.650	0.728	0.297	0.745	0.0

Table 11. Parametric Variations, AM Pile (Continued)

	Rult	Quakes Shaft	Quakes Toe	Unloading quakes Shaft	Unloading quakes Toe	Unloading shaft res. Rs-/Rs+	Soil plug	Toe gap
	KN	mm	mm	%	%	%	KN	mm
Min.	1275	2.5	5.1	90	30	4	0.0	0.0
Avg.	1500	2.5	5.9	96	33	26	0.0	1.0
Max.	1725	2.5	6.5	100	40	31	0.0	5.0
Std.	150	0.00	0.7	5	5	10	0.0	1.7
	1725	2.5	5.1	90	40	4	0.0	5.0
	1650	2.5	5.1	90	40	31	0.0	1.0
	1575	2.5	5.1	90	30	31	0.0	1.0
	1500	2.5	6.5	100	30	31	0.0	0.0
	1425	2.5	6.5	100	30	31	0.0	0.0
	1350	2.5	6.5	100	30	31	0.0	0.0
	1275	2.5	6.5	100	30	20	0.0	0.0

Table 12. Parametric Variations, LW Pile

		Resistance		Case damping		Smith damping		Toe soil damper
	Rult	Shaft	Toe	Shaft	Toe	Shaft	Toe	
	KN	KN	KN	-	-	s/m	s/m	KN/m/s
Min.	300	259.8	40.2	0.530	0.499	0.327	2.236	0.00
Avg.	712	619.9	92.2	0.705	0.661	0.882	5.560	0.20
Max.	1125	1005.5	138.7	0.913	0.950	2.183	14.070	1.86
Std.	254	225.2	30.2	0.117	0.153	0.522	3.576	0.57
	1125	1005.5	119.5	0.530	0.550	0.327	2.860	1.86
	1080	965.3	114.7	0.630	0.500	0.405	2.708	1.86
	1035	896.3	138.7	0.533	0.499	0.369	2.236	0.00
	990	857.4	132.6	0.555	0.503	0.402	2.355	0.00
	945	818.4	126.6	0.578	0.506	0.438	2.485	0.00
	900	779.4	120.6	0.600	0.510	0.478	2.628	0.00
	855	740.5	114.5	0.625	0.514	0.524	2.788	0.00
	810	701.5	108.5	0.650	0.518	0.575	2.966	0.00
	765	662.5	102.5	0.675	0.620	0.633	3.758	0.00
	720	623.5	96.5	0.701	0.624	0.698	4.022	0.00
	675	584.6	90.4	0.727	0.630	0.773	4.328	0.00
	610	528.3	81.7	0.744	0.703	0.875	5.345	0.00
	565	489.3	75.7	0.771	0.770	0.979	6.321	0.00
	520	450.4	69.6	0.799	0.775	1.102	6.913	0.00
	475	411.4	63.6	0.827	0.780	1.249	7.617	0.00
	430	372.4	57.6	0.827	0.850	1.380	9.169	0.00
	385	333.4	51.6	0.856	0.855	1.596	10.305	0.00
	345	298.8	46.2	0.856	0.950	1.781	12.772	0.00
	300	259.8	40.2	0.913	0.910	2.183	14.070	0.00

Table 12. Parametric Variations, LW Pile (Continued)

	Rult	Quakes Shaft	Toe	Unloading quakes Shaft	Toe	Unloading shaft res. Rs-/Rs+	Soil plug	Toe gap
	KN	mm	mm	%	%	%	KN	mm
Min.	300	2.5	5.0	0	40	0	0.55	0.0
Avg.	712	2.6	5.0	28	75	0	0.55	0.0
Max.	1125	3.0	5.0	100	100	0	0.55	0.0
Std.	254	0.2	0.0	36	30	0	0.00	0.0
	1125	3.0	5.0	1	40	0	0.55	0.0
	1080	3.0	5.0	1	40	0	0.55	0.0
	1035	2.5	5.0	1	40	0	0.55	0.0
	990	2.5	5.0	0	40	0	0.55	0.0
	945	2.5	5.0	0	40	0	0.55	0.0
	900	2.5	5.0	1	40	0	0.55	0.0
	855	2.5	5.0	1	40	0	0.55	0.0
	810	2.5	5.0	1	40	0	0.55	0.0
	765	2.5	5.0	10	100	0	0.55	0.0
	720	2.5	5.0	10	100	0	0.55	0.0
	675	2.5	5.0	10	100	0	0.55	0.0
	610	2.5	5.0	20	100	0	0.55	0.0
	565	2.5	5.0	30	100	0	0.55	0.0
	520	2.5	5.0	30	100	0	0.55	0.0
	475	2.5	5.0	60	100	0	0.55	0.0
	430	2.5	5.0	60	100	0	0.55	0.0
	385	2.5	5.0	100	100	0	0.55	0.0
	345	2.5	5.0	100	100	0	0.55	0.0
	300	2.5	5.0	100	100	0	0.55	0.0

Table 13. Resistance Distribution in JI Pile

Rult	Soil element number									
(KN)	3	4	5	6	7	8	9	10	11	12
1500	1.1	1.1	1.1	1.1	58.7	49.5	0.1	0.1	25.1	25.1
1450	1.1	1.1	1.1	1.1	53.6	38.1	1.6	1.6	24.3	24.3
1400	1.0	1.0	1.0	1.0	51.8	36.8	23.5	23.5	1.6	1.6
1350	1.0	1.0	1.0	1.0	49.9	35.5	22.6	22.6	1.5	1.5
1300	0.6	0.6	0.6	0.6	49.6	34.2	21.8	21.8	1.5	1.5
1250	0.6	0.6	0.6	0.6	47.7	32.9	20.9	20.9	1.4	1.4
1200	0.6	0.6	0.6	0.6	45.8	31.6	20.1	20.1	1.3	1.3
1150	0.6	0.6	0.6	0.6	43.9	30.2	19.2	19.2	1.3	1.3
1100	0.5	0.5	0.5	0.5	38.8	26.7	17.0	17.0	1.1	1.1
1050	0.5	0.5	0.5	0.5	35.9	24.7	15.7	15.7	1.0	1.0
1000	0.4	0.4	0.4	0.4	34.2	23.6	15.0	15.0	1.0	1.0
950	0.4	0.4	0.4	0.4	32.5	22.4	14.2	14.2	0.9	0.9
900	0.4	0.4	0.4	0.4	31.2	21.5	13.7	13.7	0.9	0.9
Min.	0.4	0.4	0.4	0.4	31.2	21.5	0.1	0.1	0.9	0.9
Avg.	0.7	0.7	0.7	0.7	44.1	31.4	15.8	15.8	4.8	4.8
Max.	1.1	1.1	1.1	1.1	58.7	49.5	23.5	23.5	25.1	25.1

Table 13. Resistance Distribution in JI Pile (Continued)

Rult	Soil element number								
(KN)	13	14	15	16	17	18	19	20	21	Toe

Rult (KN)	13	14	15	16	17	18	19	20	21	Toe
1500	13.4	75.6	73.5	137.7	227.9	171.1	3.7	0.8	1.0	632.3
1450	12.9	73.1	71.0	133.2	230.0	189.5	3.6	0.7	1.0	587.1
1400	12.5	70.5	68.6	128.6	246.2	183.0	3.5	0.7	0.9	542.7
1350	12.0	68.0	66.1	124.0	285.7	176.5	3.4	0.7	0.9	475.1
1300	11.6	65.5	63.7	119.3	274.6	194.3	3.3	0.7	0.9	433.3
1250	11.1	62.9	61.2	114.8	264.4	186.8	3.1	0.6	0.8	416.7
1200	10.7	60.4	58.8	110.2	253.5	179.4	3.0	0.6	0.8	400.0
1150	10.2	57.9	56.3	105.6	243.0	171.9	60.4	11.1	16.1	300.0
1100	9.0	51.2	49.8	93.3	214.9	151.9	53.4	29.0	33.4	310.4
1050	8.4	47.4	46.1	86.4	175.8	209.8	26.3	26.8	7.8	319.2
1000	8.0	45.1	43.9	82.2	167.4	200.0	25.0	25.6	7.4	304.0
950	7.6	42.9	41.7	78.1	199.1	190.0	3.8	4.3	7.0	288.8
900	7.3	41.2	40.1	75.1	191.3	142.7	0.8	0.3	0.0	317.7
Min.	7.3	41.2	40.1	75.1	167.4	142.7	0.8	0.3	0.0	288.8
Avg.	10.4	58.6	57.0	106.8	228.8	180.5	14.9	7.8	6.0	409.8
Max.	13.4	75.6	73.5	137.7	285.7	209.8	60.4	29.0	33.4	632.3

Table 14. Resistance Distribution in JA Pile

Rult (KN)	Soil element number 1	2	3	4	5	6	7	8	9	10	11
650	19.4	20.3	20.9	16.8	17.8	28.8	49.0	75.2	91.2	57.6	57.6
625	17.8	21.2	25.8	21.2	18.7	32.9	55.7	83.6	194.9	8.8	0.6
600	16.6	19.9	24.2	19.9	17.5	30.8	52.2	78.2	182.4	8.2	0.5
575	16.0	19.0	23.2	19.0	16.8	29.5	50.0	75.0	174.8	7.9	0.5
550	15.3	18.2	22.2	18.2	16.0	28.2	47.8	71.7	167.3	7.5	0.5
525	14.2	17.0	20.7	17.0	14.9	26.3	44.5	66.8	155.7	7.0	0.5
500	13.2	15.7	19.2	15.7	13.9	24.4	41.3	61.9	144.5	6.5	0.4
475	12.5	14.9	18.2	15.0	13.2	23.2	39.3	58.8	137.2	6.2	0.4
450	11.9	14.2	17.2	14.2	12.5	21.9	37.2	55.7	129.9	5.9	0.4
Min.	11.9	14.2	17.2	14.2	12.5	21.9	37.2	55.7	91.2	5.9	0.4
Avg.	15.2	17.8	21.3	17.4	15.7	27.3	46.3	69.7	153.1	12.8	6.8
Max.	19.4	21.2	25.8	21.2	18.7	32.9	55.7	83.6	194.9	57.6	57.6

Table 15. Resistance Distribution in AM Pile

Rult (KN)	Soil element number 1	2	3	4	5	6	7	8	9	10
1725	12.9	12.9	12.9	56.1	32.9	26.8	52.7	65.0	65.5	67.9
1650	6.9	6.1	37.2	57.5	35.9	29.3	53.2	63.9	70.7	69.3
1575	1.6	1.6	38.2	51.1	27.2	24.8	50.8	25.0	40.0	68.6
1500	1.4	1.4	33.8	45.3	24.1	21.9	45.0	52.5	52.8	60.7
1425	1.3	1.3	32.1	43.0	22.9	20.8	42.7	49.9	50.2	57.6
1350	1.2	1.2	30.4	40.7	21.6	19.7	40.5	47.2	47.6	54.6
1275	1.1	1.1	27.7	37.0	19.7	17.9	36.8	43.0	43.3	49.7
Min	1.1	1.1	12.9	37.0	19.7	17.9	36.8	25.0	40.0	49.7
Avg	3.8	3.7	30.3	47.2	26.3	23.0	46.0	49.5	52.9	61.2
Max	12.9	12.9	38.2	57.5	35.9	29.3	53.2	65.0	70.7	69.3

Table 15. Resistance Distribution in AM Pile (Continued)

Rult	Soil element number									
(KN)	11	12	13	14	15	16	17	18	19	20
1725	78.4	97.9	85.1	59.2	64.8	78.2	81.9	66.6	1.2	1.2
1650	67.8	88.0	80.9	57.9	64.4	79.2	75.5	52.7	21.7	2.4
1575	80.6	93.4	80.0	59.4	65.9	77.8	83.4	105.6	0.8	5.9
1500	71.3	82.7	70.8	52.6	58.3	68.9	73.8	93.4	0.7	5.2
1425	67.7	78.6	67.2	50.0	55.4	65.4	70.1	138.8	0.7	5.0
1350	64.2	74.4	63.7	47.3	52.5	62.0	86.4	151.5	0.6	4.7
1275	58.4	67.7	57.9	43.0	47.7	56.4	105.9	119.6	0.6	4.3
Min	58.4	67.7	57.9	43.0	47.7	56.4	70.1	52.7	0.6	1.2
Avg	69.8	83.2	72.2	52.8	58.4	69.7	82.4	104.0	3.8	4.1
Max	80.6	97.9	85.1	59.4	65.9	79.2	105.9	151.5	21.7	5.9

Table 15. Resistance Distribution in AM Pile (Continued)

Rult	Soil element number								
(KN)	21	22	23	24	25	26	27	28	Toe
1725	1.2	6.7	22.4	1.6	1.5	1.6	1.6	1.5	666.8
1650	2.4	2.4	32.1	34.5	20.9	9.7	9.8	22.9	494.8
1575	9.2	10.1	12.5	12.2	7.1	2.7	2.7	2.7	534.1
1500	8.1	8.9	11.1	10.8	6.3	2.4	2.4	2.4	531.0
1425	7.5	8.5	10.5	10.3	6.0	2.3	2.3	2.3	454.6
1350	7.3	8.0	10.0	9.7	5.7	2.1	2.1	2.1	391.0
1275	6.6	7.3	9.1	8.9	5.2	2.0	2.0	2.0	393.1
Min	1.2	2.4	9.1	1.6	1.5	1.6	1.6	1.5	391.0
Avg	6.0	7.4	15.4	12.6	7.5	3.3	3.3	5.1	495.1
Max	9.2	10.1	32.1	34.5	20.9	9.7	9.8	22.9	666.8

Table 16. Resistance Distribution in LW Pile

Rult	Soil element number											
(KN)	2	3	7	8	9	10	11	12	13	14	15	16	17
1125	12	22	56	58	38	157	83	41	79	322	46	46	46
1080	12	21	54	55	36	150	80	40	76	309	44	44	44
1035	11	21	51	53	35	144	77	38	92	277	33	33	33
990	11	20	49	51	33	138	73	36	88	265	31	31	31
945	10	19	47	49	32	132	70	35	84	253	30	30	30
900	10	18	44	46	30	125	67	33	80	241	29	29	29
855	9	17	42	44	29	119	63	31	76	229	27	27	27
810	9	16	40	42	27	113	60	30	72	217	26	26	26
765	8	15	38	39	26	106	57	28	68	205	24	24	24
720	8	14	36	37	24	100	53	26	64	193	23	23	23
675	7	13	33	35	23	94	50	25	60	181	21	21	21
610	7	12	30	31	20	85	45	22	54	218	1	1	1
565	6	11	28	29	19	79	42	21	50	202	1	1	1
520	6	10	26	27	17	72	39	19	46	186	1	1	1
475	5	9	23	24	16	66	35	17	42	170	1	1	1
430	5	9	21	22	14	60	32	16	38	154	1	1	1
385	4	8	19	20	13	54	29	14	34	138	1	1	1
345	4	7	17	18	12	48	26	13	31	124	1	1	1
300	3	6	15	15	10	42	22	11	27	107	1	1	1
Min	3	6	15	15	10	42	22	11	27	107	1	1	1
Avg	8	14	35	37	24	99	53	26	61	210	18	18	18
Max	12	22	56	58	38	157	83	41	92	322	46	46	46

Table 17. Load Transfer in JI Pile

Rult				Depth (m)						
(KN)	1.0	6.1	8.1	10.2	12.2	14.2	16.3	18.3	20.3	22.4
1500	1500	1499	1498	1497	1496	1437	1387	1387	1387	1362
1450	1450	1449	1448	1447	1446	1392	1354	1352	1351	1326
1400	1400	1399	1398	1397	1396	1344	1307	1284	1260	1259
1350	1350	1349	1348	1347	1346	1296	1261	1238	1215	1214
1300	1300	1299	1299	1298	1298	1248	1214	1192	1170	1169
1250	1250	1249	1249	1248	1248	1200	1167	1146	1125	1124
1200	1200	1199	1199	1198	1198	1152	1120	1100	1080	1079
1150	1150	1149	1149	1148	1148	1104	1074	1054	1035	1034
1100	1100	1100	1099	1099	1098	1059	1033	1016	999	997
1050	1050	1050	1049	1049	1048	1012	987	972	956	955
1000	1000	1000	999	999	998	964	941	926	911	910
950	950	950	949	949	948	916	894	879	865	864
900	900	900	899	899	898	867	846	832	818	817
Min	900	900	899	899	898	867	846	832	818	817
Avg	1200	1199	1199	1198	1197	1153	1122	1106	1090	1085
Max	1500	1499	1498	1497	1496	1437	1387	1387	1387	1362

Table 17. Load Transfer in JI Pile (Continued)

Rult			Depth (m)							
(KN)	24.4	26.4	28.5	30.5	32.5	34.6	36.6	38.6	40.7	42.7
1500	1337	1324	1248	1175	1037	809	638	634	633	632
1450	1302	1289	1216	1145	1012	782	592	589	588	587
1400	1257	1245	1174	1106	977	731	548	544	544	543
1350	1212	1200	1132	1066	942	657	480	477	476	475
1300	1167	1156	1090	1026	907	633	438	435	434	433
1250	1122	1111	1048	987	872	608	421	418	417	417
1200	1077	1067	1006	948	837	584	404	401	401	400
1150	1033	1022	964	908	803	560	388	327	316	300
1100	996	987	936	886	793	578	426	373	344	310
1050	954	946	898	852	766	590	380	354	327	319
1000	909	901	856	812	729	562	362	337	311	304
950	863	856	813	771	693	494	304	300	296	289
900	817	809	768	728	653	461	319	318	318	318
Min	817	809	768	728	653	461	304	300	296	289
Avg	1081	1070	1012	955	848	619	439	424	416	410
Max	1337	1324	1248	1175	1037	809	638	634	633	632

Table 18. Load Transfer in JA Pile

Rult	Depth (m)										
(KN)	1.0	9.0	11.0	13.0	15.0	17.0	19.0	21.0	23.0	25.0	27.0
650	650	631	610	589	573	555	526	477	402	311	253
625	625	607	586	560	539	520	487	432	348	153	144
600	600	583	564	539	519	502	471	419	341	158	150
575	575	559	540	517	498	481	451	401	326	152	144
550	550	535	517	494	476	460	432	384	312	145	138
525	525	511	494	473	456	441	415	370	304	148	141
500	500	487	471	452	436	422	398	357	295	150	144
475	475	463	448	429	414	401	378	339	280	143	137
450	450	438	424	407	393	380	358	321	265	135	129
Min	450	438	424	407	393	380	358	321	265	135	129
Avg	550	535	517	496	478	463	435	389	319	166	153
Max	650	631	610	589	573	555	526	477	402	311	253

Table 19. Load Transfer in AM Pile

Rult	Depth (m)									
(KN)	1.0	3.0	5.0	7.0	9.1	11.1	13.1	15.1	17.1	19.1
1725	1725	1712	1699	1686	1630	1597	1571	1518	1453	1387
1650	1650	1643	1637	1600	1542	1506	1477	1424	1360	1289
1575	1575	1573	1572	1534	1483	1455	1431	1380	1355	1315
1500	1500	1499	1497	1463	1418	1394	1372	1327	1275	1222
1425	1425	1424	1422	1390	1347	1324	1304	1261	1211	1161
1350	1350	1349	1348	1317	1276	1255	1235	1195	1147	1100
1275	1275	1274	1273	1245	1208	1188	1171	1134	1091	1047
Min	1275	1274	1273	1245	1208	1188	1171	1134	1091	1047
Avg	1500	1496	1493	1462	1415	1389	1366	1320	1270	1217
Max	1725	1712	1699	1686	1630	1597	1571	1518	1453	1387

Table 19. Load Transfer in AM Pile (Continued)

Rult	Depth (m)									
(KN)	21.1	23.2	25.2	27.2	29.2	31.2	33.2	35.2	37.3	39.3
1725	1319	1241	1143	1058	999	934	856	774	707	706
1650	1220	1152	1064	983	925	861	782	706	654	632
1575	1246	1166	1072	992	933	867	789	706	600	599
1500	1161	1090	1007	936	884	825	757	683	589	589
1425	1103	1036	957	890	840	784	719	649	510	509
1350	1045	981	907	843	796	743	681	595	443	443
1275	998	939	872	814	771	723	667	561	441	441
Min	998	939	872	814	771	723	667	561	441	441
Avg	1156	1086	1003	931	878	820	750	668	564	560
Max	1319	1241	1143	1058	999	934	856	774	707	706

Table 19. Load Transfer in AM Pile (Continued)

Rult (KN)	Depth (m) 41.3	43.3	45.3	47.3	49.3	51.4	53.4	55.4	57.4
1725	705	704	697	675	673	671	670	668	667
1650	629	627	625	593	558	537	527	518	495
1575	593	584	574	562	549	542	540	537	534
1500	583	575	566	555	545	538	536	533	531
1425	504	497	488	478	467	461	459	457	455
1350	438	431	423	413	403	397	395	393	391
1275	436	430	422	413	404	399	397	395	393
Min	436	430	422	413	403	397	395	393	391
Avg	556	550	542	527	514	507	503	500	495
Max	705	704	697	675	673	671	670	668	667

Table 20. Load Transfer in LW Pile

Rult						Depth (m)							
(KN)	1.0	2.1	3.1	7.2	8.2	9.3	10.3	11.3	12.4	13.4	14.4	15.4	16.5
1125	1125	1113	1090	1035	977	940	783	700	659	579	257	211	165
1080	1080	1068	1047	993	938	902	751	672	632	556	247	203	159
1035	1035	1024	1003	952	899	864	720	644	606	514	237	204	171
990	990	979	960	911	860	827	689	616	580	492	227	195	164
945	945	935	916	869	821	789	658	588	553	469	216	186	156
900	900	890	872	828	782	752	626	560	527	447	206	178	149
855	855	846	829	786	743	714	595	532	501	425	196	169	142
810	810	801	785	745	703	676	564	504	474	402	185	160	134
765	765	757	741	704	664	639	533	476	448	380	175	151	127
720	720	712	698	662	625	601	501	448	422	358	165	142	119
675	675	668	654	621	586	564	470	420	395	335	154	133	112
610	610	603	591	561	530	509	425	379	357	303	85	84	83
565	565	559	548	520	491	472	393	351	331	281	78	77	77
520	520	514	504	478	452	434	362	324	305	258	72	71	70
475	475	470	460	437	413	397	331	296	278	236	66	65	64
430	430	425	417	396	374	359	299	268	252	214	60	59	58
385	385	381	373	354	334	322	268	239	225	191	53	53	52
345	345	341	334	317	300	288	240	215	202	171	48	47	47
300	300	297	291	276	261	251	209	187	176	149	42	41	41
Min	300	297	291	276	261	251	209	187	176	149	42	41	41
Avg	712	704	690	655	618	595	496	443	417	356	146	128	110
Max	1125	1113	1090	1035	977	940	783	700	659	579	257	211	171

Table 21. Maximum Compression Forces in JI Pile (KN)

Rult	Depth (m)											
(KN)	1.0	4.1	8.1	12.2	17.3	21.4	25.4	29.5	33.5	38.6	41.7	42.
1500	964	975	986	1017	960	989	973	970	804	435	381	41
1450	964	974	985	1012	960	991	988	991	841	425	380	41
1400	964	974	986	1018	973	957	990	995	846	411	374	41
1350	964	974	985	1016	972	959	994	1005	868	403	347	38
1300	964	974	986	1016	976	976	1009	1040	911	384	393	42
1250	964	975	987	1017	965	967	1013	1038	920	406	423	45
1200	964	974	986	1015	961	956	1011	1036	921	423	463	49
1150	964	975	988	1015	972	967	1014	1043	941	464	405	42
1100	964	977	992	1016	970	974	1026	1057	956	534	451	49
1050	964	985	1013	1024	991	995	1039	1086	991	533	541	58
1000	964	983	1009	1024	981	976	1033	1081	997	557	557	59
950	964	980	1000	1025	978	966	1043	1093	1013	563	577	61
900	964	980	996	1020	981	966	1041	1089	1003	615	639	68

Table 22. **Maximum Compression Forces in JA Pile (KN)**

Rult (KN)	Depth (m) 1.0	2.0	5.0	8.0	11.0	14.0	17.0	19.0	22.0	25.0	28.0	29.
650	1200	1241	1237	1248	1225	1156	1155	1172	1120	1091	525	467
625	1200	1238	1232	1239	1224	1150	1145	1165	1115	1126	522	364
600	1200	1238	1232	1239	1225	1151	1146	1165	1118	1130	574	449
575	1200	1238	1232	1238	1224	1151	1146	1166	1119	1132	578	454
550	1200	1237	1232	1238	1224	1151	1146	1165	1119	1131	579	456
525	1200	1237	1232	1238	1225	1151	1145	1164	1118	1130	616	523
500	1200	1237	1232	1238	1225	1152	1145	1164	1118	1130	618	528
475	1200	1247	1231	1238	1225	1152	1146	1165	1121	1134	644	569
450	1200	1245	1243	1253	1240	1173	1168	1187	1152	1160	697	631

Table 23. **Maximum Compression Forces in AM Pile (KN)**

Rult (KN)	Depth (m) 1.0	5.0	11.1	16.1	22.2	28.2	34.2	39.3	45.3	51.4	56.4	57.
1725	1969	2099	2040	1969	1833	1623	1496	1349	1344	1299	1123	120
1650	1969	2111	2034	1954	1806	1616	1485	1365	1336	1279	1113	118
1575	1969	2105	2019	1918	1840	1597	1449	1242	1229	1182	1039	111
1500	1969	2104	2020	1944	1796	1560	1418	1219	1209	1167	1027	107
1425	1969	2101	2019	1944	1799	1567	1436	1193	1183	1142	1007	104
1350	1969	2098	2017	1943	1799	1570	1457	1168	1159	1119	961	98
1275	1969	2097	2010	1932	1779	1540	1436	1115	1105	1067	962	98

Table 24. Maximum Compression Forces in LW Pile (KN)

Rult (KN)	Depth (m) 1.0	2.1	4.1	5.1	7.2	9.3	11.3	12.4	14.4	16.5	17.5
1125	1915	1971	1921	1933	2000	1937	1770	1724	1732	1212	972
1080	1915	1974	1920	1934	2008	1940	1758	1710	1712	1152	901
1035	1915	1972	1920	1933	2004	1936	1764	1718	1691	1193	984
990	1915	1973	1920	1933	2005	1938	1764	1718	1690	1190	982
945	1915	1973	1920	1934	2006	1939	1763	1718	1688	1187	981
900	1915	1974	1920	1934	2007	1940	1763	1717	1687	1184	980
855	1915	1975	1920	1934	2009	1950	1762	1717	1685	1179	978
810	1915	1975	1920	1935	2010	1943	1761	1716	1683	1175	976
765	1915	1976	1920	1936	2012	1945	1762	1716	1685	1230	1061
720	1915	1977	1919	1936	2013	1946	1761	1715	1683	1228	1061
675	1915	1977	1919	1936	2014	1948	1759	1714	1681	1226	1061
610	1915	1977	1920	1936	2015	1950	1764	1732	1717	1204	1089
565	1915	1978	1920	1937	2017	1952	1763	1731	1717	1235	1135
520	1915	1979	1919	1937	2018	1953	1762	1730	1715	1231	1132
475	1915	1980	1919	1938	2020	1954	1760	1729	1712	1226	1129
430	1915	1979	1920	1938	2019	1955	1763	1733	1718	1268	1185
385	1915	1980	1920	1938	2021	1956	1762	1731	1716	1263	1181
345	1915	1979	1920	1938	2020	1957	1765	1736	1722	1312	2147
300	1915	1981	1919	1939	2024	1959	1759	1728	1712	1271	1201

Table 25. Maximum Tension Forces in JI Pile (KN)

Rult	Depth (m)										
(KN)	1.0	4.1	8.1	12.2	17.3	21.4	25.4	29.5	33.5	38.6	41.7	42.
1500	28.3	17.9	16.8	15.5	15.0	14.5	13.8	12.9	11.8	80.5	64.2	59.
1450	28.3	17.9	16.8	15.5	15.1	14.6	13.9	13.1	12.1	75.4	60.0	55.
1400	28.3	17.9	16.8	15.5	15.0	14.4	13.8	12.9	11.8	70.0	49.5	45.
1350	28.3	17.9	16.8	15.5	14.9	14.4	13.7	12.8	11.7	57.7	40.3	32.
1300	28.3	17.9	16.8	15.5	14.9	14.4	13.8	12.9	11.9	61.6	41.6	31.
1250	28.3	17.9	16.8	15.5	14.9	14.4	13.8	12.9	11.9	57.6	39.5	32.
1200	28.3	17.9	16.8	15.5	14.9	14.4	13.8	12.9	11.9	56.5	38.0	33.
1150	28.3	17.9	16.8	15.5	15.1	14.6	14.0	13.1	12.1	11.4	50.5	46.
1100	28.3	17.9	16.8	15.5	15.1	14.6	13.9	13.1	12.0	11.2	34.4	27.
1050	28.3	17.9	16.8	15.5	13.0	11.4	10.5	8.9	7.3	9.1	12.6	4.
1000	28.3	17.9	16.8	15.5	13.0	11.4	10.7	9.0	7.3	11.1	16.7	6.
950	28.3	17.9	16.8	15.5	13.3	12.4	12.1	10.8	8.8	6.0	6.6	3.
900	28.3	17.9	16.8	15.5	14.5	13.9	13.3	12.3	10.9	8.7	9.6	7.

Table 26. Maximum Tension Forces in JA Pile (KN)

Rult (KN)	Depth (m) 1.0	2.0	5.0	8.0	11.0	14.0	17.0	19.0	22.0	25.0	28.0	29.
650	14.6	84.3	101.0	105.3	114.7	103.0	107.2	109.0	103.2	92.7	84.5	51.2
625	14.6	89.4	79.8	86.7	92.6	79.5	79.8	86.6	93.7	86.5	139.2	82.4
600	14.6	54.0	50.0	67.8	65.5	64.0	68.5	67.2	74.0	60.9	108.8	80.7
575	14.6	65.5	61.9	79.9	74.7	73.7	78.0	77.1	79.4	67.3	104.9	79.2
550	14.6	73.4	70.9	89.1	82.3	81.7	86.2	86.0	83.6	73.5	96.5	78.7
525	14.6	64.8	67.5	88.4	79.5	80.4	89.4	90.8	85.7	81.4	71.8	75.6
500	14.6	78.1	82.7	103.5	94.1	92.8	101.1	101.9	95.9	90.1	70.4	63.4
475	14.6	80.5	89.8	110.5	102.5	100.4	108.0	108.5	102.7	97.8	68.0	64.4
450	14.6	103.7	117.0	133.5	130.9	127.3	133.6	134.2	130.0	119.7	93.5	91.0

Table 27. Maximum Tension Forces in AM Pile (KN)

Rult	Depth (m)										
(KN)	1.0	5.0	11.1	16.1	22.2	28.2	34.2	39.3	45.3	51.4	56.4	57.
1725	2.9	0.0	0.0	0.0	0.0	0.0	0.0	32.3	49.8	75.9	91.1	89.
1650	2.9	0.0	0.0	0.0	0.0	0.0	0.0	0.0	0.0	0.0	0.0	0.
1575	2.9	0.0	0.0	0.0	0.0	0.0	0.0	0.0	0.0	0.0	0.0	0.
1500	2.9	0.0	0.0	0.0	0.0	0.0	0.0	0.0	0.0	0.0	0.0	0.
1425	2.9	0.0	0.0	0.0	0.0	0.0	0.0	0.0	0.0	0.0	0.0	0.
1350	2.9	0.0	0.0	0.0	0.0	0.0	0.0	0.0	0.0	0.0	0.0	0.
1275	2.9	0.0	0.0	0.0	0.0	0.0	0.0	0.0	0.0	0.0	0.0	0.

Table 28. Maximum Tension Forces in LW Pile (KN)

Rult	Depth (m)										
(KN)	1.0	2.1	4.1	5.1	7.2	9.3	11.3	12.4	14.4	16.5	17.5
1125	81.5	164.2	180.2	177.6	183.7	177.9	152.9	143.8	124.8	86.6	80.9
1080	81.5	177.3	183.5	182.5	188.7	181.3	151.4	142.5	122.0	78.3	72.6
1035	81.5	136.6	141.5	140.4	145.7	139.5	113.3	104.9	84.4	56.0	53.9
990	81.5	143.5	146.5	145.2	150.9	144.8	117.8	109.6	89.9	61.2	58.9
945	81.5	155.4	156.2	154.2	160.3	154.1	127.7	118.8	97.5	68.9	66.7
900	81.5	164.4	162.8	160.9	167.4	161.4	134.4	125.9	104.6	74.0	72.1
855	81.5	177.3	186.5	182.0	191.8	173.5	152.2	148.0	126.8	82.9	78.8
810	81.5	193.9	202.0	197.4	206.9	187.2	164.5	160.0	138.5	91.9	84.2
765	81.5	151.5	156.4	153.6	156.5	150.5	124.8	113.7	91.8	51.5	46.8
720	81.5	163.8	169.0	166.5	169.0	162.0	135.2	123.6	102.5	59.1	54.2
675	81.5	176.6	181.9	179.7	183.5	174.0	146.0	133.9	113.8	66.9	61.7
610	81.5	165.1	176.6	177.6	185.9	178.7	153.0	144.4	127.7	113.0	83.4
565	81.5	147.1	163.4	171.1	181.0	176.6	153.3	142.9	123.3	100.6	76.0
520	81.5	166.3	180.6	187.7	197.4	191.6	166.7	155.5	134.9	98.7	82.7
475	81.5	133.4	144.0	150.3	164.8	164.4	148.6	139.7	122.7	106.6	104.9
430	81.5	150.8	160.0	165.4	178.9	176.5	159.4	152.7	136.7	112.7	111.6
385	81.5	141.2	145.6	149.2	161.1	156.6	142.5	139.0	143.3	135.8	135.1
345	81.5	156.8	161.5	164.5	175.1	170.0	157.0	153.0	151.9	141.3	140.7
300	81.5	193.3	195.9	198.4	208.1	200.1	181.9	175.1	172.4	145.3	145.8

Table 29. Maximum Element Velocities in JI Pile (m/s)

Rult	Depth (m)											
(KN)	1.0	4.1	8.1	12.2	17.3	21.4	25.4	29.5	33.5	38.6	41.7	42.
1500	2.5	2.5	2.4	2.3	2.3	2.2	2.0	1.8	1.6	1.8	1.9	1.
1450	2.5	2.5	2.4	2.4	2.3	2.2	2.1	1.8	1.6	1.8	1.9	1.
1400	2.5	2.5	2.4	2.3	2.2	2.2	2.1	1.8	1.6	1.8	1.8	1.
1350	2.5	2.5	2.4	2.3	2.3	2.2	2.1	1.8	1.6	1.8	1.9	1.
1300	2.5	2.5	2.4	2.3	2.3	2.3	2.1	1.8	1.6	1.8	1.7	1.
1250	2.5	2.5	2.4	2.3	2.3	2.3	2.1	1.8	1.6	1.8	1.7	1.
1200	2.5	2.5	2.4	2.3	2.3	2.3	2.1	1.8	1.6	1.7	1.7	1.
1150	2.5	2.5	2.4	2.3	2.3	2.3	2.1	1.8	1.6	1.7	1.7	1.
1100	2.5	2.5	2.4	2.3	2.3	2.3	2.1	1.8	1.6	1.7	1.7	1.
1050	2.5	2.5	2.4	2.3	2.3	2.2	2.1	1.8	1.6	1.8	1.8	1.
1000	2.5	2.5	2.4	2.3	2.3	2.3	2.1	1.8	1.6	1.7	1.7	1.
950	2.5	2.5	2.4	2.3	2.3	2.2	2.1	1.8	1.6	1.7	1.6	1.
900	2.5	2.5	2.4	2.3	2.3	2.2	2.1	1.8	1.6	1.6	1.7	1.

Table 30. Maximum Element Velocities in JA Pile (m/s)

Rult	Depth (m)										
(KN)	1.0	2.0	5.0	8.0	11.0	14.0	17.0	19.0	22.0	25.0	28.0	29.
650	3.0	3.0	3.0	2.9	2.8	2.6	2.5	2.4	2.1	2.0	2.4	2.4
625	3.0	3.0	3.0	2.9	2.8	2.6	2.5	2.4	2.1	2.0	2.5	2.6
600	3.0	3.0	3.0	2.9	2.8	2.6	2.5	2.4	2.1	1.8	2.3	2.4
575	3.0	3.0	3.0	2.9	2.8	2.6	2.5	2.4	2.1	1.8	2.3	2.4
550	3.0	3.0	3.0	2.9	2.8	2.6	2.5	2.4	2.1	1.8	2.3	2.4
525	3.0	3.0	3.0	2.9	2.8	2.6	2.5	2.4	2.1	1.7	2.2	2.3
500	3.0	3.0	3.0	2.9	2.8	2.6	2.5	2.4	2.1	1.7	2.2	2.3
475	3.0	3.0	3.0	2.9	2.8	2.6	2.5	2.4	2.0	1.7	2.1	2.2
450	3.0	3.0	3.0	2.9	2.8	2.6	2.5	2.4	2.0	1.7	2.0	2.1

Table 31. Maximum Element Velocities in AM Pile (m/s)

Rult	Depth (m)											
(KN)	1.0	5.0	11.1	16.1	22.2	28.2	34.2	39.3	45.3	51.4	56.4	57.
1725	5.0	4.9	4.6	4.4	4.1	3.8	3.4	3.3	3.3	3.3	3.7	3.
1650	5.0	4.8	4.6	4.4	4.1	3.7	3.4	3.3	3.2	3.1	3.4	3.
1575	5.0	4.8	4.6	4.4	4.0	3.6	3.2	3.1	3.0	2.9	3.2	3.
1500	5.0	4.8	4.6	4.3	3.9	3.5	3.1	3.0	2.9	2.8	3.1	3.
1425	5.0	4.8	4.6	4.3	3.9	3.6	3.1	2.9	2.8	2.8	3.1	3.
1350	5.0	4.8	4.6	4.3	3.9	3.6	3.1	2.9	2.8	2.7	3.1	3.
1275	5.0	4.8	4.6	4.3	3.9	3.5	3.0	2.7	2.7	2.6	2.8	2.

Table 32. **Maximum Element Velocities in LW Pile (m/s)**

Rult	Depth (m)										
(KN)	1.0	2.1	4.1	5.1	7.2	9.3	11.3	12.4	14.4	16.5	17.5
1125	3.1	3.1	3.1	3.0	2.9	2.7	2.5	2.4	2.1	2.4	2.7
1080	3.1	3.1	3.1	3.0	2.9	2.7	2.5	2.4	2.1	2.3	2.6
1035	3.1	3.1	3.1	3.0	2.9	2.7	2.5	2.4	2.1	2.3	2.6
990	3.1	3.1	3.1	3.0	2.9	2.7	2.5	2.4	2.1	2.3	2.6
945	3.1	3.1	3.1	3.0	2.9	2.7	2.5	2.4	2.1	2.3	2.5
900	3.1	3.1	3.1	3.0	2.9	2.7	2.5	2.4	2.1	2.3	2.5
855	3.1	3.1	3.1	3.0	2.9	2.7	2.5	2.3	2.1	2.3	2.5
810	3.1	3.1	3.1	3.0	2.9	2.7	2.5	2.3	2.1	2.3	2.5
765	3.1	3.1	3.1	3.0	2.9	2.7	2.5	2.3	2.0	2.1	2.3
720	3.1	3.1	3.1	3.0	2.9	2.6	2.5	2.3	2.0	2.1	2.3
675	3.1	3.1	3.1	3.0	2.9	2.6	2.5	2.3	2.0	2.1	2.3
610	3.1	3.1	3.1	3.0	2.9	2.6	2.5	2.3	2.0	2.0	2.2
565	3.1	3.1	3.1	3.0	2.9	2.6	2.4	2.3	2.0	2.0	2.1
520	3.1	3.1	3.1	3.0	2.9	2.6	2.4	2.3	2.0	2.0	2.1
475	3.1	3.1	3.0	3.0	2.9	2.6	2.4	2.3	2.0	1.9	2.1
430	3.1	3.1	3.1	3.0	2.9	2.6	2.4	2.3	2.0	1.9	2.0
385	3.1	3.1	3.1	3.0	2.9	2.6	2.4	2.3	1.9	1.9	2.0
345	3.1	3.1	3.1	3.0	2.9	2.6	2.4	2.3	2.0	1.8	1.9
300	3.1	3.1	3.0	3.0	2.9	2.6	2.4	2.2	1.9	1.8	1.9

Table 33. **Maximum Element Displacements in JI Pile (mm)**

Rult (KN)	Depth (m) 1.0	4.1	8.1	12.2	17.3	21.4	25.4	29.5	33.5	38.6	41.7	42.
1500	30.5	28.5	26.5	24.3	22.3	20.9	19.5	18.2	17.1	16.7	16.8	16.
1450	30.5	28.6	26.6	24.6	22.3	20.9	19.4	18.0	16.9	16.5	16.5	16.
1400	30.5	28.5	26.5	24.4	22.3	20.9	19.5	18.1	17.0	16.6	16.7	16.
1350	30.5	28.6	26.6	24.6	22.3	20.8	19.4	17.9	16.7	16.3	16.3	16.
1300	30.5	28.6	26.6	24.6	22.1	20.5	19.0	17.5	16.2	15.9	15.9	16.
1250	30.5	28.6	26.7	24.6	22.1	20.5	18.9	17.5	16.3	16.0	16.0	16.
1200	30.5	28.6	26.7	24.6	22.1	20.3	18.8	17.3	16.2	15.9	16.0	16.
1150	30.5	28.6	26.7	24.7	22.2	20.6	19.1	17.7	16.4	15.9	15.9	16.
1100	30.5	28.5	26.6	24.5	22.0	20.0	18.4	17.2	16.2	15.8	15.8	15.
1050	30.5	28.5	26.4	24.3	21.8	20.0	18.0	16.1	14.7	13.5	13.0	12.
1000	30.5	28.5	26.5	24.5	22.0	20.1	18.4	16.6	15.1	13.9	13.4	13.
950	30.5	28.5	26.6	24.6	22.2	20.4	18.6	16.9	15.4	14.2	13.8	13.
900	30.5	28.5	26.6	24.6	22.2	20.5	18.7	17.0	15.5	14.3	13.8	13.

Table 34. Maximum Element Displacements in JA Pile (mm)

Rult	Depth (m)										
(KN)	1.0	2.0	5.0	8.0	11.0	14.0	17.0	19.0	22.0	25.0	28.0	29.
650	12.6	12.2	11.7	11.2	10.6	9.9	9.3	8.9	8.3	7.9	7.5	7.5
625	12.6	12.2	11.8	11.2	10.5	9.9	9.3	8.8	8.3	7.9	7.8	7.8
600	12.6	12.1	11.6	11.0	10.3	9.6	9.0	8.6	8.1	7.7	7.5	7.5
575	12.6	12.1	11.7	11.1	10.4	9.8	9.2	8.8	8.2	7.9	7.7	7.7
550	12.6	12.1	11.7	11.1	10.5	9.9	9.3	8.9	8.4	8.0	7.8	7.9
525	12.6	12.1	11.6	11.0	10.3	9.7	9.1	8.7	8.2	7.8	7.7	7.7
500	12.6	12.1	11.6	11.0	10.4	9.8	9.2	8.9	8.4	8.0	7.8	7.6
475	12.6	12.0	11.5	11.0	10.3	9.8	9.2	8.9	8.4	8.0	7.9	7.9
450	12.6	12.0	11.6	11.0	10.4	9.8	9.3	8.9	8.4	8.1	7.9	7.9

Table 35. Maximum Element Displacements in AM Pile (mm)

Rult	Depth (m)											
(KN)	1.0	5.0	11.1	16.1	22.2	28.2	34.2	39.3	45.3	51.4	56.4	57.
1725	28.6	25.9	22.7	20.8	18.4	16.2	14.2	13.1	12.7	12.4	12.3	12.
1650	28.6	25.8	22.5	20.3	17.9	15.6	13.6	12.1	10.7	9.1	8.2	8.
1575	28.6	25.8	22.6	20.5	17.9	15.4	13.2	11.7	10.4	9.1	8.2	8.
1500	28.6	25.9	22.8	20.7	18.2	15.9	13.6	12.1	10.6	9.1	8.2	8.
1425	28.6	25.9	22.7	20.6	18.1	15.7	13.4	12.0	10.7	9.2	8.3	8.
1350	28.6	25.9	22.7	20.7	18.2	15.8	13.5	12.3	11.0	9.8	8.9	8.
1275	28.6	26.0	22.9	20.8	18.3	15.8	13.6	12.3	11.0	9.8	8.8	8.

Table 36. Maximum Element Displacements in LW Pile (mm)

Rult	Depth (m)									
(KN)	1.0	2.1	4.1	5.1	7.2	9.3	11.3	12.4	14.4	16.5	17.5
1125	10.3	9.7	9.3	9.0	8.5	8.0	7.5	7.3	7.0	6.9	6.9
1080	10.3	9.7	9.3	9.0	8.5	8.0	7.5	7.4	7.1	7.0	7.0
1035	10.3	9.7	9.3	9.0	8.5	8.0	7.6	7.4	7.1	7.0	7.0
990	10.3	9.7	9.3	9.1	8.6	8.1	7.7	7.5	7.2	7.1	7.1
945	10.3	9.7	9.3	9.1	8.6	8.2	7.8	7.6	7.3	7.2	7.2
900	10.3	9.8	9.4	9.1	8.7	8.2	7.8	7.7	7.4	7.3	7.4
855	10.3	9.8	9.4	9.2	8.7	8.3	7.9	7.8	7.5	7.5	7.5
810	10.3	9.8	9.4	9.2	8.8	8.4	8.0	7.9	7.6	7.6	7.6
765	10.3	9.7	9.3	9.0	8.6	8.2	7.8	7.7	7.5	7.4	7.4
720	10.3	9.7	9.3	9.1	8.6	8.2	7.9	7.8	7.6	7.5	7.5
675	10.3	9.7	9.3	9.1	8.7	8.3	8.0	7.9	7.7	7.6	7.6
610	10.3	9.7	9.3	9.1	8.7	8.3	8.0	7.9	7.7	7.7	7.8
565	10.3	9.6	9.2	9.0	8.6	8.2	7.9	7.8	7.7	7.7	7.7
520	10.3	9.6	9.2	9.0	8.6	8.3	8.0	7.9	7.8	7.8	7.8
475	10.3	9.7	9.2	9.0	8.7	8.3	8.1	8.0	7.9	7.8	7.9
430	10.3	9.6	9.2	9.0	8.6	8.3	8.1	8.0	7.8	7.8	7.9
385	10.3	9.6	9.2	9.0	8.7	8.3	8.1	8.0	7.9	7.9	7.9
345	10.3	9.6	9.2	9.0	8.6	8.3	8.0	7.9	7.8	7.8	7.8
300	10.3	9.6	9.2	9.0	8.6	8.4	8.1	8.1	7.9	7.9	8.0

Table 37. Deviation of Maximum Rult from Average Rult

Pile	Ultimate Soil Resistance Minimum (KN)	Maximum (KN)	Average (KN)	(Max.-Avg.)/Avg. (%)
JI	900	1500	1200	25
JA	450	650	550	18
AM	1275	1725	1500	15
LW	300	1125	712.5	58

Table 38. Maximum, Minimum Rult as a Percentage of Reference Rult

Pile	Ultimate Soil Resistance Minimum (KN)	Maximum (KN)	Ref.+ (KN)	Min./Ref. (%)	Max./Ref. (%)
JI	900	1500	1000	90	150
JA	450	650	575	78	113
AM	1275	1725	1500	85	115
LW	300	1125	900	33	125

+ Reference Rult

Table 39. Relative Variation+ of CAPWAP Parameters

Pile	JI	JA	AM	LW	Avg.
Ultimate resistance	16	12	10	36	18.5
Shaft resistance	11	13	8	36	17.0
Toe resistance	28	12	18	33	22.8
Shaft Case damping	63	7	44	17	32.8
Toe Case damping	27	32	5	23	21.8
Shaft Smith damping	71	18	51	59	49.8
Toe Smith damping	18	39	16	64	34.3
Toe soil damper	92	0	245	292	157.3
Shaft quakes	35	33	0	6	18.5
Toe quakes	13	29	12	0	13.5
Shaft unld. quakes	69	0	5	128	50.5
Toe unld. quakes	39	186	14	40	69.8
Shaft unld. resistance	64	215	38	0	79.3
Soil plug	0	0	0	0	0.0
Toe gap	39	150	169	0	89.5

+ Standard deviation / Mean (%)

Table 40. Variation of Static Resistance, JI Pile

Rult	Static Resistance Shaft (KN)	Toe (KN)	Percent of Rult Shaft (%)	Toe (%)
1500	867.7	632.3	57.8	42.2
1450	862.9	587.1	59.5	40.5
1400	857.3	542.7	61.2	38.8
1350	874.9	475.1	64.8	35.2
1300	866.7	433.3	66.7	33.3
1250	833.3	416.7	66.7	33.3
1200	800.0	400.0	66.7	33.3
1150	850.0	300.0	73.9	26.1
1100	789.6	310.4	71.8	28.2
1050	730.8	319.2	69.6	30.4
1000	696.0	304.0	69.6	30.4
950	661.2	288.8	69.6	30.4
900	582.3	317.7	64.7	35.3

Table 41. Variation of Static Resistance, JA Pile

Rult	Static Resistance Shaft (KN)	Toe (KN)	Percent of Rult Shaft (%)	Toe (%)
650	454.7	195.3	70.0	30.0
625	481.2	143.8	77.0	23.0
600	450.4	149.6	75.1	24.9
575	431.7	143.3	75.1	24.9
550	412.9	137.1	75.1	24.9
525	384.6	140.4	73.3	26.7
500	356.7	143.3	71.3	28.7
475	338.9	136.1	71.3	28.7
450	321.0	129.0	71.3	28.7

Table 42. Variation of Static Resistance, AM Pile

Rult	Static Resistance Shaft (KN)	Toe (KN)	Percent of Rult Shaft (%)	Toe (%)
1725	1058.3	666.7	61.4	38.6
1650	1155.2	494.8	70.0	30.0
1575	1040.8	534.2	66.1	33.9
1500	968.8	531.2	64.6	35.4
1425	970.4	454.6	68.1	31.9
1350	959.3	390.7	71.1	28.9
1275	881.5	393.5	69.1	30.9

Table 43. Variation of Static Resistance, LW Pile

Rult	Static Resistance Shaft (KN)	Toe (KN)	Percent of Rult Shaft (%)	Toe (%)
1125	1005.5	119.5	89.4	10.6
1080	965.3	114.7	89.4	10.6
1035	896.3	138.7	86.6	13.4
990	857.4	132.6	86.6	13.4
945	818.4	126.6	86.6	13.4
900	779.4	120.6	86.6	13.4
855	740.5	114.5	86.6	13.4
810	701.5	108.5	86.6	13.4
765	662.5	102.5	86.6	13.4
720	623.5	96.5	86.6	13.4
675	584.6	90.4	86.6	13.4
610	528.3	81.7	86.6	13.4
565	489.3	75.7	86.6	13.4
520	450.4	69.6	86.6	13.4
475	411.4	63.6	86.6	13.4
430	372.4	57.6	86.6	13.4
385	333.4	51.6	86.6	13.4
345	298.8	46.2	86.6	13.4
300	259.8	40.2	86.6	13.4

Table 44. Compilation of Basic CAPWAP Results (After Fellenius, 1988)

PARTICIPANT	TOTAL CAPACITY (KN)				SHAFT QUAKES (mm)				TOE QUAKE (mm)				SHAFT DAMPING (s/m)				TOE DAMPING (s/m)			
#	JI	JA	AM	LW	JI	JA	AM	LW	JI	JA	AM	LW	JI	JA	AM	LW	JI	JA	AM	LW
1	1100	666	2072	851	3.1	2.6	4.0	2.0	3.0	4.8	6.0	1.0	0.07	0.25	0.06	0.90	0.92	1.26	1.06	1.12
2	1103	632	1810	780	2.5	2.5	5.0	2.5	2.8	4.0	5.0	2.5	0.00	0.57	0.03	0.95	1.16	1.65	1.54	1.62
3	1122	645	1681	927	1.0	1.5	4.0	1.5	2.8	2.0	2.8	2.0	0.11	0.17	0.07	1.05	0.31	3.94	1.16	0.58
4	1103	647	1715	908	2.5	2.5	2.5	3.5	8.9	0.4	2.5	1.3	0.26	0.53	0.34	0.95	0.25	1.23	0.22	0.93
5	1081	629	2617	958	0.3	1.4	0.5	1.4	5.0	1.0	4.0	7.0	0.08	0.46	0.03	0.76	0.59	0.32	0.07	0.70
6	1030	540	1734	688	2.2	3.0	3.0	2.6	13.5	6.5	1.8	3.3	0.09	0.97	0.31	1.37	0.60	0.15	0.05	2.08
7	1065	624	1919	988	1.6	2.5	2.5	2.5	5.1	2.5	3.9	3.7	0.48	0.56	3.71	0.73	0.14	1.15	0.12	0.90
8	1000	575	1500	900	2.0	2.5	2.5	2.5	4.0	5.0	6.5	5.0	0.06	0.63	0.17	0.48	0.74	1.16	0.49	2.63
9	1122	583	1667	838	6.0	2.0	8.0	1.5	6.0	5.0	3.0	1.5	0.12	0.47	0.03	0.90	0.62	12.28	2.39	12.61
10	1021	609	1799	721	4.2	2.5	5.0	3.2	8.0	4.5	6.0	4.0	0.42	0.86	0.26	1.46	0.17	0.29	0.29	1.17
11	1132	644	1891	803	2.0	2.3	3.9	3.0	4.0	2.5	3.9	3.0	0.17	0.53	0.40	0.99	0.08	0.47	0.13	1.19
12	1166	670	1799	778	2.0	2.5	6.0	2.5	4.0	2.5	6.5	2.5	0.11	0.30	0.07	1.10	0.09	1.01	1.03	1.23
13	1051	621	1696	636	1.5	3.0	4.0	3.0	5.0	3.0	4.0	3.0	0.38	0.36	0.13	0.93	0.35	2.19	1.76	4.94
14	1091	687	1819	1042	3.5	3.5	4.5	3.0	8.0	0.8	3.0	3.0	0.06	0.22	0.07	0.58	0.73	1.57	0.68	1.08
15	1006	608	1684	725	1.4	2.2	3.5	1.0	6.9	2.5	3.0	8.1	0.22	0.59	0.21	1.14	0.32	0.86	0.50	1.26
16	1051	621	1696	636	2.8	1.8	2.0	1.7	7.0	4.5	2.6	2.0	0.34	0.36	0.36	0.82	0.25	0.30	0.27	0.65
17	1144	622	1726	960	2.5	2.8	3.0	2.0	5.5	3.3	6.5	6.5	0.11	0.64	0.25	0.83	0.39	0.38	0.18	0.96
18	1126	580	1770	921	2.9	2.5	6.5	3.2	8.8	2.5	6.5	6.5	0.14	0.74	0.27	0.95	0.39	0.38	0.18	0.96
AVERAGE (KN):	1084	622	1811	837	2.5	2.4	3.9	2.4	6.0	3.2	4.3	3.7	0.18	0.51	0.38	0.94	0.45	1.78	0.70	2.10
STD.DEV.(KN):	49	37	235	123																
STD.DEV.(%) :	5	6	13	15																

Table 45. Relative Variation+ of Maximum Dynamic Quantities

Pile	Depth / Length (%) 5	15	25	35	45	55	65	75	85	95	Toe
Maximum compression forces											
JI	0.4	0.9	0.4	0.9	1.3	2.1	3.8	7.1	15.5	19.6	19.0
JA	0.3	0.3	0.4	0.4	0.6	0.6	0.6	1.0	1.5	8.9	15.0
AM	0.2	0.5	0.8	1.1	1.8	1.8	6.9	6.7	6.6	5.8	7.4
LW	0.0	0.1	0.0	0.1	0.3	0.4	0.1	0.4	1.0	3.2	23.2
Maximum tension forces											
JI	0.0	0.0	0.0	5.5	8.5	9.0	12.2	16.1	72.3	51.1	62.4
JA	18.1	24.2	19.0	20.9	20.1	19.8	19.8	16.8	19.5	23.2	15.5
AM	0.0	0.0	0.0	0.0	0.0	0.0	244.9	244.9	244.9	244.9	244.9
LW	0.0	10.5	10.4	9.9	9.8	9.2	11.6	12.9	18.2	31.0	34.0
Maximum element velocities											
JI	0.0	0.0	1.2	1.2	2.2	1.3	0.0	0.0	3.6	5.3	4.2
JA	0.0	0.0	0.0	0.0	0.0	0.0	0.0	2.0	6.4	6.3	5.7
AM	0.7	0.0	1.1	2.2	2.7	4.6	6.8	7.0	7.7	8.2	6.7
LW	0.0	0.0	1.0	0.0	0.0	1.9	2.0	2.4	3.2	9.1	11.0
Maximum element displacements											
JI	0.2	0.3	0.5	0.7	1.5	2.4	3.4	4.5	6.9	8.4	8.8
JA	0.6	0.7	0.7	1.0	1.0	1.1	1.2	1.3	1.4	1.8	1.9
AM	0.2	0.5	0.8	1.0	1.5	2.1	3.3	6.5	11.3	15.4	15.8
LW	0.0	0.7	0.7	0.7	0.9	1.5	2.4	2.9	3.8	4.3	4.4

+ Standard deviation / Mean (%)

F I G U R E S

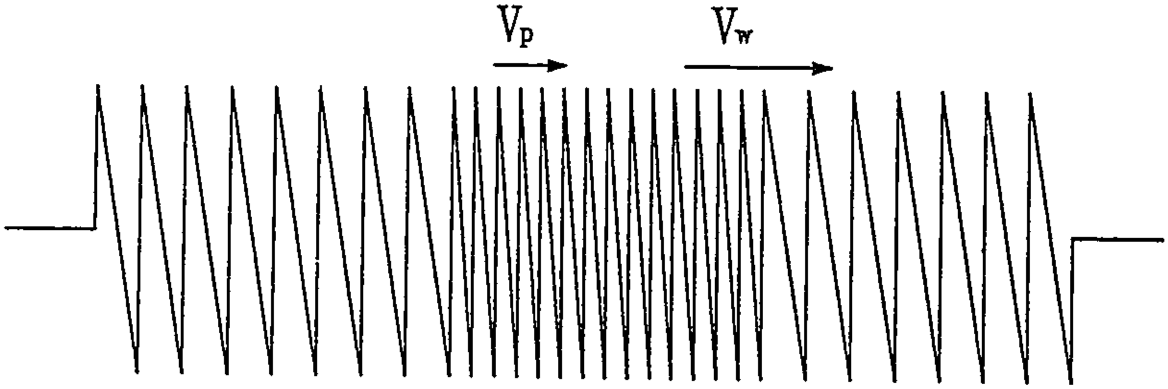

(a) Longitudinal wave

Particules vibrate in the direction of wave movement

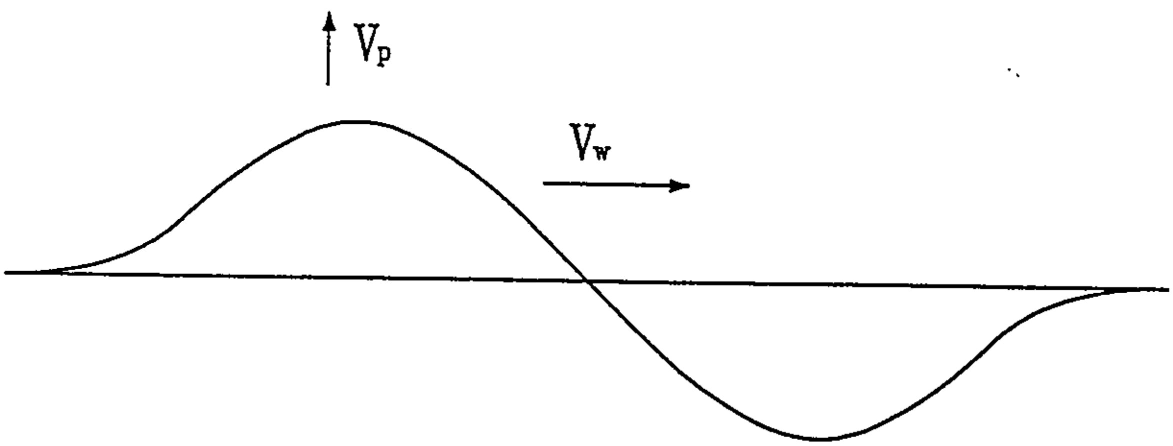

(b) Transverse wave

Particules vibrate in perpendicular direction to wave movement

Fig. 2.1 Definition of Mechanical Waves

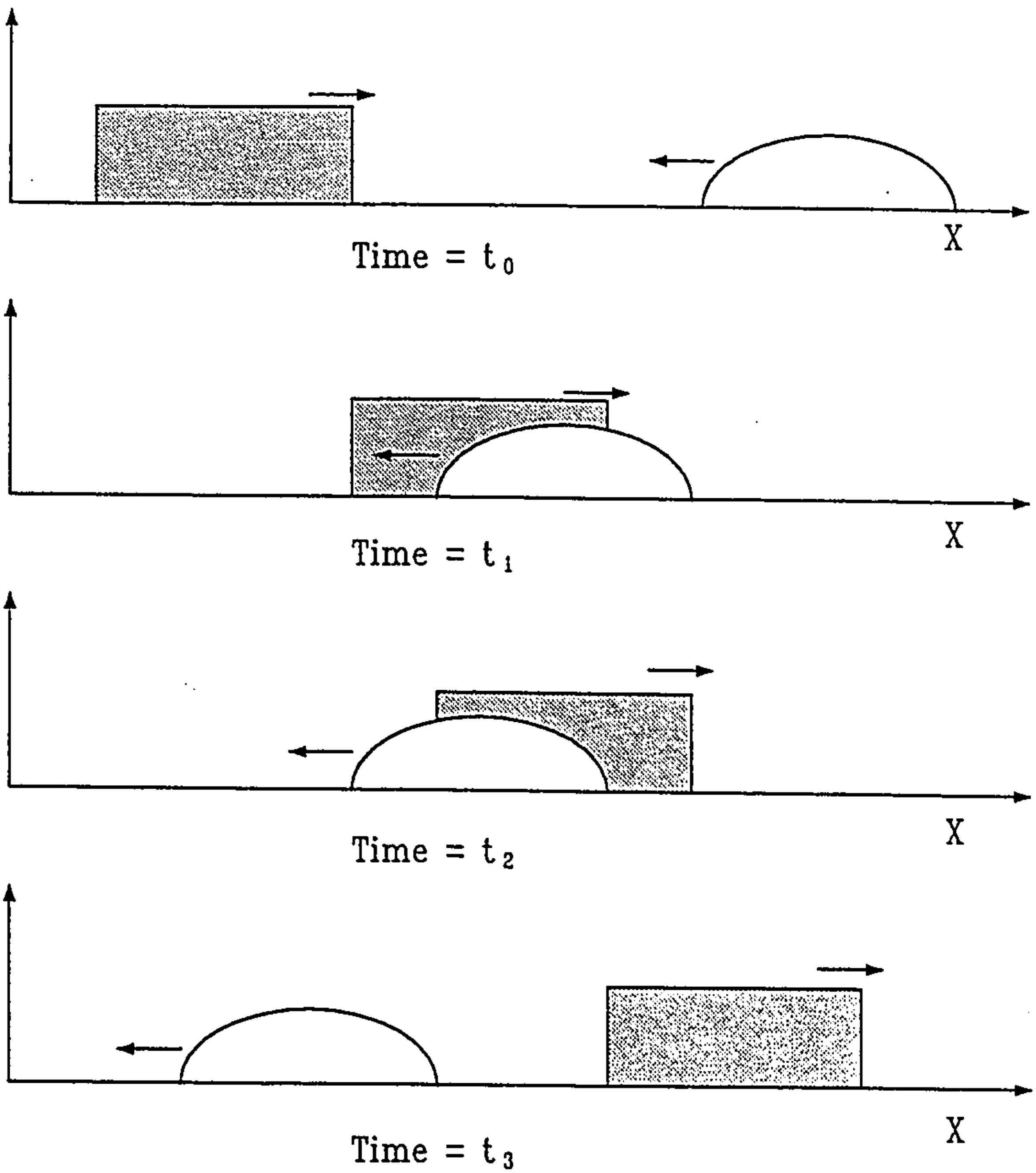

Fig. 2.2 Principle of Superposition

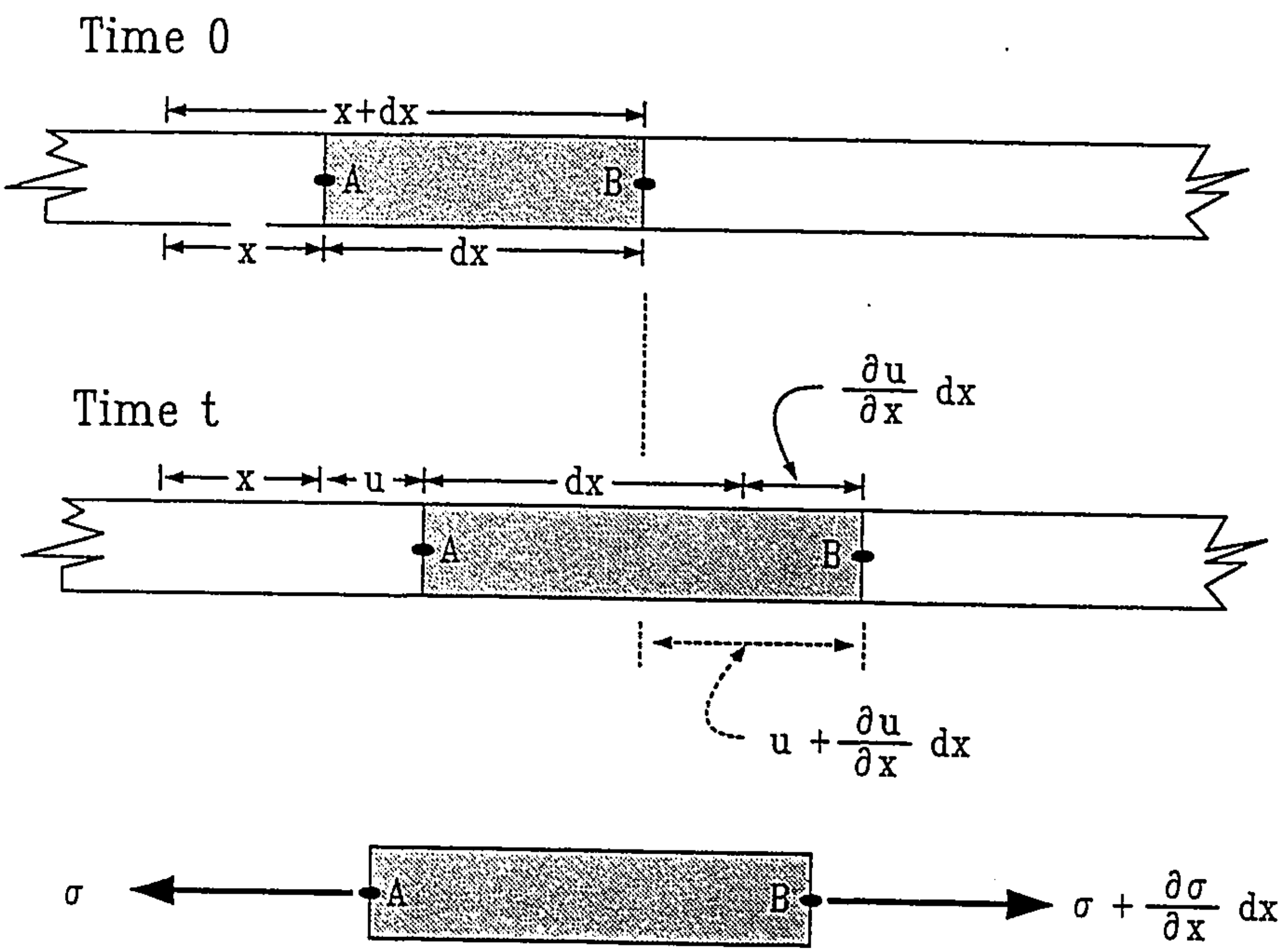

Fig. 2.3 Derivation of Wave Equation

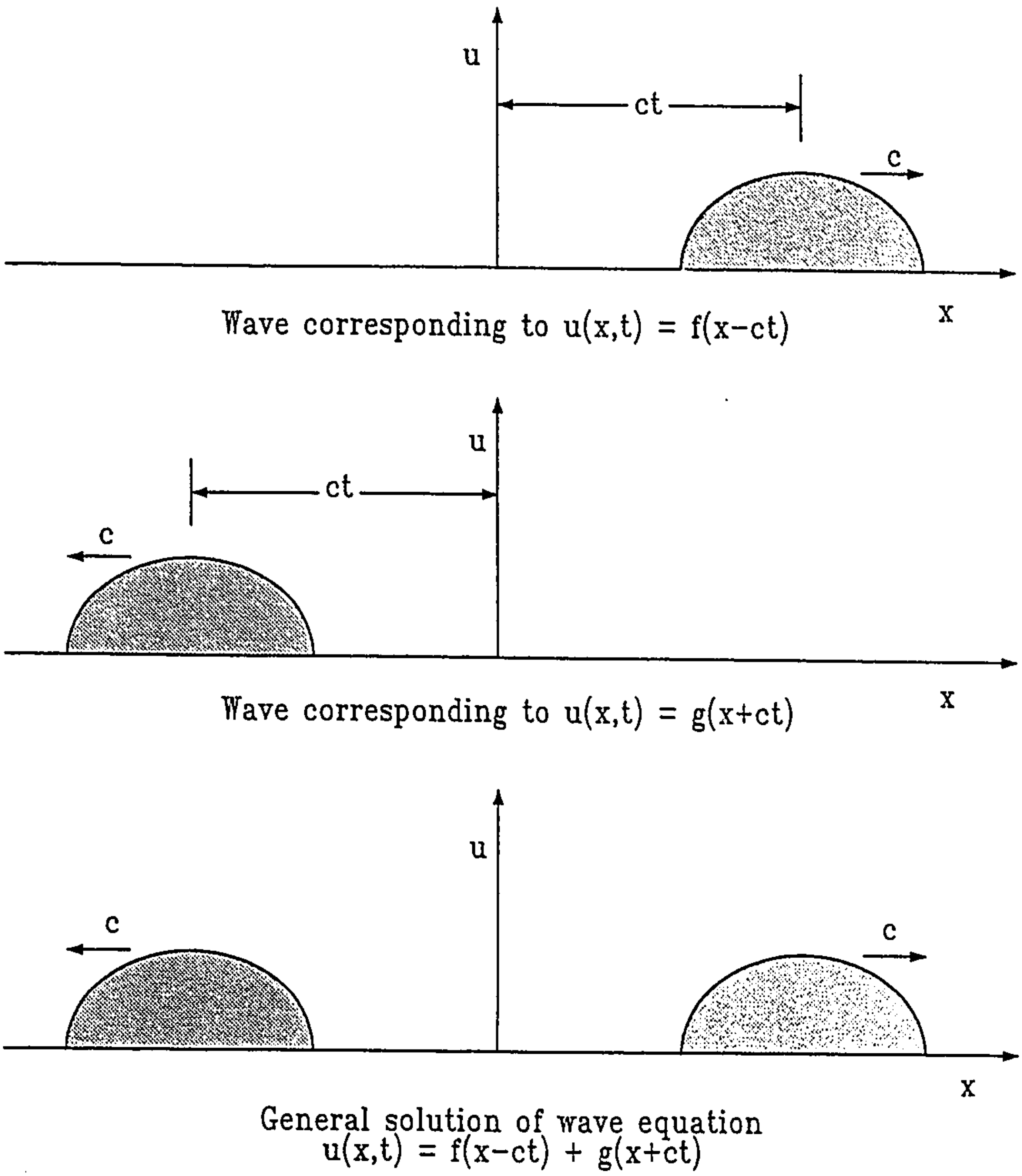

Fig. 2.4 General Solution of Wave Equation

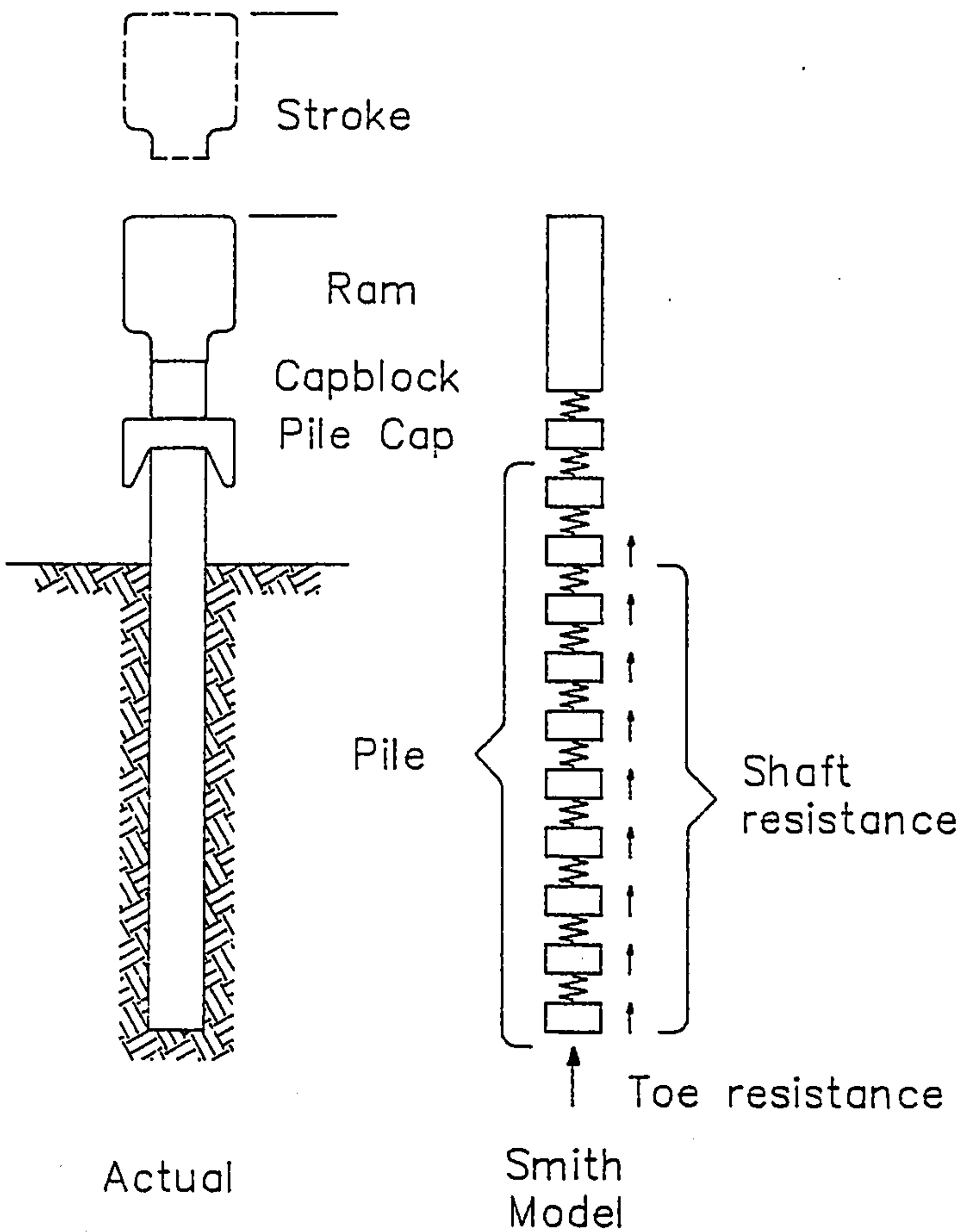

Fig. 2.5 Smith Model

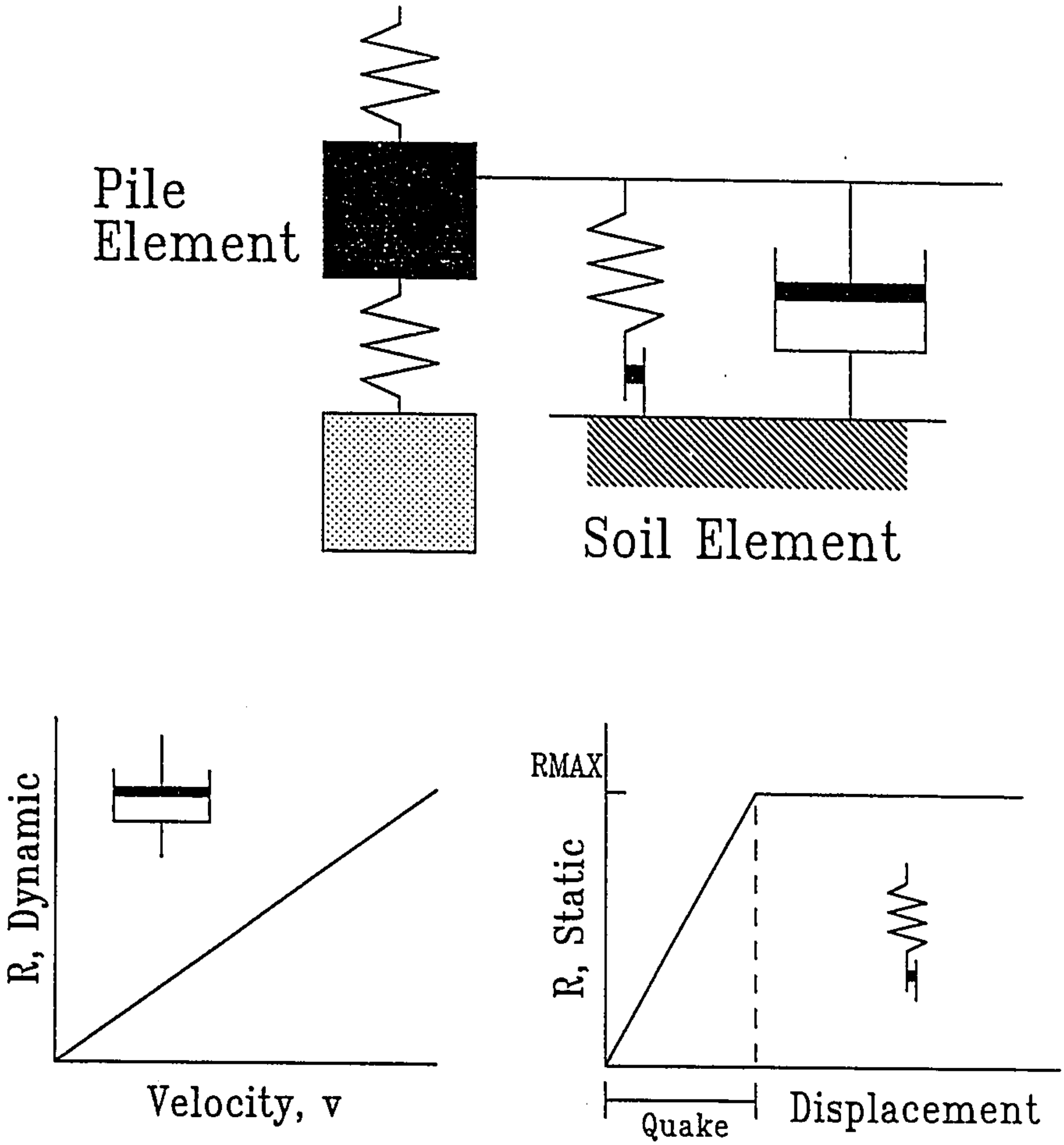

Fig. 2.6 Smith Soil Model

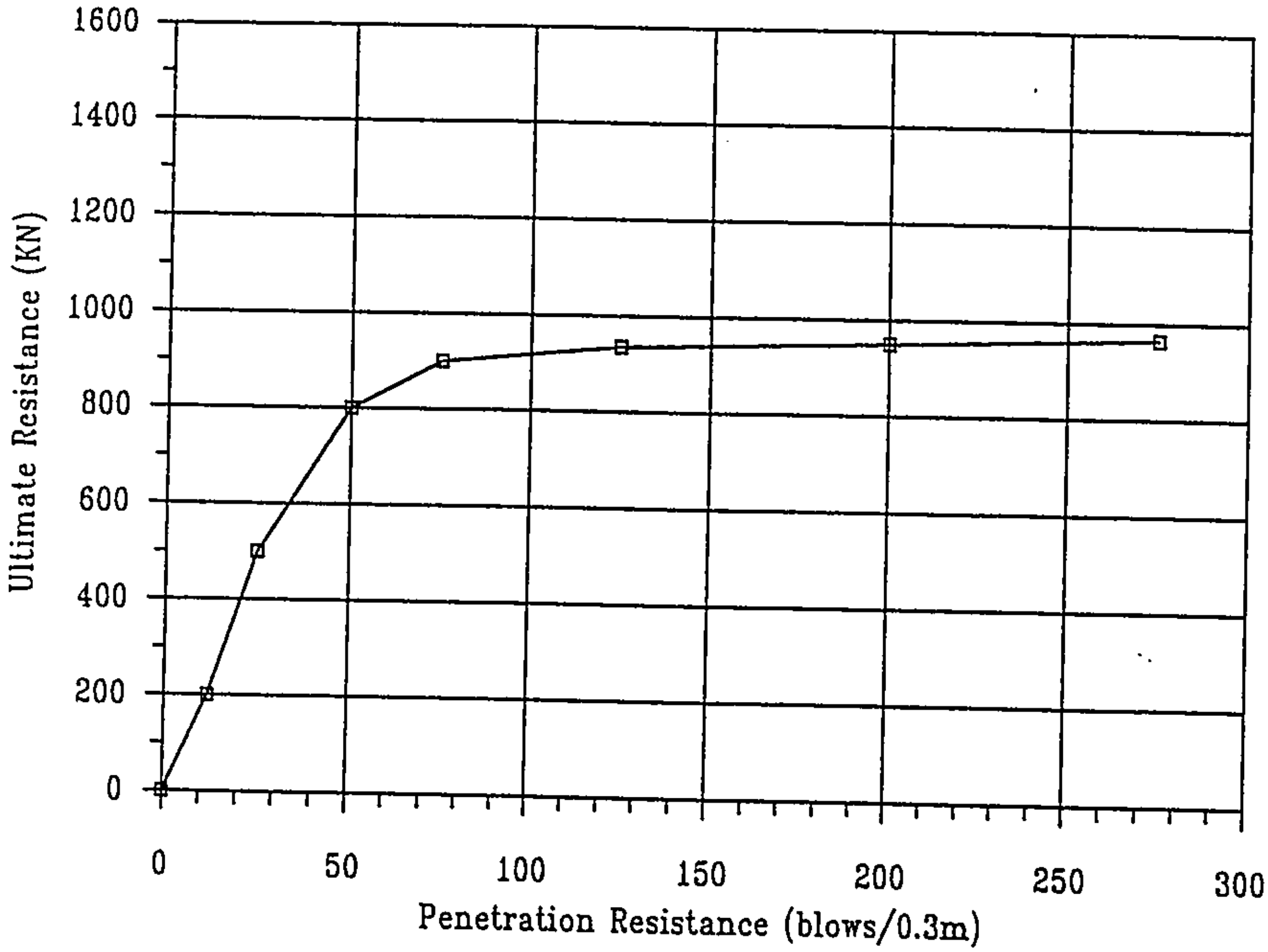

Fig. 2.7 Typical Bearing Graph

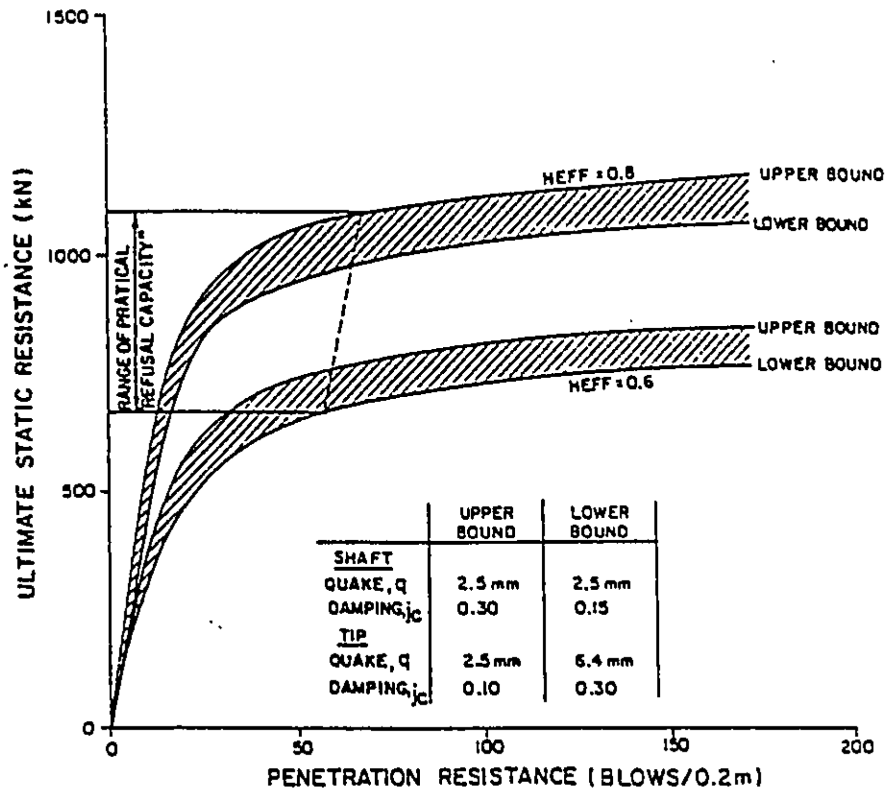

Results of Wave Equation Analyses of a closed-end pipe pile driven with a drop hammer. Comparison is made between two hammer efficiences (HEFF), and a range of quake values and damping factors. (W = 28 KN, H = 1.0 m, L = 12.2 m, D = 275 mm, RULT-SHFT = 450 KN).

Fig. 2.8 Sensitivity of the Wave Equation

(After Authier and Fellenius, 1983)

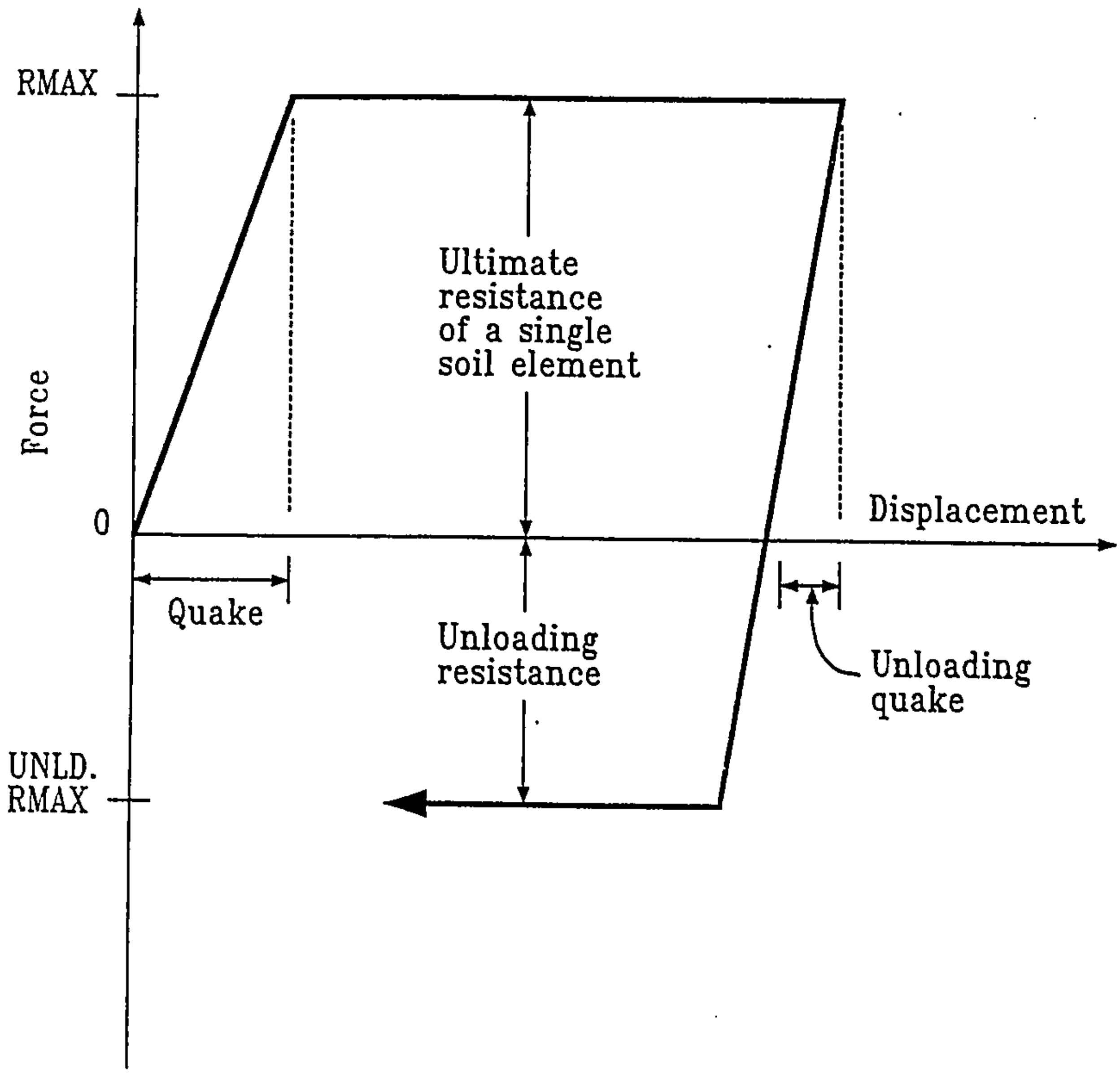

Fig. 2.9   Unloading Parameters

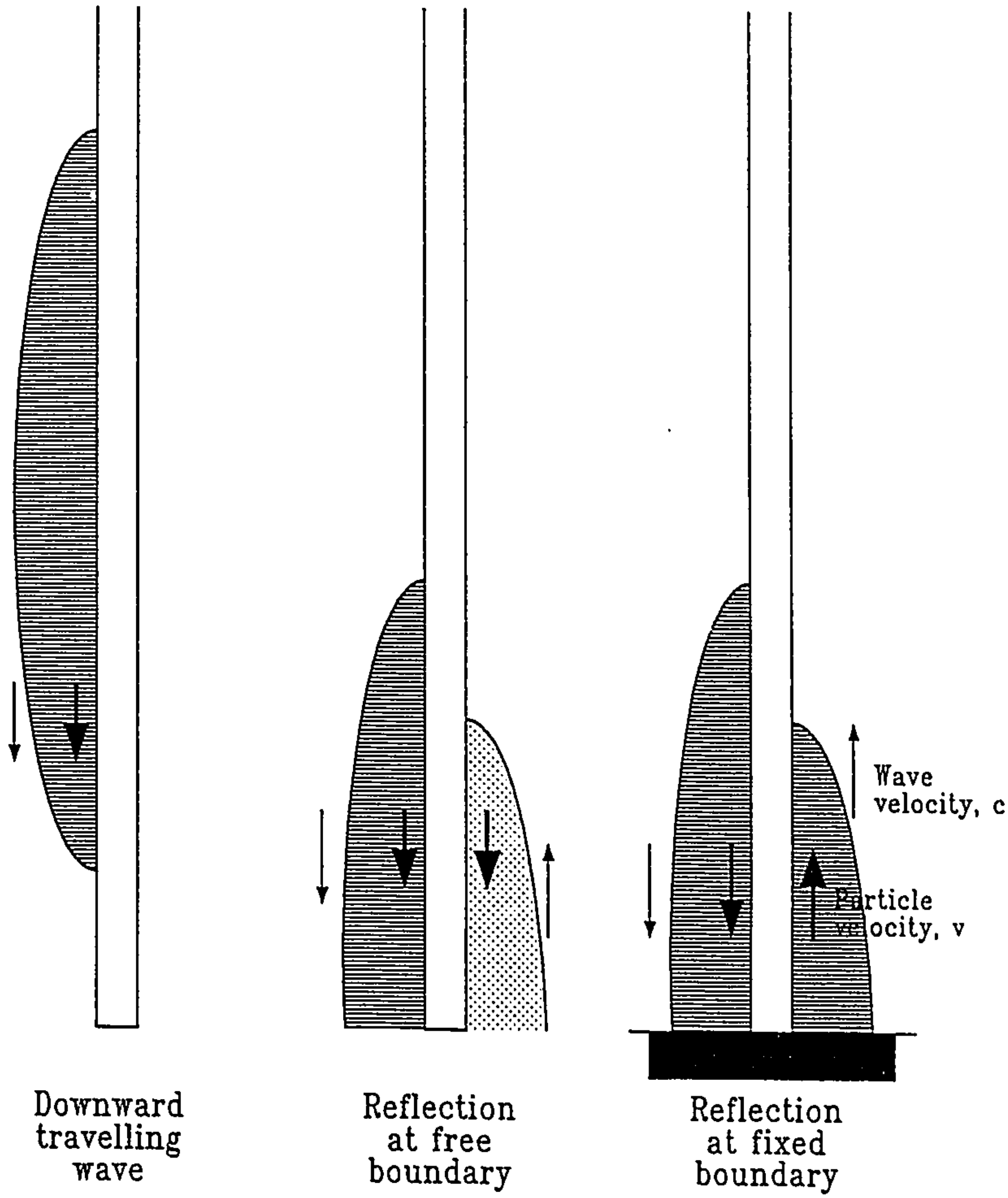

Fig. 2.10 Wave Reflections and Boundary Conditions

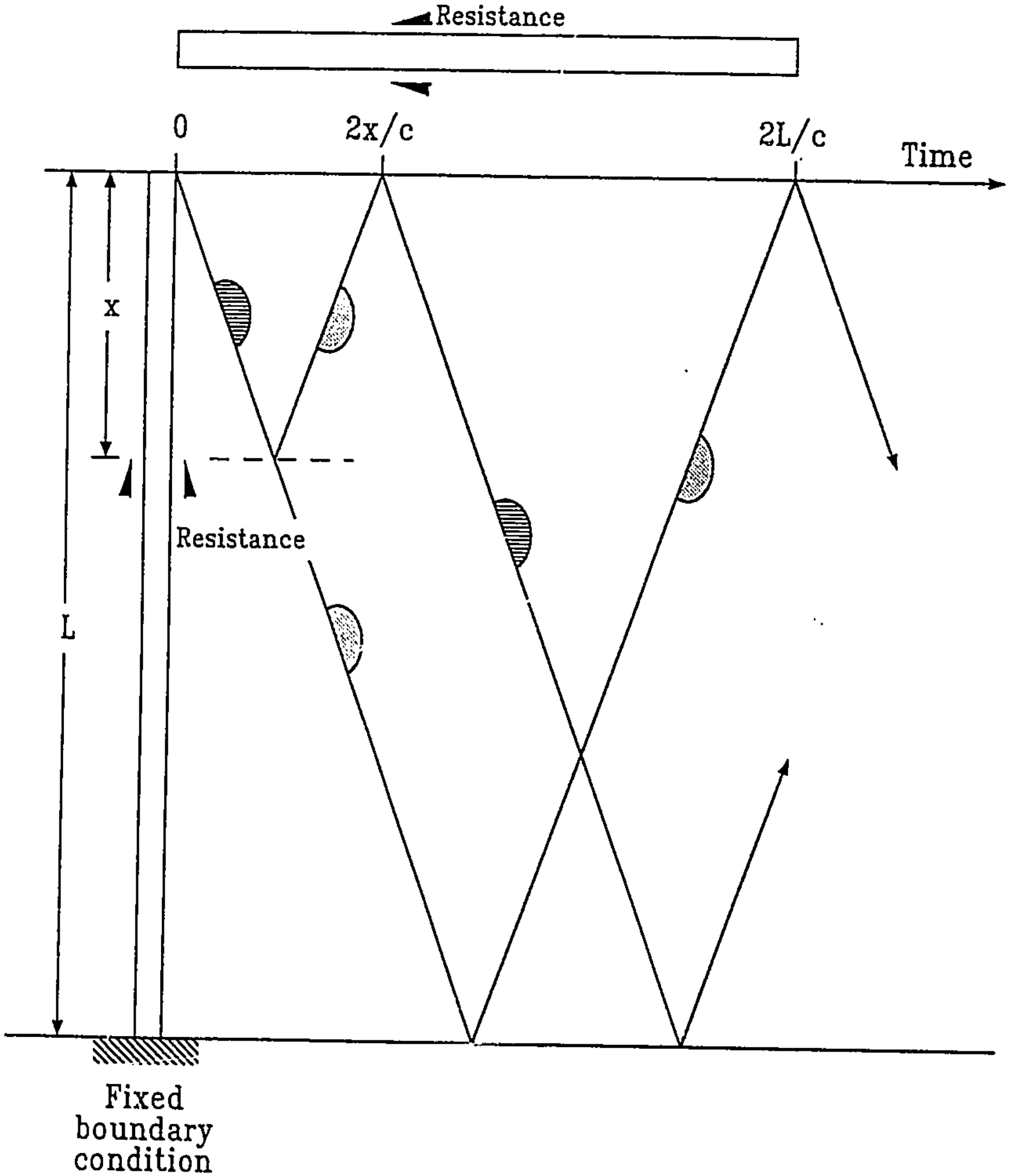

Fig. 2.11 Resistance Waves

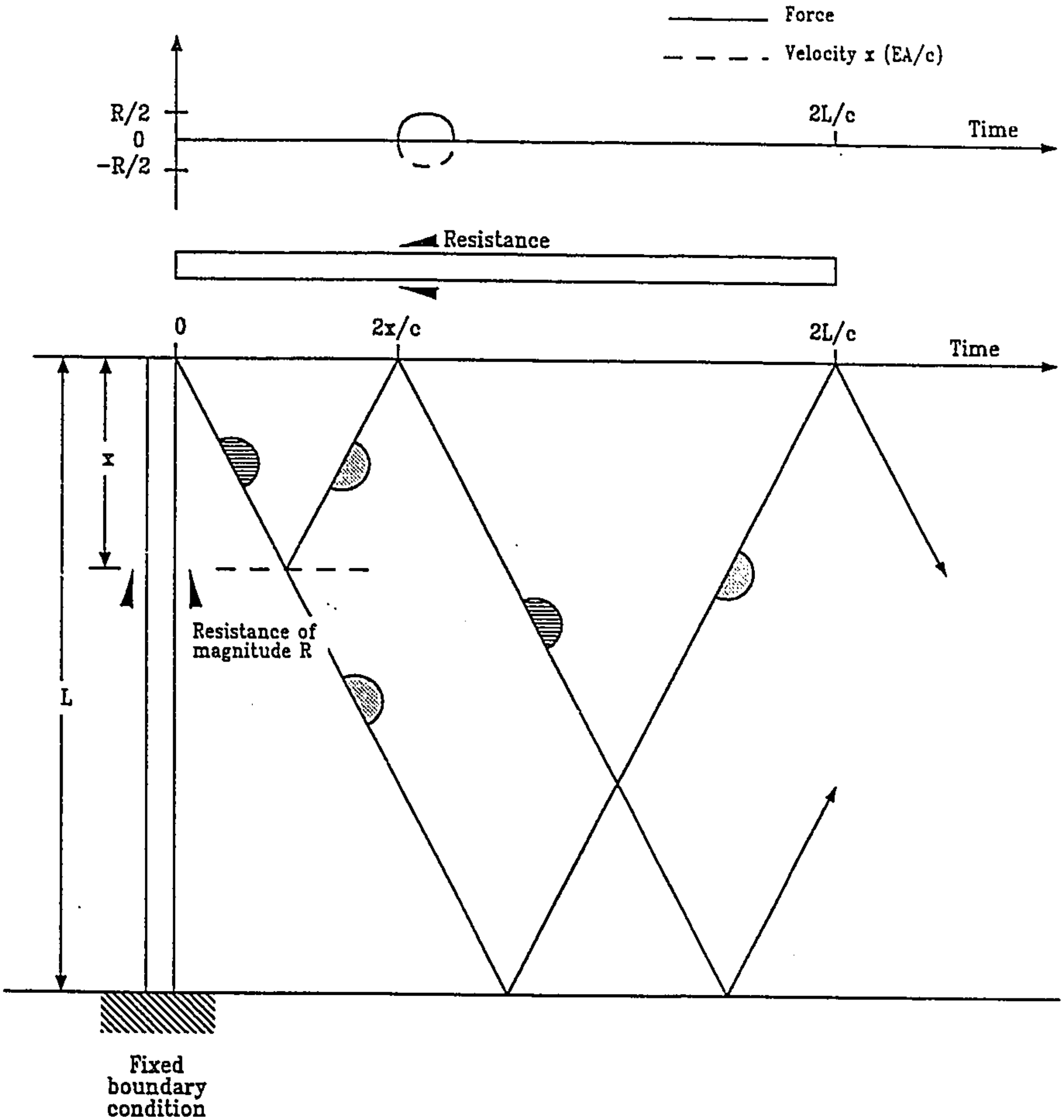

Fig. 2.12 Determination of Soil Resistance from Resistance Waves

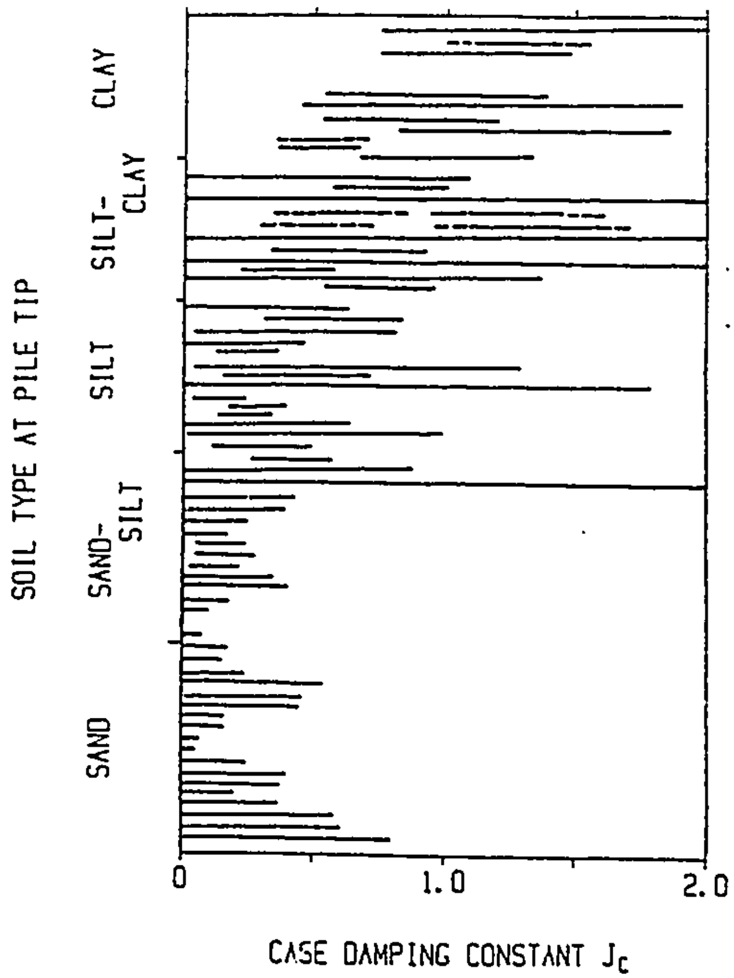

Damping Constant Determination by
Correlation with Field Measurements

± 20% of Static Load Test Result

Soil Type in Bearing Strata	Suggested range J_c	Correlation Value J_c
Sand	0.05 - 0.20	0.05
Silty Sand or Sandy Silt	0.15 - 0.30	0.15
Silt	0.20 - 0.45	0.30
Silty Clay and Clayey Silt	0.40 - 0.70	0.55
Clay	0.60 - 1.10	1.10

Fig. 2.13 Correlation Study for Determining Values of Case Damping Coefficient (After Hannigan, 1986)

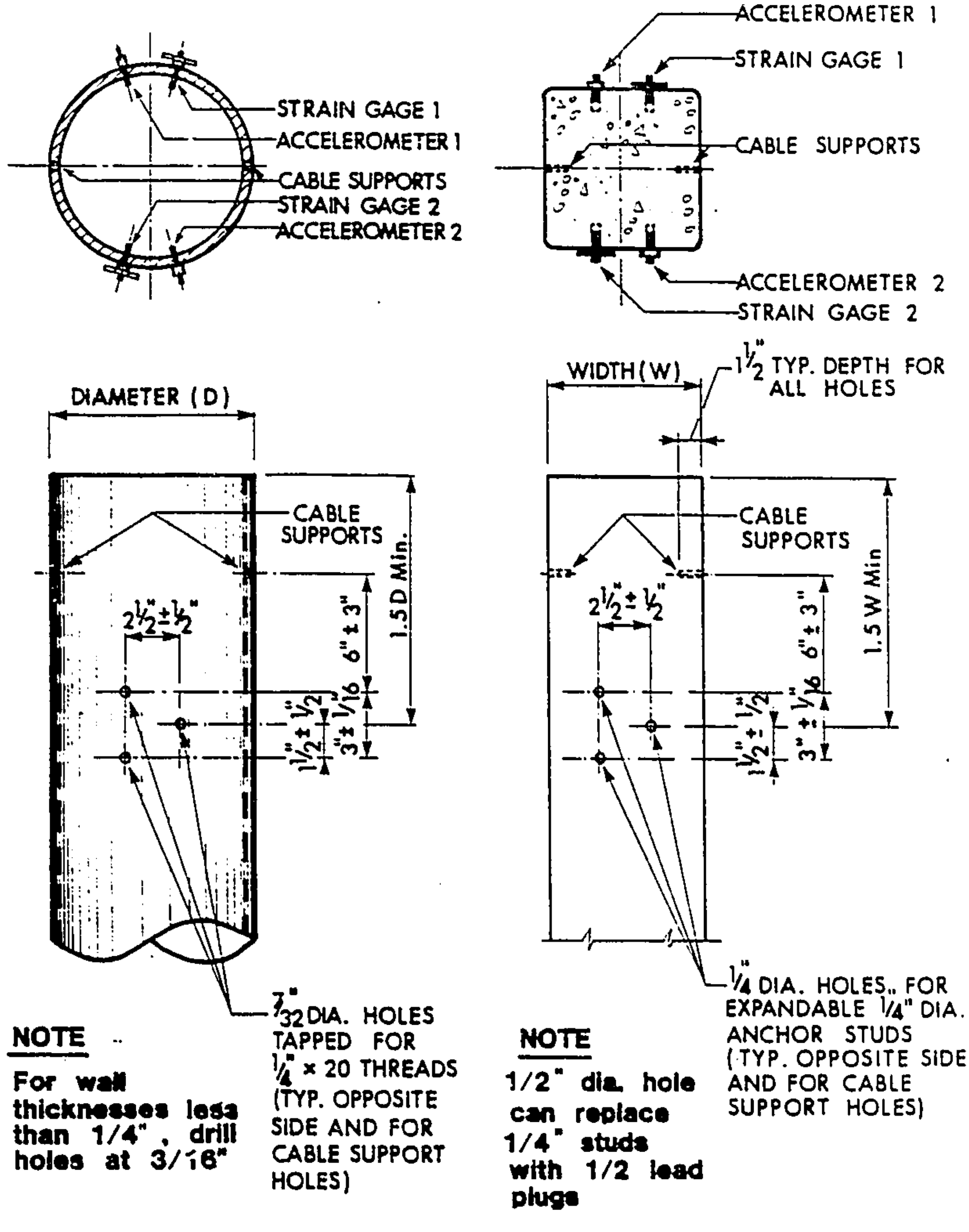

Fig. 3.1 Typical Arrangement for Attaching Transducers (After ASTM, 1986)

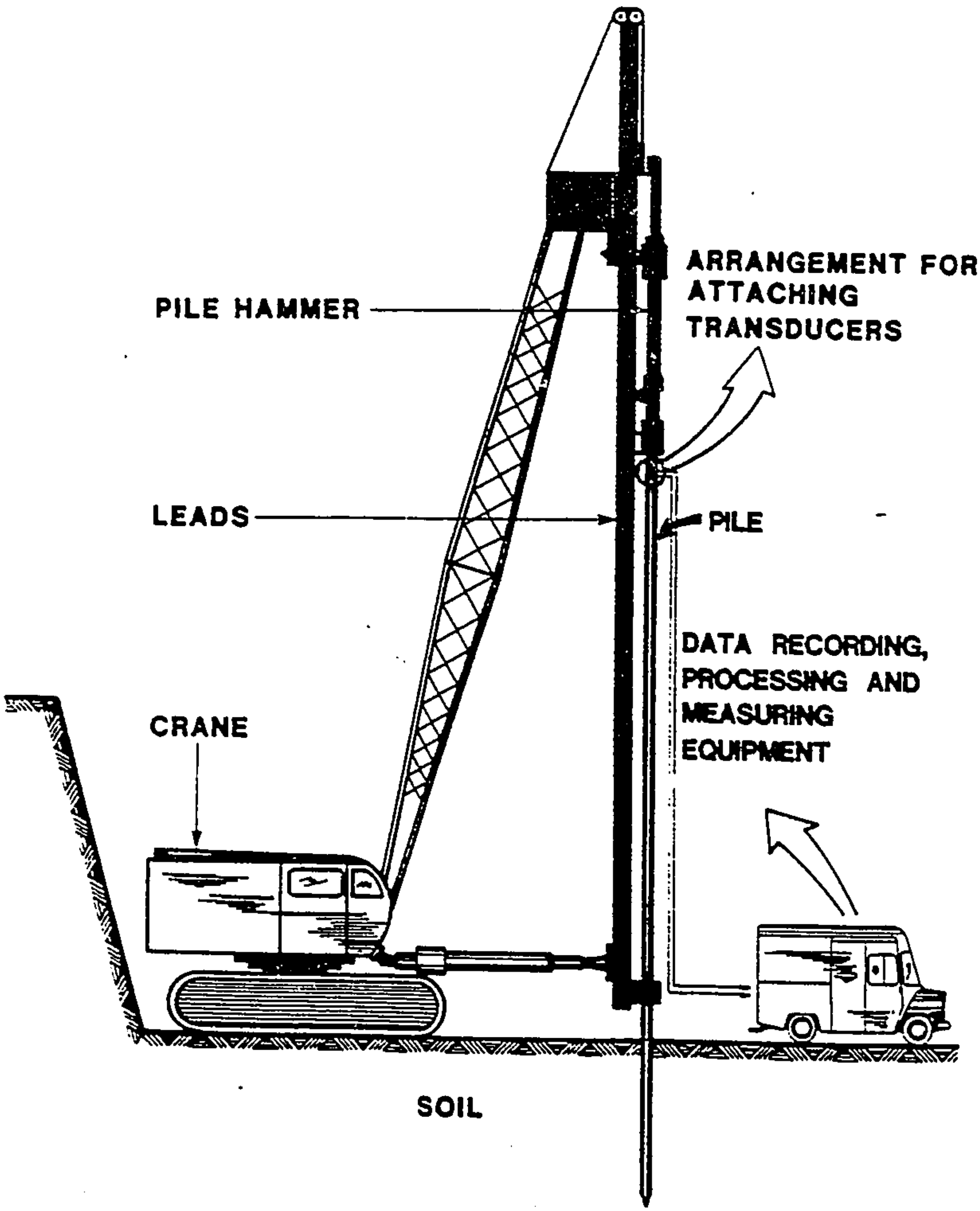

Fig. 3.2 Typical Arrangement for High Strain Dynamic Testing of Piles (After ASTM, 1986)

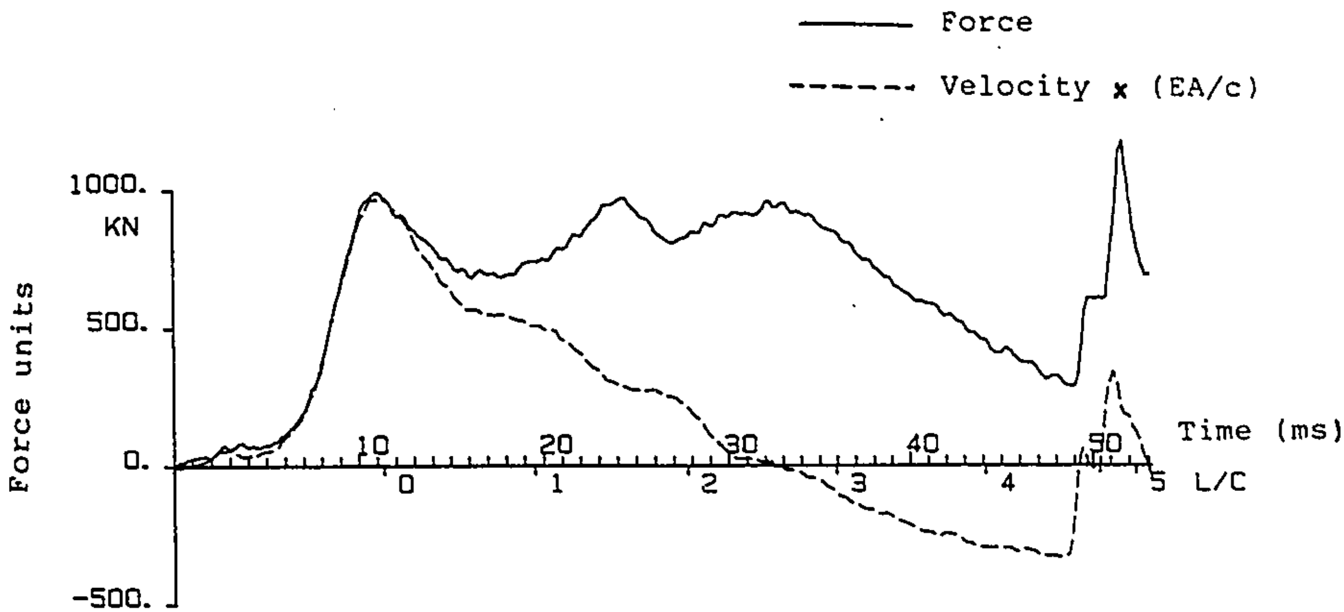

Fig. 5.3 Dynamic Measurements

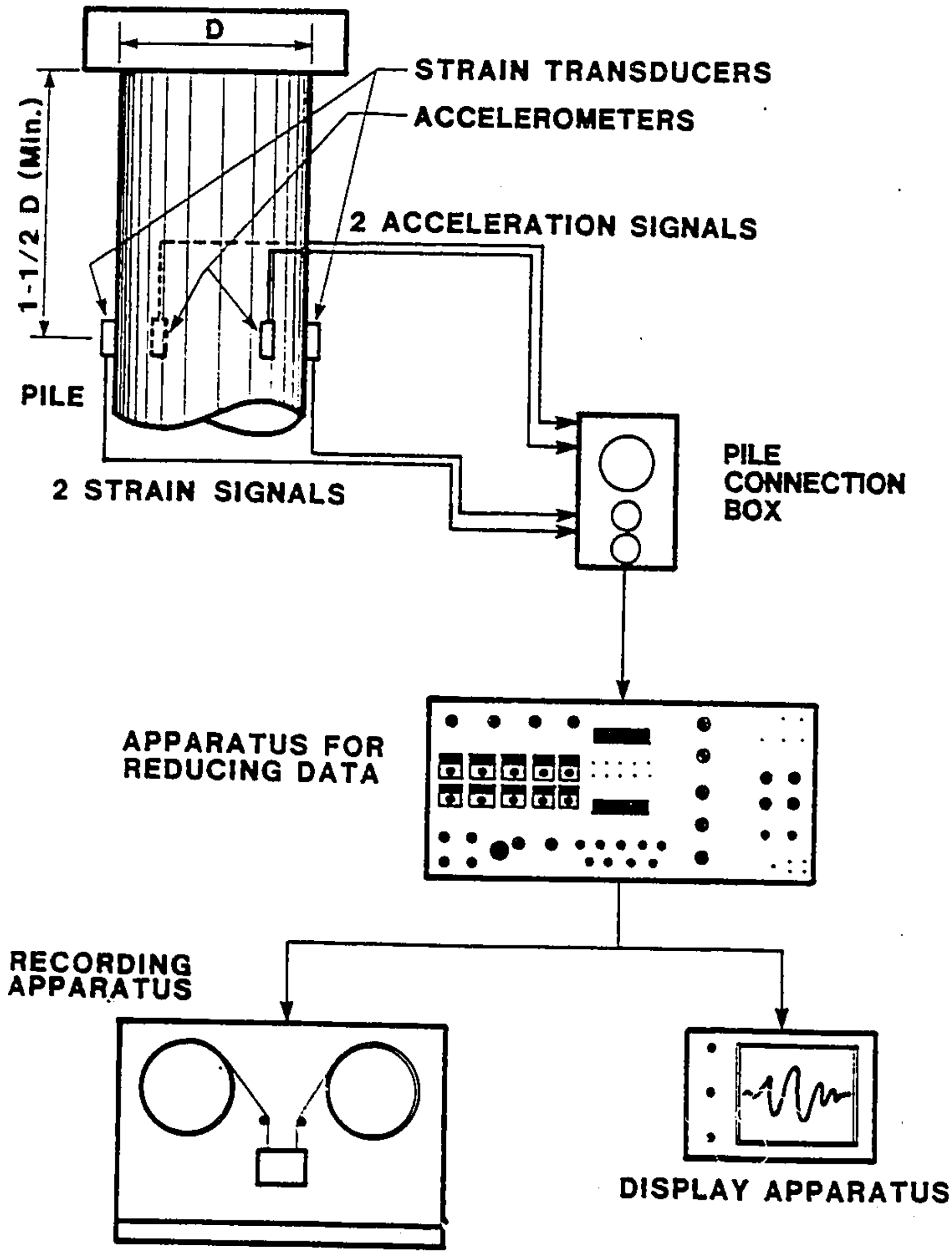

Fig. 3.4 Dynamic Data Aquisition System

(After ASTM, 1986)

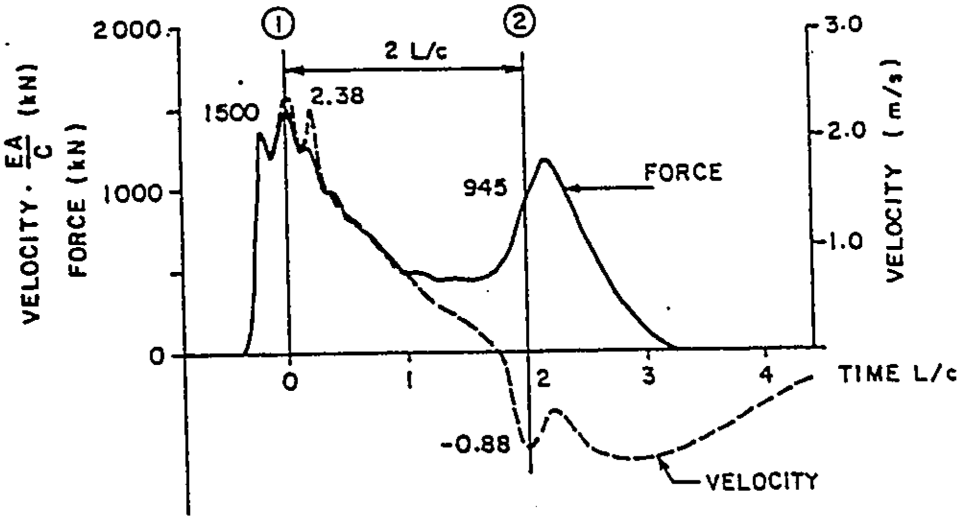

$$\text{MOBILIZED RESISTANCE} = \frac{F_1 + F_2}{2} + \frac{EA}{C} \cdot \frac{1}{2} (V_1 - V_2)$$

(dynamic and static)

$$= \frac{1500 + 945}{2} + 638 \cdot \frac{1}{2} (2.38 + 0.88)$$

$$= 2260 \text{ kN}$$

Example of measured force and velocity as wave traces drawn against time, and calculation of mobilized total soil resistance according to the Case method (Precast concrete pile: L = 34 m, A = 0.080 m^2).

Fig. 3.5 Example of Case Method Computations

(After Authier and Fellenius, 1983)

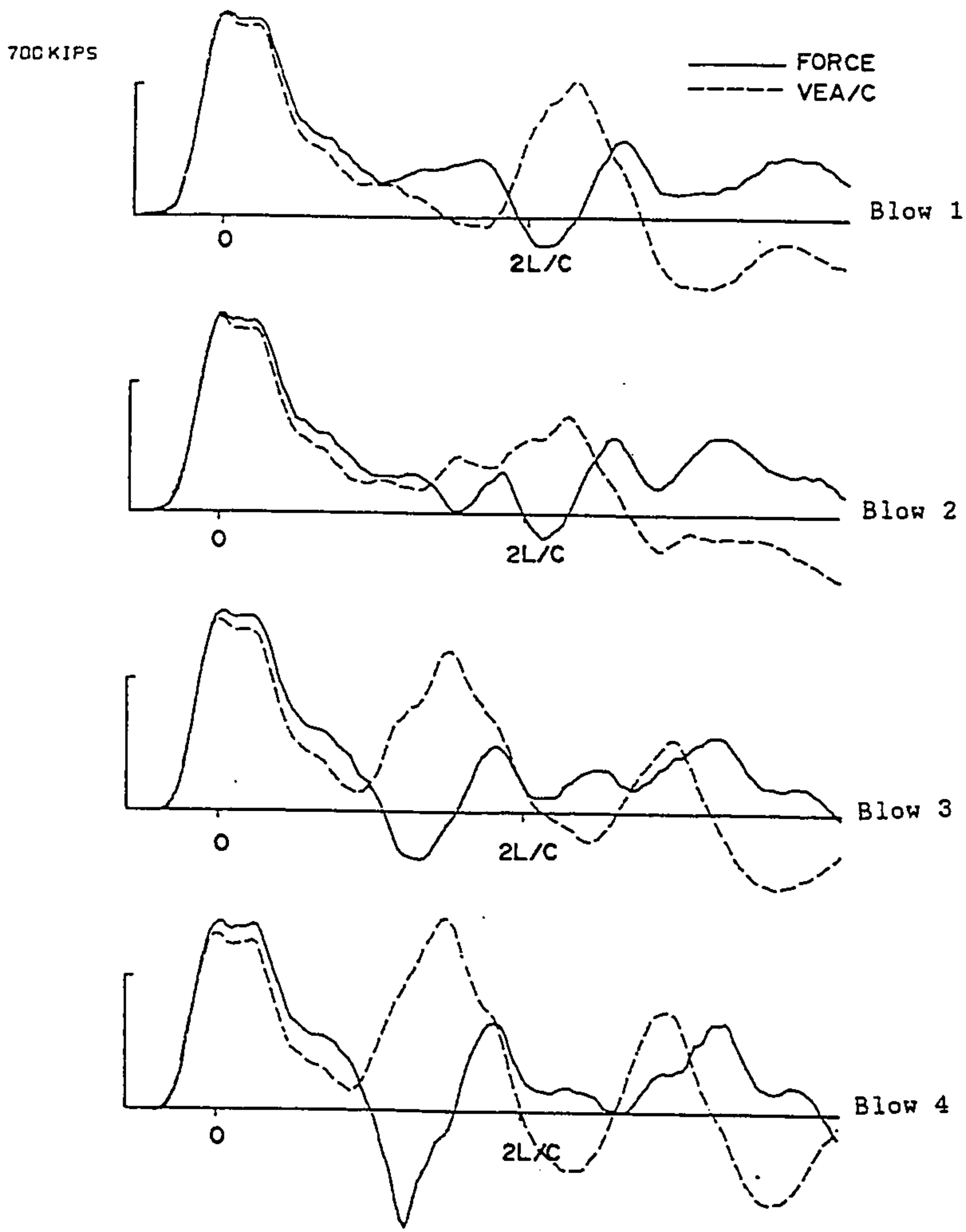

Fig. 3.6 Progressive Failure of a Concrete Pile
(After Hannigan, 1986)

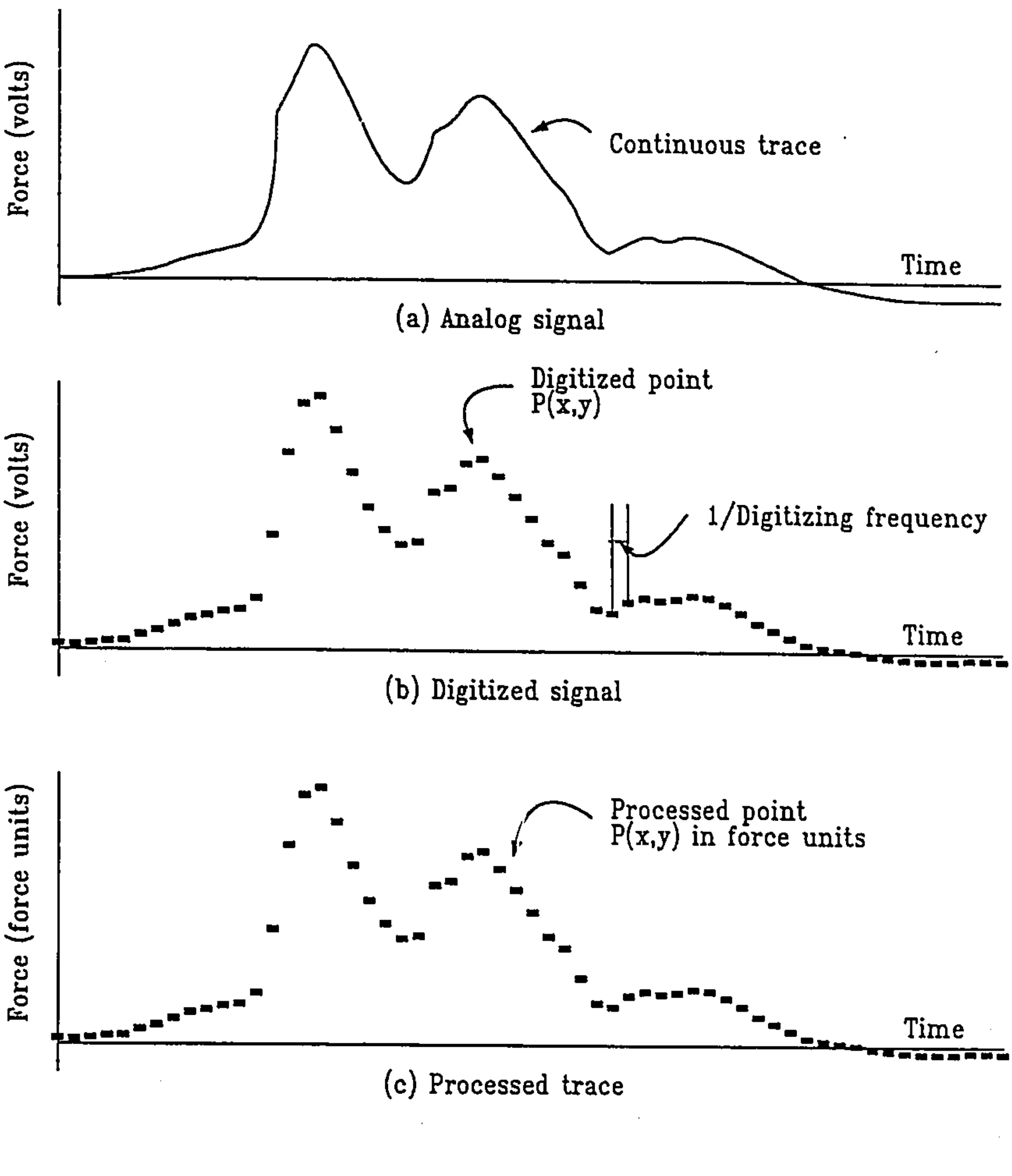

Fig. 3.7 Data Digitizing and Processing

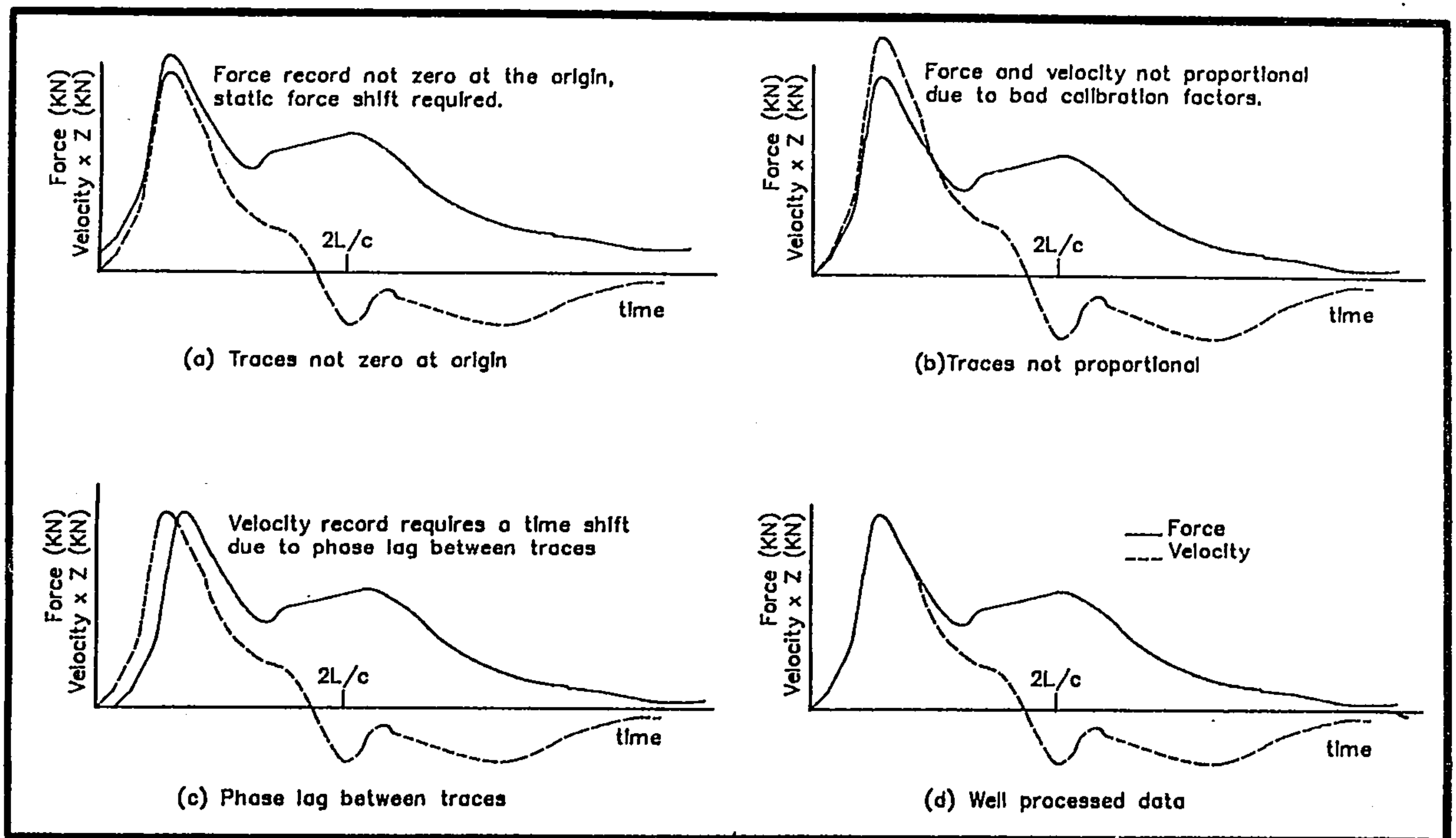

Fig. 3.8 Examples of Data Processing

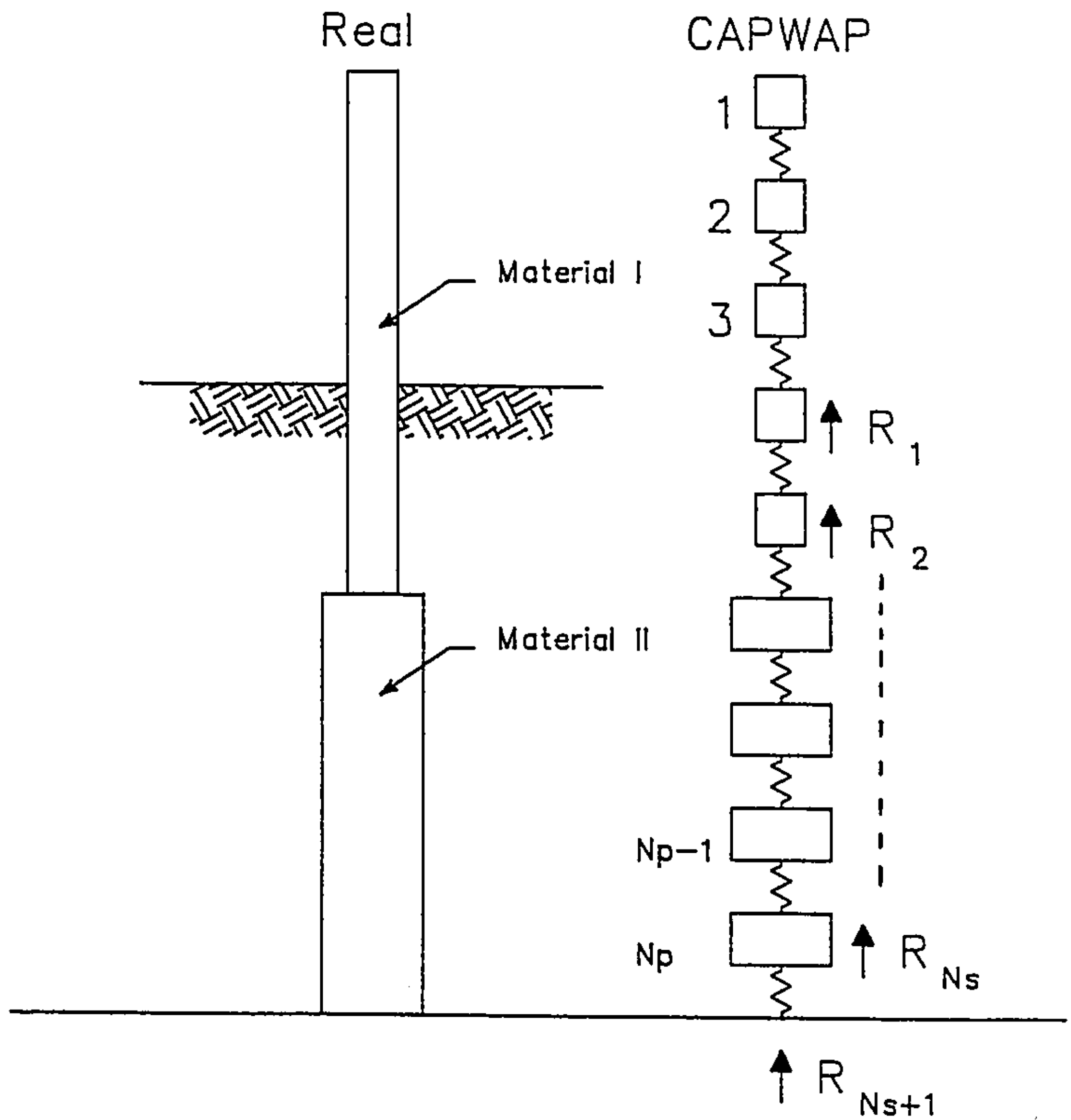

Fig. 4.1 Lumped Mass CAPWAP Model

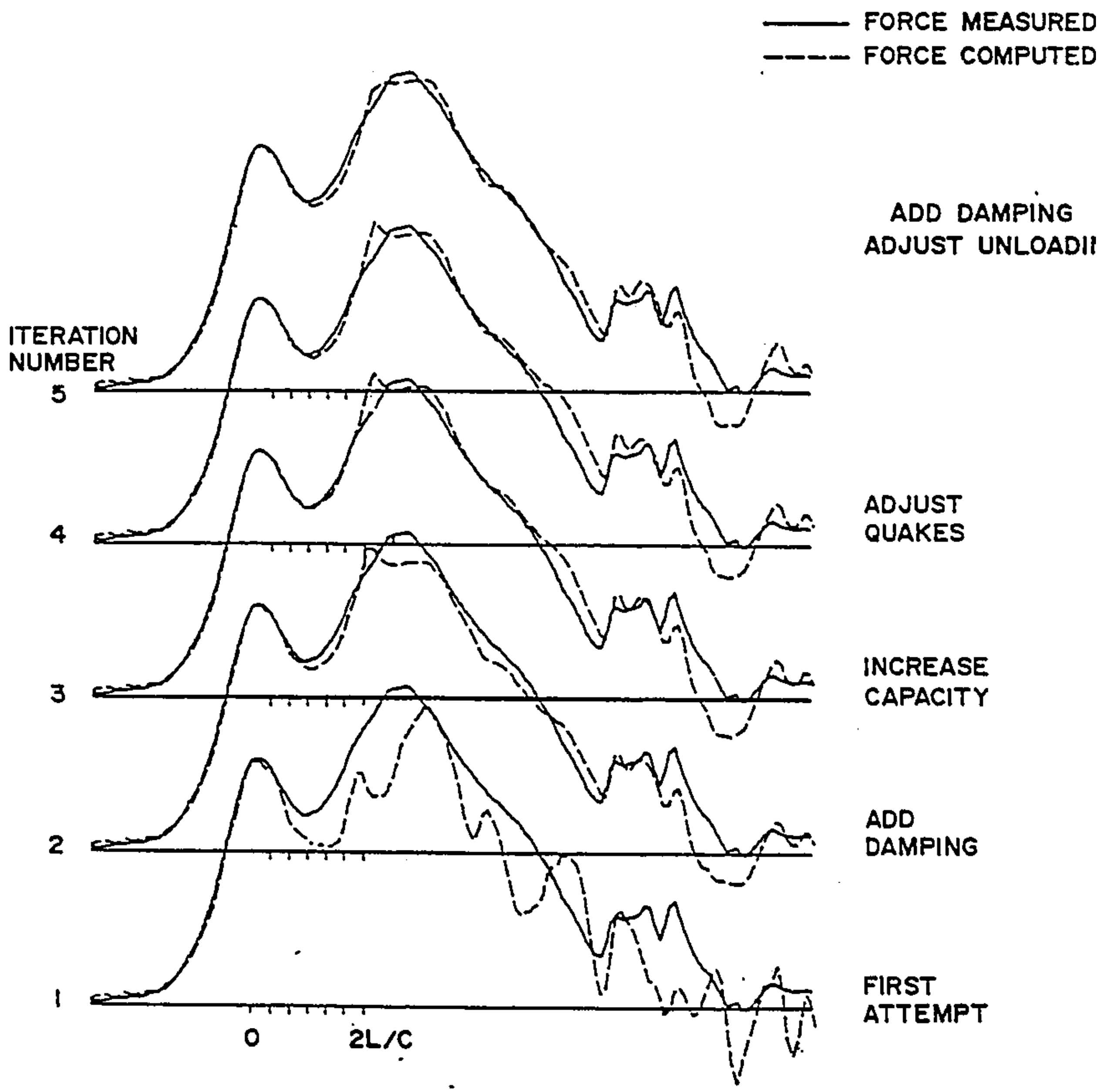

Fig. 4.2 Example of CAPWAP Iterations

(After Hannigan, 1986)

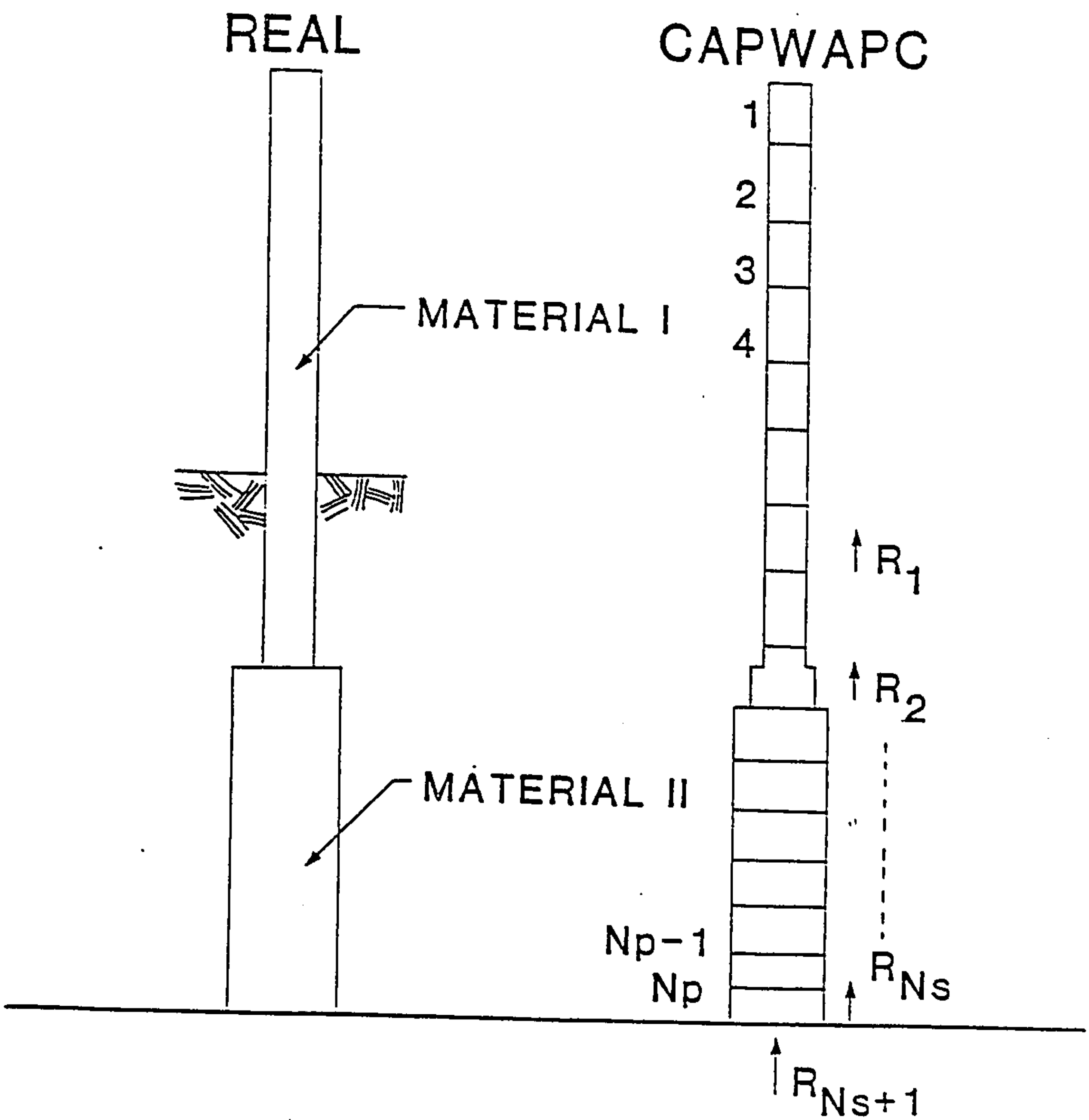

Fig. 4.3 Continuous CAPWAP Model
(After Rausche, 1986)

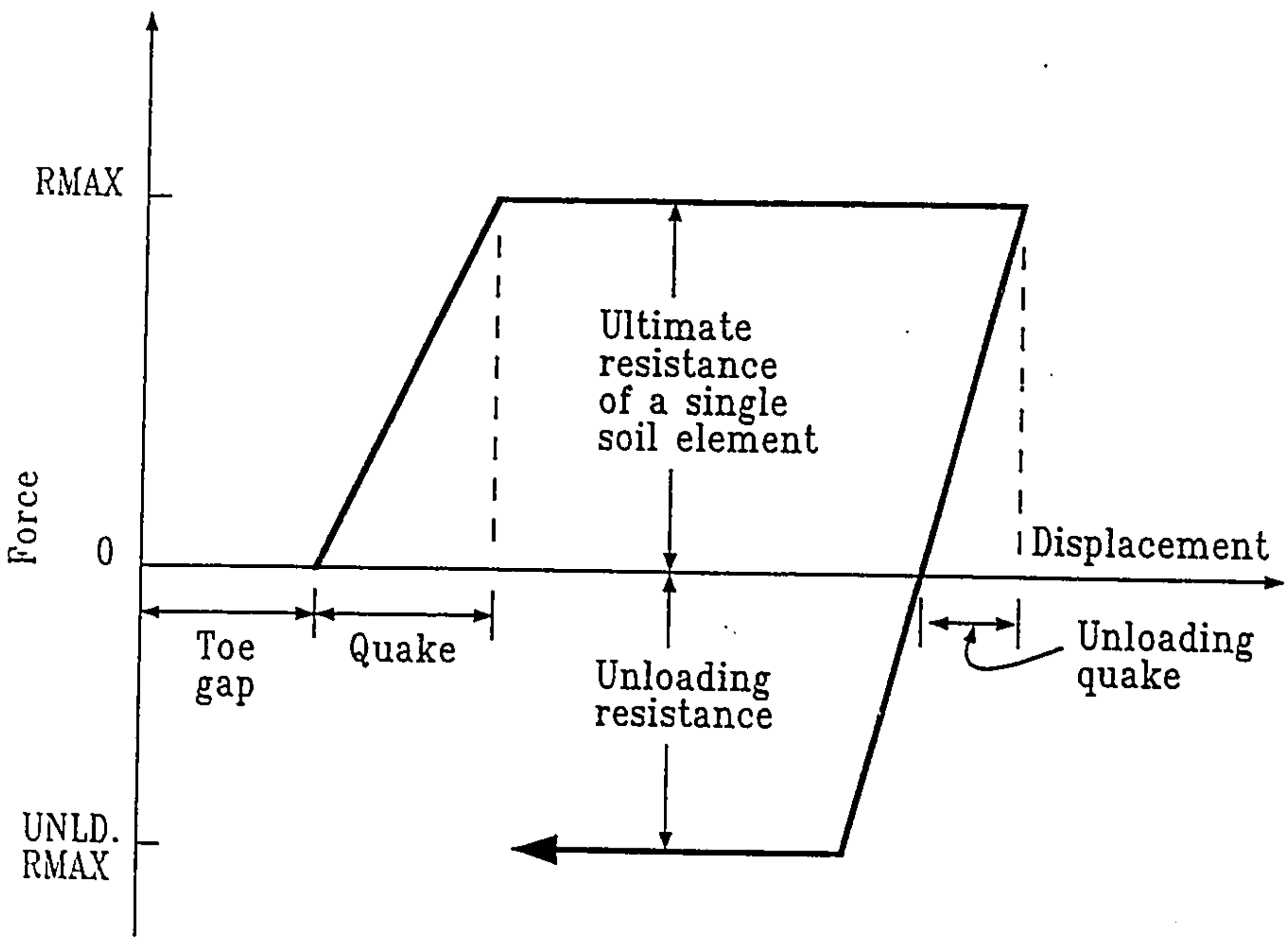

Fig. 4.4 Toe Gap

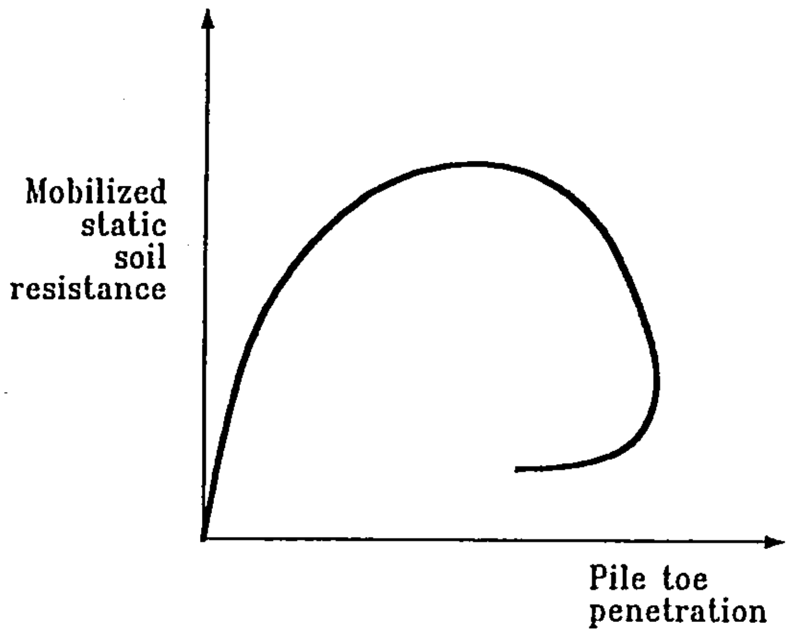

(a)
Force-Displacement curve for pile driving in rock

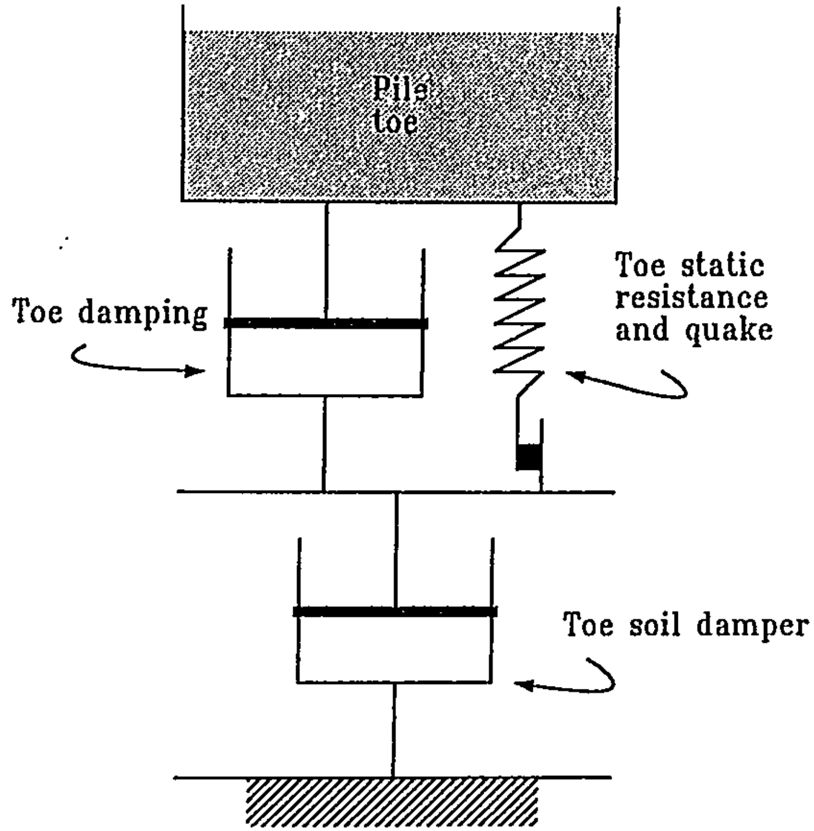

(b)
Toe soil damper

Fig. 4.5 Toe Soil Damper

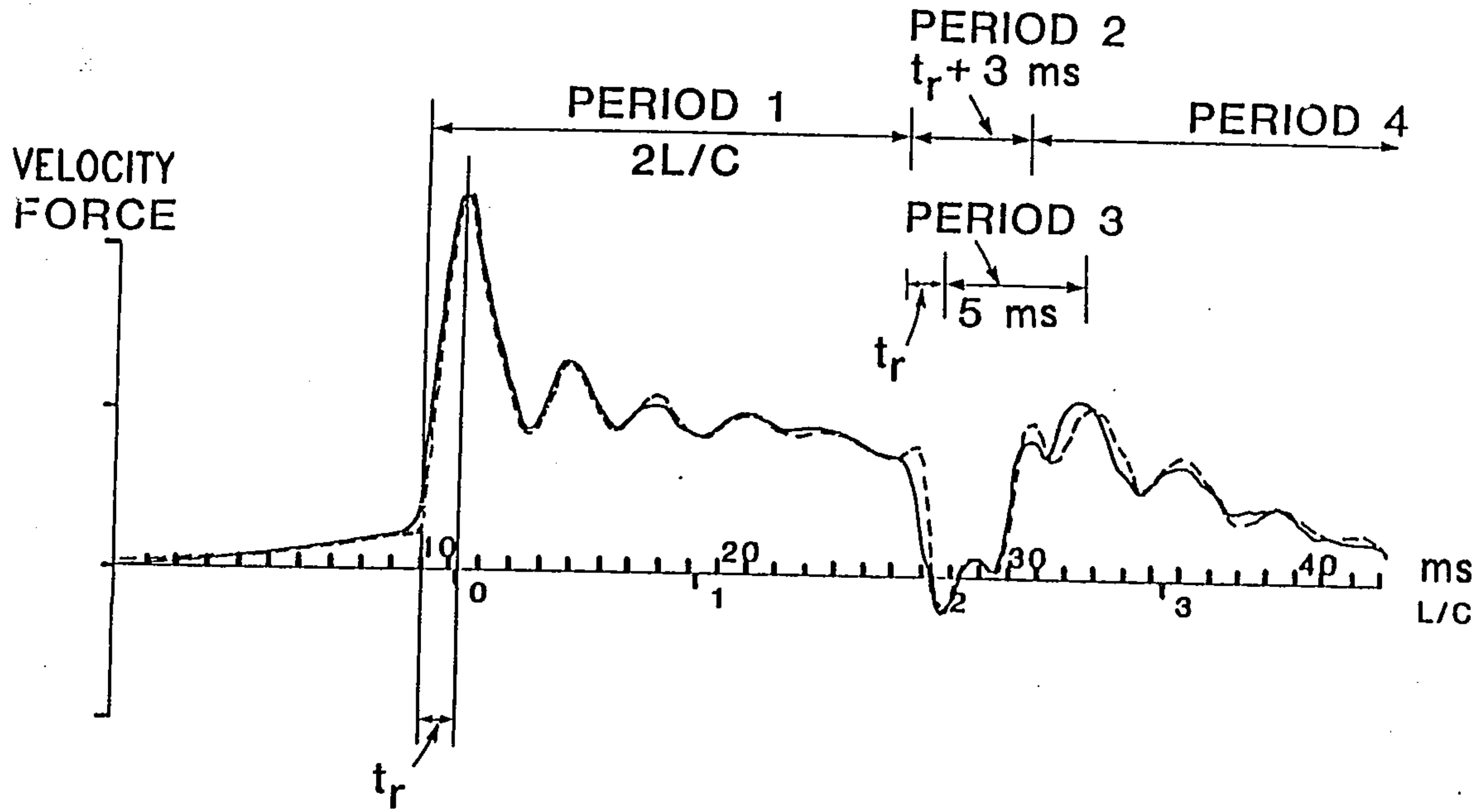

Fig. 4.6 Subdivisions of a CAPWAP Trace

(After Rausche, 1986)

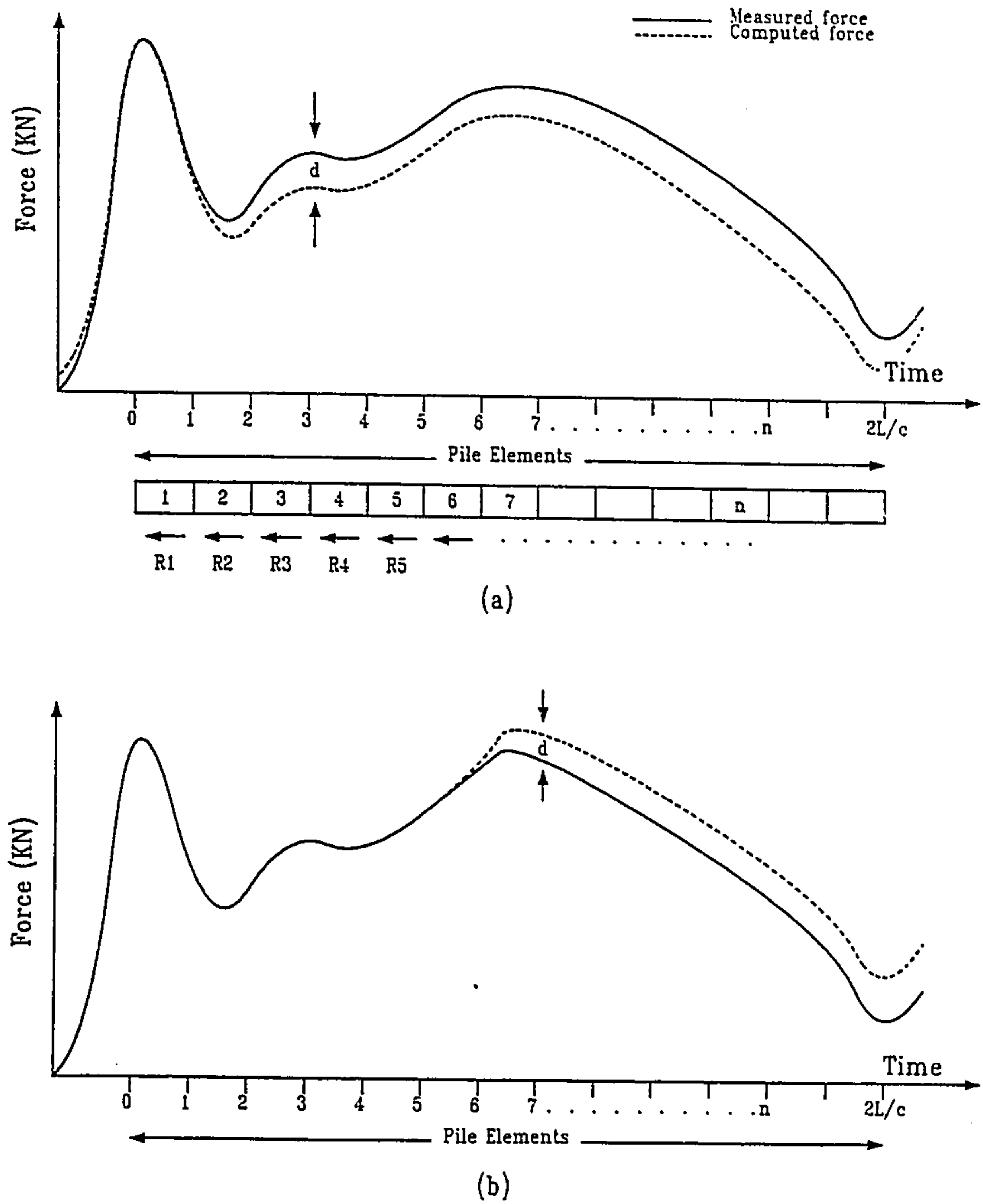

Fig. 4.7 Effect of Soil Resistance Distribution

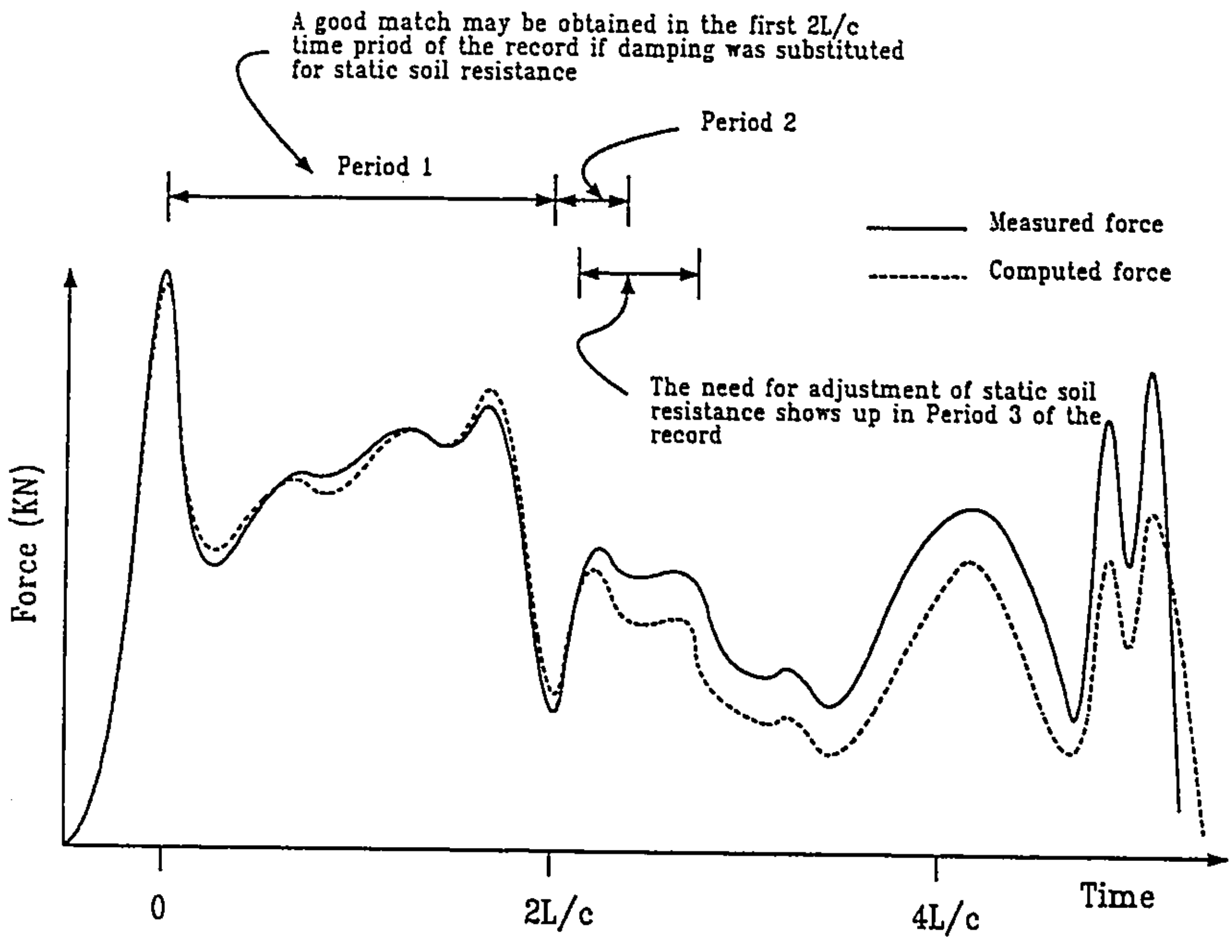

Fig. 4.8 Effect of Ultimate Soil Resistance

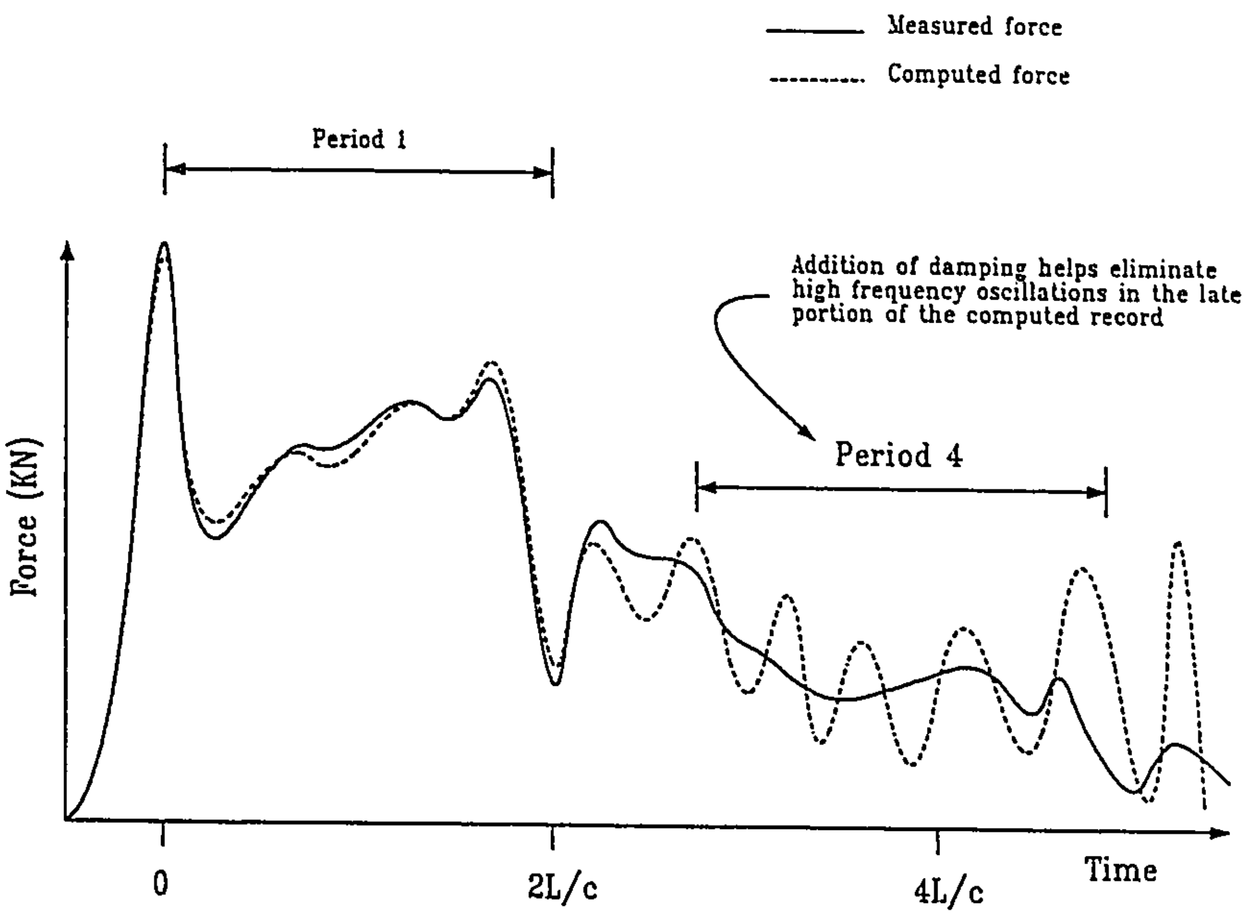

Fig. 4.9 Effect of Damping

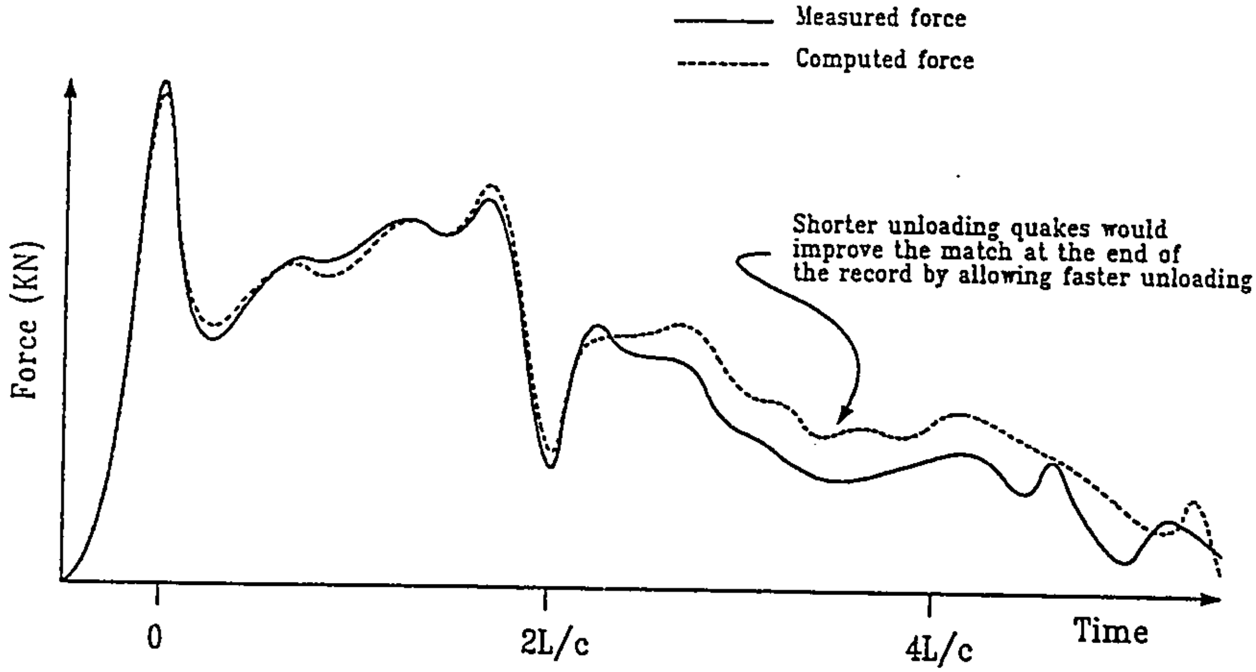

(a)

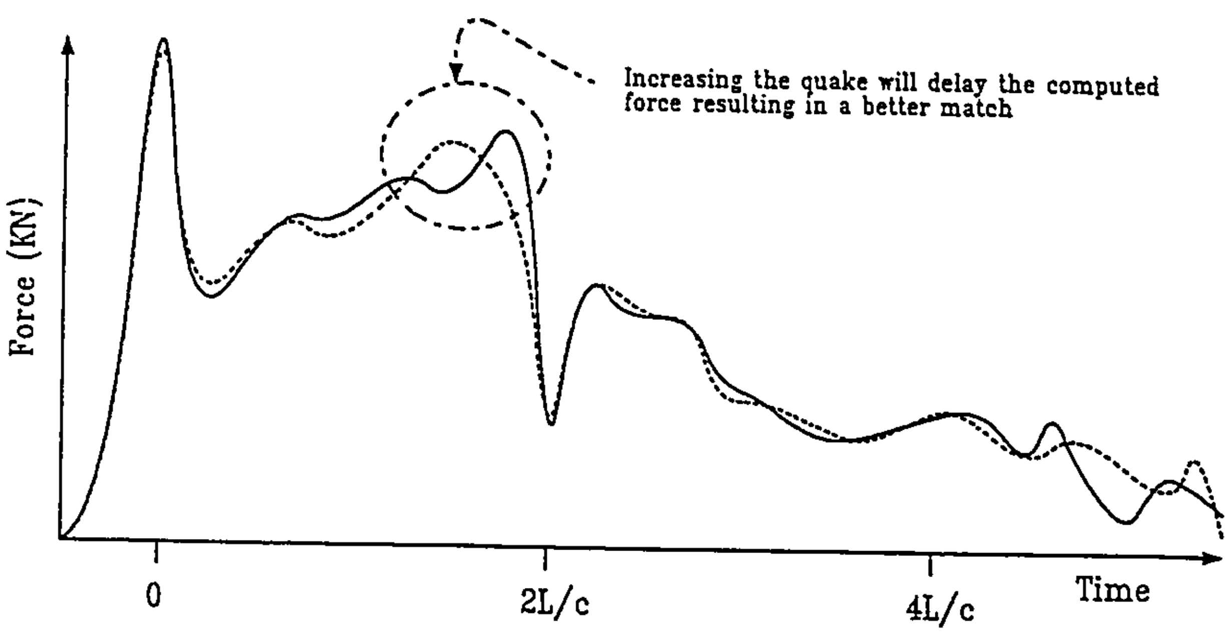

(b)

Fig. 4.10 Effect of Quakes

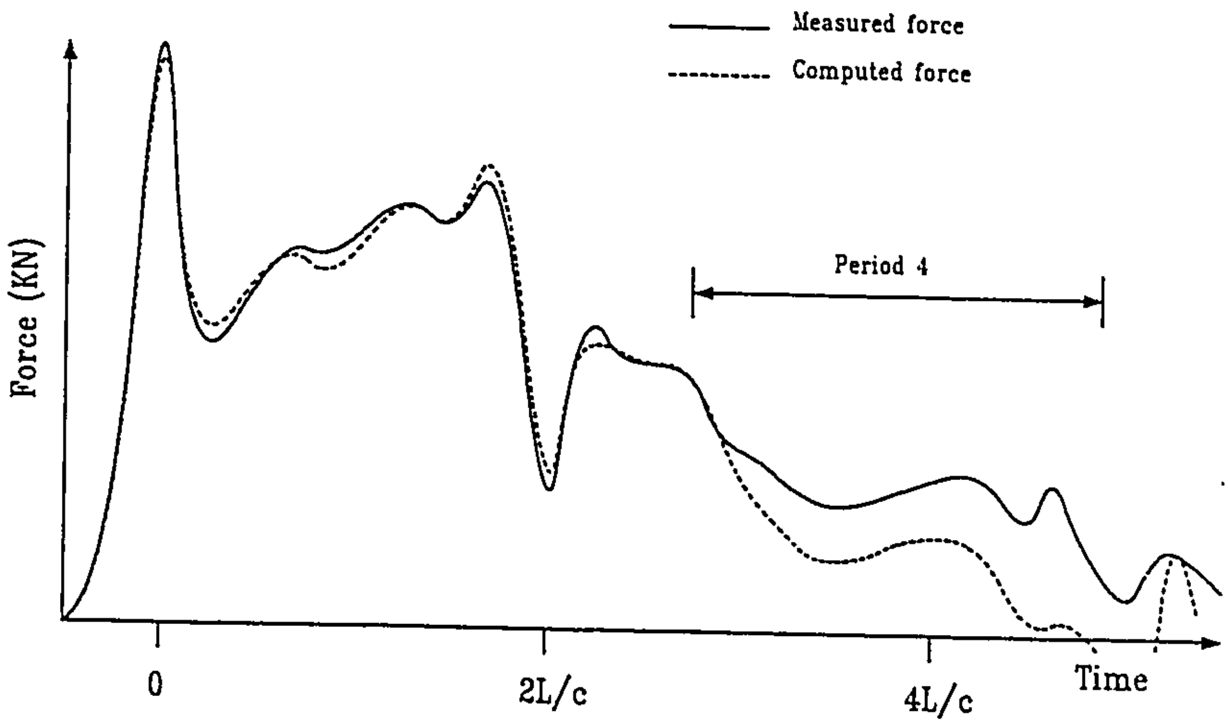

Fig. 4.11 Effect of Unloading Resistance

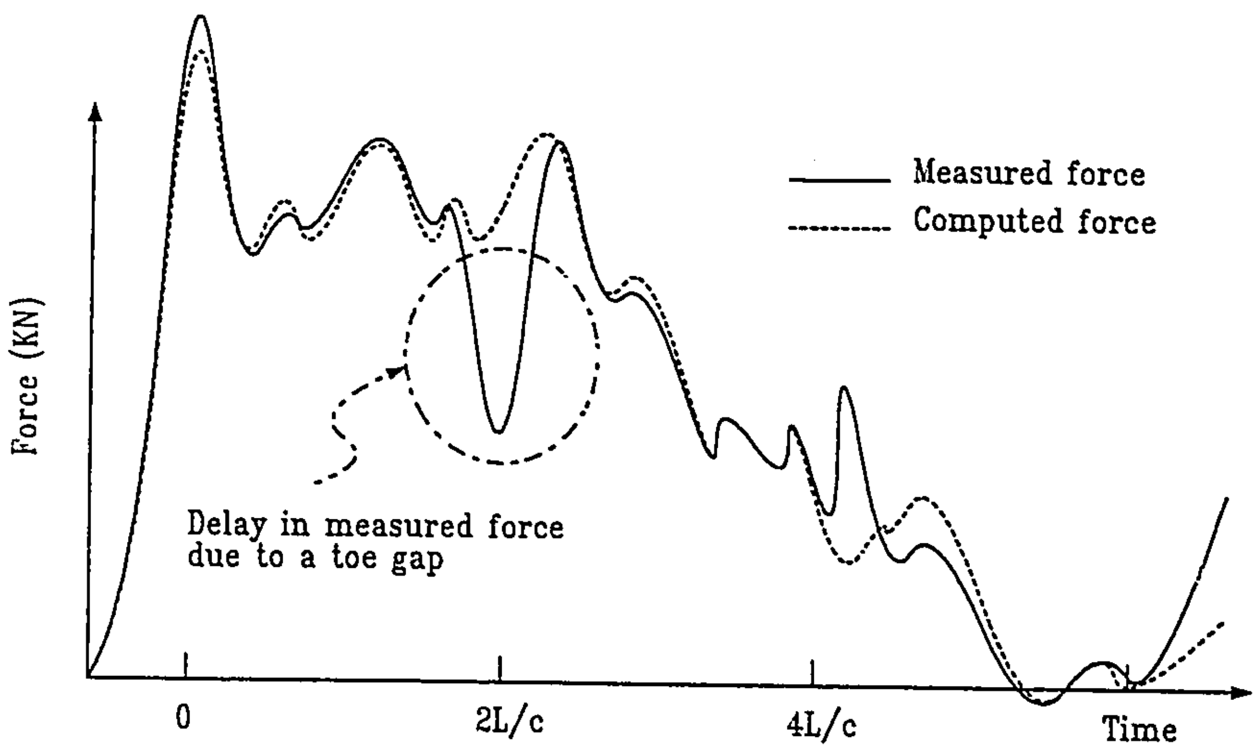

Fig. 4.12 Effect of a Toe Gap

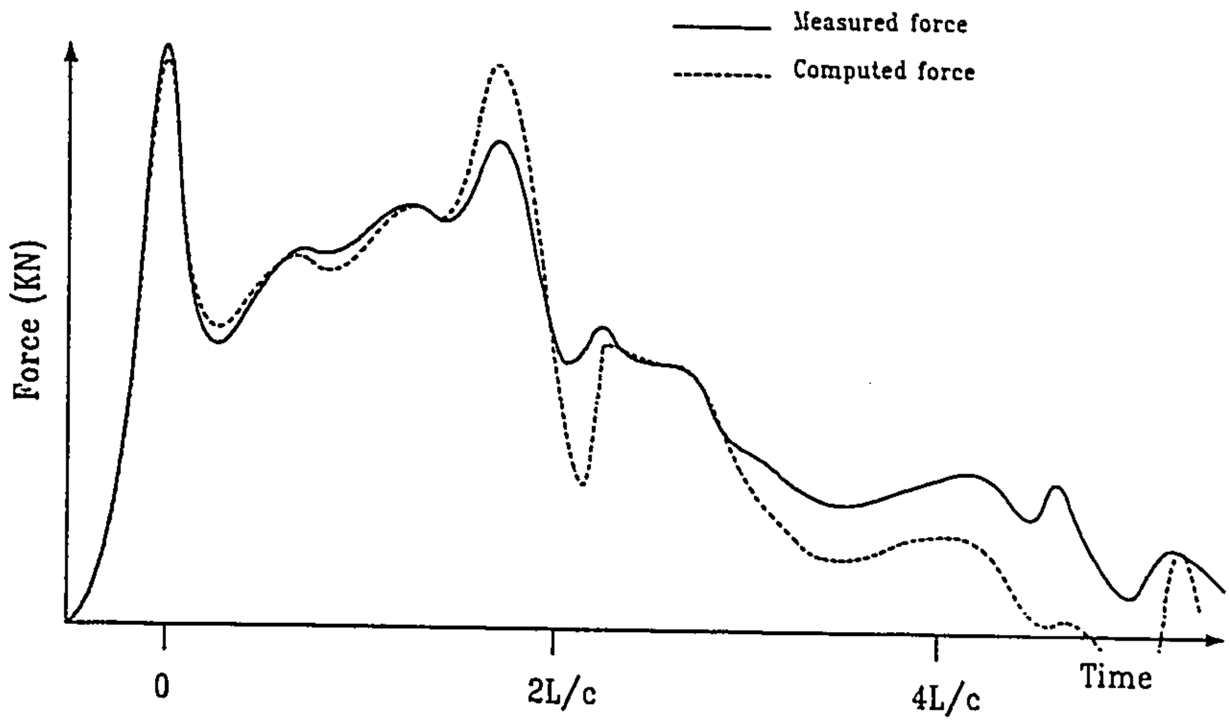

Fig. 4.13 Effect of a Soil Plug

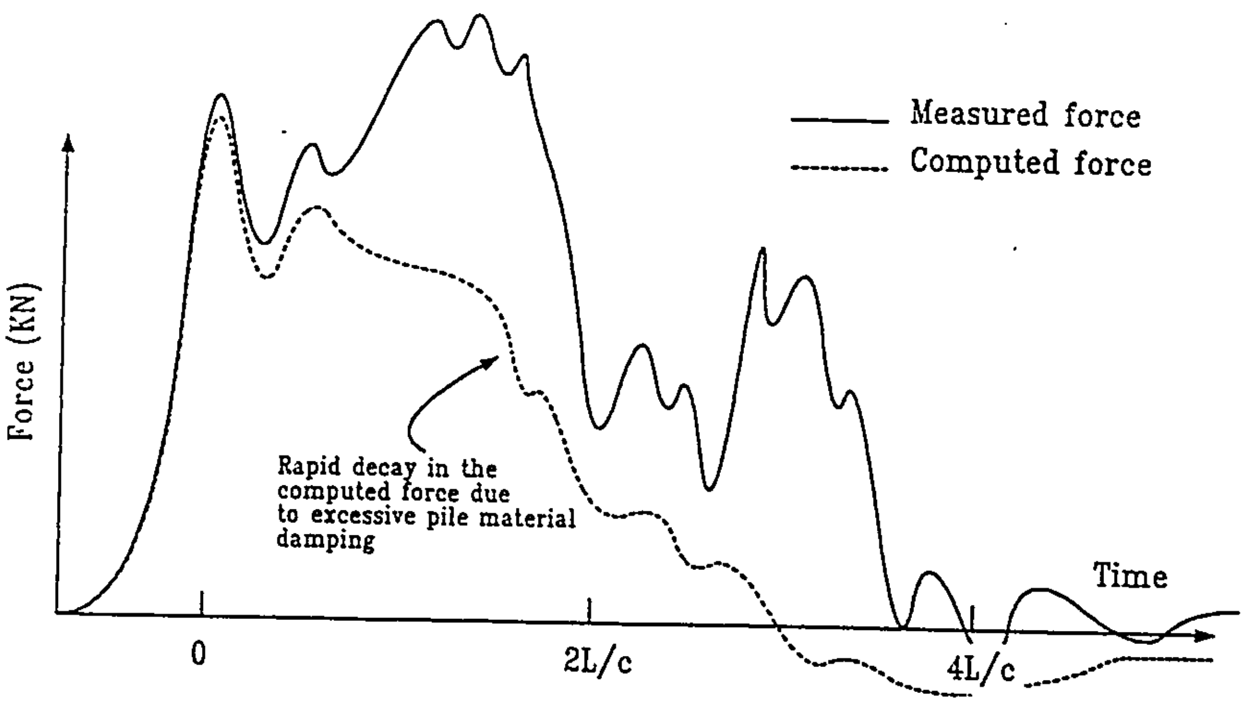

(a)

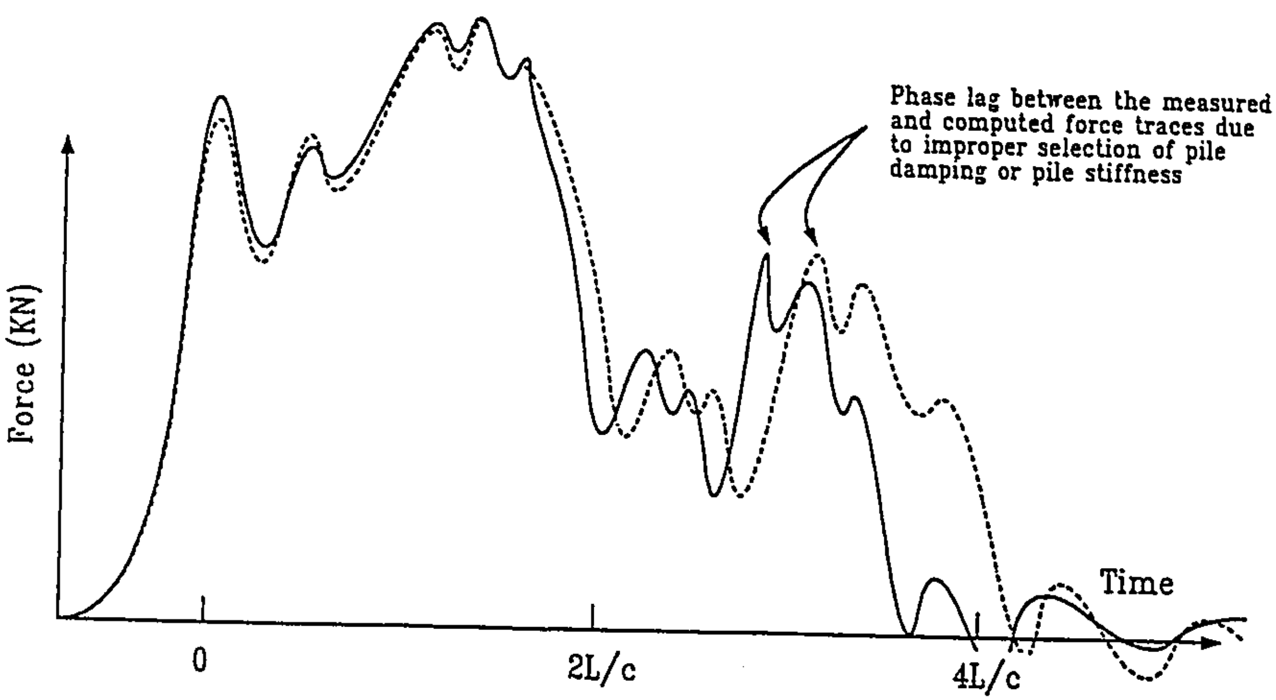

(b)

Fig. 4.14 Effect of Pile Parameters

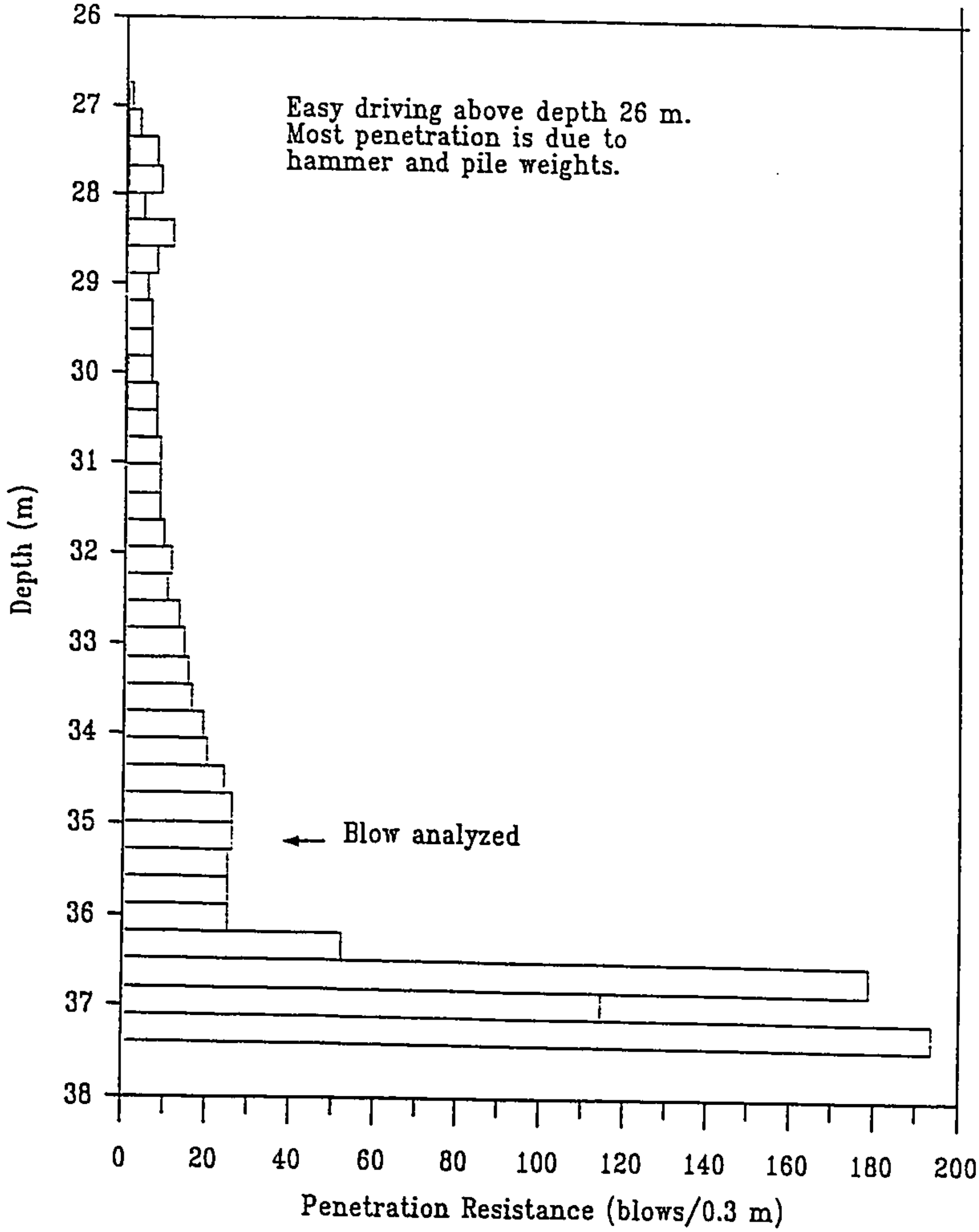

Fig. 5.1 Pile Driving Diagram, JI Pile

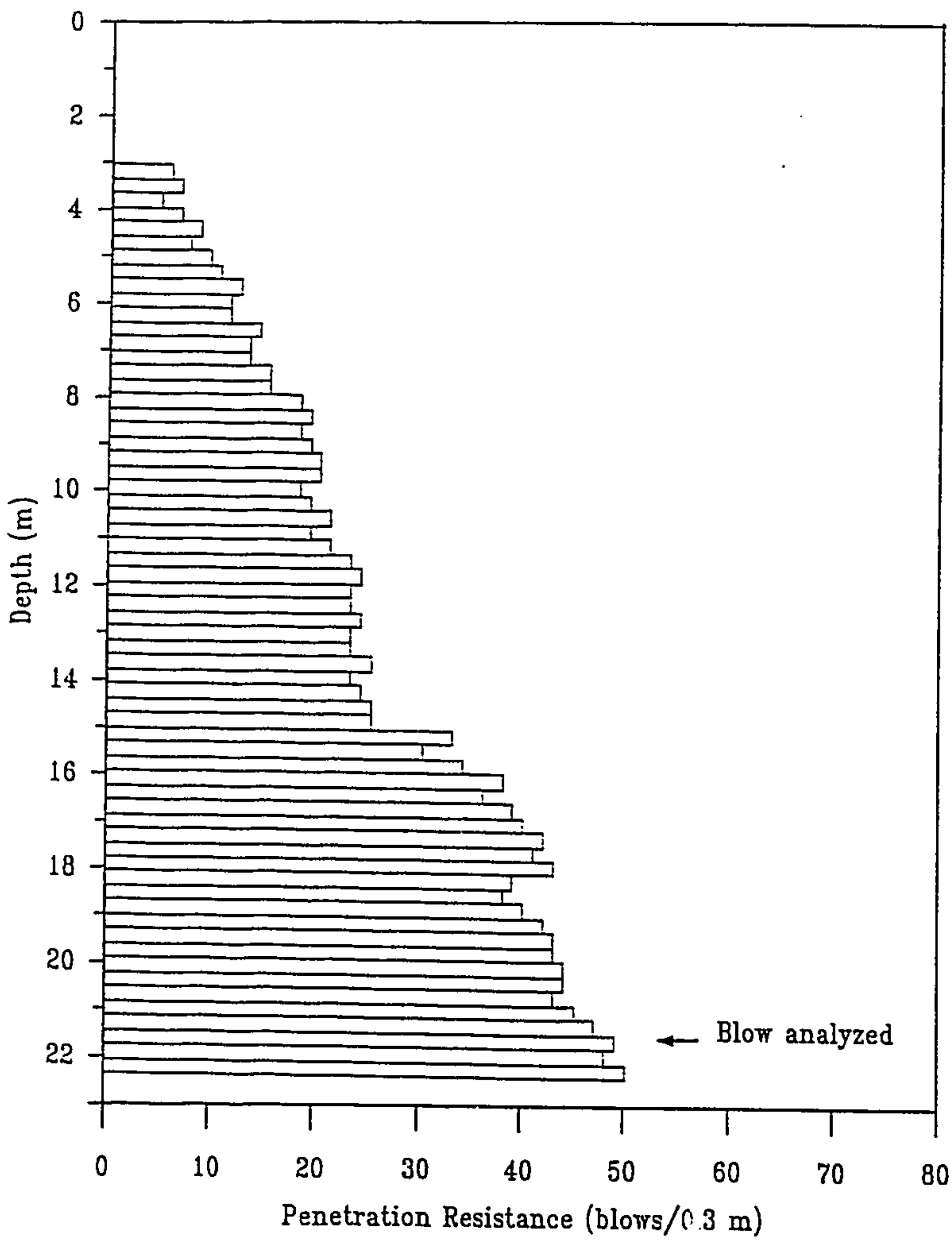

Fig. 5.2 Pile Driving Diagram, JA Pile

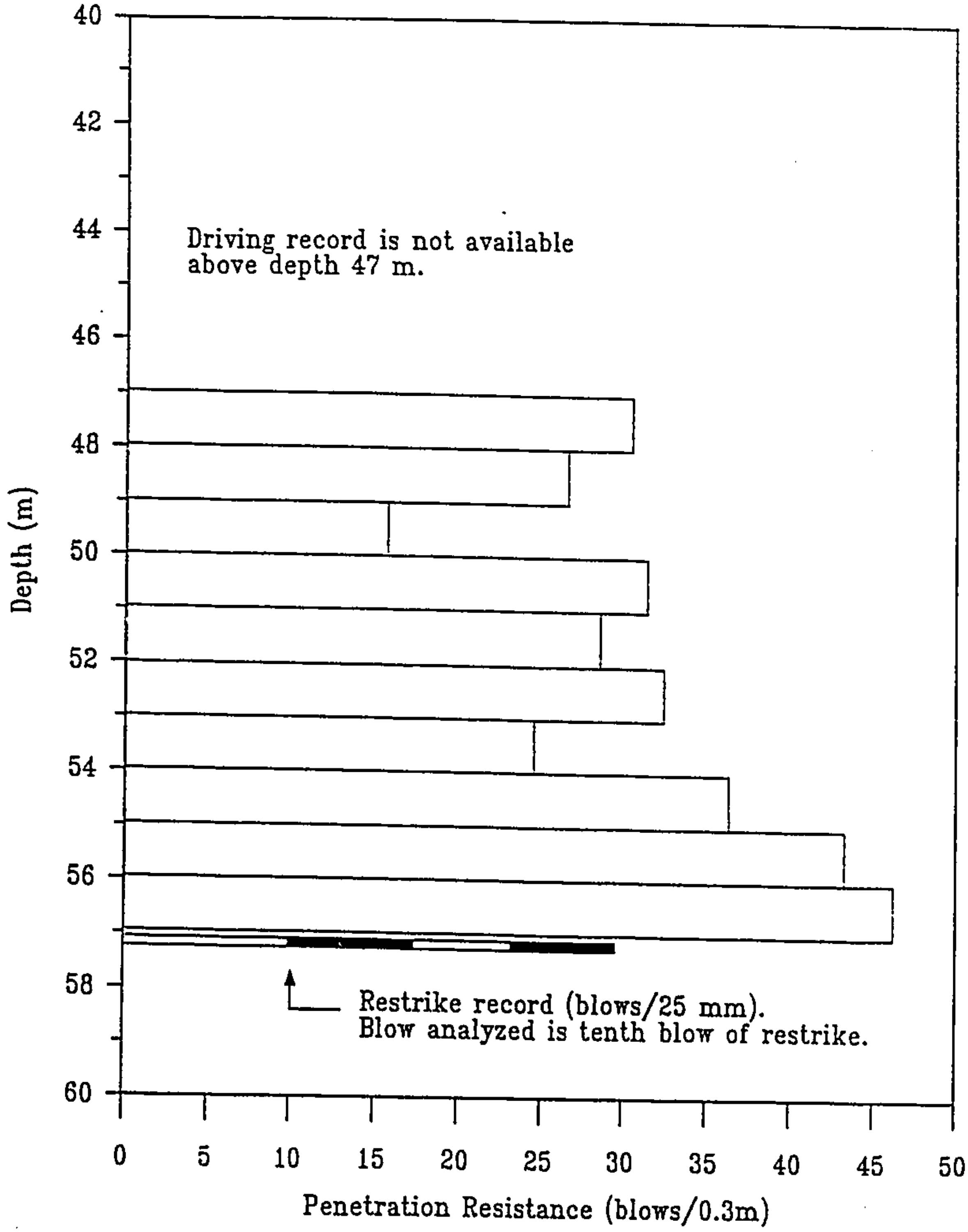

Fig. 5.3 Pile Driving Diagram, AM Pile

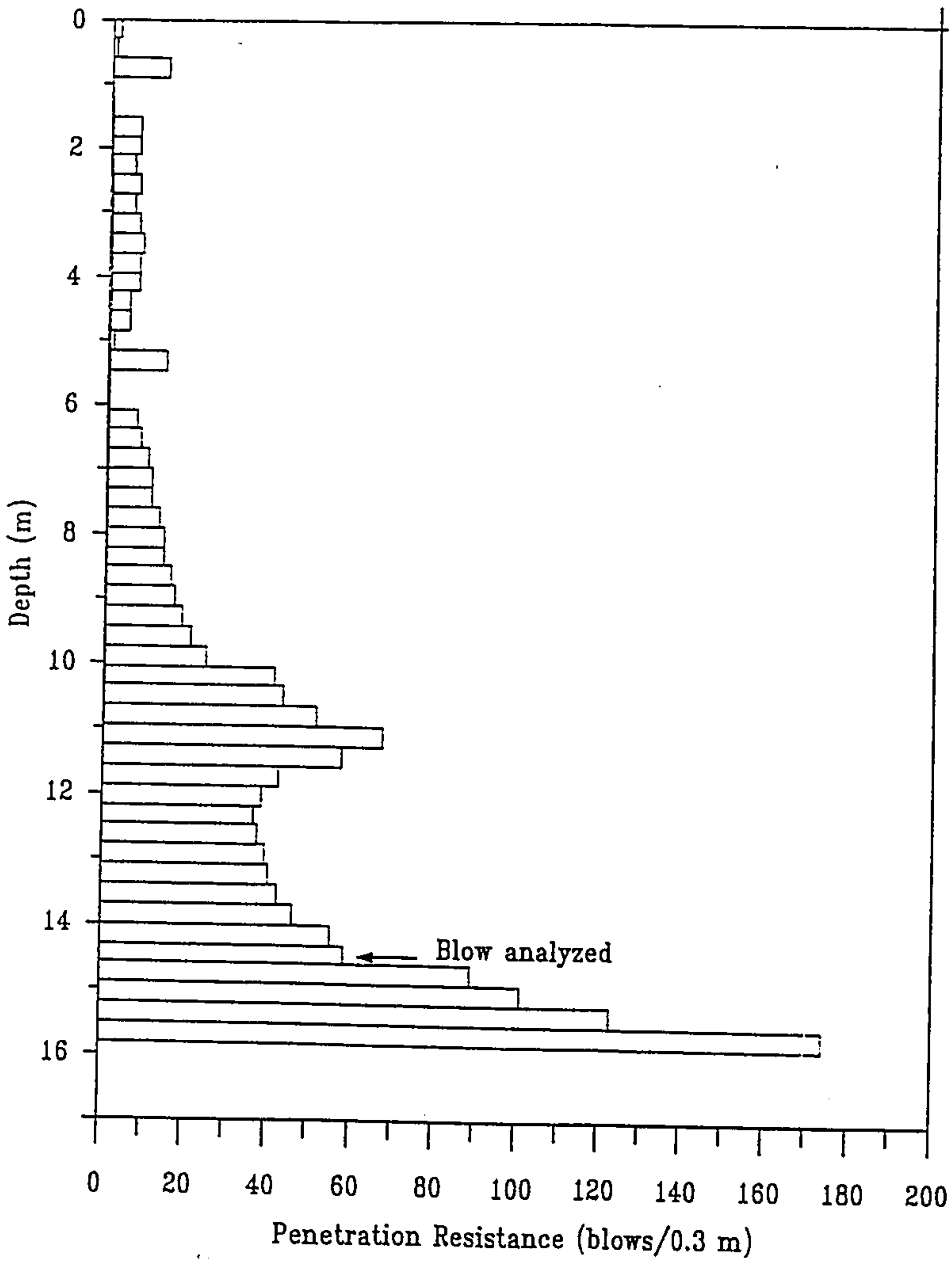

Fig. 5.4 Pile Driving Diagram, LW Pile

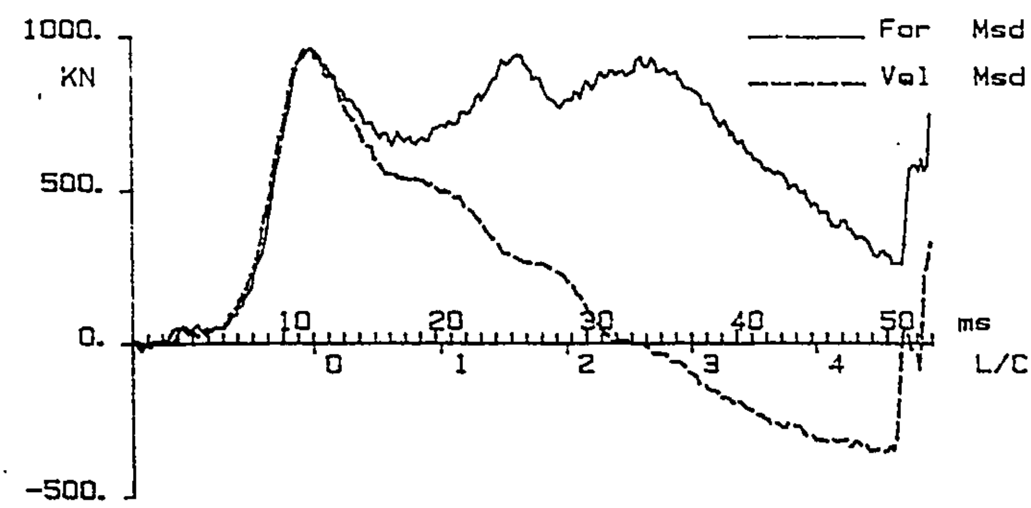

Fig. 5.5 Dynamic Data, JI Pile

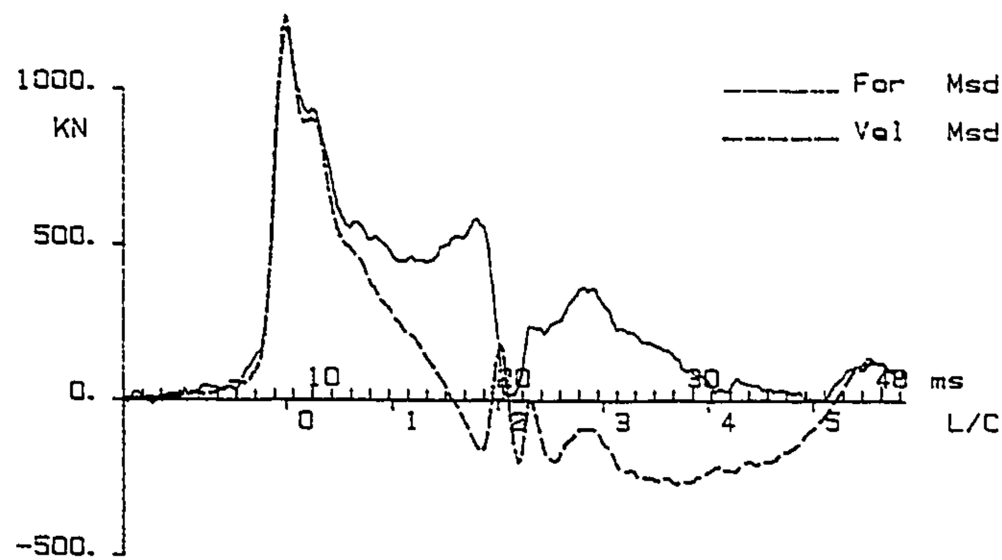

Fig. 5.6 Dynamic Data, JA Pile

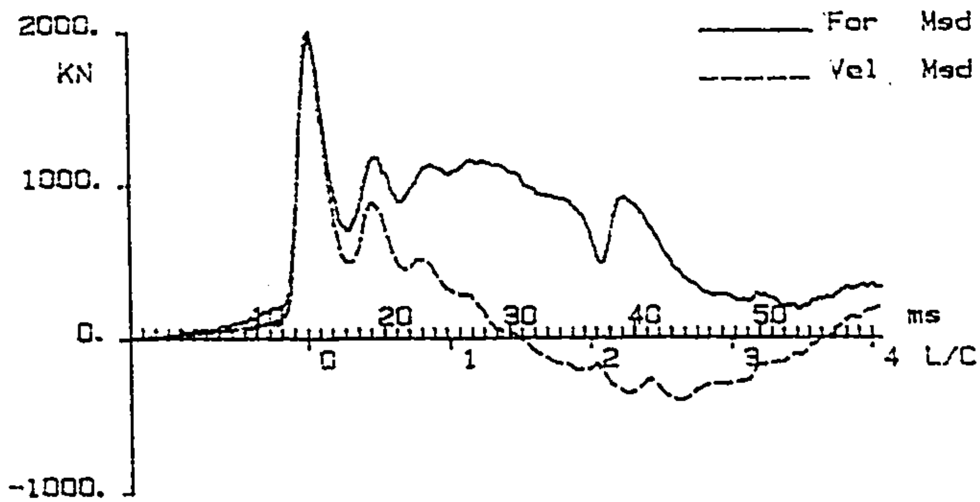

Fig. 5.7 Dynamic Data, AM Pile

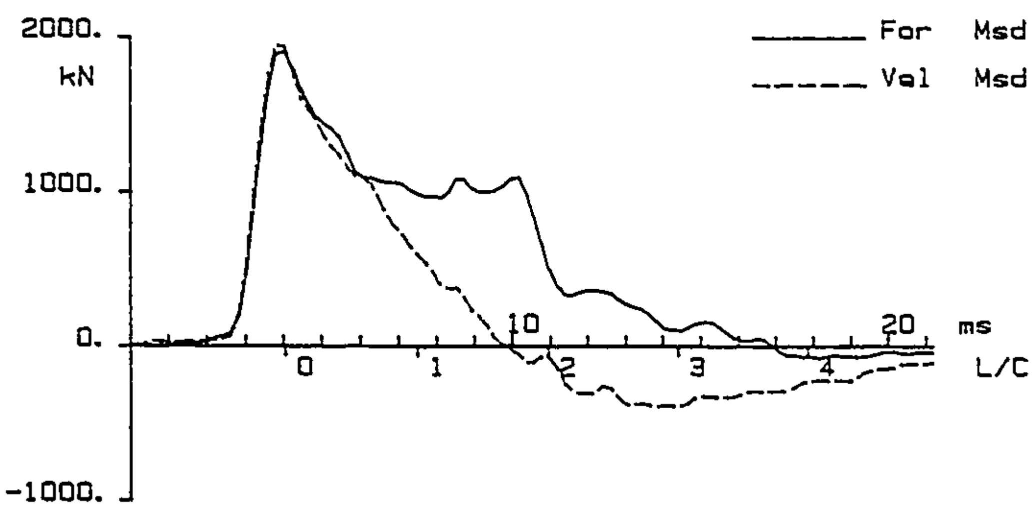

Fig. 5.8 Dynamic Data, LW Pile

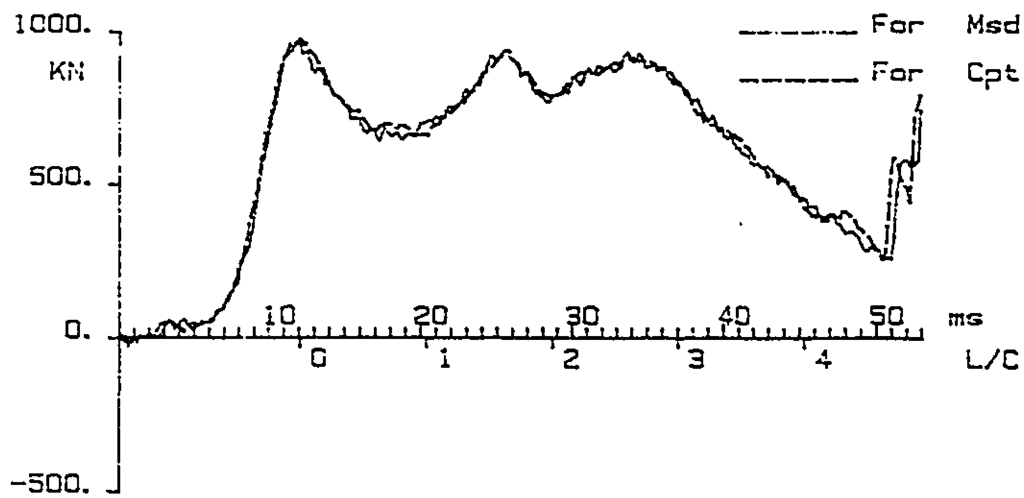

(a) CAPWAP Solution at 1000 KN

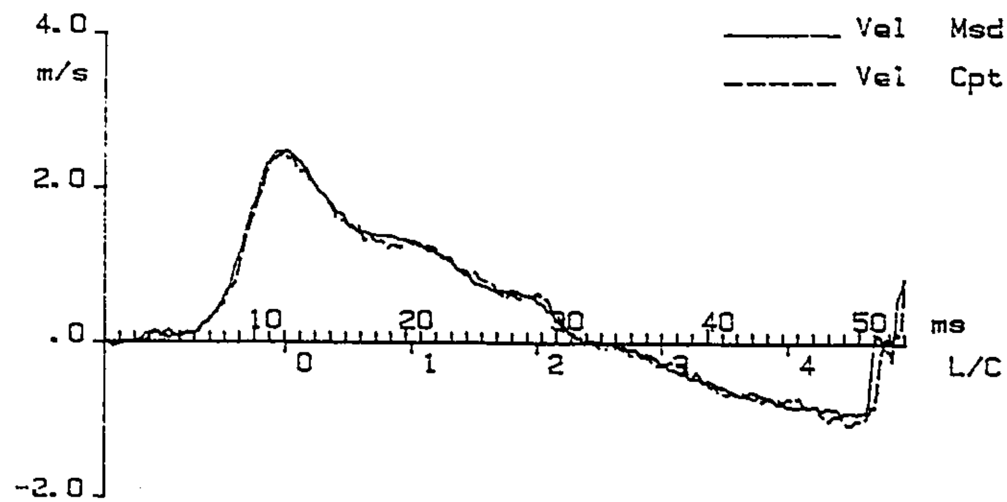

(b) WAPCAP Solution at 1000 KN

Fig. 6.1 JI Pile, Reference Matches

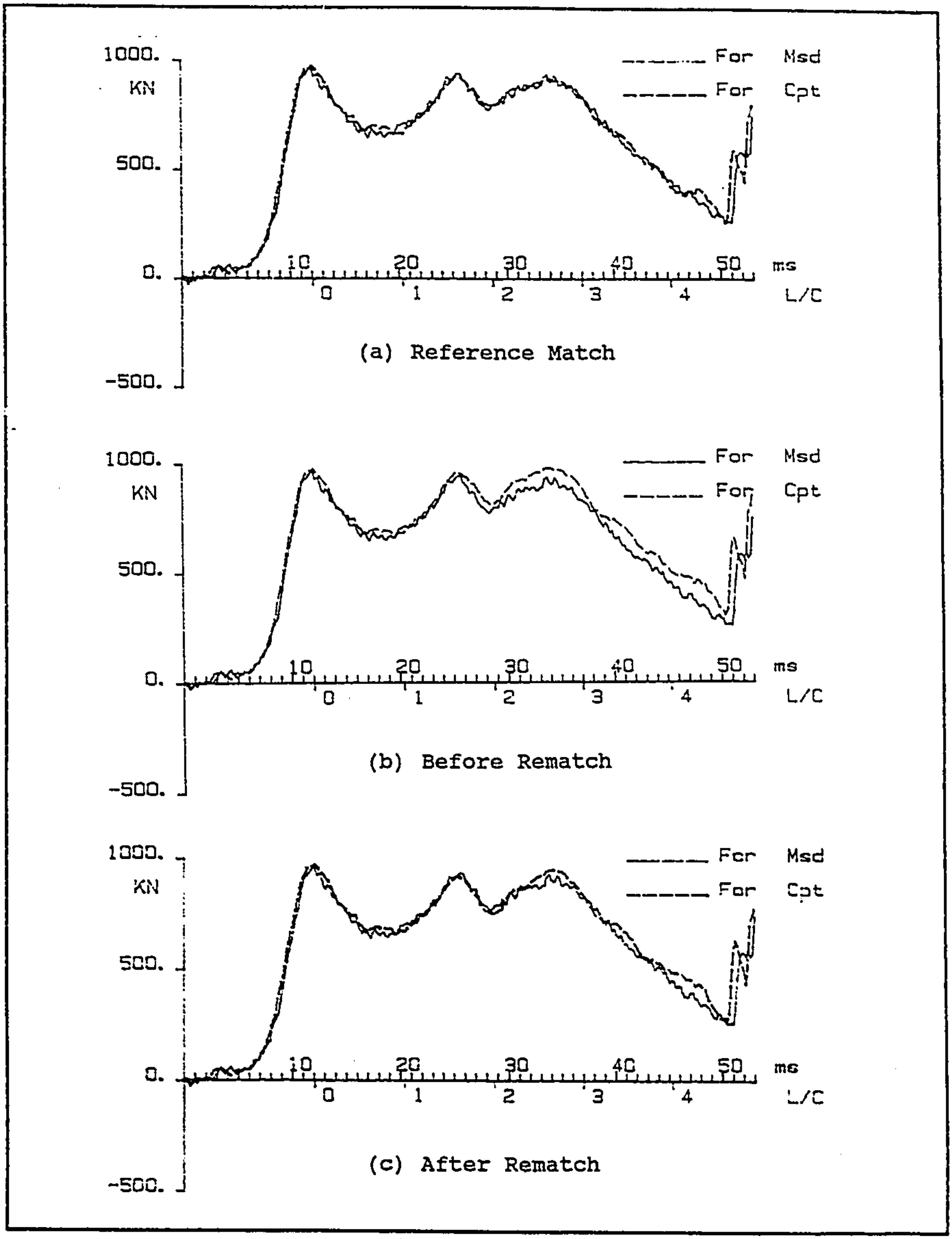

Fig. 6.2 JI Pile, CAPWAP Solution at 1050 KN

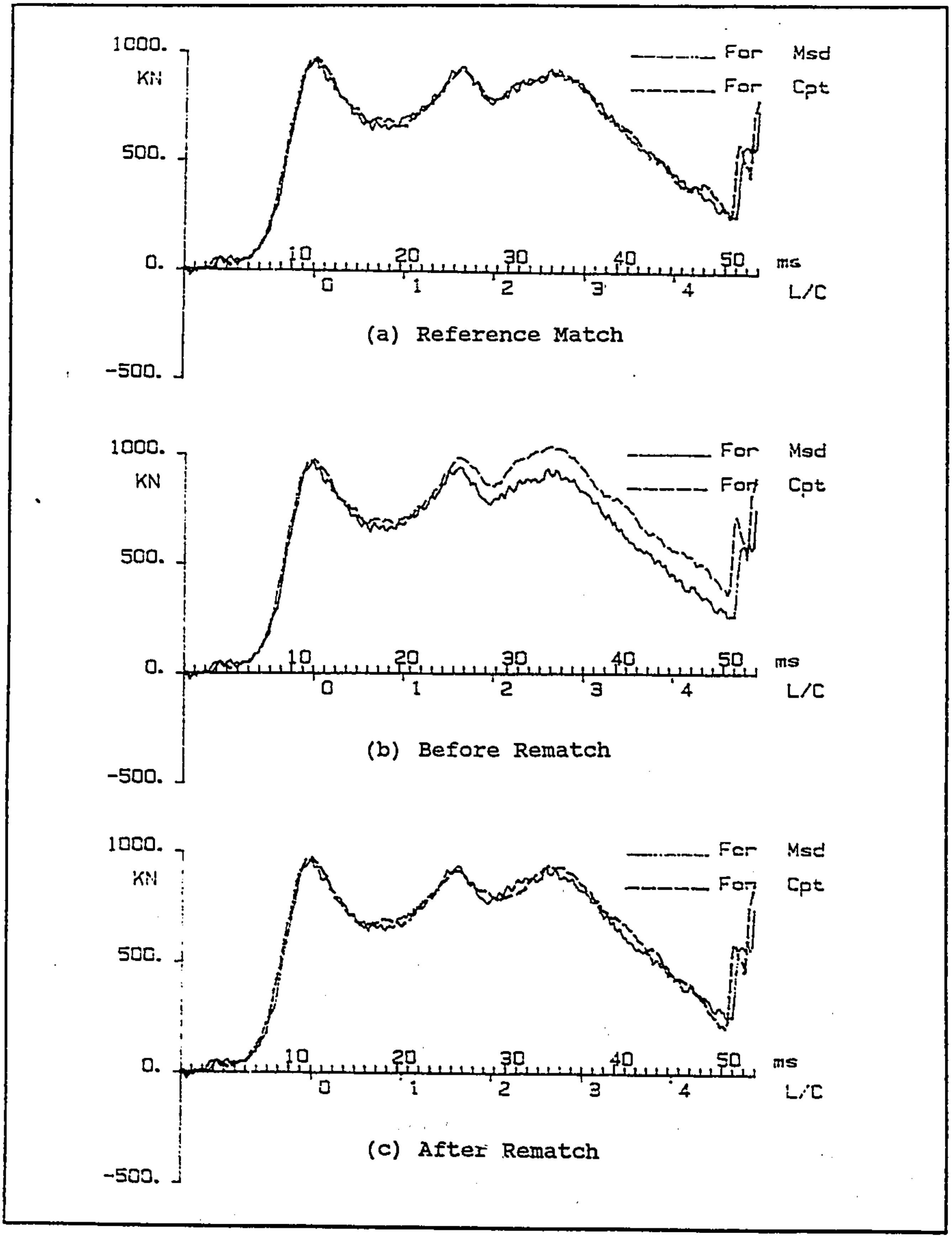

Fig. 6.3 JI Pile, CAPWAP Solution at 1100 KN

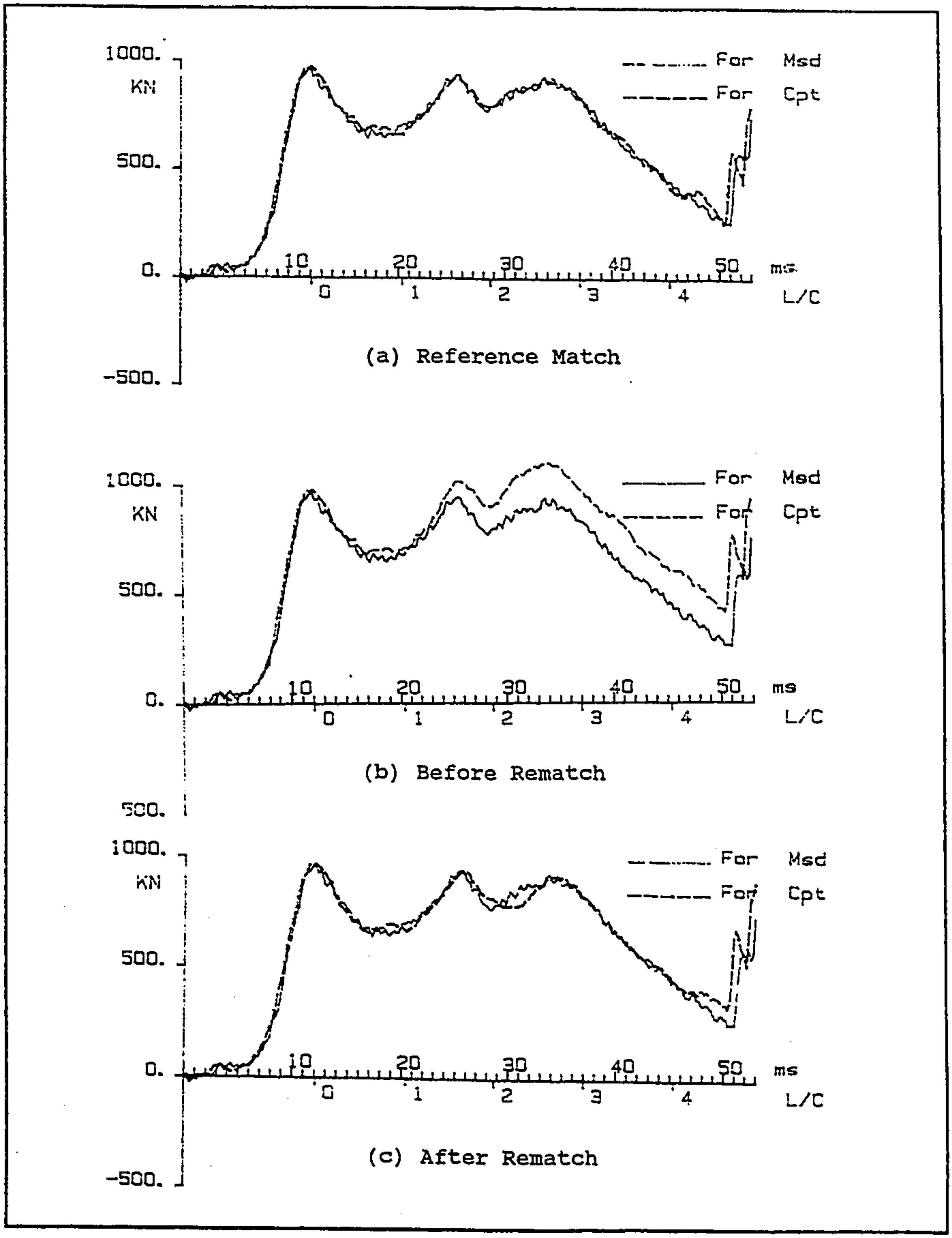

Fig. 6.4 JI Pile, CAPWAP Solution at 1150 KN

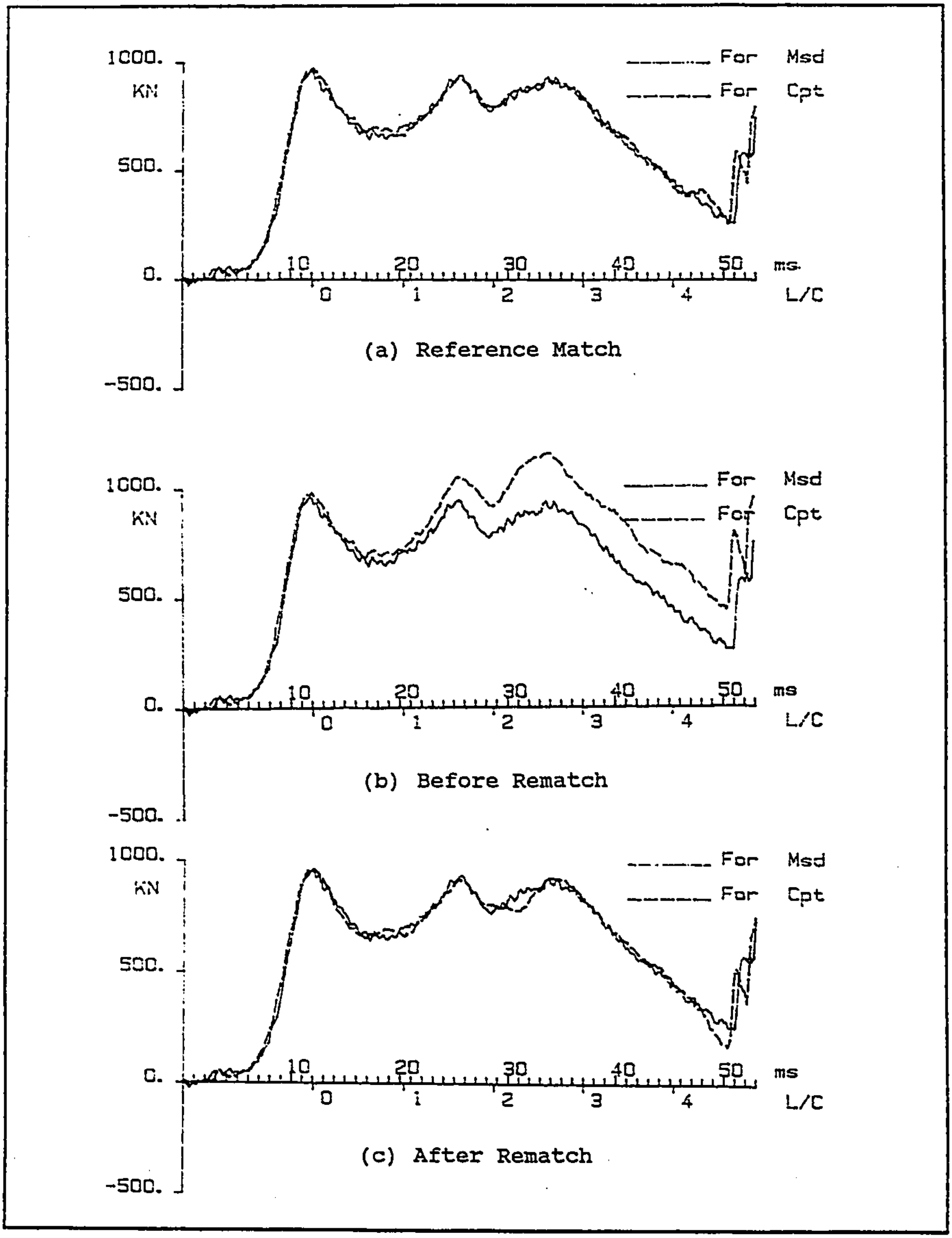

Fig. 6.5 JI Pile, CAPWAP Solution at 1200 KN

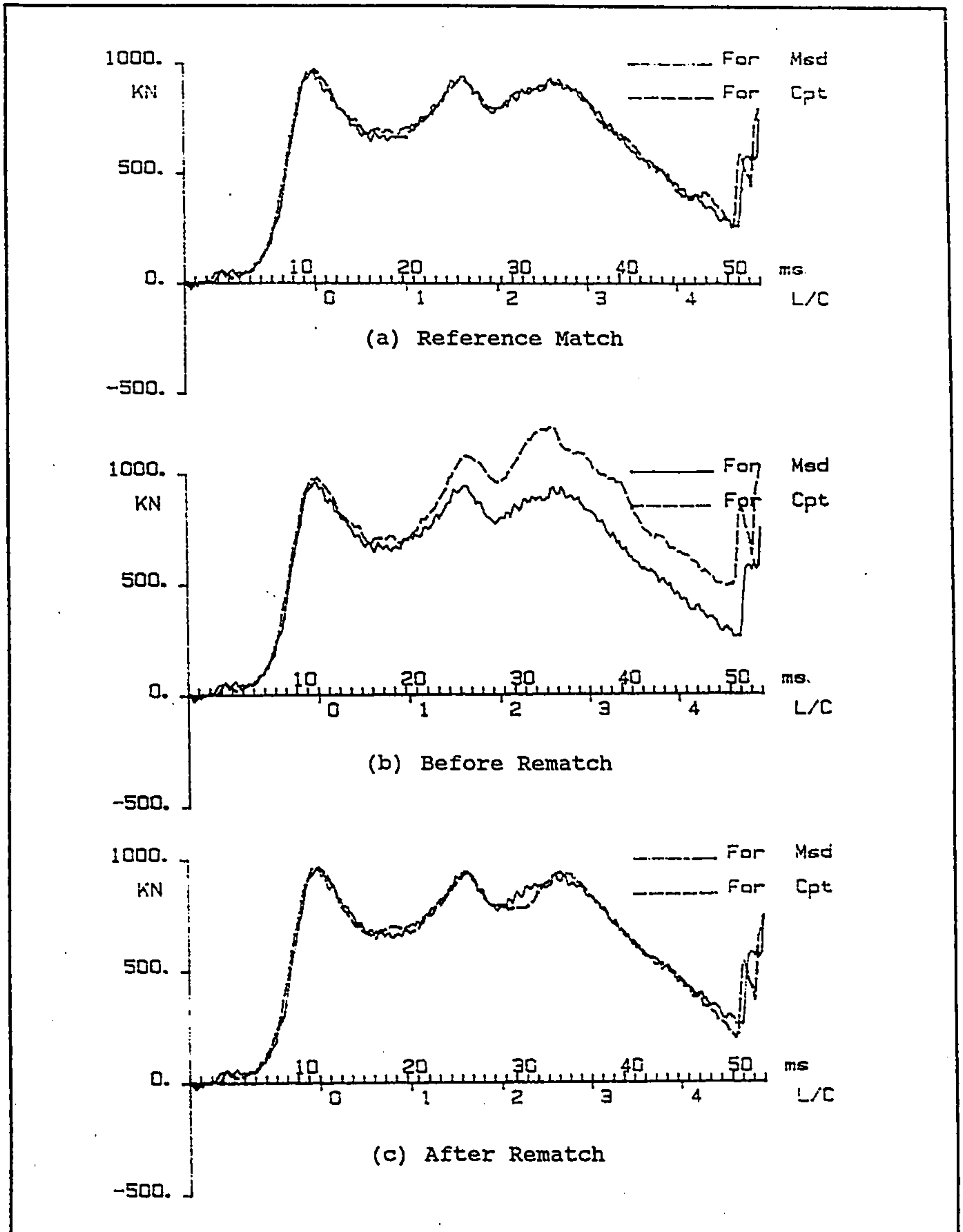

Fig. 6.6 JI Pile, CAPWAP Solution at 1250 KN

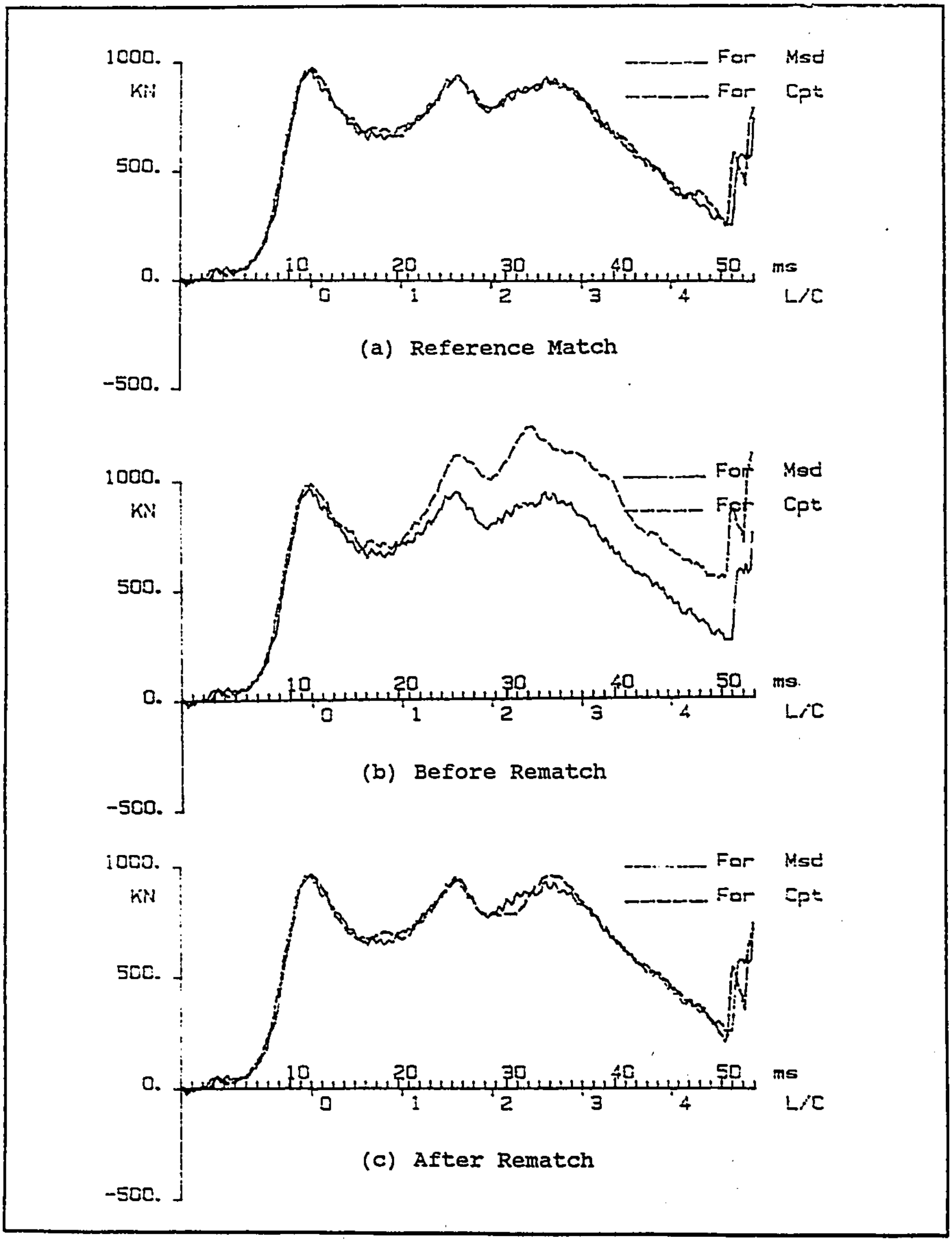

Fig. 6.7 JI Pile, CAPWAP Solution at 1300 KN

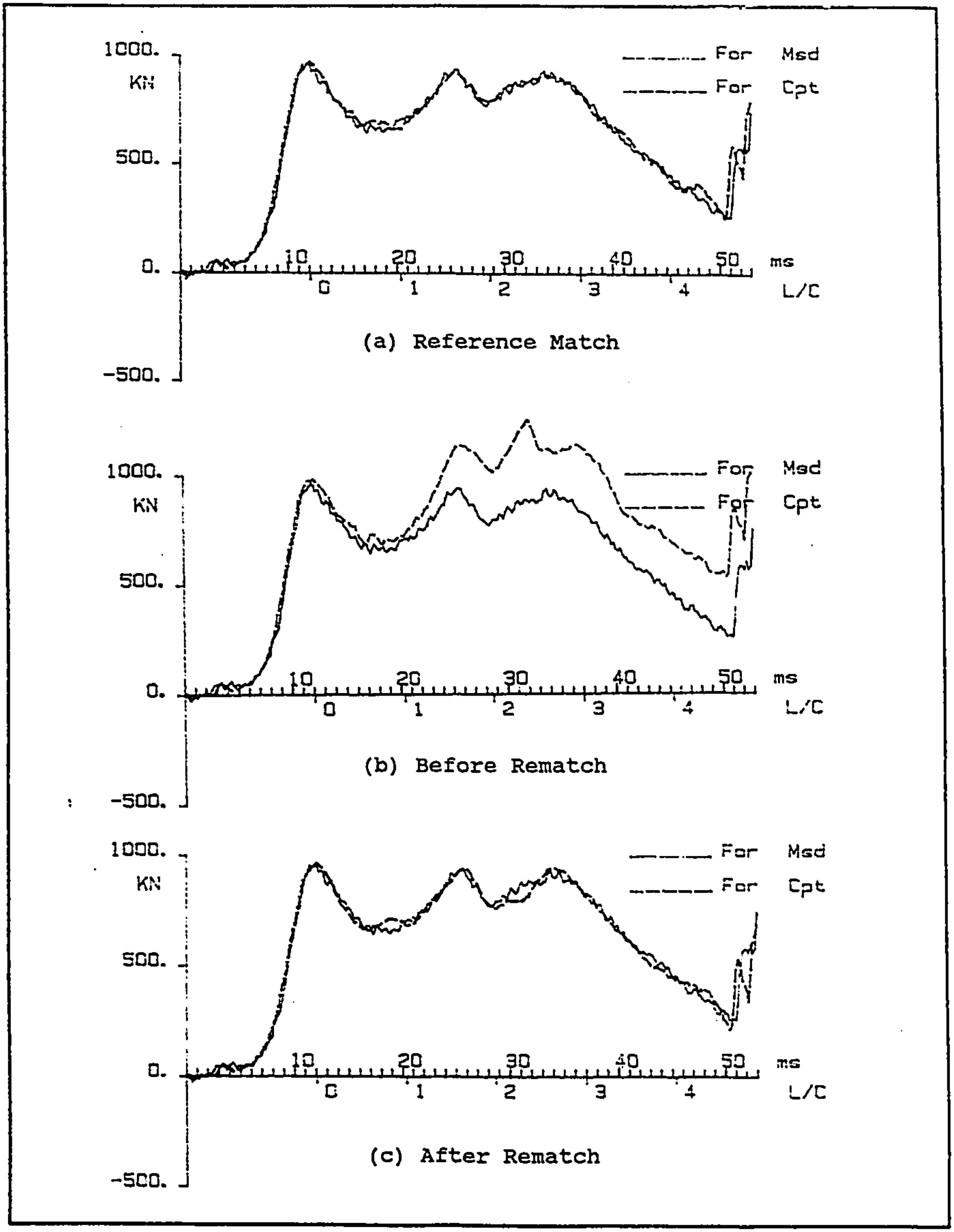

Fig. 6.8 JI Pile, CAPWAP Solution at 1350 KN

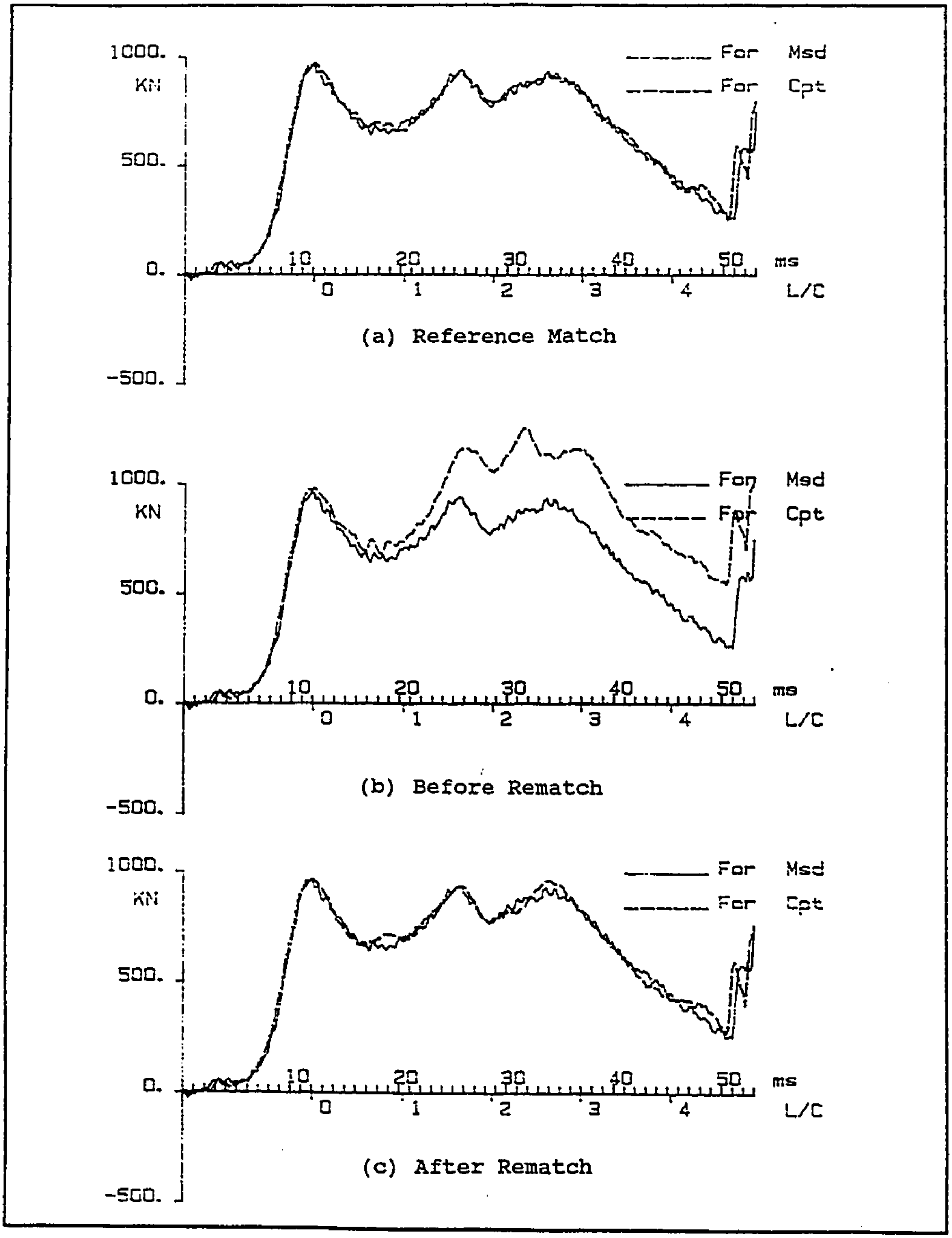

Fig. 6.9 JI Pile, CAPWAP Solution at 1400 KN

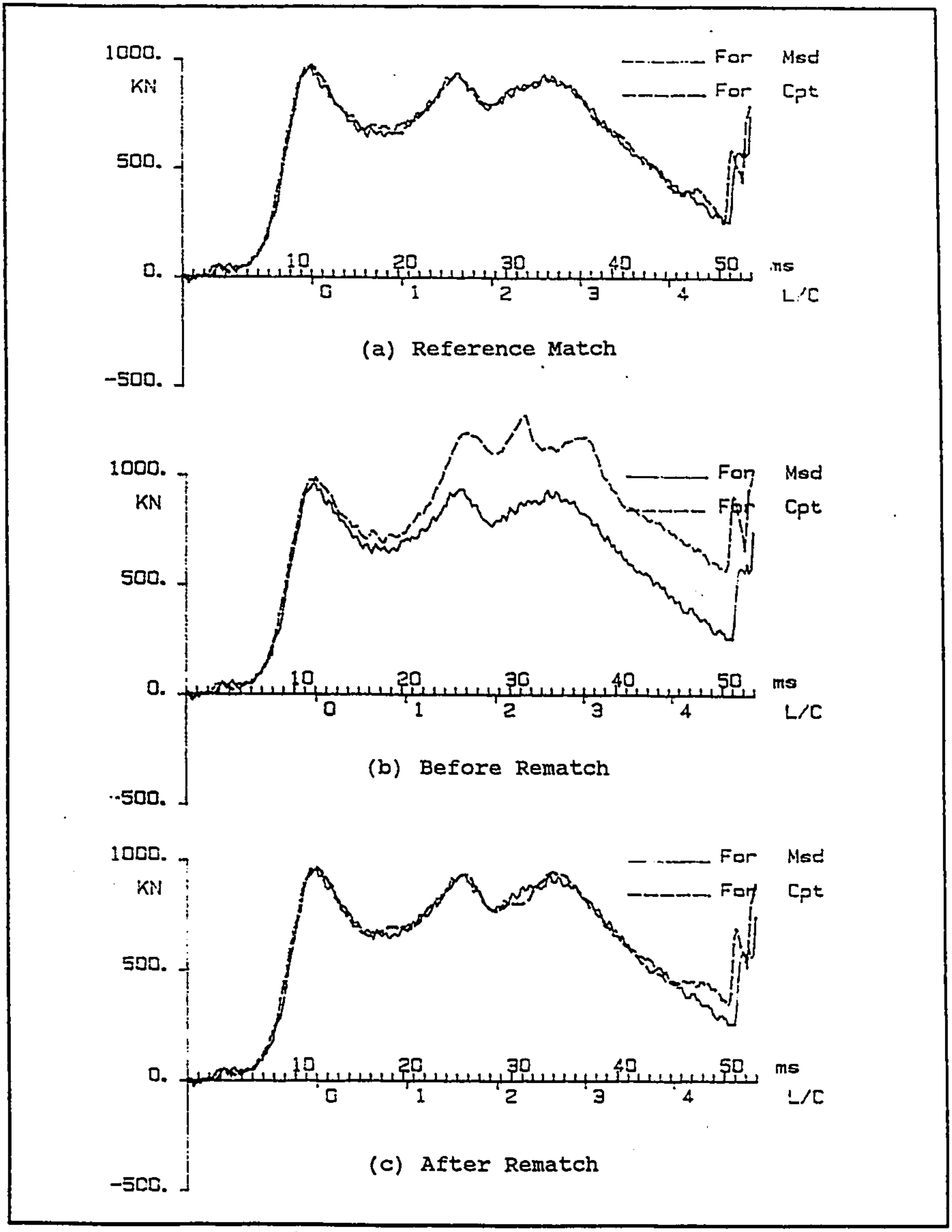

Fig. 6.10 JI Pile, CAPWAP Solution at 1450 KN

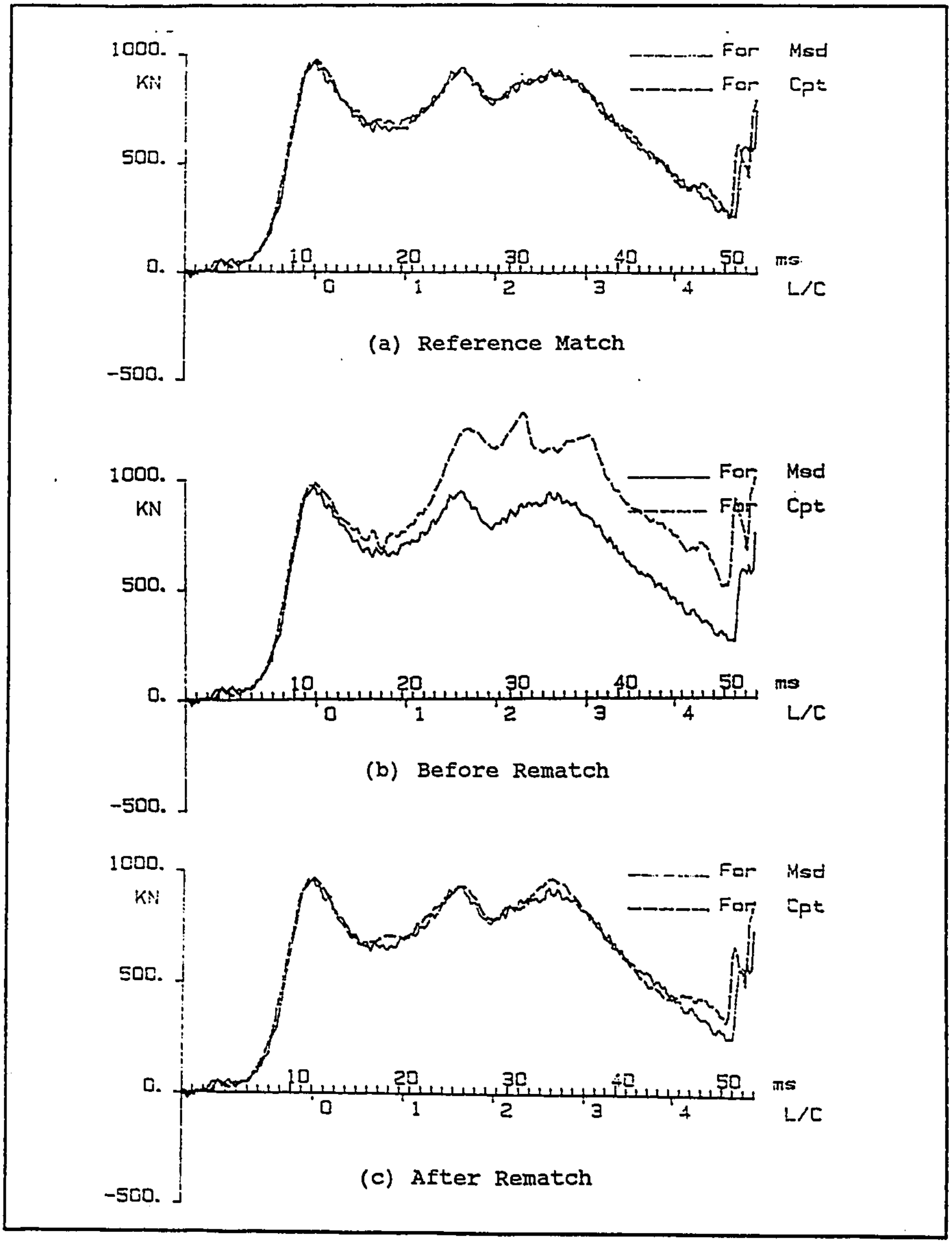

Fig. 6.11 JI Pile, CAPWAP Solution at 1500 KN

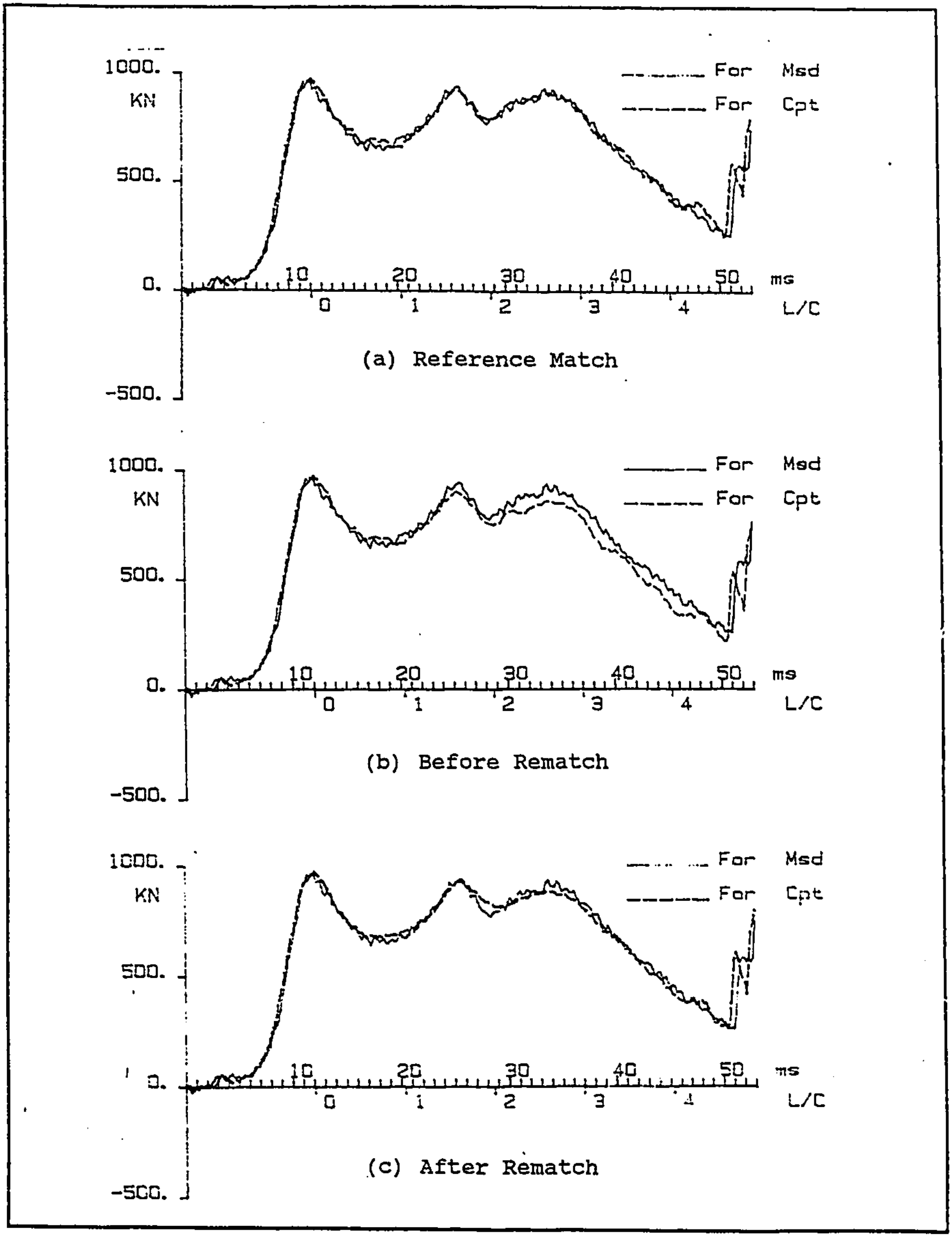

Fig. 6.12 JI Pile, CAPWAP Solution at 950 KN

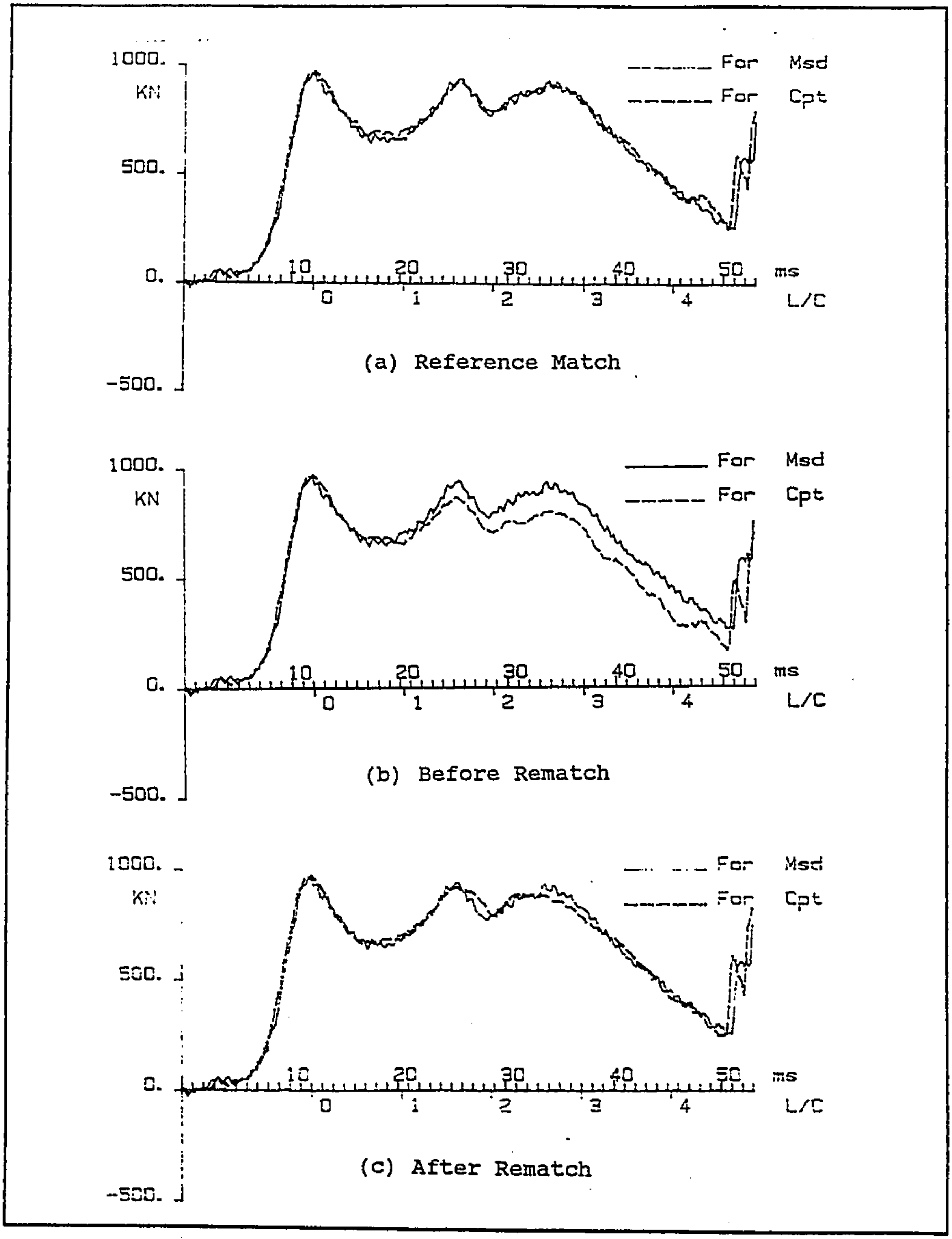

Fig. 6.13 JI Pile, CAPWAP Solution at 900 KN

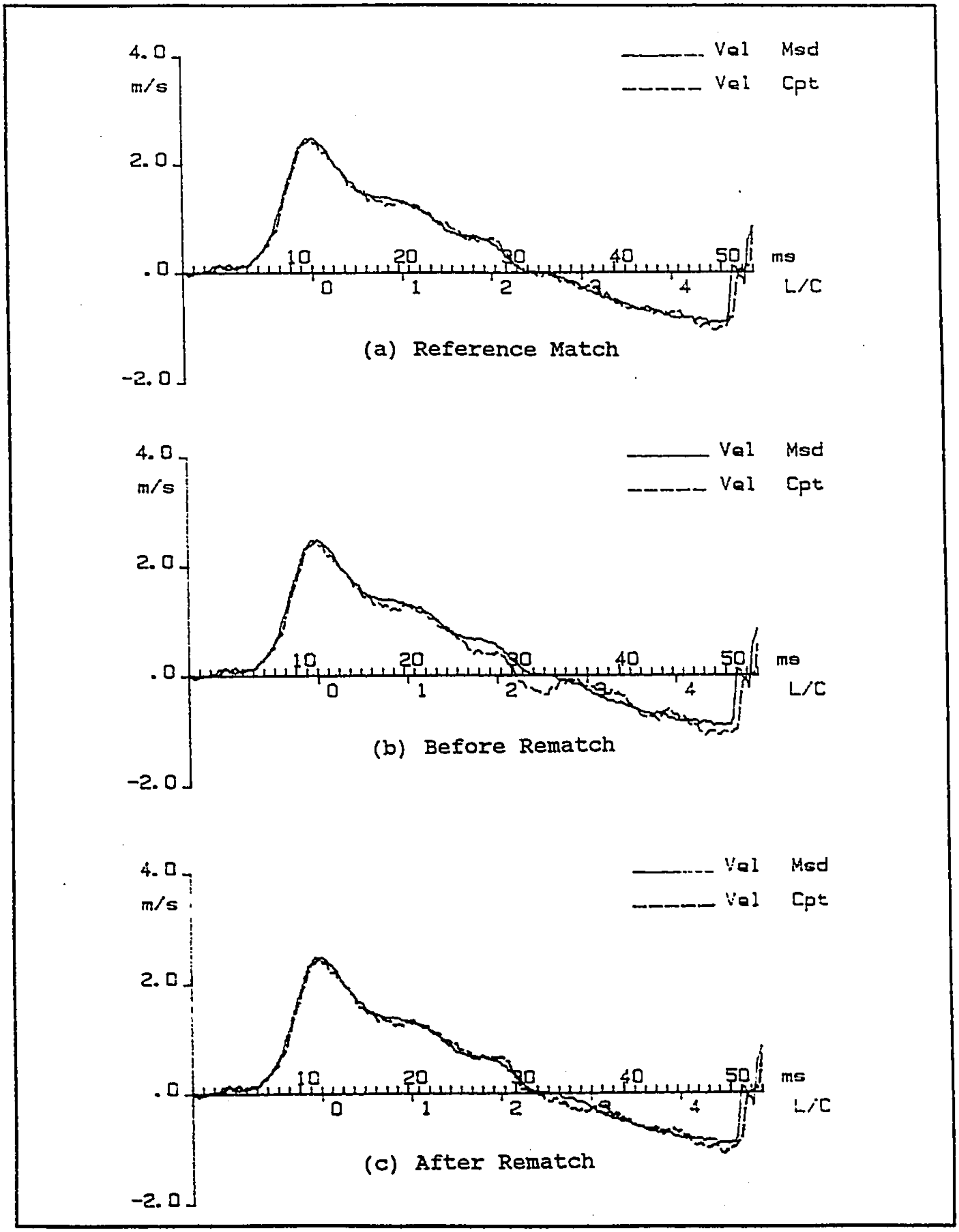

Fig. 6.14 JI Pile, WAPCAP Solution at 1050 KN

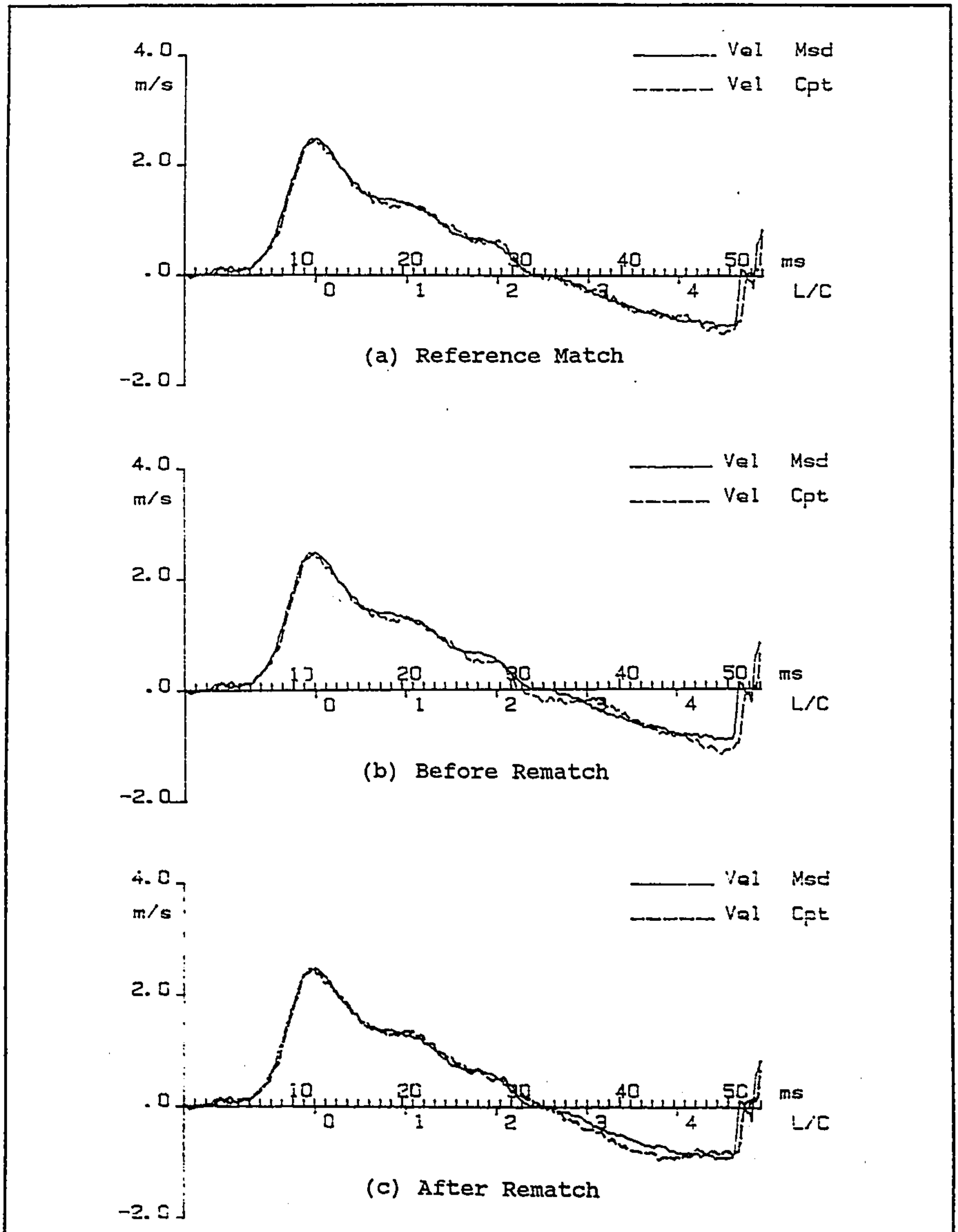

Fig. 6.15 JI Pile, WAPCAP Solution at 1100 KN

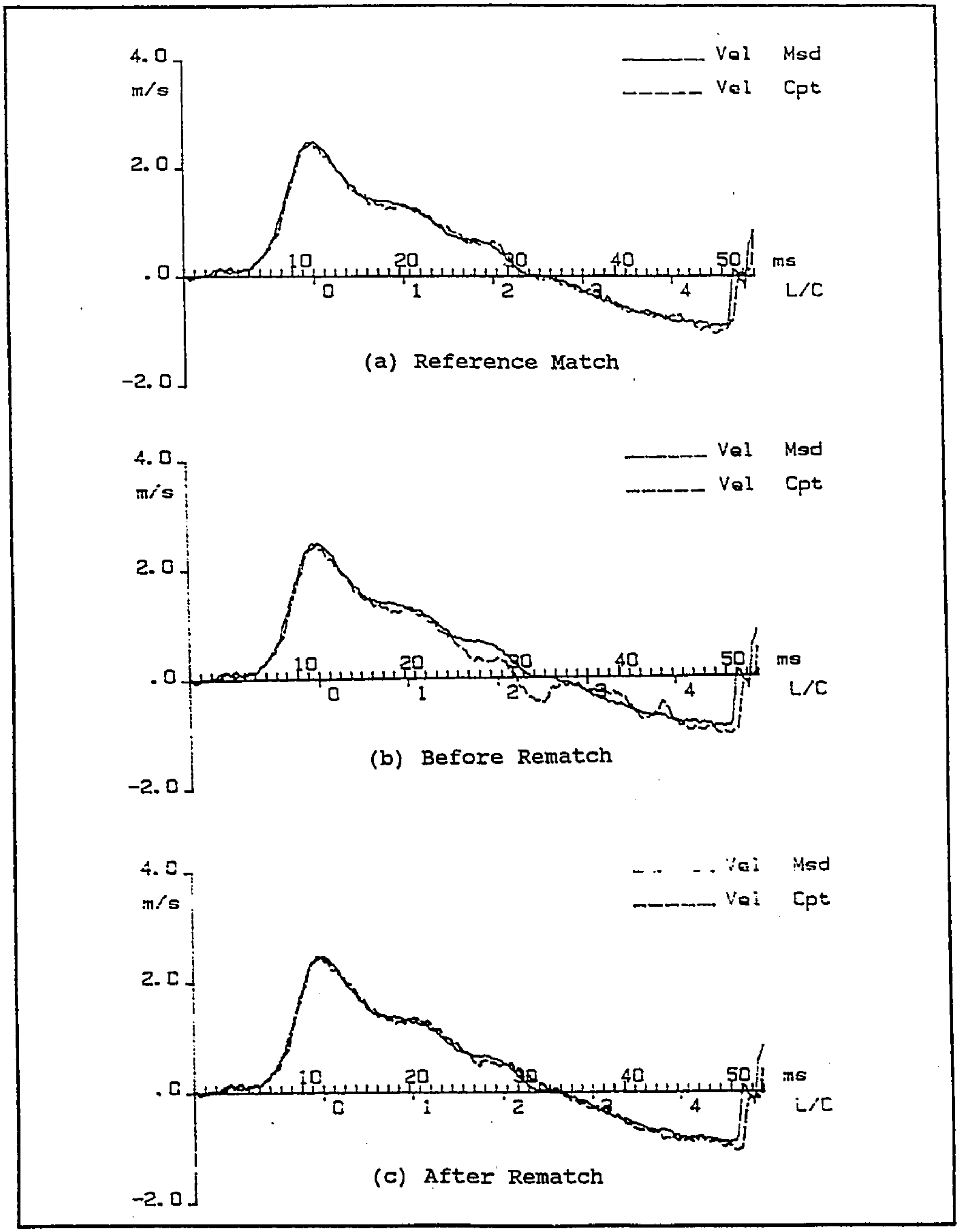

Fig. 6.16 JI Pile, WAPCAP Solution at 1150 KN

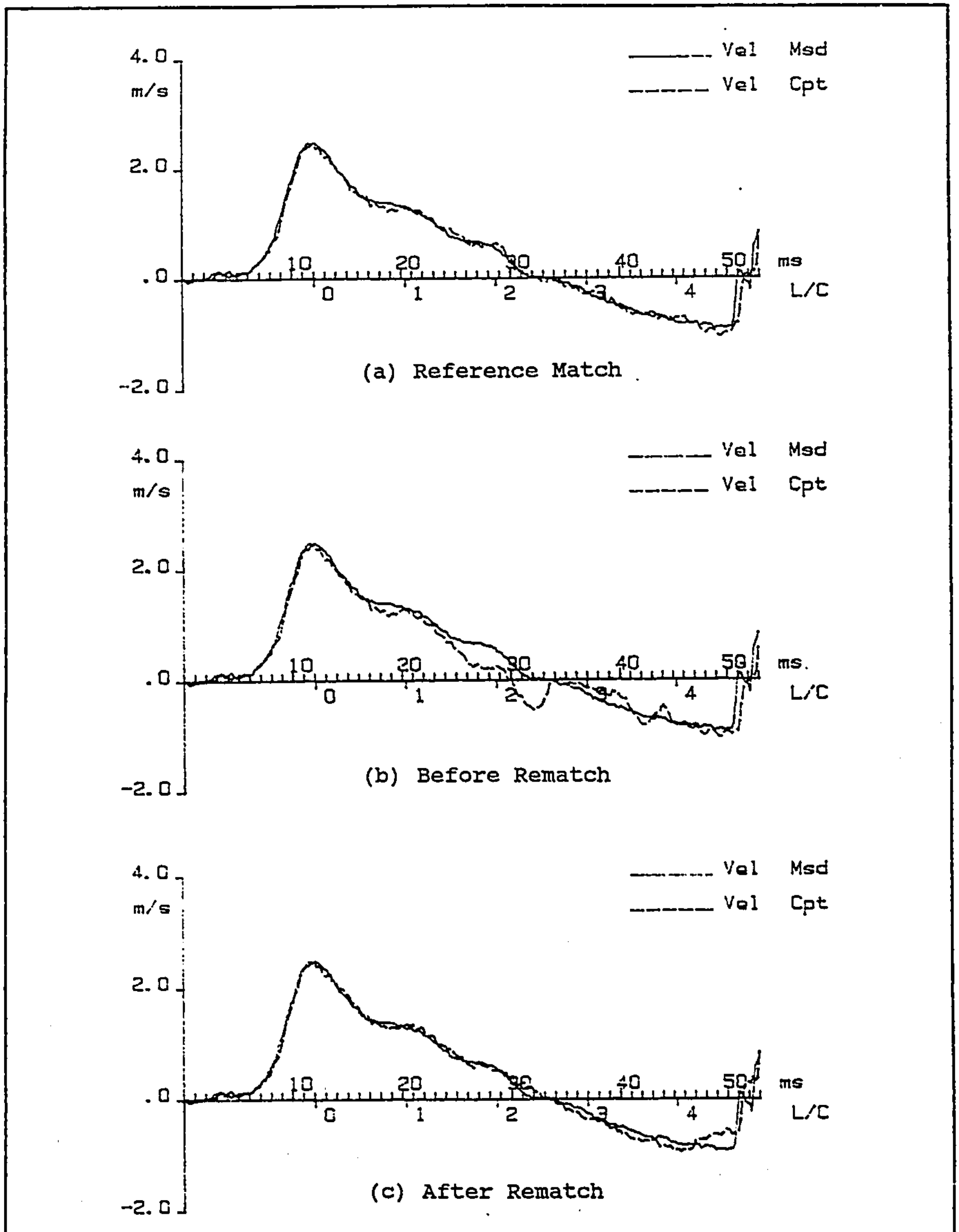

Fig. 6.17 JI Pile, WAPCAP Solution at 1200 KN

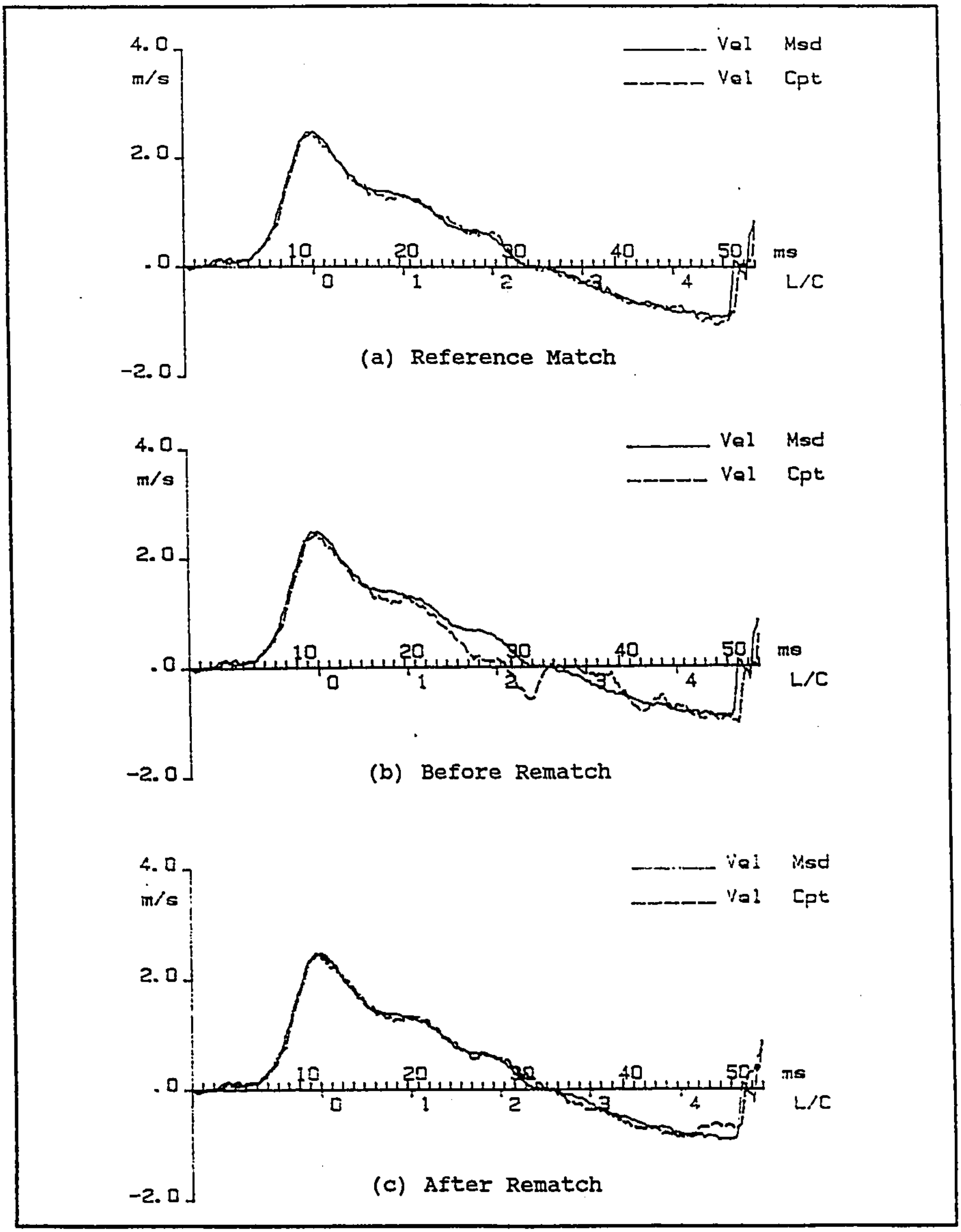

Fig. 6.18 JI Pile, WAPCAP Solution at 1250 KN

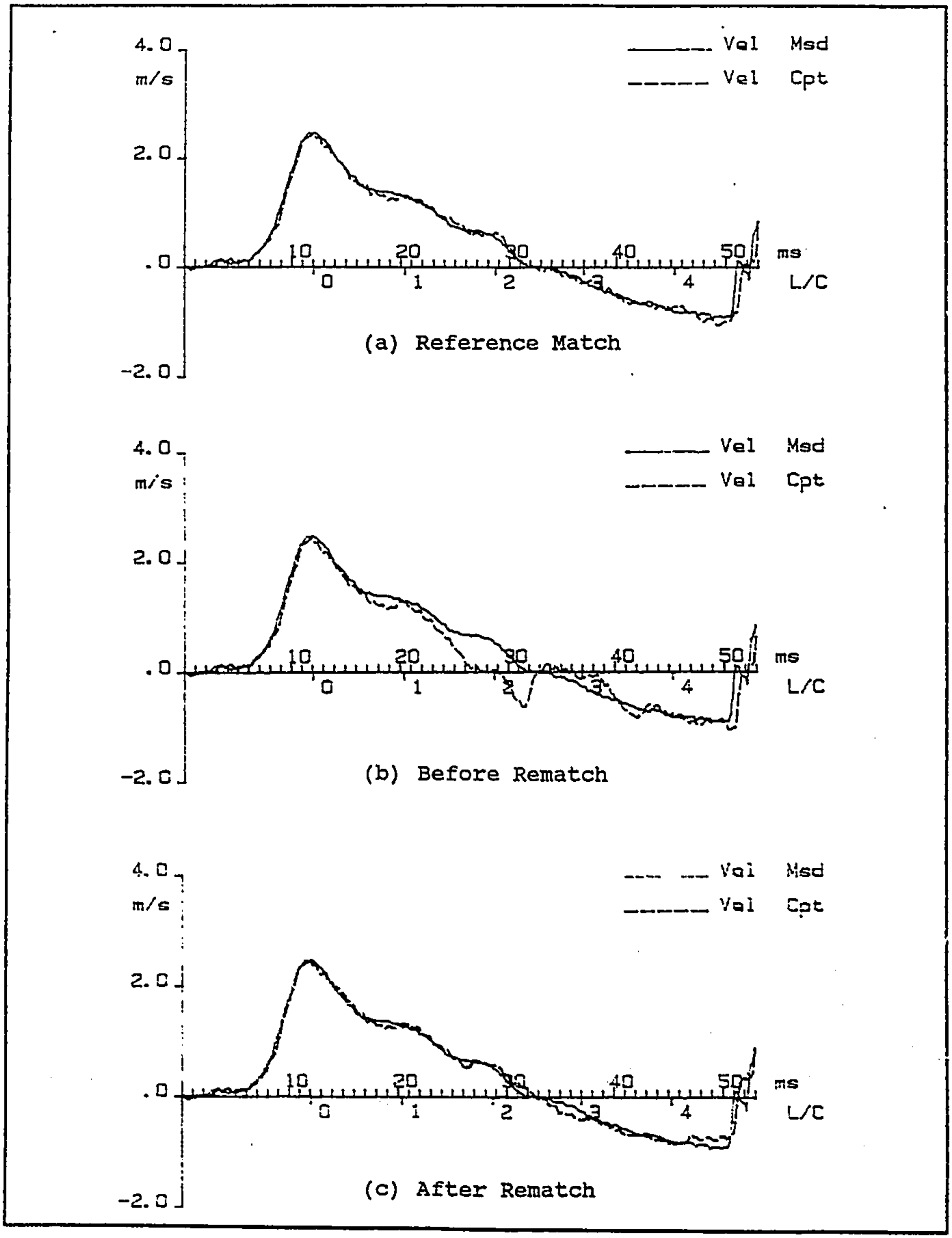

Fig. 6.19 JI Pile, WAPCAP Solution at 1300 KN

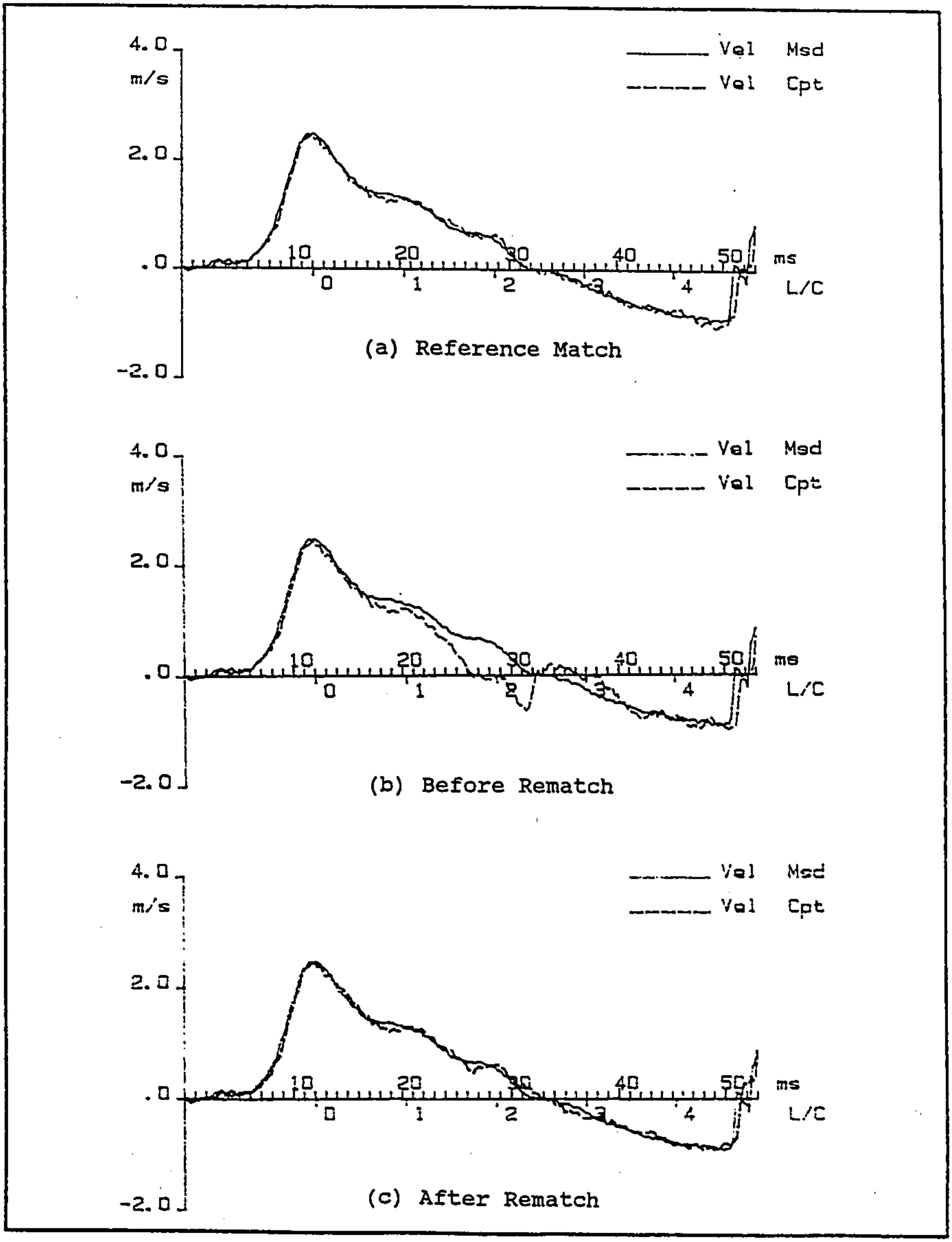

Fig. 6.20 JI Pile, WAPCAP Solution at 1350 KN

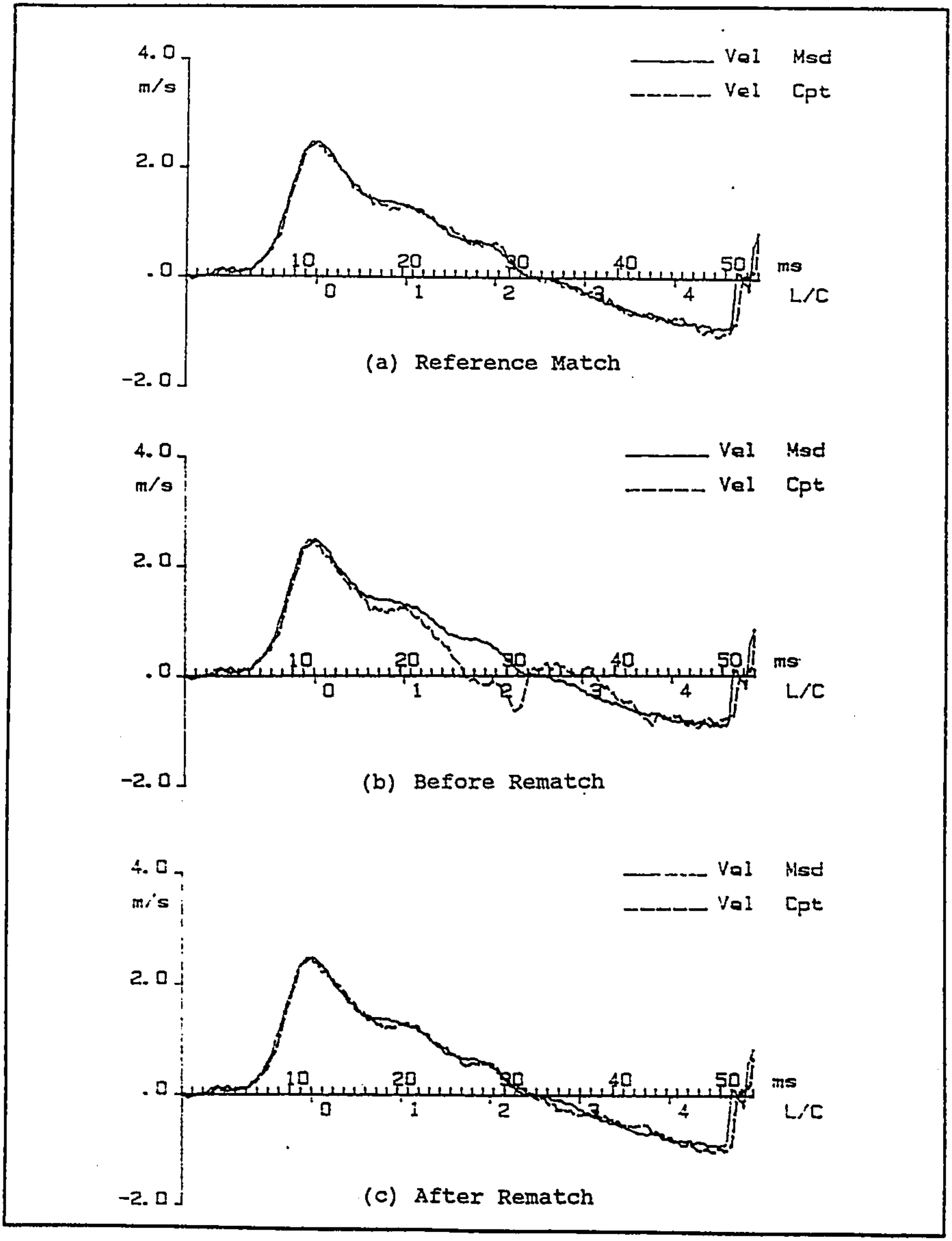

Fig. 6.21 JI Pile, WAPCAP Solution at 1400 KN

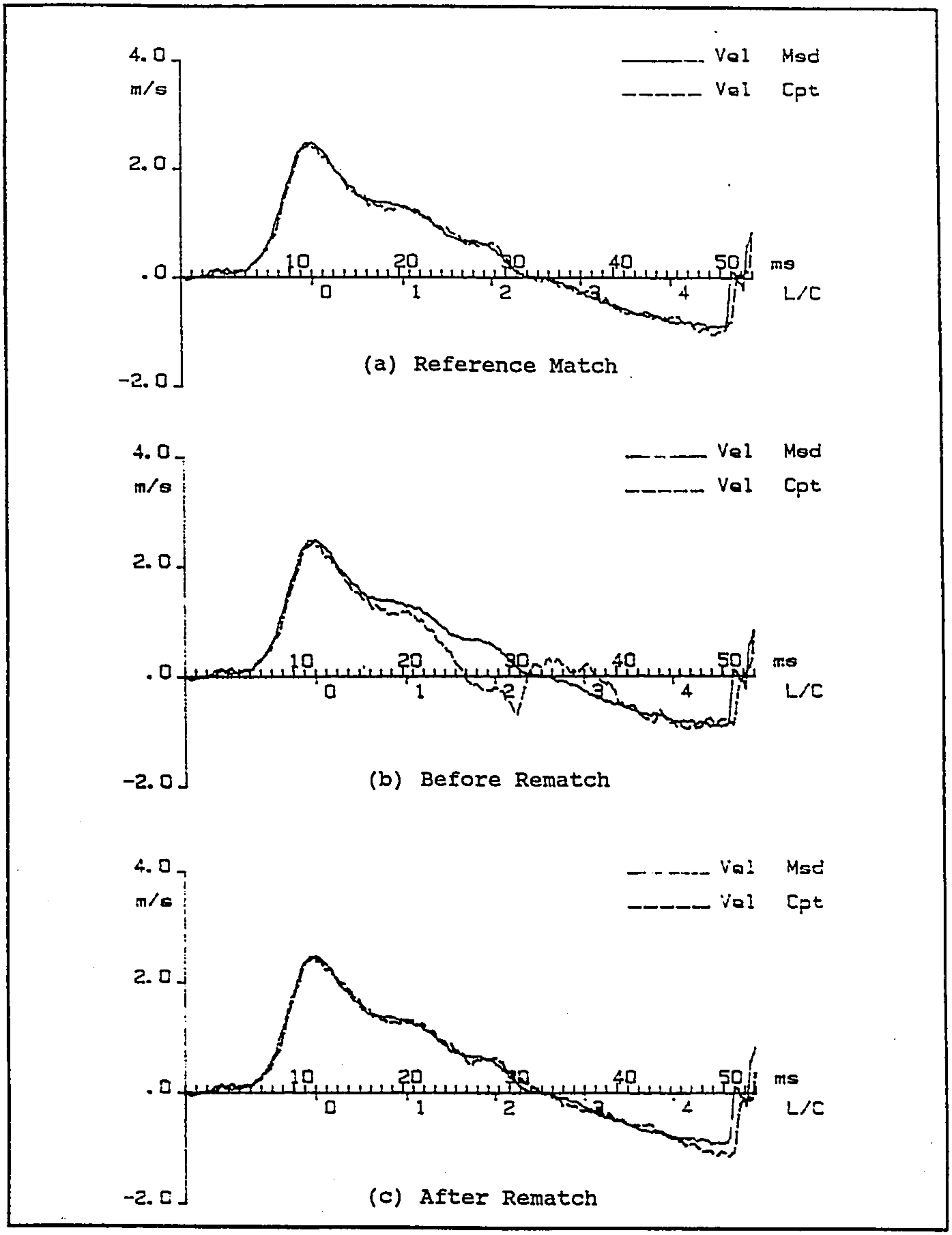

Fig. 6.22 JI Pile, WAPCAP Solution at 1450 KN

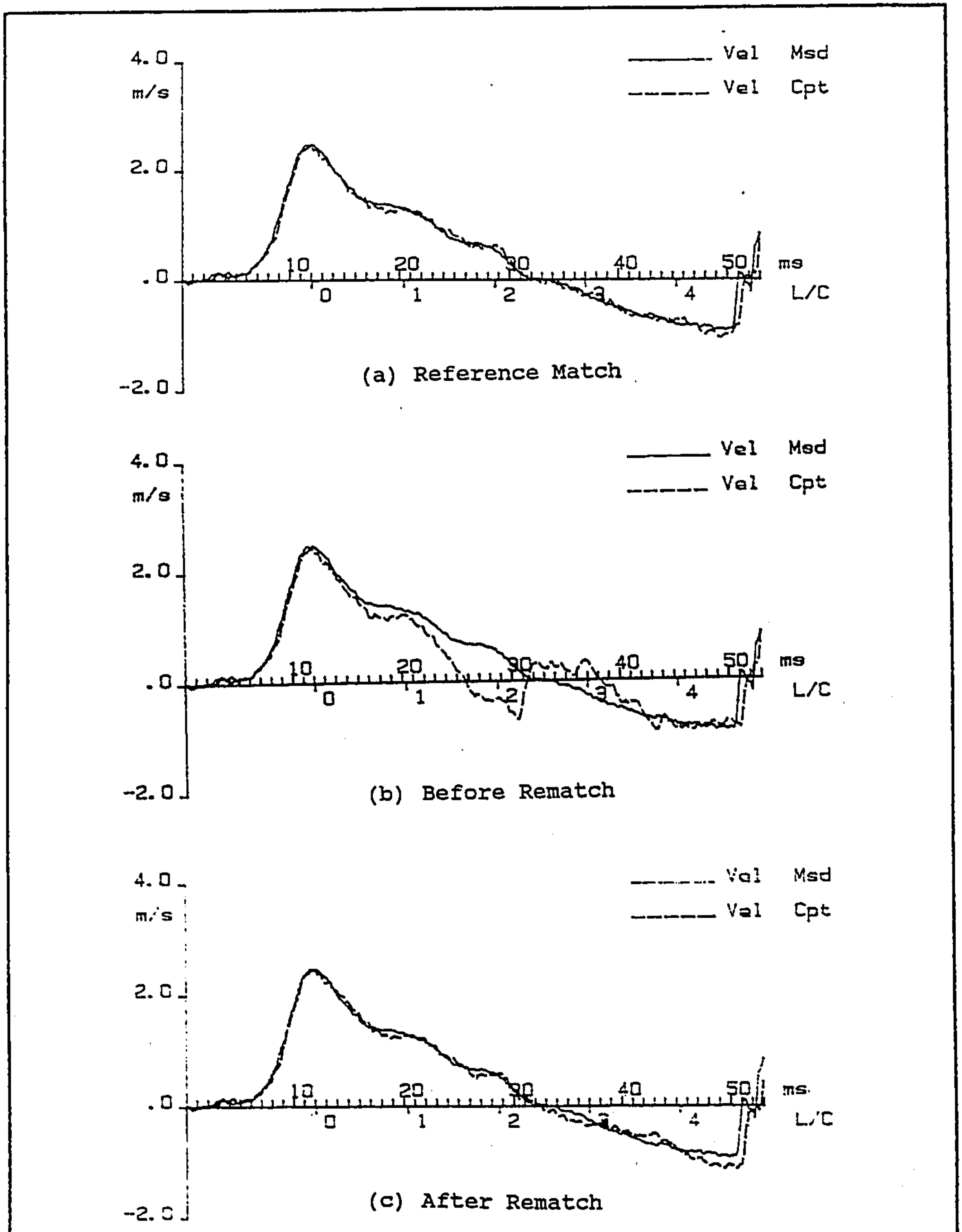

Fig. 6.23 JI Pile, WAPCAP Solution at 1500 KN

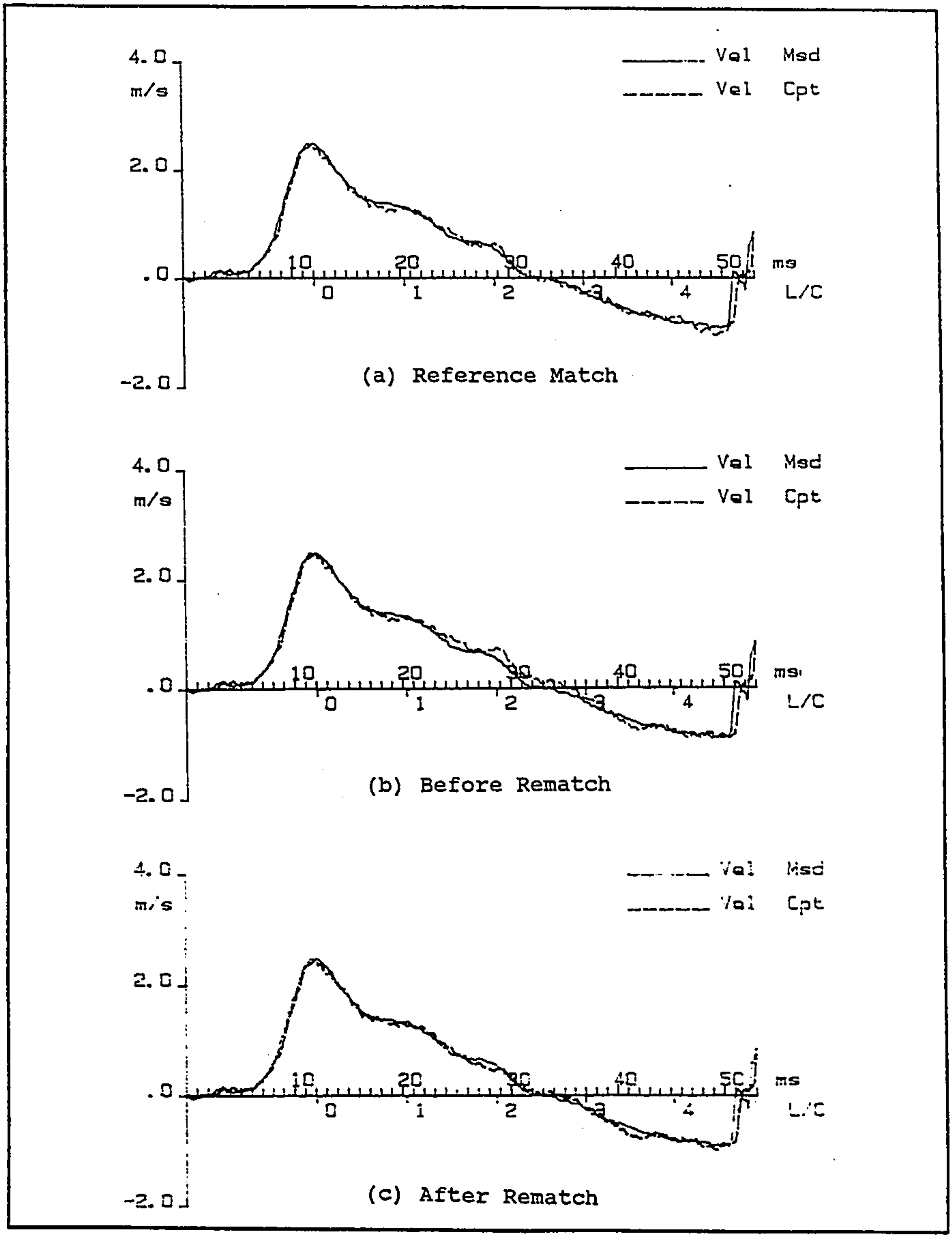

Fig. 6.24 JI Pile, WAPCAP Solution at 950 KN

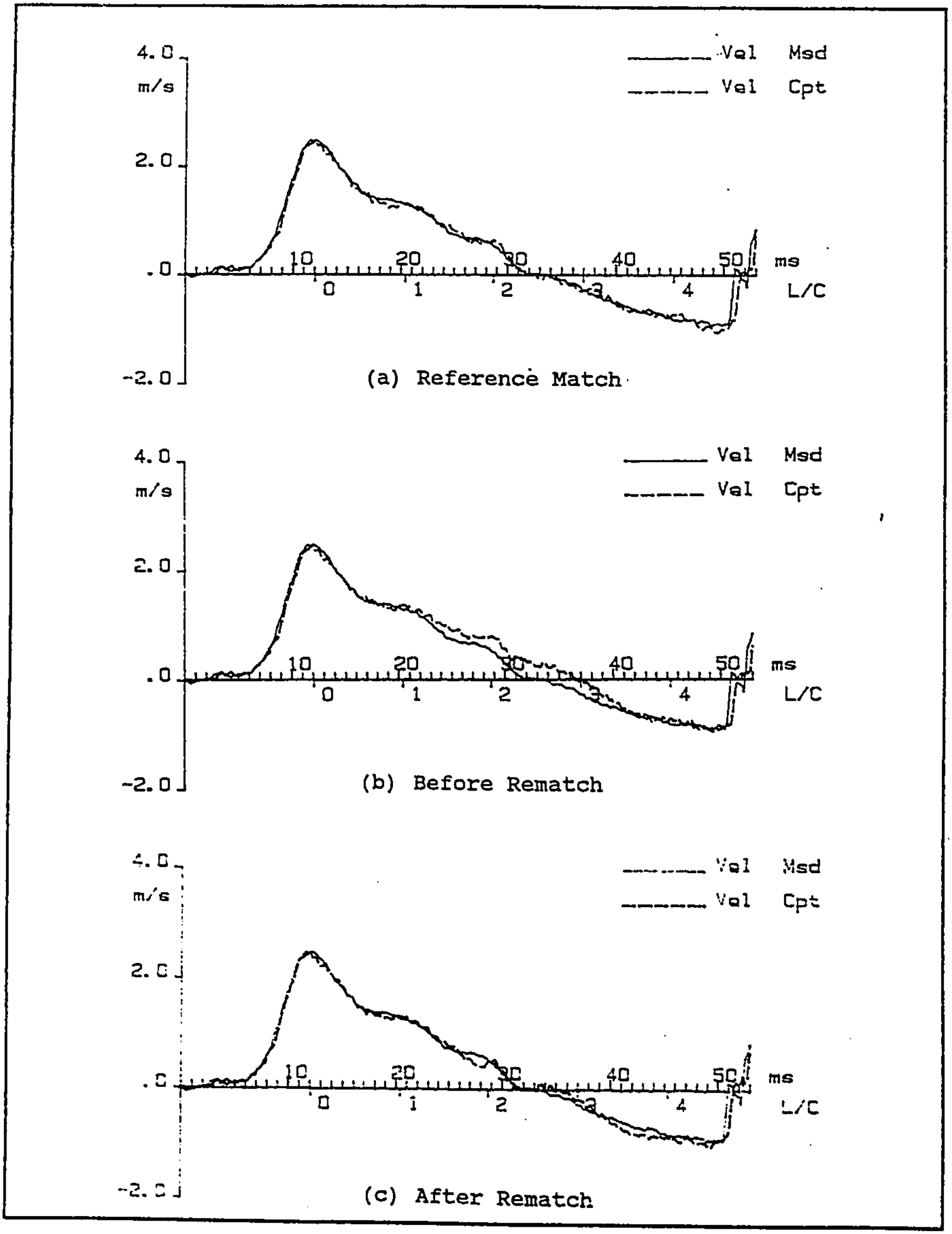

Fig. 6.25 JI Pile, WAPCAP Solution at 900 KN

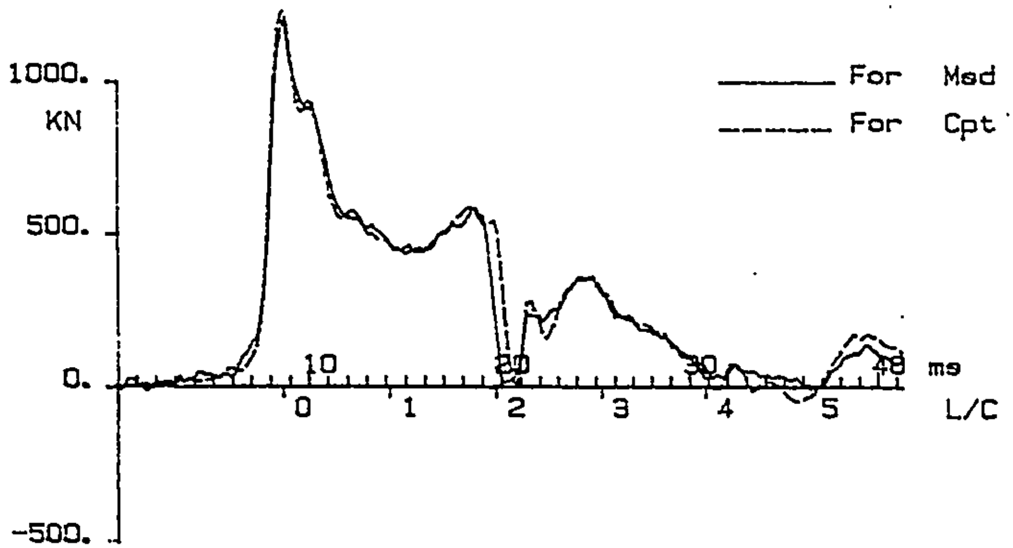

(a) CAPWAP Solution at 575 KN

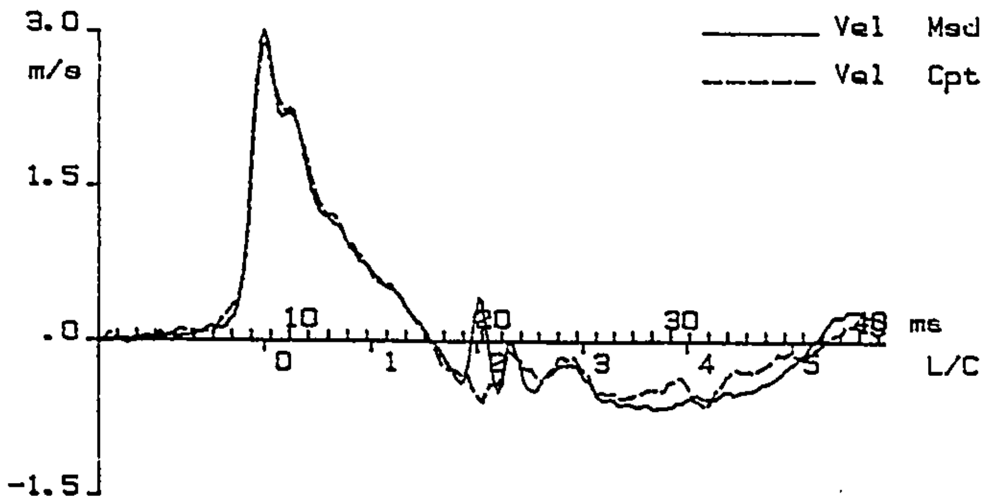

(b) WAPCAP Solution at 575 KN

Fig. 6.26 JA Pile, Reference Matches

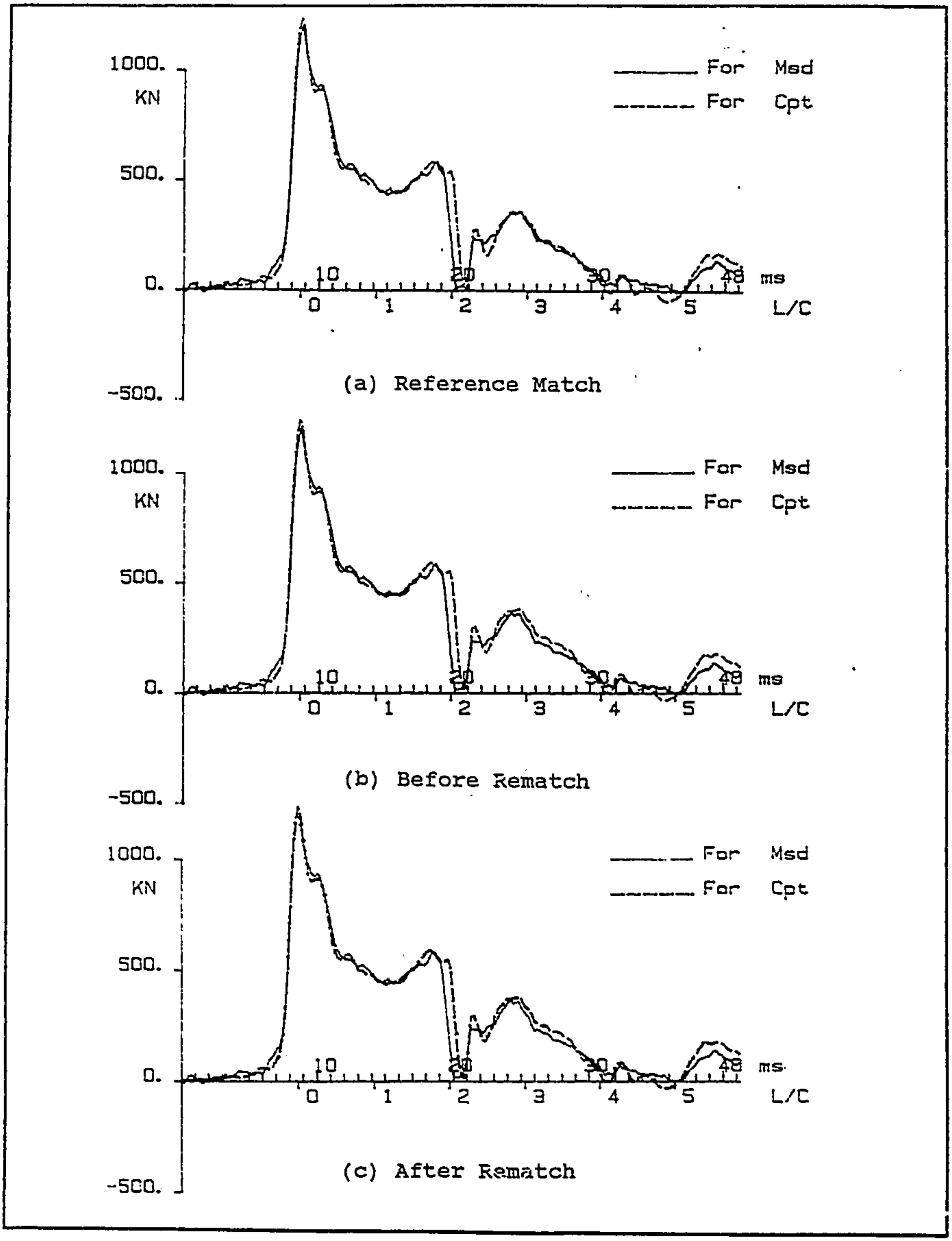

Fig. 6.27 JA Pile, CAPWAP Solution at 600 KN

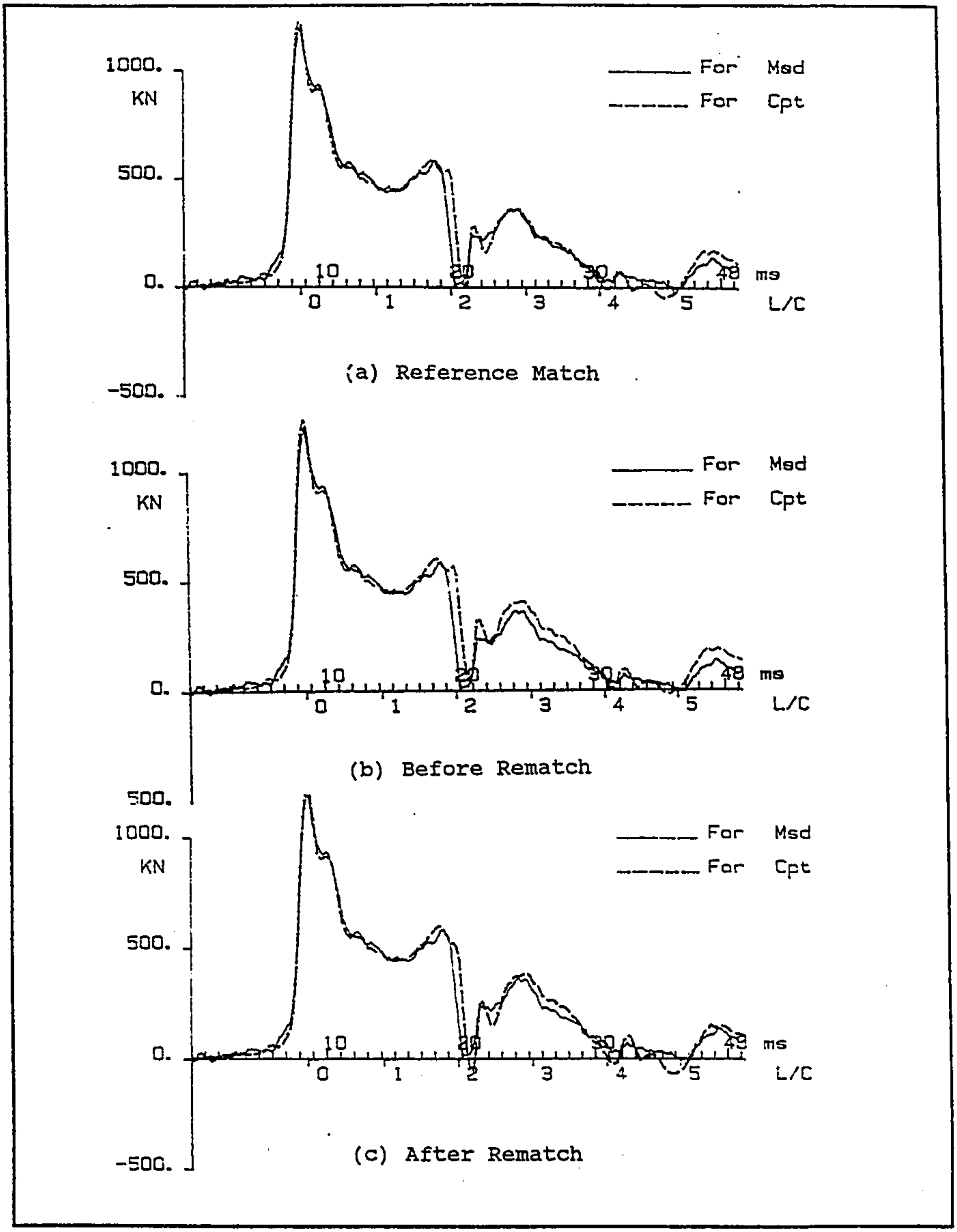

Fig. 6.28 JA Pile, CAPWAP Solution at 625 KN

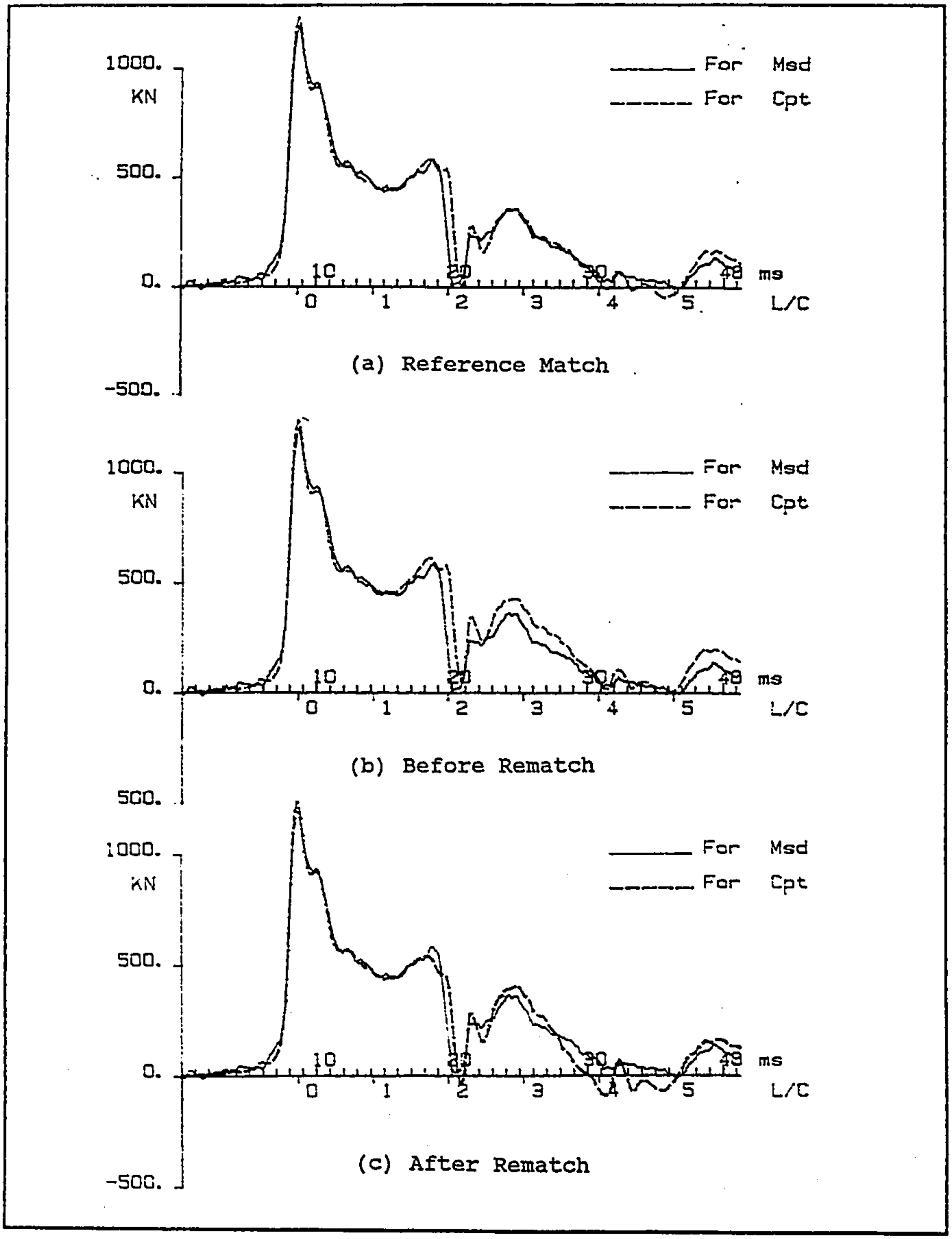

Fig. 6.29 JA Pile, CAPWAP Solution at 650 KN

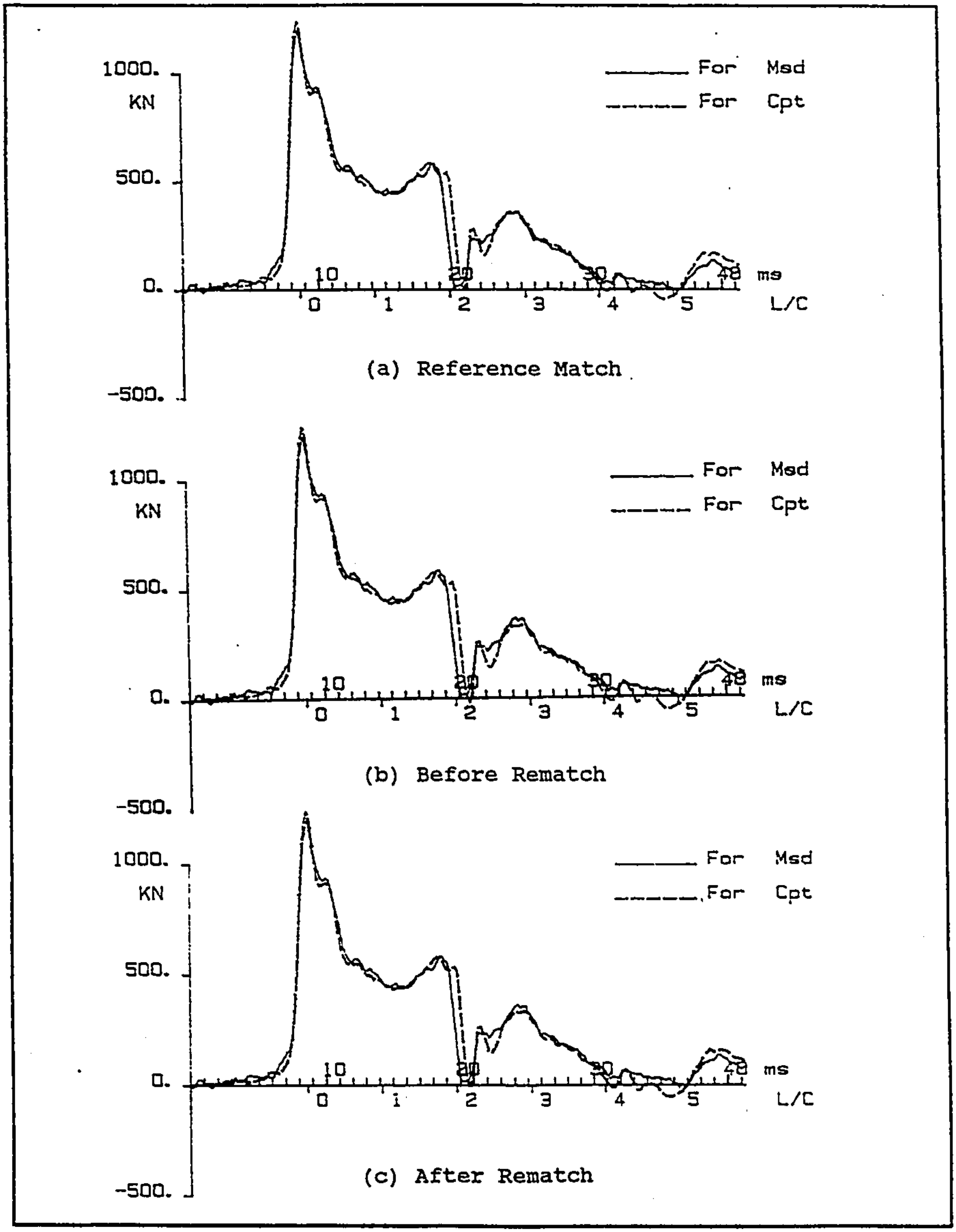

Fig. 6.30 JA Pile, CAPWAP Solution at 550 KN

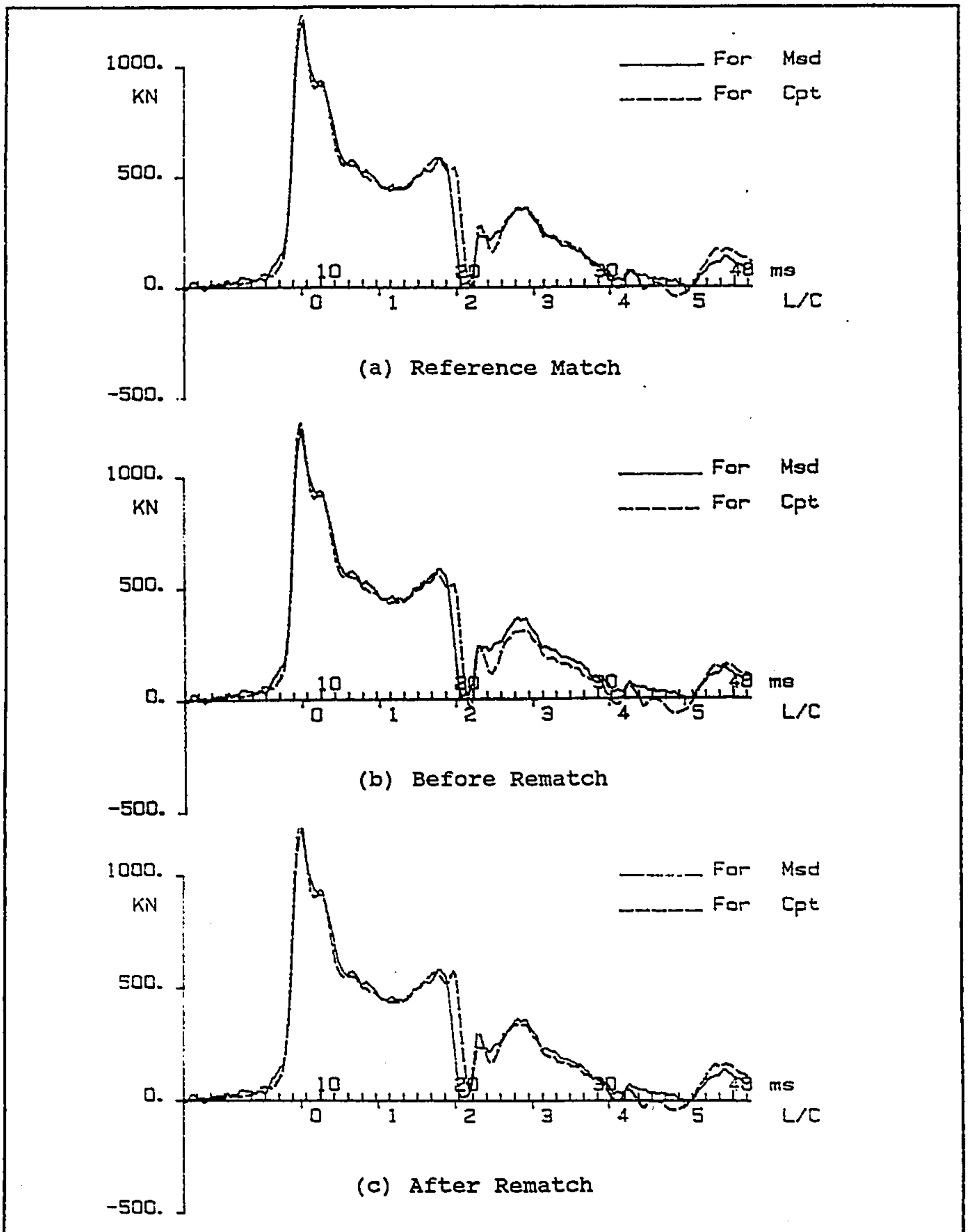

Fig. 6.31 JA Pile, CAPWAP Solution at 525 KN

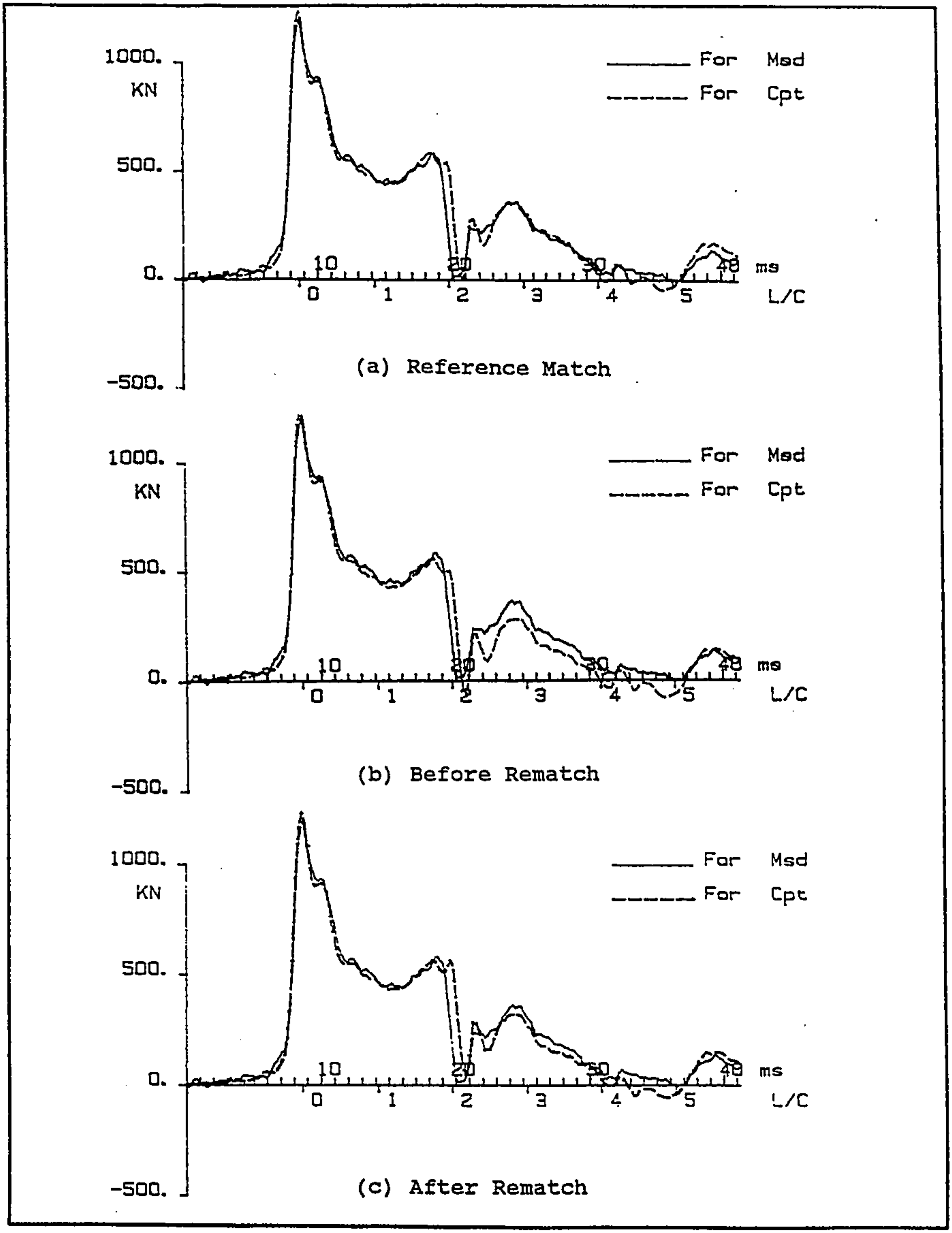

Fig. 6.32 JA Pile, CAPWAP Solution at 500 KN

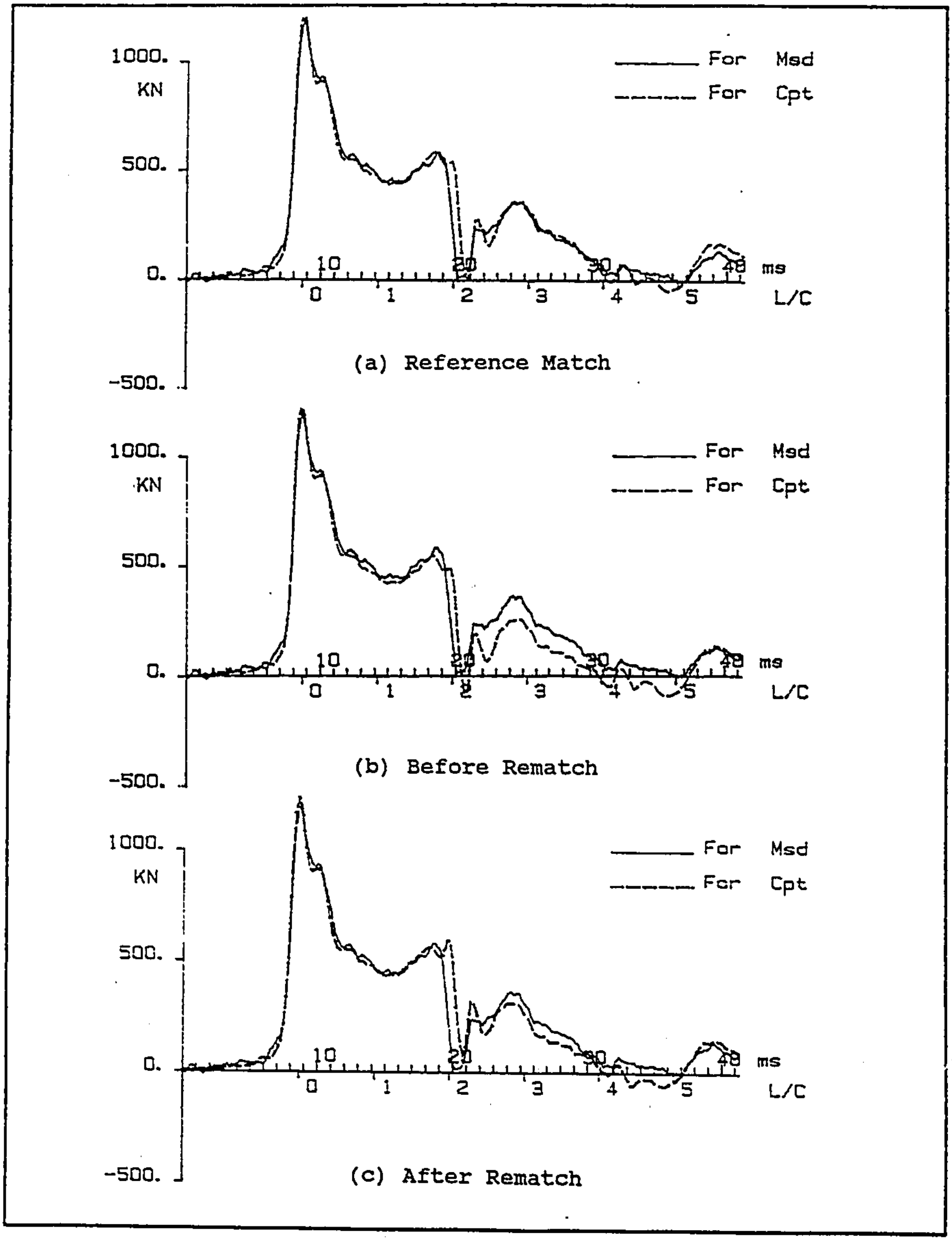

Fig. 6.33 JA Pile, CAPWAP Solution at 475 KN

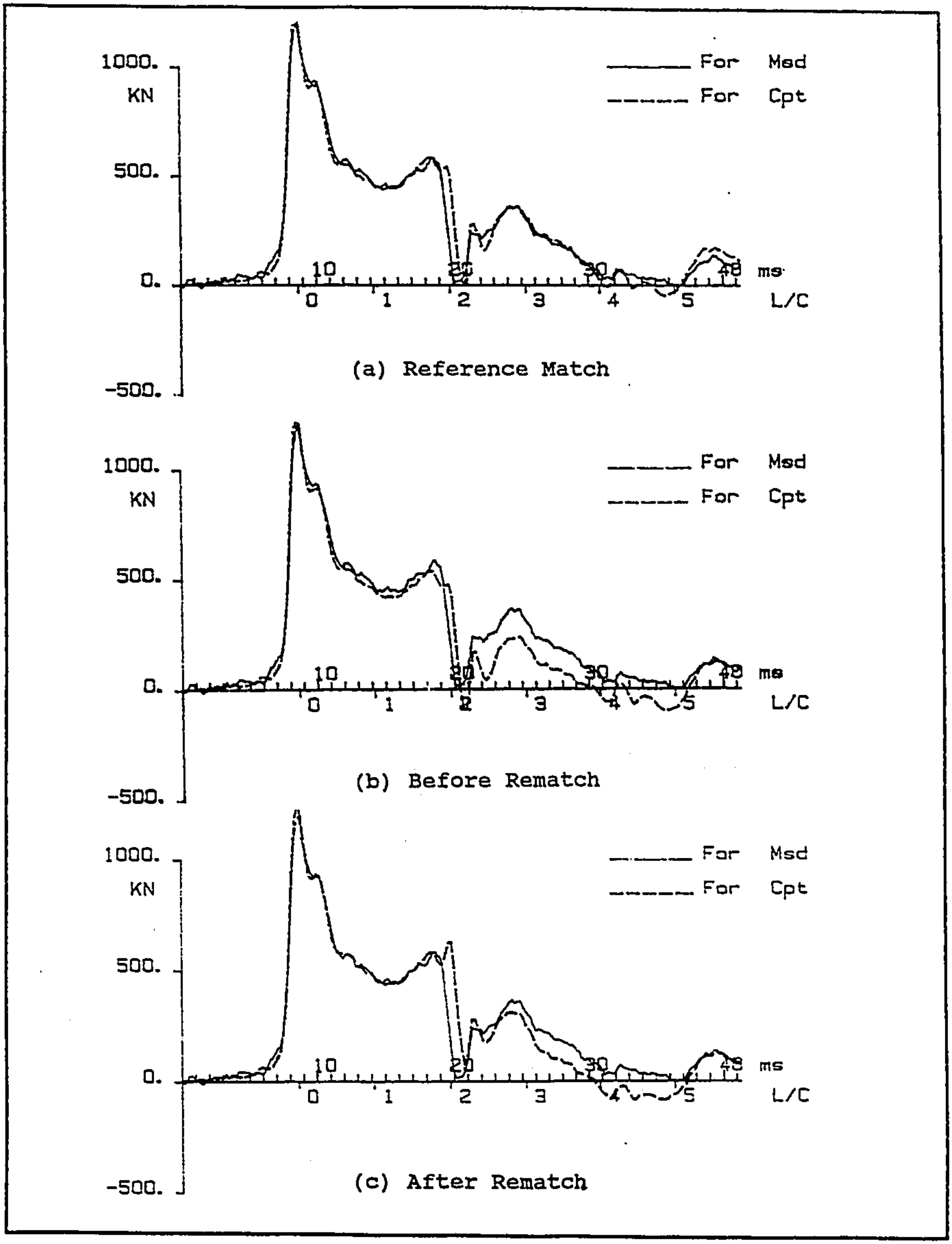

Fig. 6.34 JA Pile, CAPWAP Solution at 450 KN

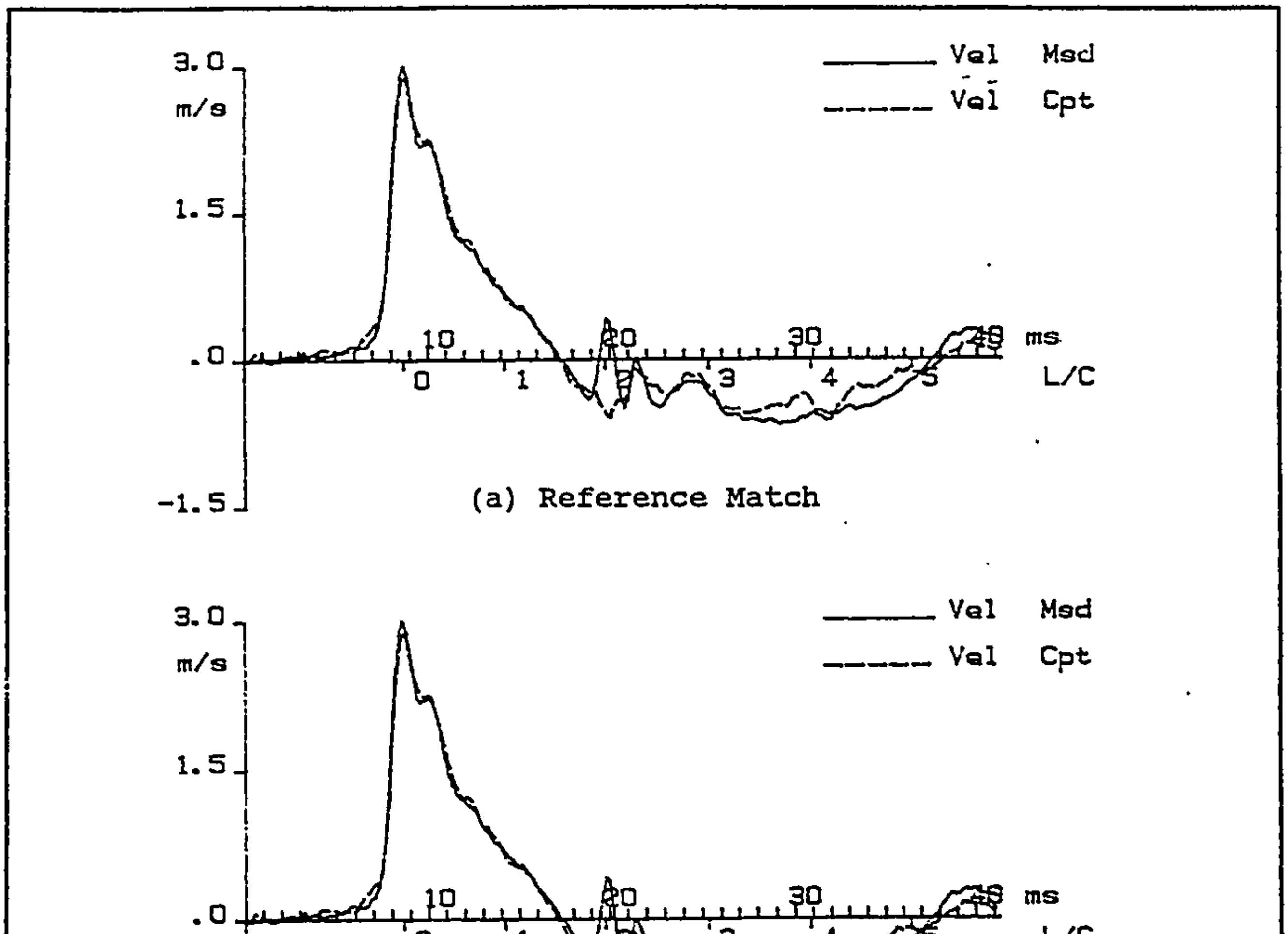

Fig. 6.35 JA Pile, WAPCAP Solution at 600 KN

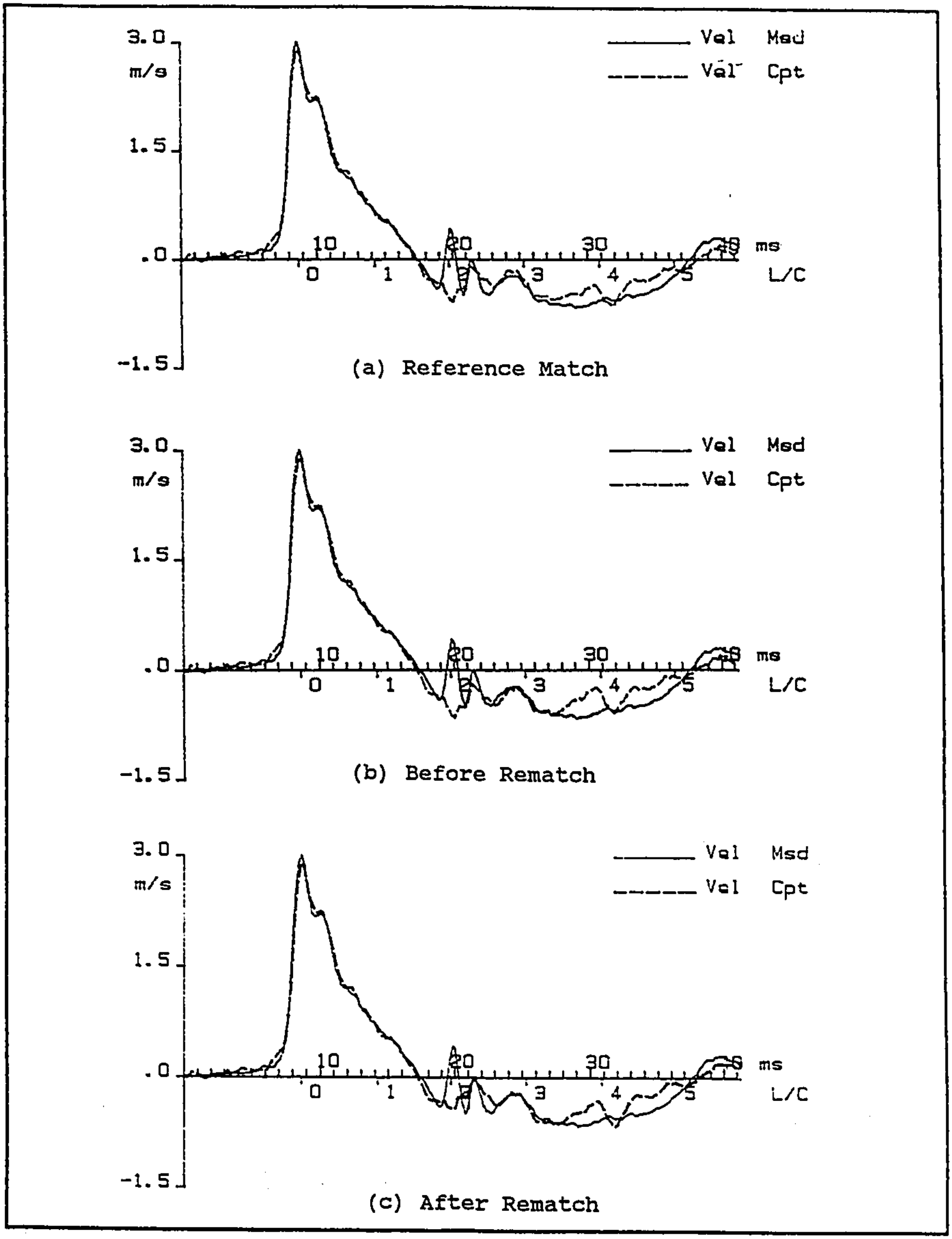

(a) Reference Match

(b) Before Rematch

(c) After Rematch

Fig. 6.36 JA Pile, WAPCAP Solution at 625 KN

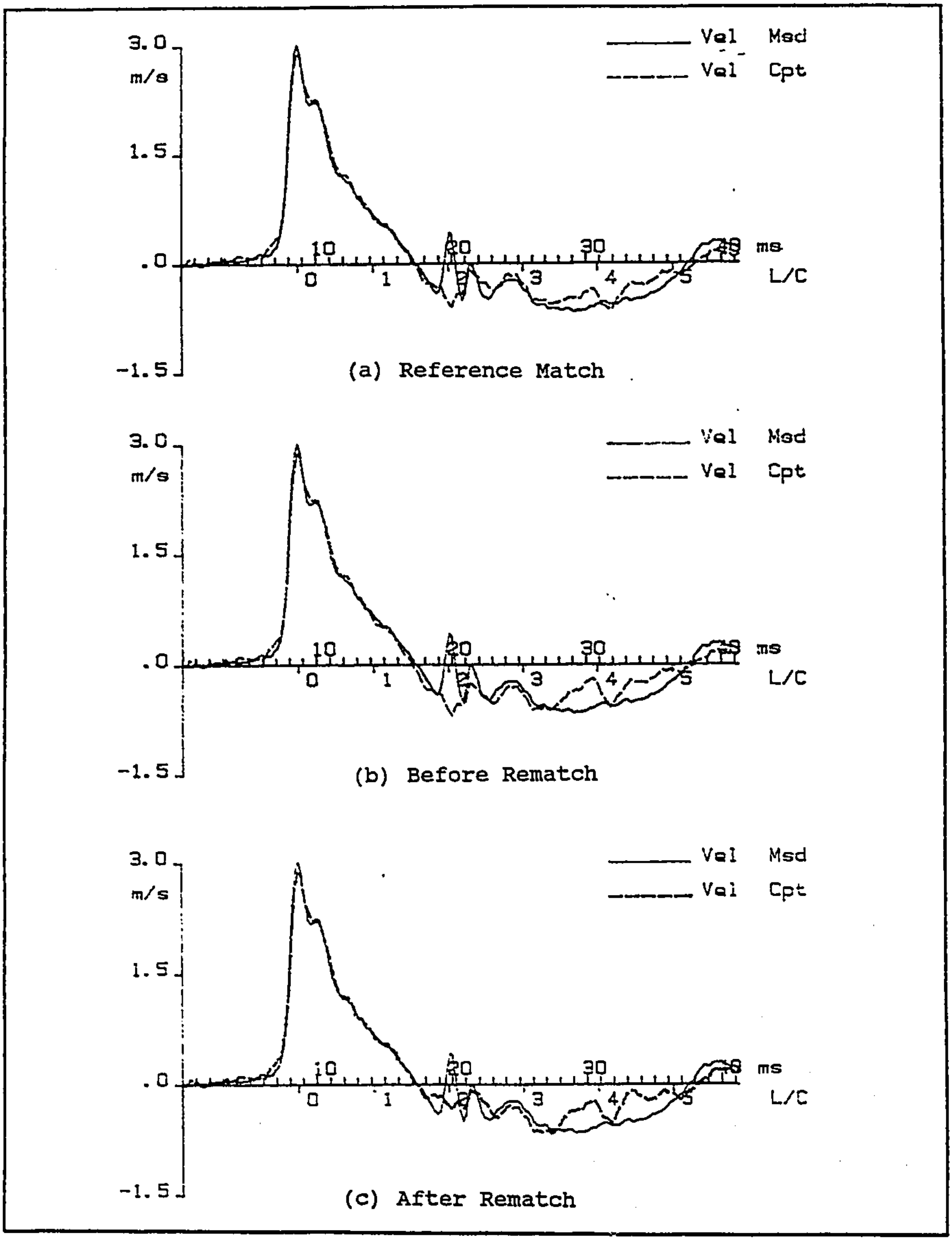

Fig. 6.37 JA Pile, WAPCAP Solution at 650 KN

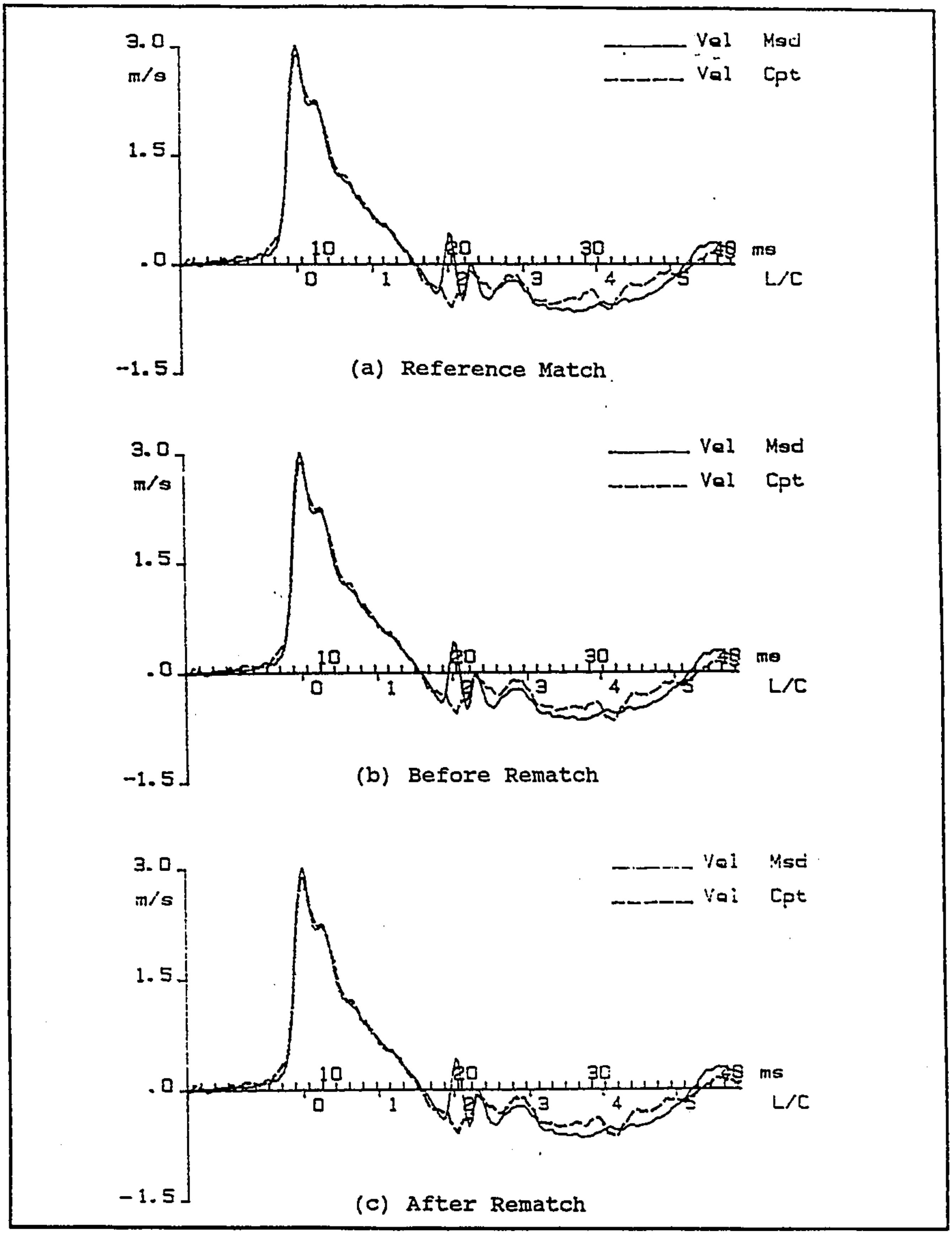

Fig. 6.38 JA Pile, WAPCAP Solution at 550 KN

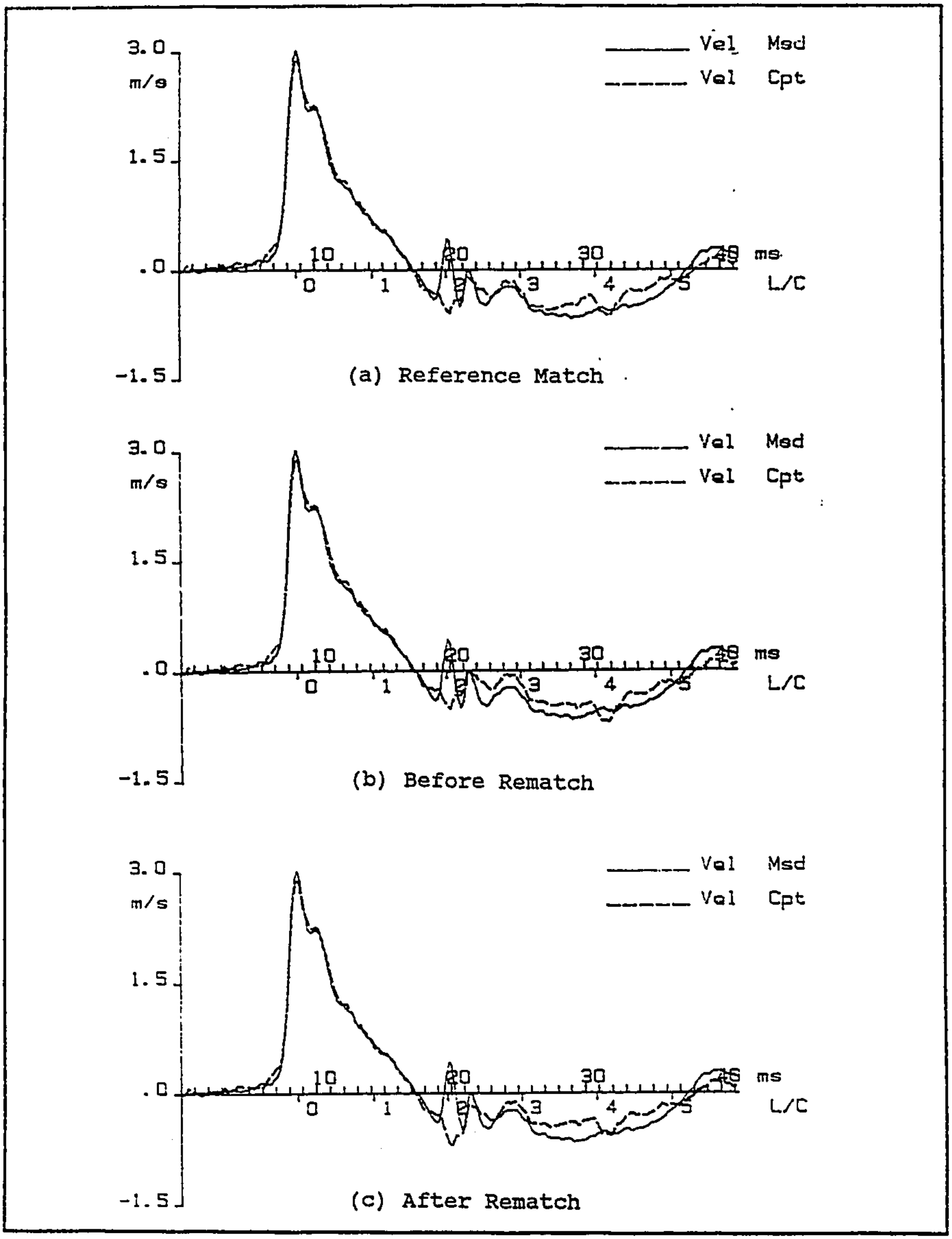

Fig. 6.39 JA Pile, WAPCAP Solution at 525 KN

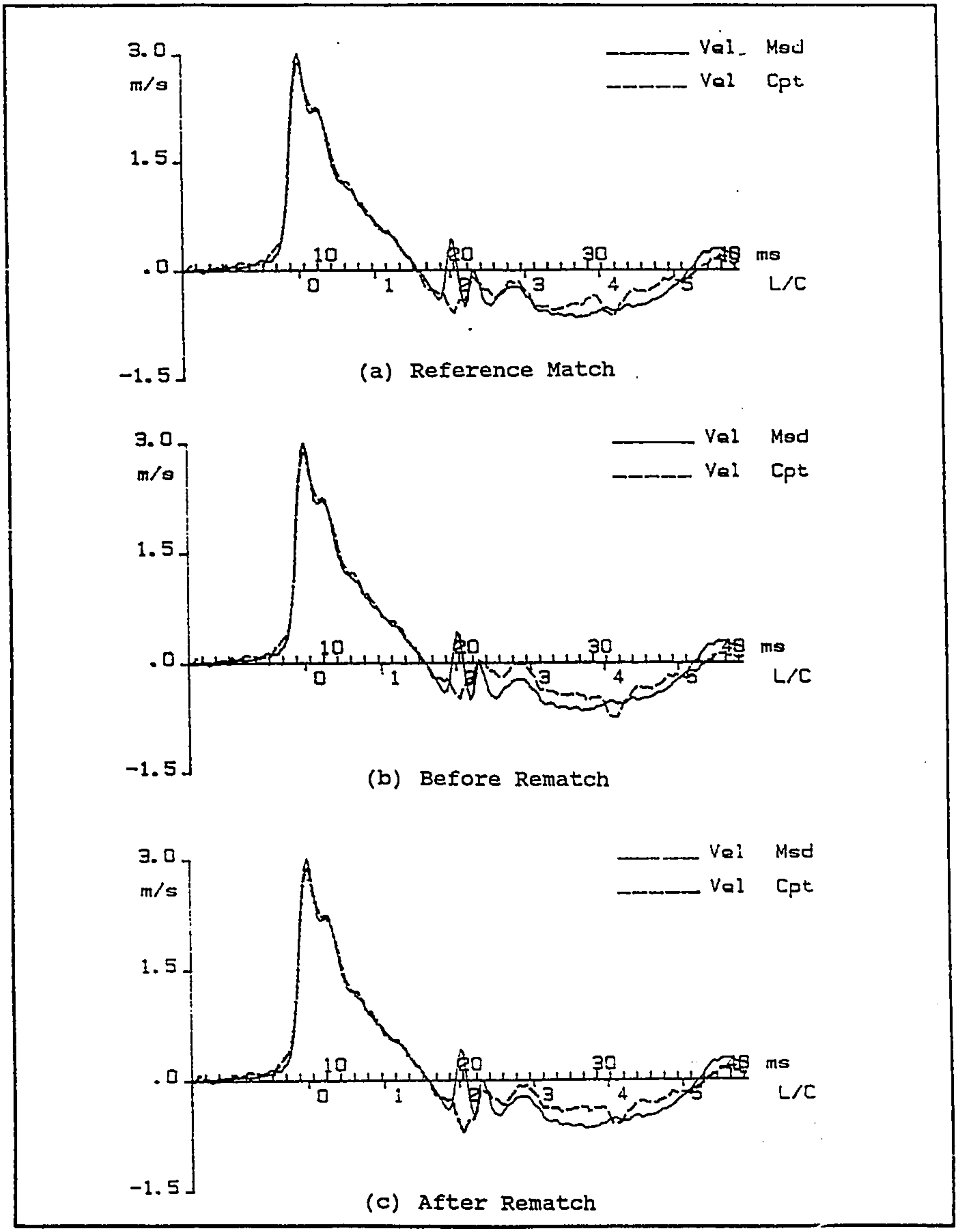

Fig. 6.40 JA Pile, WAPCAP Solution at 500 KN

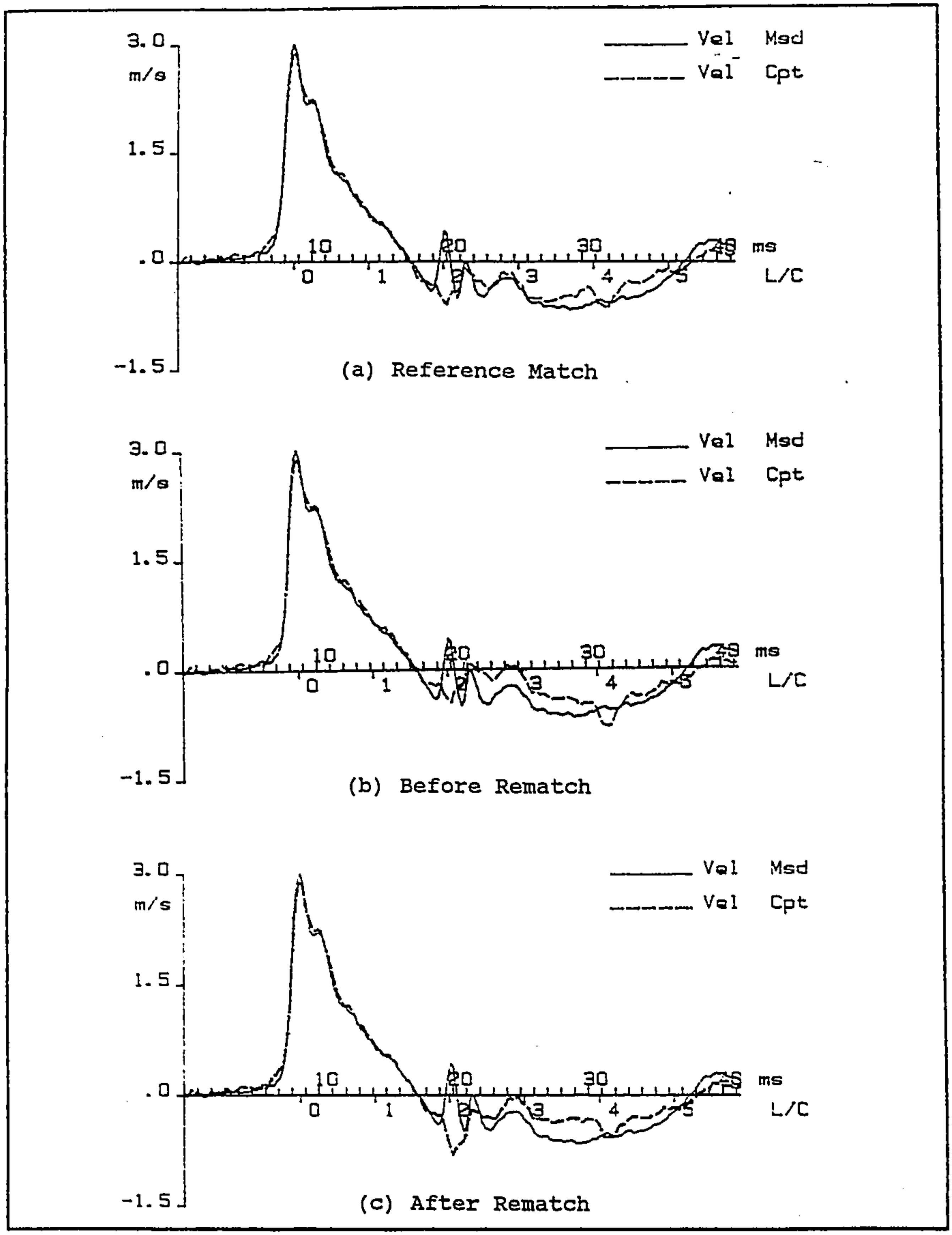

Fig. 6.41 JA Pile, WAPCAP Solution at 475 KN

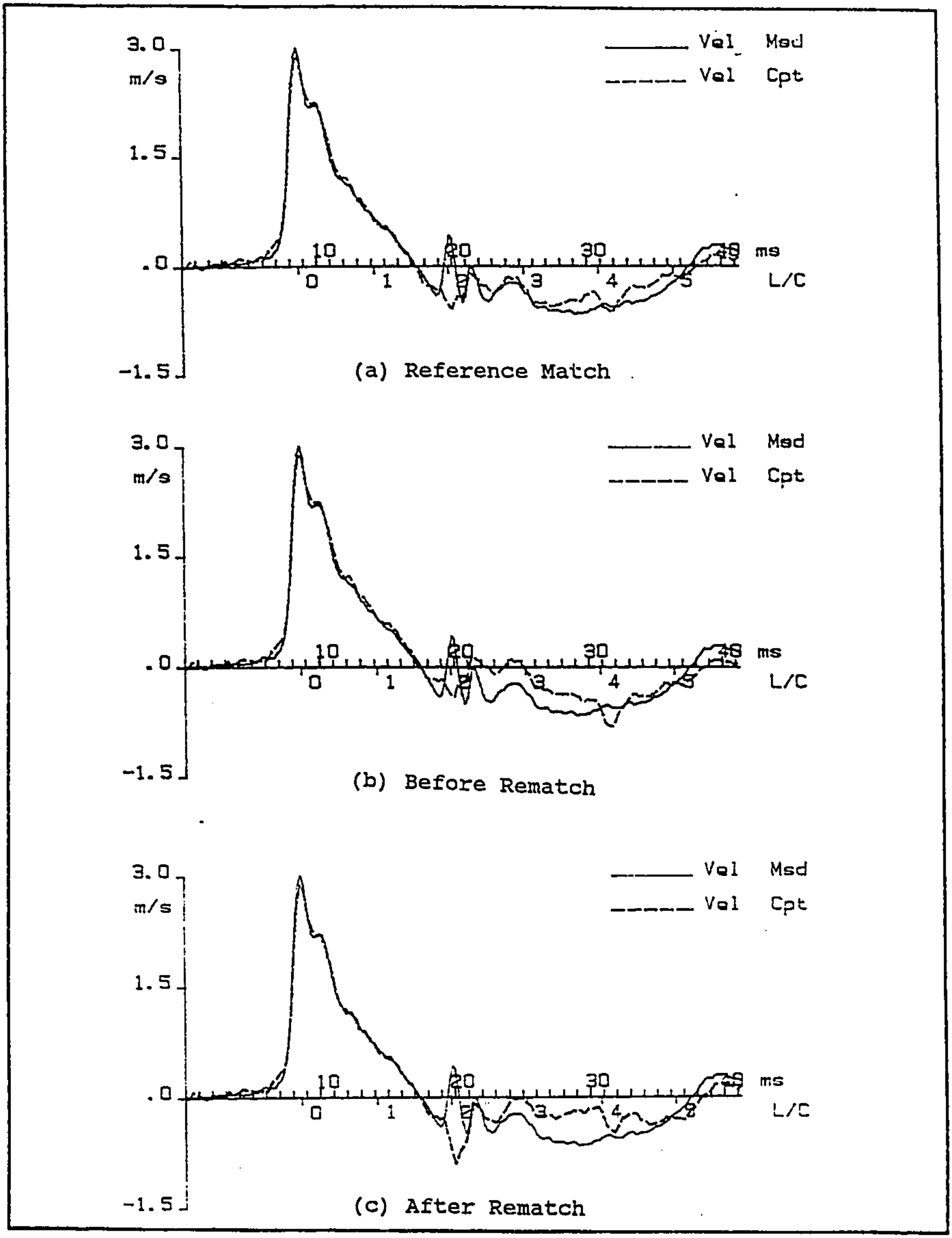

Fig. 6.42 JA Pile, WAPCAP Solution at 450 KN

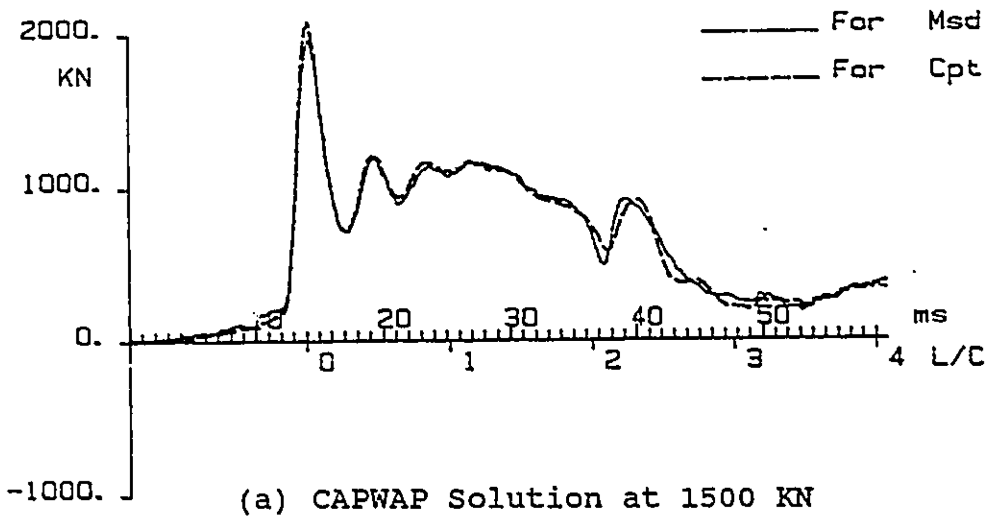

(a) CAPWAP Solution at 1500 KN

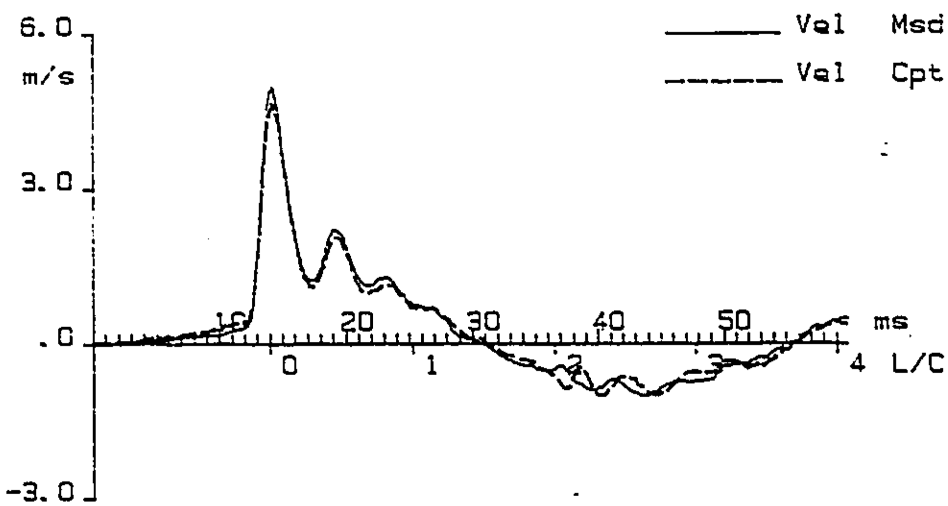

(b) WAPCAP Solution at 1500 KN

Fig. 6.43 AM Pile, Reference Matches

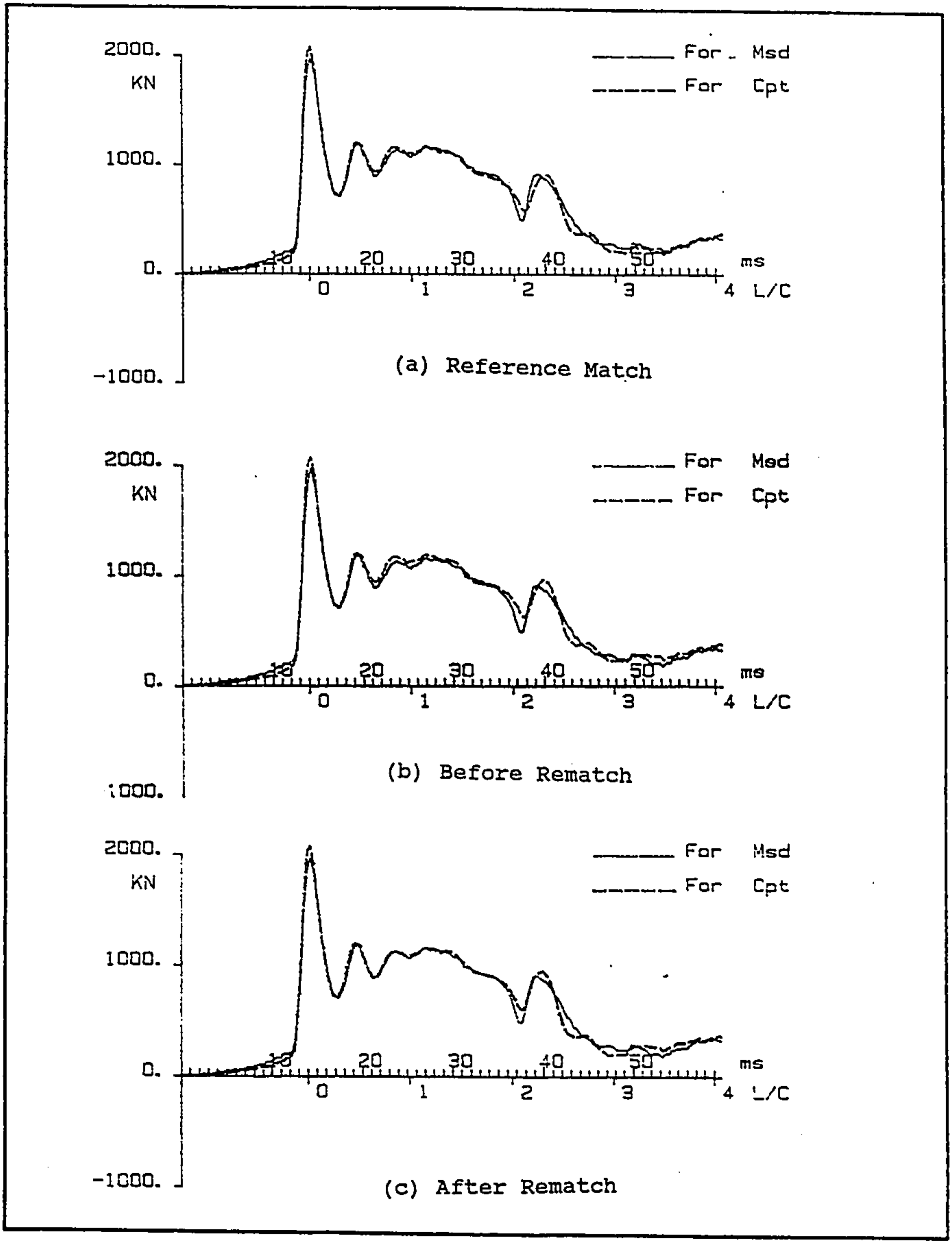

Fig. 6.44 AM Pile, CAPWAP Solution at 1575 KN

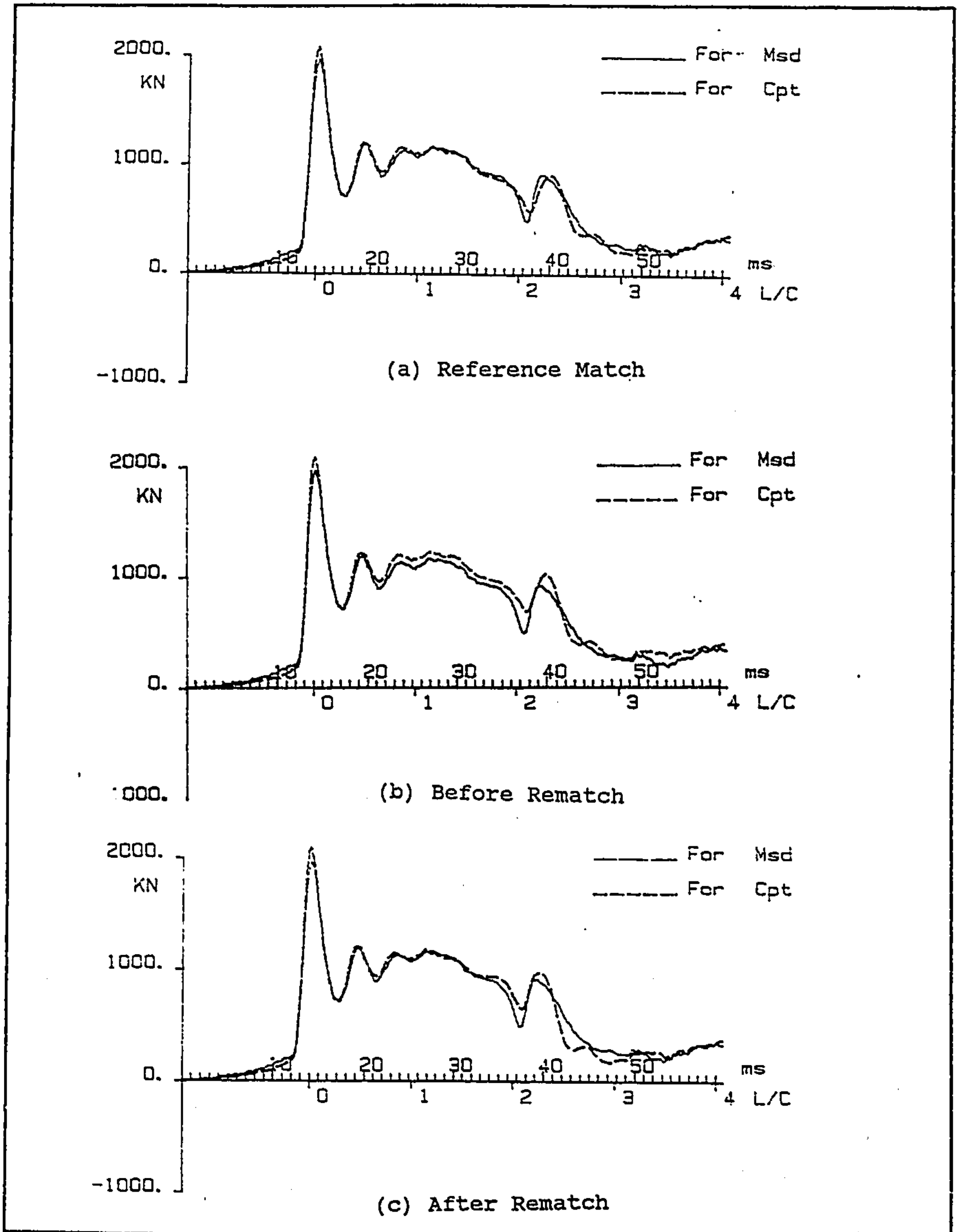

Fig. 6.45 AM Pile, CAPWAP Solution at 1650 KN

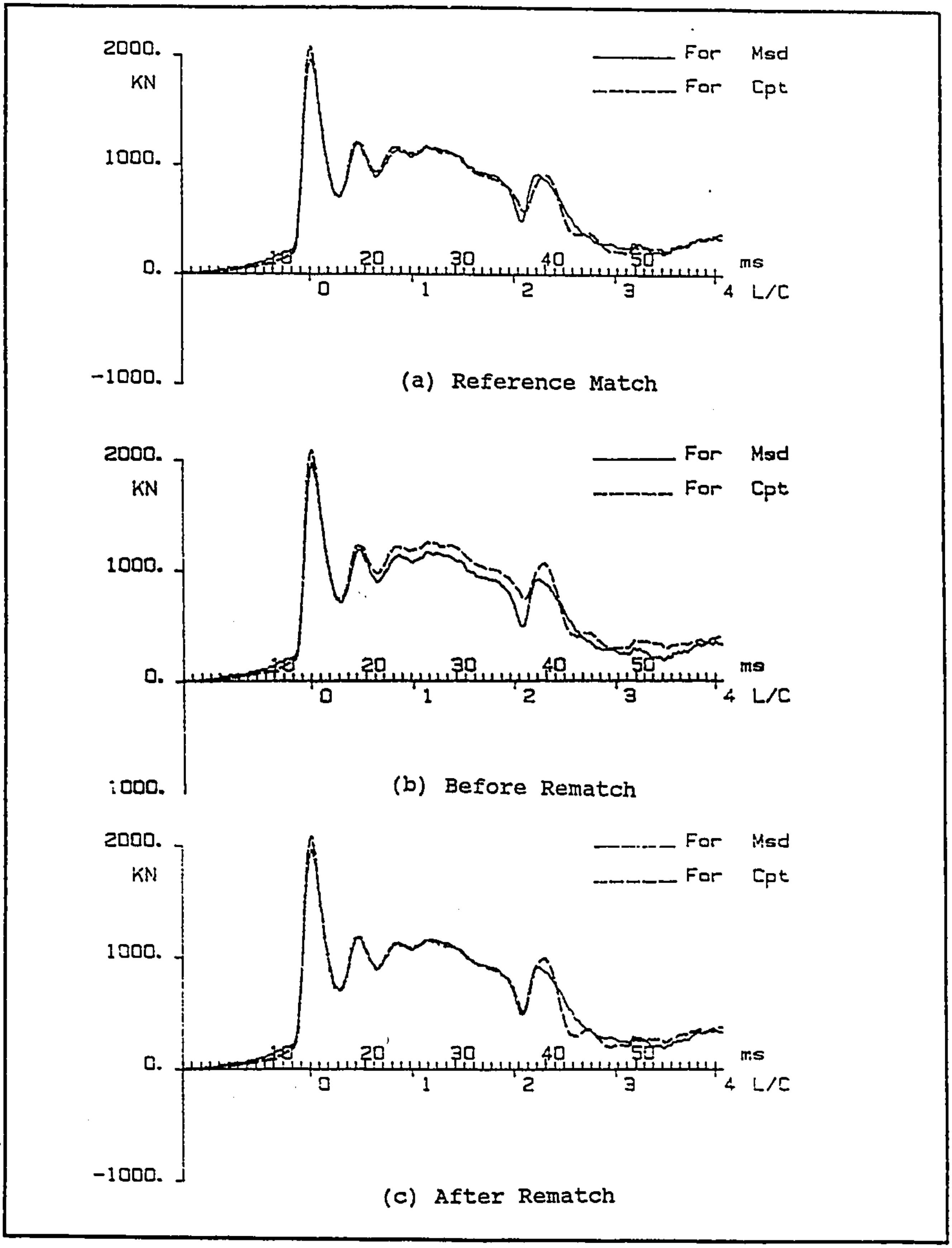

Fig. 6.46 AM Pile, CAPWAP Solution at 1725 KN

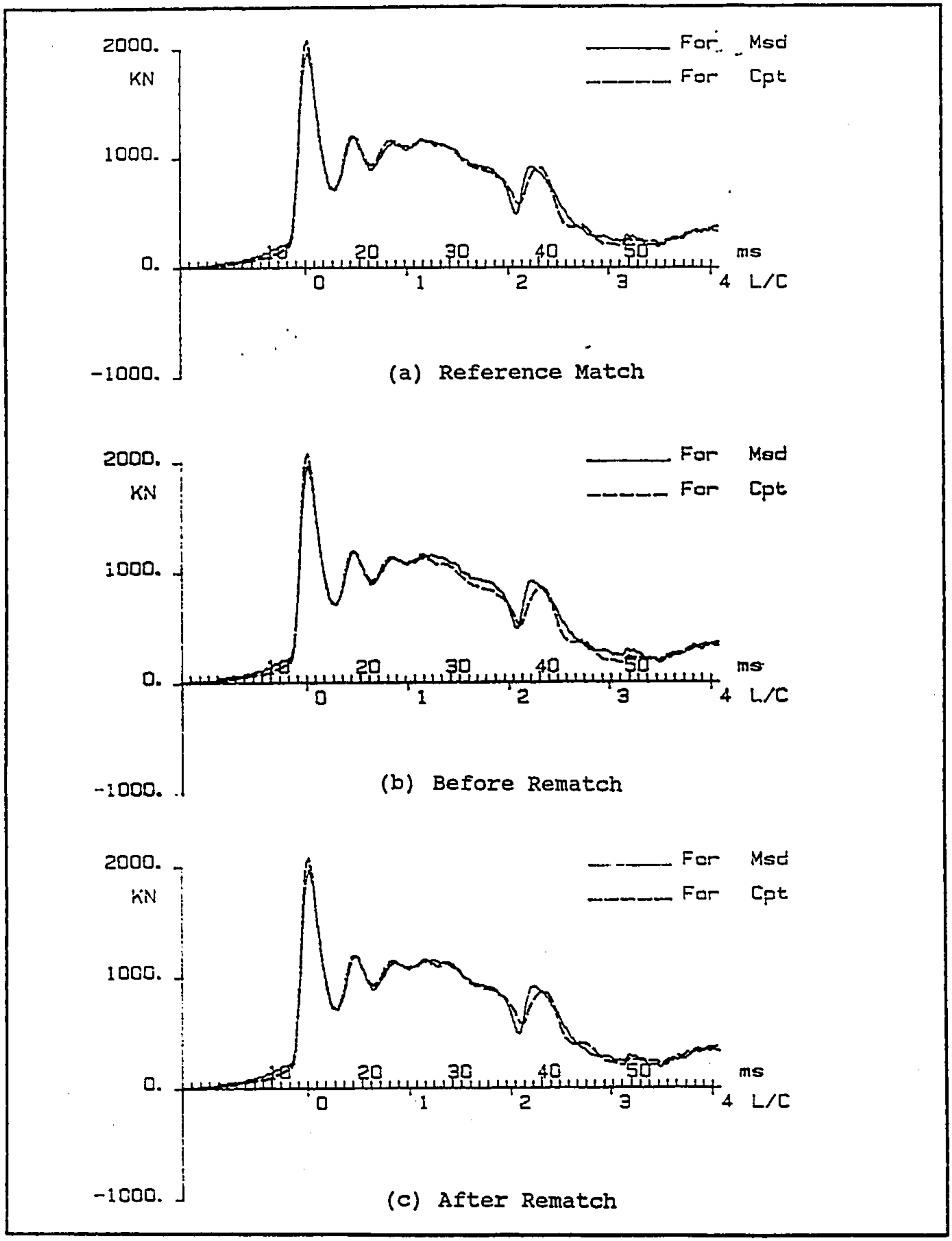

Fig. 6.47 AM Pile, CAPWAP Solution at 1425 KN

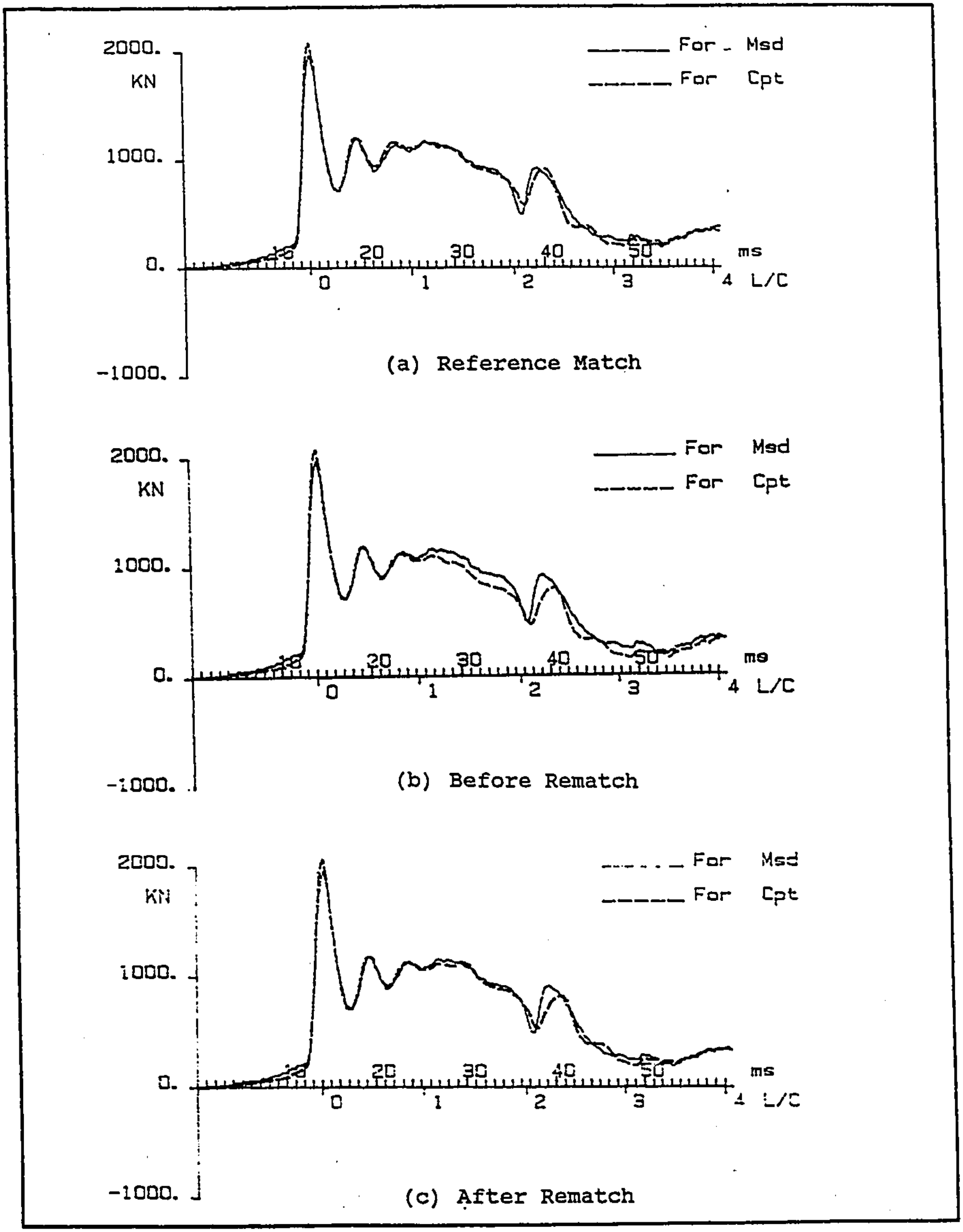

Fig. 6.48 AM Pile, CAPWAP Solution at 1350 KN

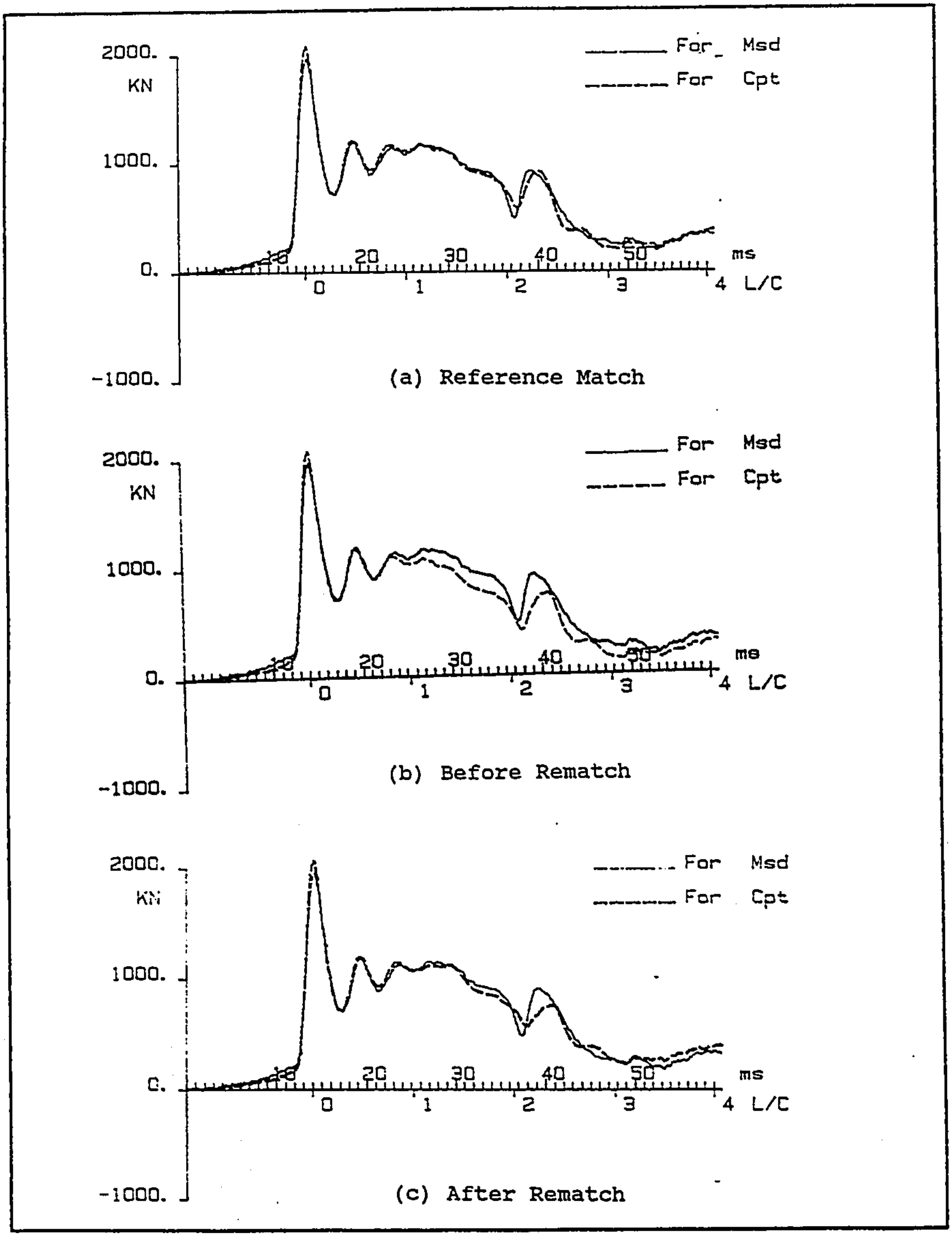

Fig. 6.49 AM Pile, CAPWAP Solution at 1275 KN

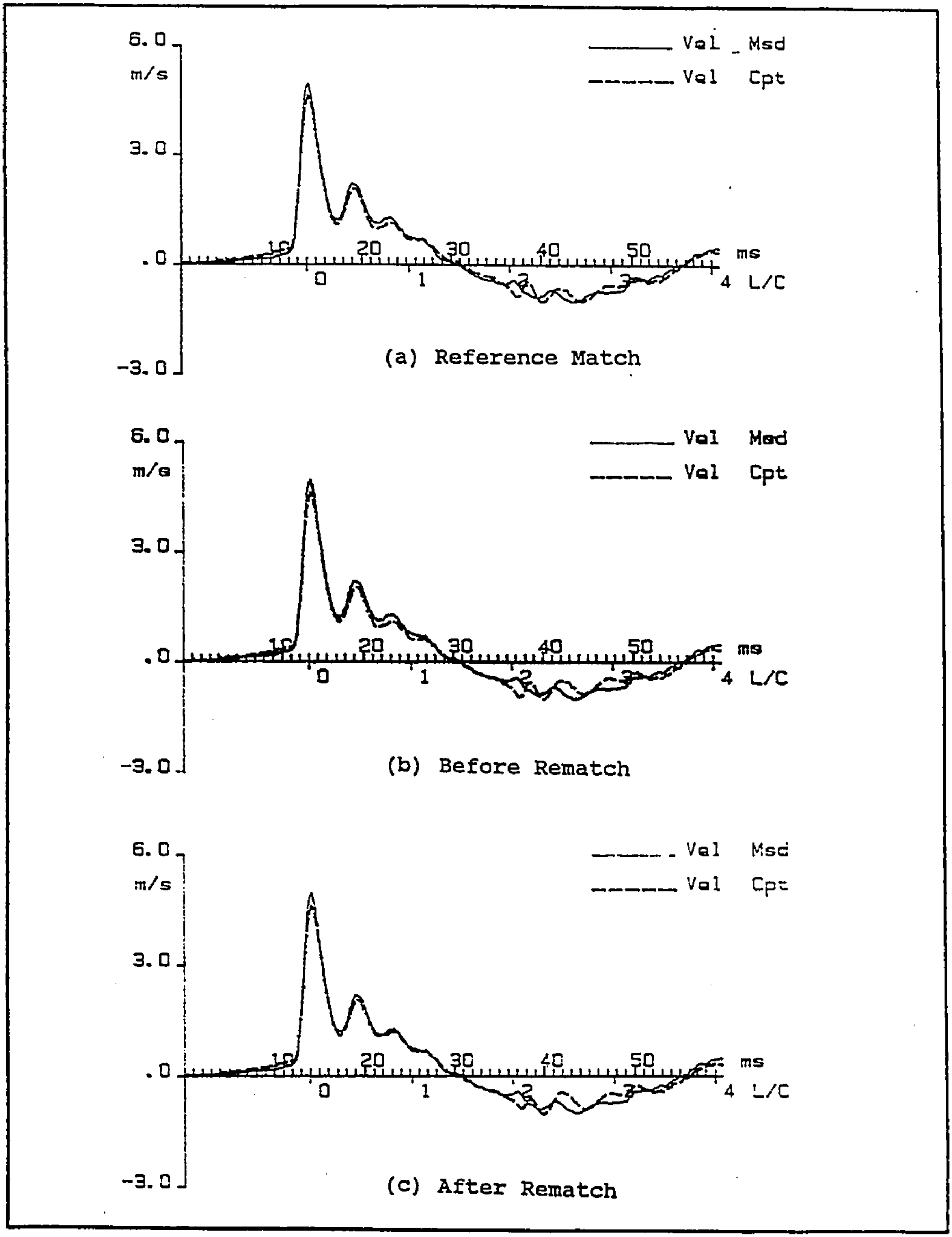

Fig. 6.50 AM Pile, WAPCAP Solution at 1575 KN

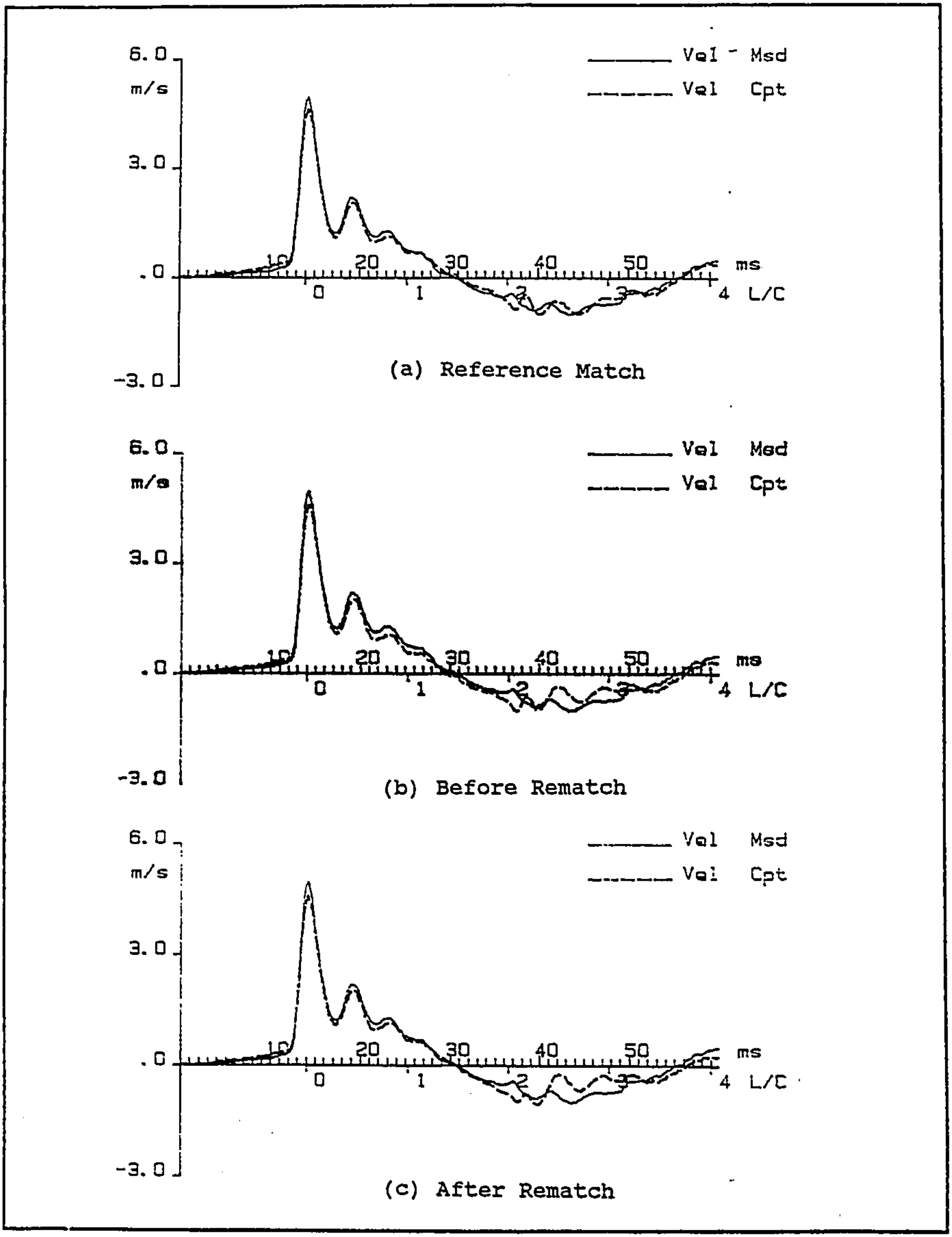

Fig. 6.51 AM Pile, WAPCAP Solution at 1650 KN

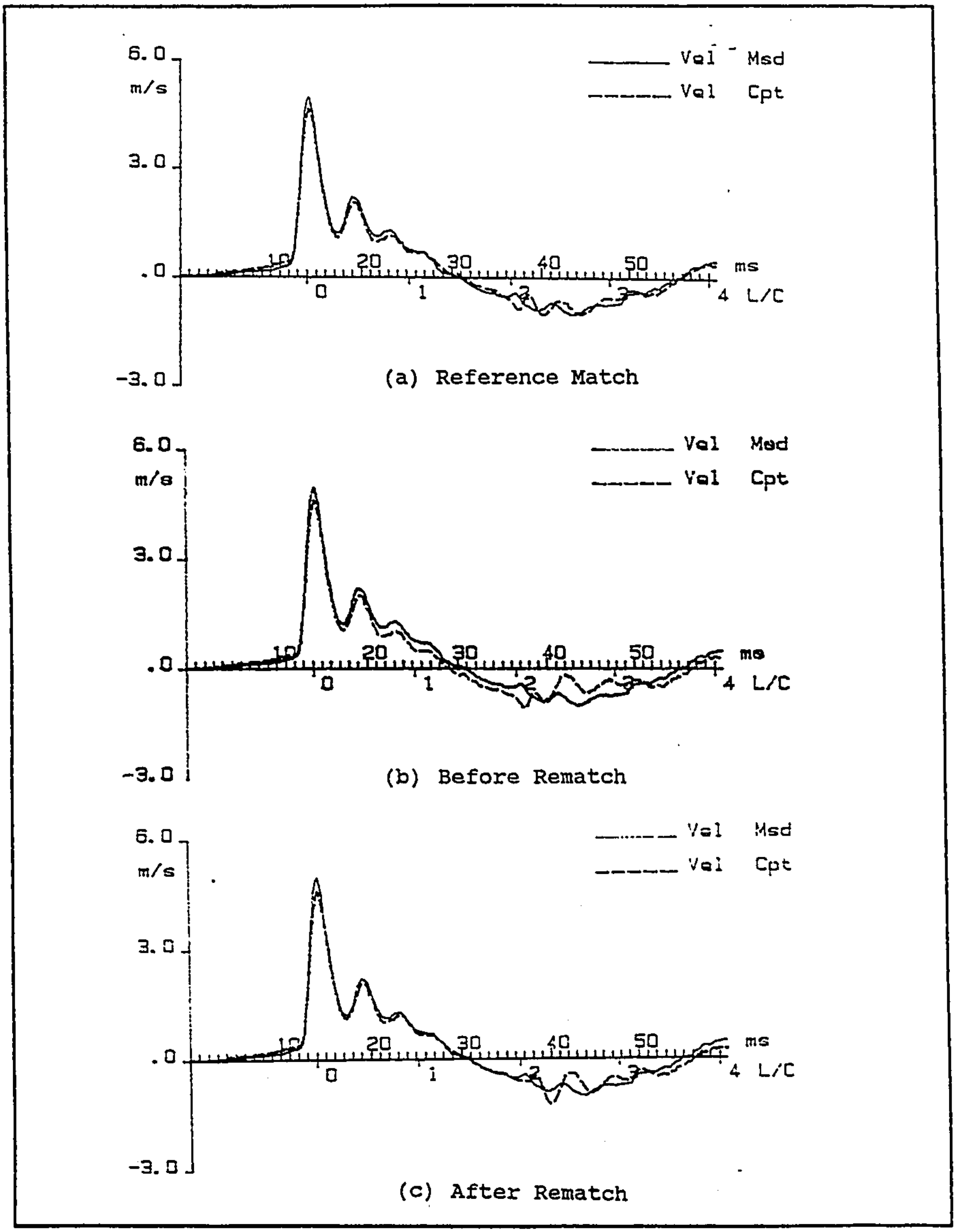

Fig. 6.52 AM Pile, WAPCAP Solution at 1725 KN

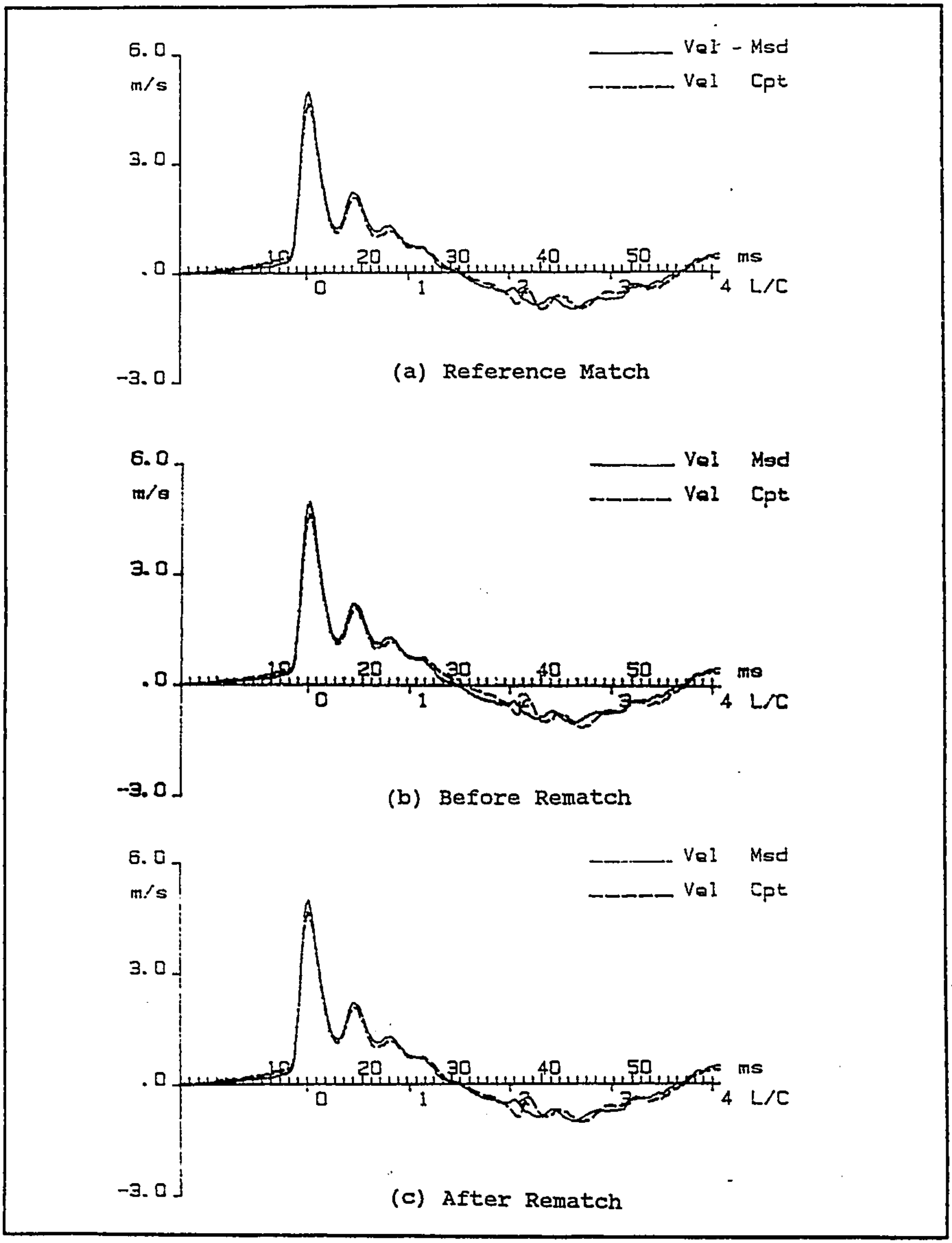

Fig. 6.53 AM Pile, WAPCAP Solution at 1425 KN

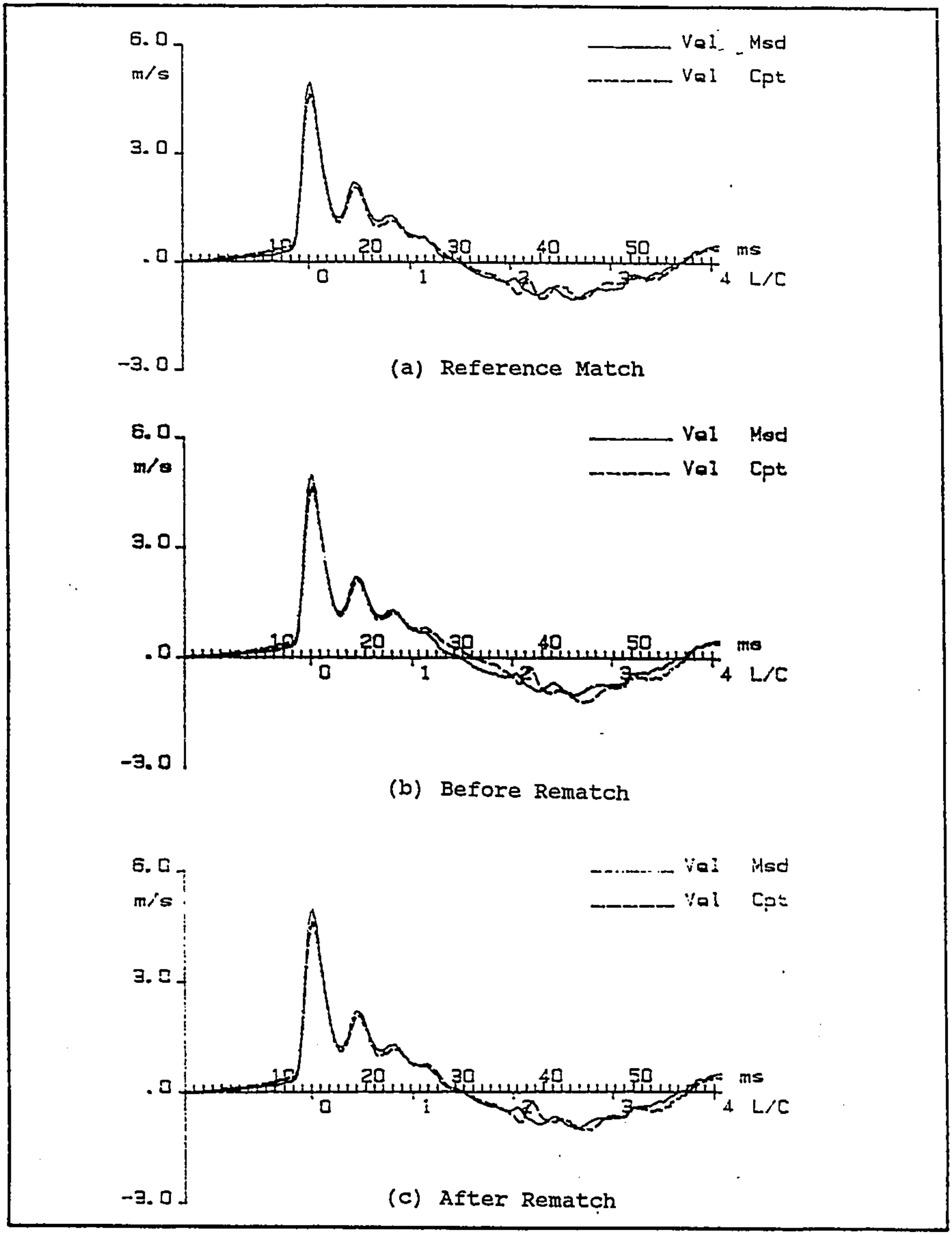

Fig. 6.54 AM Pile, WAPCAP Solution at 1350 KN

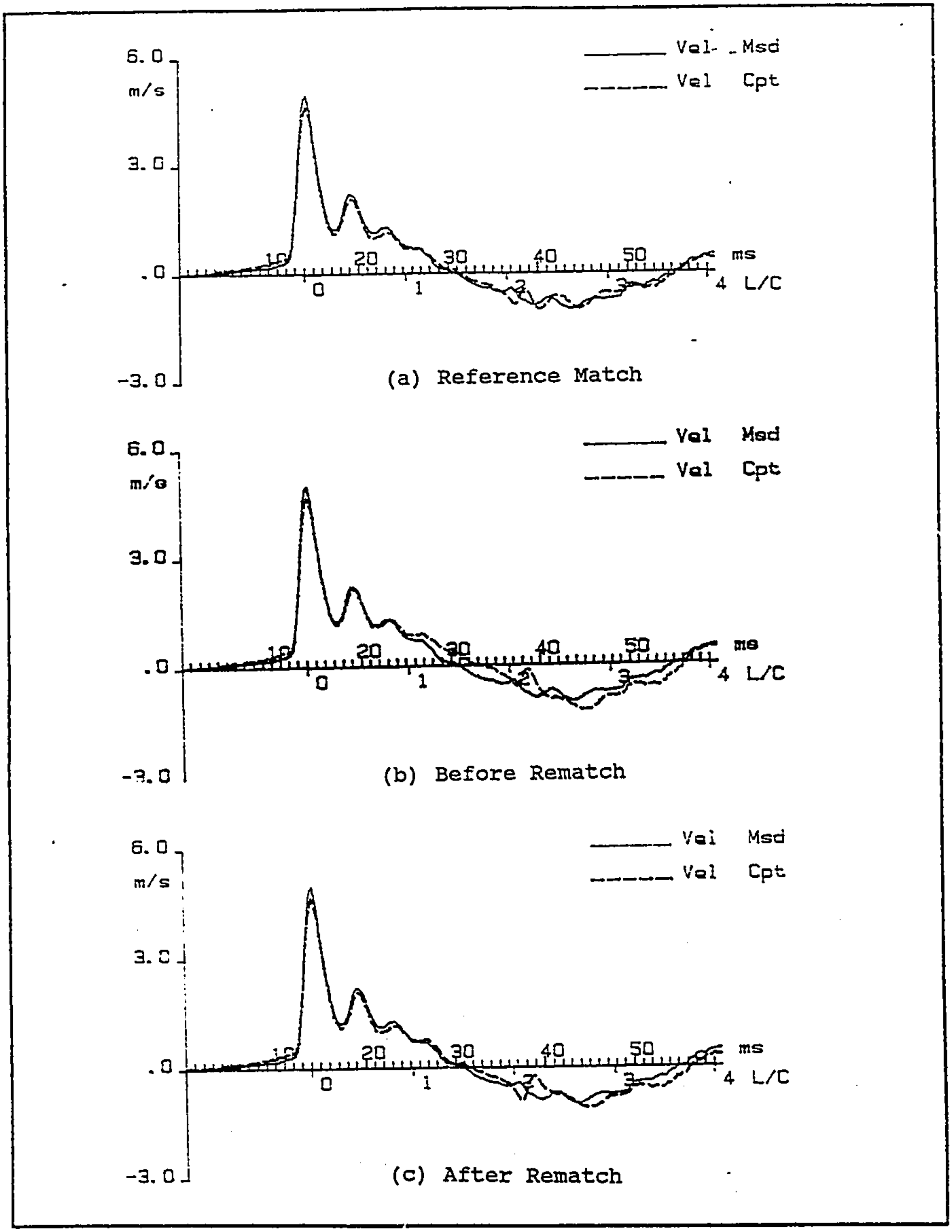

Fig. 6.55 AM Pile, WAPCAP Solution at 1275 KN

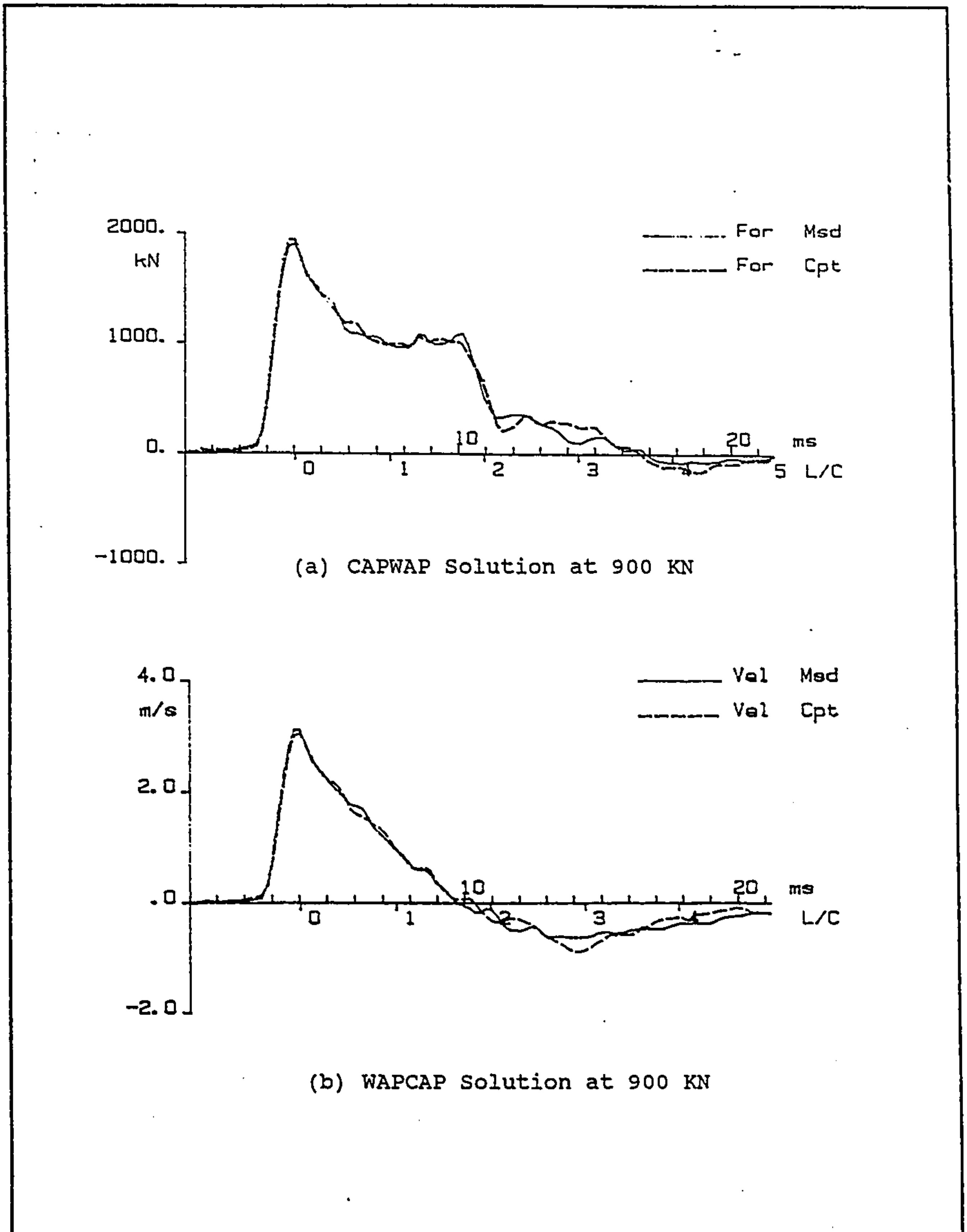

Fig. 6.56 LW Pile, Reference Matches

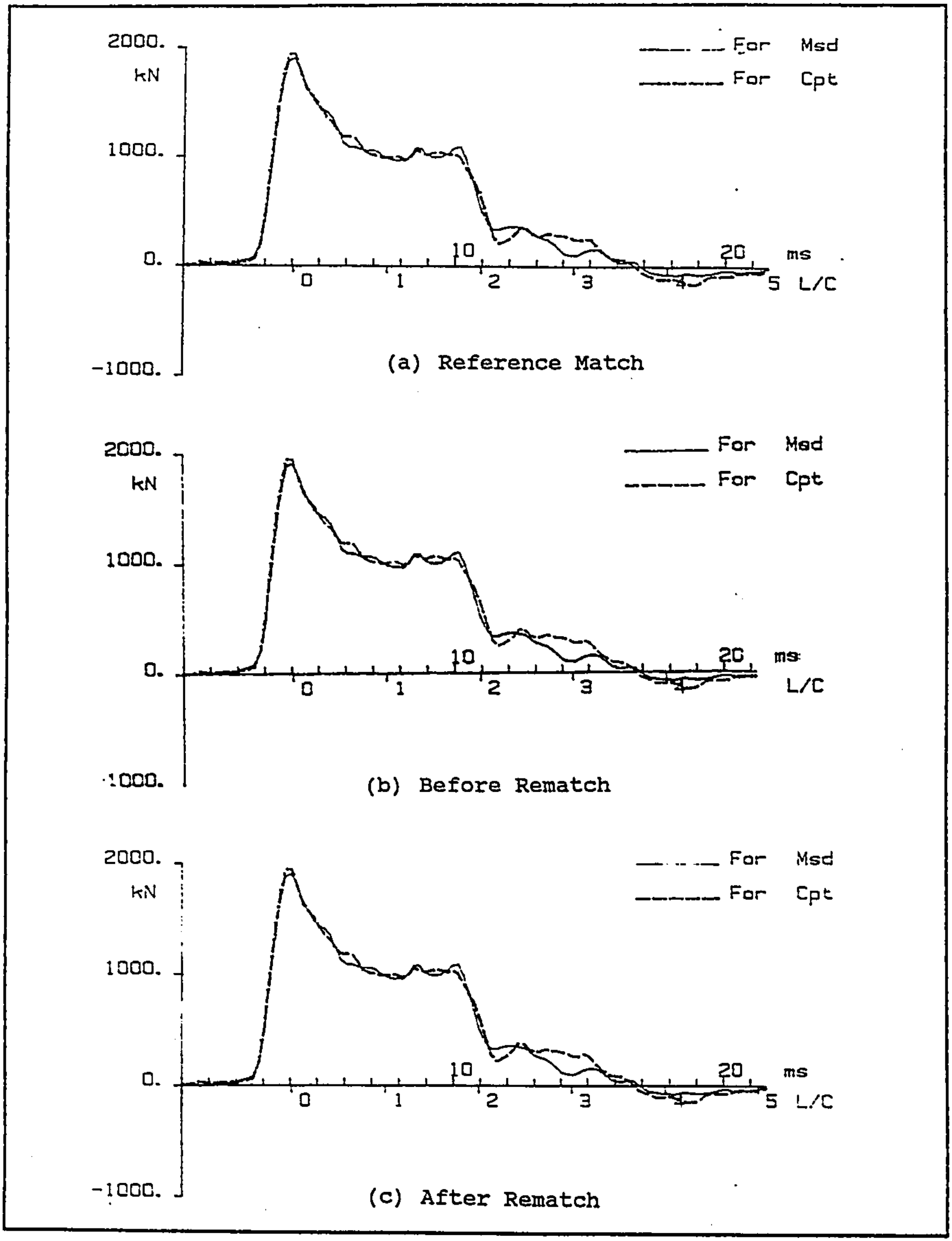

Fig. 6.57 LW Pile, CAPWAP Solution at 945 KN

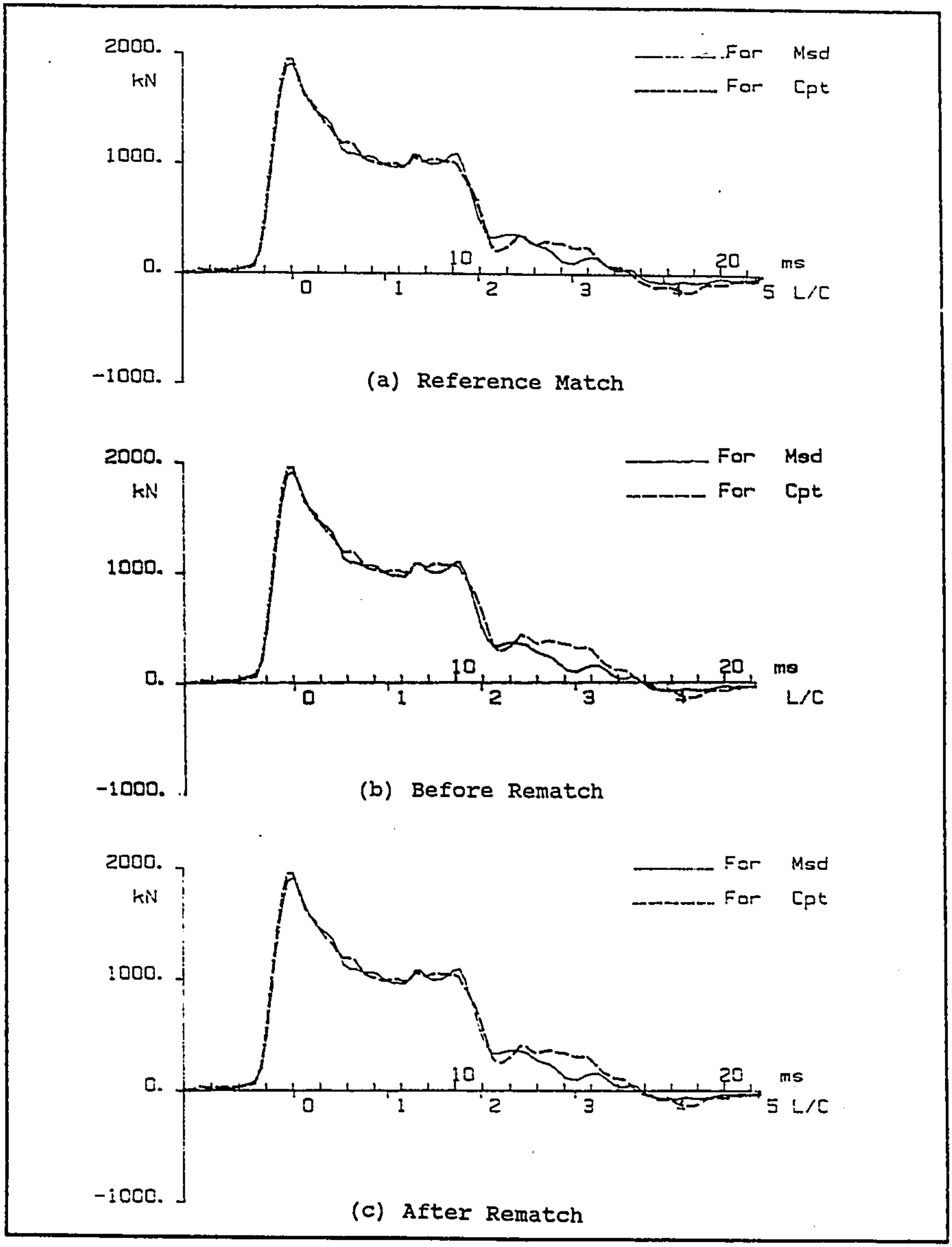

Fig. 6.58 LW Pile, CAPWAP Solution at 990 KN

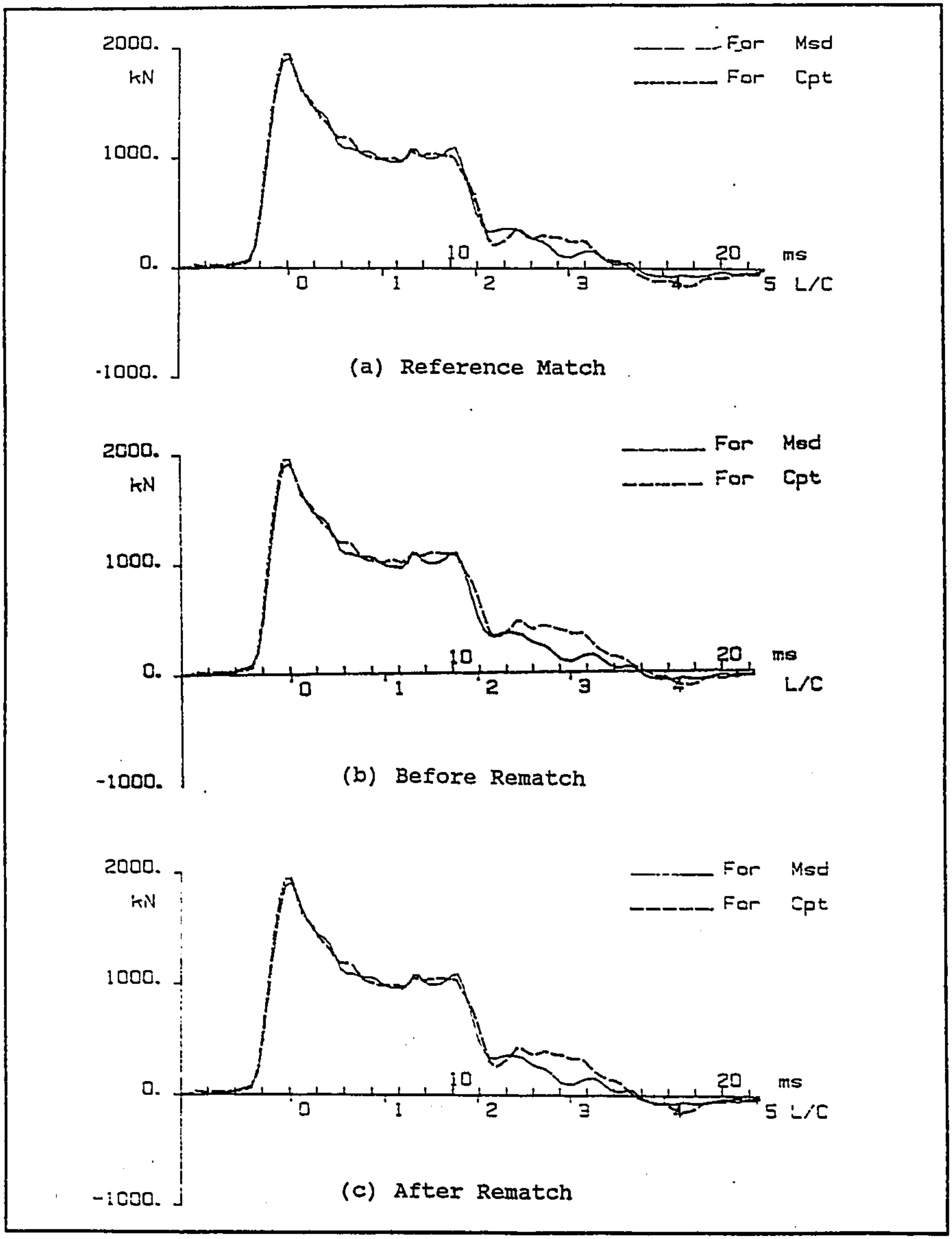

Fig. 6.59 LW Pile, CAPWAP Solution at 1035 KN

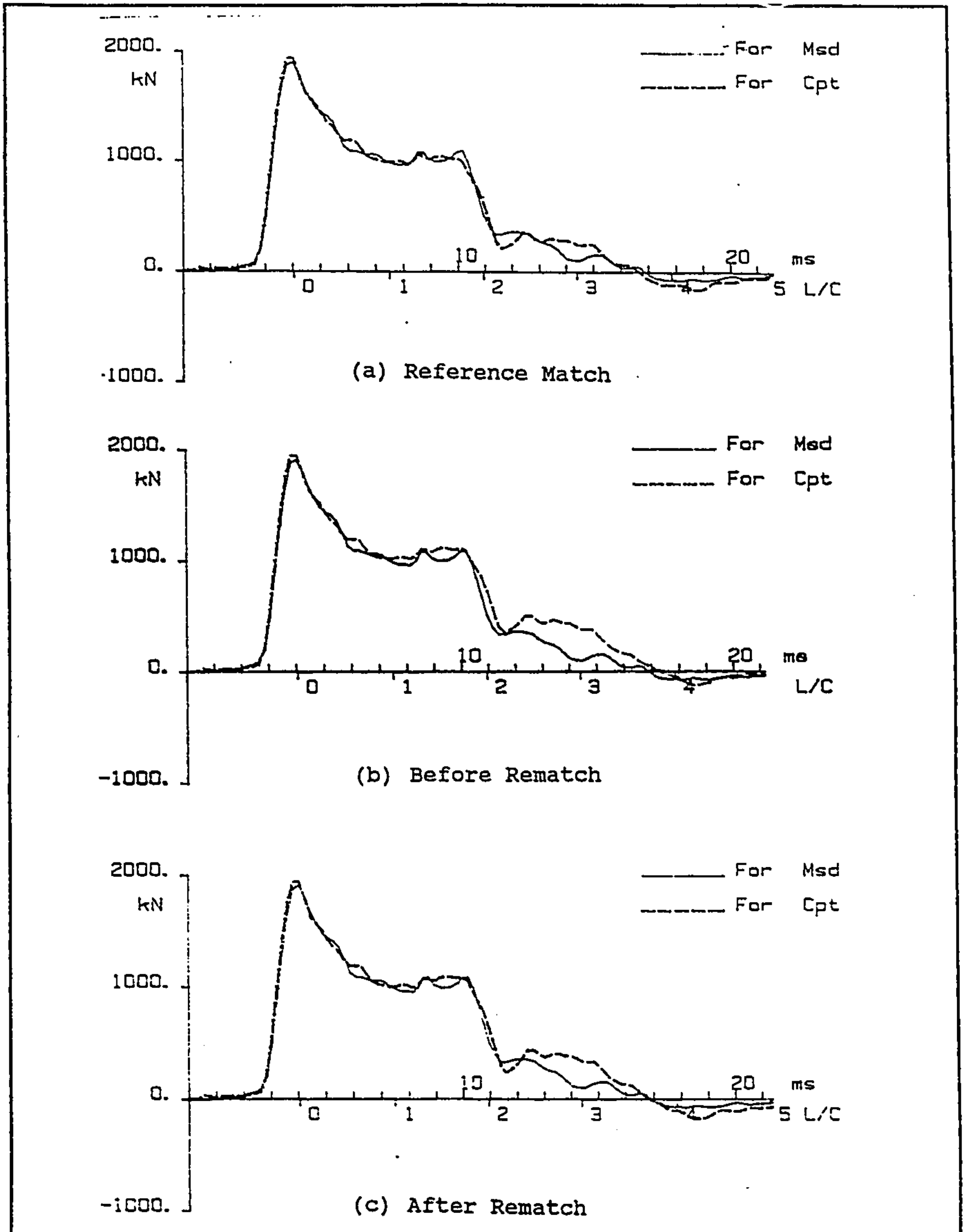

Fig. 6.60 LW Pile, CAPWAP Solution at 1080 KN

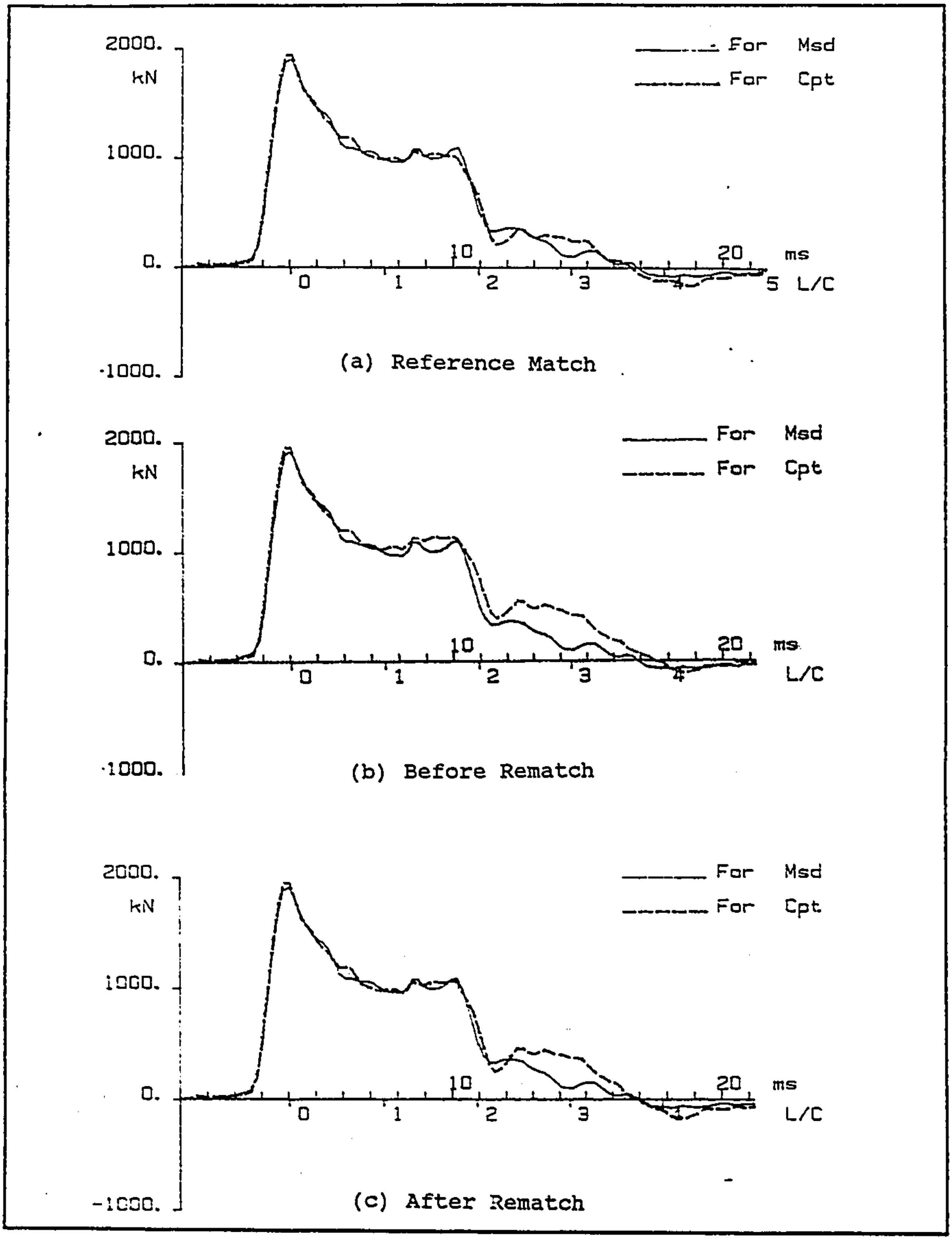

Fig. 6.61 LW Pile, CAPWAP Solution at 1125 KN

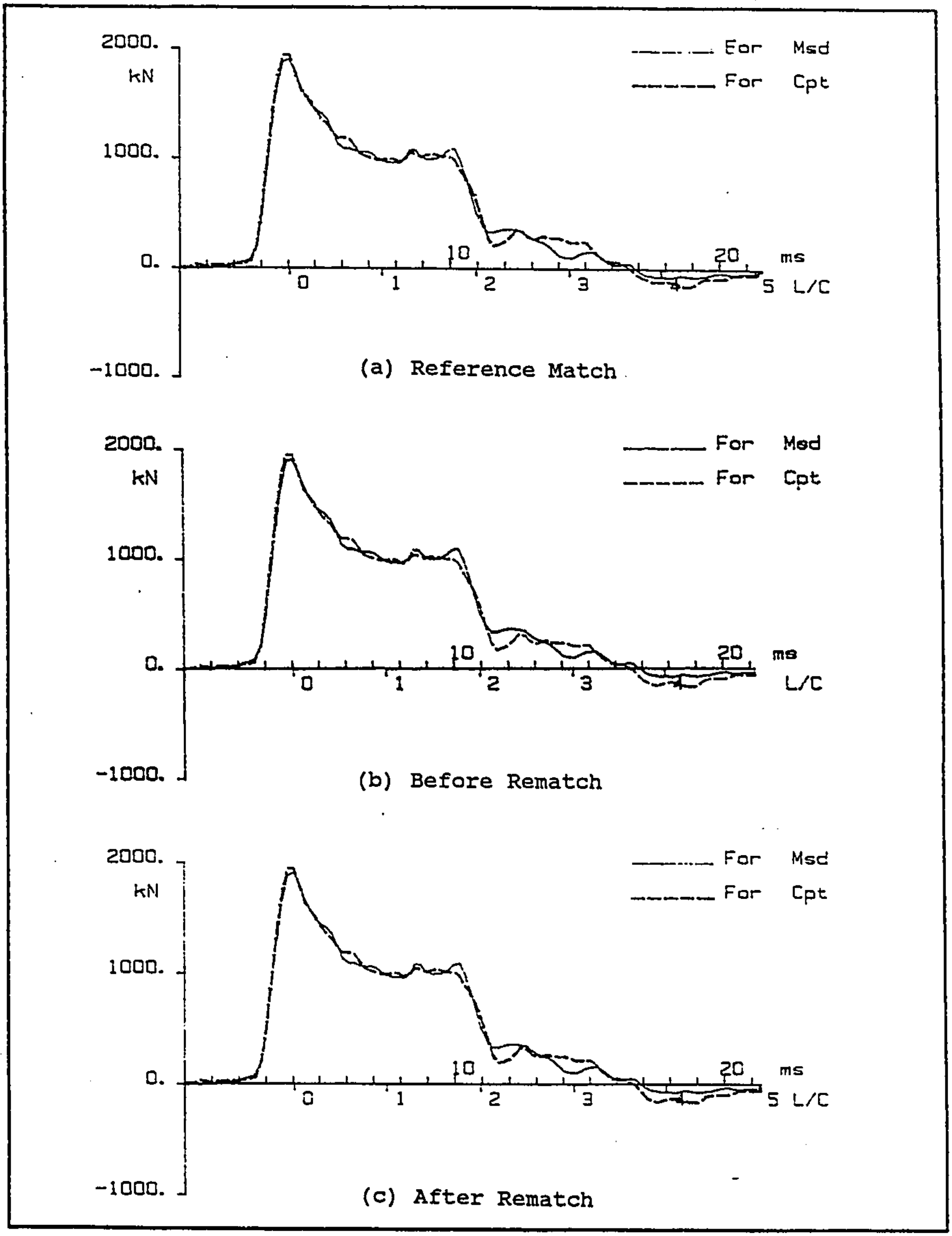

Fig. 6.62 LW Pile, CAPWAP Solution at 855 KN

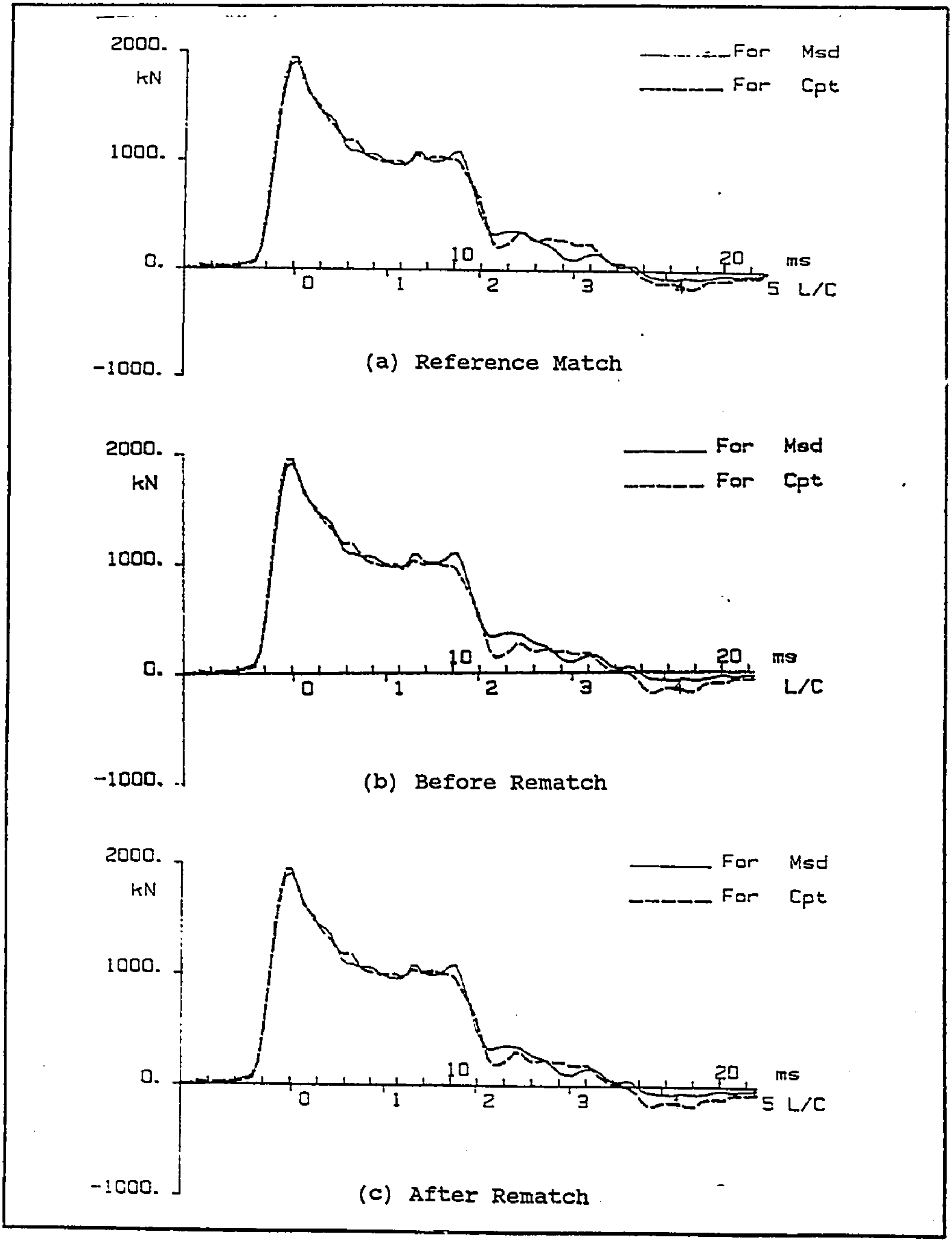

Fig. 6.63 LW Pile, CAPWAP Solution at 810 KN

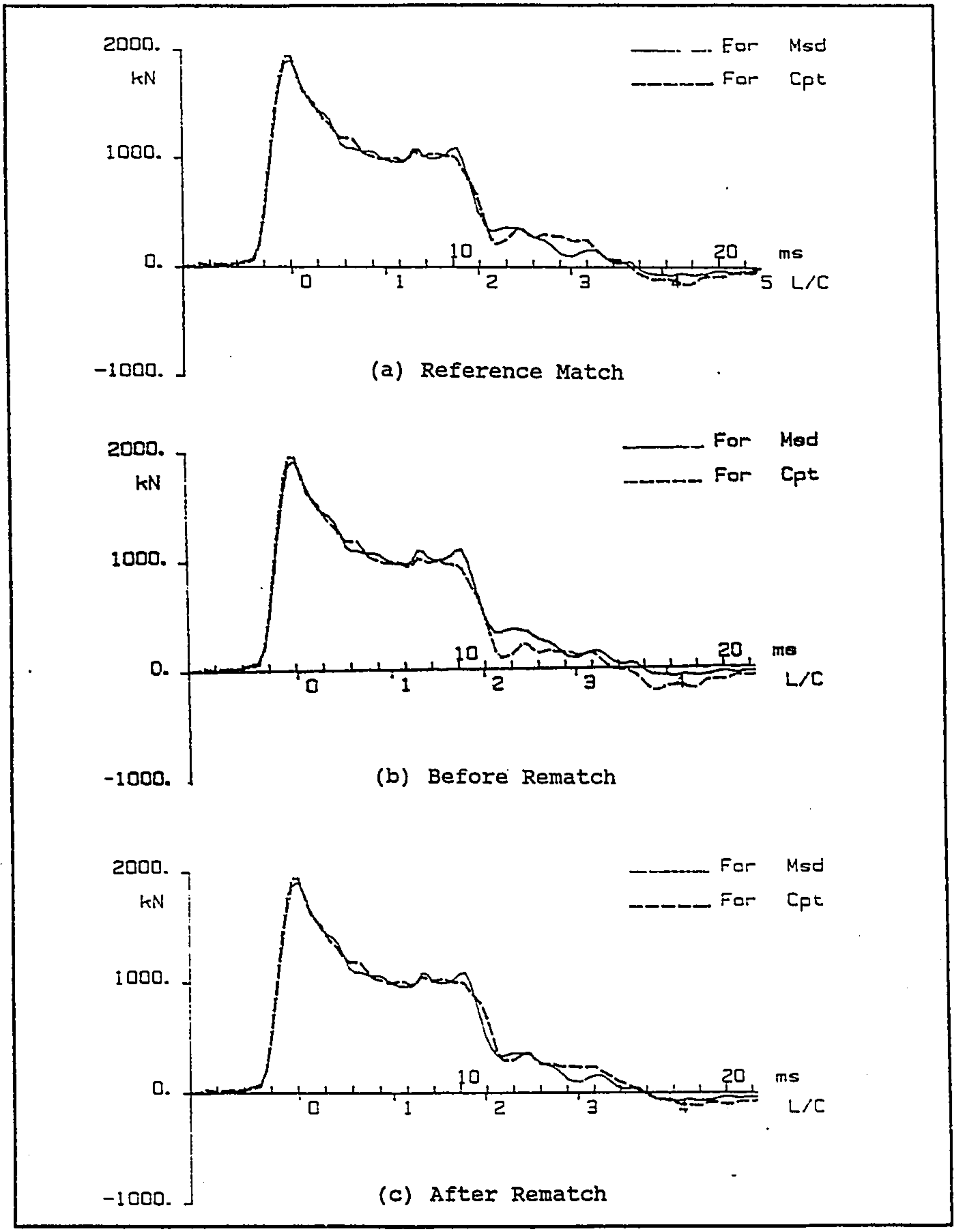

Fig. 6.64 LW Pile, CAPWAP Solution at 765 KN

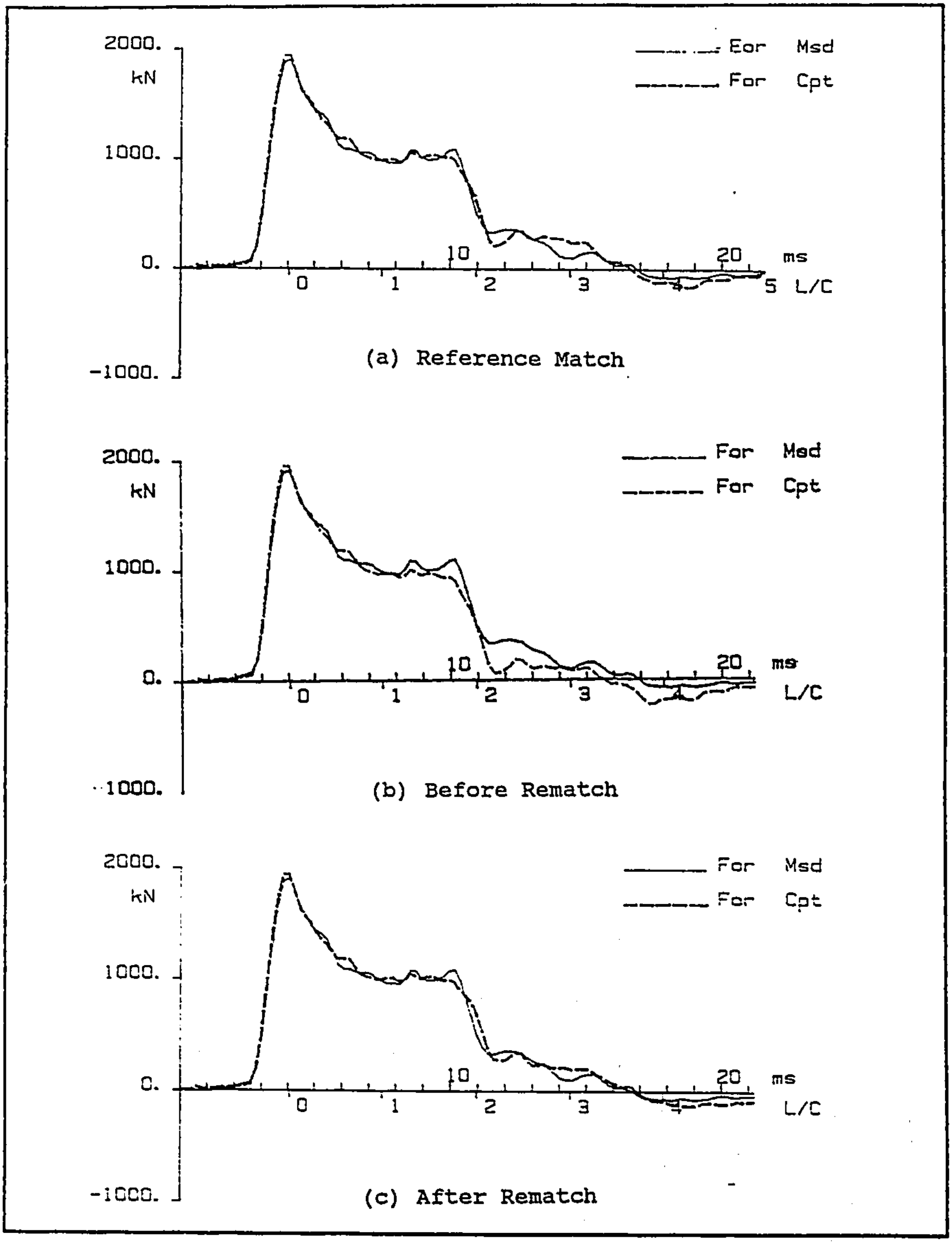

Fig. 6.65 LW Pile, CAPWAP Solution at 720 KN

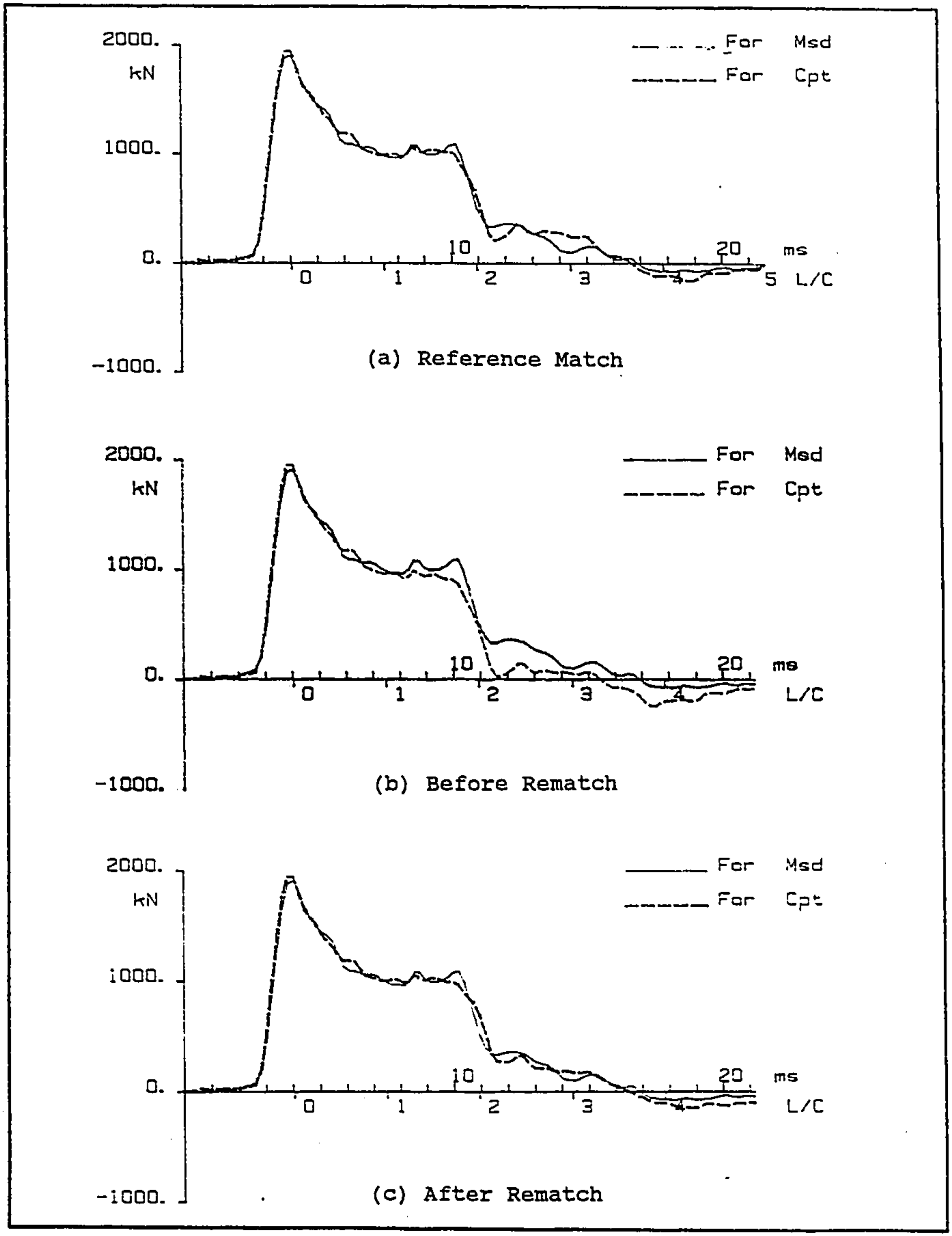

Fig. 6.66 LW Pile, CAPWAP Solution at 675 KN

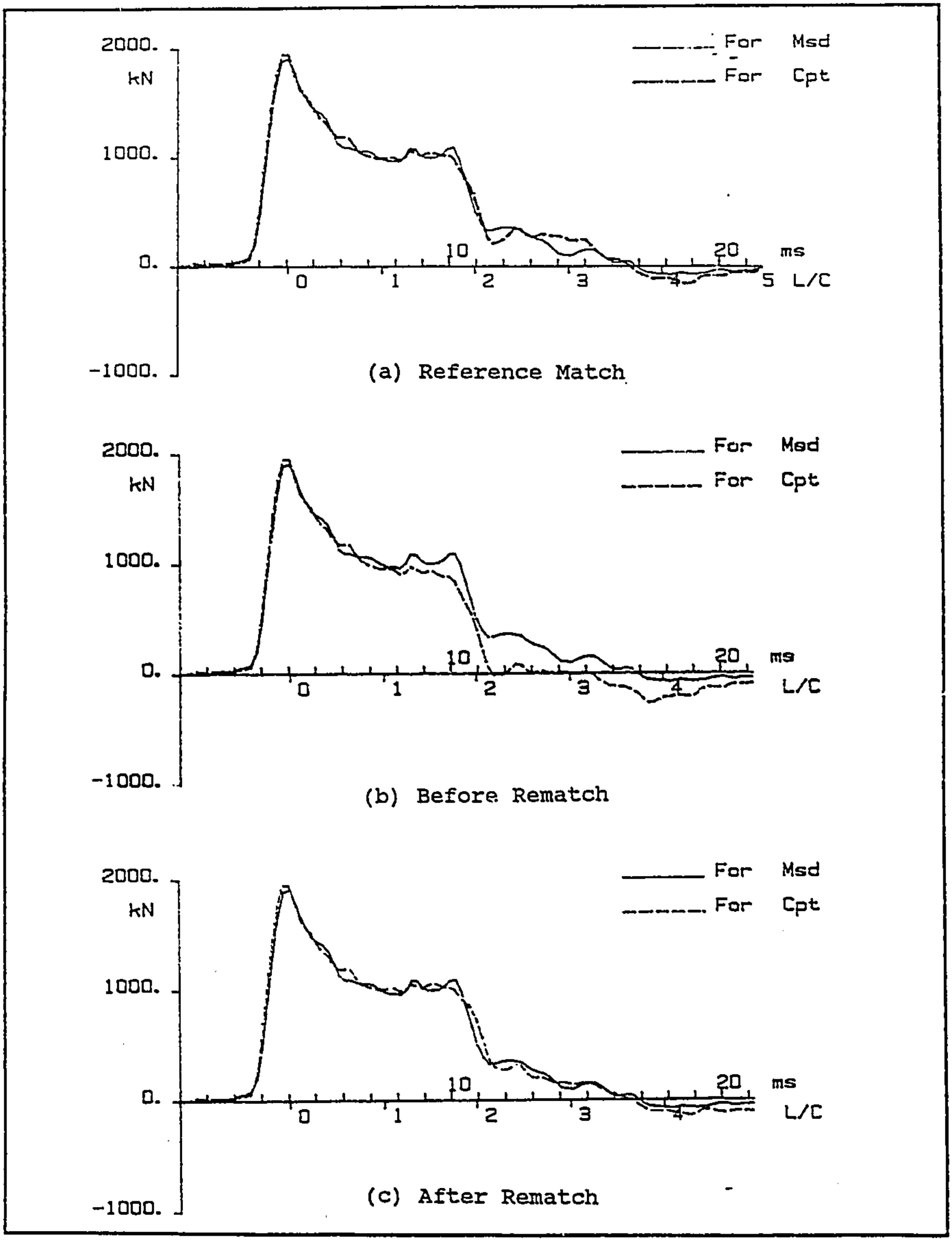

Fig. 6.67 LW Pile, CAPWAP Solution at 610 KN

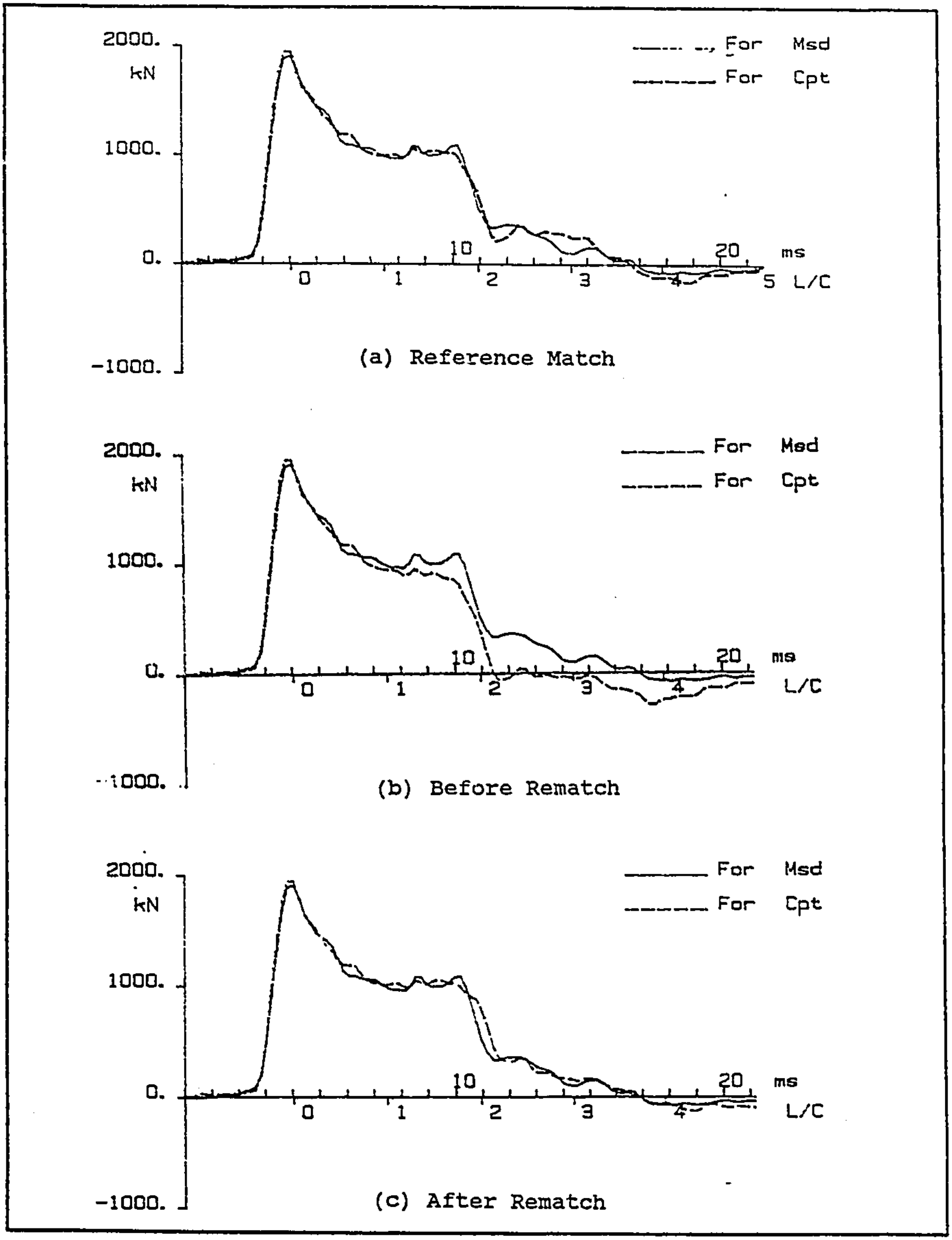

Fig. 6.68 LW Pile, CAPWAP Solution at 565 KN

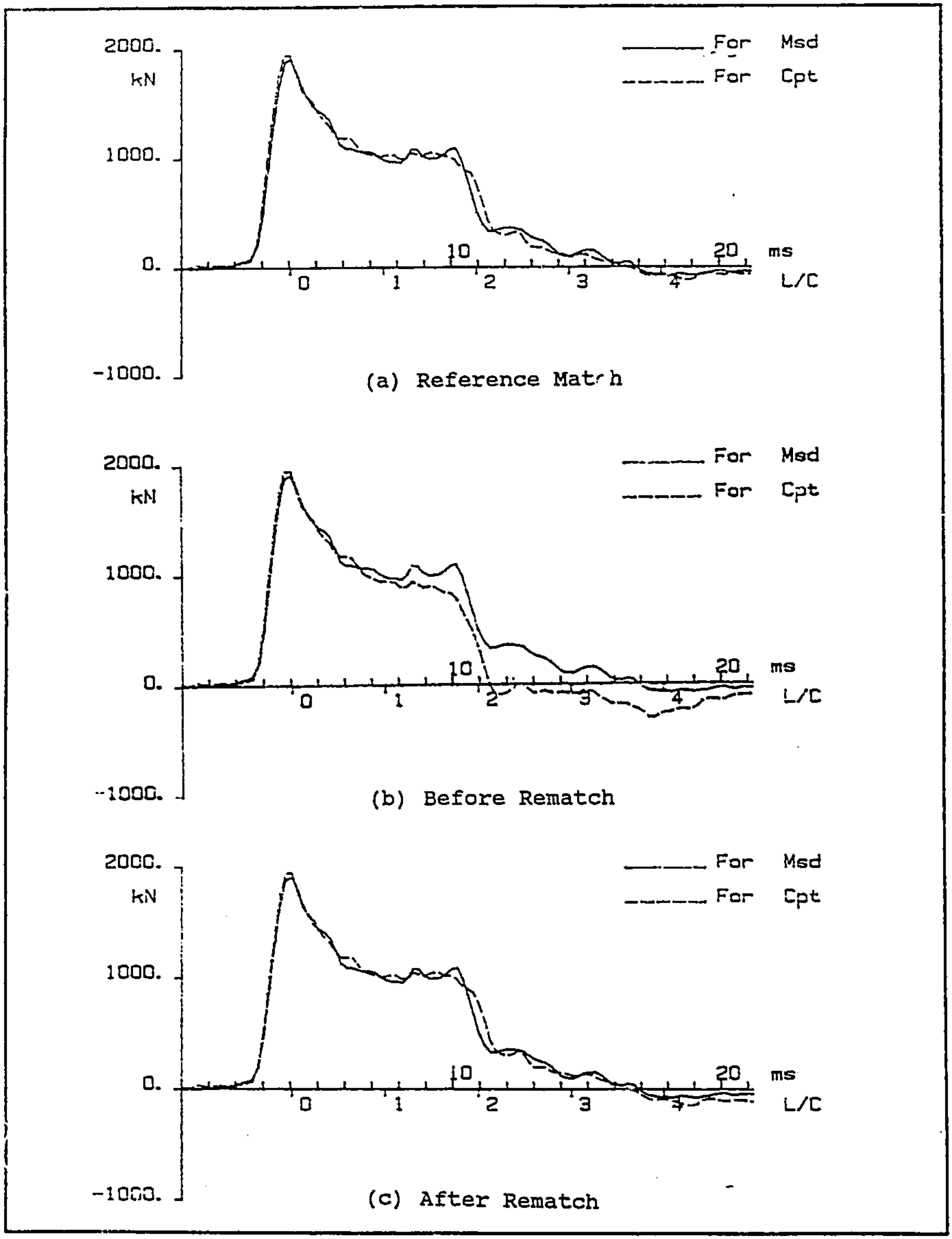

Fig. 6.69 LW Pile, CAPWAP Solution at 520 KN

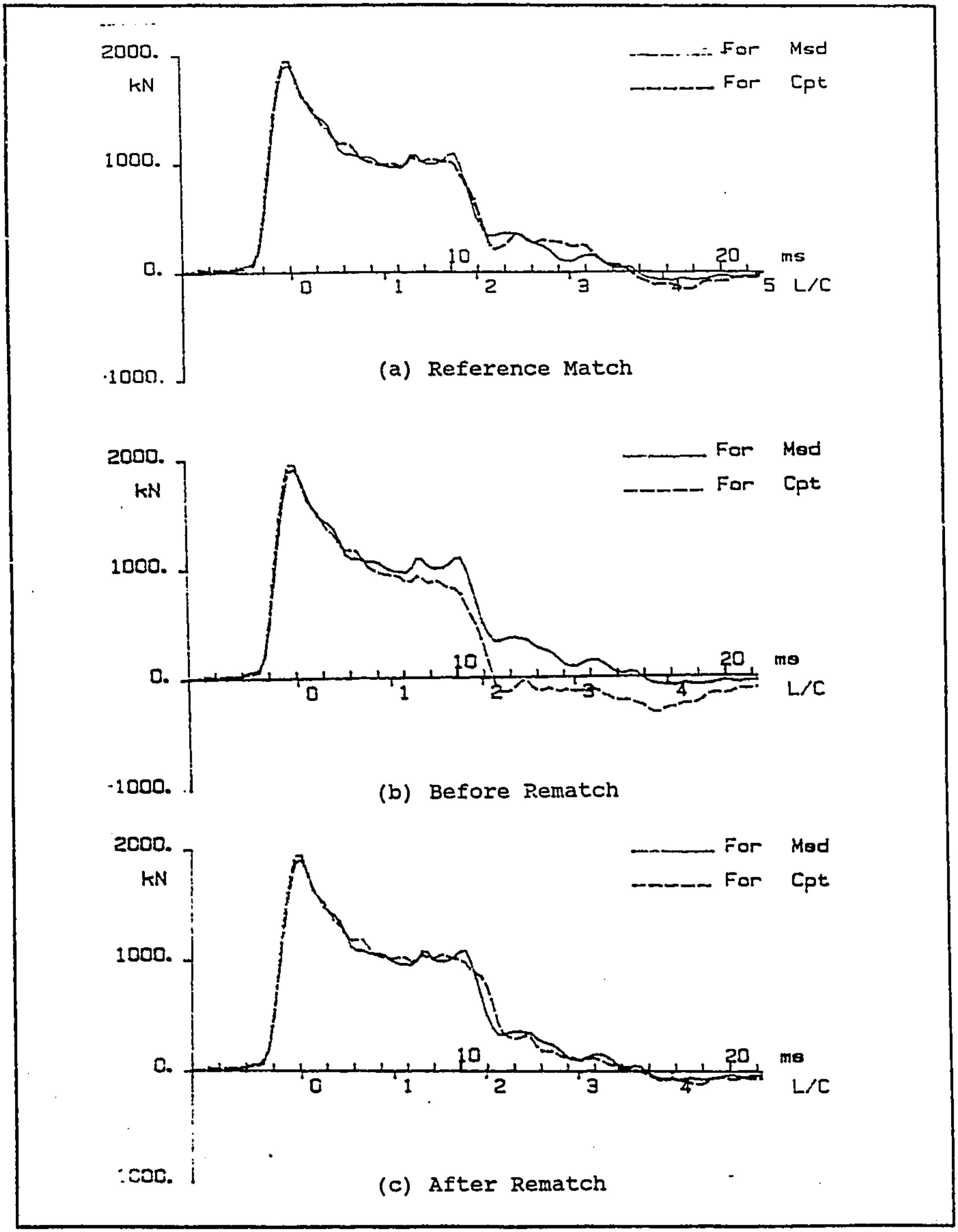

Fig. 6.70 LW Pile, CAPWAP Solution at 475 KN

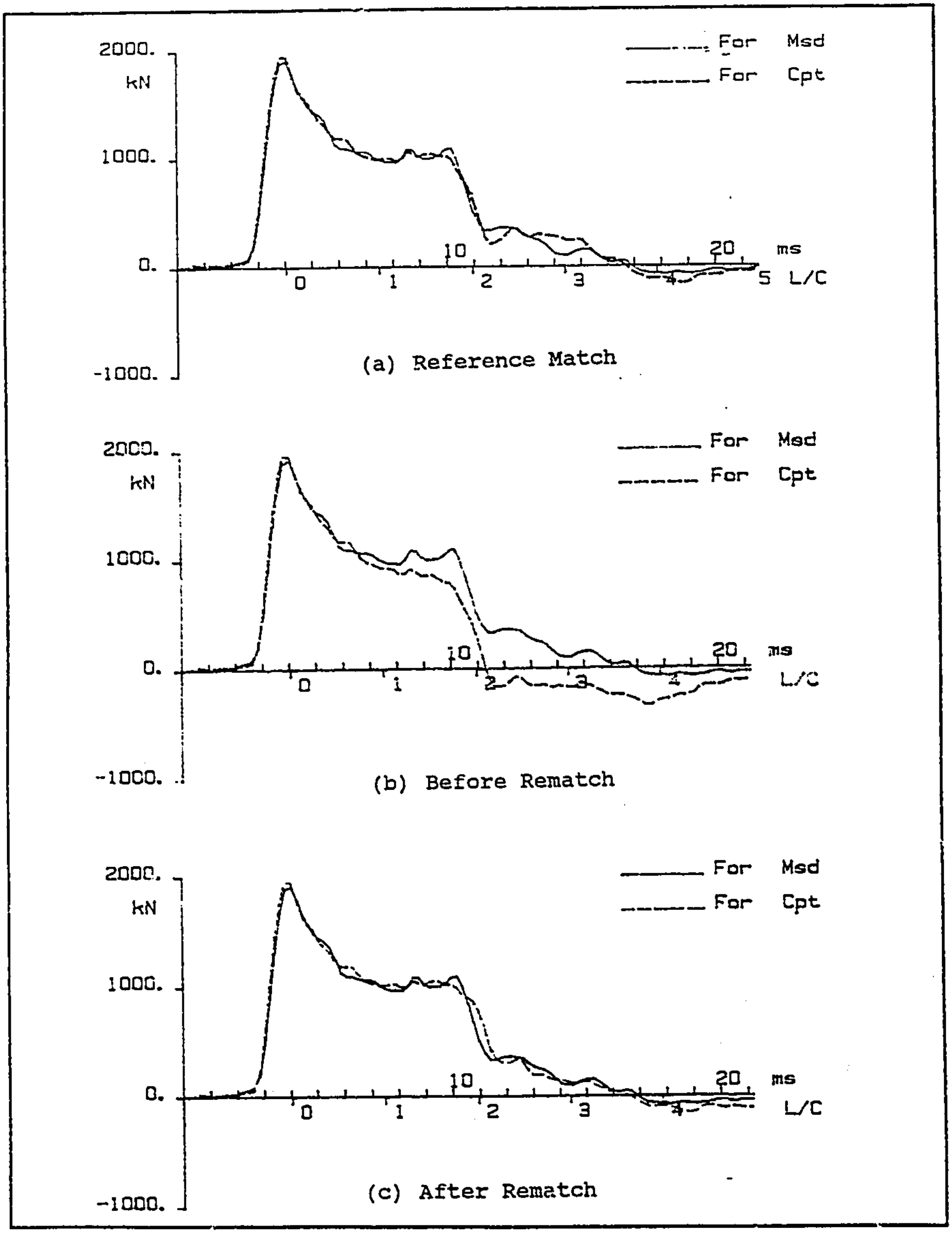

Fig. 6.71 LW Pile, CAPWAP Solution at 430 KN

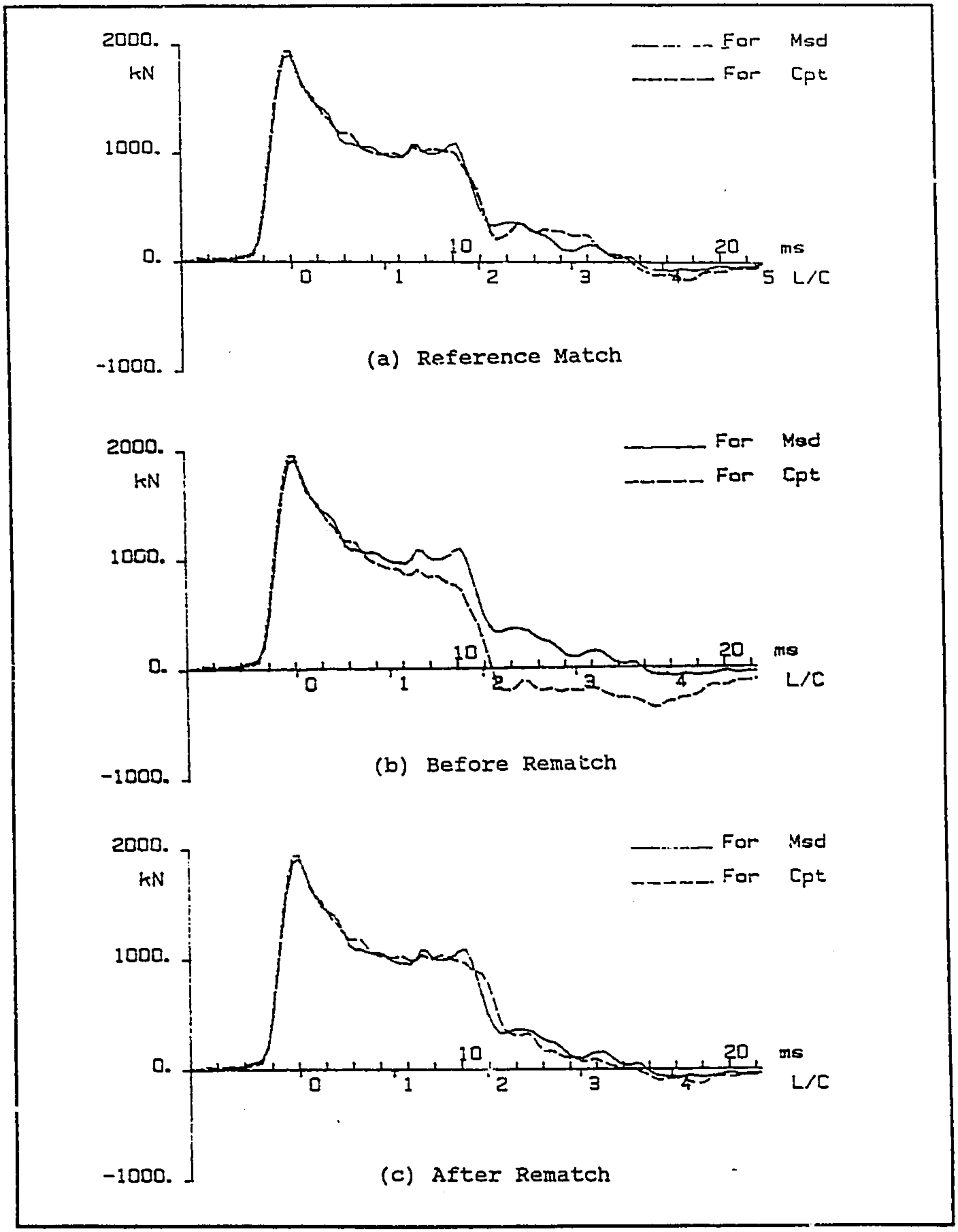

Fig. 6.72 LW Pile, CAPWAP Solution at 385 KN

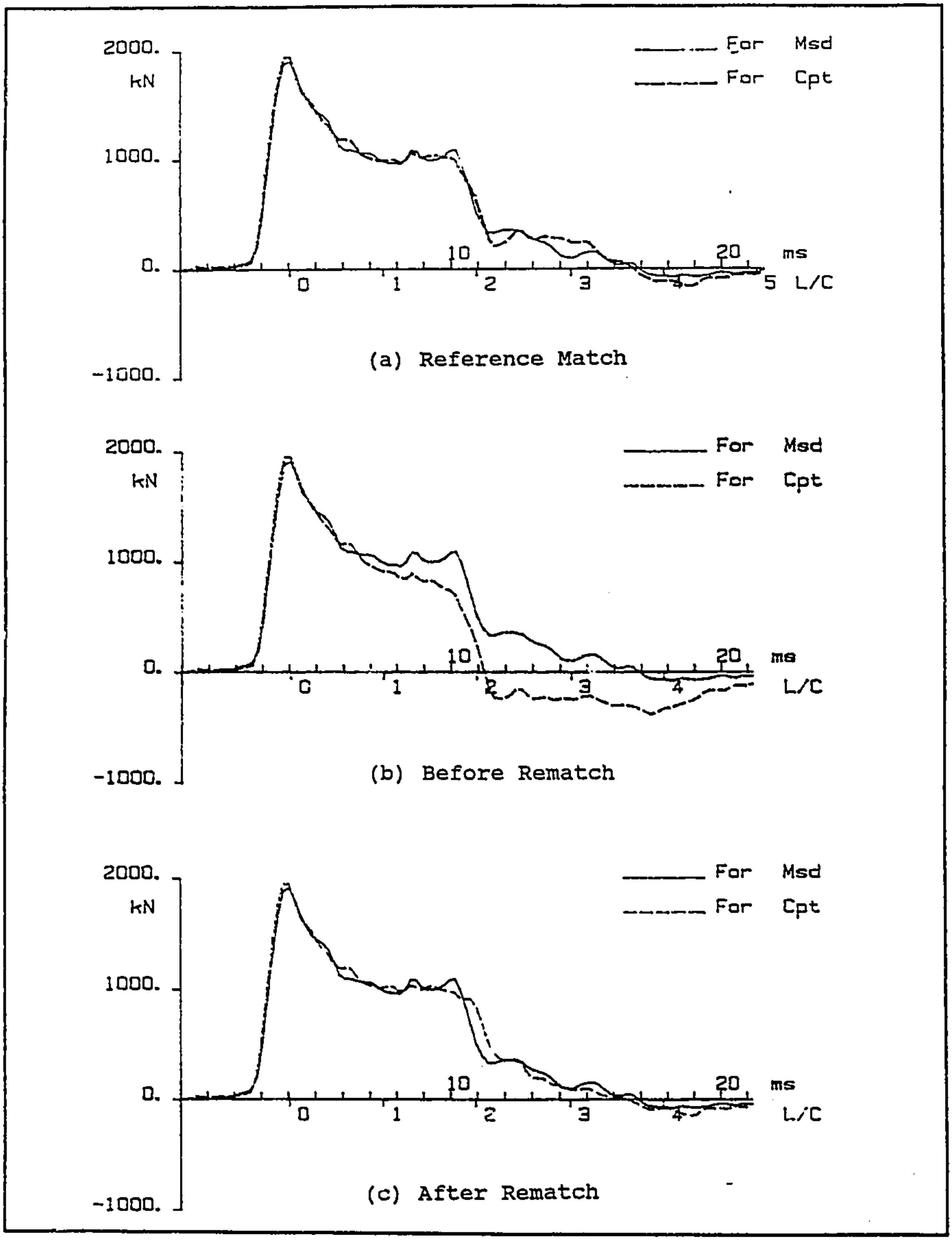

Fig. 6.73 LW Pile, CAPWAP Solution at 345 KN

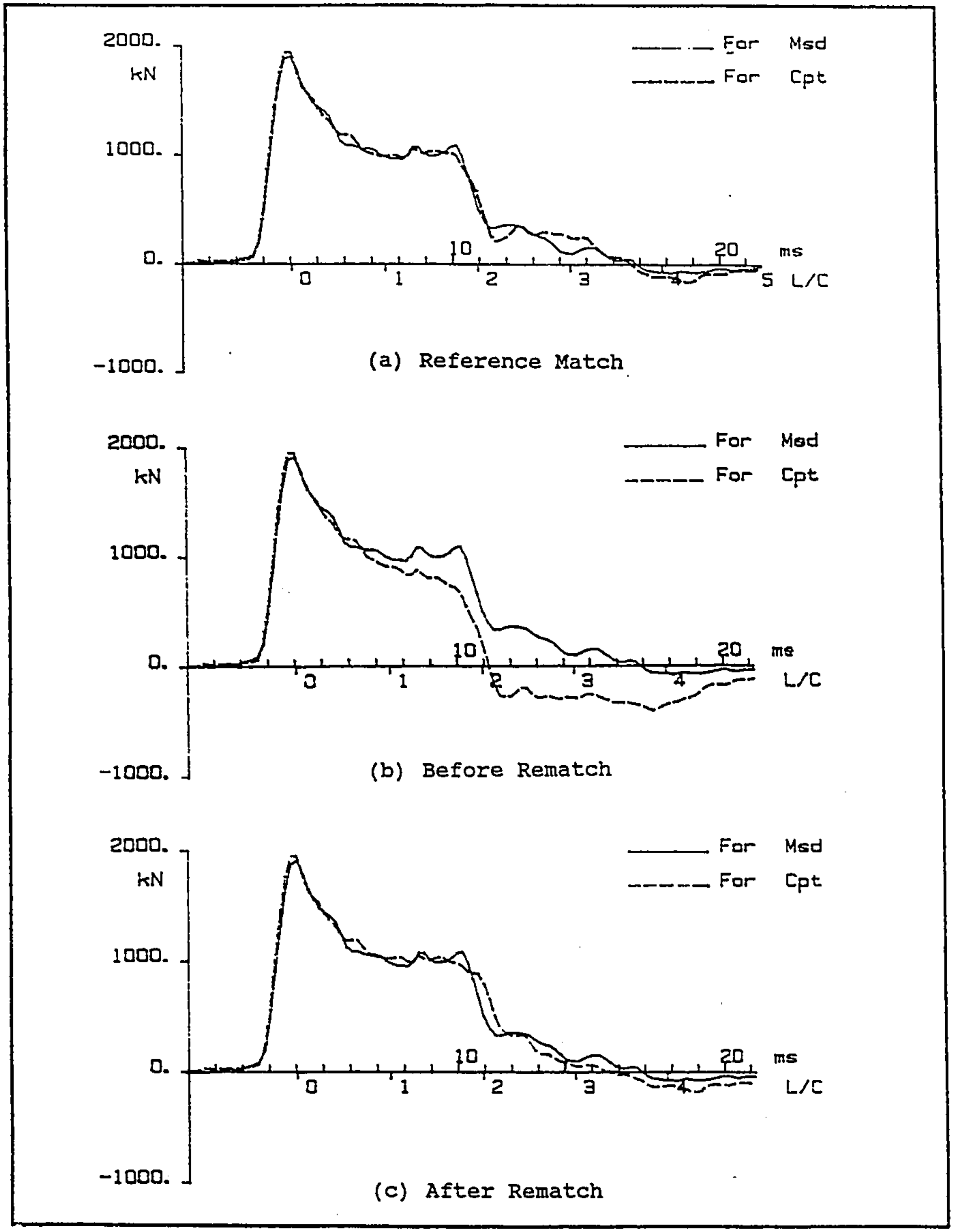

Fig. 6.74 LW Pile, CAPWAP Solution at 300 KN

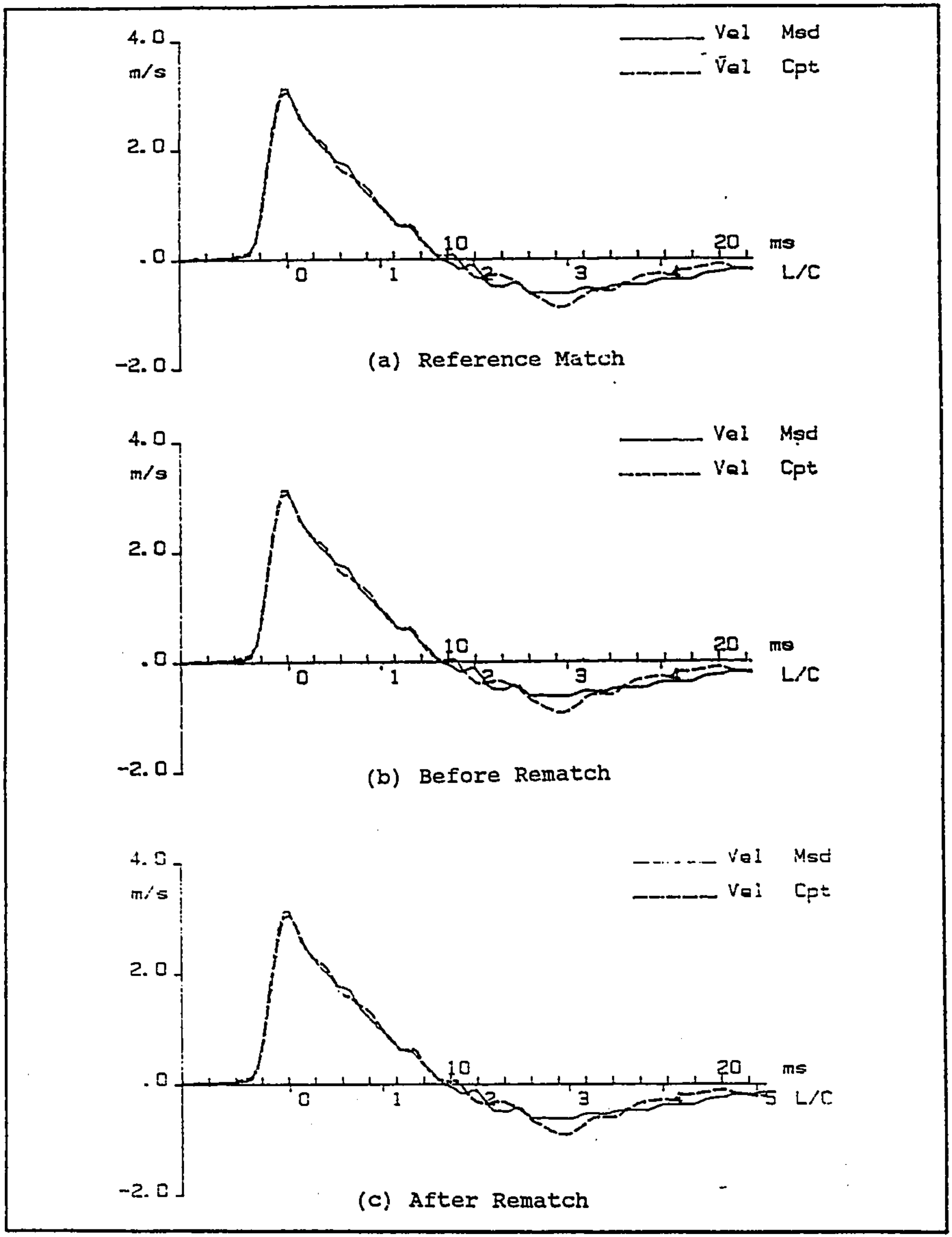

Fig. 6.75 LW Pile, WAPCAP Solution at 945 KN

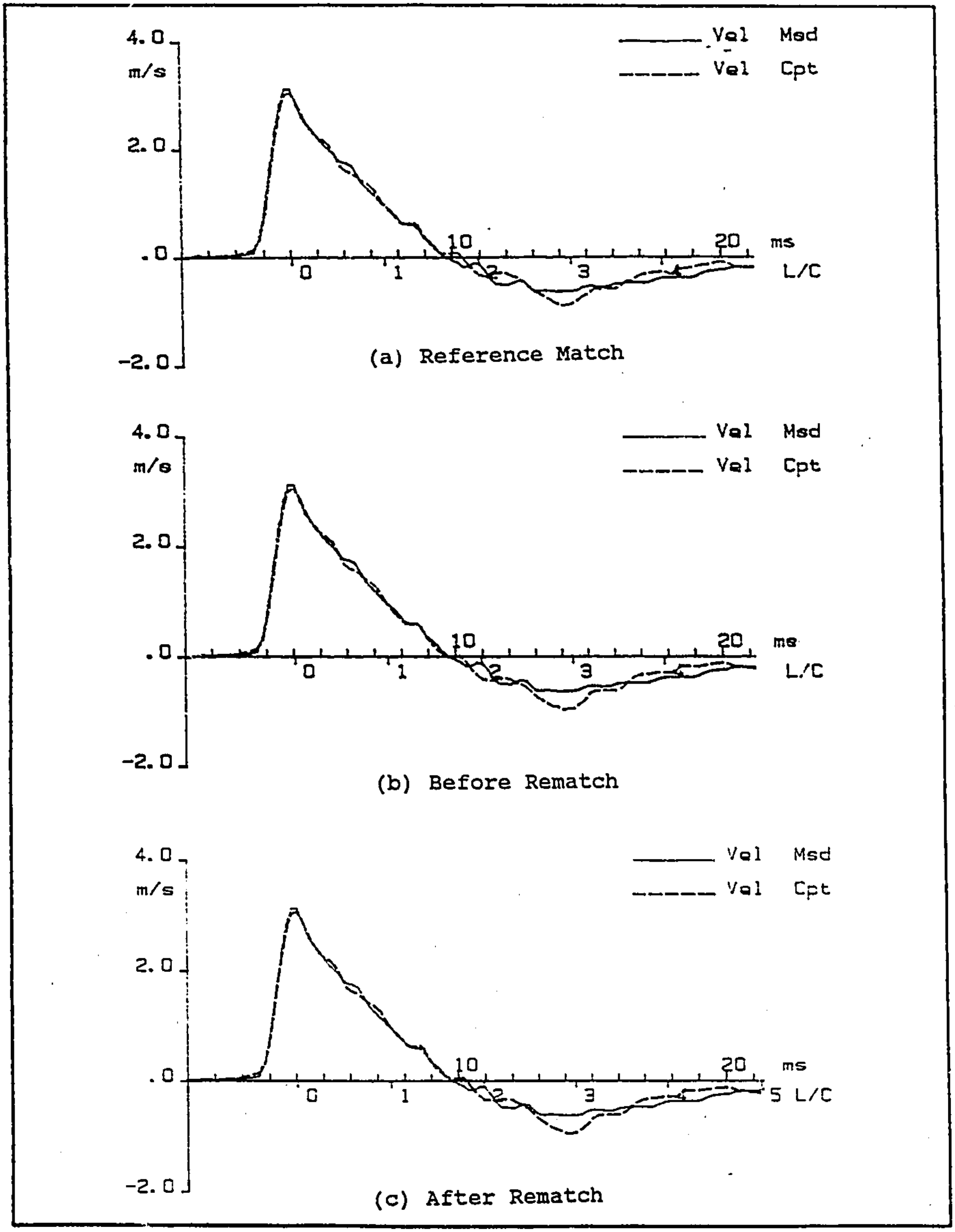

Fig. 6.76 LW Pile, WAPCAP Solution at 990 KN

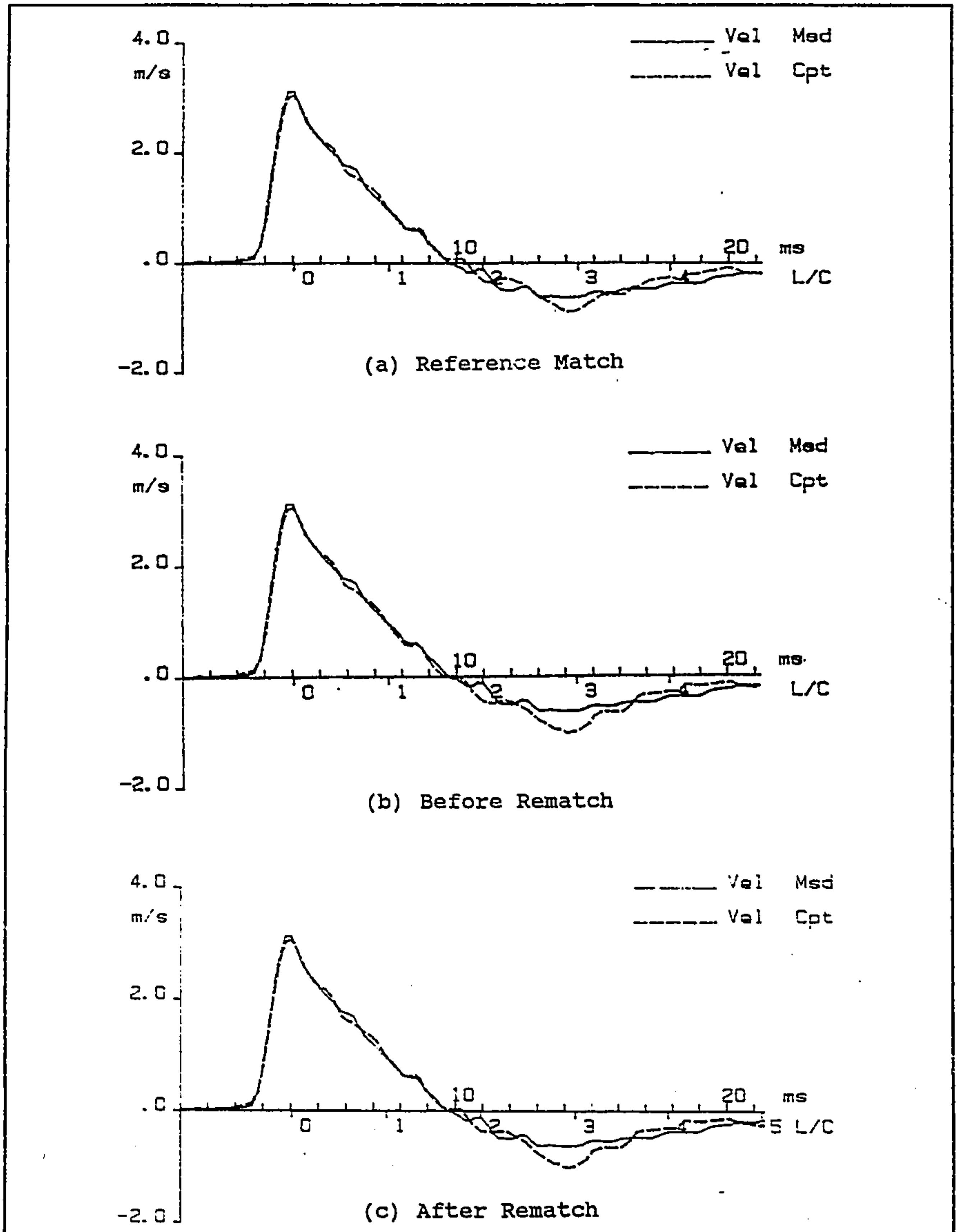

Fig. 6.77 LW Pile, WAPCAP Solution at 1035 KN

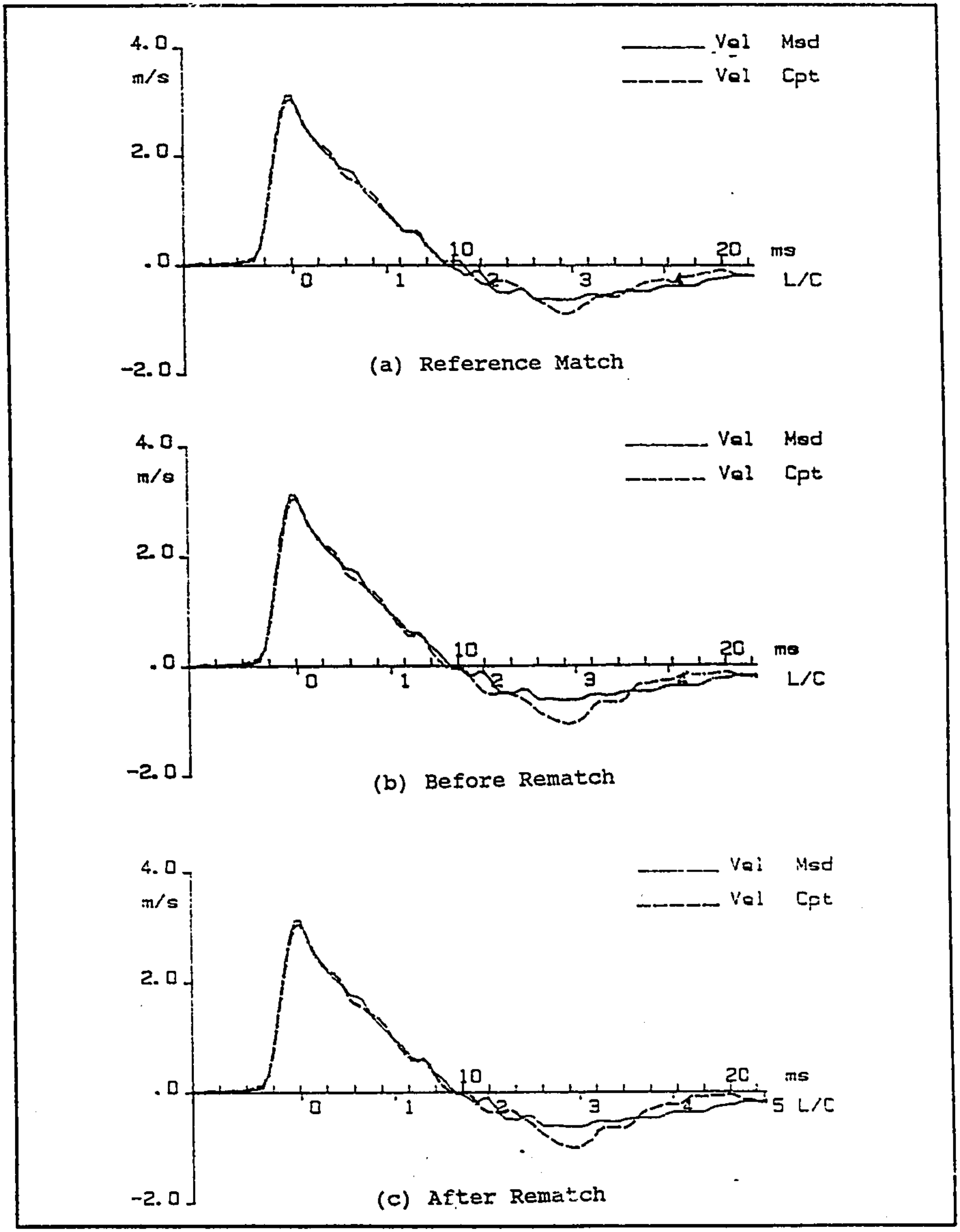

Fig. 6.78 LW Pile, WAPCAP Solution at 1080 KN

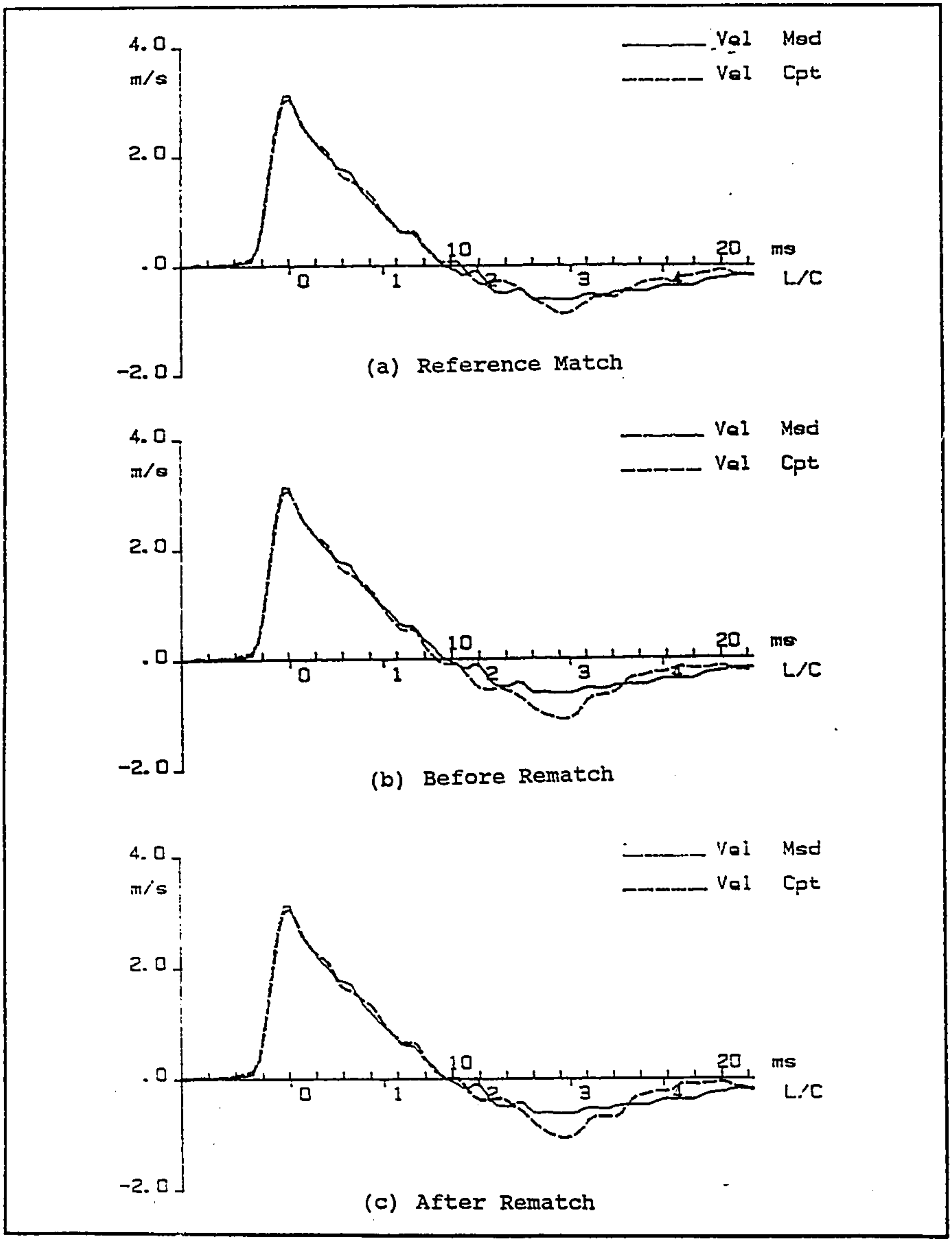

Fig. 6.79 LW Pile, WAPCAP Solution at 1125 KN

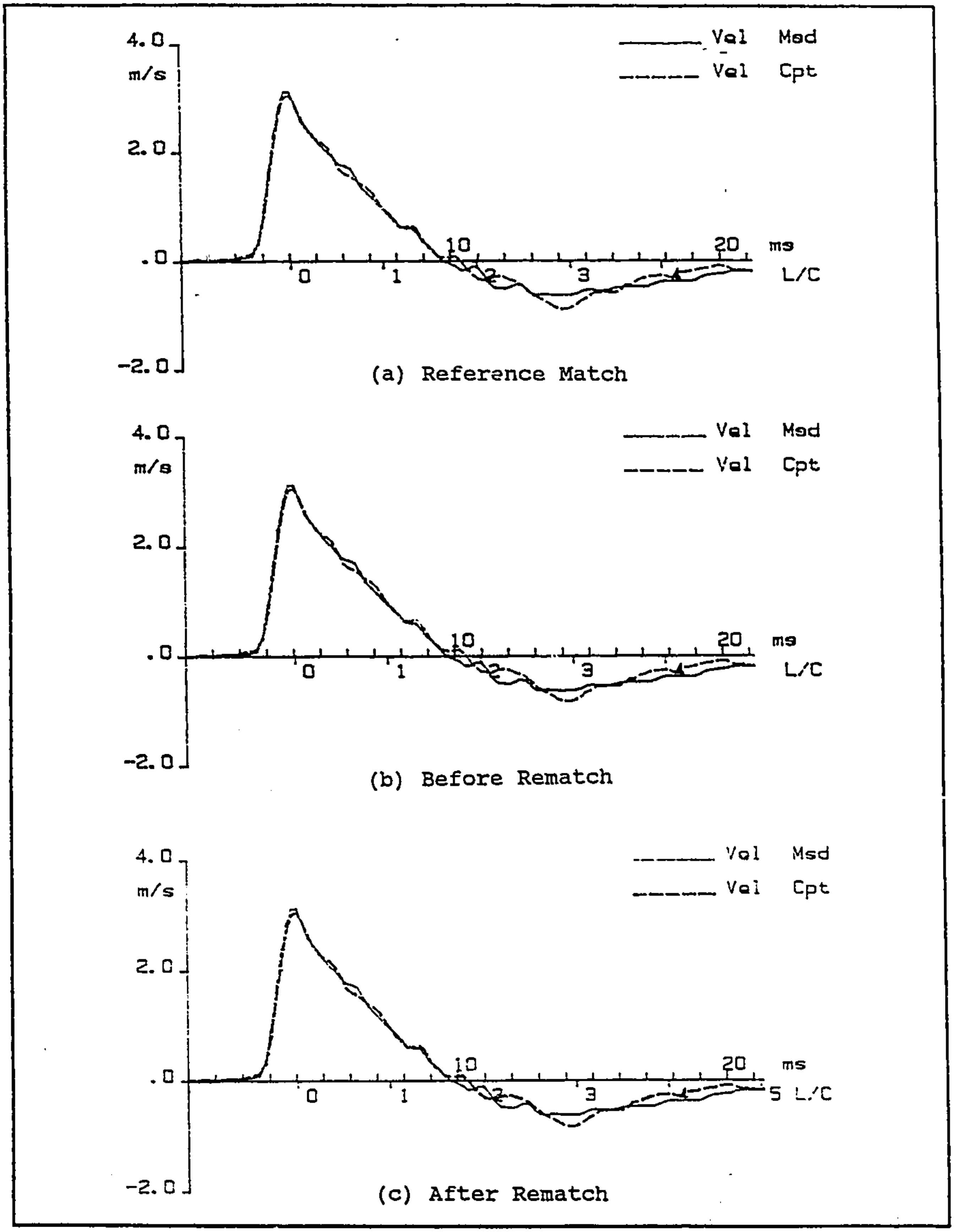

Fig. 6.80 LW Pile, WAPCAP Solution at 855 KN

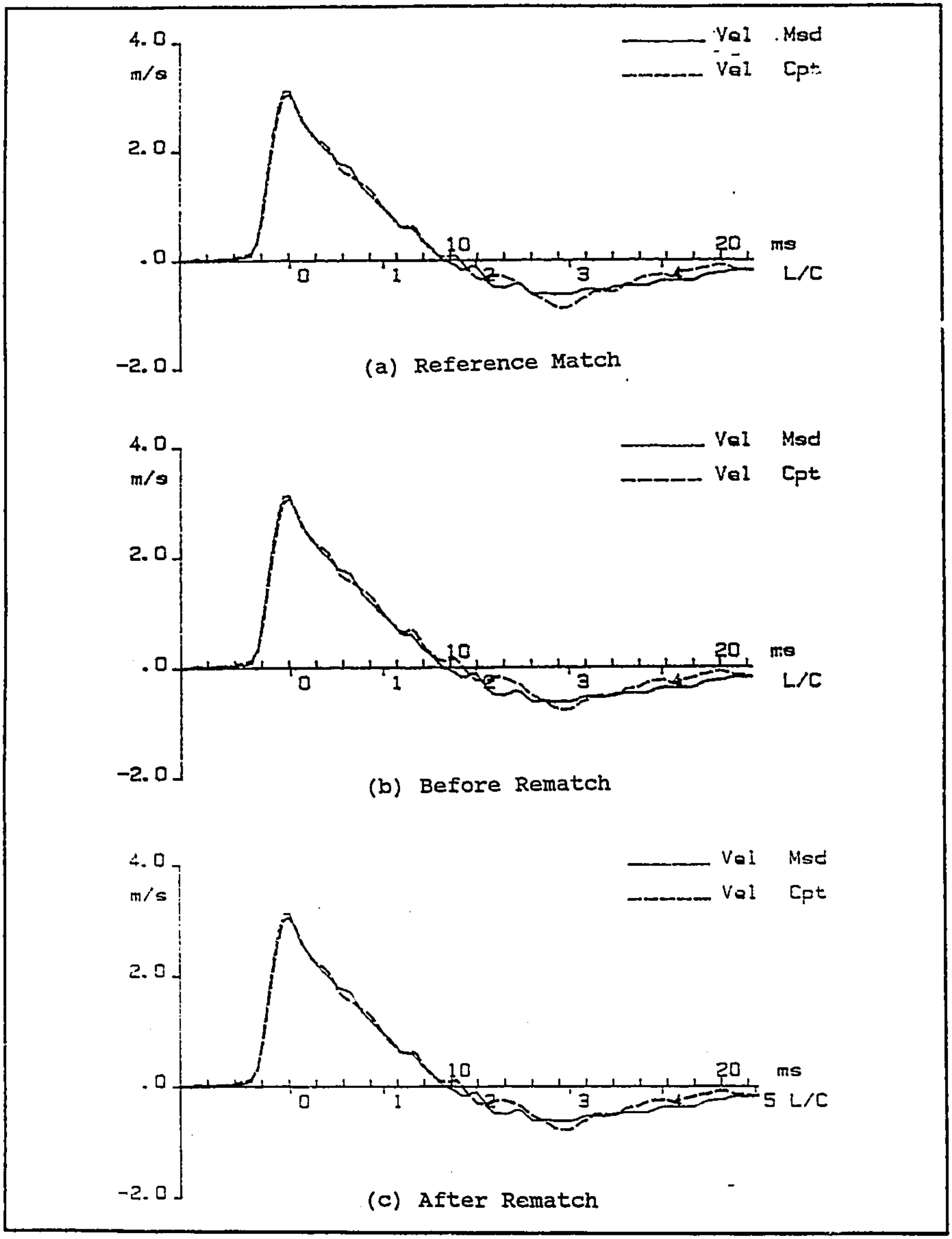

Fig. 6.81 LW Pile, WAPCAP Solution at 810 KN

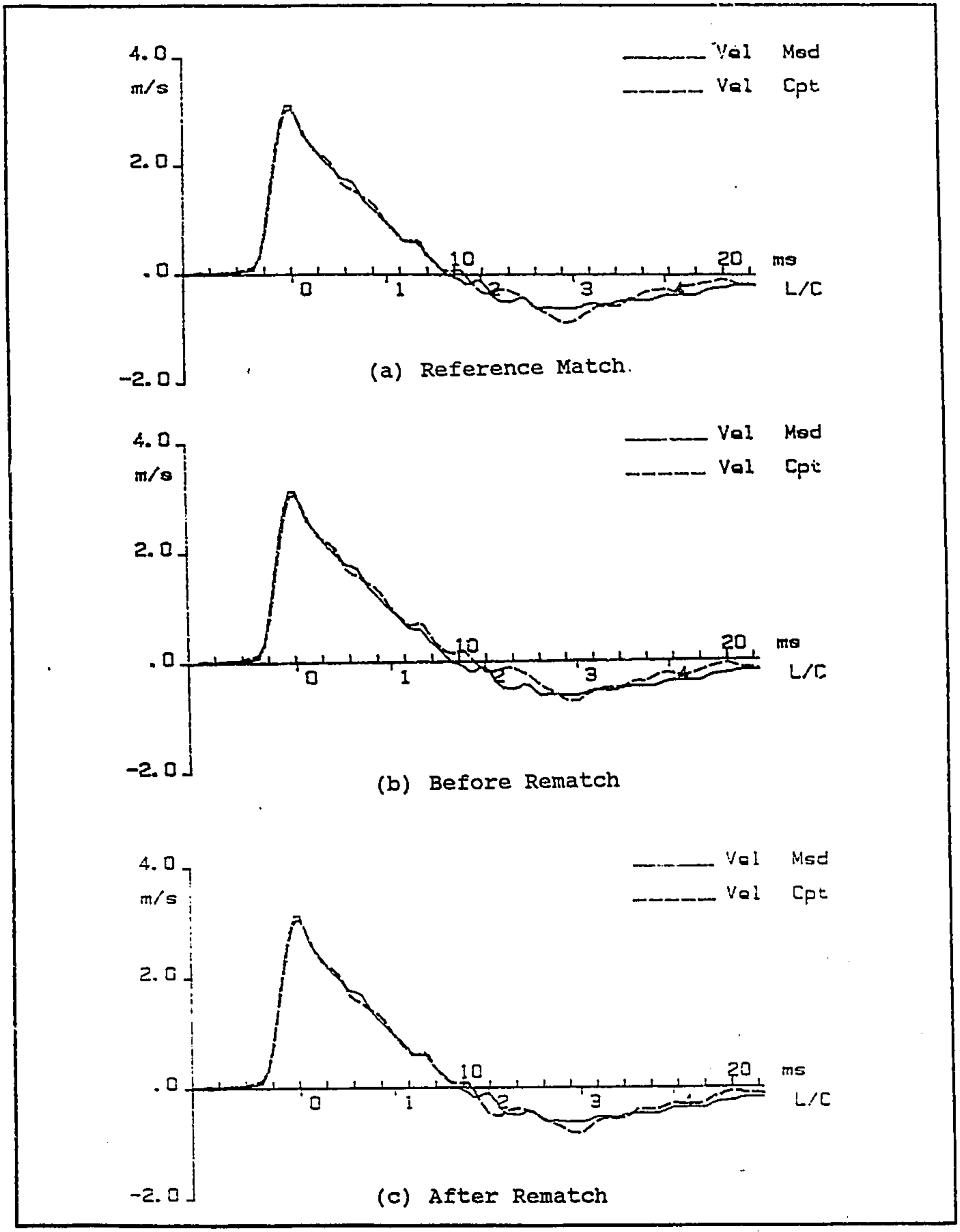

Fig. 6.82 LW Pile, WAPCAP Solution at 765 KN

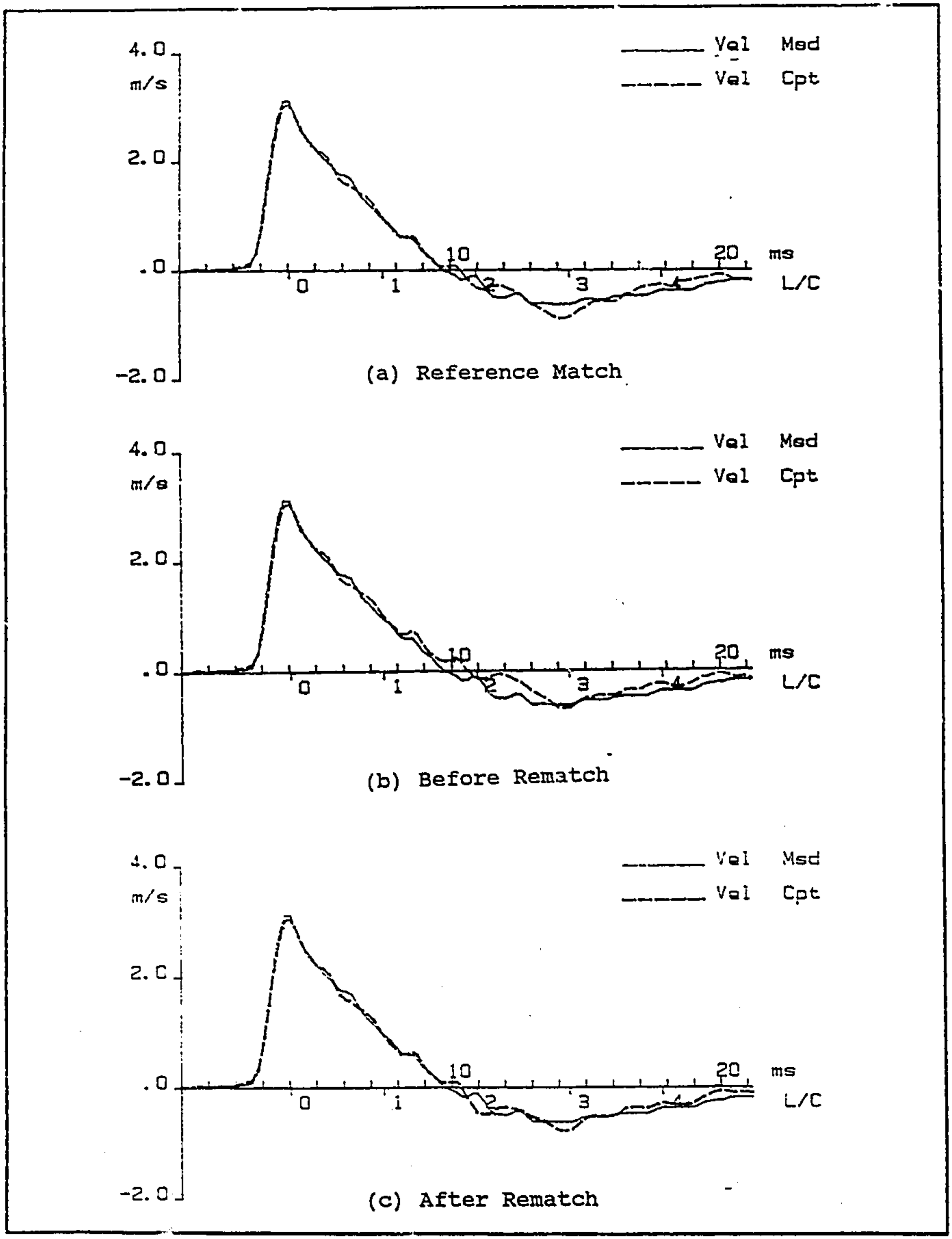

Fig. 6.83 LW Pile, WAPCAP Solution at 720 KN

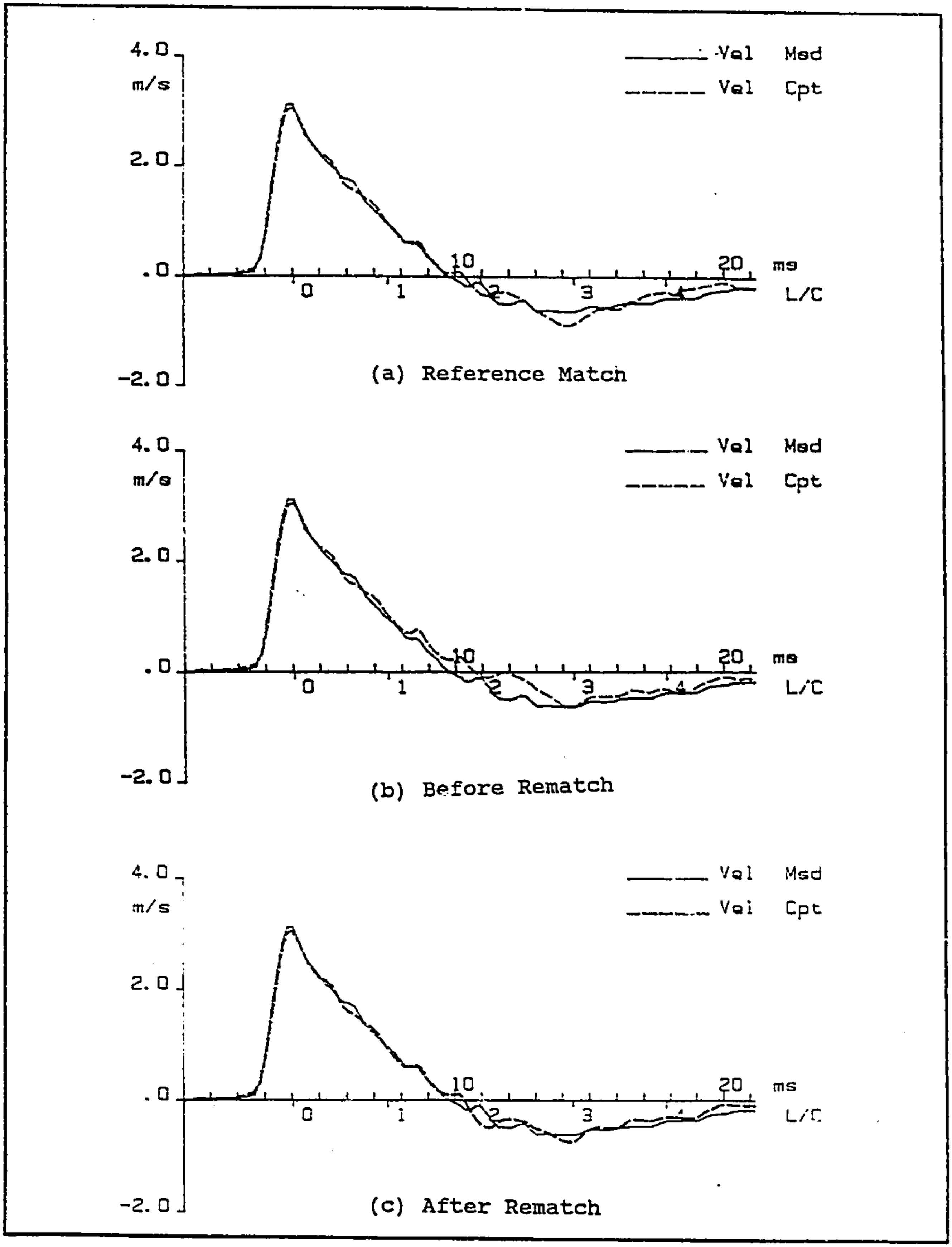

Fig. 6.84 LW Pile, WAPCAP Solution at 675 KN

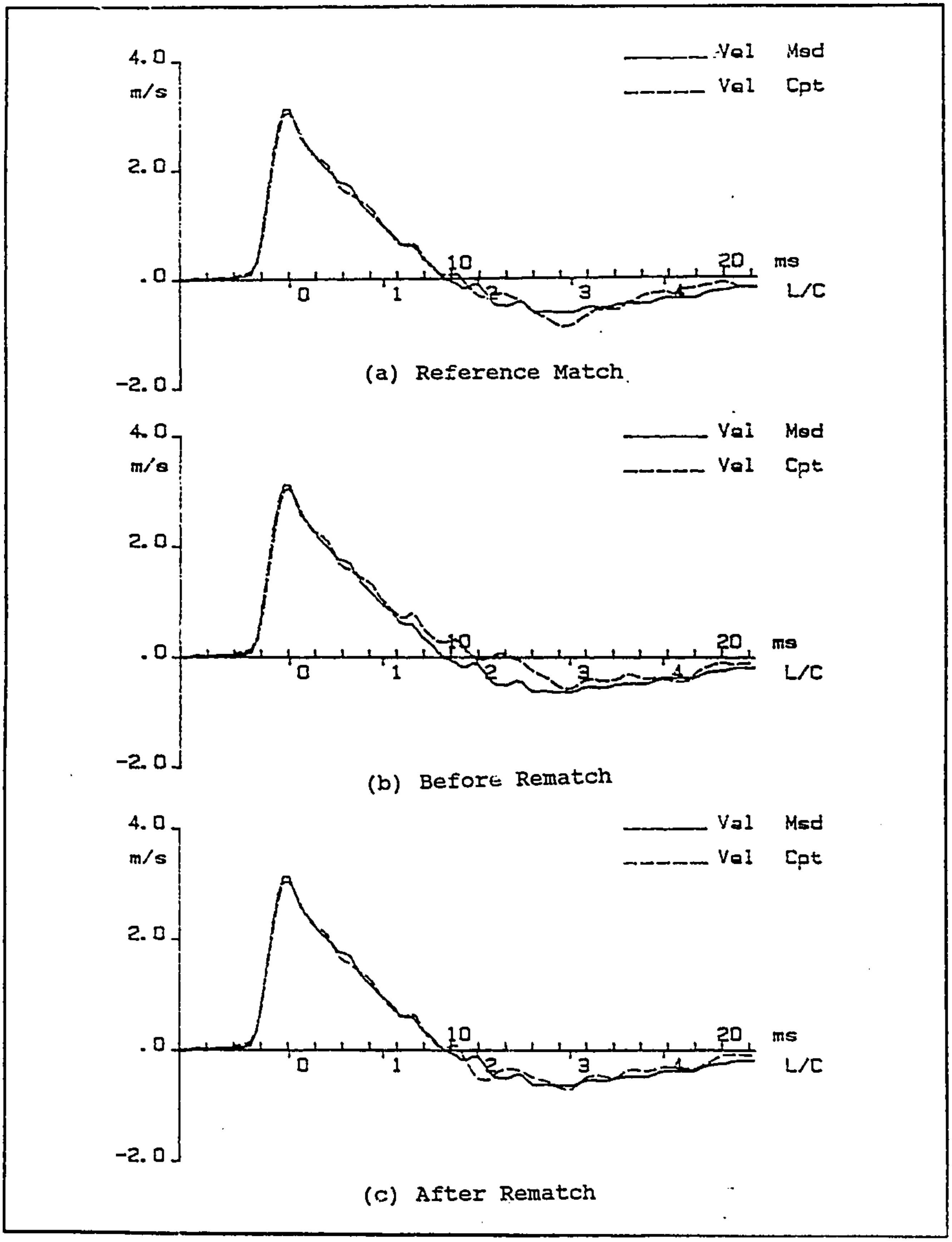

Fig. 6.85 LW Pile, WAPCAP Solution

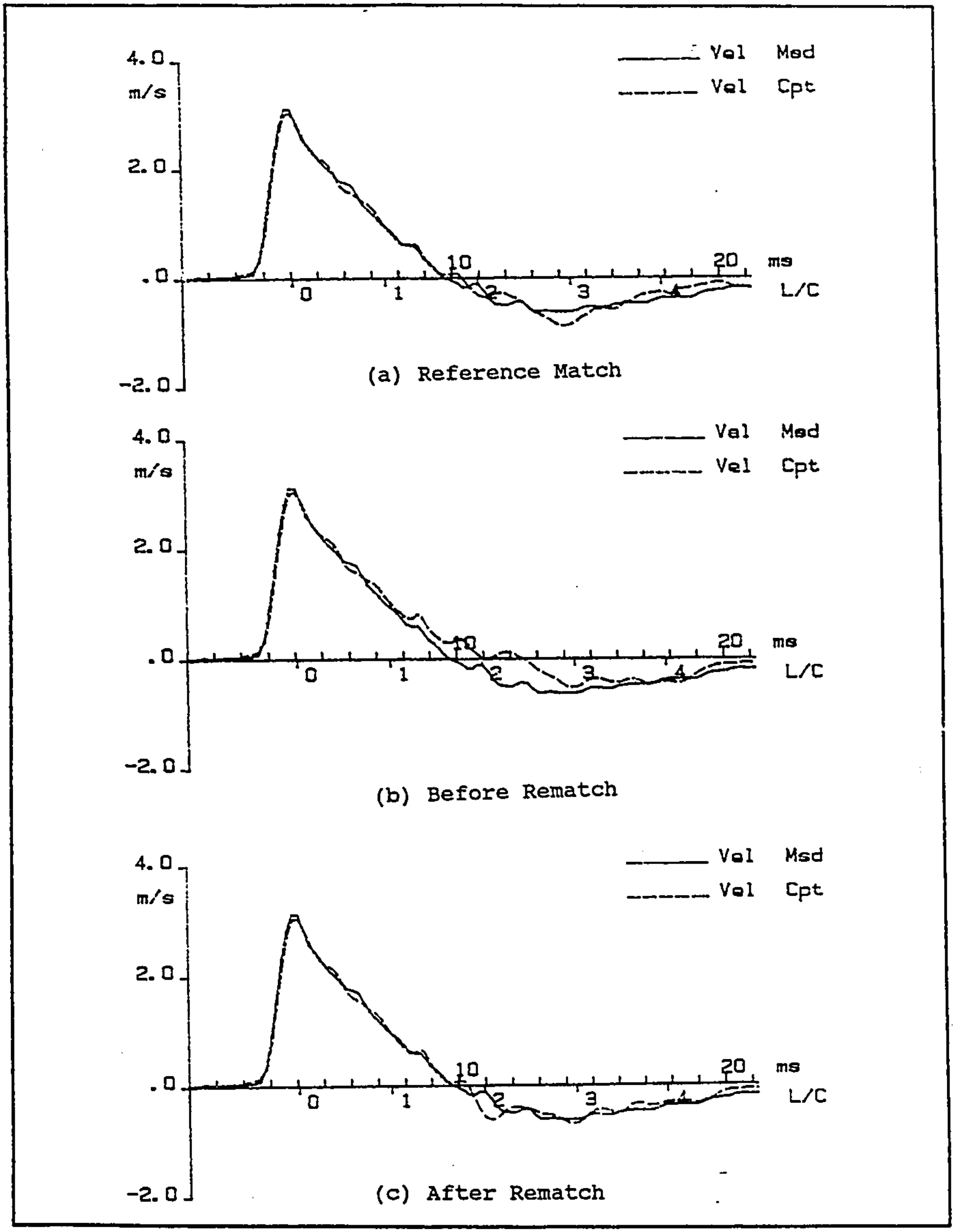

Fig. 6.86 LW Pile, WAPCAP Solution at 565 KN

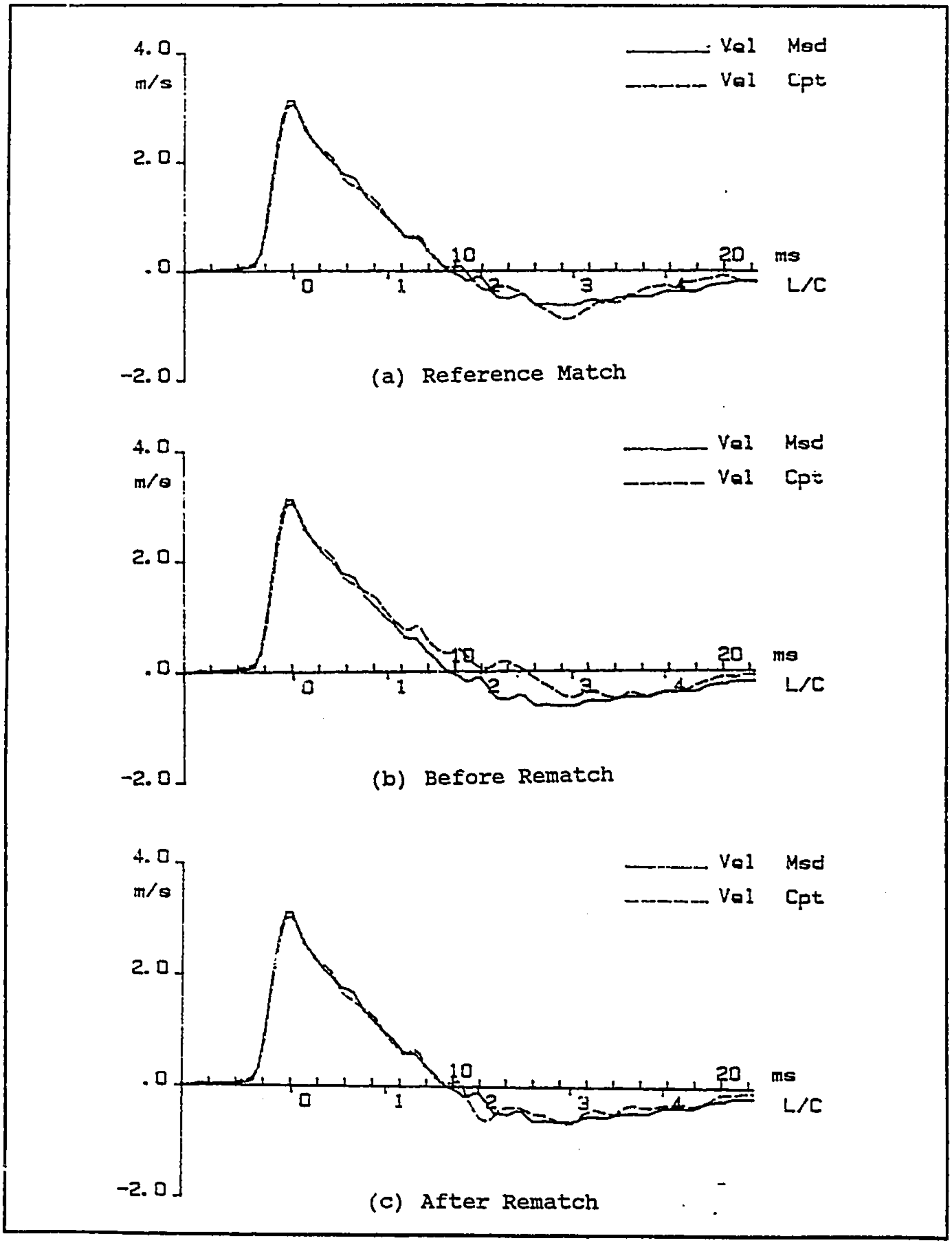

Fig. 6.87 LW Pile, WAPCAP Solution at 520 KN

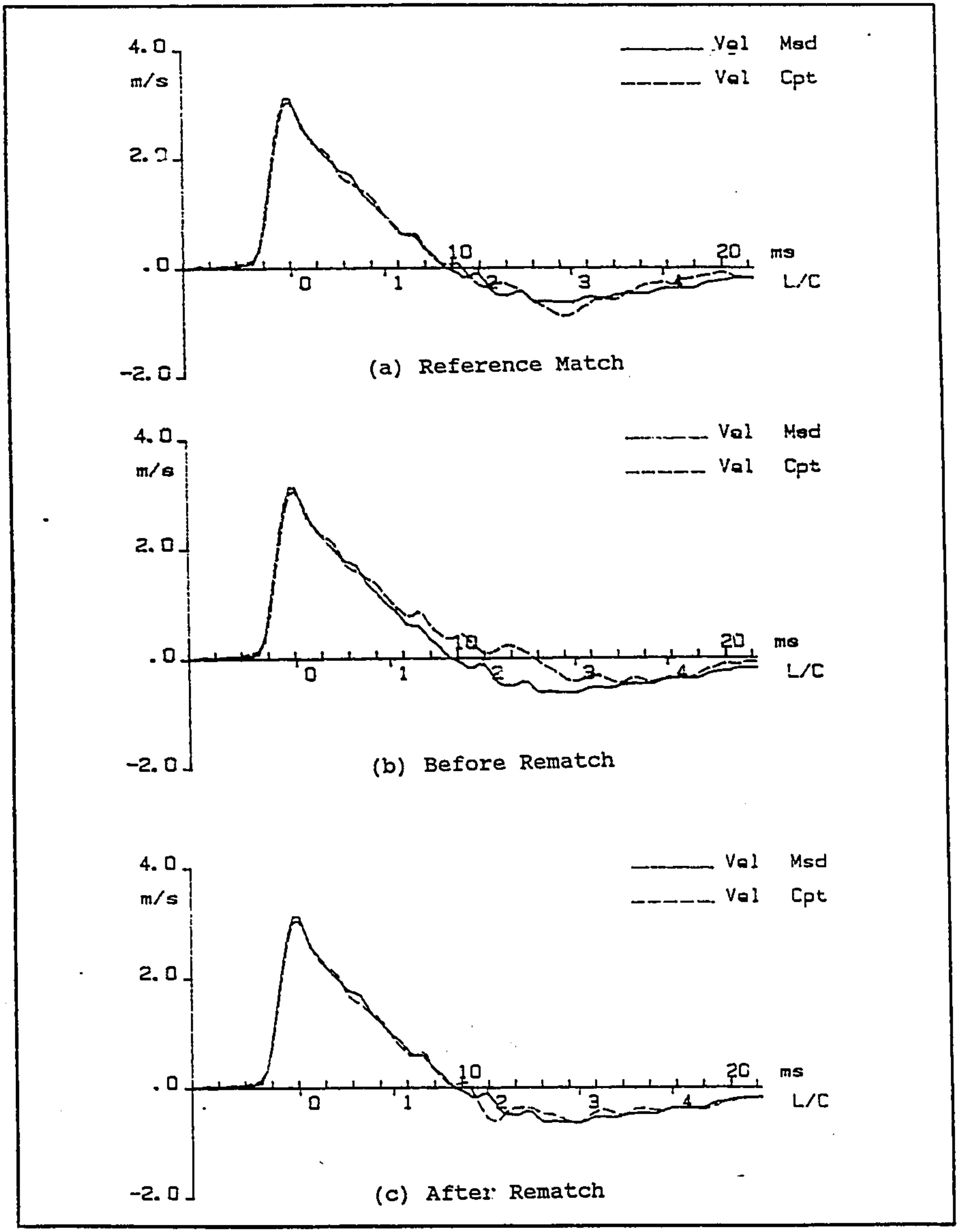

Fig. 6.88 LW Pile, WAPCAP Solution at 475 KN

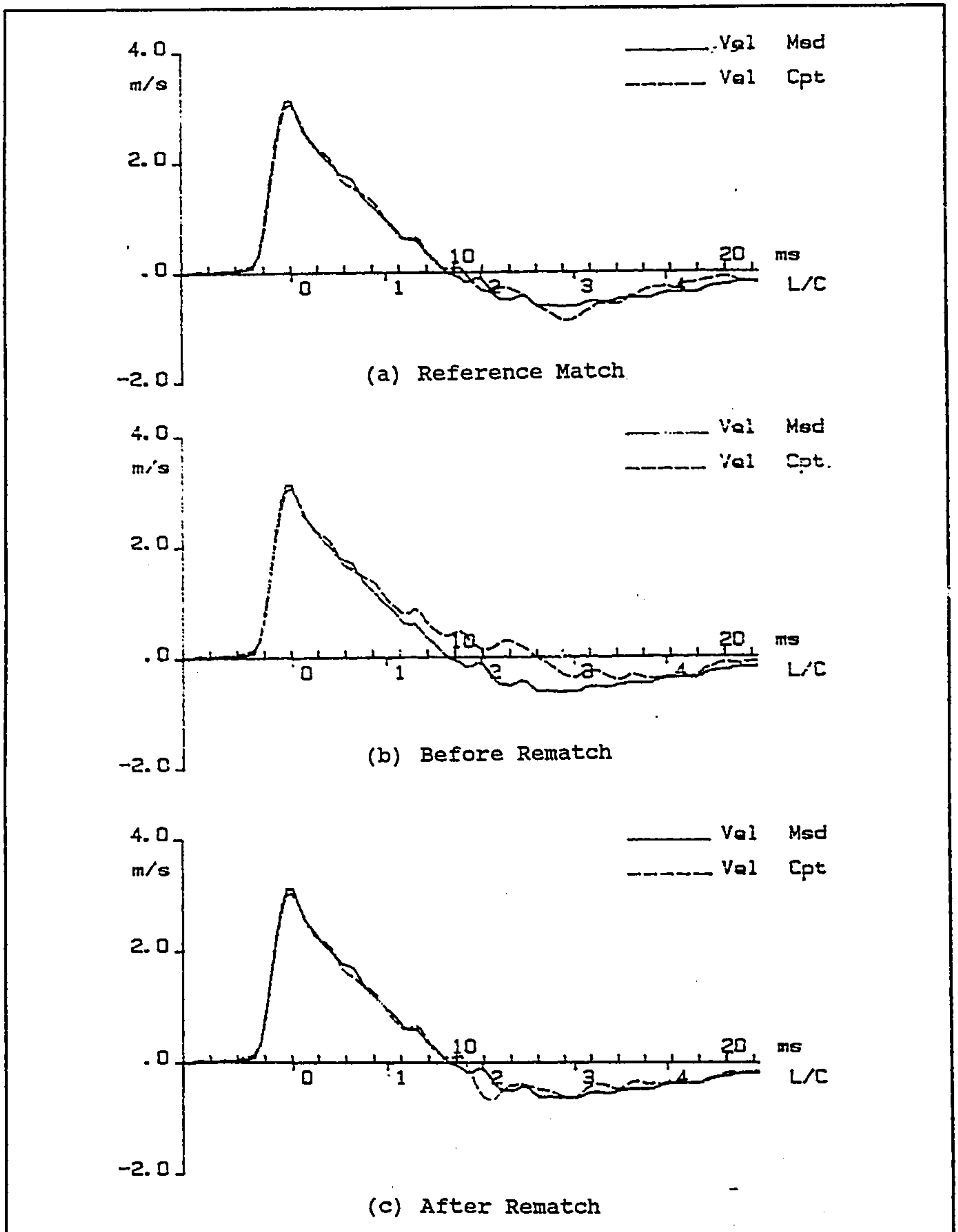

Fig. 6.89 LW Pile, WAPCAP Solution at 430 KN

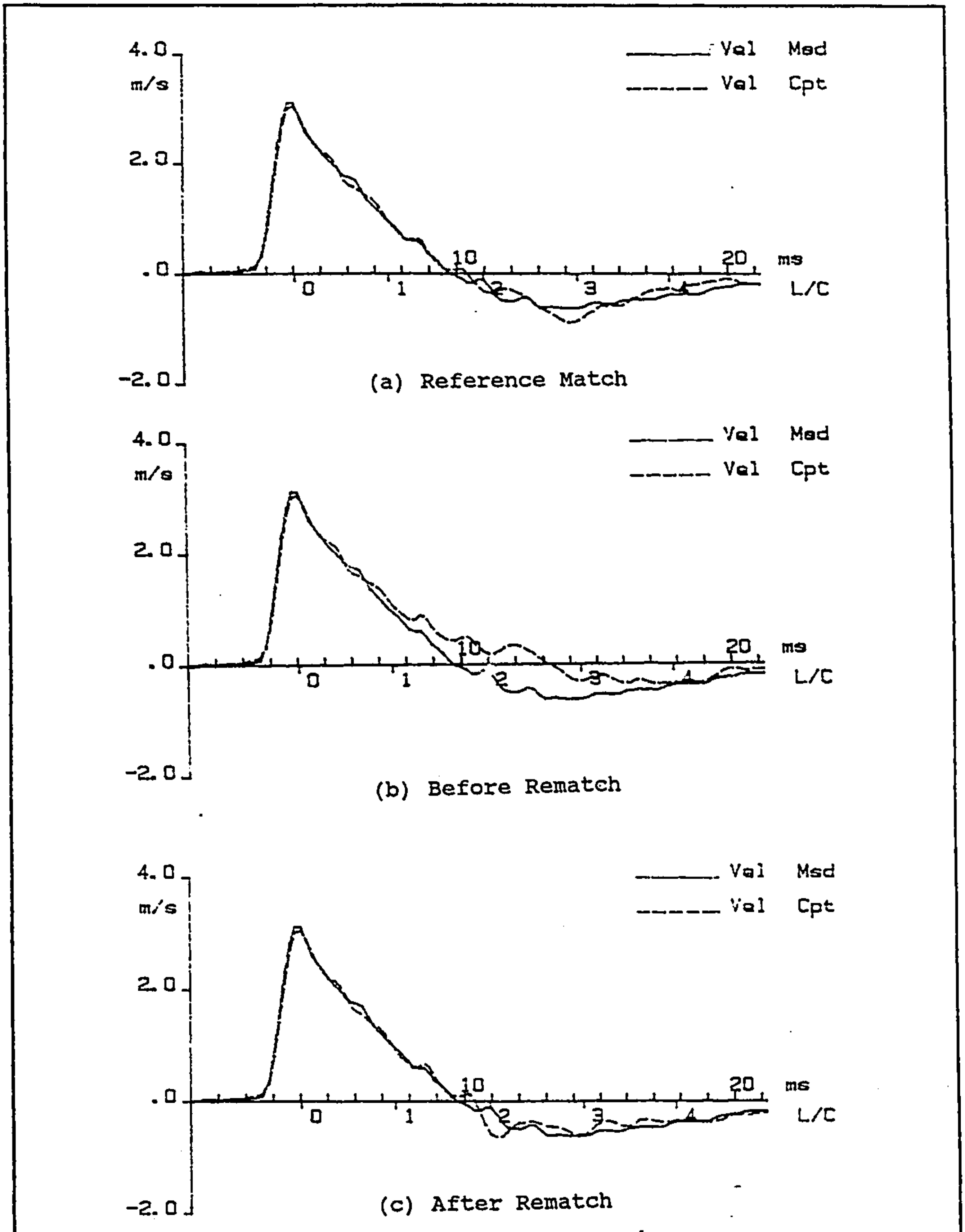

Fig. 6.90 LW Pile, WAPCAP Solution at 385 KN

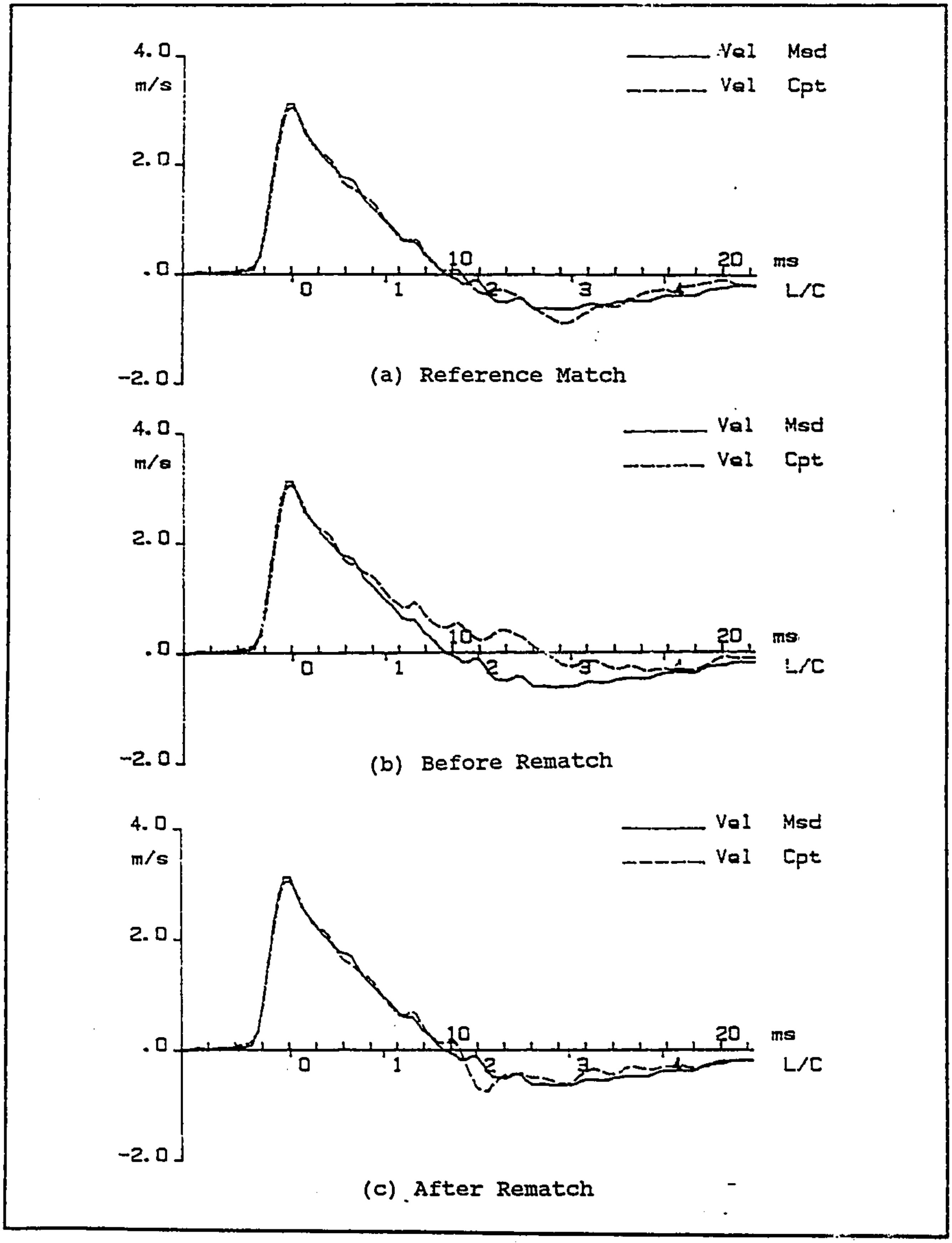

Fig. 6.91 LW Pile, WAPCAP Solution at 345 KN

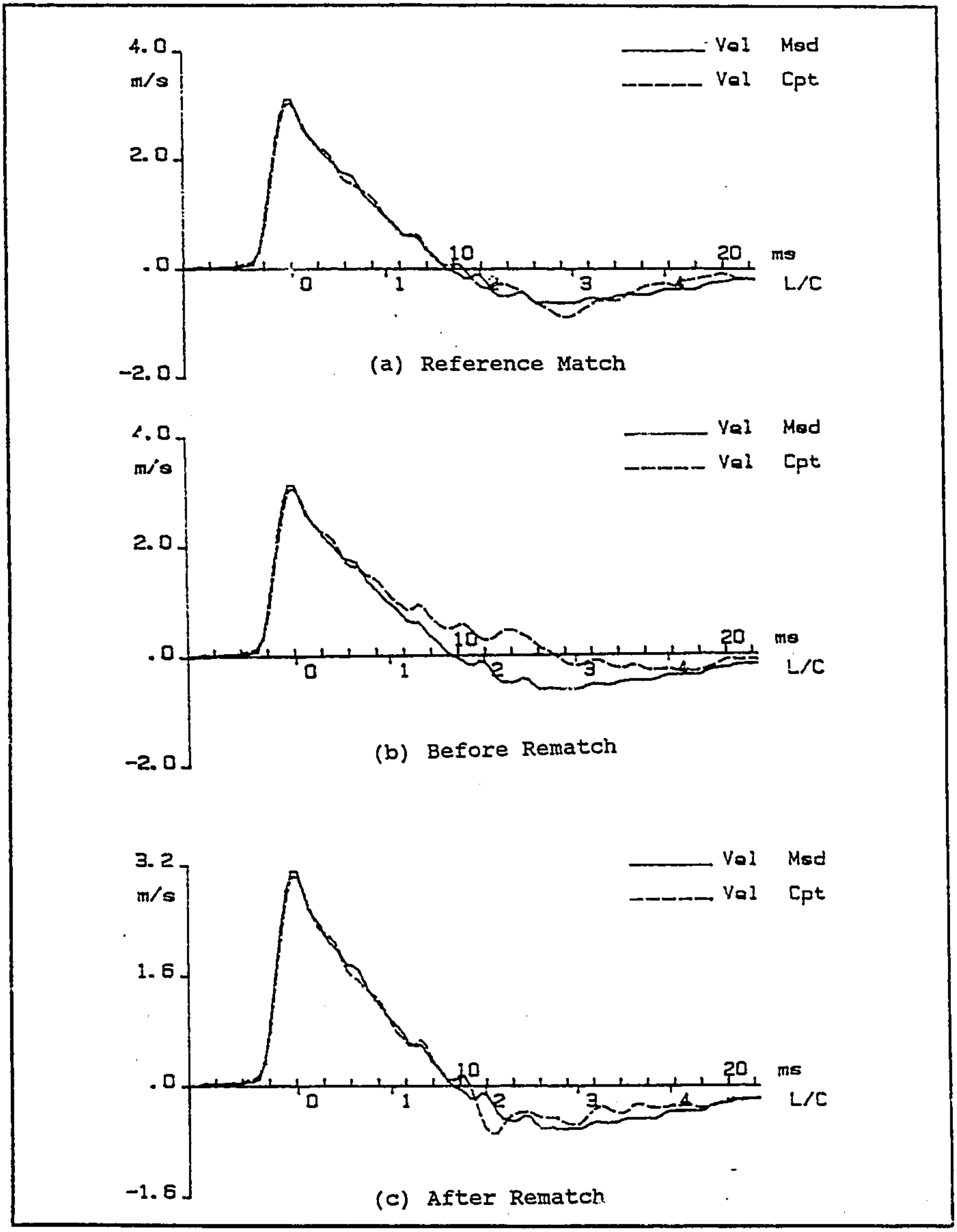

Fig. 6.92 LW Pile, WAPCAP Solution at 300 KN

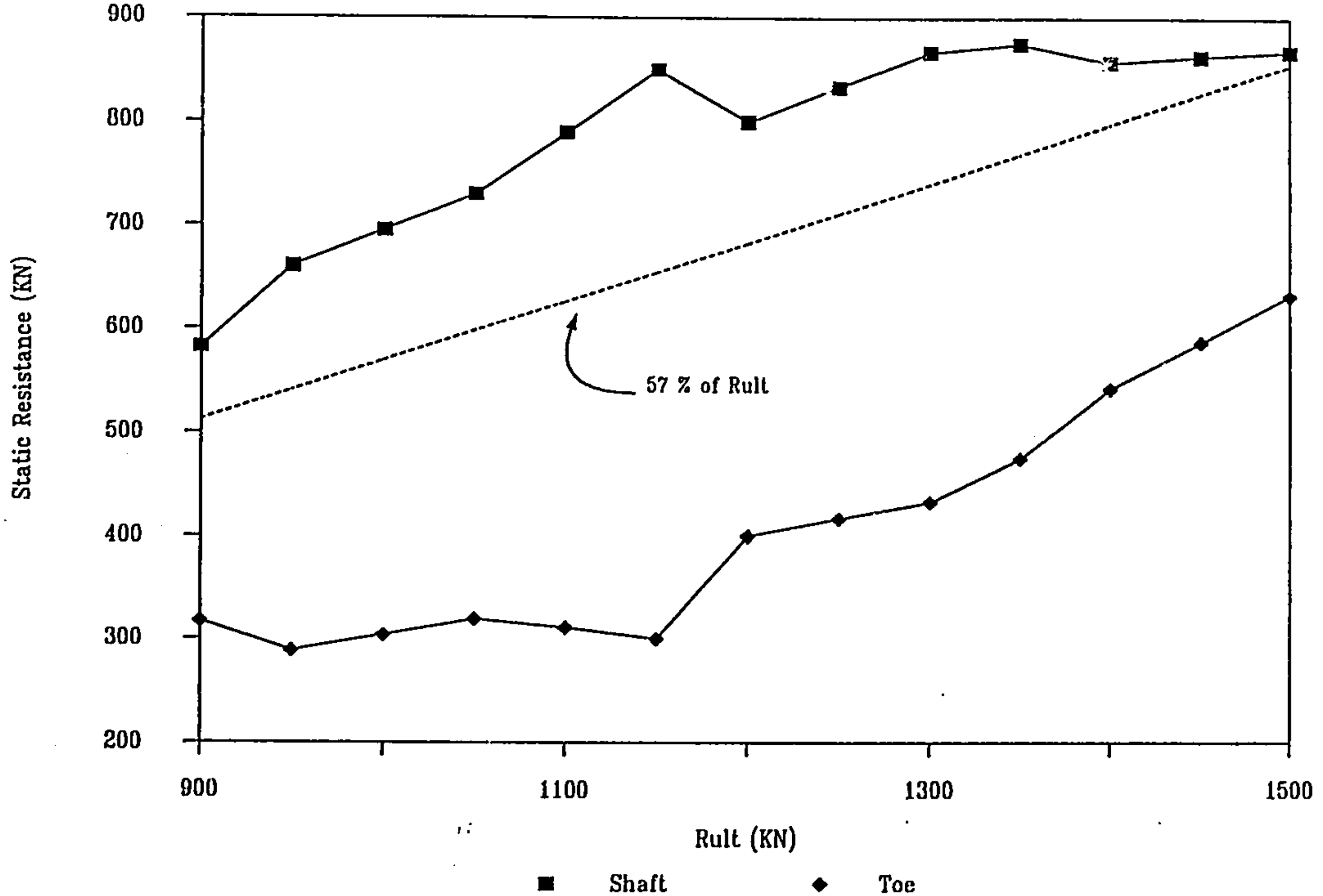

Fig. 6.93 Static Resistance, JI Pile

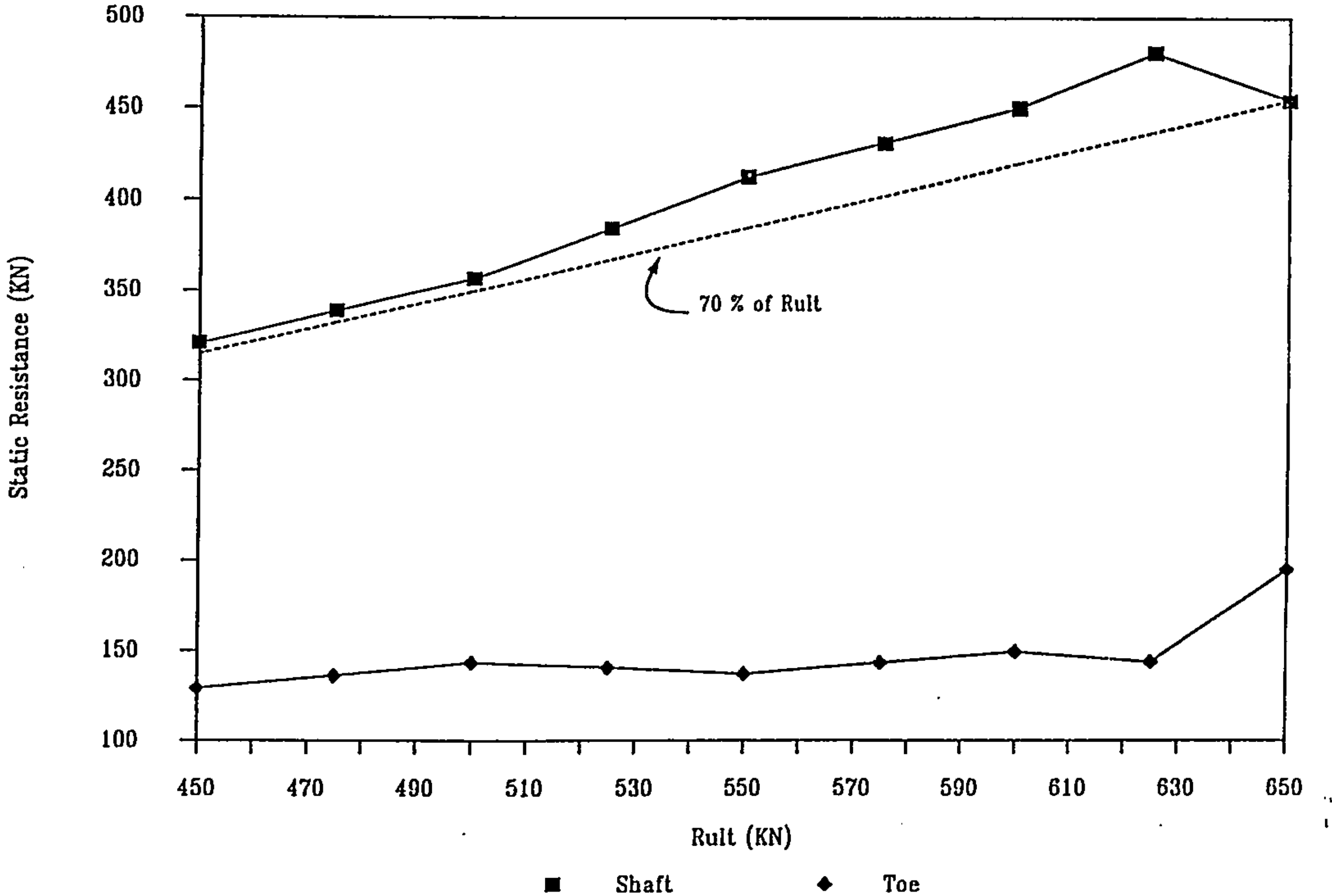

Fig. 6.94 Static Resistance, JA Pile

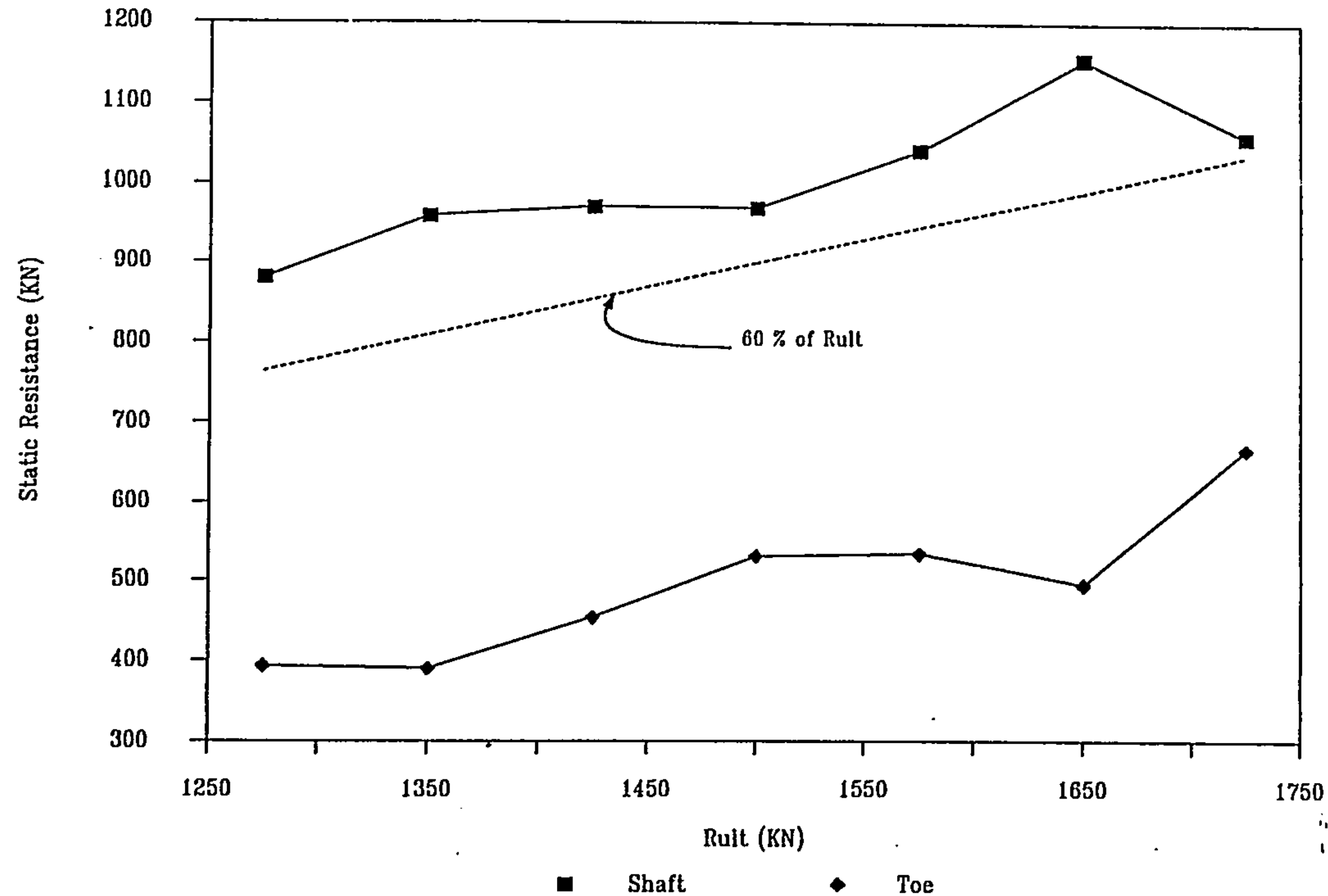

Fig. 6.95 Static Resistance, AM Pile

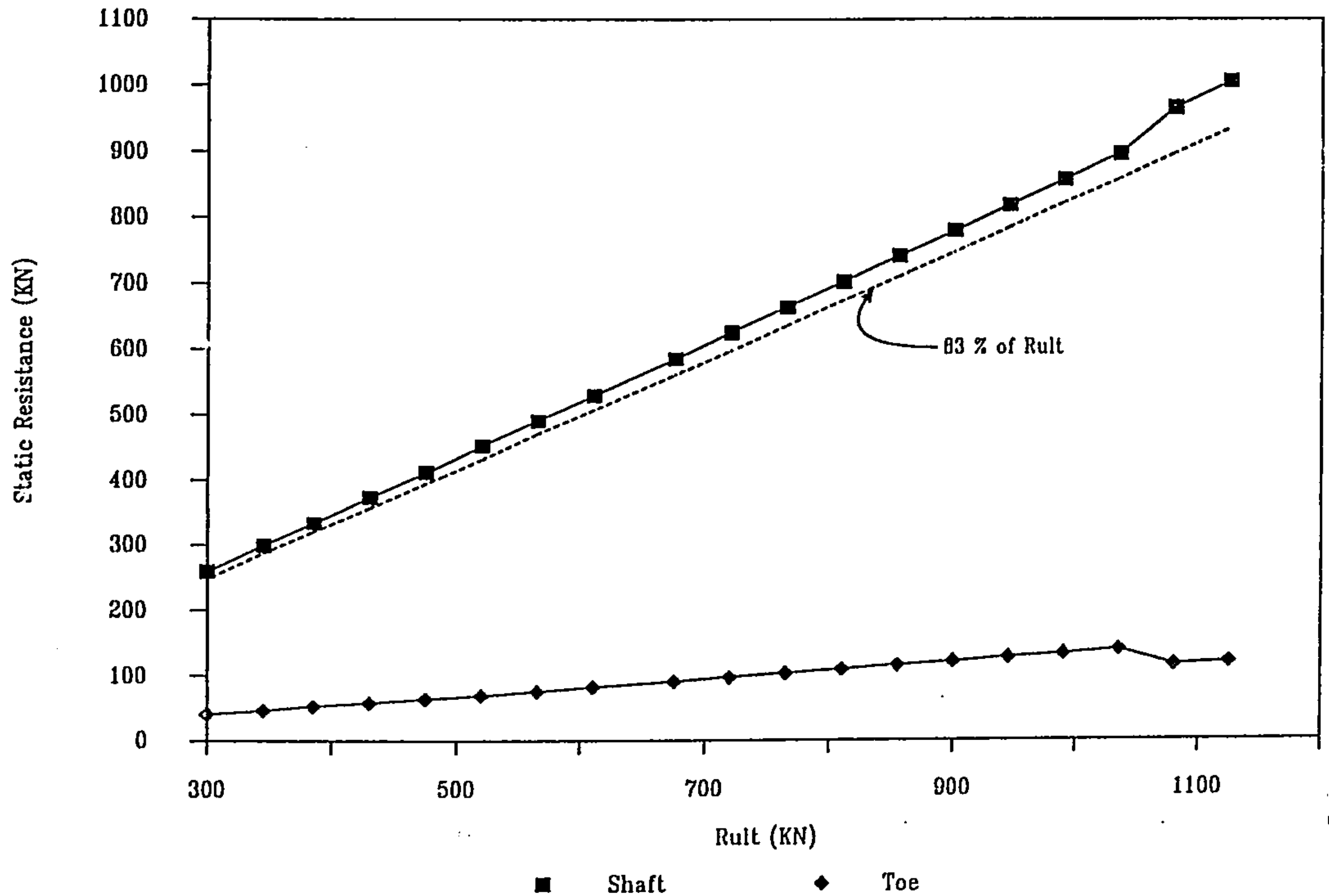

Fig. 6.96 Static Resistance, LW Pile

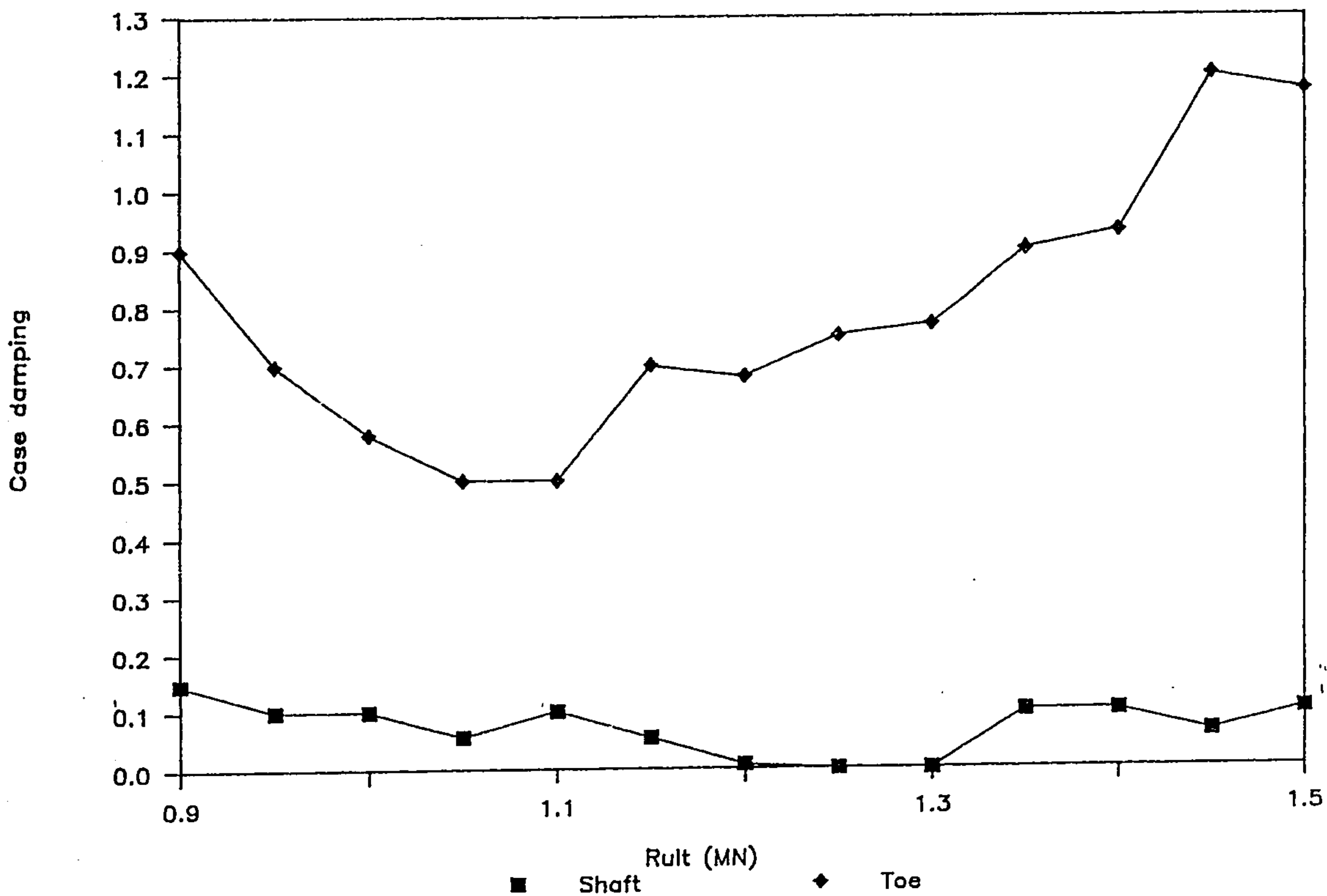

Fig. 6.97 Case Damping, JI Pile

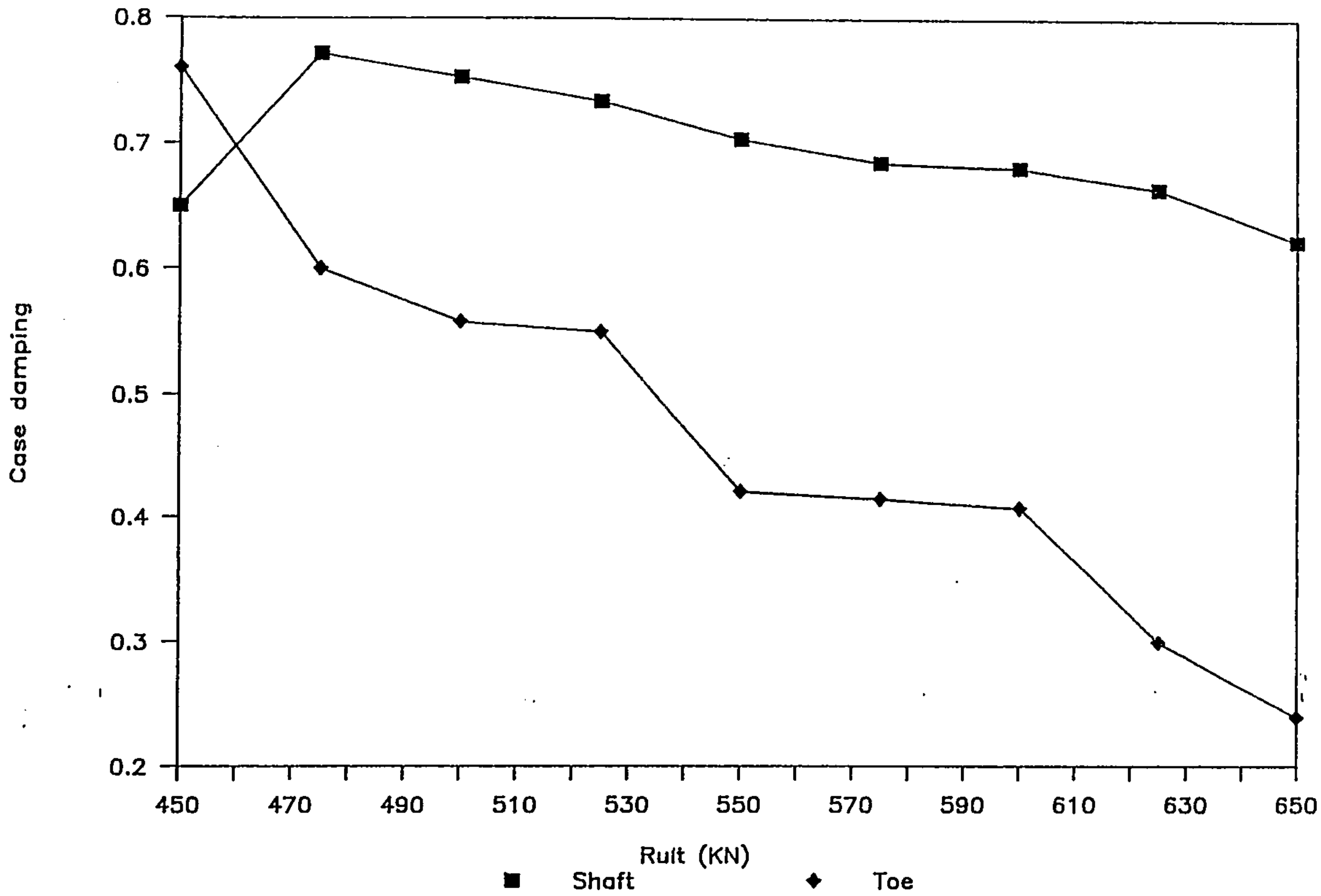

Fig. 6.98 Case Damping, JA Pile

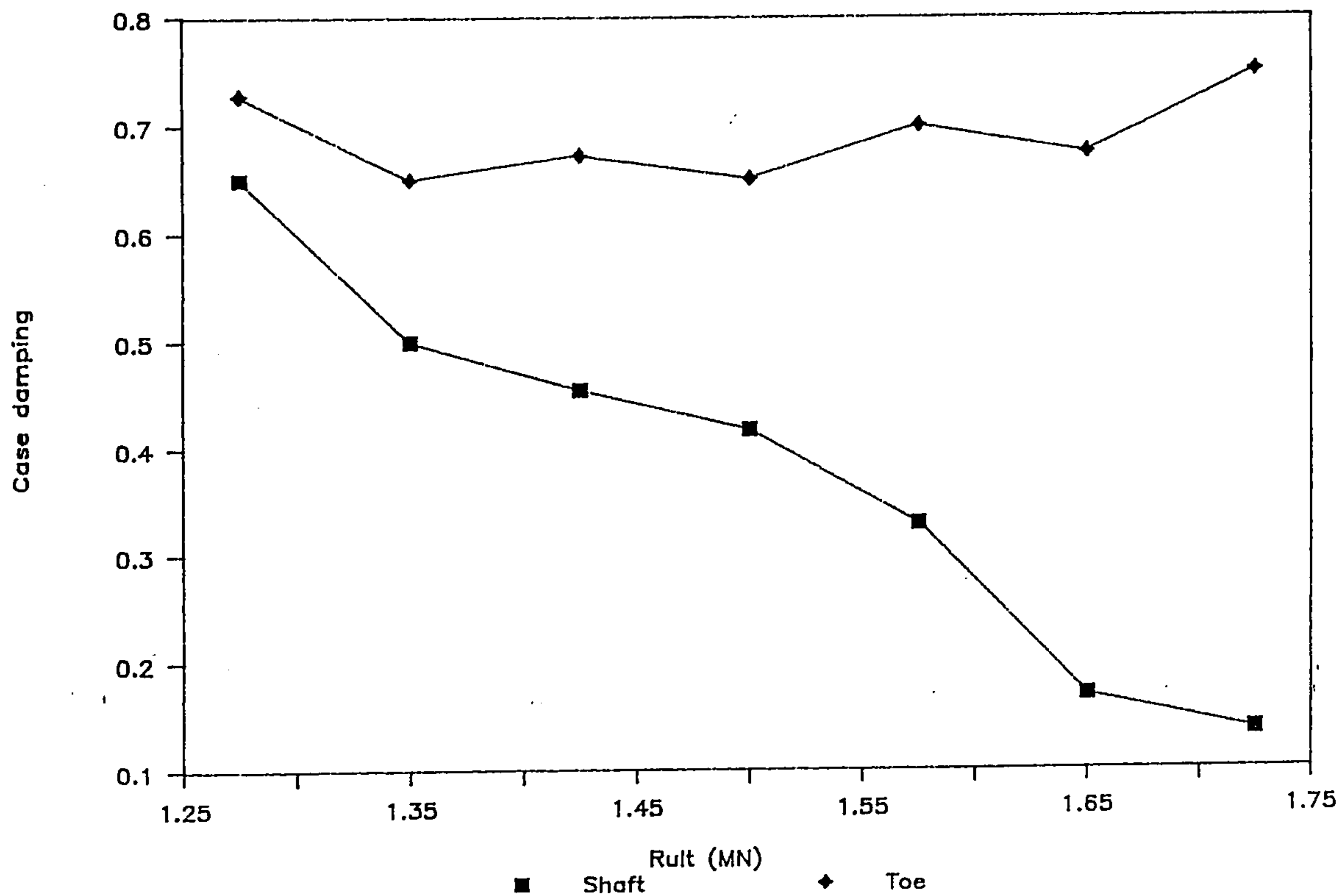

Fig. 6.99 Case Damping, AM Pile

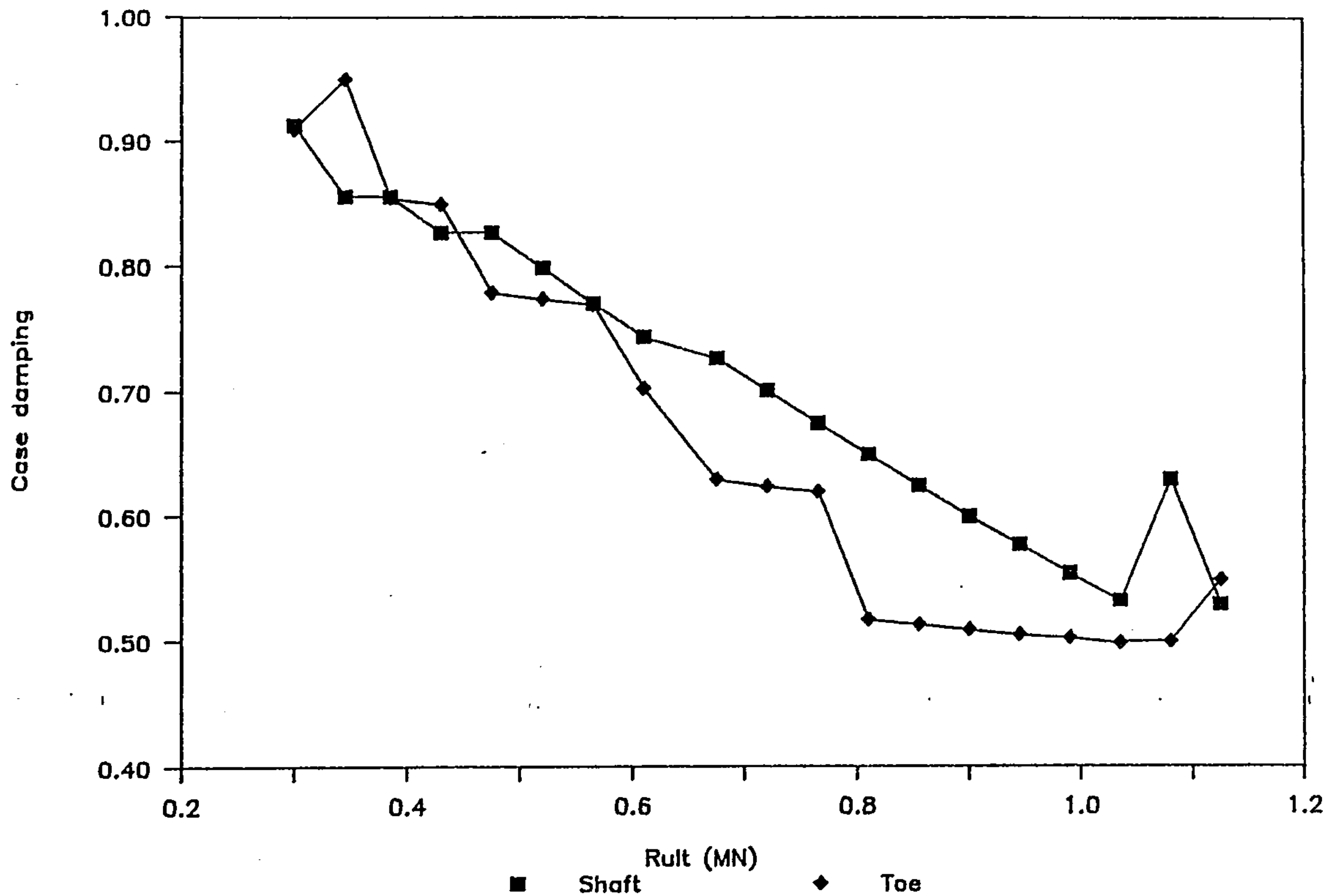

Fig. 6.100 Case Damping, LW Pile

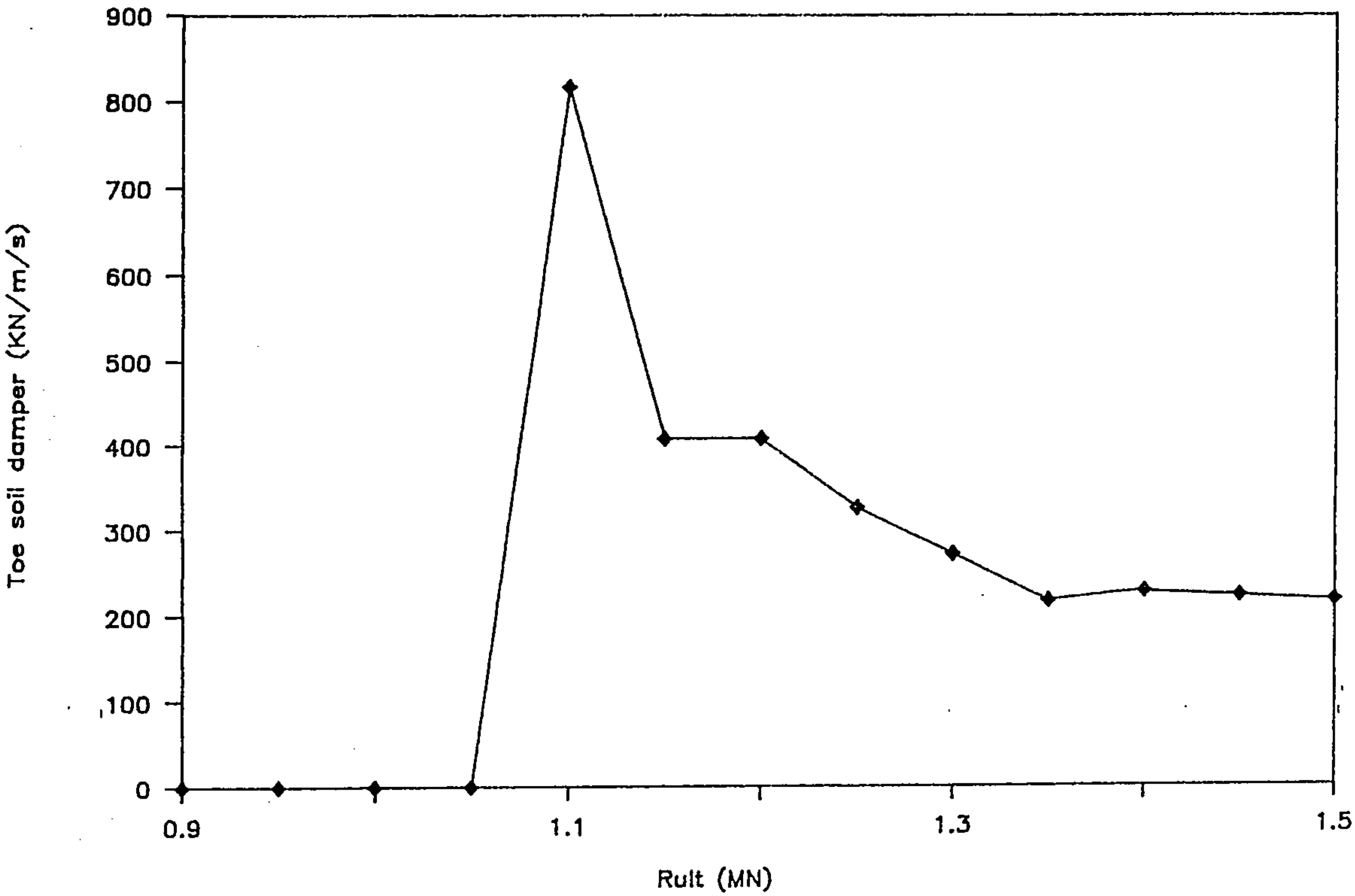

Fig. 6.101 Toe Soil Damper, JI Pile

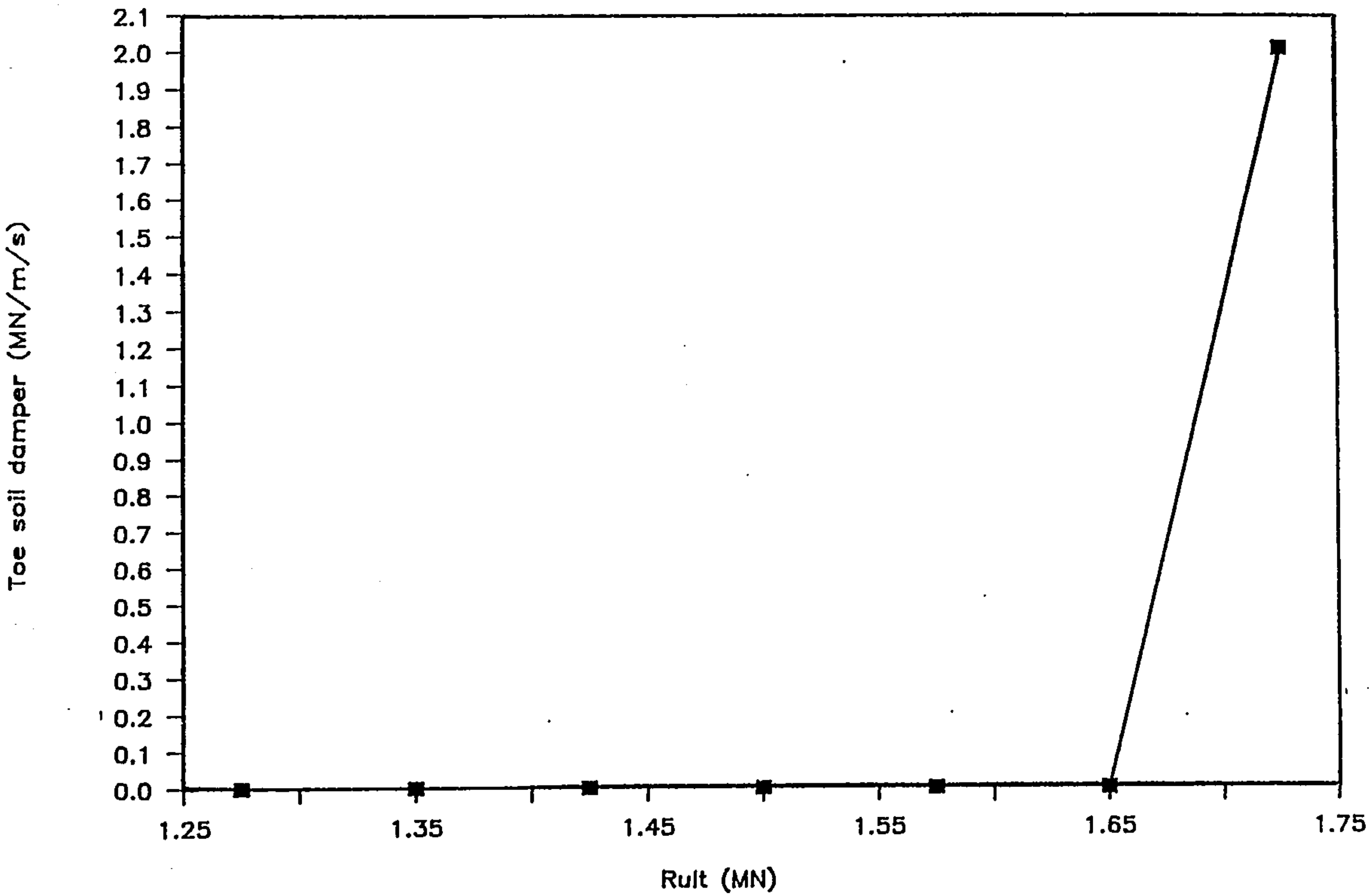

Fig. 6.102 Toe Soil Damper, AM Pile

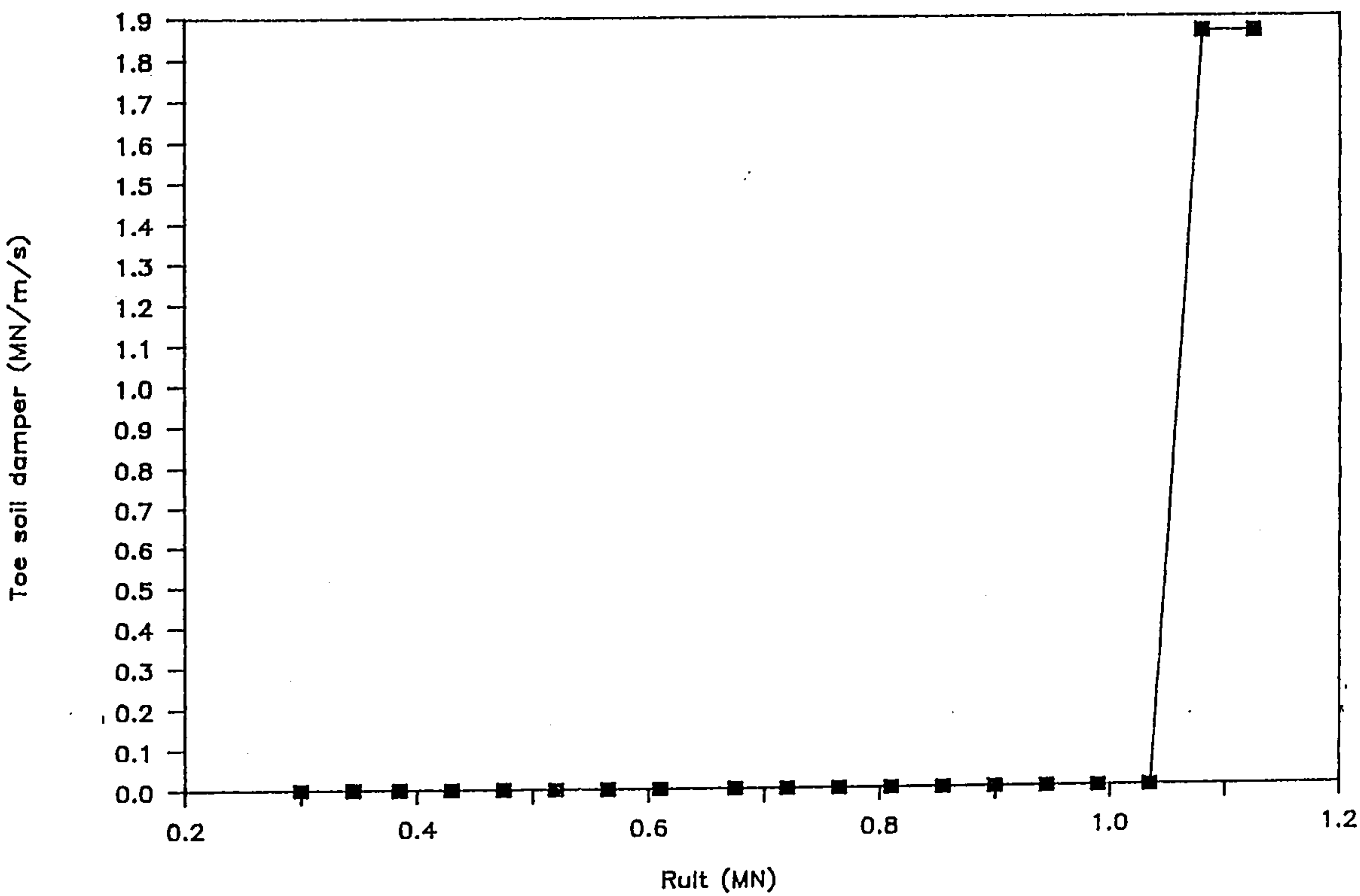

Fig. 6.103 Toe Soil Damper, LW Pile

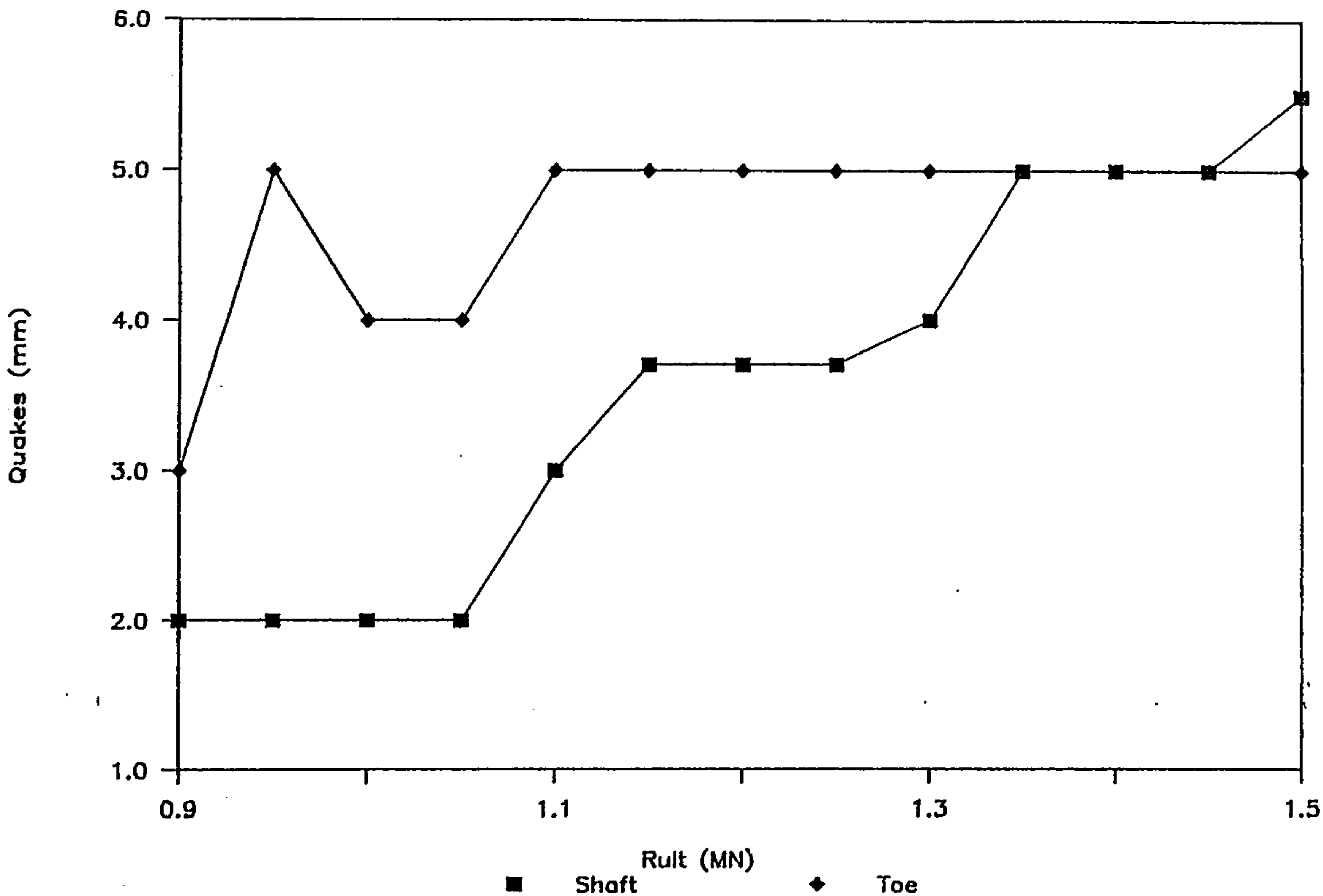

Fig. 6.104 Quakes, JI Pile

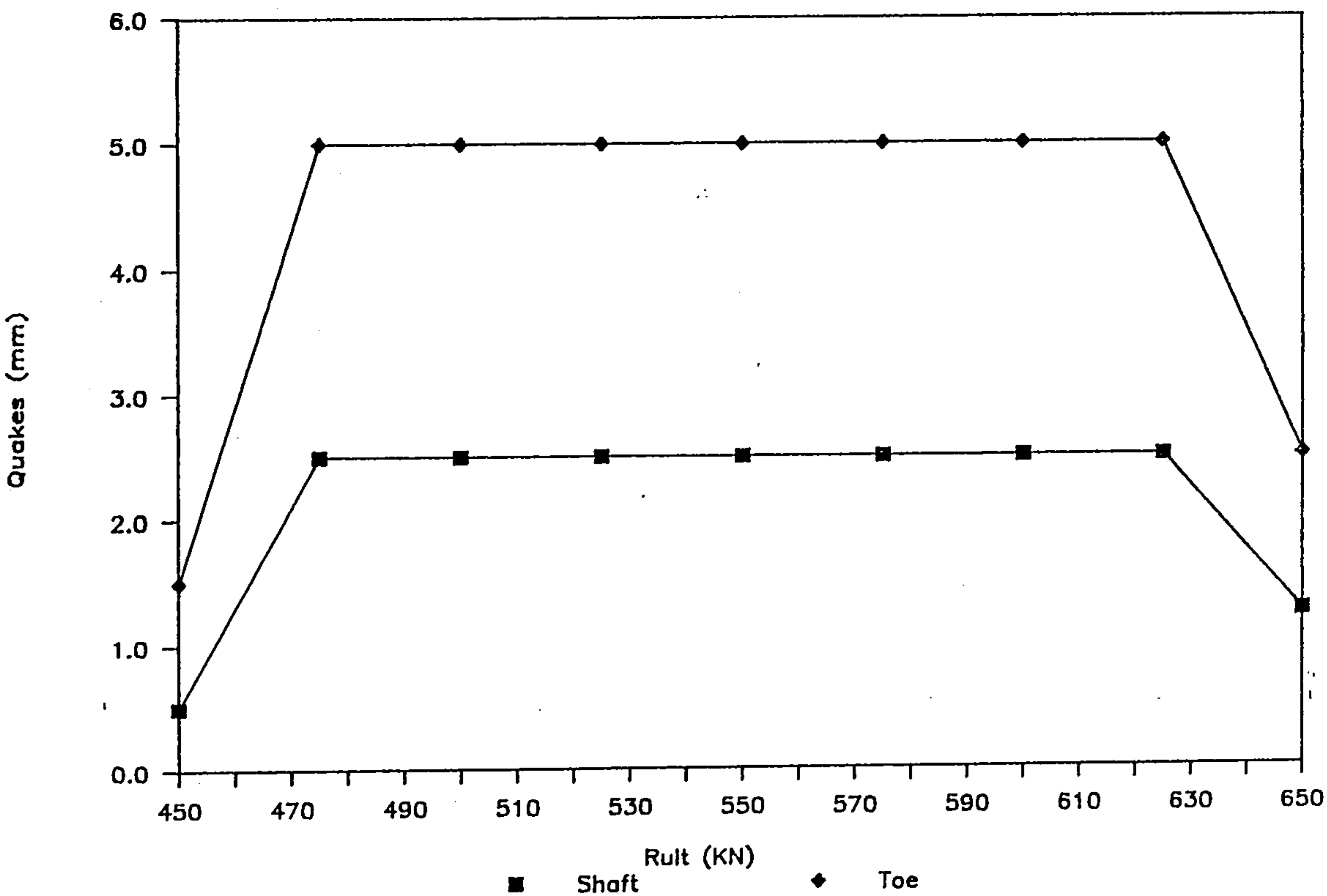

Fig. 6.105 Quakes, JA Pile

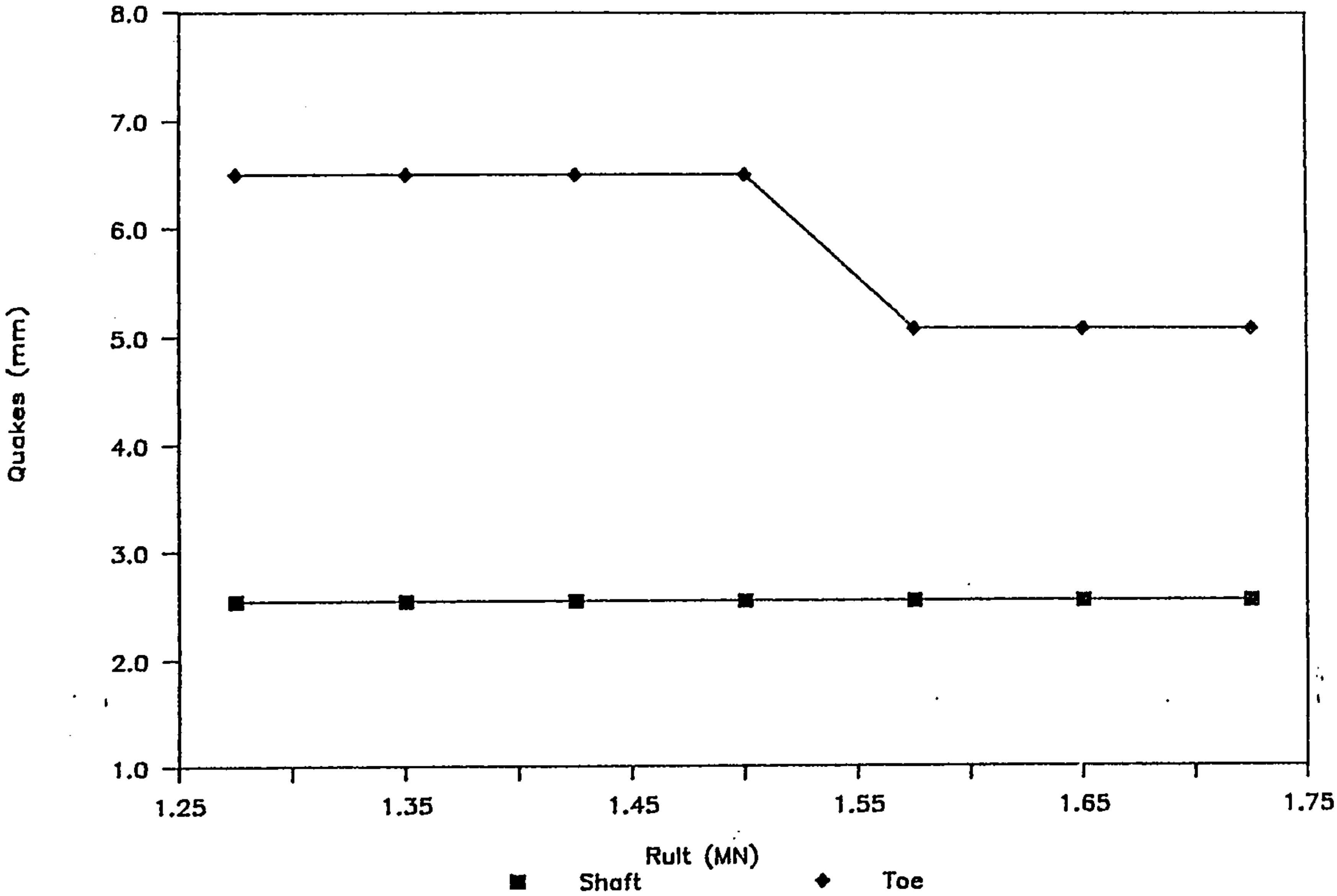

Fig. 6.106 Quakes, AM Pile

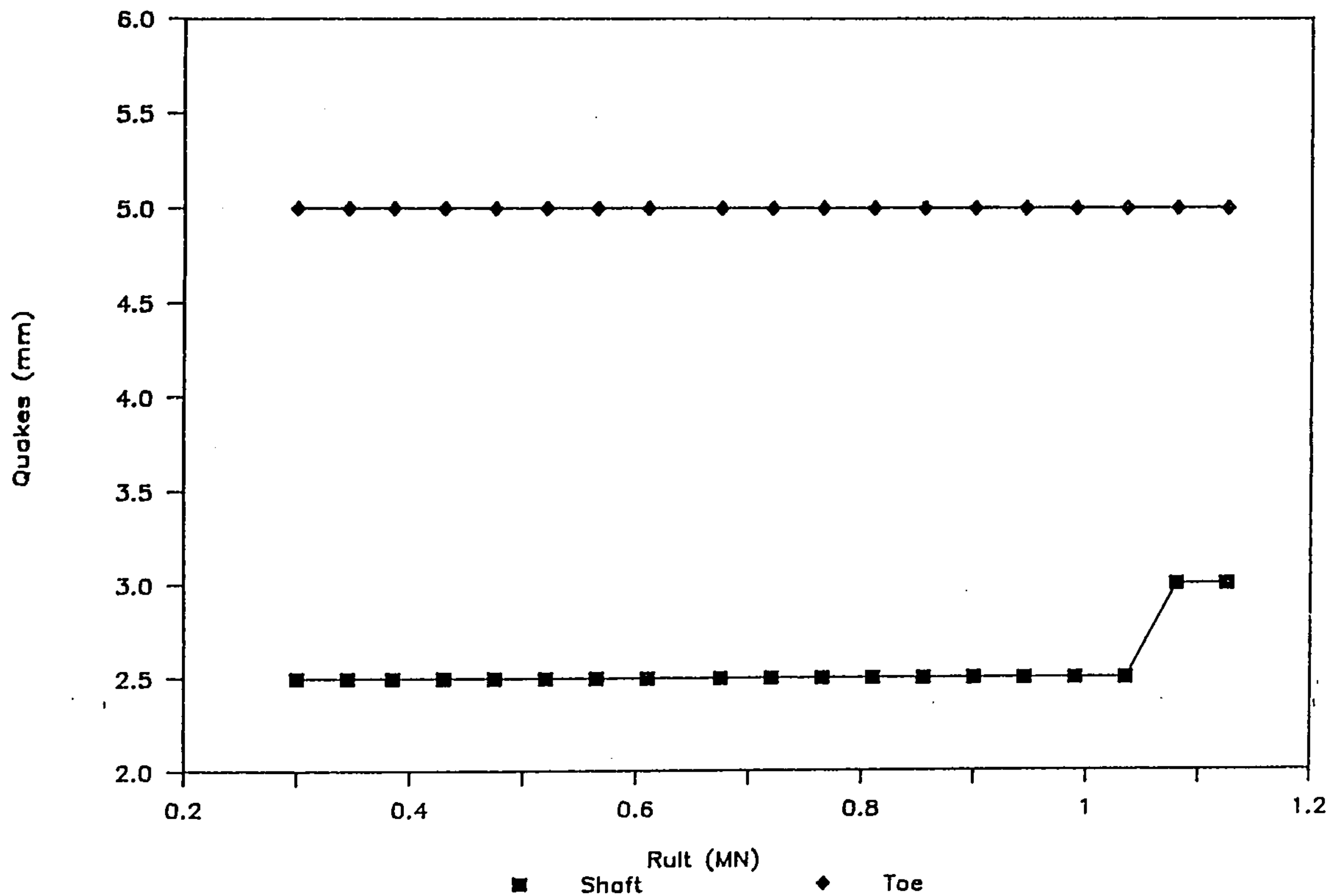

Fig. 6.107 Quakes, LW Pile

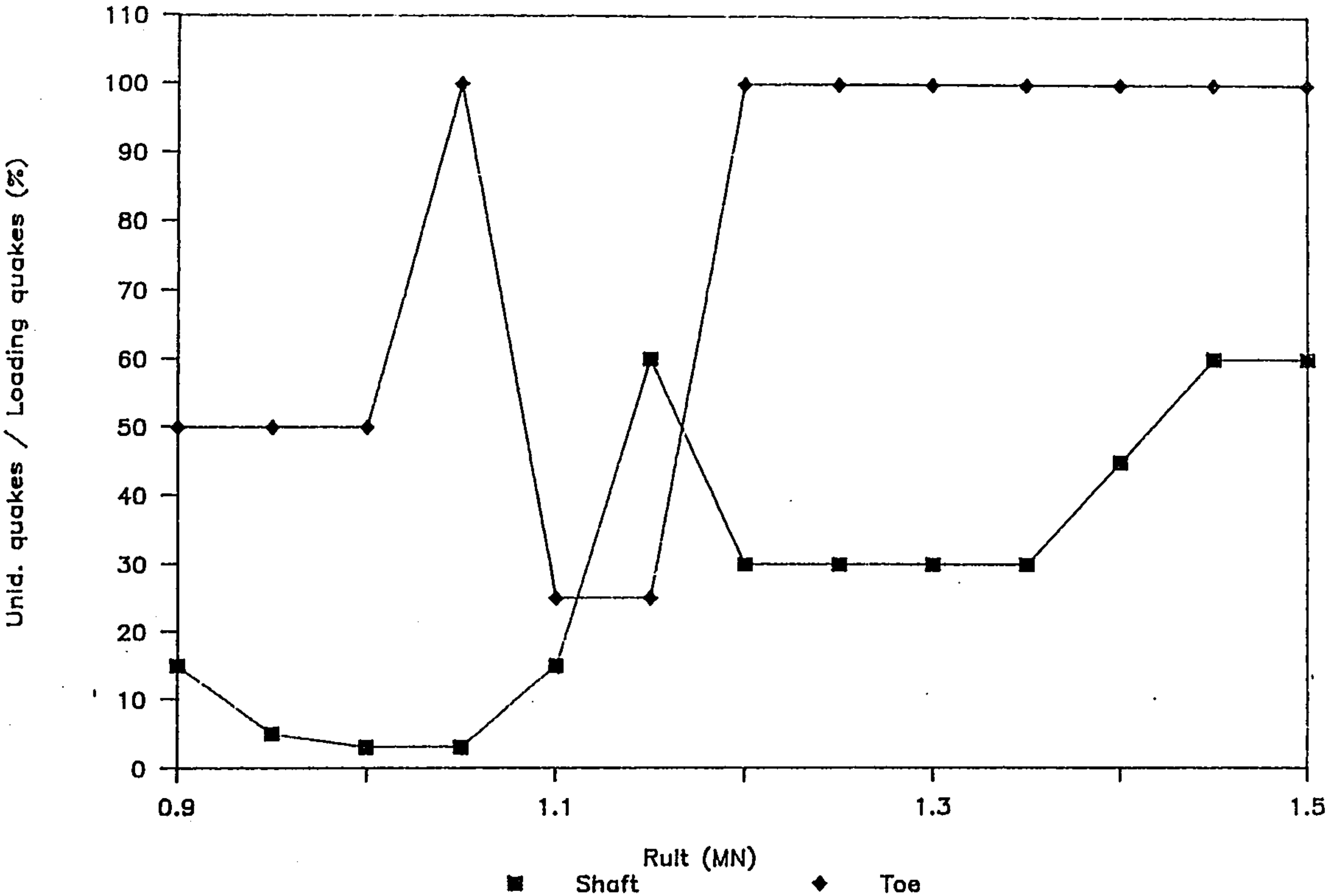

Fig. 6.108 Unloading Quakes, JI Pile

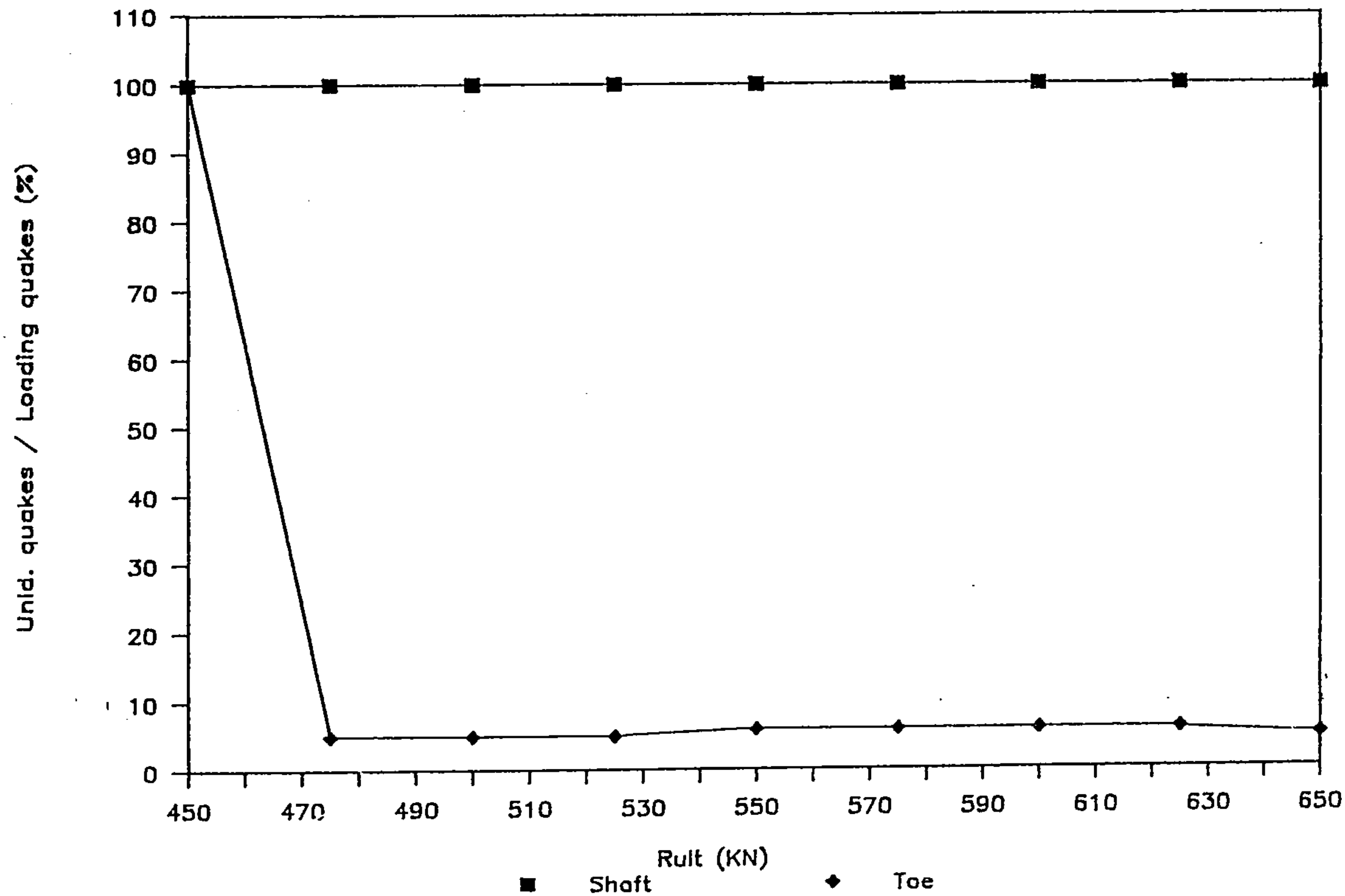

Fig. 6.109 Unloading Quakes, JA Pile

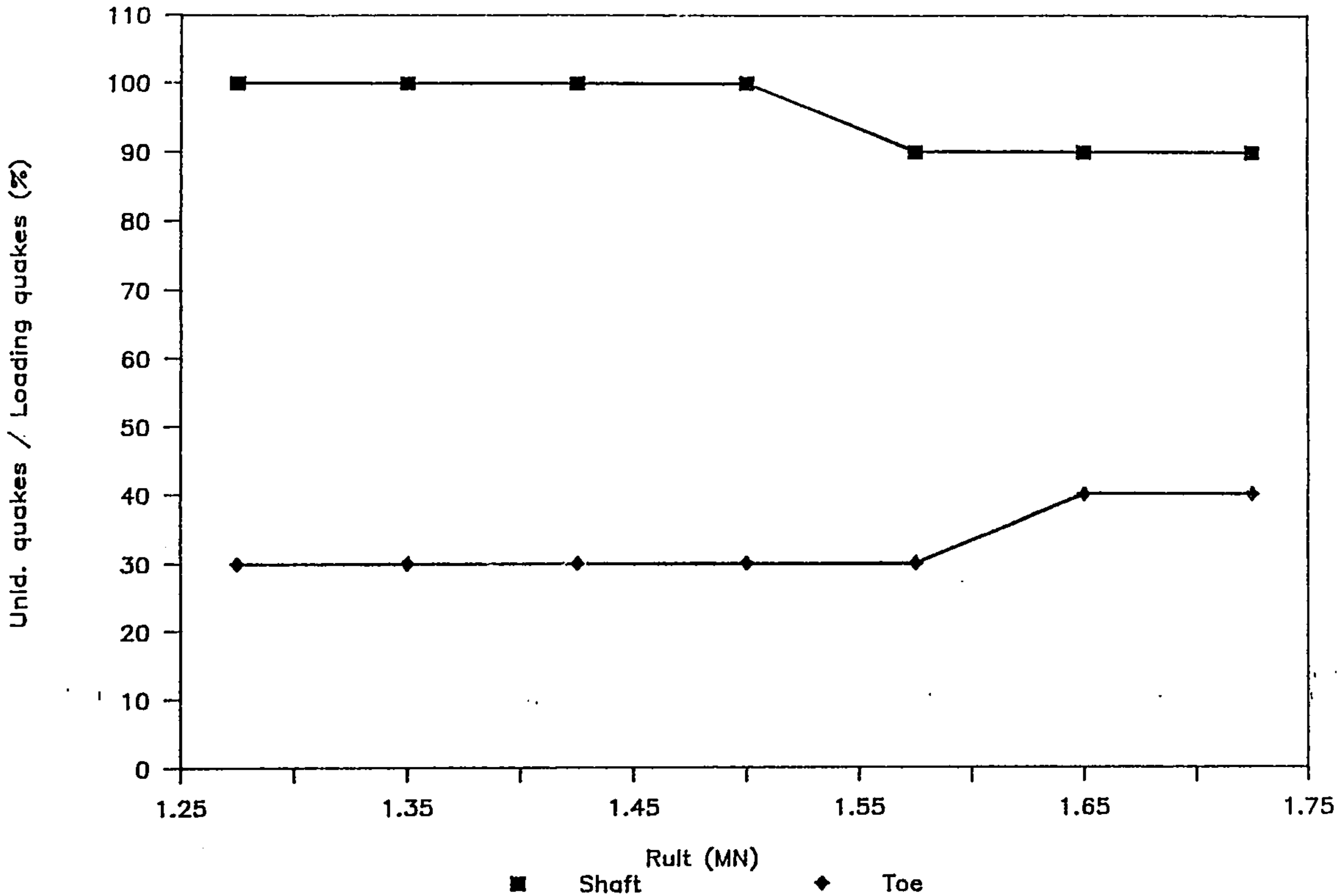

Fig. 6.110 Unloading Quakes, AM Pile

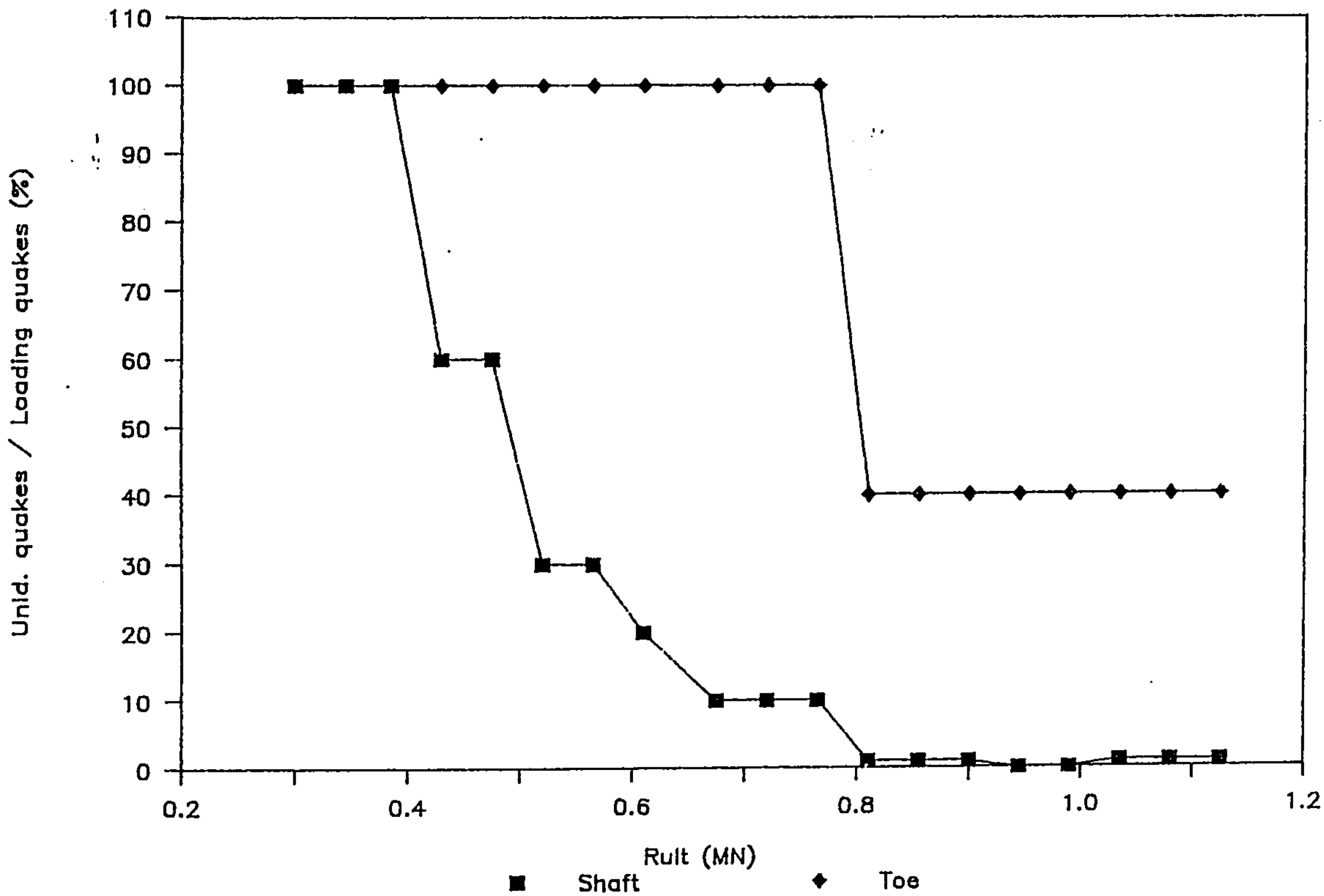

Fig. 6.111 Unloading Quakes, LW Pile

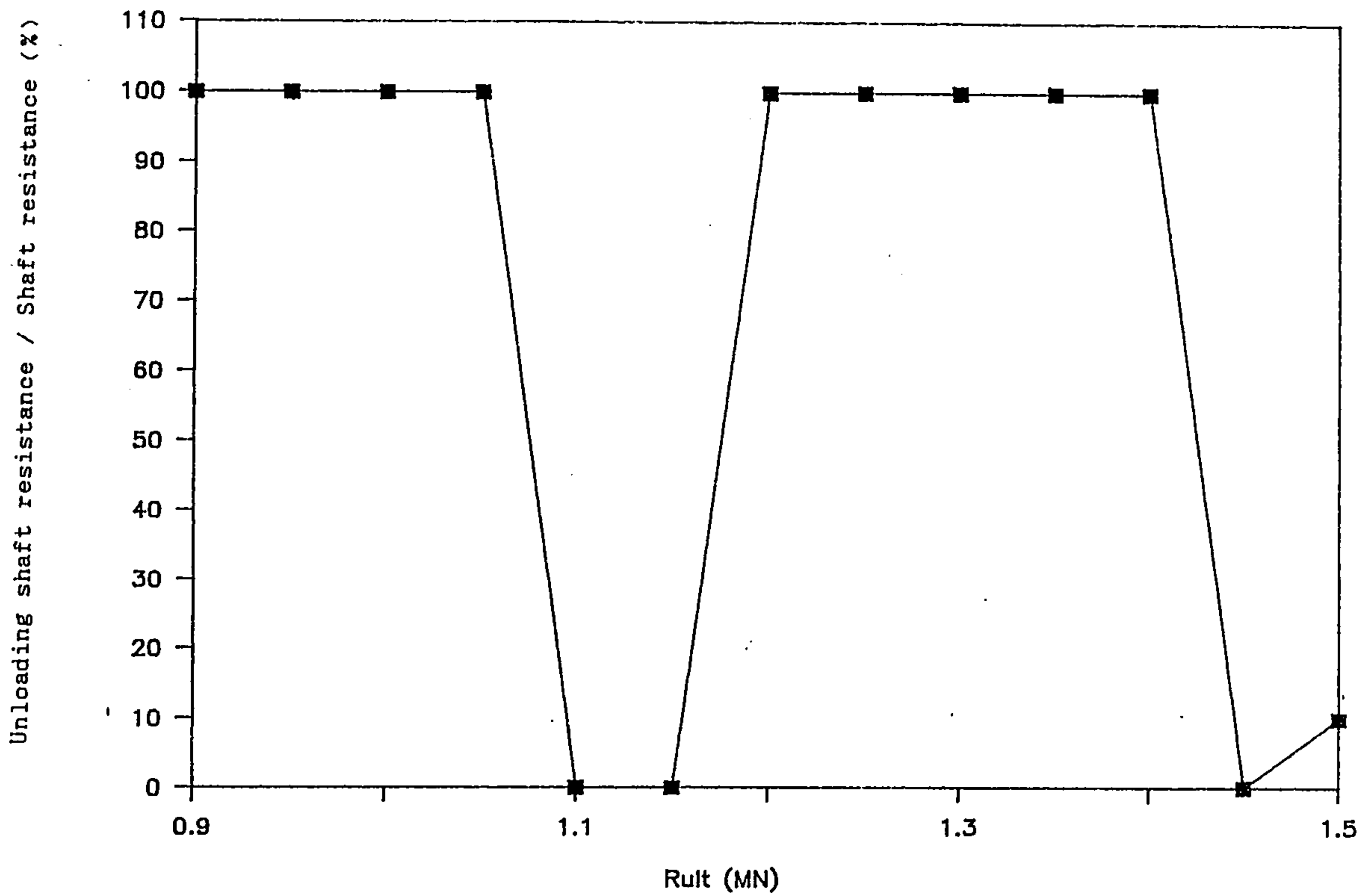

Fig. 6.112 Unloading Resistance, JI Pile

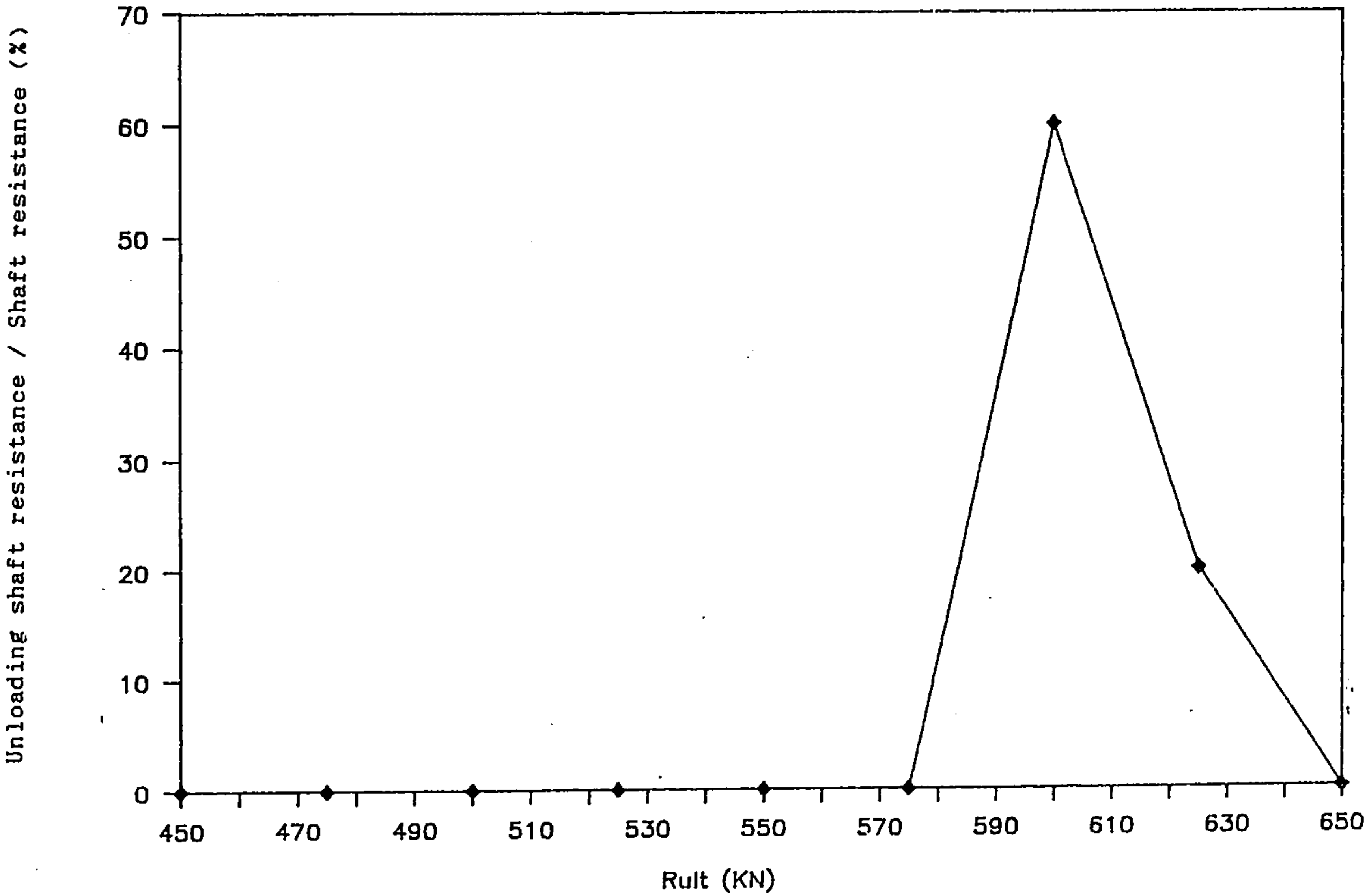

Fig. 6.113 Unloading Resistance, JA Pile

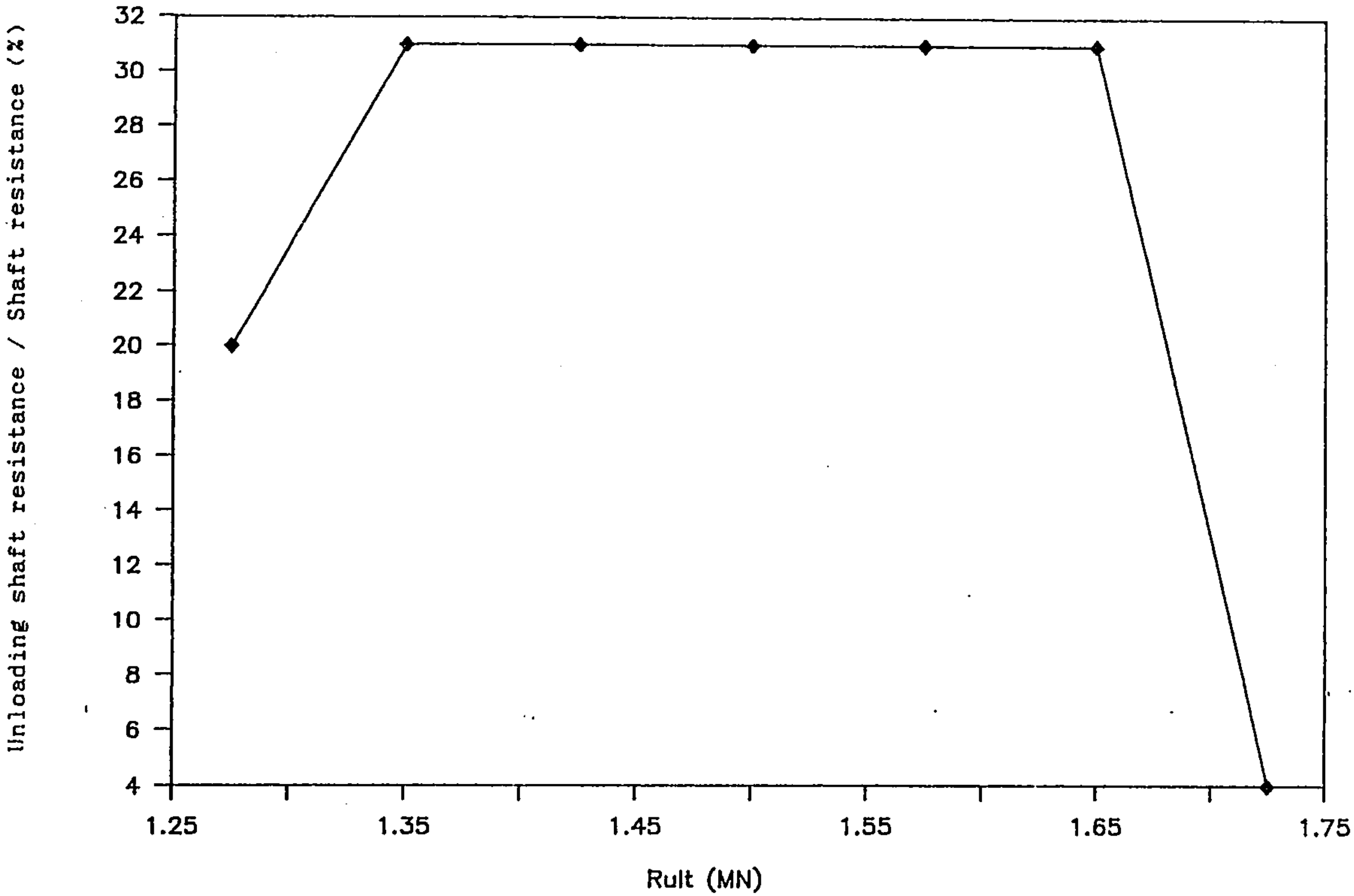

Fig. 6.114 Unloading Resistance, AM Pile

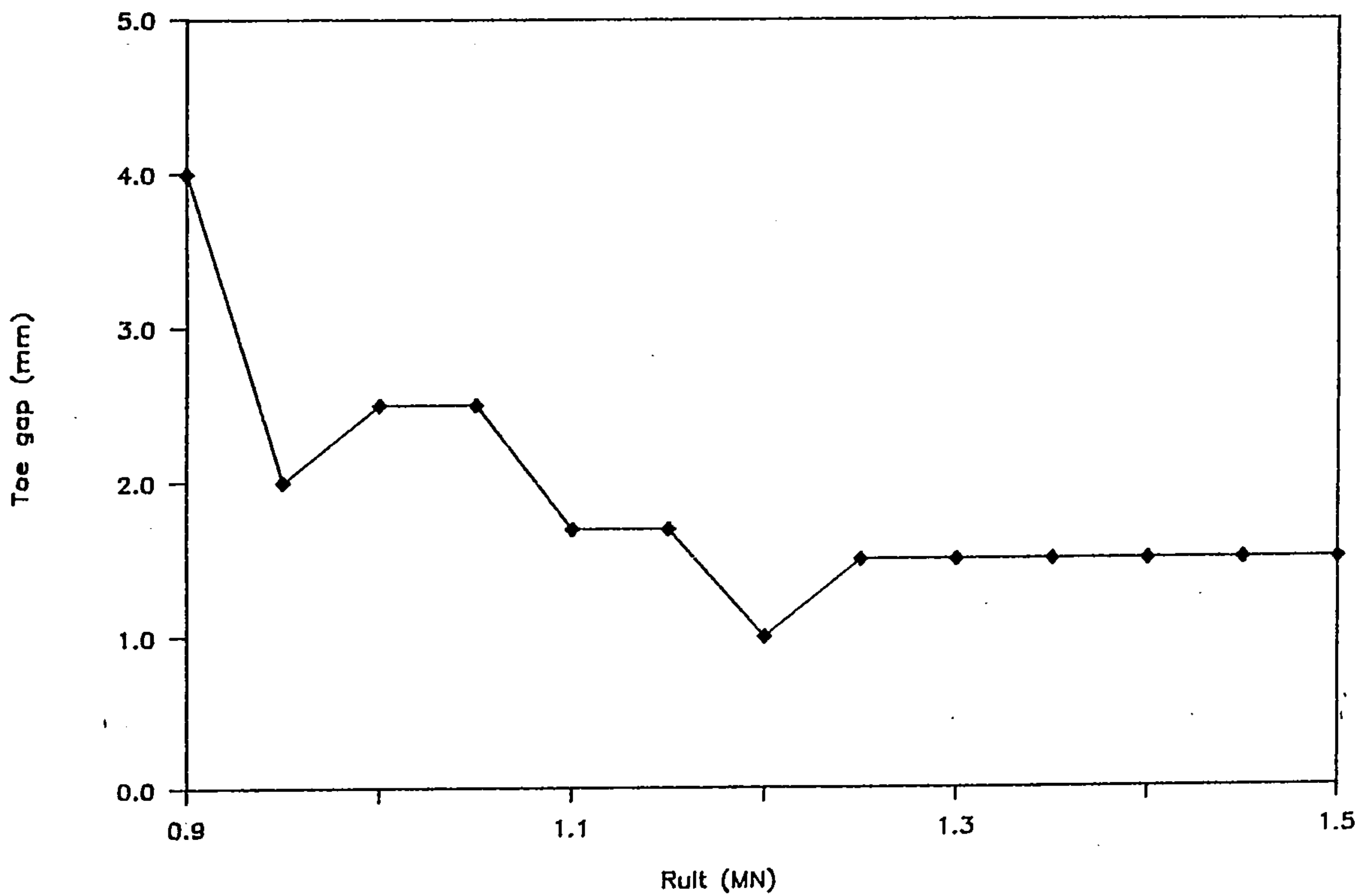

Fig. 6.115 Toe Gap, JI Pile

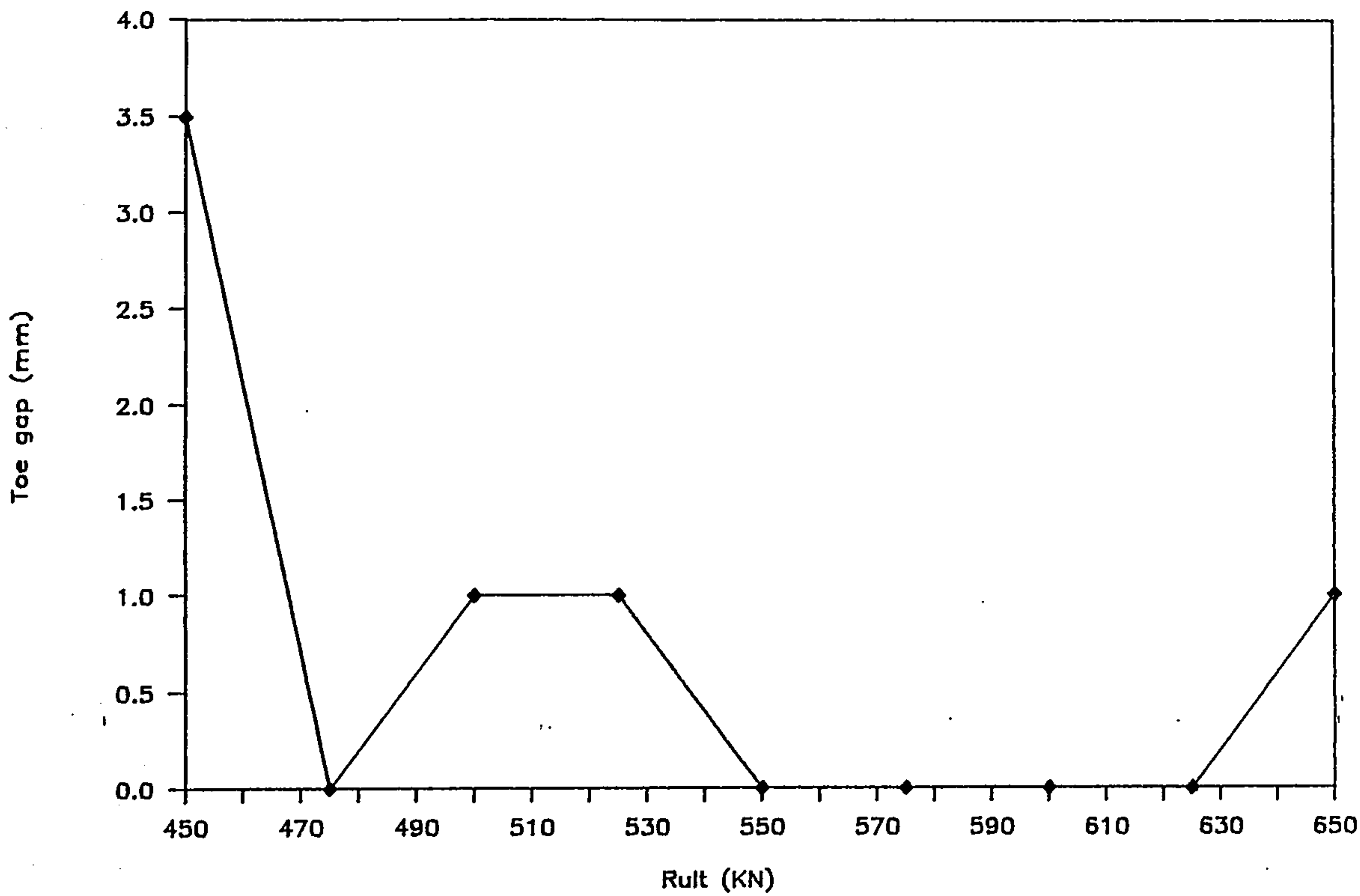

Fig. 6.116 Toe Gap, JA Pile

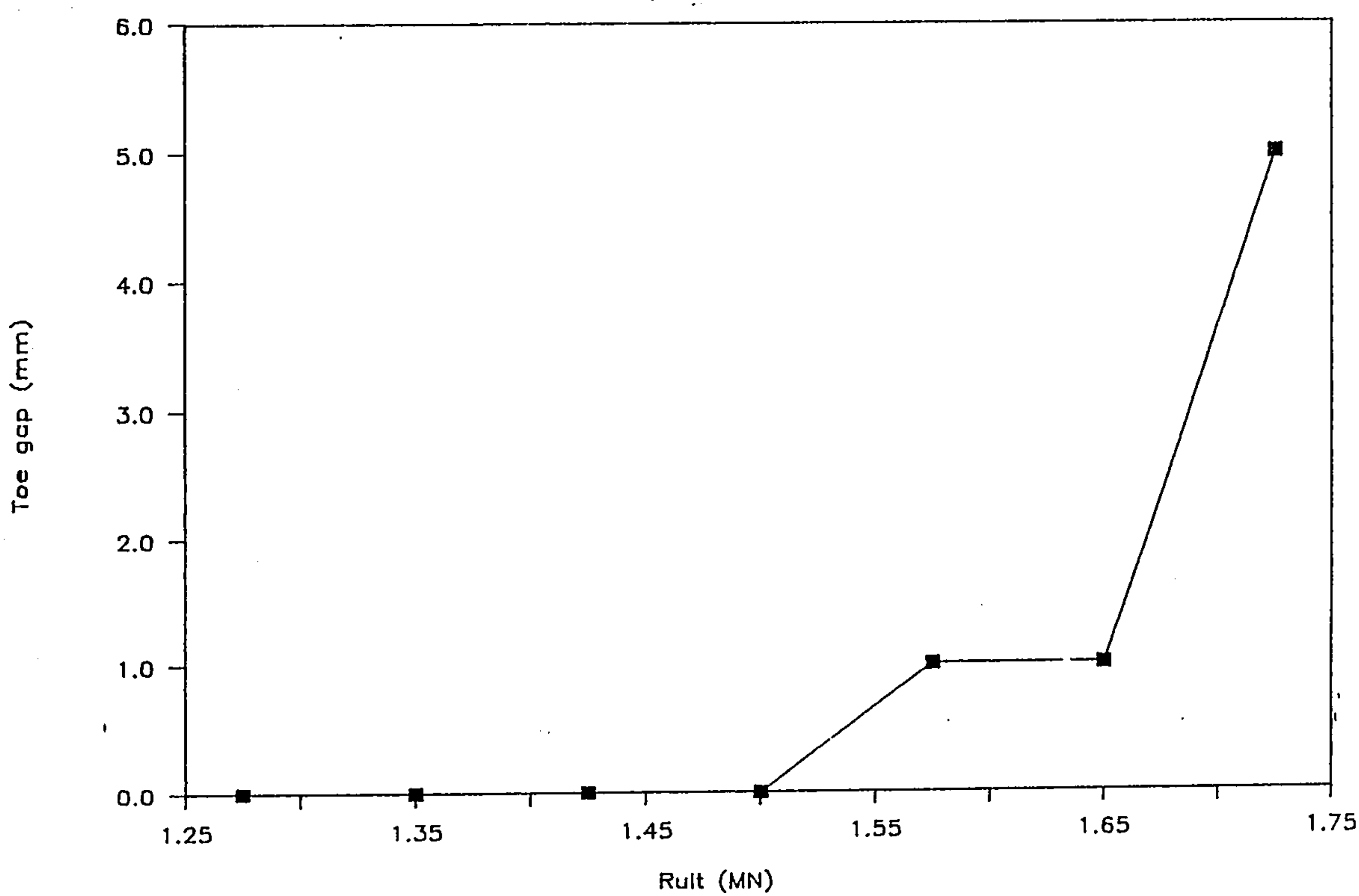

Fig. 6.117 Toe Gap, AM Pile

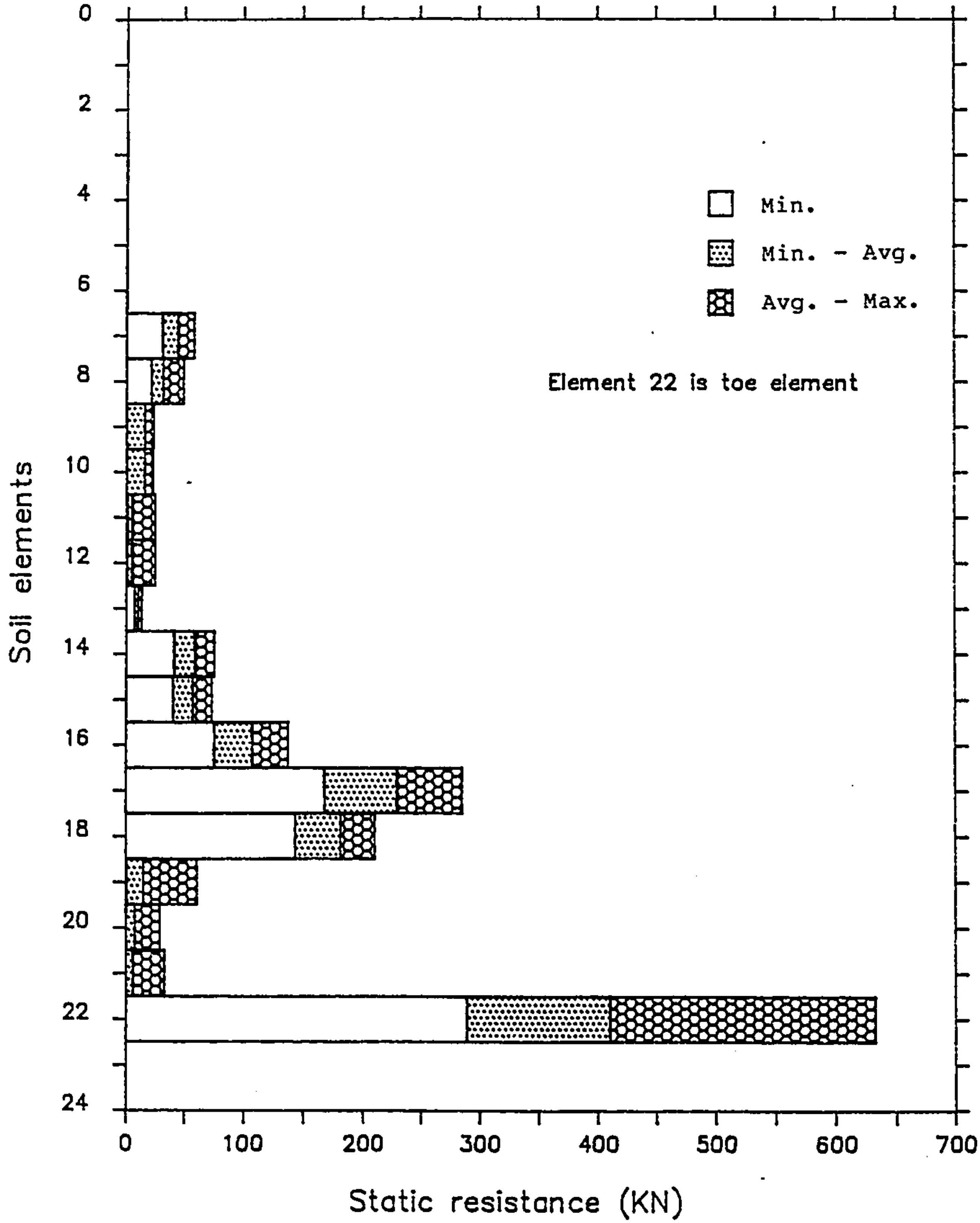

Fig. 6.118 Static Resistance Distribution, JI Pile

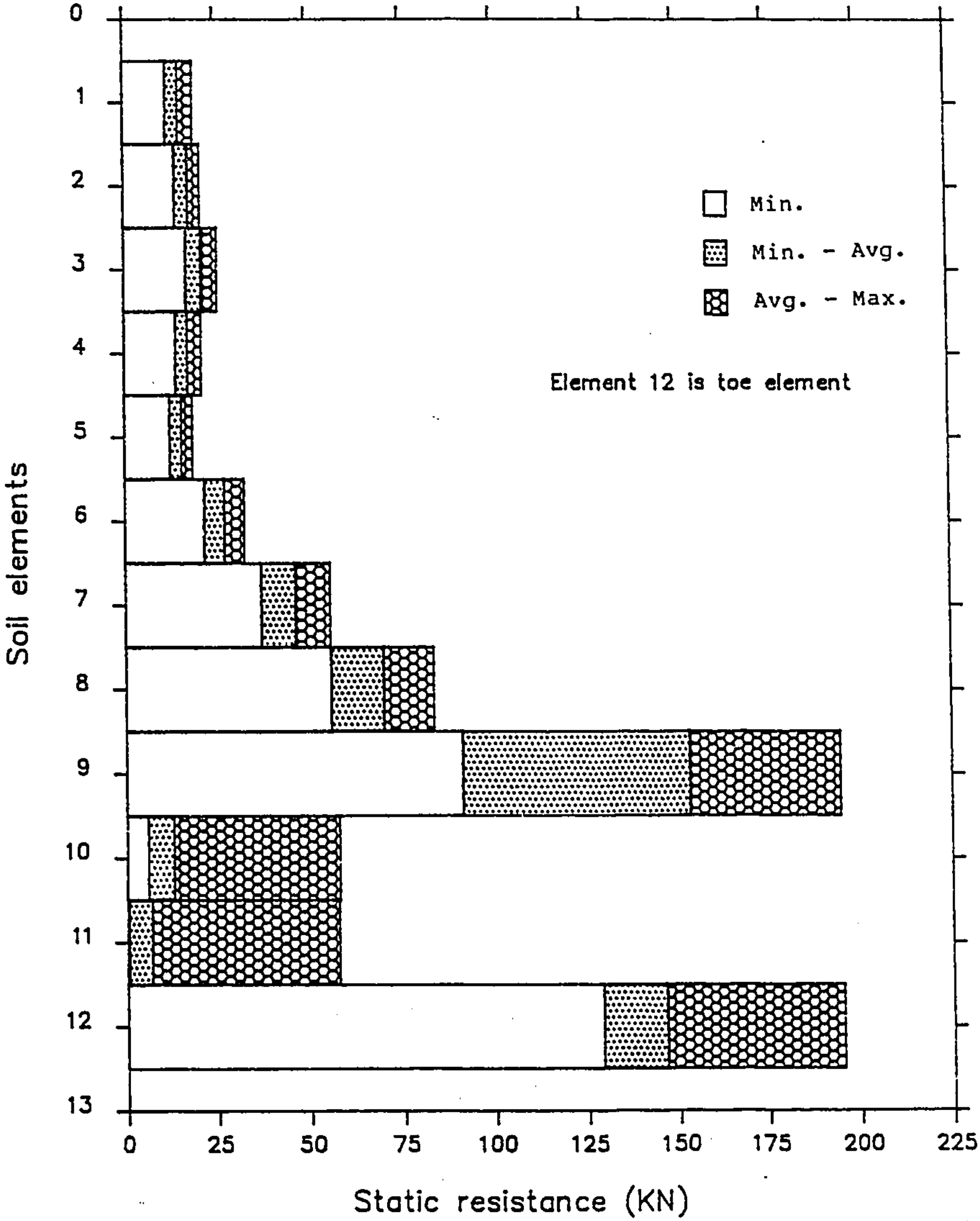

Fig. 6.119 Static Resistance Distribution, JA Pile

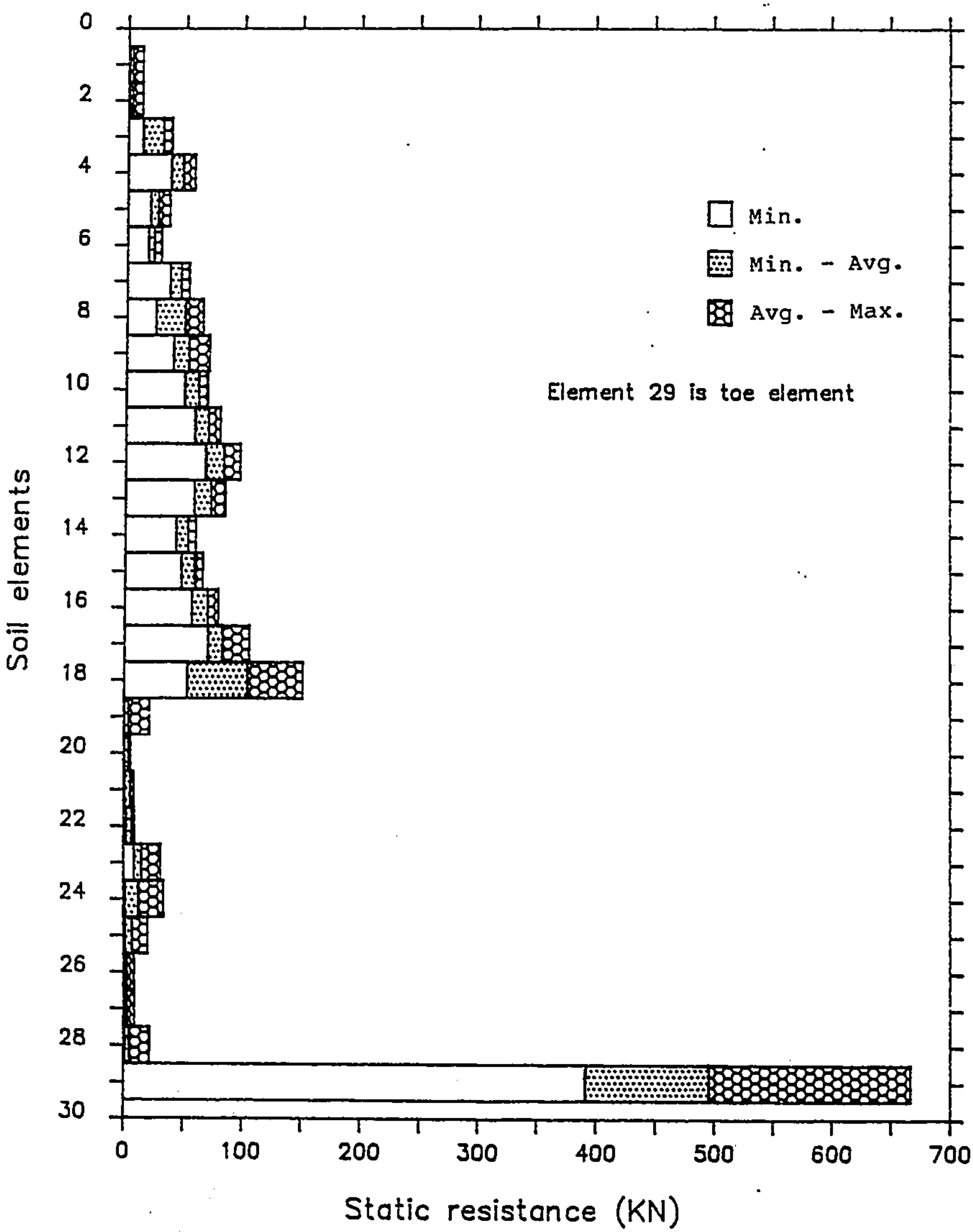

Fig. 6.120 Static Resistance Distribution, AM Pile

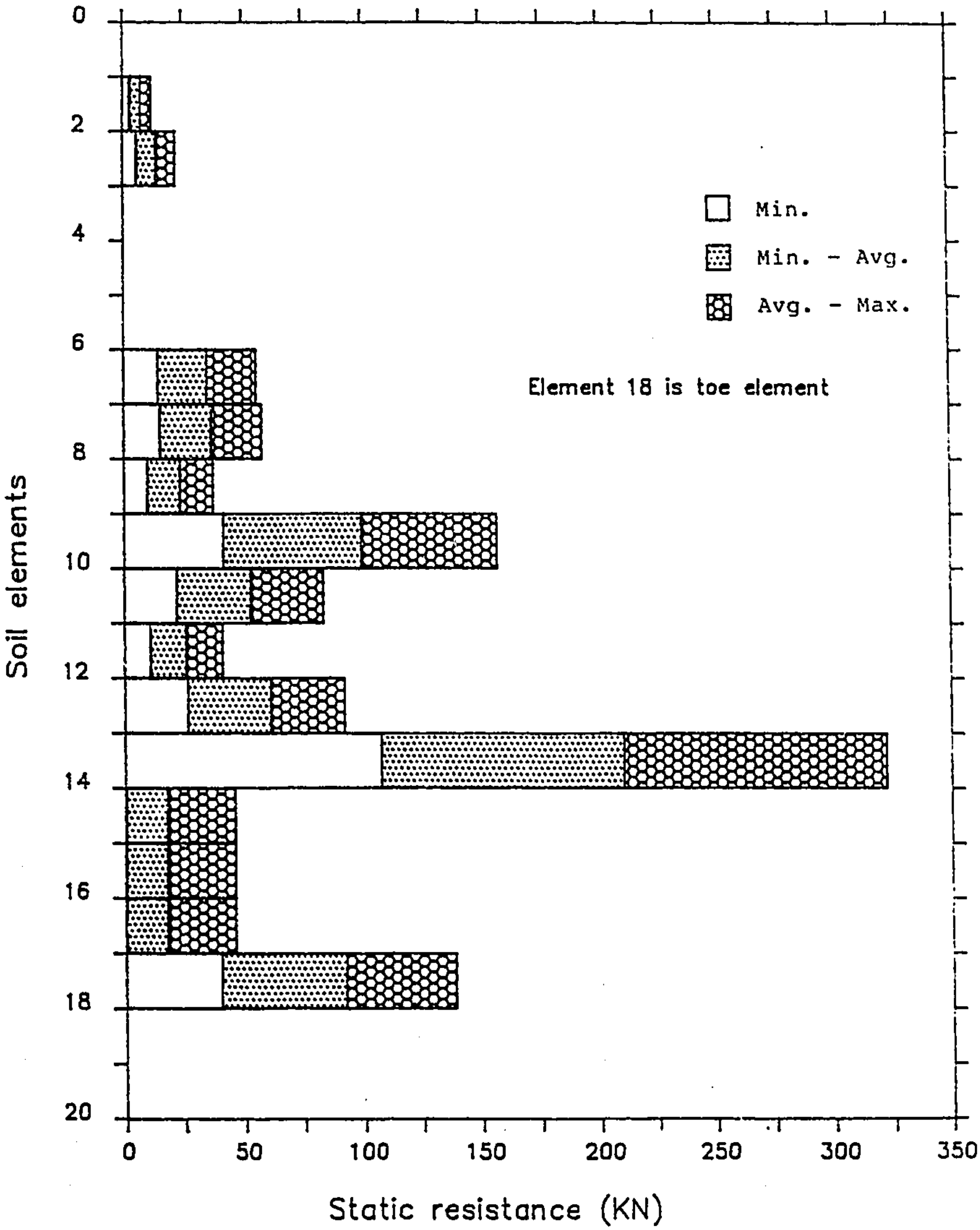

Fig. 6.121 Static Resistance Distribution, LW Pile

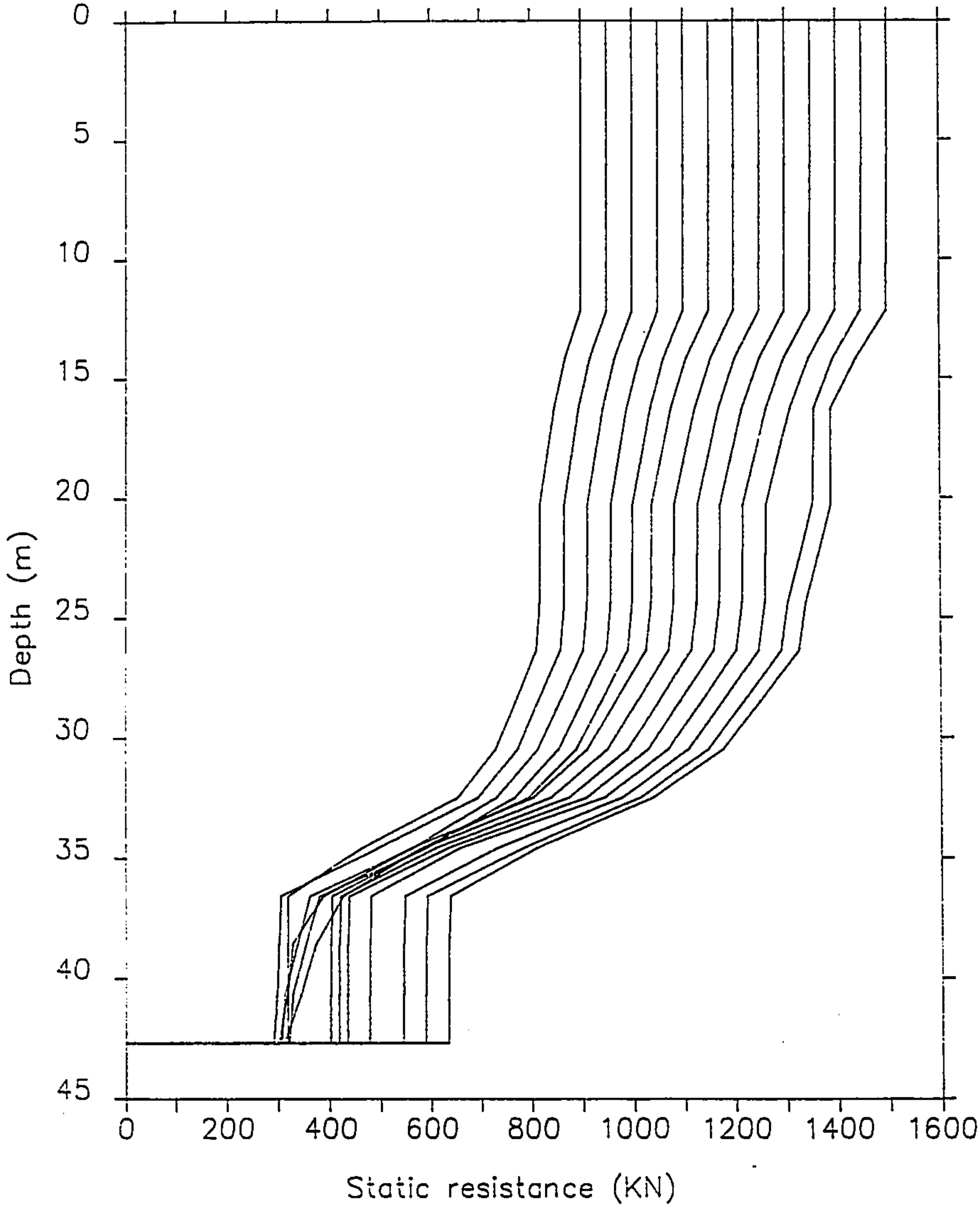

Fig. 6.122 Load Transfer in JI Pile

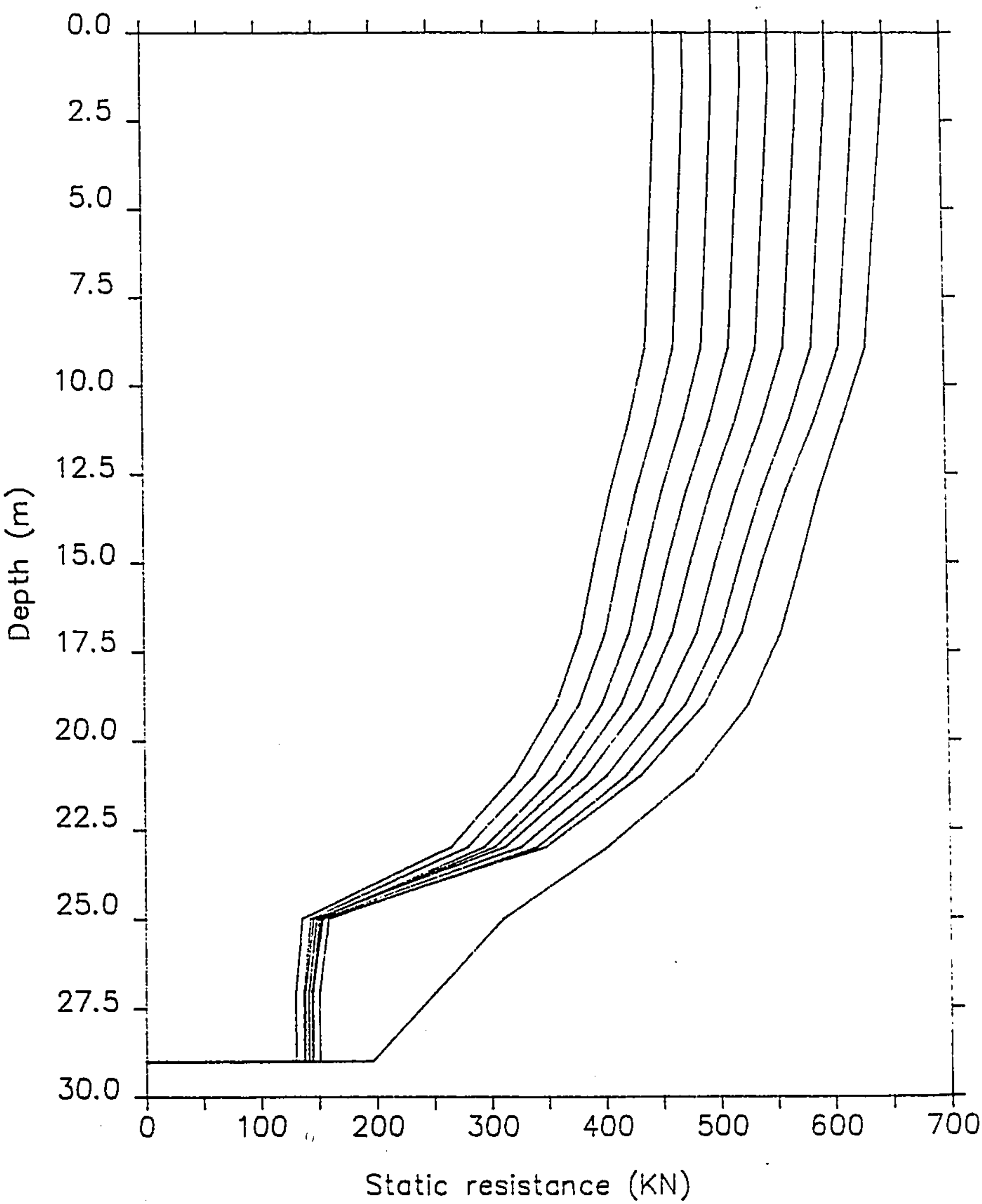

Fig. 6.123 Load Transfer in JA Pile

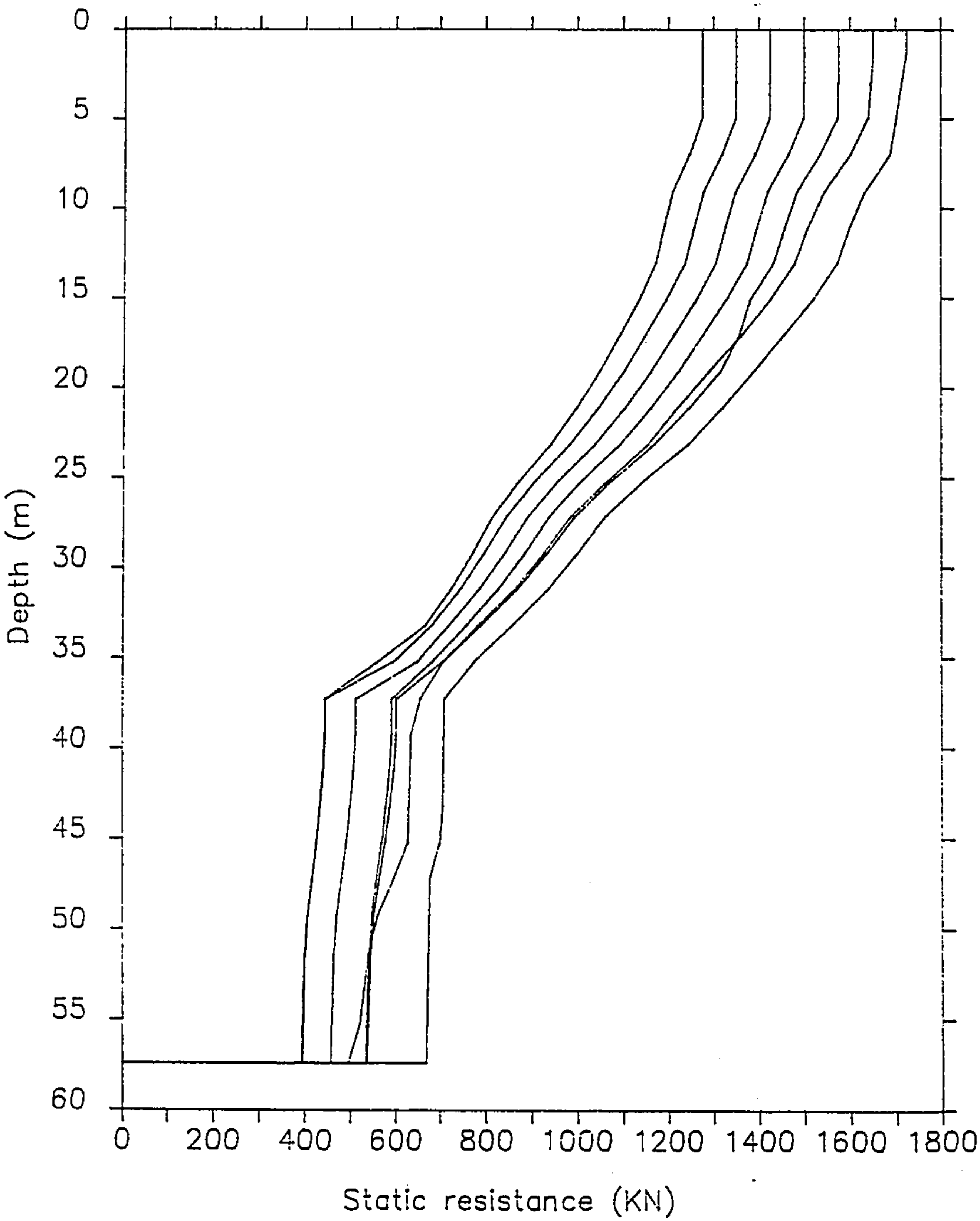

Fig. 6.124 Load Transfer in AM Pile

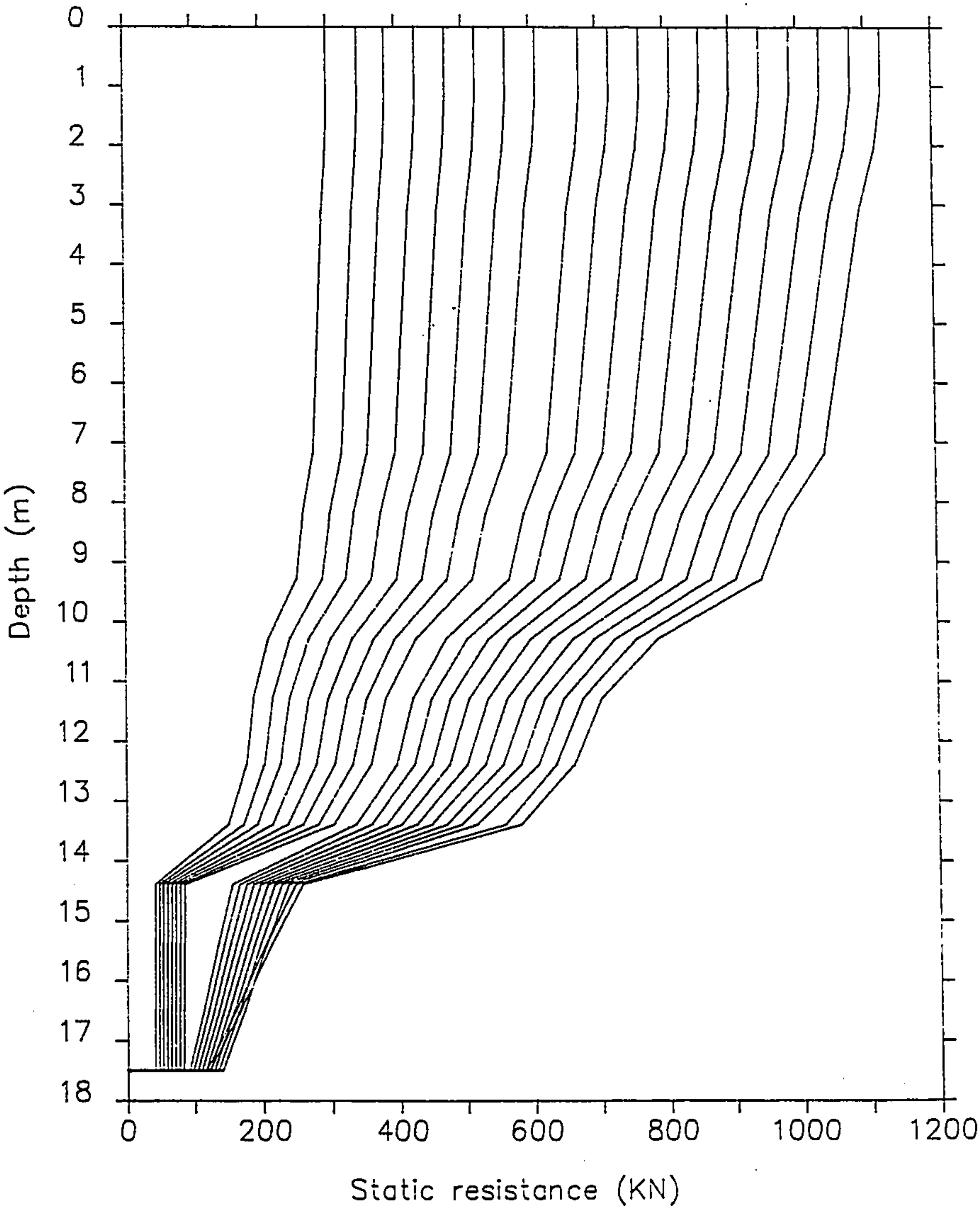

Fig. 6.125 Load Transfer in LW Pile

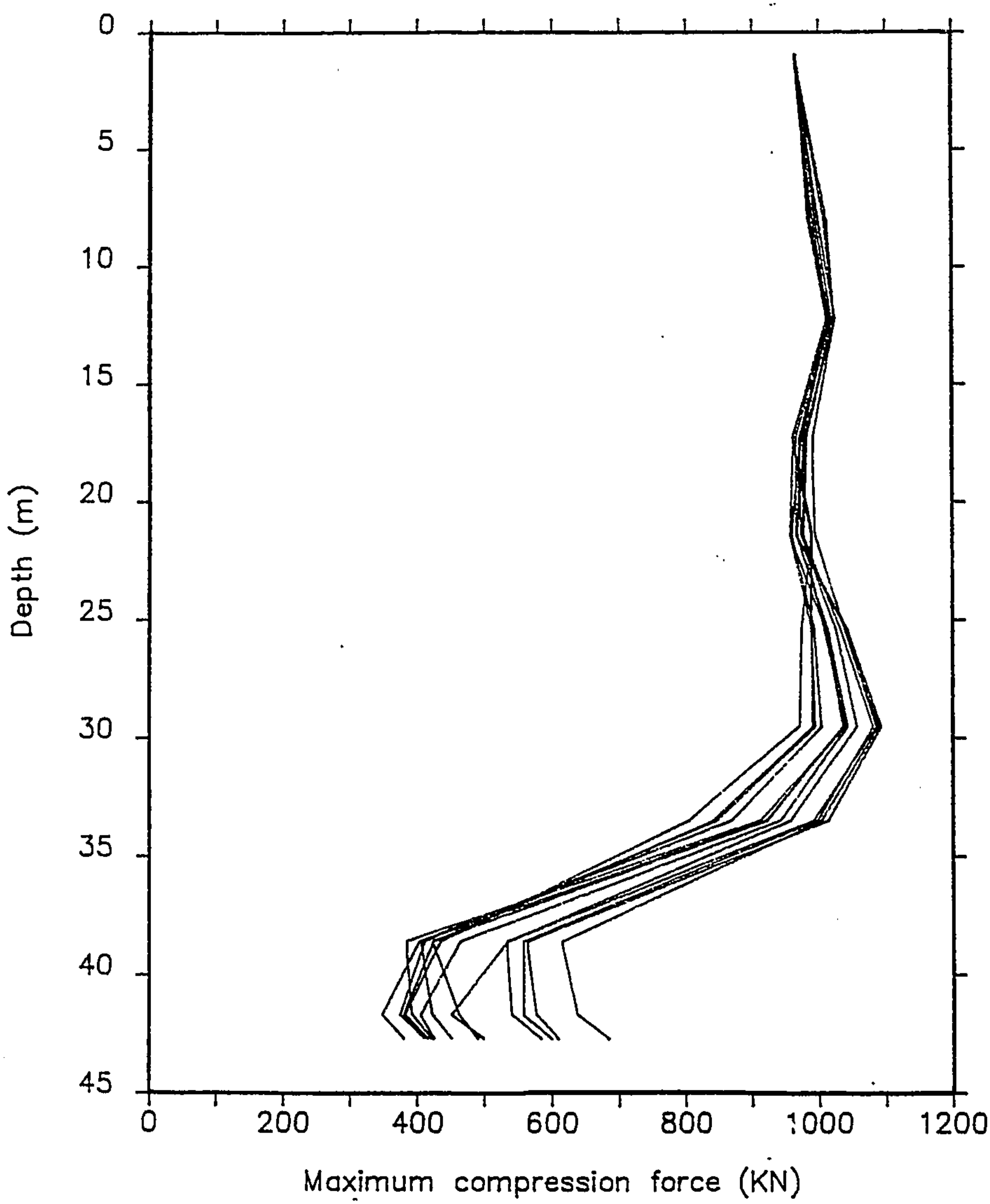

Fig. 6.126 Maximum Compression Forces, JI Pile

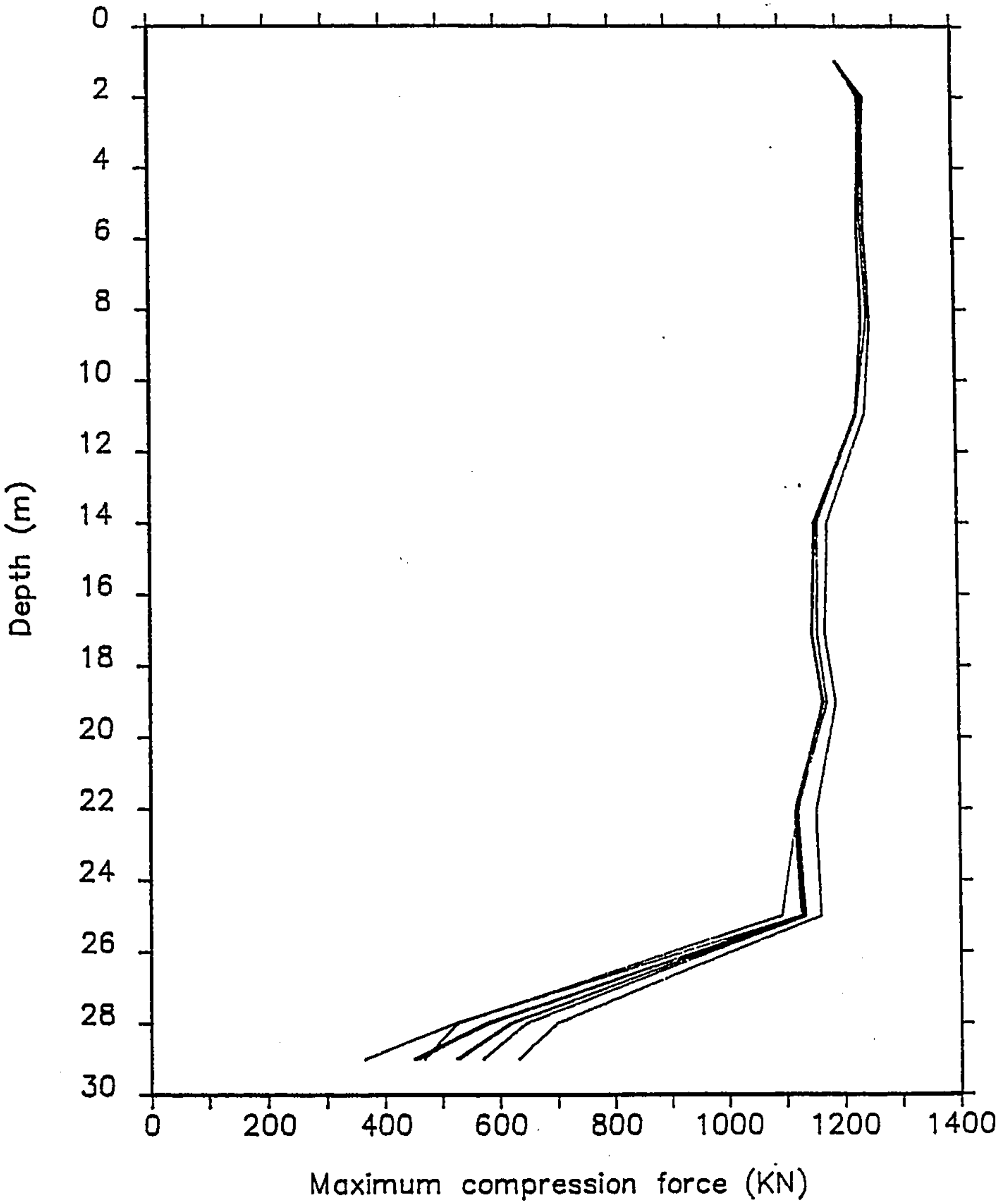

Fig. 6.127 Maximum Compression Forces, JA Pile

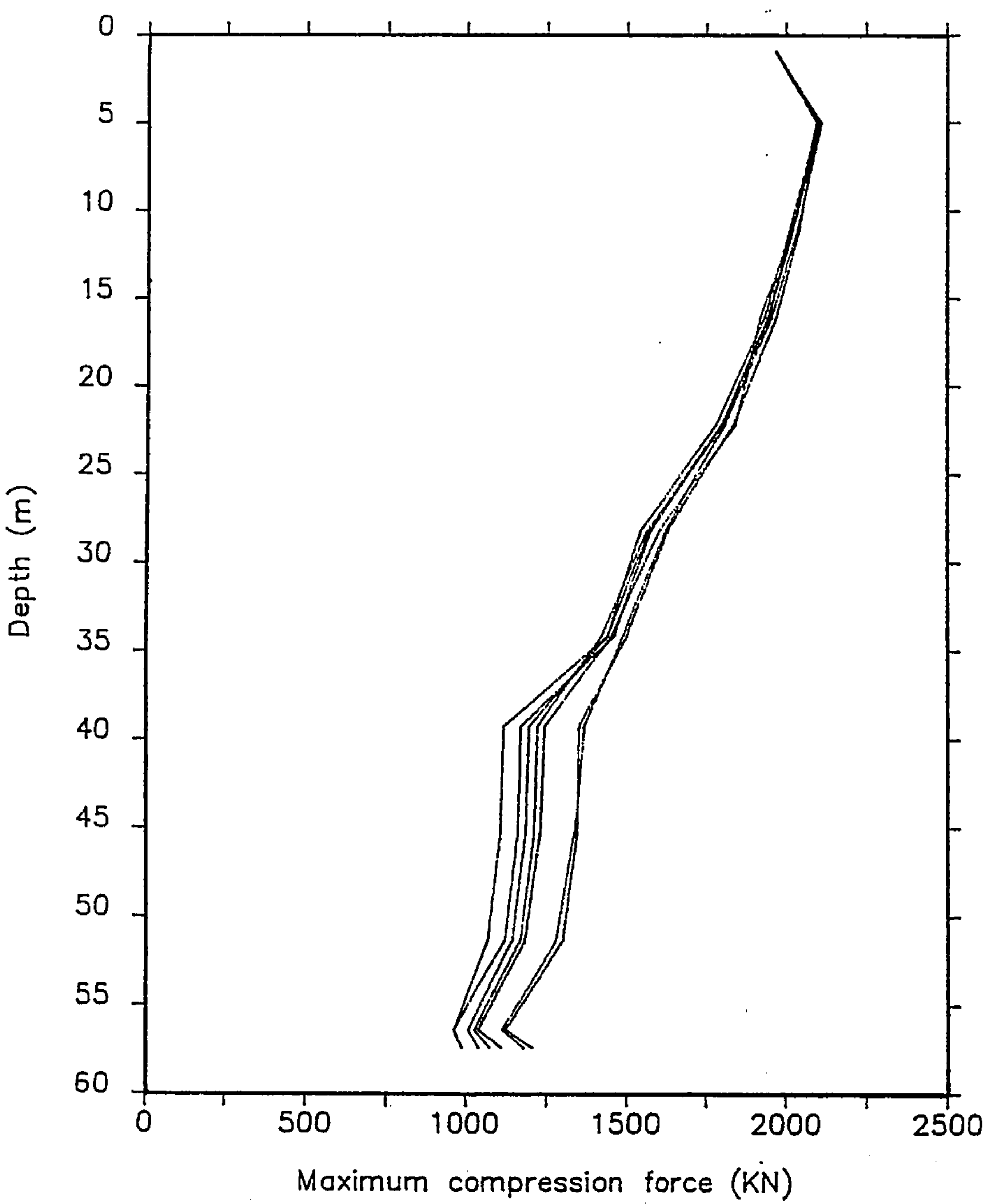

Fig. 6.128 Maximum Compression Forces, AM Pile

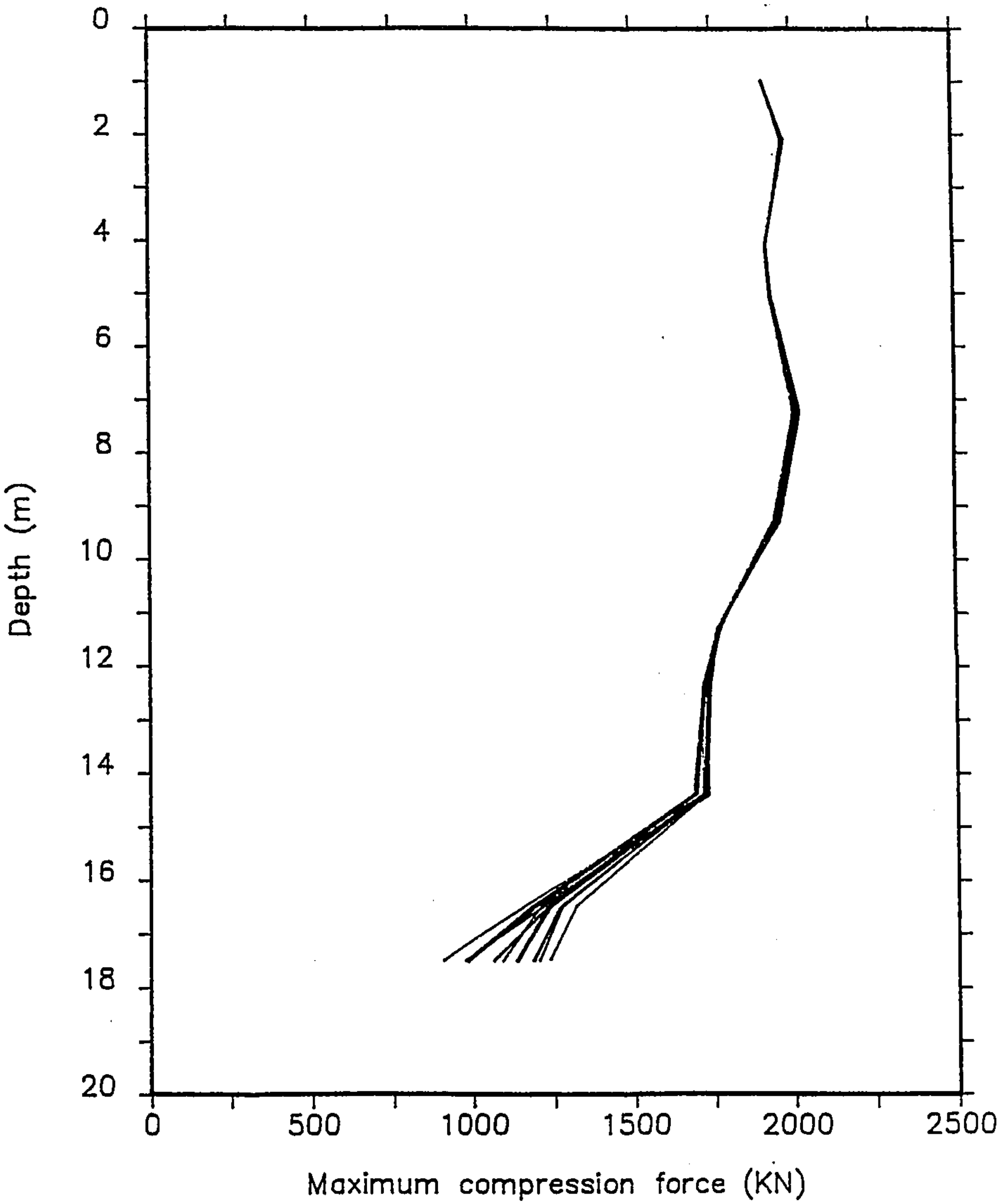

Fig. 6.129 Maximum Compression Forces, LW Pile

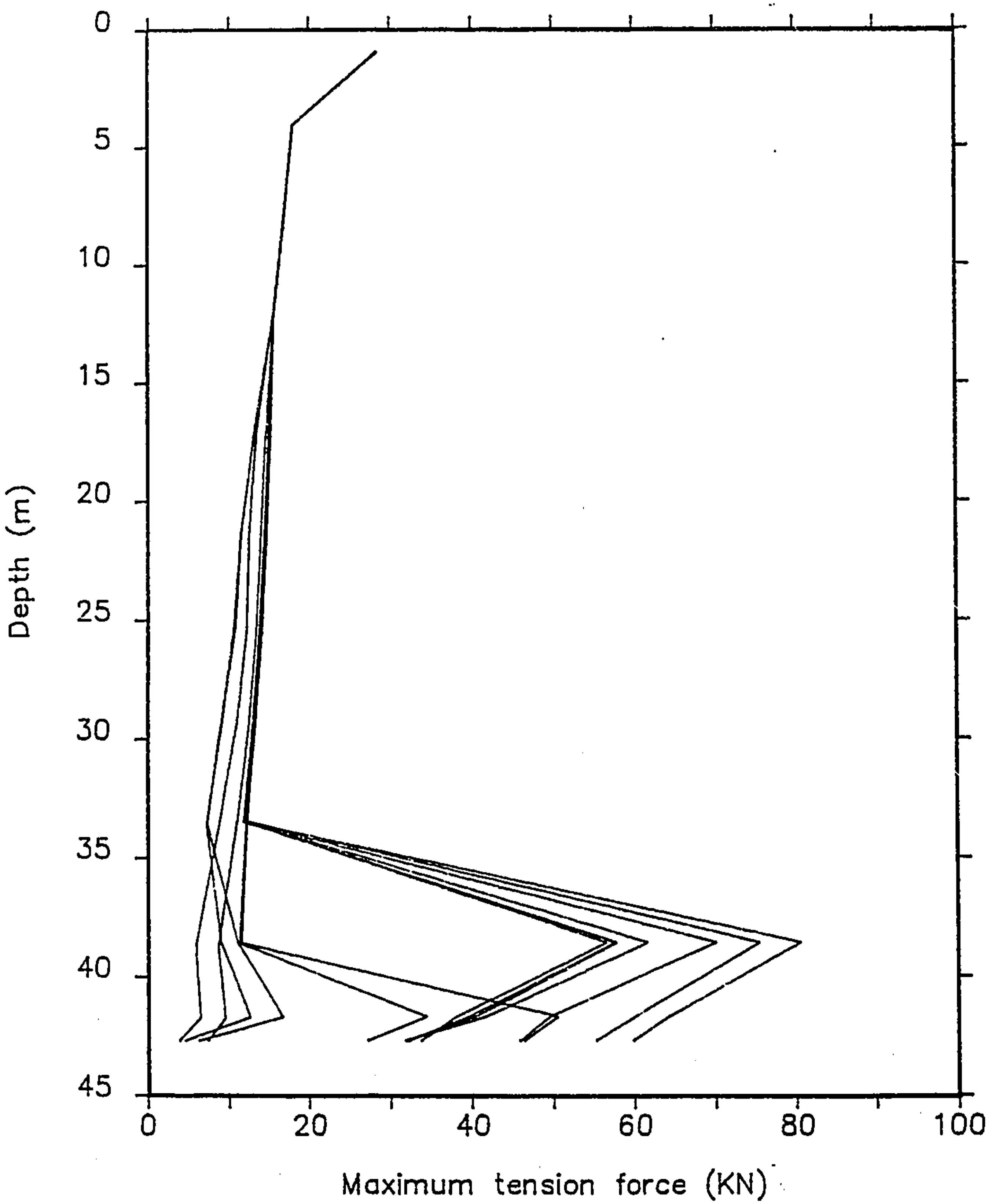

Fig. 6.130 Maximum Tension Forces, JI Pile

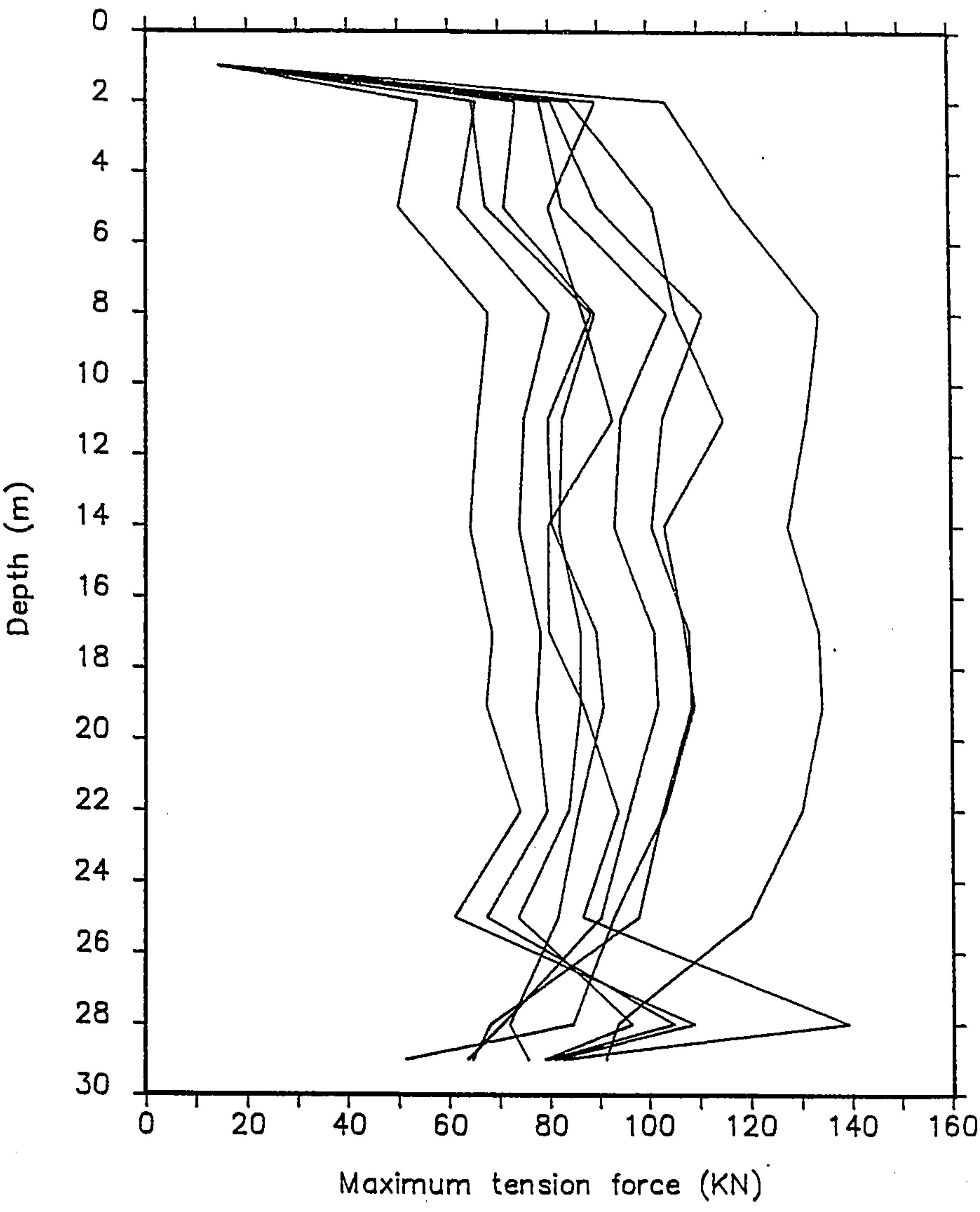

Fig. 6.131 Maximum Tension Forces, JA Pile

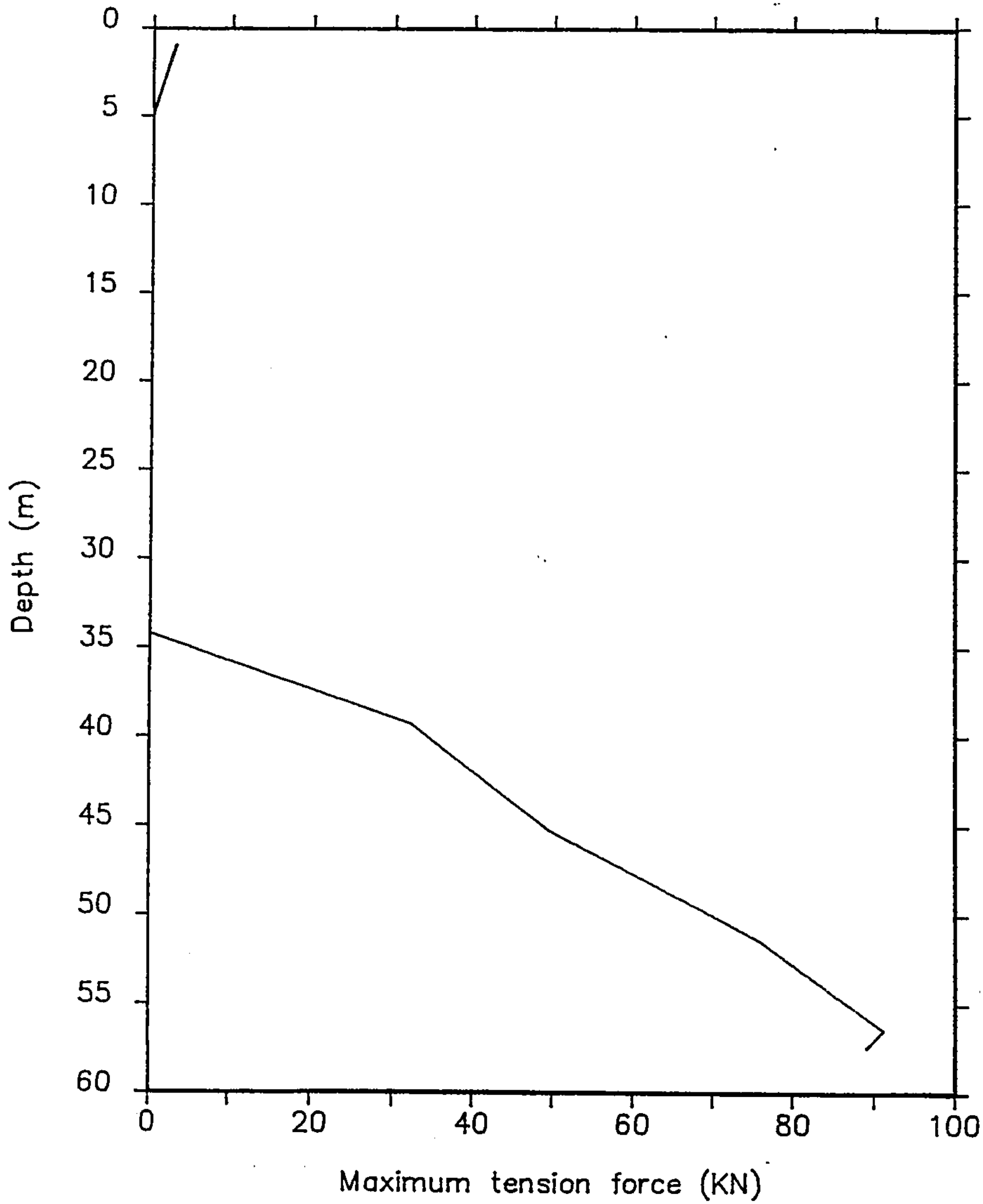

Fig. 6.132 Maximum Tension Forces, AM Pile

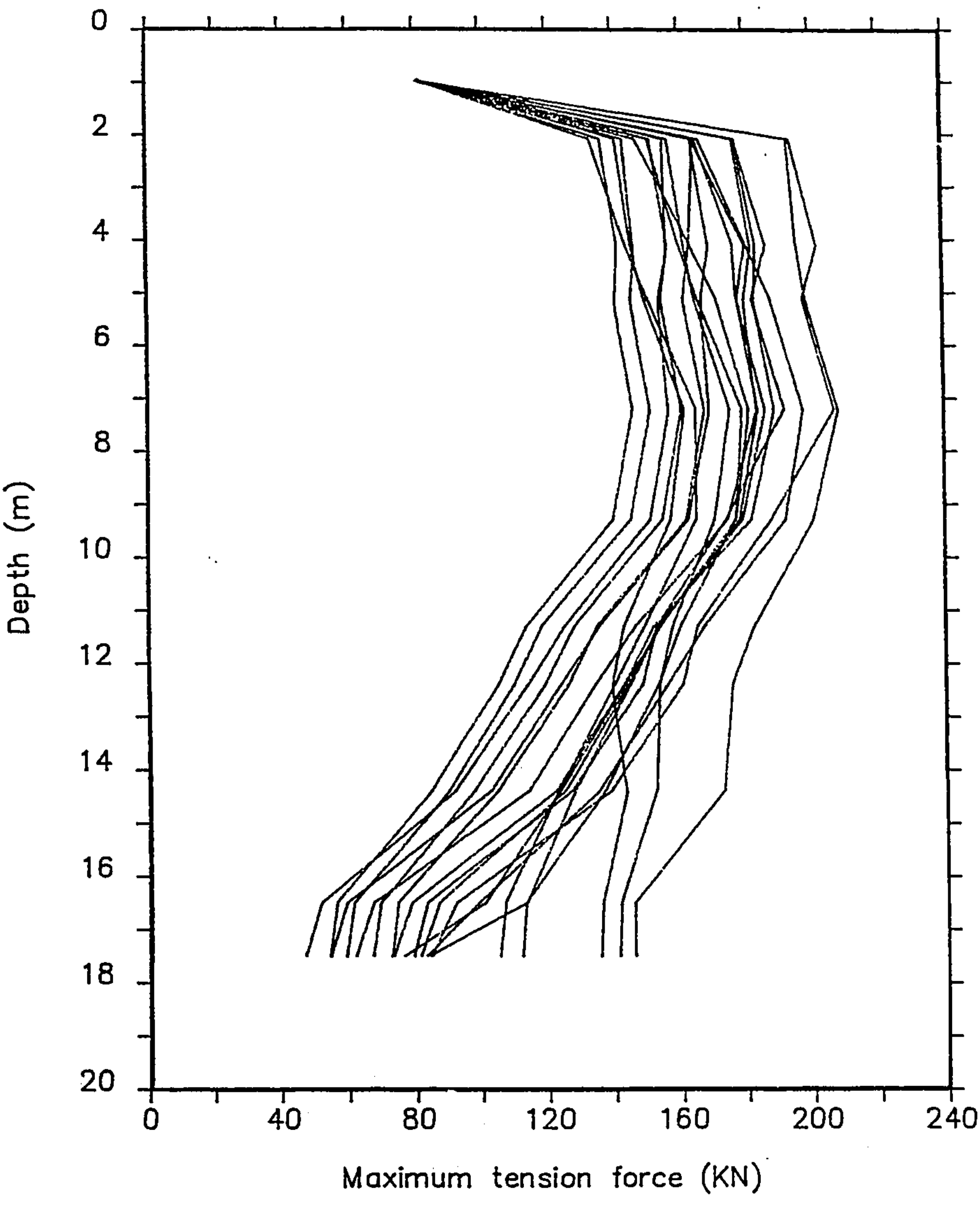

Fig. 6.133 Maximum Tension Forces, LW Pile

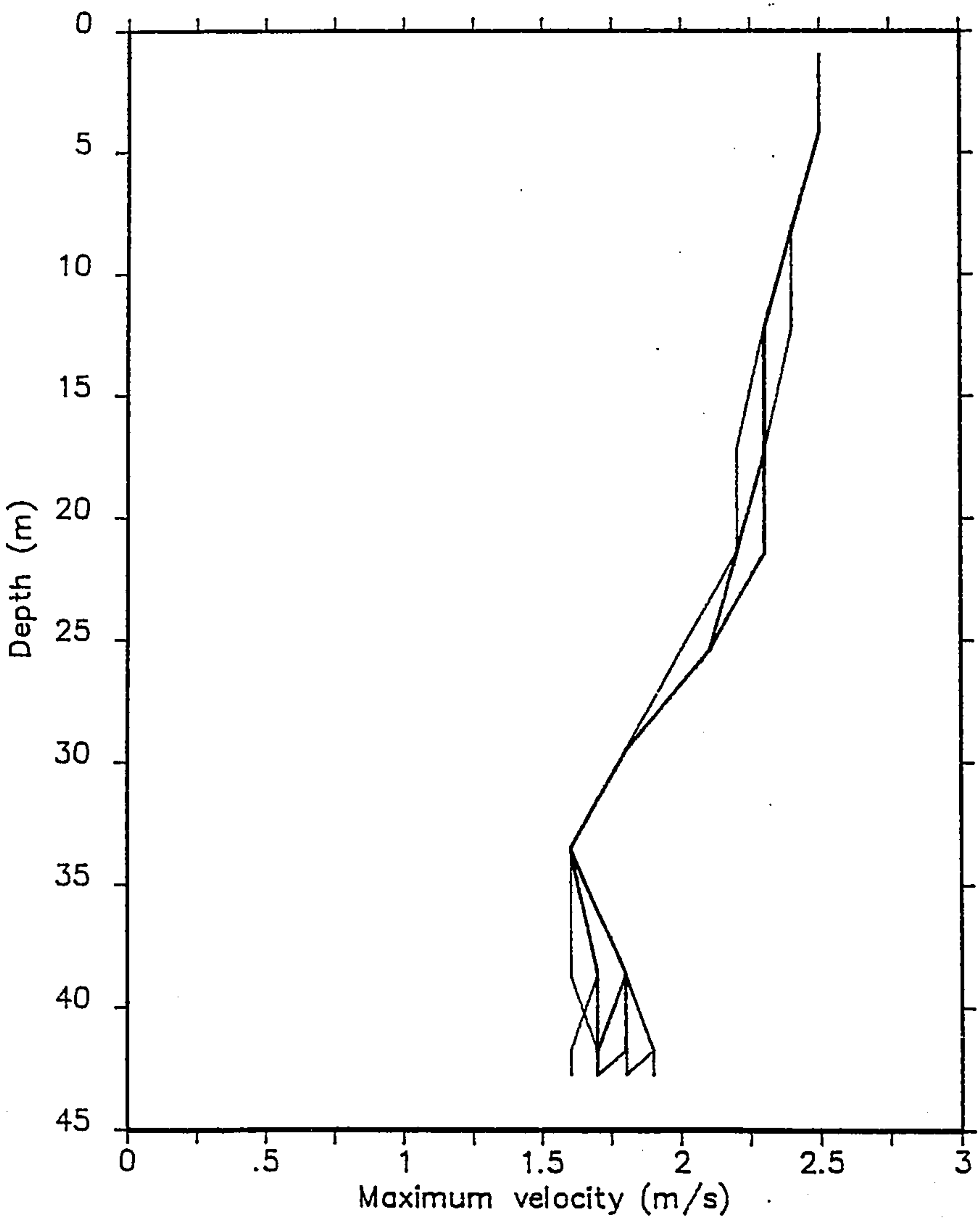

Fig. 6.134 Maximum Element Velocities, JI Pile

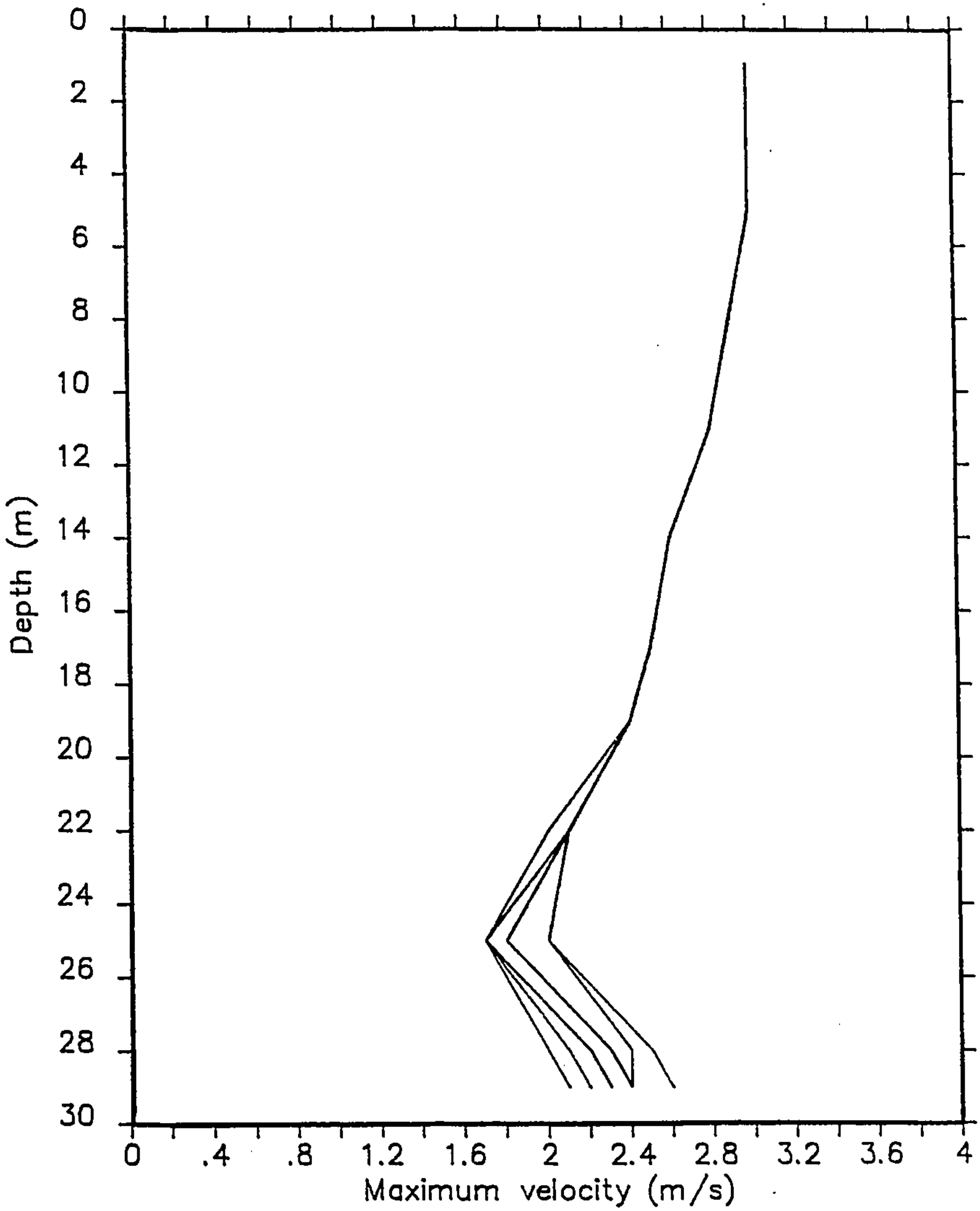

Fig. 6.135 Maximum Element Velocities, JA Pile

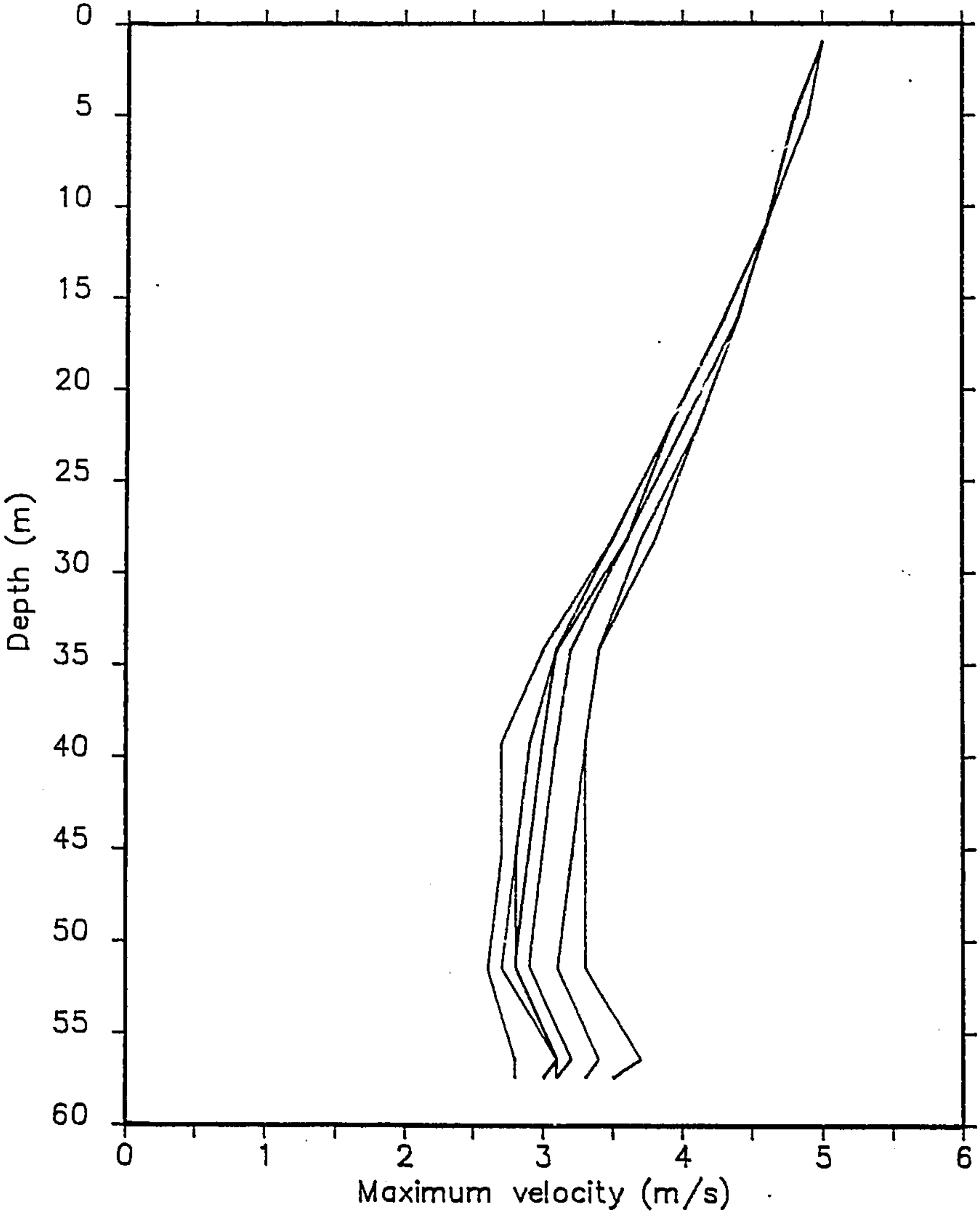

Fig. 6.136 Maximum Element Velocities, AM Pile

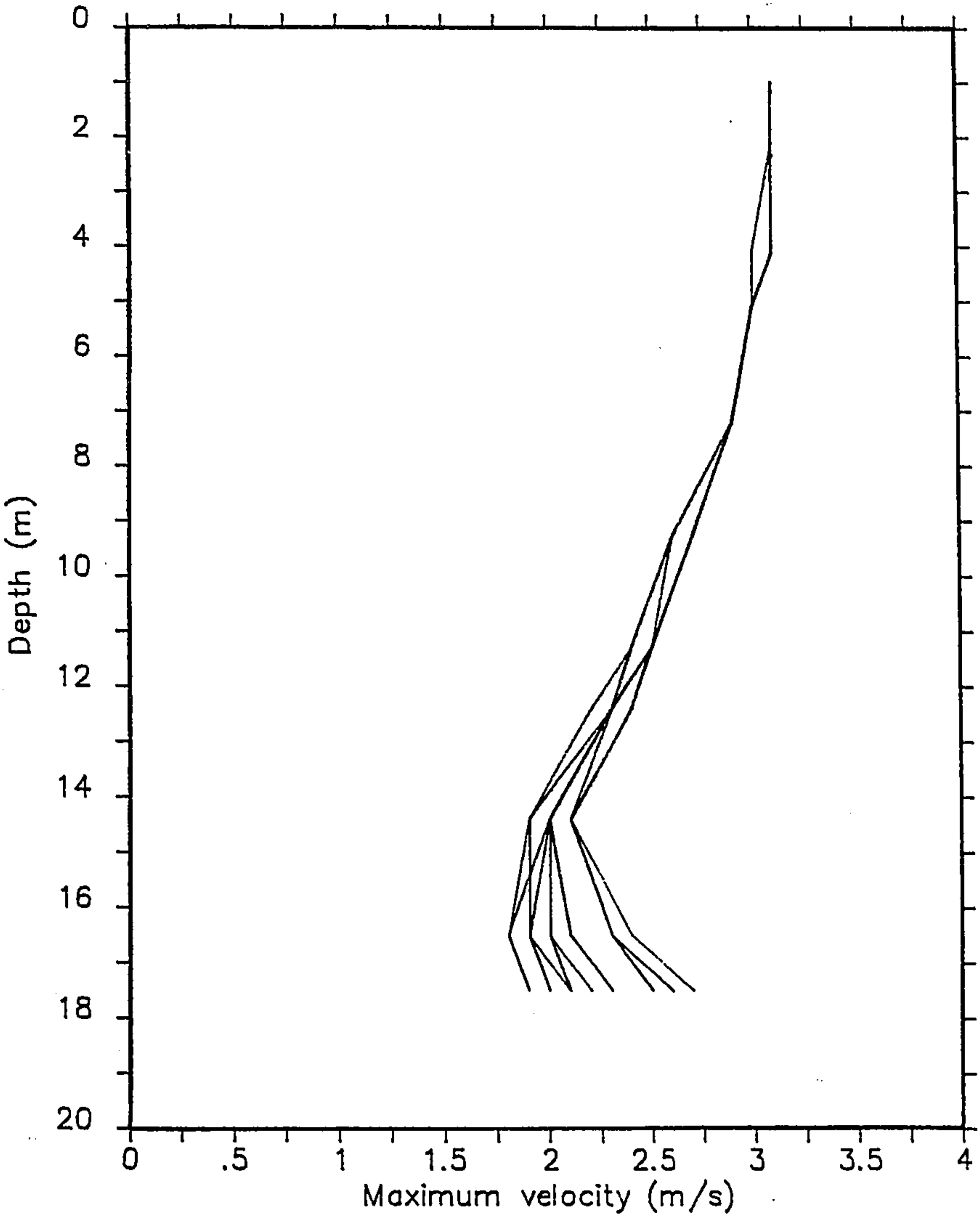

Fig. 6.137 Maximum Element Velocities, LW Pile

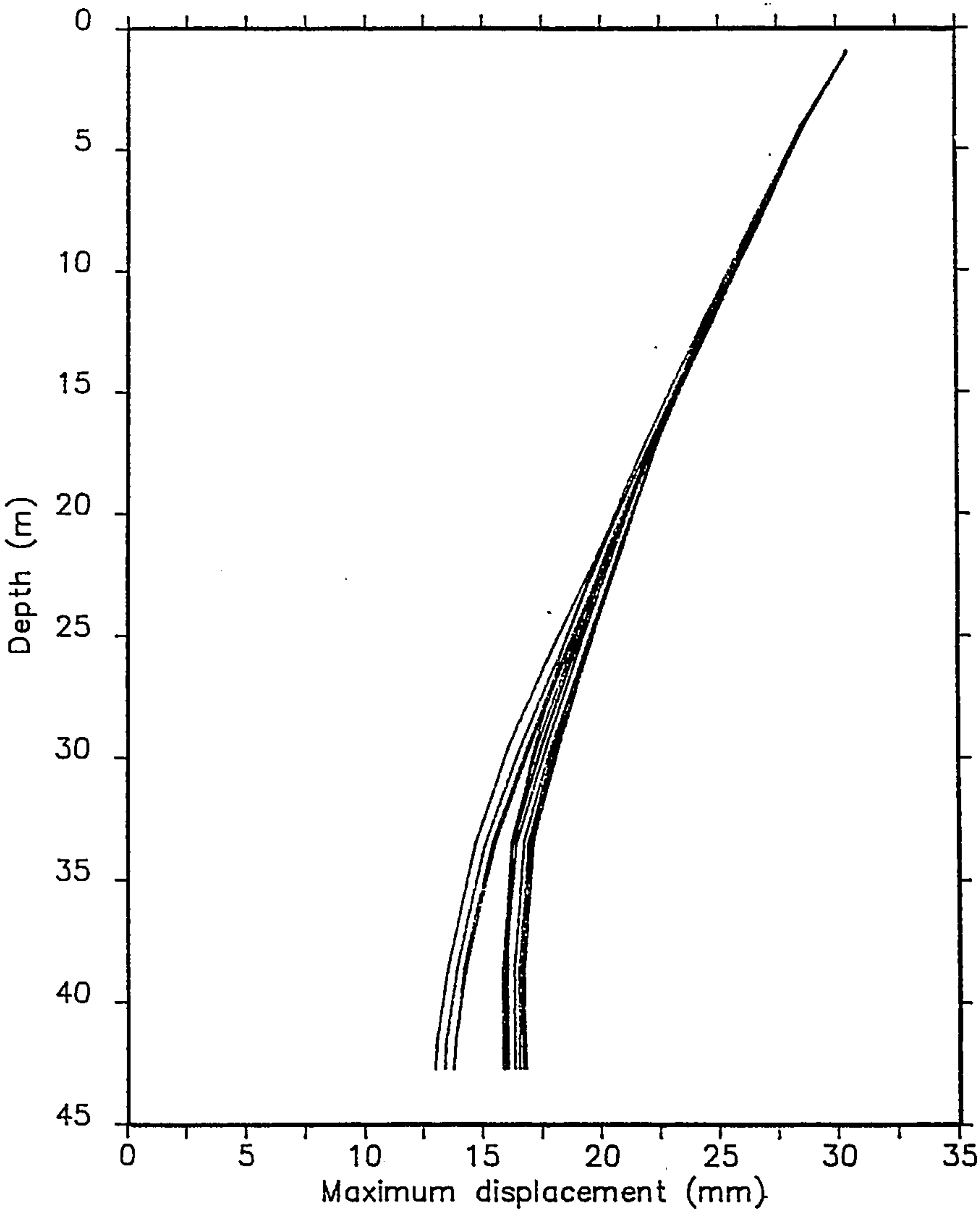

Fig. 6.138 Maximum Element Displacements, JI Pile

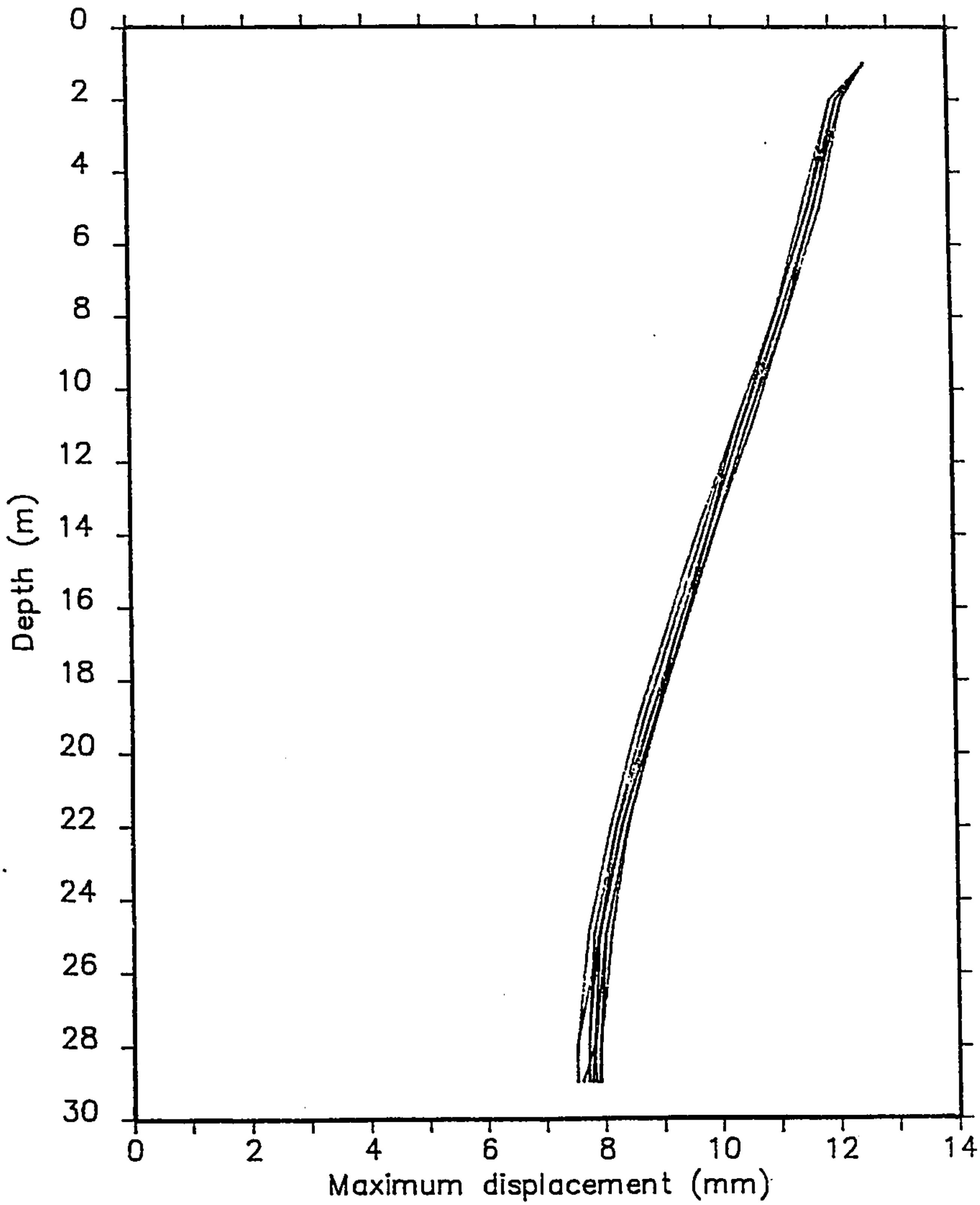

Fig. 6.139 Maximum Element Displacements, JA Pile

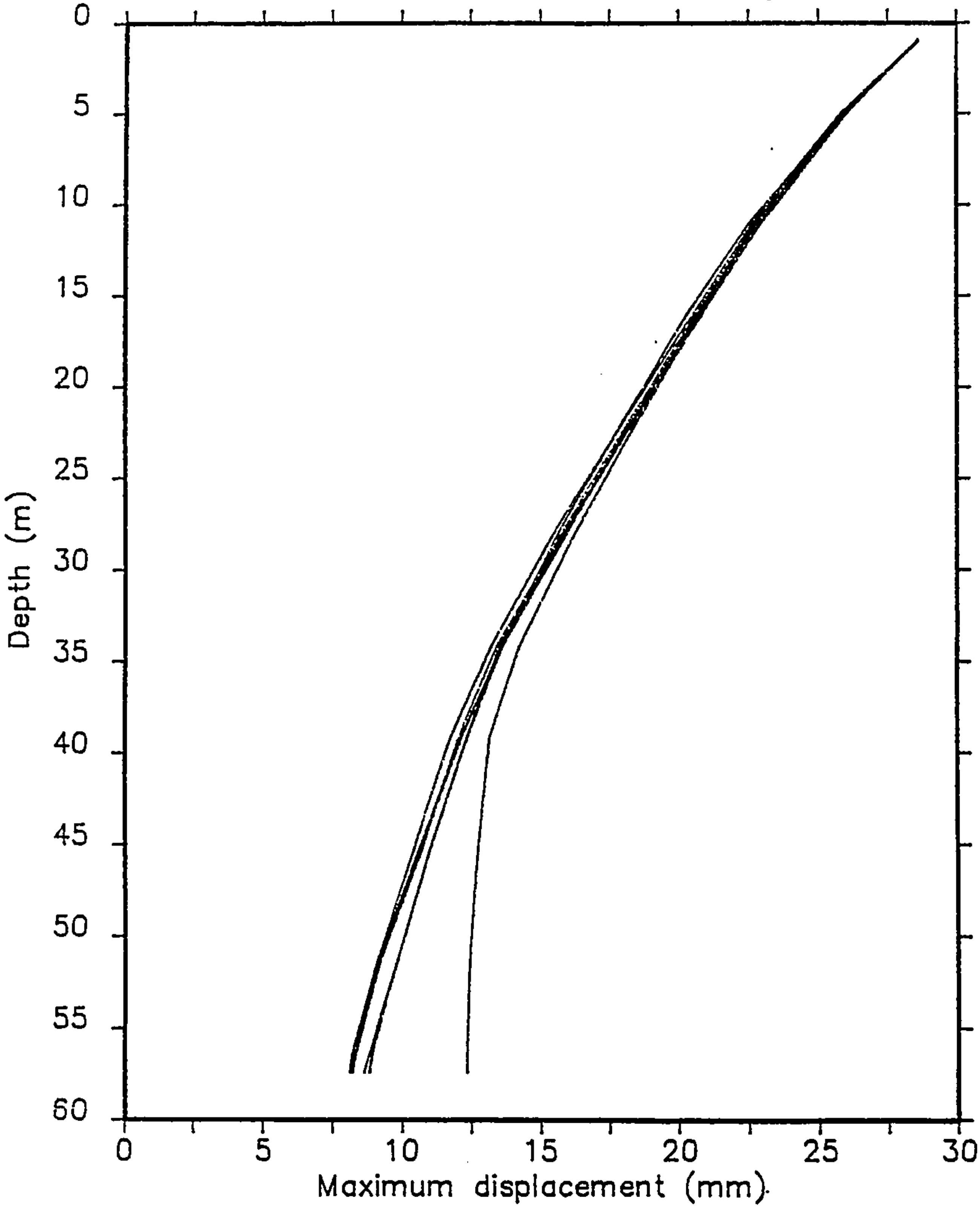

Fig. 6.140 Maximum Element Displacements, AM Pile

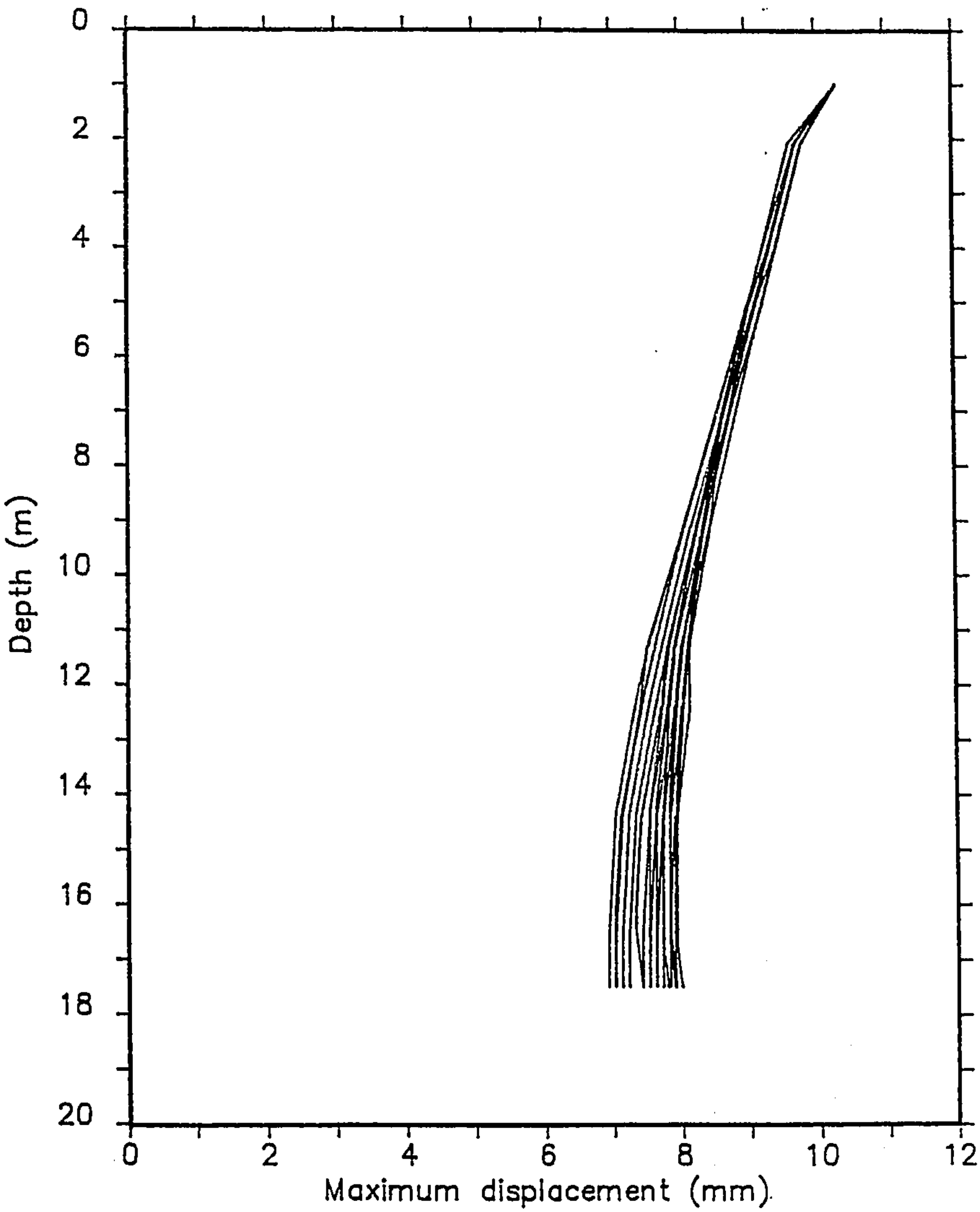

Fig. 6.141 Maximum Element Displacements, LW Pile

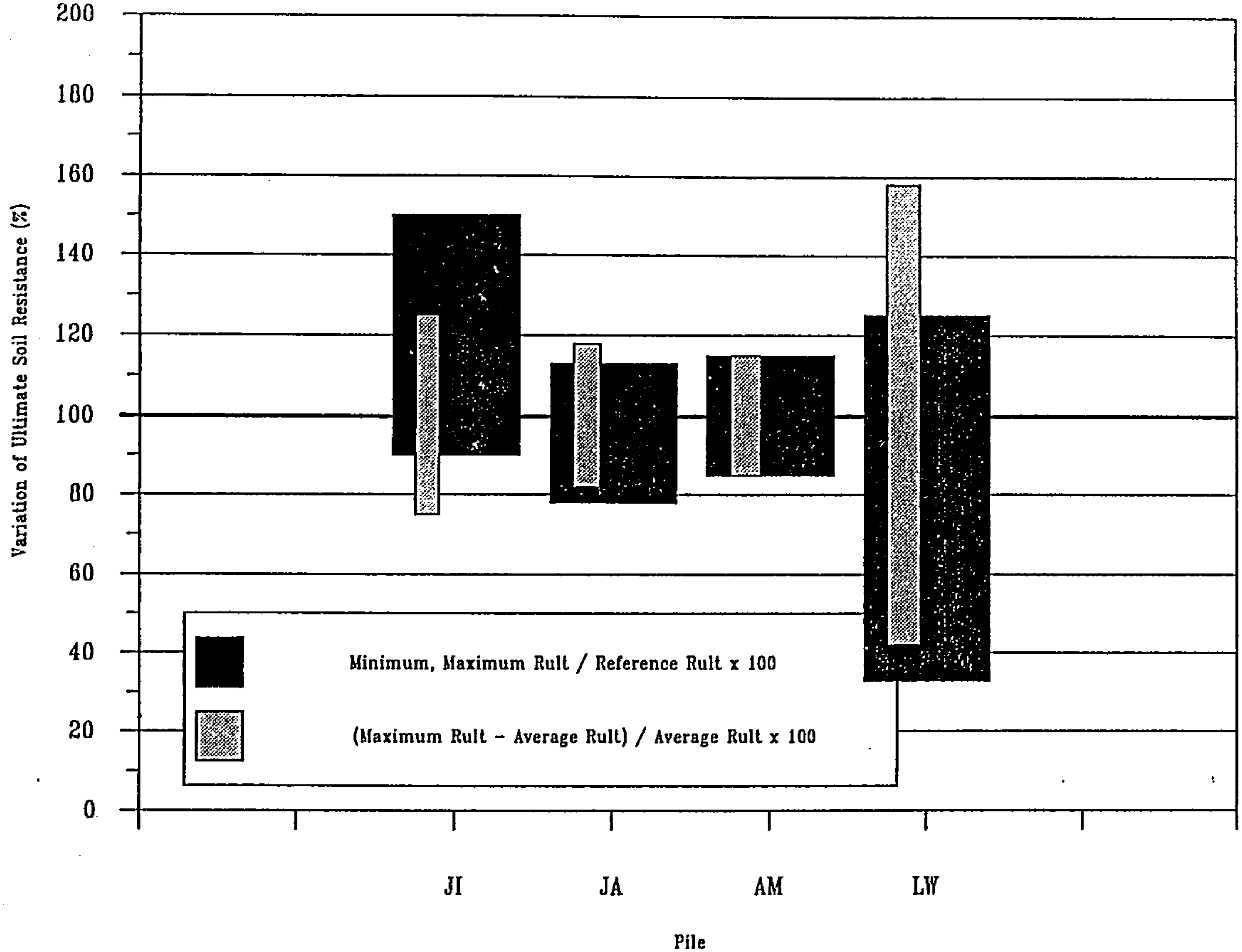

Fig. 7.1 Variation of Ultimate Soil Resistance

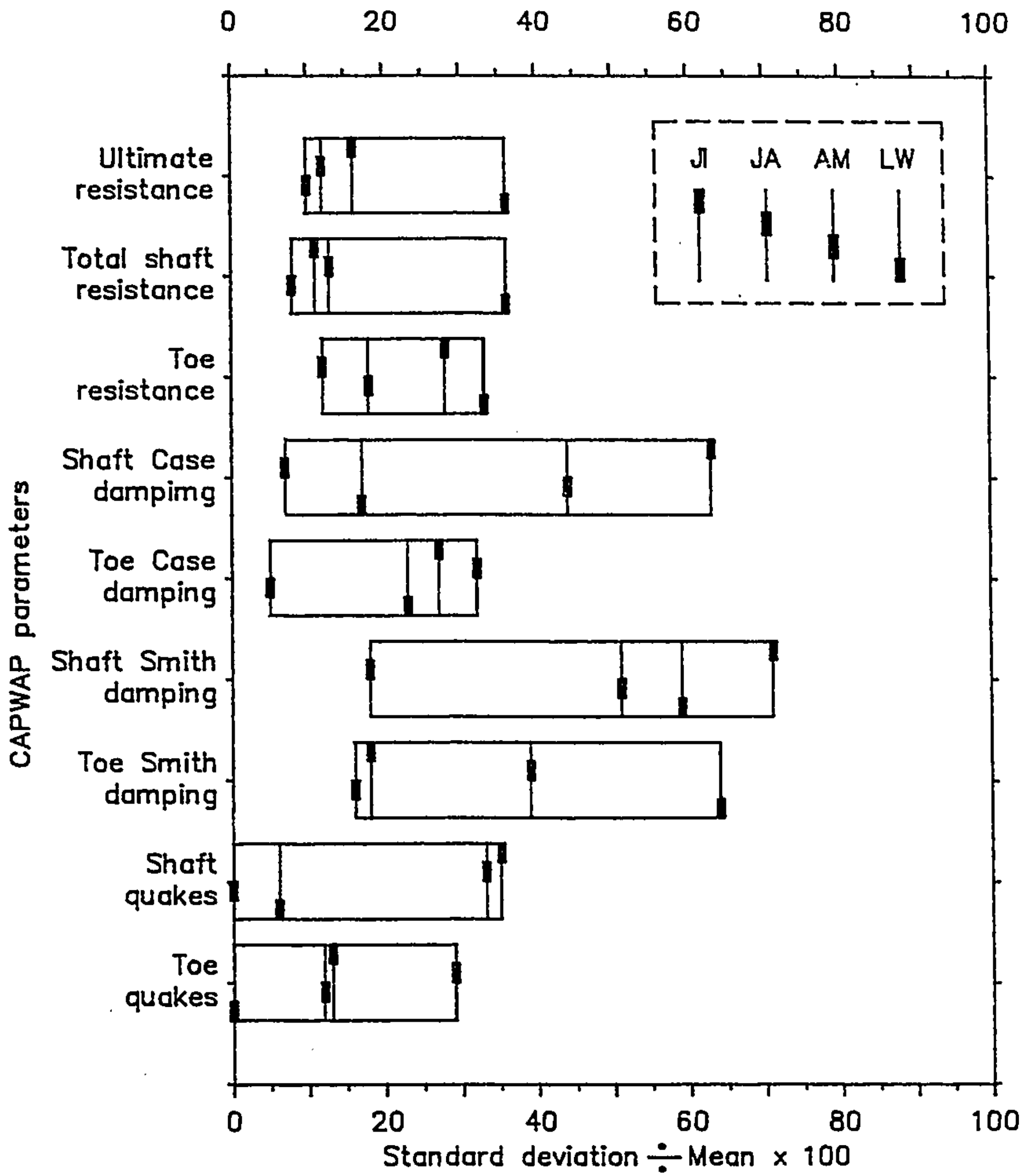

Fig. 7.2 Coefficient of Variation for Basic CAPWAP Parameters

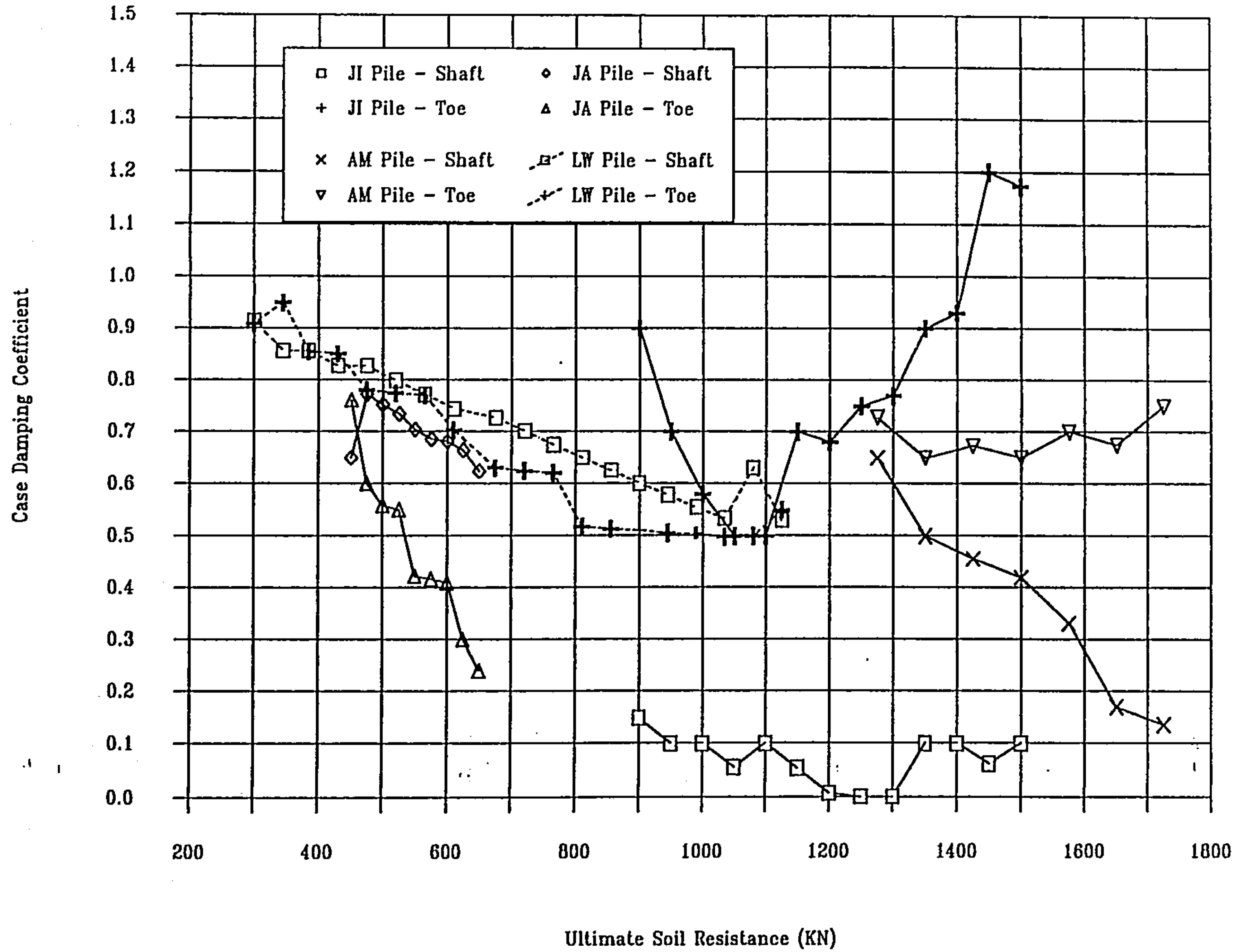

Fig. 7.3 Variation of Case Damping

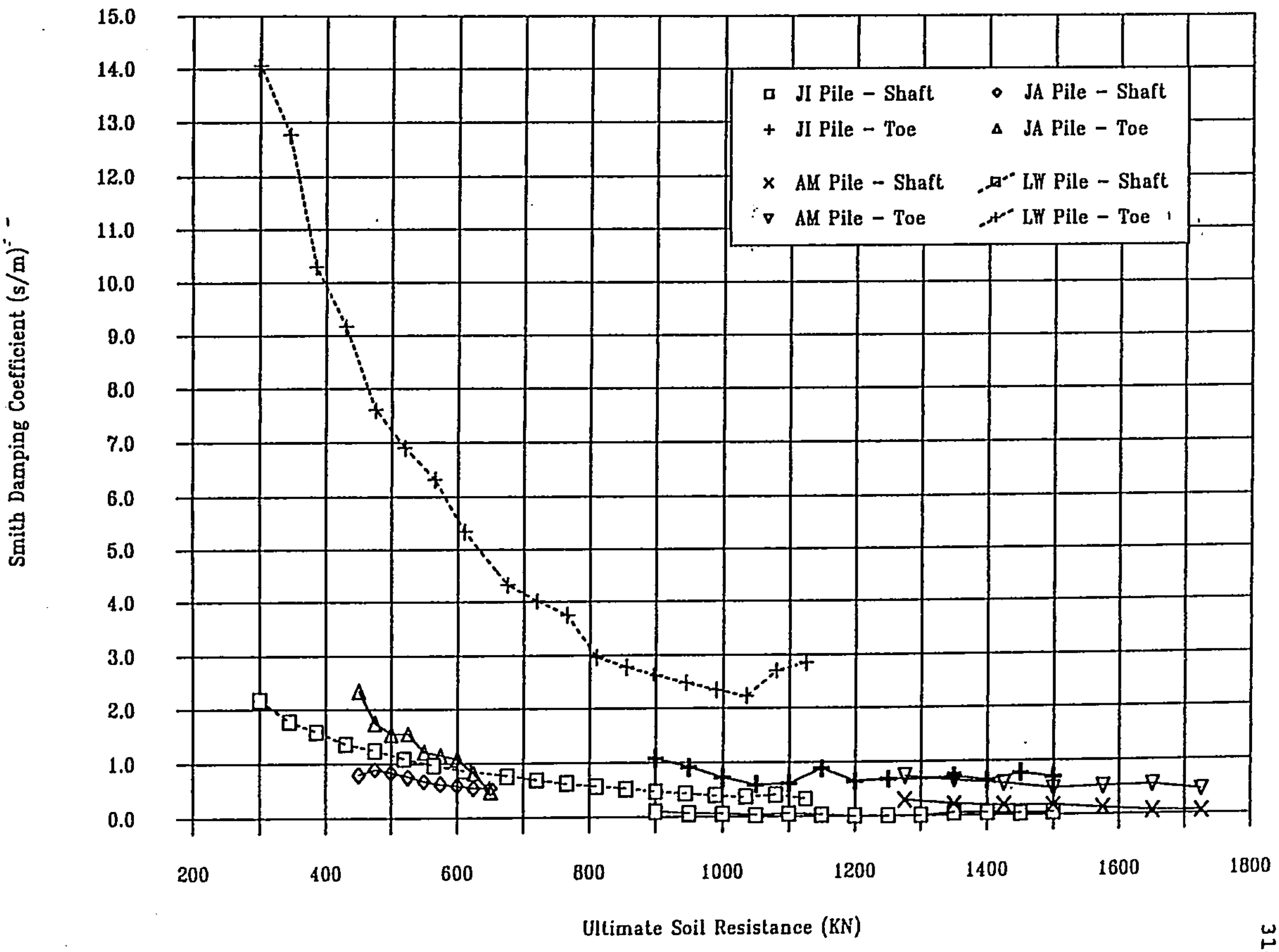

Fig. 7.4 Variation of Smith Damping

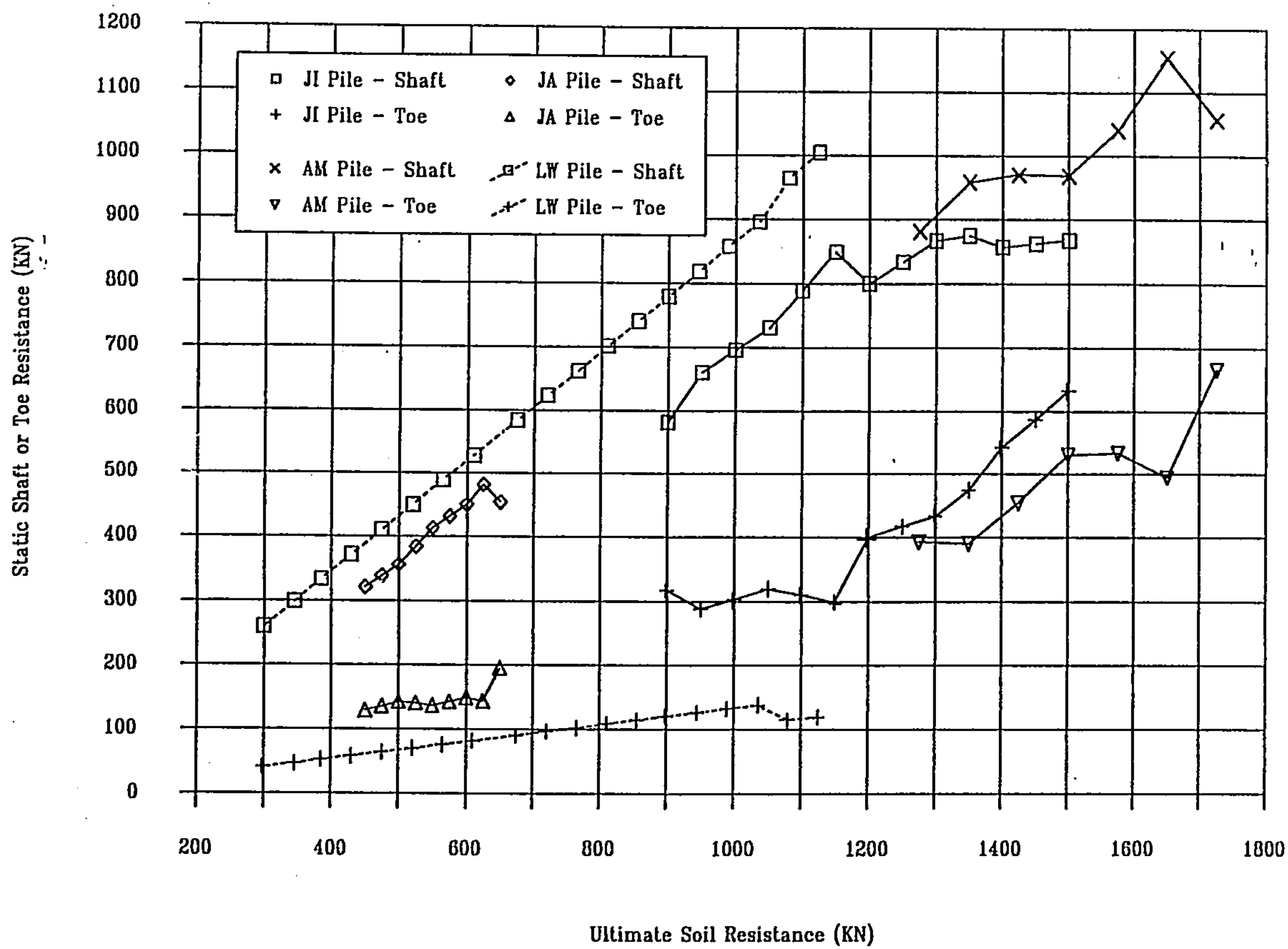

Fig. 7.5 Variation of Static Shaft and Toe Resistance

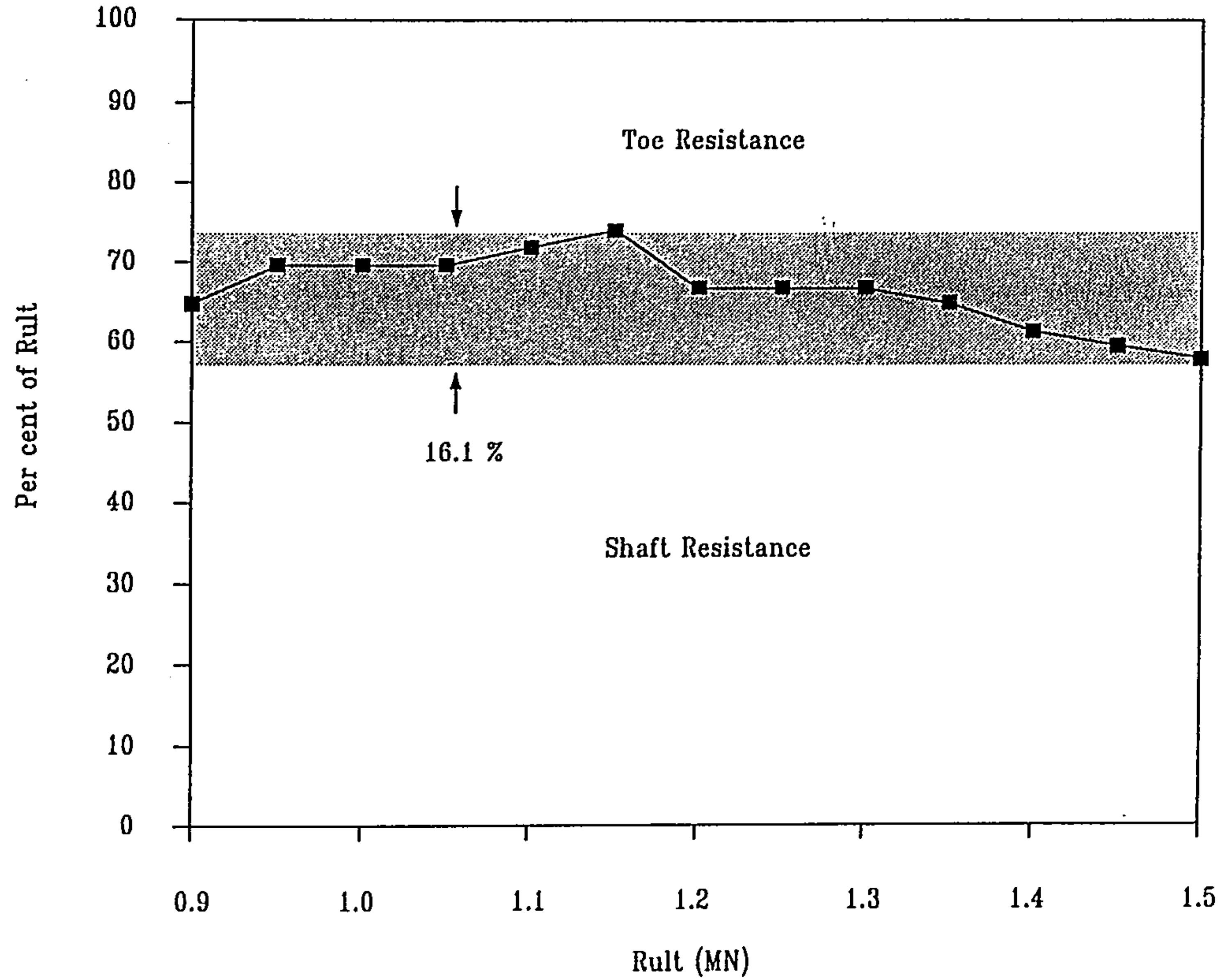

Fig. 7.6 Relative Variation of Static Resistance, JI Pile

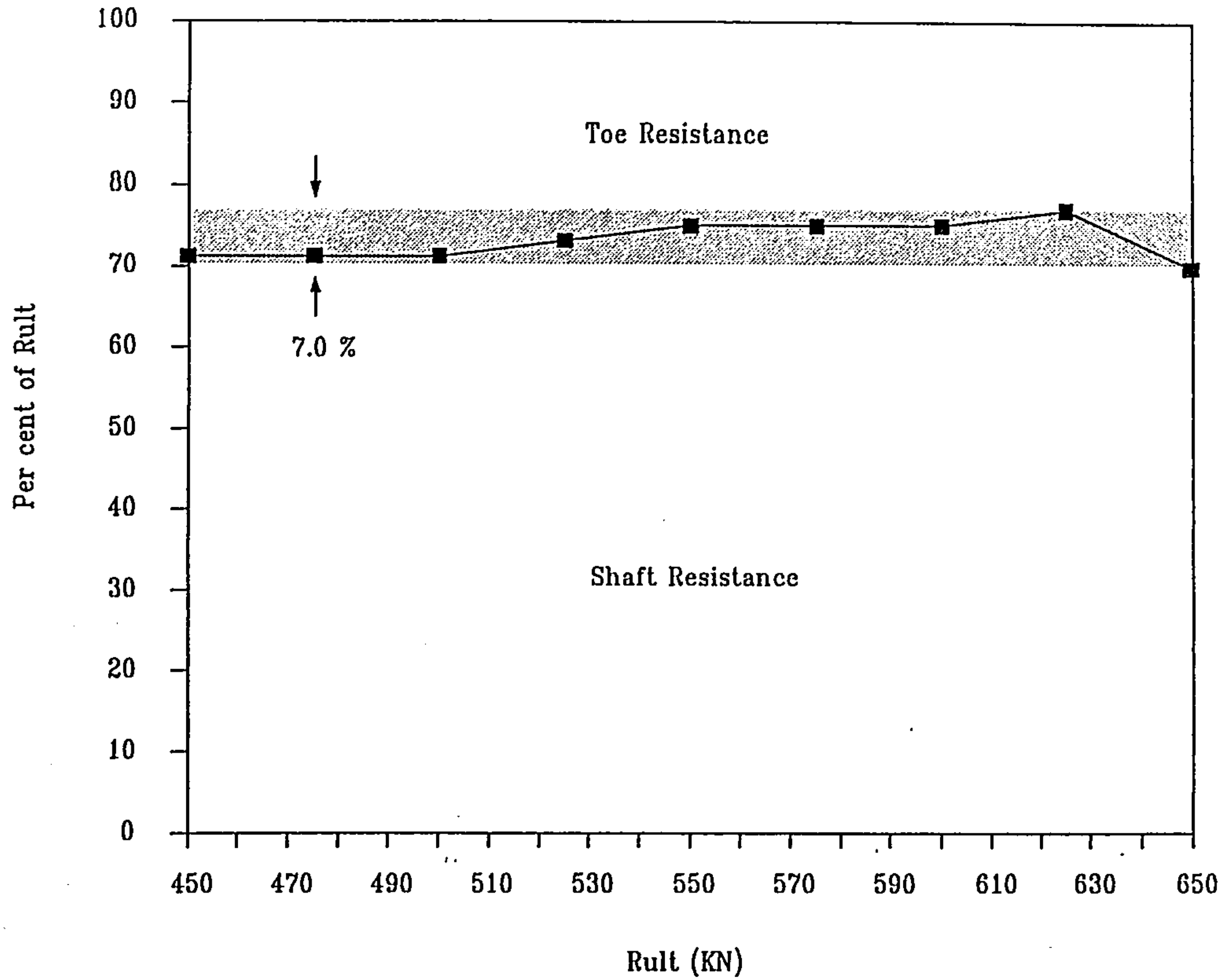

Fig. 7.7 Relative Variation of Static Resistance, JA Pile

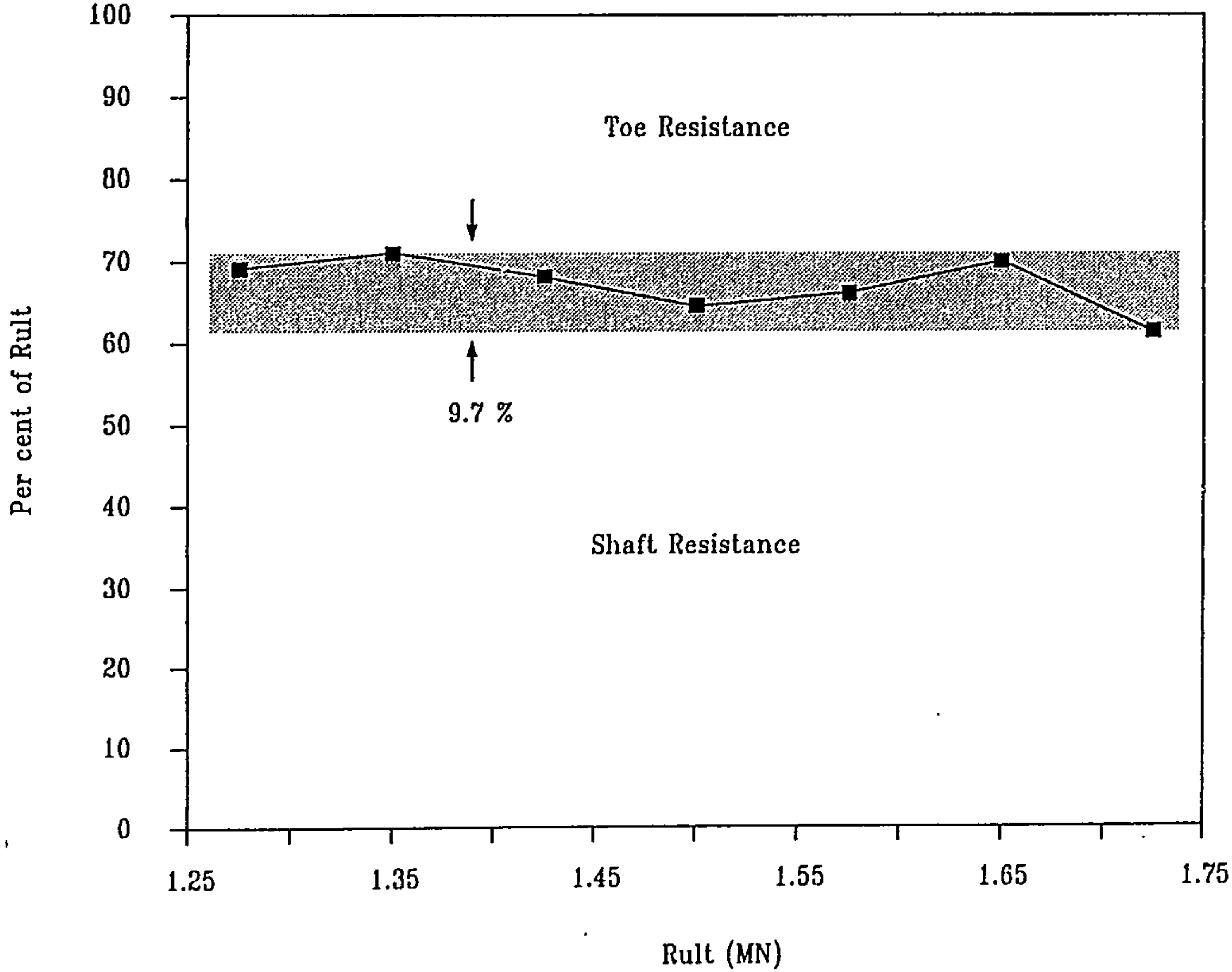

Fig. 7.8 Relative Variation of Static Resistance, AM Pile

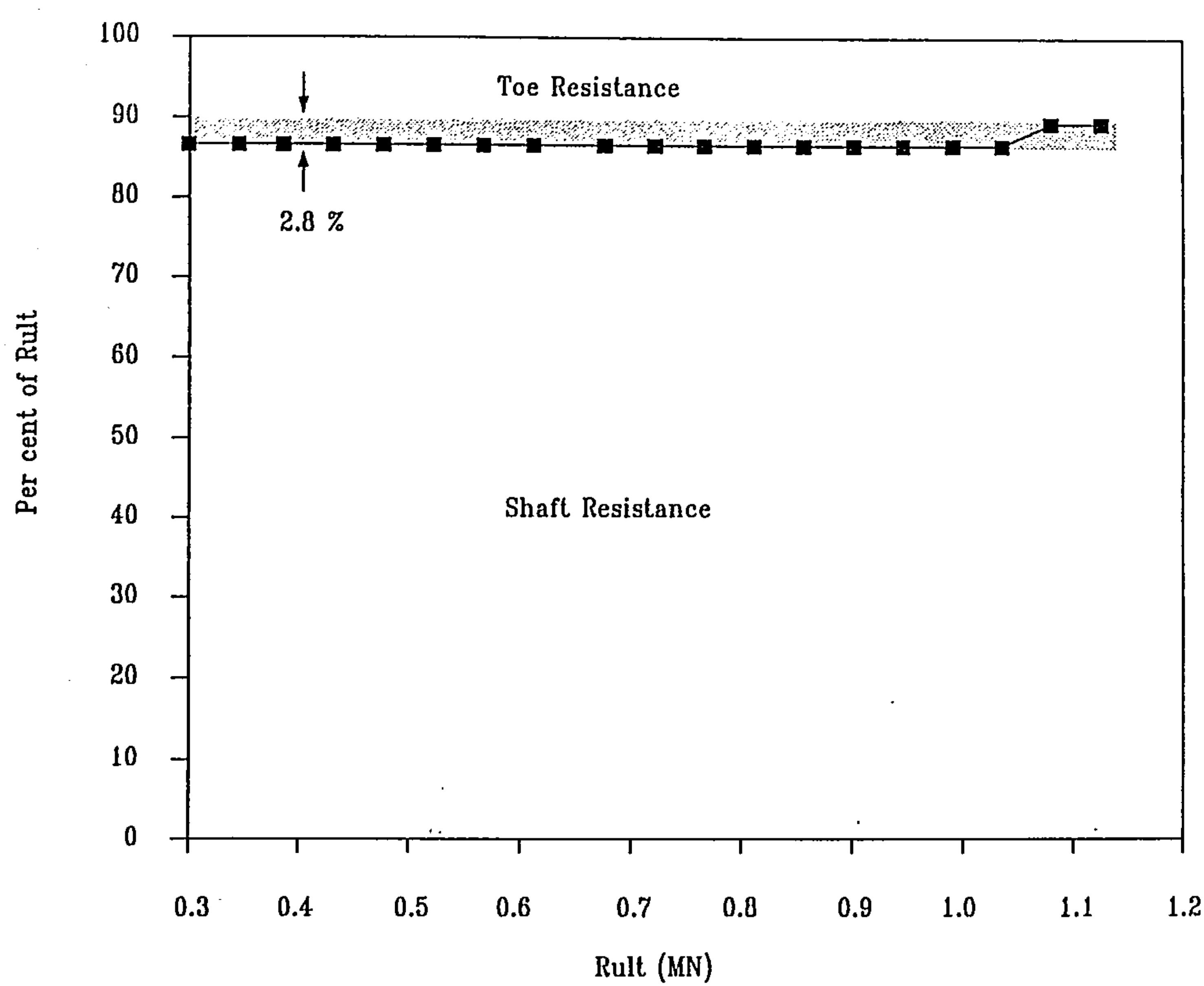

Fig. 7.9 Relative Variation of Static Resistance, LW Pile

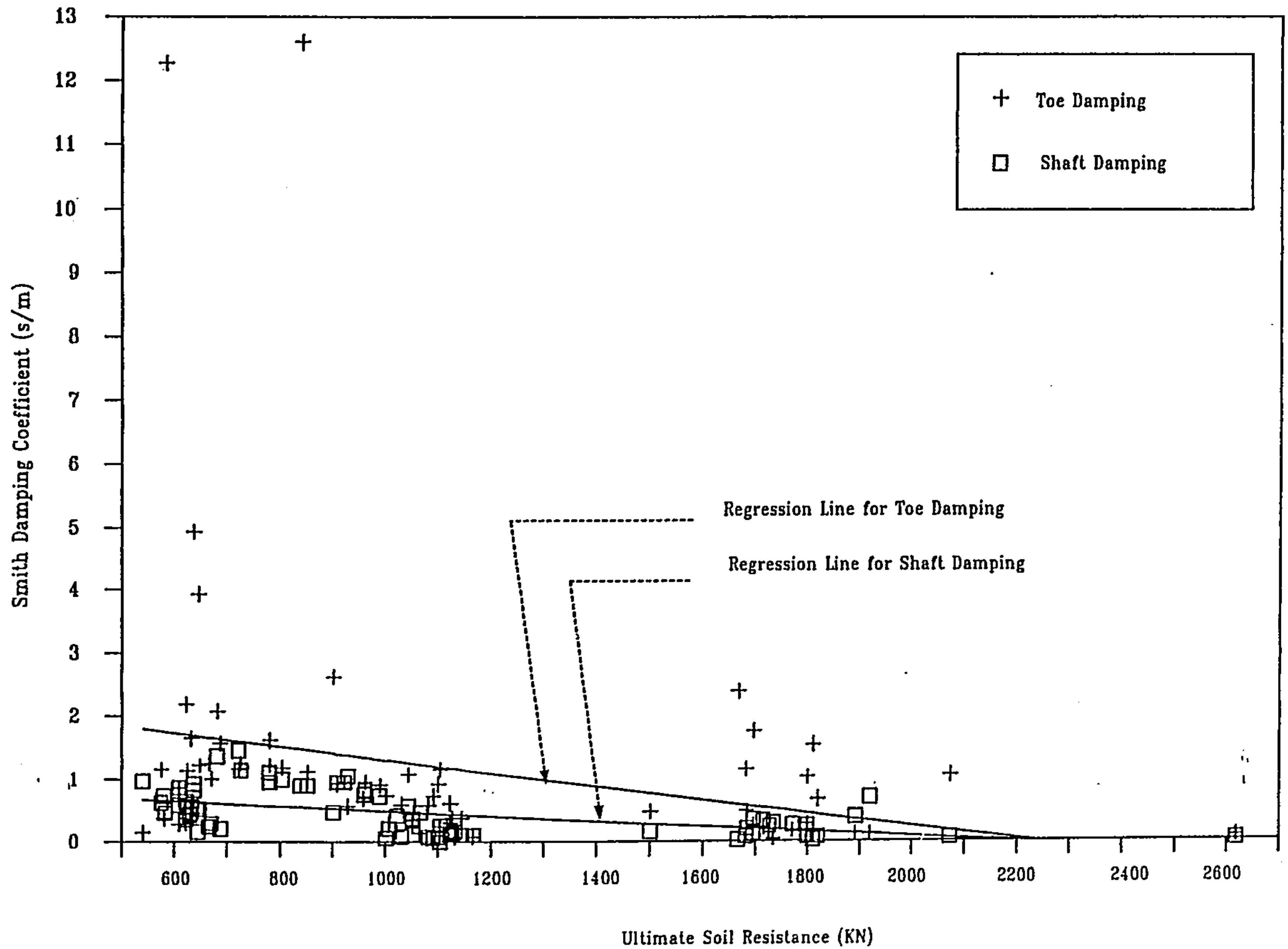

Fig. 7.10 Variation of Smith Damping as a Function of Rult

(Data After Fellenius, 1988)

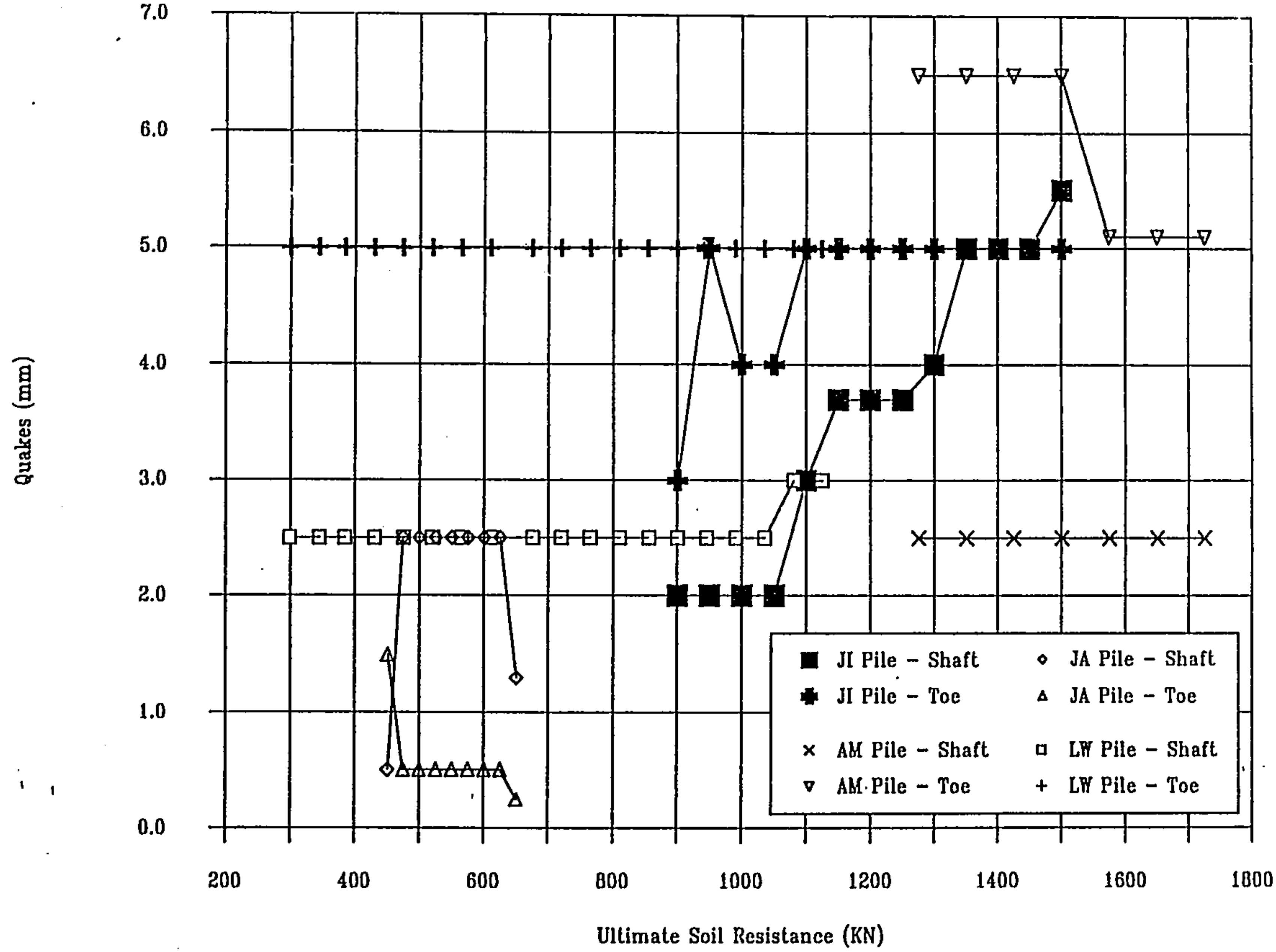

Fig. 7.11 Variation of Quakes

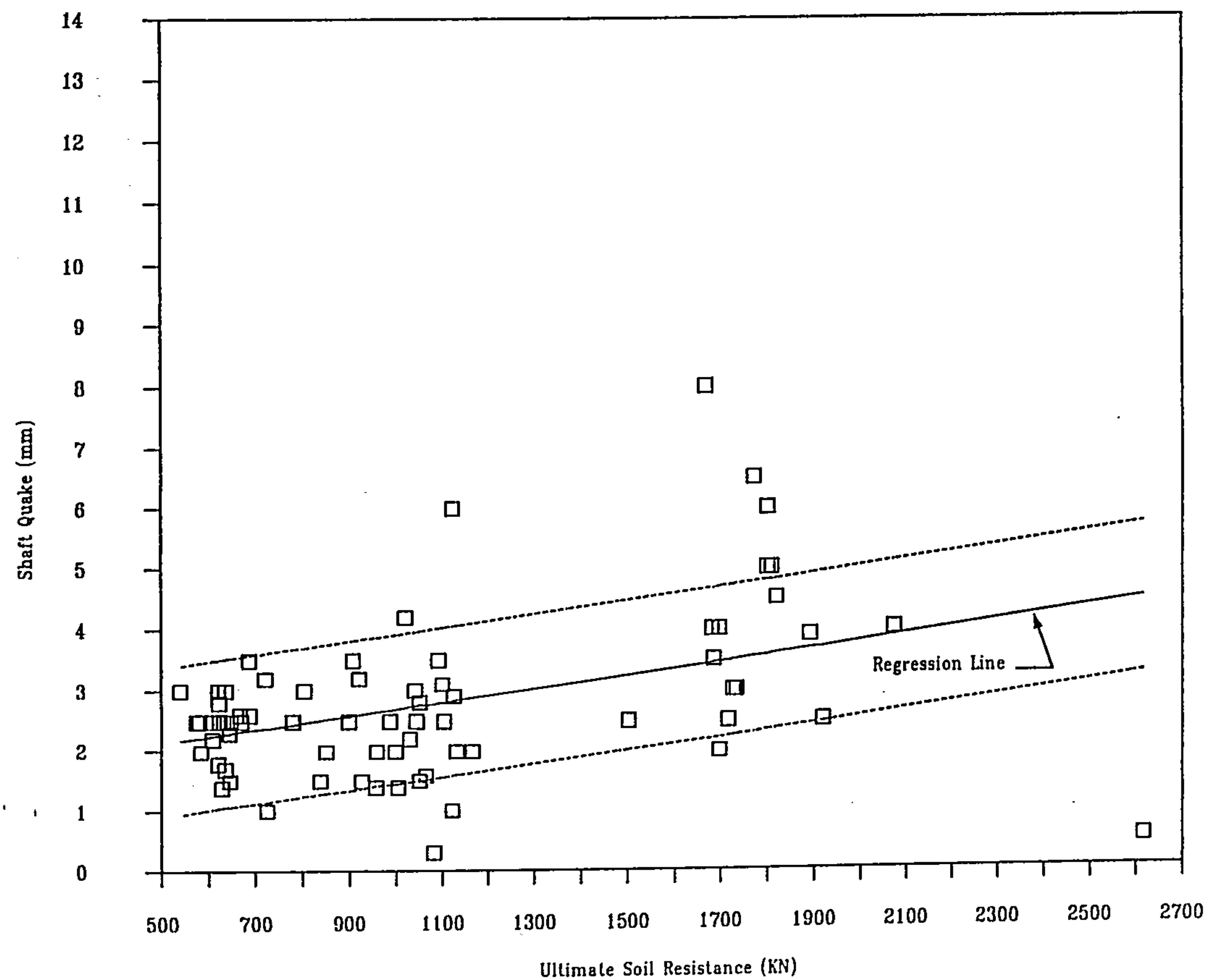

Fig. 7.12 Shaft Quakes as a Function of Rult
(Data After Fellenius, 1988)

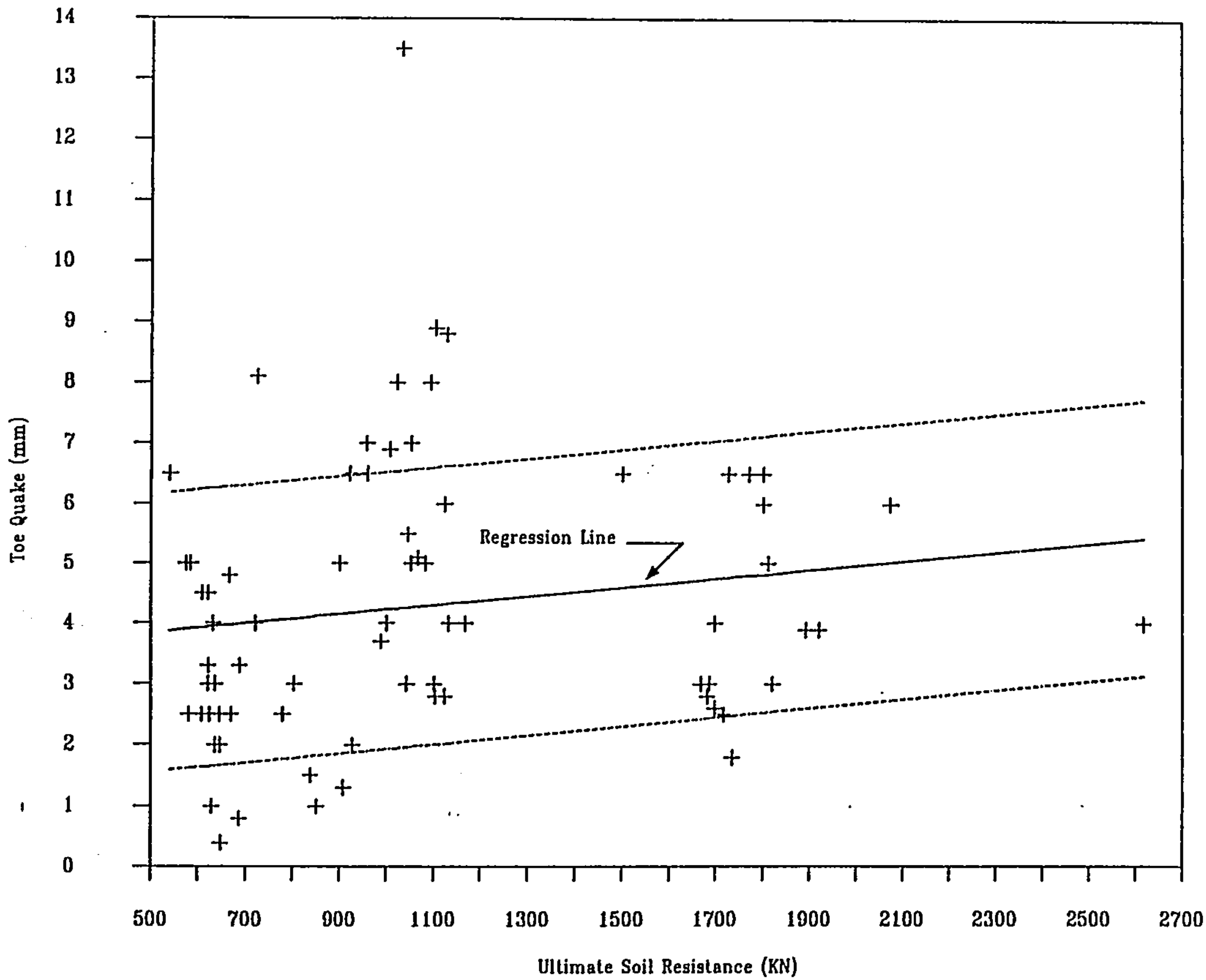

Fig. 7.13 Toe Quakes as a Function of Rult

(Data After Fellenius, 1988)

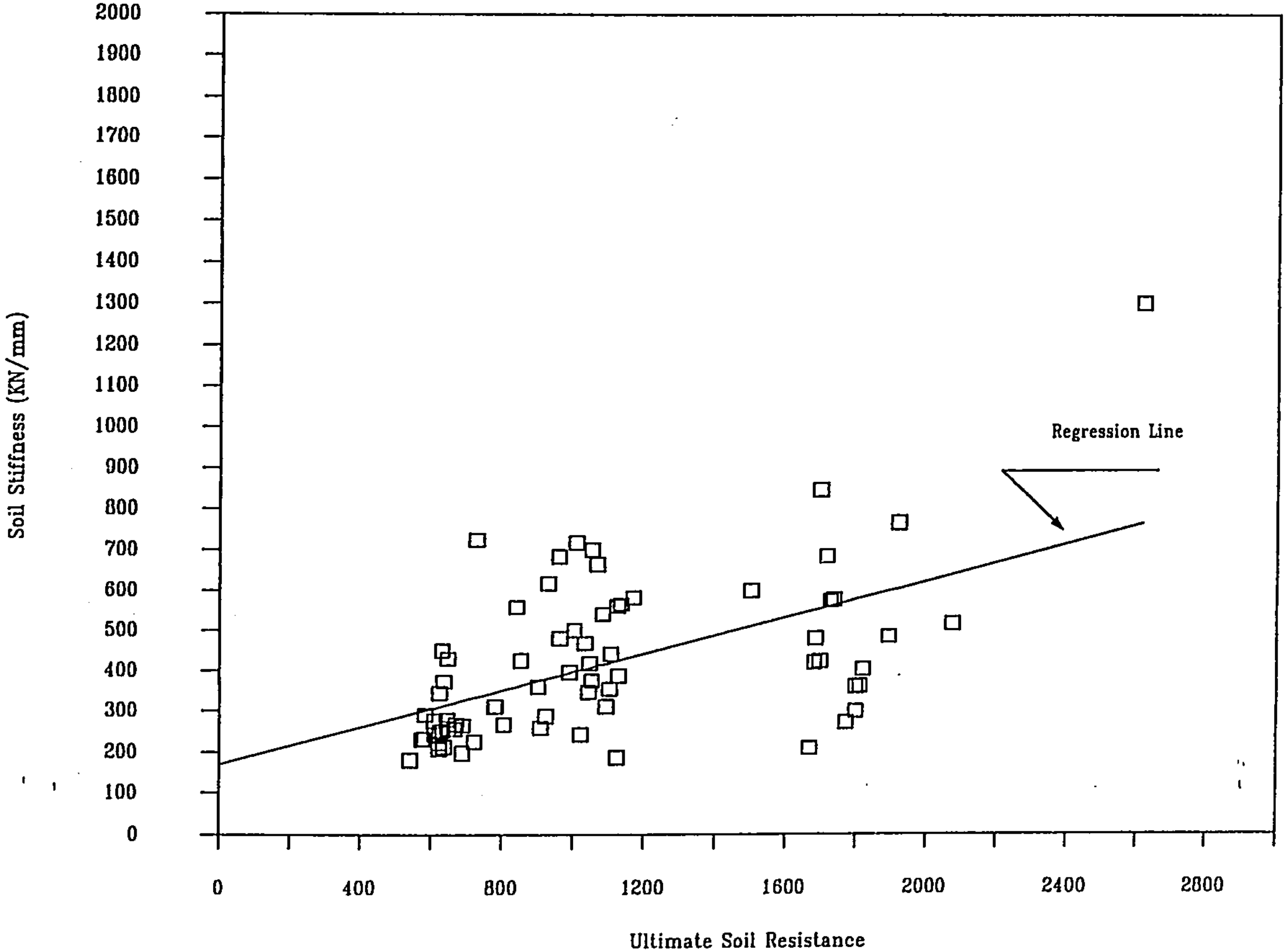

Fig. 7.14 Computed Soil Stiffness as a Function of Ultimate Soil Resistance (Data After Fellenius, 1988)

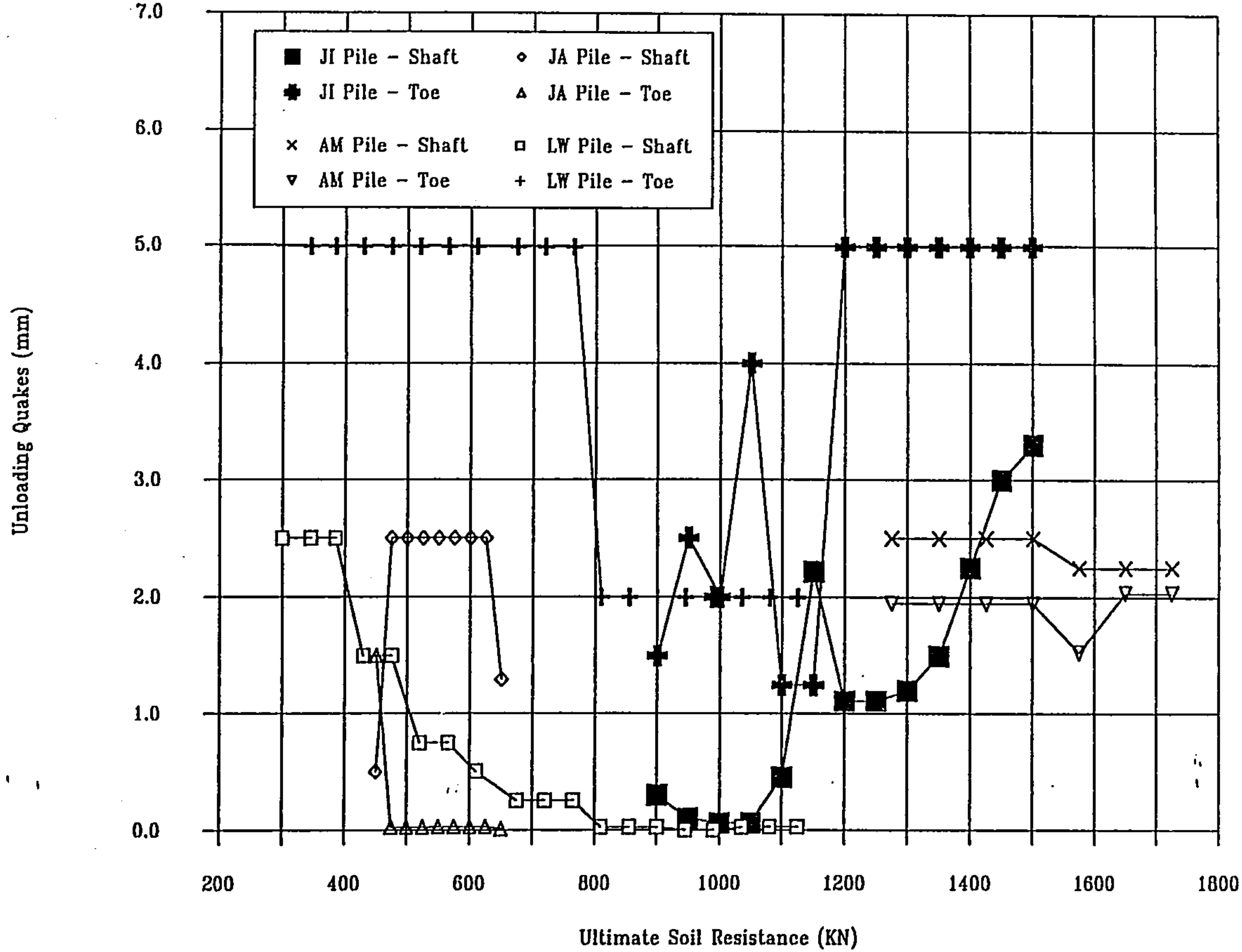

Fig. 7.15 Variation of Unloading Quakes

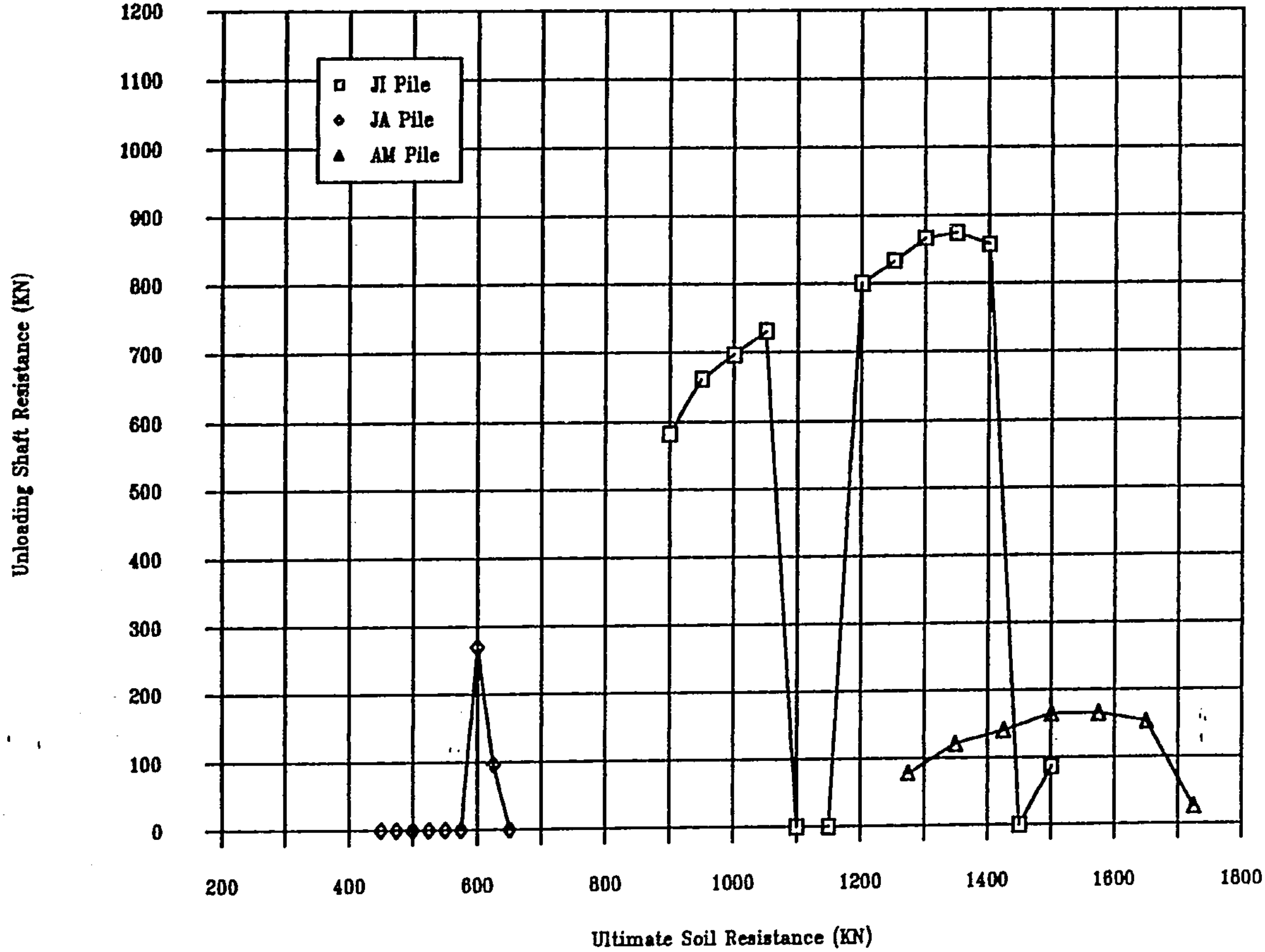

Fig. 7.16 Variation of Unloading Shaft Resistance

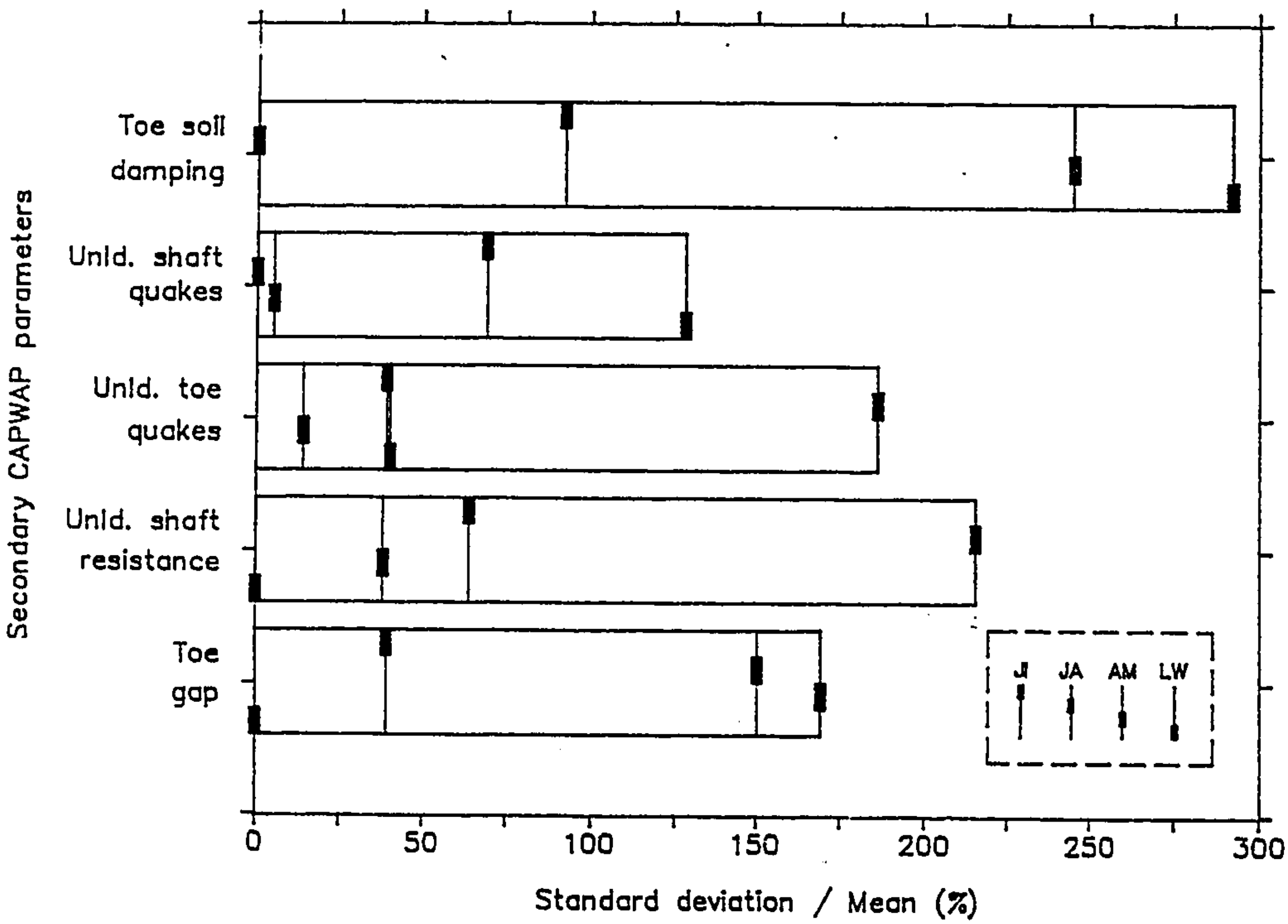

Fig. 7.17 Coefficients of Variation for Secondary CAPWAP Parameters

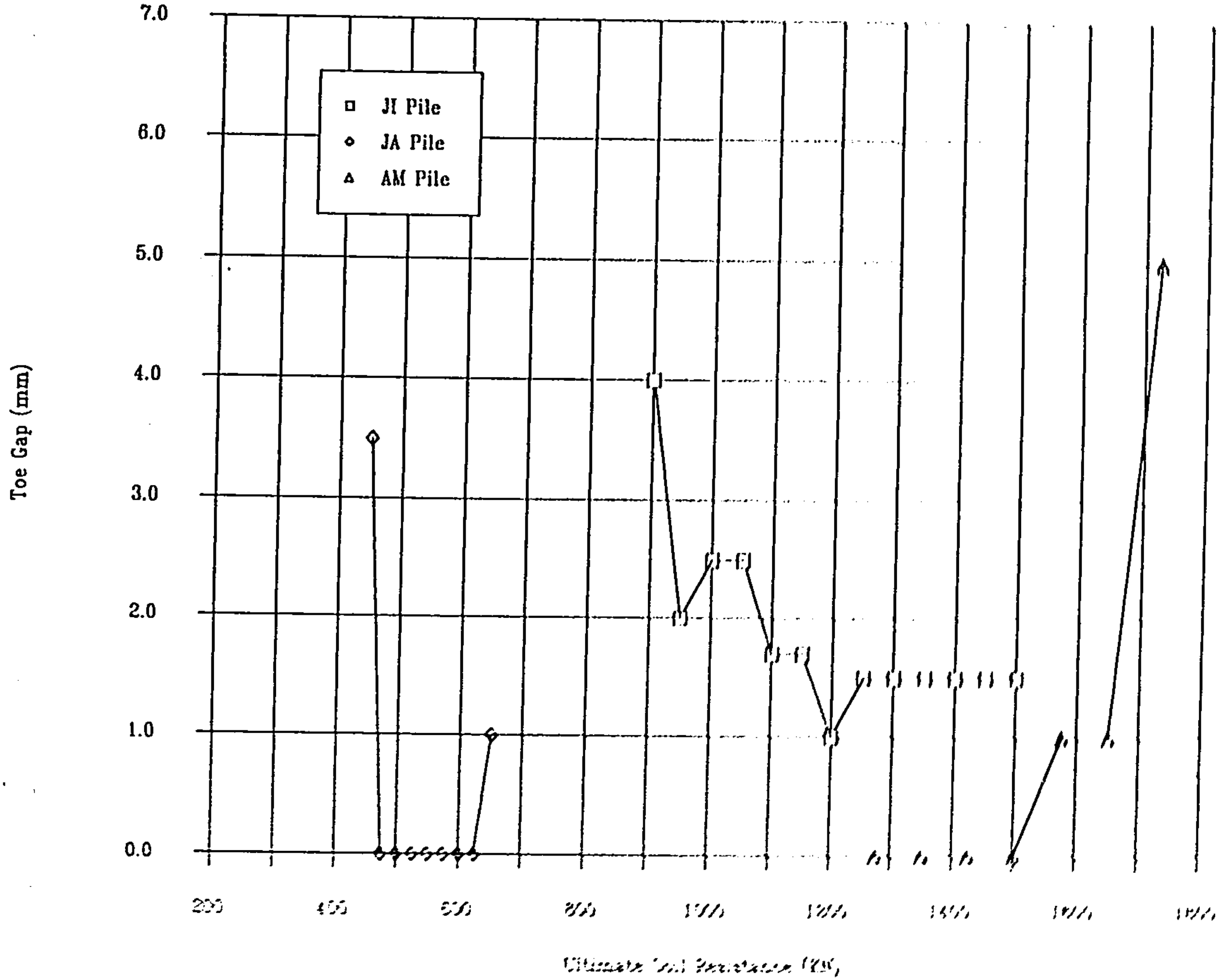

Fig. 7.18 Variation of Toe Gap

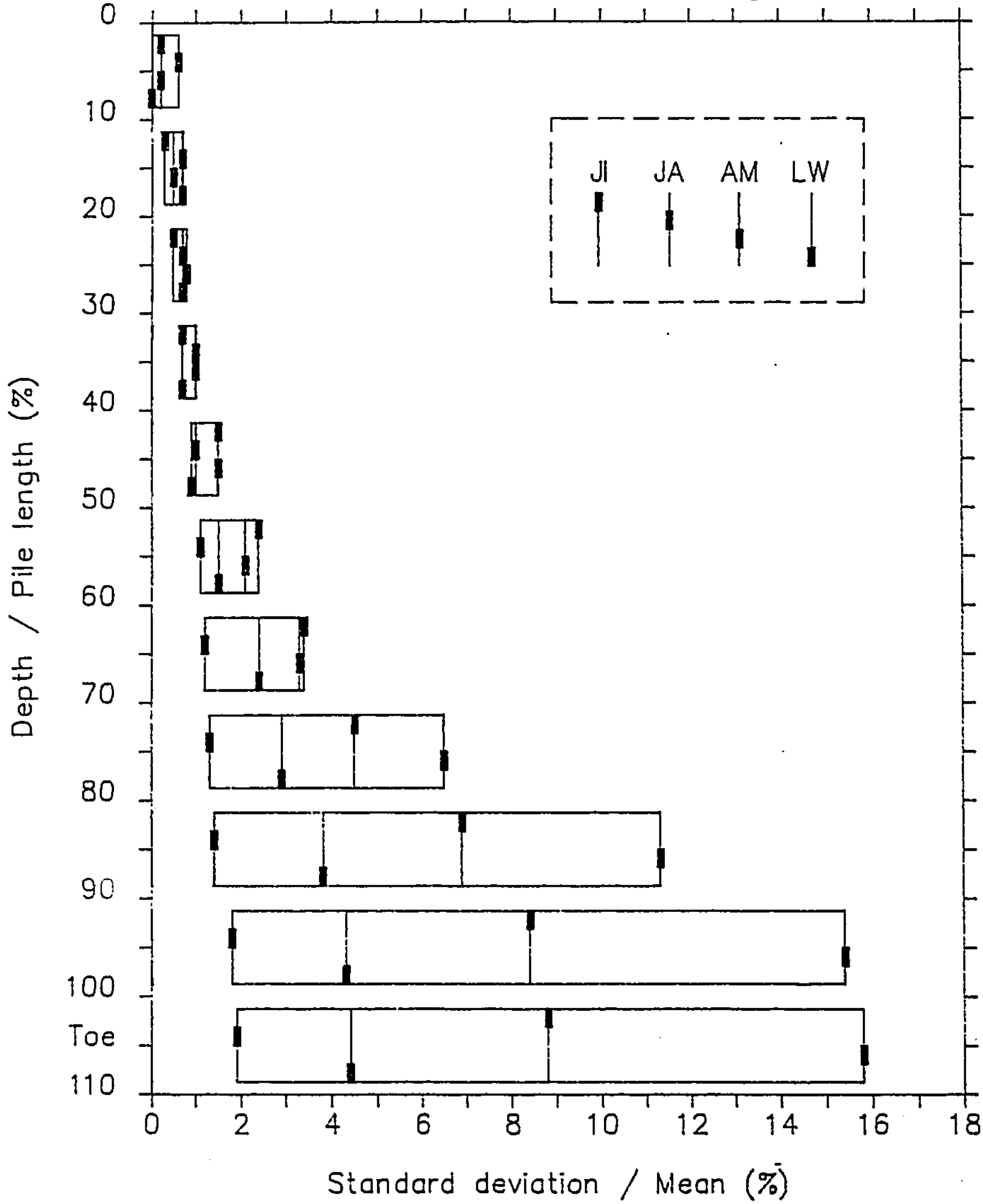

Fig. 7.19 Coefficients of Variation for Maximum Element Displacements

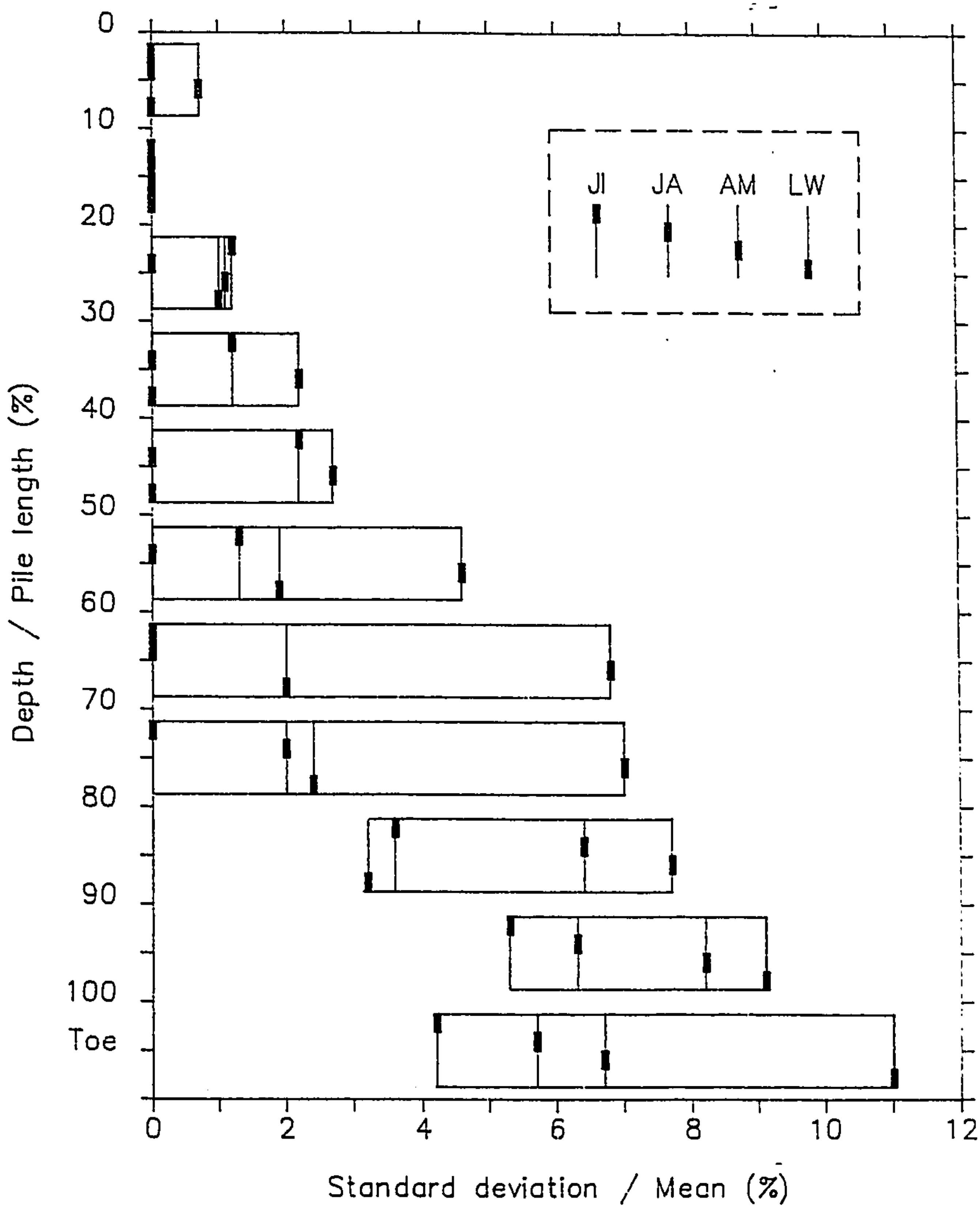

Fig. 7.20 Coefficients of Variation for Maximum Element Velocities

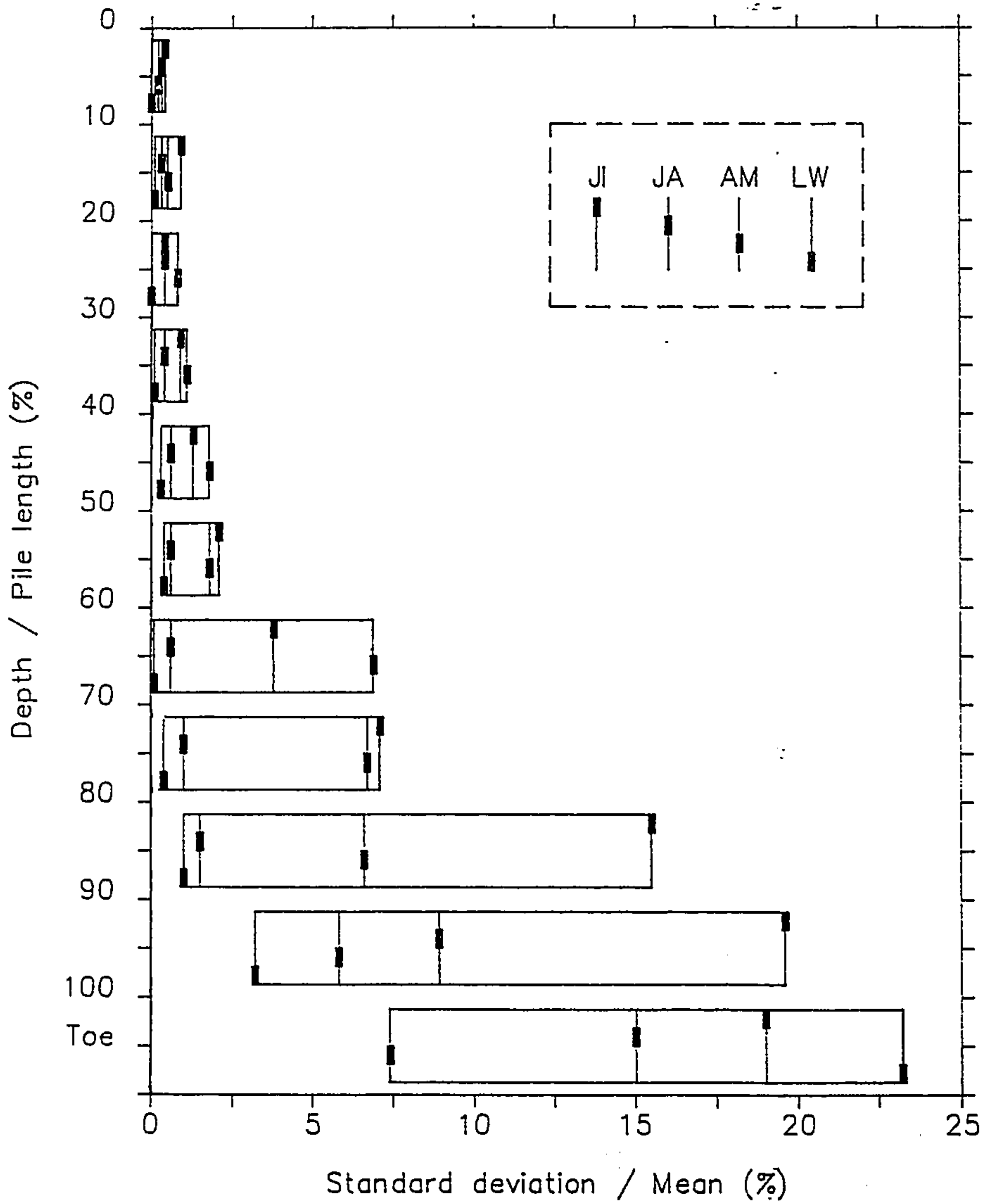

Fig. 7.21 Coefficients of Variation for Maximum Compression Forces

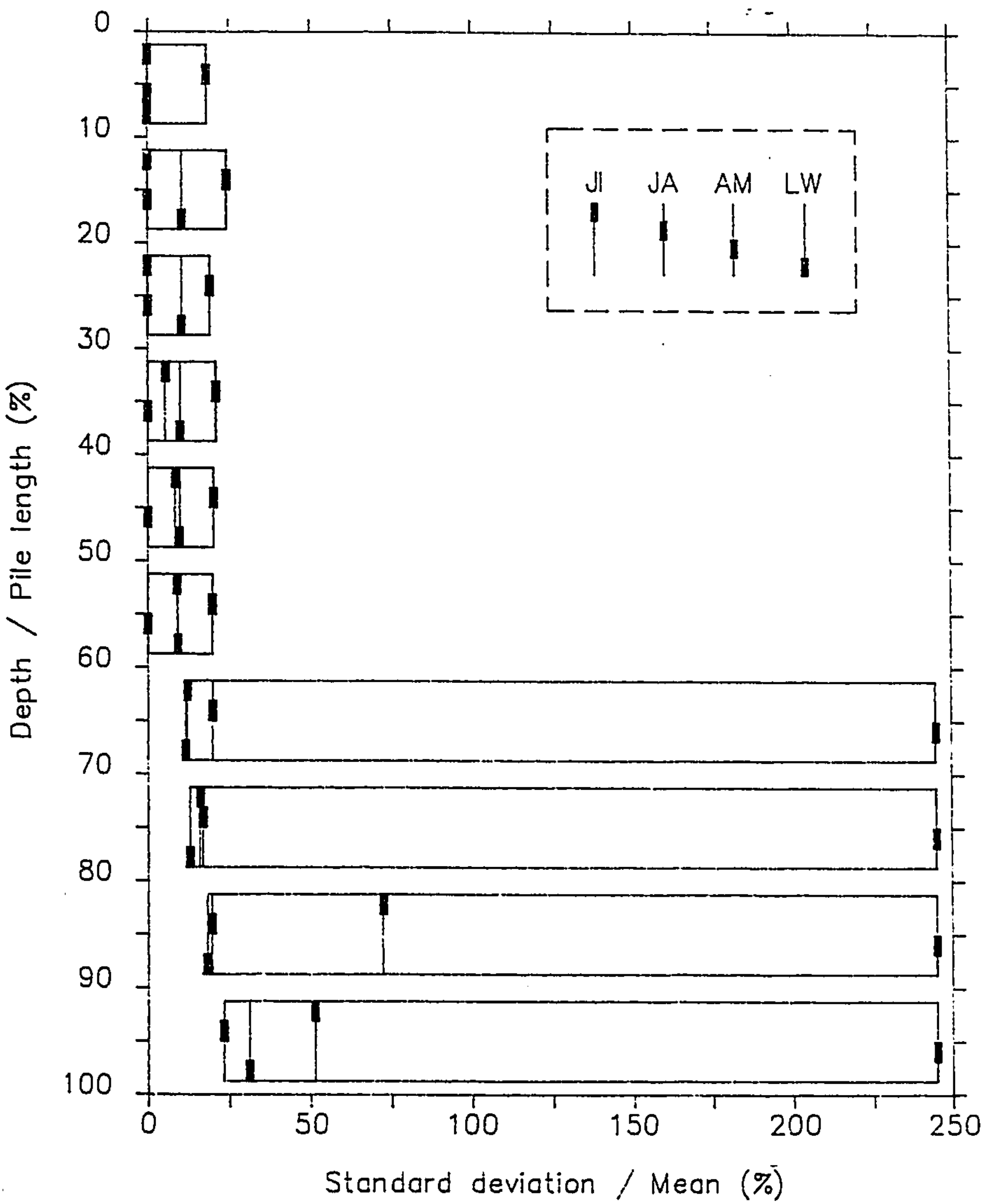

Fig. 7.22 Coefficients of Variation for Maximum Tension Forces

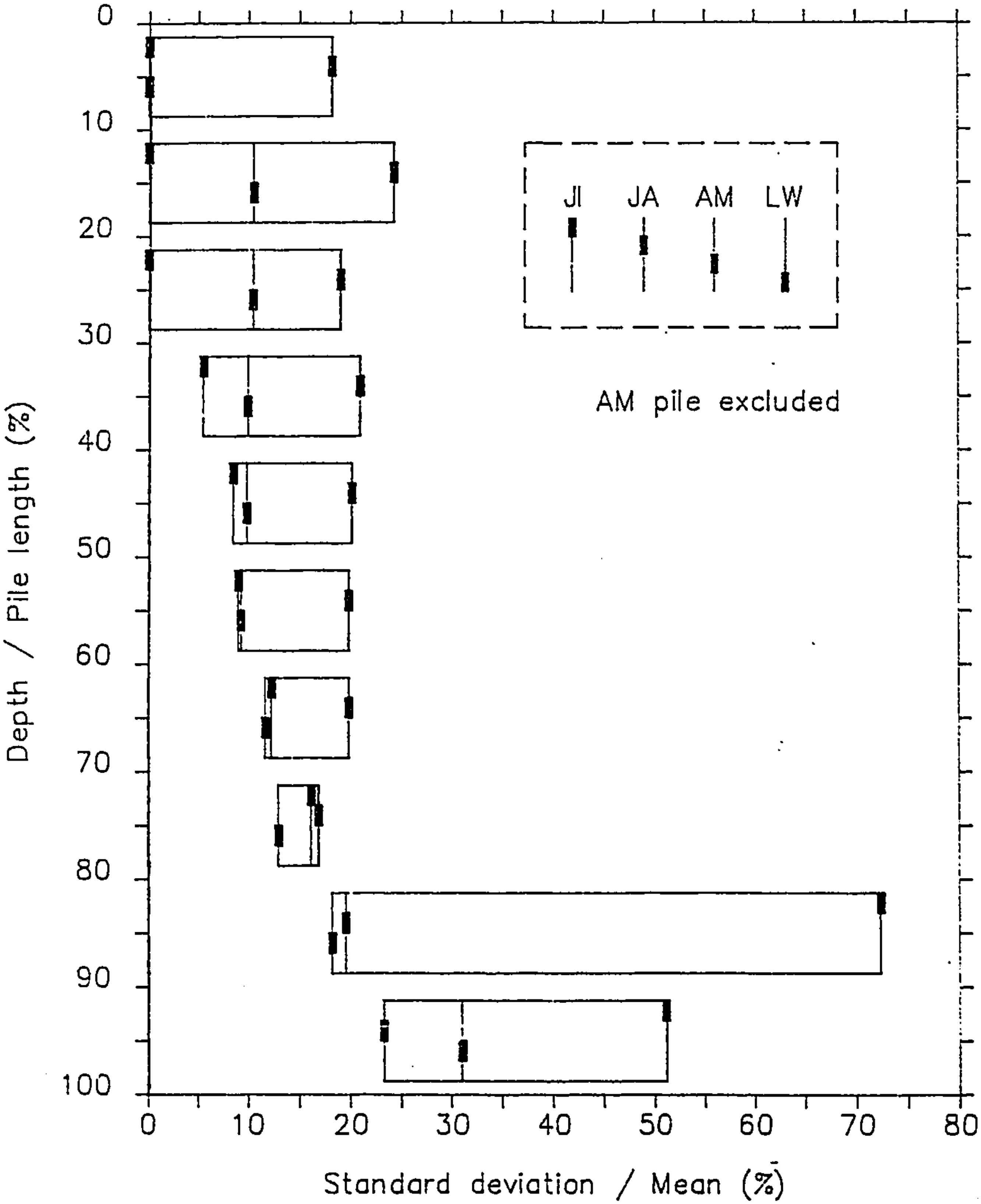

Fig. 7.23 Coefficients of Variation for Maximum Tension Forces Excluding AM Pile